

ULTIMATE STRENGTHS OF WELDED JOINTS IN
TUBULAR STEEL STRUCTURES

A thesis submitted for the degree of
Doctor of Philosophy awarded by the
Council for National Academic Awards.

by

Keith David Sparrow B.Sc.

BEST COPY

AVAILABLE

Variable print quality

TEXT BOUND INTO

THE SPINE

**TEXT
CUT OFF IN THE
ORIGINAL**

ULTIMATE STRENGTHS OF WELDED JOINTS IN TUBULAR STEEL STRUCTURES

by Keith David Sparrow B.Sc.

SUMMARY

An experimental and theoretical investigation of the strength of welded T-joints has been carried out, and the following tests were conducted:-

- 17 No. tests for ultimate axial strength (P_u)
- 17 No. tests for ultimate bending strength (M_u)
- 71 No. tests for combined axial and bending strength

The parameter ranges of the tests were:-

brace diameter/chord diameter:	0.42, 0.53, 0.67, 0.77, 1.0
chord diameter/chord thickness:	18, 21, 23, 32
brace thickness/chord thickness:	0.63 - 1.4

All test specimens were steel to BS Grade 43C, with an average nominal yield strength of 350N/mm^2 .

The interaction between axial and bending strength has been studied experimentally and theoretically and a relationship has been established. Formulae are proposed for calculating the ultimate axial strengths of welded T-joints and the ultimate bending strengths of welded T-joints.

Numerical analysis of the experimental test results has been carried out using regression methods. A computer program has been developed to facilitate this task. Design equations have been deduced as a result of the regression analysis.

A theoretical study of T-joint stress distribution under axial and bending loads has been carried out using an elastic finite element system called LUSAS, which has been developed at Imperial College, London by Dr. P. Lyons. Results have been plotted using programs developed at Kingston Polytechnic.

A review of the twenty existing methods for calculating the ultimate static strengths of welded T, Y, X, K and N-joints in circular hollow steel sections has also been carried out. Calculated loads have been compared with 450 existing test loads, and the results have been analysed statistically. Each formula has been reviewed and discussed and, as a result of the statistical analysis, recommendations for design formulae for K, N and X-joints have been made.

INDEX

	<u>Page No.</u>
SUMMARY	i
ACKNOWLEDGEMENTS	xii
NOTATION	xiii
1. INTRODUCTION	1
1.1. Applications of Hollow Steel Sections (HSS)	2
1.1.1. Architectural Structures	2
1.1.2. Office Buildings	2
1.1.3. Industrial Buildings	3
1.1.4. Towers	4
1.1.5. Bridges	4
1.1.6. Space Frames	4
1.1.7. Marine Structures	5
1.1.8. Other Uses	5
1.2. Utilisation of the Void in Structural Hollow Sections (SHS)	6
1.3. Development of SHS Worldwide	6
1.3.1. United Kingdom	6
1.3.2. Canada	8
1.3.3. Japan	9
1.3.4. France	10
1.3.5. Germany	10
1.4. Advantages of SHS	11
2. JOINTS IN HOLLOW STRUCTURAL SECTIONS	25
2.1. Types of Joint	25
2.1.1. T-Joints	25
2.1.2. K-Joints	25

	<u>Page No.</u>
2.1.3. N-Joints	25
2.1.4. Y-Joints	25
2.1.5. X-Joints	25
2.1.6. Multiple Joints	25
2.2. Categories of Joint	25
2.2.1. Bolted Joints	25
2.2.2. Welded Joints	26
2.3. Reinforcement of Joints	26
2.3.1. Joint Cans	26
2.3.2. Gusset Plates	27
2.3.3. Joint Plates	27
2.3.4. Concrete Filling	27
2.4. Characteristics of Joint Types	27
2.4.1. T-Joint	27
2.4.2. Y-Joint	27
2.4.3. K- and N-Joints	28
2.4.4. Joints with Three Bracing Members	28
2.5. Types of Loading	28
2.5.1. T-Joint	28
2.5.2. Y-Joint	28
2.5.3. K-Joint	29
2.5.4. N-Joint	29
2.5.5. X-Joint	29
2.5.6. Joint with Three Bracing Members	29
2.6. Tubular Joint Strength - General	29
2.7. The Present Investigation	30

	<u>Page No.</u>
3. EXISTING METHODS FOR CALCULATING THE STATIC STRENGTH OF T, Y, K AND N JOINTS IN CHS, WHICH ARE AVAILABLE FOR AXIAL LOADS ONLY	37
3.1. Introduction	37
3.2. Existing Methods for Calculating Either the Working Strength or the Ultimate Strength of a Welded Tubular Connection	39
3.2.1. Shear Area	39
3.2.2. Column Analogy	41
3.2.3. Roark Method 1	43
3.2.4. Roark Method 2 - Empirical	45
3.2.5. Kellogg Method	46
3.2.6. Kurobane Method	49
3.2.7. Naka, Kato, Kanatani Method	53
3.2.8. Washio, Togo Method	56
3.2.9. J. Blair Reber Method	57
3.2.10. Toprac & Marshall Method	63
3.2.11. Kato Method	66
3.2.12. A.P.I. Method	68
3.2.13. A.W.S. Method	71
3.2.14. Stelco Method (Bouwkamp)	72
3.2.15. Det Norske Veritas	76
3.2.16. Visser Method	81
3.2.17. Harlicot, Mouty, Tournay Verification Formulae	83
3.2.17.1. Y and T-Joints	83
3.2.17.2. N and K-Joints	84
3.2.17.3. X-Joints	85
3.2.18. Harlicot, Mouty, Tournay Envelope Formulae	85
3.2.18.1. T and Y-Joints	85
3.2.18.2. N and K-Joints	85
3.2.18.3. X-Joints	86

	<u>Page No.</u>
3.3. Summary of Existing Recommendations on T, K, Y and N-Joints	86
3.3.1. T-Joint Recommendations	87
3.3.2. K and N-Joint Recommendations	87
3.4. Calculation of Ultimate Loads Using the Existing Design Formulae	89
3.5. Discussion of Results Obtained for Each Existing Formula	90
3.5.1. Shear Area	90
3.5.2. Column Analogy	91
3.5.3. Roark 1	91
3.5.4. Roark 2	91
3.5.5. Kellogg	92
3.5.6. Kurobane	92
3.5.7. Naka, Kato, Kanatani	93
3.5.8. Washio, Togo	93
3.5.9. Reber	93
3.5.10. Toprac	94
3.5.11. Kato	94
3.5.12. A.P.I.	94
3.5.13. A.W.S.	94
3.5.14. Stelco (Bouwkamp)	94
3.5.15. Det Norske Veritas	95
3.5.16. Visser	95
3.5.17. Harlicot, Mouty, Tournay Verification Formulae	96
3.5.17.1. T and Y-Joints	96
3.5.17.2. K and N-Joints	96
3.5.18. Harlicot, Mouty, Tournay Envelope Formulae	97
3.6. Recently Available Experimental and Theoretical Data	98
3.6.1. Pan, Plummer Method	98
3.6.2. Kurobane, Makino, Mitsui	99
3.6.3. Ultimate Strength of X-Joints	100
3.6.4. Discussion and Conclusion	102

	<u>Page No.</u>
4. FINITE ELEMENT METHOD USED IN THE PRESENT INVESTIGATION FOR ANALYSING T-JOINTS	118
4.1. Finite Element Computer System	118
4.1.1. General	118
4.1.2. Machine Independence and Requirements	118
4.1.3. Modular Internal Data Structure	119
4.1.4. Modular Computer System Structure	119
4.1.5. Independent User Options	119
4.1.6. The Computer System	120
4.1.7. Data Processors	120
4.1.8. Finite Element Library	122
4.1.9. Pre-Solution Processor	122
4.1.10. Random Access Front Processor	123
4.1.11. Post-Solution Processor	129
4.2. Thin Plate Flexure Elements	130
4.2.1. Introduction	130
4.2.2. Requirements for Thin Plate Flexure Elements	133
4.3. Theory for Constrained Thin Plate Elements	134
4.3.1. Basic Assumptions	134
4.3.2. Derivation of Thin Plate Theory	135
4.3.3. Unconstrained Displacement Fields	139
4.3.4. Hierarchical Shape Functions	140
4.3.5. Hierarchical Mapping and the Jacobian Matrix	141
4.3.6. Strain-Displacement Relations	146
4.3.7. Shape Function Array	148
4.3.8. Kinematic Constraints	149
4.3.9. Numerically Integrated Stiffness Matrix	153
4.3.10. Nodal and Distributed Loading	154
4.4. Reduced Numerical Integration	155
4.5. Stress Smoothing	156

	<u>Page No.</u>
4.6. Semi-Loof Element	157
4.6.1. General	157
4.6.2. The Element	158
4.6.3. In Plane Behaviour	160
4.6.4. Out of Plane Behaviour	160
4.6.5. Shear Constraints	162
4.7. Notation for Finite Element System (LUSAS)	164
5. RESULTS OF FINITE ELEMENT ANALYSIS OF T-JOINTS WHICH WERE TESTED IN THE PRESENT INVESTIGATION FOR AXIAL AND BENDING LOADS	181
5.1. Finite Element Analysis	181
5.2. Results of Finite Element Analysis of T-Joints	182
5.3. Conclusions	184
6. EXPERIMENTAL PROCEDURE FOR THE PRESENT INVESTIGATION	220
6.1. General	220
6.2. Welding	222
6.3. Strength of Fillet Welds	222
6.4. Present Program	223
6.5. Experimental Apparatus	226
6.5.1. Testing Rig	226
6.5.2. Load Application	233
6.5.3. Instrumentation	233
6.5.4. Test Specimens	234

7.	PRESENT EXPERIMENTAL INVESTIGATION OF T-JOINTS UNDER AXIAL LOAD, BENDING LOAD, AND COMBINED AXIAL AND BENDING LOAD - RESULTS AND DISCUSSION	255
7.1.	T-Joints - Axial Load Only	255
7.1.1.	$d_1/d_o = 0.42$	255
7.1.2.	$d_1/d_o = 0.53$	257
7.1.3.	$d_1/d_o = 0.67$	259
7.1.4.	$d_1/d_o = 0.77$	261
7.1.5.	$d_1/d_o = 1.0$	263
7.1.6.	General Conclusions	264
7.2.	T-Joints - Moment Load Only	265
7.2.1.	$d_1/d_o = 0.42$	265
7.2.2.	$d_1/d_o = 0.53$	267
7.2.3.	$d_1/d_o = 0.67$	268
7.2.4.	$d_1/d_o = 0.77$	269
7.2.5.	$d_1/d_o = 1.0$	270
7.2.6.	General Conclusions	271
7.3.	T-Joints - Combined Axial Load and Bending Moment	272
7.3.1.	General	272
7.3.2.	Interaction Tests for Combined Axial and Moment Loading	273
7.3.3.	$d_1/d_o = 0.42$	273
7.3.4.	$d_1/d_o = 0.53$	273
7.3.5.	$d_1/d_o = 0.67$	274
7.3.6.	$d_1/d_o = 0.77$	274
7.3.7.	$d_1/d_o = 1.0$	274
7.3.8.	Relationship Between f_{bu} , f_{au} and f_a	275
7.3.9.	General Conclusions	277
8.	MULTIPLE REGRESSION FOR ANALYSIS OF THE ULTIMATE LOAD TESTS ON T-JOINTS	338
8.1.	Definitions	338
8.1.1.	Linear Regression	338

8.1.2.	Correlation	338
8.1.3.	Correlation and Regression	340
8.2.	Methods of Multiple Regression	341
8.2.1.	Full Multiple Regression	341
8.2.2.	Backward Elimination	342
8.2.3.	Forward Selection Procedure	343
8.2.4.	Stepwise Regression Procedure	344
8.2.4.1.	Introduction	344
8.2.4.2.	General Procedure for Computer Method	344
8.2.4.3.	Stepwise Procedure	347
8.2.5.	A Computer Program - Stepwise Procedure	354
9.	REGRESSION ANALYSIS APPLIED TO THE RESULTS OF ULTIMATE LOAD TESTS ON T-JOINTS UNDER AXIAL AND MOMENT LOADS, CARRIED OUT IN THE PRESENT INVESTIGATION	362
9.1.	Ultimate Axial Load (P_u)	362
9.1.1.	Analysis of Test Results	362
9.1.2.	Results	364
9.1.3.	Discussion	366
9.1.4.	Conclusions and Proposed Formulae	369
9.2.	Ultimate Moment Load (M_u)	370
9.2.1.	Analysis of Test Results	370
9.2.2.	Results	371
9.2.3.	Discussion	372
9.2.4.	Conclusions and Proposed Formulae	374
10.	FINAL CONCLUSIONS	380
10.1.	Equations Proposed From the Present Experimental Study	380

	<u>Page No.</u>
10.1.1. Ultimate Axial Load (Pu)	380
10.1.2. Ultimate Moment Load (Mu)	380
10.1.3. Combined Axial and Moment Load	380
10.2. Equations Proposed From Statistical Review	381
10.2.1. K-Joints	381
10.2.2. X-Joints	381
10.3. General	382
10.3.1. T-Joints	382
10.3.2. K-Joints	383
10.3.3. X-Joints	383
11. RECOMMENDATIONS FOR FURTHER RESEARCH	384
11.1. Analytical Work	384
11.2. Experimental Work	385
11.2.1. T-Joints	385
11.2.2. K-Joints	385
REFERENCES	386
APPENDIX A	
Table 1 - Data for Statistical Review in Chapter 3	1A
Table 2 - Calculated Loads for Statistical Review in Chapter 3	5A
APPENDIX B	
Multiple Regression Computer Program Listing	1B
Strain Gauge Profiles for Experimental Results	10B
Intersection Lengths U_b and U_c (L_2 and L_1) - Formulae	40B

ACKNOWLEDGEMENTS

The research described herein was carried out in the School of Civil Engineering at Kingston Polytechnic. During the course of the research the author received helpful suggestions from many persons. In particular the author wishes to express his gratitude to the following:-

To Mr. D. Simm for the Helpful way in which he accommodated the project as Head of School, and for his encouragement throughout the research period.

To Dr. A. Stamenković for acting as supervisor for this work, for his help and guidance throughout the duration of the project. The author would also like to acknowledge Dr. Stamenković for initiating the research program.

To Mr. T. Giddings, Mr. N. Yeomans, and others at the Research Centre of the British Steel Corporation's Tubes Division at Corby for their guidance, and their assistance in providing the test specimens for the experimental work.

To Mr. E. N. Bromhead for his advice and help in matters relating to computing work.

To Dr. P. Lyons for permitting the author the use of his finite element system at Imperial College (LUSAS).

To Miss F. Javadi for her tireless advice and assistance in carrying out the finite element computing part of this research.

To Mr. R. Stevens for his advice and assistance in carrying out the experimental work; for constructing and assembling the testing rig.

To my wife, Christine, for typing the manuscript and for her support in general.

NOTATION

An Cross-sectional area of tube member

n = 0, for chord member

n = 1, for compression branch member

n = 2, for tension branch member

The significance of n is the same wherever used as a suffix in these abbreviations.

dmin Minimum nominal diameter of two branch members at a joint.

dn Diameter of tube member.

e Eccentricity - usually of a 'K' type joint.

fcn Applied axial stress in tube member.

fbcn Applied bending stress in tube member.

Fn Applied axial member load.

fyn Specified yield strength (stress) of tube material.

g Gap between branch members along chord member crown - usually of a 'K' or 'N' type joint.

go Ratio of gap (g) divided by chord diameter (do).

K₁ Joint strength parameter for bracing member angle.

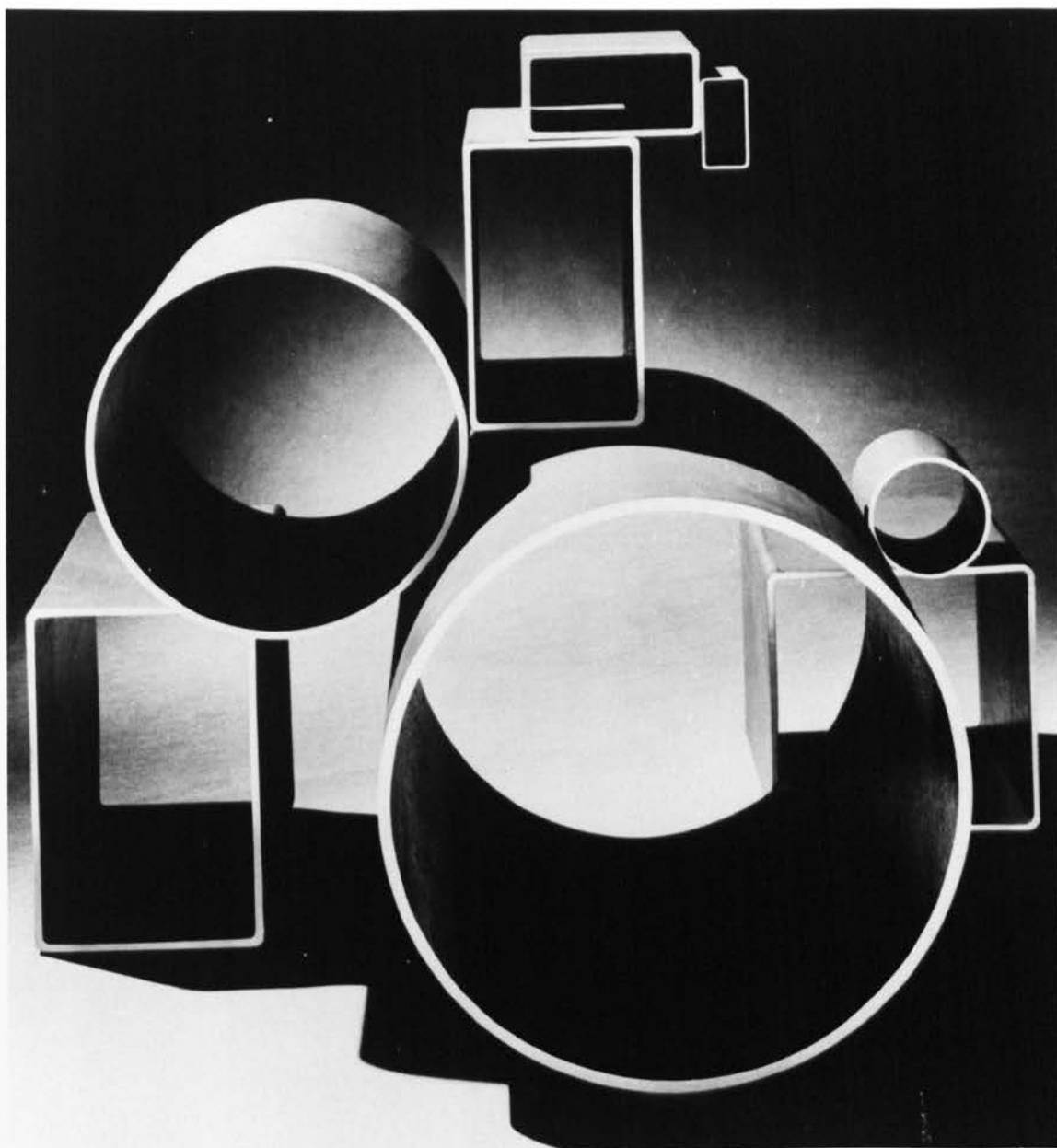
K₂ Joint strength parameter for chord prestress.

K₃ Joint strength parameter for gap.

K₄ Joint strength parameter for local bending effects.

k_A	Intersection length factor ($L_A = Lk_A$)
k_B	Intersection section factor ($Z_B = Zk_B$)
L	Intersection length between brace and chord members.
M	Applied moment at joint.
M_u	Ultimate moment of joint.
M_y	Yield moment of joint.
N	Applied axial force in chord member.
N_u	Ultimate axial force in chord member.
n	Dimensionless group $N/f_y \cdot A_o$.
P	Applied axial force at joint in branch member.
P_N	Allowable normal force in chord at a joint.
P_n	Safe working load of a joint.
P_u	Ultimate axial force at joint in branch member.
q	Overlap of branch members usually in 'K' or 'N' type joint.
R_n	Radius of tube member.
t_n	Thickness of tube member.
U_b	Of an overlapped K or N-joint: the intersection length between the two overlapping branch members.
U_c	Of an overlapped K or N-joint: the intersection length between the compression branch only and the chord member.

Z_n	Inclined length of branch member diameter, along chord crown ($Z_n = d_n/2\sin\theta_n$)
α	$\sin^{-1} d_1/d_o$
β	d_1/d_o
γ	R_o/t_o
τ	t_1/t_o
θ_n	Angle of inclination of branch member.
ν	Poisson's ratio.



CHAPTER 1

INTRODUCTION

In 1952 the British company of Stewarts and Lloyds rolled the first rectangular hollow steel sections (RHS) which were used as stair treads in the walkways of the first big jib - the walking dragline W1400 - built at Corby to strip the overburden in the open cast iron-ore quarries. From these small beginnings, structural hollow sections (SHS) have developed to the point where they are a fully accepted type of structural steel section. Not all countries have reached the same stage of development, but in many, a full range of structural hollow sections is being produced and used in all types of structural applications. Hollow steel sections (HSS) are used as columns, or as members in truss structures, either simple frames, or complex space frames. Jointing has always been a major problem for this type of structure and many ingenious methods have been evolved. The most popular method for jointing relatively small sections has been one which involved some type of bolted connector. The NODUS system for circular sections developed by the British Steel Corporation is an example of this joint.

Recent developments in the use of hollow steel sections have required the use of welded connections, braced and unbraced, between members. The welding procedure is fairly straightforward in RHS, but becomes more complex for circular hollow sections (CHS). Straight cut circular sections may only be welded to a curved surface provided that the weld gap caused by the curve does not exceed some maximum value e.g. 3.17mm. Where this is exceeded the branch tube must be profile shaped (known as saddling). The profile cutting of ends may be carried out by flame cutting, or by flame cutting and subsequent grinding to clean up the edges. Machines are available which will flame cut and profile shape the ends of any combination of diameters and angles required. They will also chamfer the ends for butt welding.

1.1. Applications of HSS

1.1.1. Architectural Structures

The covered walkway in Figure 1 is constructed in SHS and glass to a height of 15 metres. This combination of materials creates a light and airy internal walkway, appreciated by pedestrians in cold weather. Designers do not like to be confined to rectilinear forms. One of the advantages of SHS is that designers can use it to create curves in any three-dimensional form. The clean, good looks of SHS has long been recognised by Architects, who have often used it in situations where the steel frame is dramatically exposed to view. Typical applications include banking halls, swimming pools, ice rinks, stadiums and exhibition pavilions.

1.1.2. Office Buildings

The structural hollow section has the highest compression strength to weight ratio of any steel section. Its application to columns in office buildings is thus quite natural. In addition to structural efficiency, the compact shape of SHS gives clearer floor areas. A good example is the Estel Headquarters in Holland which features SHS not only in the structural framework but also in the facade units which incorporate the central heating system.

A ten storey office tower at Hanley uses 304.8 square SHS, commencing with a thickness of 16mm at the ground floor and reducing to 12.5mm at the upper floor. The columns were supplied in three storey lengths with temporary shelf angles tack welded to the ends. On site these were removed after butt welding the two exposed sides, and the butt welding was completed. The use of HSS in this way eliminated the need for temporary bracing and made alignment of the columns easier.

The danger of earthquakes in Japan means that their high rise office buildings must be extremely rigid. Frames using 500 x 500mm RHS columns with thicknesses up to 50mm have been used. Unique shop fabricated connections consisting of column, internal diaphragms

at the connection point, and short beam stubs, are popular. These connections are rigid under bending moments and have the necessary strength to resist seismic shearing forces.

1.1.3. Industrial Buildings

These structures must be rugged and economical. SHS is rugged but can only be economical where an expertise has been acquired in its application. A very large construction project, presently in progress, will eventually double the Steel Company of Canada's steelmaking capacity. Phase 1, which will add 1½ million tons per year, will start in 1980. Over 80,000t of structural steel were used in the complex including 8,000t of structural hollow sections. SHS were used exclusively for roof trusses, most of which had a 32m span. The high compressive and torsional strength of HSS gave a more economical design than was possible using conventional hot rolled sections. HSS trusses are extremely rigid and can be lifted from one point, therefore, reducing erection costs. SHS was also used to provide aesthetic pipe racks, conveyor supports and sign structures. About 6km of pipe racks have been constructed from 300 x 300mm and 250 x 250mm RHS.

Industrial halls are more common and in total represent a larger market for SHS. An example is the Jumbo jet hangar at London's Heathrow Airport (Figures 2, 3 & 4). The building is 138m x 81m and 30m high. The main girders in the roof span 138m between columns, and the transverse Pratt (N) girders span 45m. The high efficiency of SHS in compression easily accommodates the larger effective lengths required in this type of construction. The savings in joint fabrication more than offset the slight weight penalty. In this structure the rainwater pipes from the roof run within the RHS columns.

SHS storage structures have been widely used to cover bulk materials such as wood chips, cement, and potash.

SHS has been accepted for use in the construction of pipe racks, flare towers and stair towers in heavy water plants and in clear generating stations.

1.1.4. Towers

SHS has been widely used for all types of towers in the communications and electrical industries. All governments are under strong pressure to conserve the environment. The aesthetics offered by SHS give an improved appearance (Figure 5).

Tall microwave towers have to be designed to meet very severe deflection requirements imposed by the communications industry. The low drag coefficient of SHS makes it the natural choice for such towers.

1.1.5. Bridges

The aesthetic qualities of SHS combined with its structural efficiency is the reason why it is widely used in pedestrian footbridge construction. The CN Tower in Canada is the tallest free-standing structure in the World. One of its features is a glass enclosed pedestrian passageway serving as the Tower's main entrance; the bridge consists of three continuous spans over two concrete piers. The welded 135m long truss structure is made from 300 x 300mm RHS chord and 250 x 250mm RHS web (branch) members. The whole structure is 3.5m deep and 4.0m wide.

Pipeline bridges of the type shown in Figure 6 are becoming more popular since the application of CHS gives a light, flexible structure, which compares favourably costwise with the alternatives e.g. tunnelling or pipe jacking.

1.1.6. Space Frames

Since the recent advent of jointing systems the use of SHS in space frame construction has increased (Figure 7). Large clear spans are available, with the possibility of accessible storage space incorporated in the roof of a structure.

1.1.7. Marine Structures

Round SHS (CHS) has found wide application in pile foundations. It is the only piling material that can be inspected after driving to check for out-of-straightness and end damage. Tubular piling is readily joined in the field to form any desired length.

The Japanese have taken the development of tubular piling one step further. Through the addition of interlocking devices along the edges of CHS, a tubular form of sheet piling is obtained. The high bending strength of this type of pile gives increased lateral strength for coffer dams and retaining walls. The tubular shape can also accept harder driving than conventional sheet piling.

SHS has been extensively used in all of the offshore oil rigs fabricated throughout the world. It has also been used for dolphins and mooring towers which are required for loading and unloading the oil industry's super tankers, (Figure 8).

1.1.8. Other Uses

These are numerous and include such diverse uses as, scaffolding, agricultural buildings and machinery, cattle pens, roll bars for agricultural and earth moving equipment, jibs of cranes, (Figures 9, 10, 11), lorry chassis, bents and trusses to support conveyors, railway ties and crossings, and road sign supports and safety barriers.

1.2. Utilisation of the Void in SHS

As mentioned earlier, one use of the void in SHS is as a passageway for water pipes, drainpipes and/or electrical conduits.

A recent development has been the increase in fire protection by filling the void with water. Provided the water supply is maintained the resulting structure provides infinite fire resistance. The structure behaves exactly like a boiler.

For many years, SHS piling has been concrete filled. Recently, however, concrete filled SHS columns are being used in structures. The concrete substantially increases the strength of the column in addition to providing increased fire resistance.

Recent papers give more details of research developments in both these fields of application^{1,2,3}.

1.3. Development of SHS Around the World

1.3.1. United Kingdom

A full range of RHS and CHS are manufactured in the U.K. by the British Steel Corporation. RHS are available as square from 20 x 20 x 2mm to 400 x 400 x 12.5mm or rectangular from 50 x 30 x 2.4mm to 450 x 250 x 16.0mm. CHS are available from 21.3 x 3.2mm to 457 x 40mm.

The steel is supplied in accordance with BS 4360 Grades 43C, 50C, 55C, and WR 50 (weathering steel). In addition, during 1976, a new steel "ROPSTEEL" was introduced for use in the construction of tractor cab and roll over protection structures. This steel is tested for impact at -29°C according to the specimen size.

Plane Trusses

At the shopping centre in the new town of Craigavon, 30 miles south of Belfast, Northern Ireland, there are plane lattice girders in a roof which is supported by suspension cables from 21m high masts of HSS "ladder form" in Stalcrest weathering steel to give a clear span of 48m. The building size is 96m x 120m giving 11,000m² of floor space. The 12m span lattice roof girders are 1m deep using 88.9 square HSS top chords; 76.2 x 50.8 HSS bottom chords with 42.4 diameter CHS web members.

Triangulated Roof Trusses

On the new town development at Runcorn, on the south bank of the Mersey, is a factory structure called the TKK Building. The roof trusses are triangulated and span 30m at 11.25m centres. The trusses are 3.75m wide and were fabricated and delivered in halves for site jointing prior to erection. Alternate trusses are supported on twin columns 9m high, the remaining trusses being carried on lattice girders spanning between the twin columns.

The roof sheeting is galvanized steel trough decking 85mm deep with vapour barrier, insulation, three layers of roofing felt and finished with limestone chippings.

The roof decking spans directly onto the top chords of the triangular girders, which have 114.3 square HSS top chord with a 139.7 diameter CHS bottom chord. Supporting columns are 254 square HSS set outside the building for architectural effect. The building was awarded one of the BSC/BCSA Structural Design Awards for 1975.

Space Frames

With the development of the Nodus jointing system by the British Steel Corporation, large truss space frames are now in use. The Harrow Leisure Centre uses Nodus to cover 43.2 x 43.2m making it one of the largest clear areas completed in the U.K.

HSS has also been extensively used in other areas such as for columns in structures, for bridges and parapets, and for handrails, scaffolding etc.

1.3.2. Canada

Since 1962 Stelco's HSS has been produced by the continuous weld (CW) process. The maximum sizes available from this method are CHS up to 114.3mm O.D., square HSS up to 100 x 100mm, and RHS up to 127 x 76.2mm. The maximum wall thickness is 9.5mm. In 1967 larger sizes were introduced, square SHS up to 305 x 305mm, RHS up to 305 x 203mm and CHS up to 406mm O.D. The standard yield strength was raised by 248N/mm^2 to 350N/mm^2 , and the maximum wall thickness for 350N/mm^2 yield strength HSS became 11.4mm. These larger sections were produced by the Electric Resistance weld (ERW) process.

SHS have been extensively used in Canada in most of the structures mentioned previously. Stelco have published design rules for welded joints in SHS based on a joint efficiency concept⁴. These will be discussed in a later section.

A typical example of the use of HSS in Canada is the Royal Bank of Toronto. The office complex includes two triangular office towers of 41 and 26 storeys, linked by a 130ft high glass-enclosed banking hall. The hall is clear spanned by a two-way truss system made entirely from HSS the roof structure is 34.0m wide by 85.3m long and was assembled on the ground. The two-way truss system is basically a series of 4.3m cube modules constructed from 305 x 305mm HSS chords and 152 x 152mm HSS diagonal members. The roof weighed 350 tonnes and was hydraulically jacked up to its final position.

The two long sides of the roof are supported by the two towers and the two shorter sides by vertical Vierendeel trusses. In addition to carrying a portion of the roof load, the Vierendeel trusses give wind resistance to the structure. The connection design of the trusses was verified by testing at McMaster University. The Vierendeel trusses are framed with glass.

1.3.3. Japan

The structural use of tubular steel products in Japan amounts to 0.4 million tons per year at present, which represents 26% of total steel tube production. Square HSS of 100 x 100mm were introduced in 1960. Presently such sections are produced by various methods such as cold forming, pressing and hot rolling in sizes up to 1000 x 1000mm. The larger sizes are used for structures, while the smaller are used for structures and a wide range of other applications e.g. doors, fences, handrails etc. Standards for square HSS are specified in the Japanese Industrial Standard JIS G 3466 in which the materials, sizes, tolerances, and chemical composition are included. The maximum size at present, is 300 x 300 x 8, but this is shortly to be revised. Some of the applications in Japan are:-

Electric Transmission Towers

Recent developments have required higher towers for the pylon function. STK55 is the newest steel developed in Japan for this purpose. This increase in material strength for HSS has been stimulated by the field of electric transmission towers.

Tubular towers constitute 40% of Japanese transmission towers, and the demand for this use is about 35,000 tons per year.

Buildings

There is an ever increasing trend to use HSS in building structures. CHS columns are used extensively in multi-storey building frames. Popular sections for these columns, which are used in office buildings

which require unbraced figures, are centrifugally cast steel pipes and heavy square hollow sections.

Other areas of use are in bridges, offshore structures, piles, poles and tunnel supports.

1.3.4. France

Spectacular progress has been made in the use of HSS in France due to the research and development carried out by Cometube and the French Association of Manufacturers of Steel Tubes. From the small sections manufactured by early craftsmen, a full range of HSS is now produced and used in a wide variety of structures. Hollow hexagonal sections have become popular because they simplify assembly by simple flat cuts.

Traditional builders found savings of between 20% and 30% of the weight of steel utilized. The main attraction being the constant outer dimension of HSS with a variable thickness available.

Much research and development has been carried out in France into the use of water filled HSS columns for fire resistance, and concrete filled HSS columns for increased strength, and improved fire resistance.

1.3.5. Germany

Before the automatic pipe cutting machine had been developed by the firm of Mueller in Opladen in Germany, the application of CHS for steel structures had been restricted to their use as columns for taking axial load and moments on all sides. The production of RHS was started in Germany in 1962, and became popular with fabricators because they required plain intersection only.

In Germany seamless tubes are hot rolled up to an outer diameter of 660mm in accordance with DIN 2448. For welded tubes DIN 2458 gives the dimensions. The maximum diameter permitted is limited only by the available facilities for transport.

Rectangular hollow sections are specified in DIN 59410, in which the sizes and tolerances are included. The maximum size in this standard is 400 x 400mm in square HSS and 400 x 260mm in RHS. Figure 12 shows the production program for square HSS of the German producers of RHS. The difference between the dimensions of hot rolled and cold formed sections can be seen clearly. Cold formed sections are of smaller size, starting from a width of 15mm, while hot rolled sections cover the middle and higher dimensions from 40 x 40mm to 260 x 260mm. The maximum size for RHS is 260 x 180mm.

Steel properties according to German standard DIN 17100 are:-

R St 37-2 tensile strength 360-440N/mm²
 yield strength 235N/mm²

St 52-3 tensile strength 510-610N/mm²
 yield strength 355N/mm²

A recent recommendation for higher grade steels has been made:-

St E 47 tensile strength 560-730N/mm²
 yield strength 460N/mm²

St E 70 tensile strength 770-960N/mm²
 yield strength 690N/mm²

The values for higher grade steels reduce as wall thickness increases.

1.4. Summary of Advantages of Using Hollow Steel Sections in Structures

Ease of fabrication and construction.

Considerable saving in weight, and therefore reduced transport and erection costs.

Larger spans, possible because of the lighter sections.

Ease of accessibility for maintenance, due to smaller surface areas.

Effects of wind forces are smaller because of shape. CHS are particularly useful in offshore structures where the low drag coefficient reduces the effects of wind and waves.

Torsional rigidity is greater than that of conventional sections.

No weak axis in bending.

Comparable cross-section to conventional sections.

Reduction in stress due to flange instability does not occur.

Contact areas for welding are smaller.

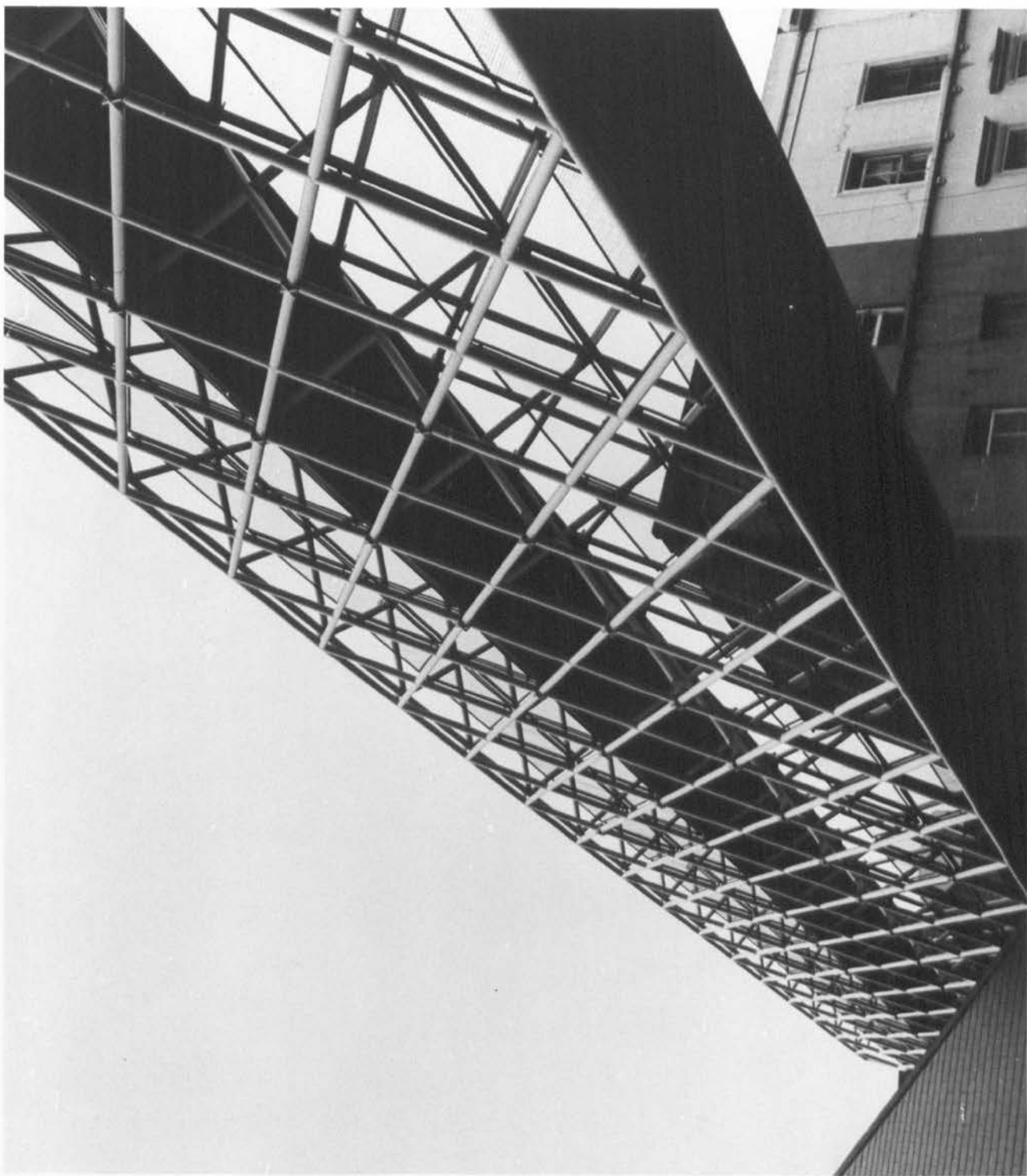


Figure 1 - Covered Walkway in CHS

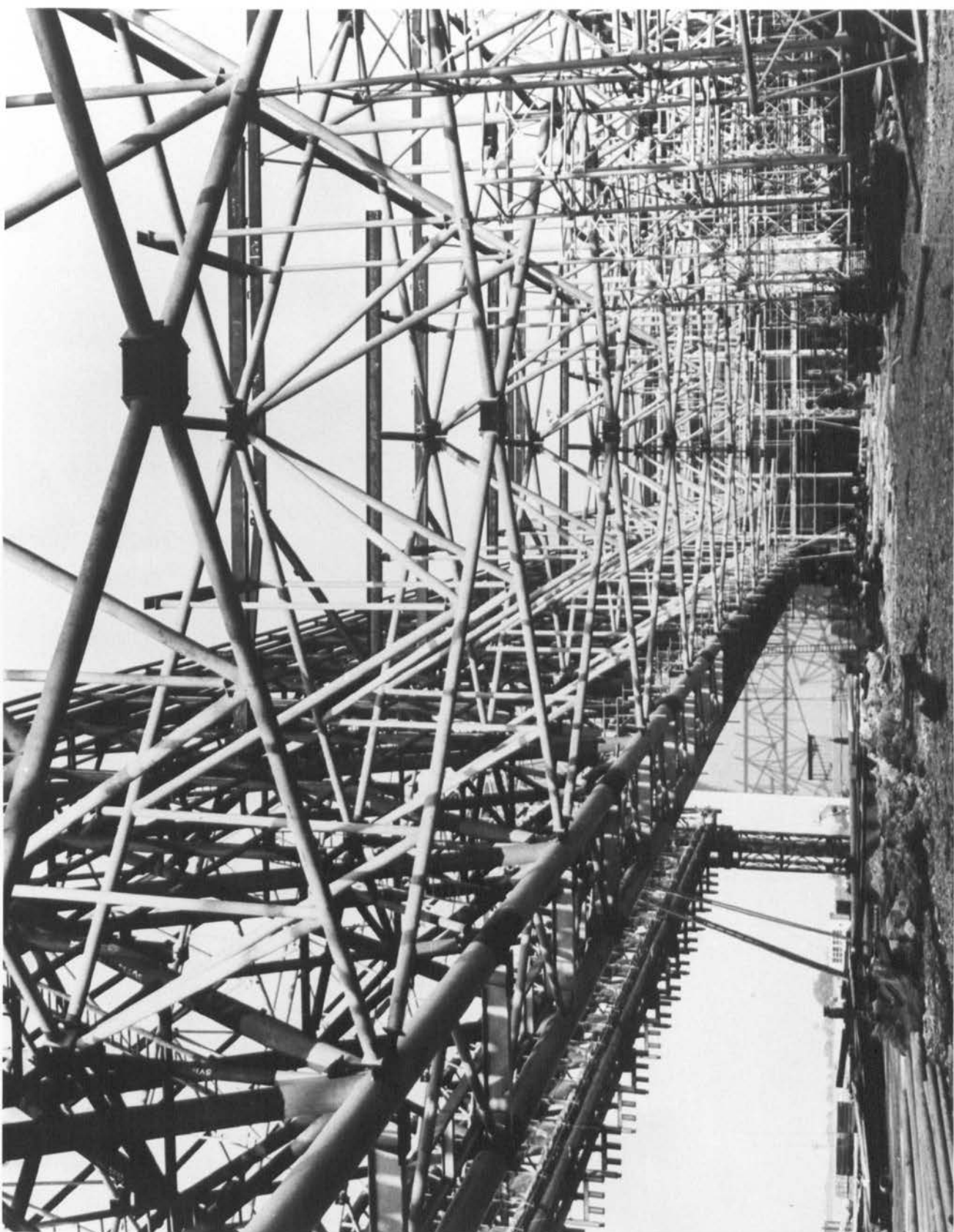


Figure 2 - Jumbo Jet Hangar at Heathrow Airport (CHS)



Figure 3 - Jumbo Jet Hangar at Heathrow Airport (CHS)

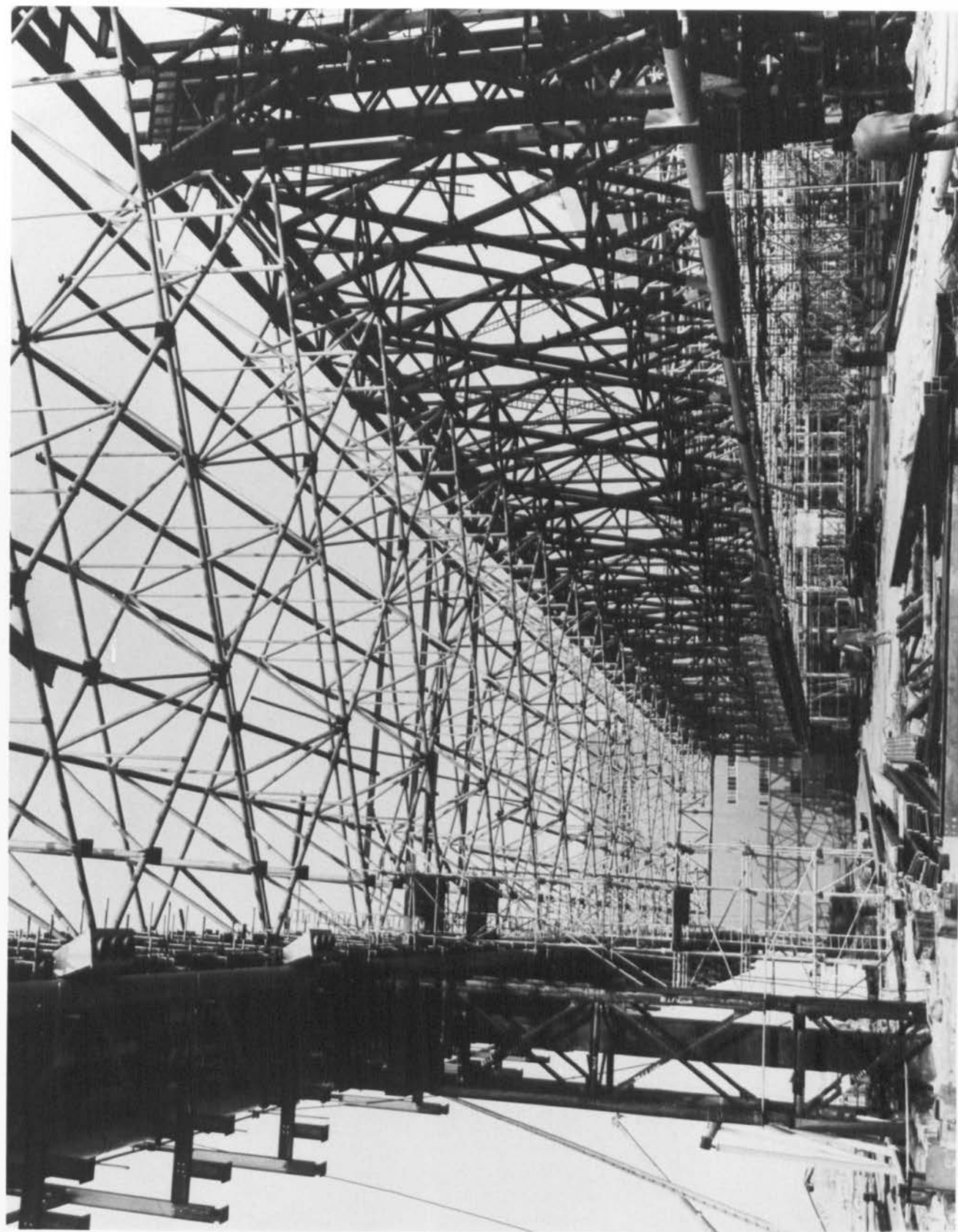


Figure 4 - Jumbo Jet Hangar at Heathrow Airport (CHS)



Figure 5 - Tower Structure (CHS and RHS)



Figure 6 - Pipeline Bridge

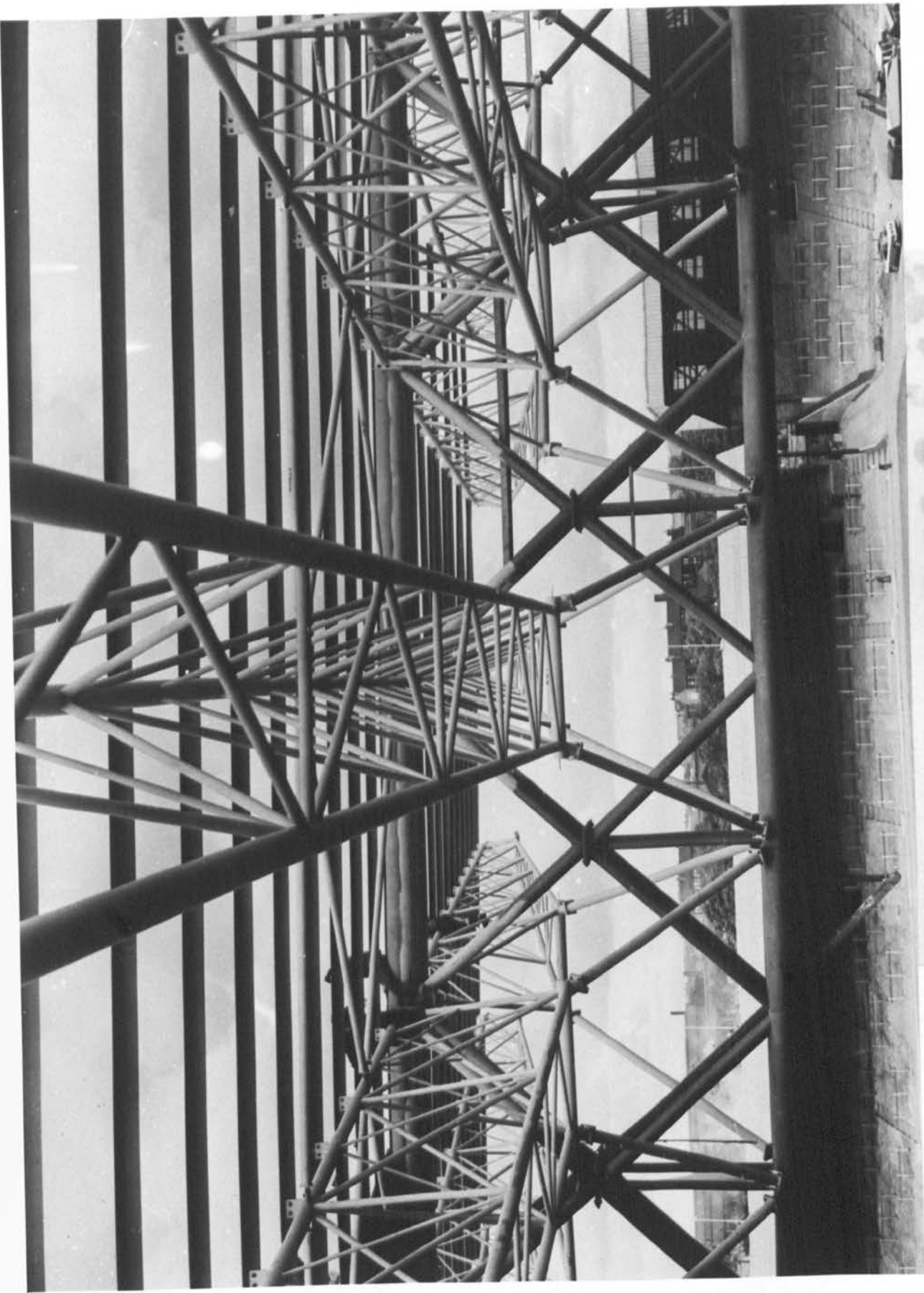


Figure 7 - Roof Structure - Celtic Football Ground



Figure 8 - Jetty Construction - CHS Piles

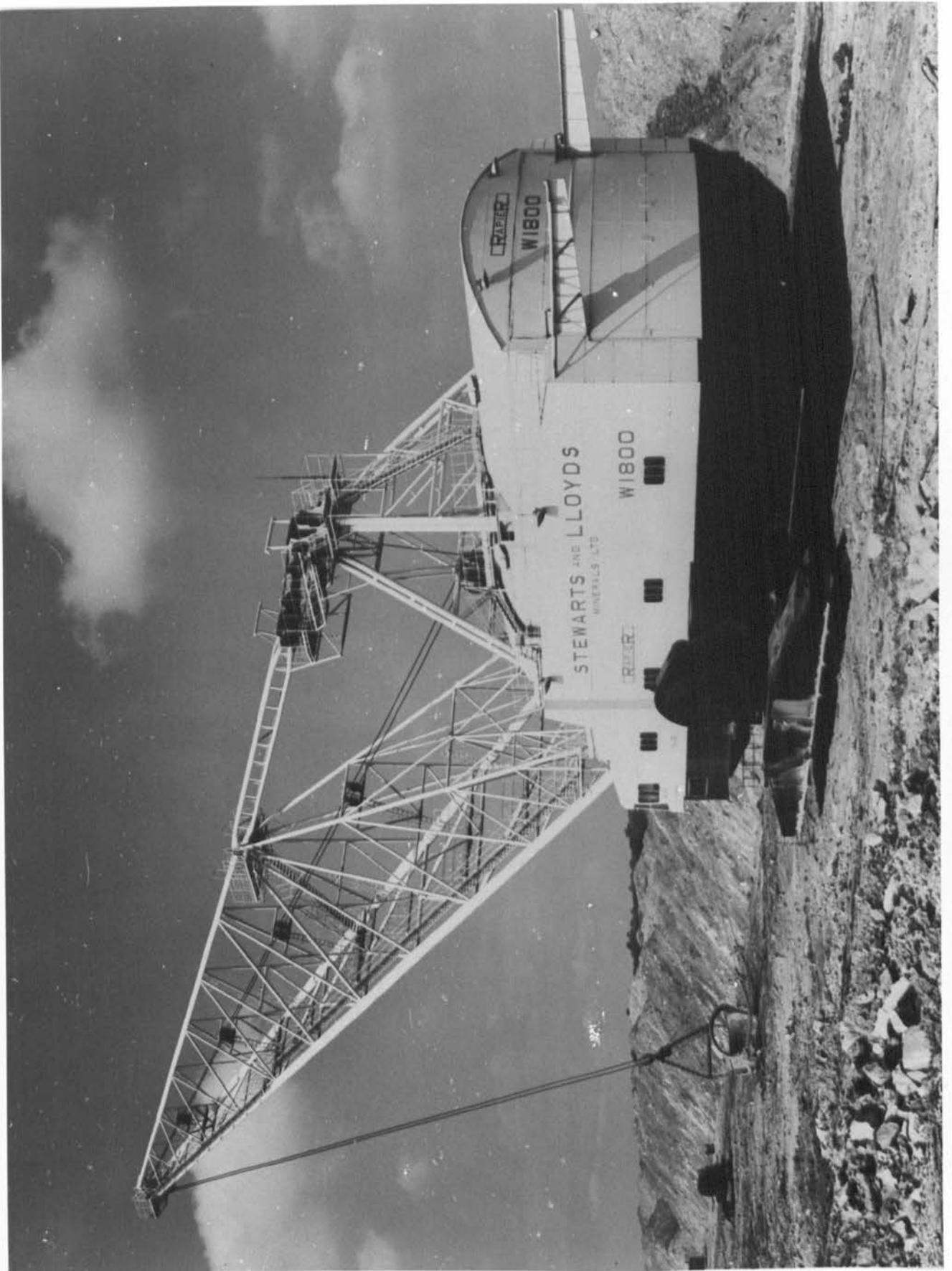


Figure 9 - Walking Dragline

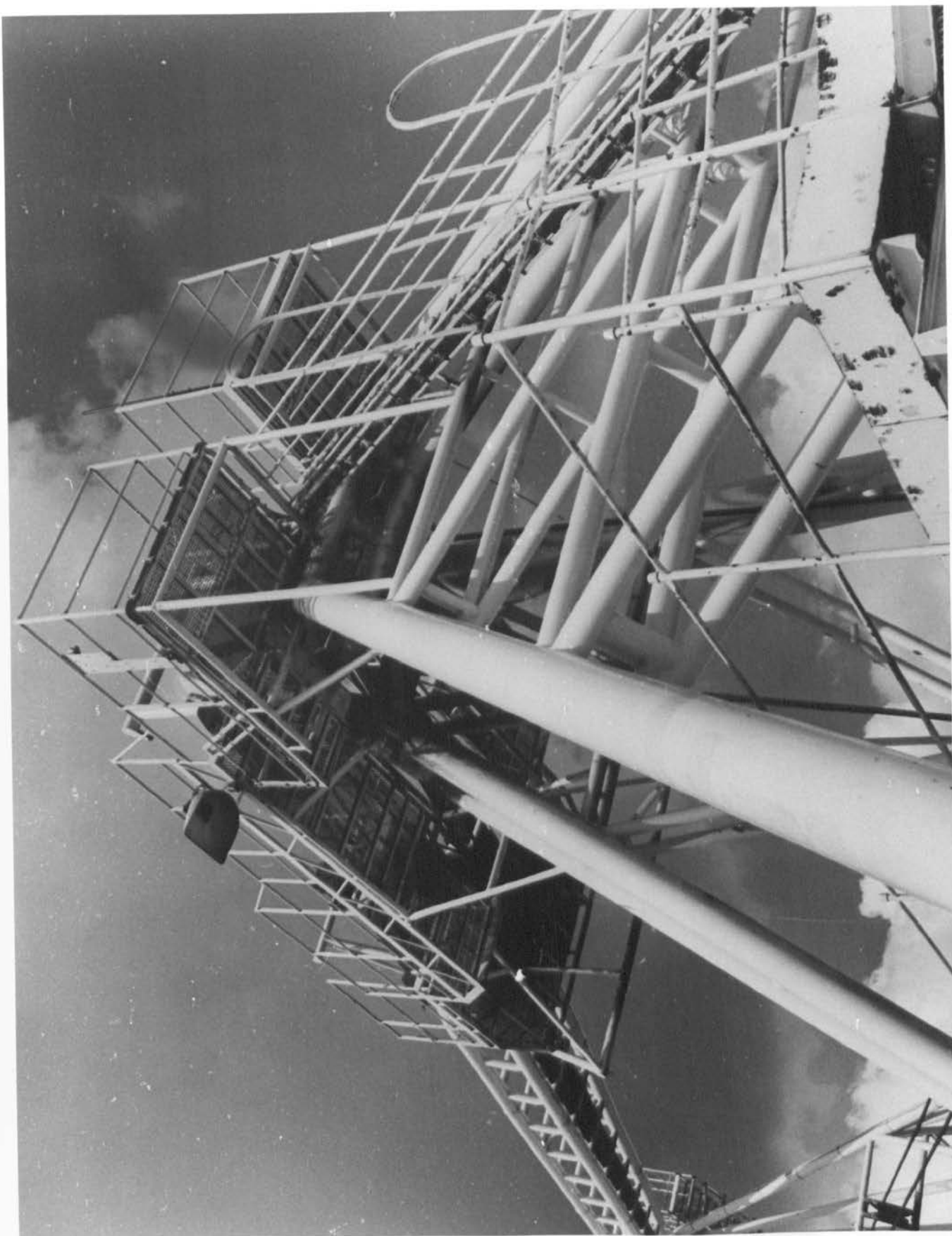


Figure 10 - CHS Joints On Walking Dragline



Figure 11 - Mobile Crane

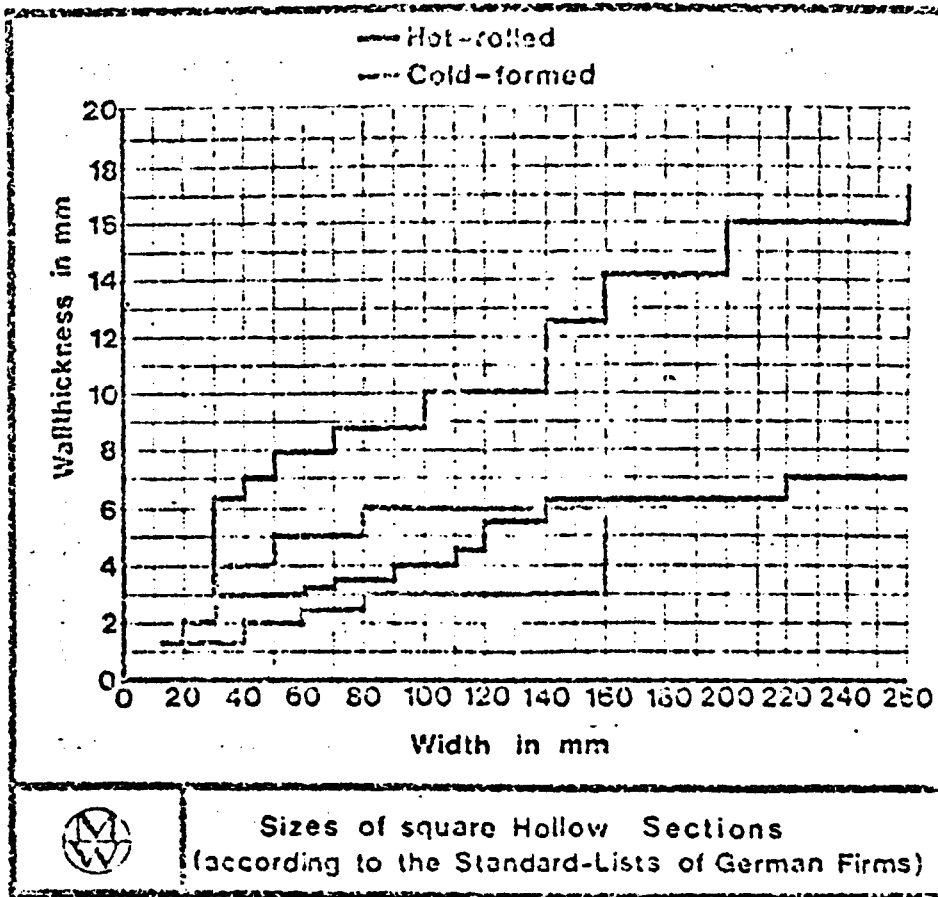


Figure 12 - Production Program for Square HSS - Germany

CHAPTER 2

JOINTS IN HOLLOW STRUCTURAL SECTIONS

2.1. Types of Joint

The main types of joint used in structures using HSS are shown in Figures 13-16. They are:-

2.1.1. T-Joints

Found generally in Vierendeel structures but may be used elsewhere.

2.1.2. K-Joints

Found generally in Warren girder structures.

2.1.3. N-Joints

Found generally in Pratt girder structures.

2.1.4. Y-Joints

These are a variation of the 'T' joint and may be seen in various types of girder structure.

2.1.5. Cross-Joints

These are not common except in tower structures.

2.1.6. Multiple Joints

These involve several bracing members connecting to a chord member, possibly in more than one plane. This type of joint is often seen in large three-dimensional offshore rig structures. (Figure 14(c)).

2.2. Categories of Joint

Joints fall into the following categories:-

2.2.1. Bolted Joints

Reinforced or unreinforced.

Braced or unbraced.

2.2.2. Welded Joints

Reinforced or Unreinforced.

Braced or unbraced.

The bolted joints include such proprietary systems as the British Steel Corporation's NODUS system. The majority of bolted joints must be simple and involve welding the members at either side of a joint to plates which are then bolted together. Because of the fabrication problems involved bolted connections are used mostly at end frame connections.

Welded joints in CHS are easier to fabric since the advent of automatic tube profiling machines. The welded joint gives a cleaner appearance, and provided the welding is carried out correctly then the weld property normally ceases to be a joint strength parameter. Various types of welding condition are shown in Figures 14-16. The choice of joint type depends upon several considerations, not the least of which is the load that is required to be transmitted by the joint.

Until fairly recently joints in HSS have been designed fairly conservatively, employing simplified assumptions. While these assumptions are not incorrect they have lead to some very conservative designs, especially where joints have been further reinforced above their design strength.

2.3. Reinforcement of Joints

This may be achieved in various ways:-

2.3.1. Joint-Cans

This procedure involves thickening of the chord in the vicinity of the joint. It has been used fairly extensively, but involves extra fabrication procedures.

2.3.2. Gusset Plates

Here the joint is reinforced by welding gusset plates either side of the branch member in a similar manner to the method used in conventional sections.

2.3.3. Joint Plates

Shown in Figure 15. Joint plates and gusset plates tend to make joint strength indeterminate. They also have the effect of increasing stress concentration in the joint.

2.3.4. Concrete Filling

Research⁵ is presently continuing to study the effects of concrete filled chord members. The expected result would be that, since this would make the chord member very stiff, then the failure mode would always be either a buckling or shear failure in one of the branch members.

2.4. Characteristics of the Various Joint Types

2.4.1. T-Joint

The T-joint occurs most often in Vierendeel types of structure. The joint itself is, therefore, normally subject to a combination of axial load in the branch member and bending moment applied through the same member. It is the effect of this combined loading on T-joints in CHS that is described in this present experimental investigation.

2.4.2. Y-Joint

The Y-joint may occur in any type of truss where a diagonal member is inserted to provide extra bracing, or to reduce the effective length of a compression chord. For large angles of intersection ($90^\circ > \theta > 60^\circ$) the Y-joint can be considered to act similarly to a T-joint, with the appropriate angular correction factor for the applied load.

2.4.3. K-Joint, of Which the N-joint is a Special Case

K-joints may be either gapped, in which case there is a discernible gap between the two bracing members, or overlapped, where as the name suggests the two bracing members overlap at the joint.

Overlapping K-joints is a method of improving the strength of a joint since an additional bracing effect is introduced between the two branch members. It does, however, involve additional tube end profiling in CHS which increases the joint cost.

Overlapping K-joints also has the effect of making the joint strength less predictable and invariably leads to a conservative design.

2.4.4. Joints with Three Bracing Members (Figure 17)

Joints with three bracing members have been studied and design rules for them have been proposed. These are based on a method which reduces the effect of loads from three bracing members to an equivalent effect from two bracing members.

2.4.5. X-Joints

This type of joint occurs mainly in towers and larger structures. It is generally assumed that loads are axial in the branch members.

2.5. Types of Loading

2.5.1. T-Joint

- i. Compressive axial load and moment in branch member.
- ii. Tensile axial load in branch member.

2.5.2. Y-Joint

- i. Compressive axial load and moment in branch member.
- ii. Tensile axial load in branch member.

2.5.3. K-Joint

- i. Tensile axial load in one branch member, and compressive axial load in the other.
- ii. Tensile axial load in both branch members.
- iii. Compressive axial load in both branch members.

2.5.4. N-Joint

As K-joint above.

2.5.5. X-Joint

- i. Compressive axial load in both branch members.
- ii. Tensile axial load in both members.

2.5.6. Joint With Three Branch Members

See Figure 17 for the various combinations of loading possible.

2.6. Tubular Joint Strength - General

Considerable research into the strength of 'T', 'Y', 'K' and 'N' joints has recently been carried out. Initially, experimental results were compared with theoretical results obtained from yield line analyses. However, this approach was generally conservative, particularly for CHS, and recently more sophisticated analyses were carried out based on shell equation solutions⁶, and finite element methods⁷. This research has been carried out at various centres in America⁸⁻¹², Japan¹³⁻¹⁷, and Europe¹⁸⁻²¹ and it has lead to a number of proposed empirical and semi-empirical design formulae. In most of the experimental and theoretical work the following joint parameters have been considered:-

- i. Ratio of branch member width or diameter to chord member width or diameter (d_1/d_0).
- ii. Ratio of thickness of chord member to width or diameter of chord member (d_0/t_0).

- iii. Ratio of thickness of chord member to thickness of branch member (t_1/t_0).
- iv. Effect on joint strength of chord member length.
- v. Effect on joint strength of chord member support conditions.

The last two parameters above relate to the scale effects encountered when comparing model test results with full scale truss behaviour.

- vi. Effect on joint strength of concrete filled chords.
- vii. Effect on joint strength of different welding conditions.

In most of the test specimens axial loads have been applied to branch members only; in some cases axial loads have also been applied to the main chord member. Toprac⁹, however, considered CHS joints in which the branch tube was subjected to a combined axial and bending load. No results were published for these tests. The effects of positive, zero and negative eccentricities have been studied in CHS K-joints¹³.

Attempts have been made to correlate the results of existing experimental and theoretical research. Problems, however, have arisen when comparing and correlating test results in RHS and CHS, due mainly to the different sizes of test specimens and a lack of data on material properties and failure criteria. Furthermore, these attempts have lacked a systematic and unified approach to the problem of joint strength. This has had an adverse effect on the usefulness and even the validity of existing design recommendations, especially in the case of joints in CHS.

2.7. The Present Investigation

The present investigation, therefore, consists of a review of existing research and design recommendations for 'T', 'Y', 'K' and 'N' joints in CHS and a presentation of the results of current experimental and theoretical research into the effects of combined

axial load and bending moment in T-joints in CHS. The research program has been carried out at Kingston Polytechnic where a test-rig has been constructed. The test-rig permits combined loads to be applied to the joint being tested while deflections, strains and general joint behaviour are monitored. Theoretical work has included:-

- i. Finite element analysis of CHS T-joint behaviour using LUSAS, the London University Structures Analysis System developed by Dr. Paul Lyons at Imperial College.
- ii. Statistical evaluation of all existing design formulae for joints in CHS, using available test data.
- iii. Regression analysis of existing T-joint test results.
- iv. Regression analysis of T-joint test results obtained from the present investigation.
- v. Evaluation and presentation of results.
- vi. Proposed design formulae for:-

Ultimate axial load of welded T-joints in CHS.

Ultimate moment load of welded T-joints in CHS.

Combined load cases for welded T-joints in CHS.

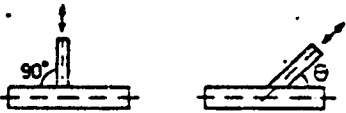
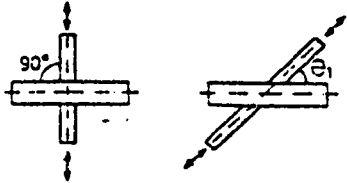
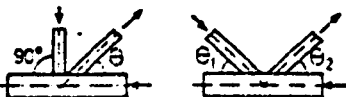

TYPES OF JOINTS	
T- AND Y-JOINT	X-JOINT
	
N- AND K-JOINT	K-T JOINT
	

Figure 13(a) - Types of Joints in HSS

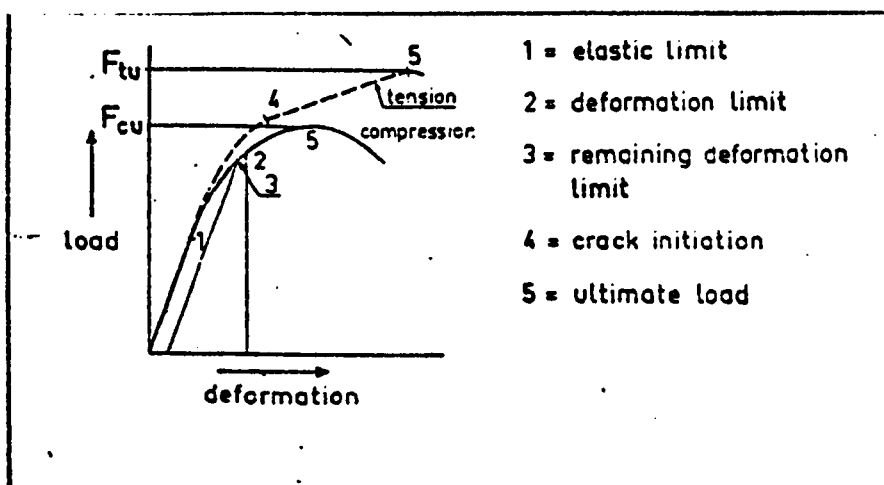


Figure 13(b) - Criteria of Failure

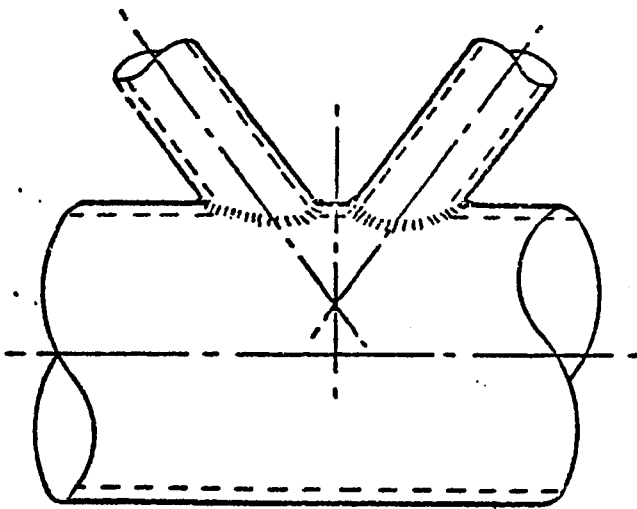


Figure 14(a) - Gapped K-Joint

- Negative Eccentricity

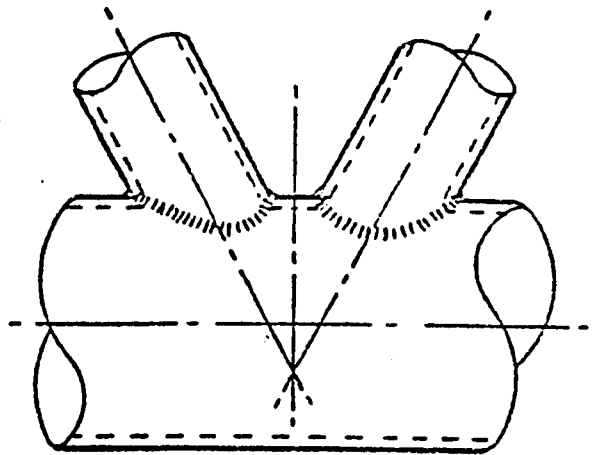


Figure 14(b) - Gapped K-Joint

- Positive Eccentricity

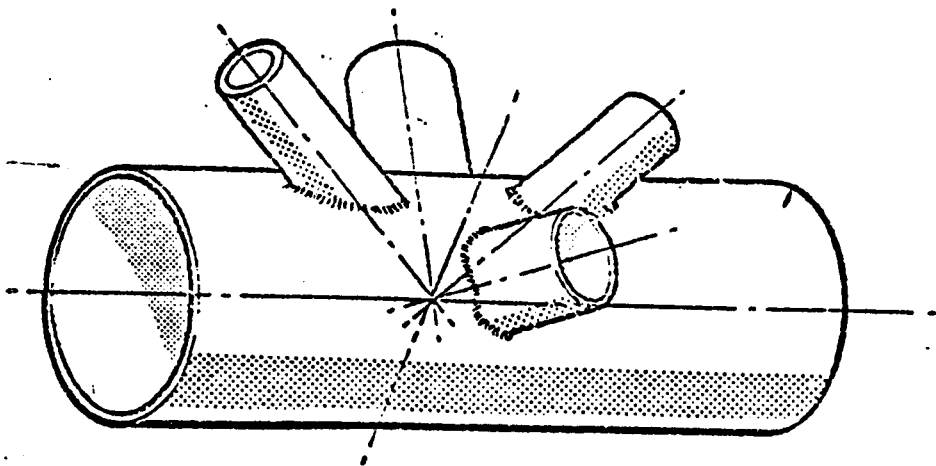


Figure 14(c) - Multiple Joint

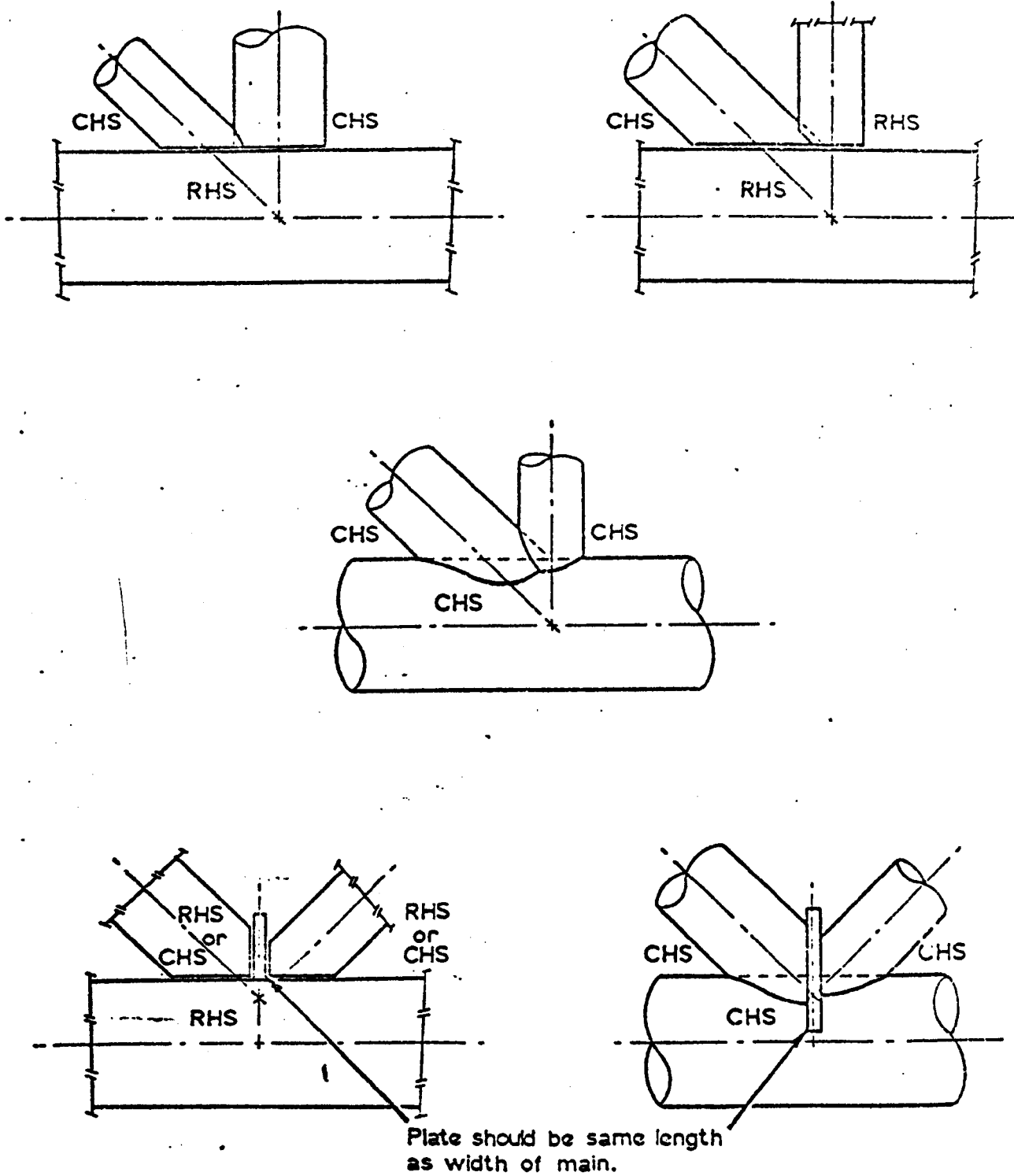


Figure 15 - Welding Conditions for Joints in HSS - Using Joint Plates

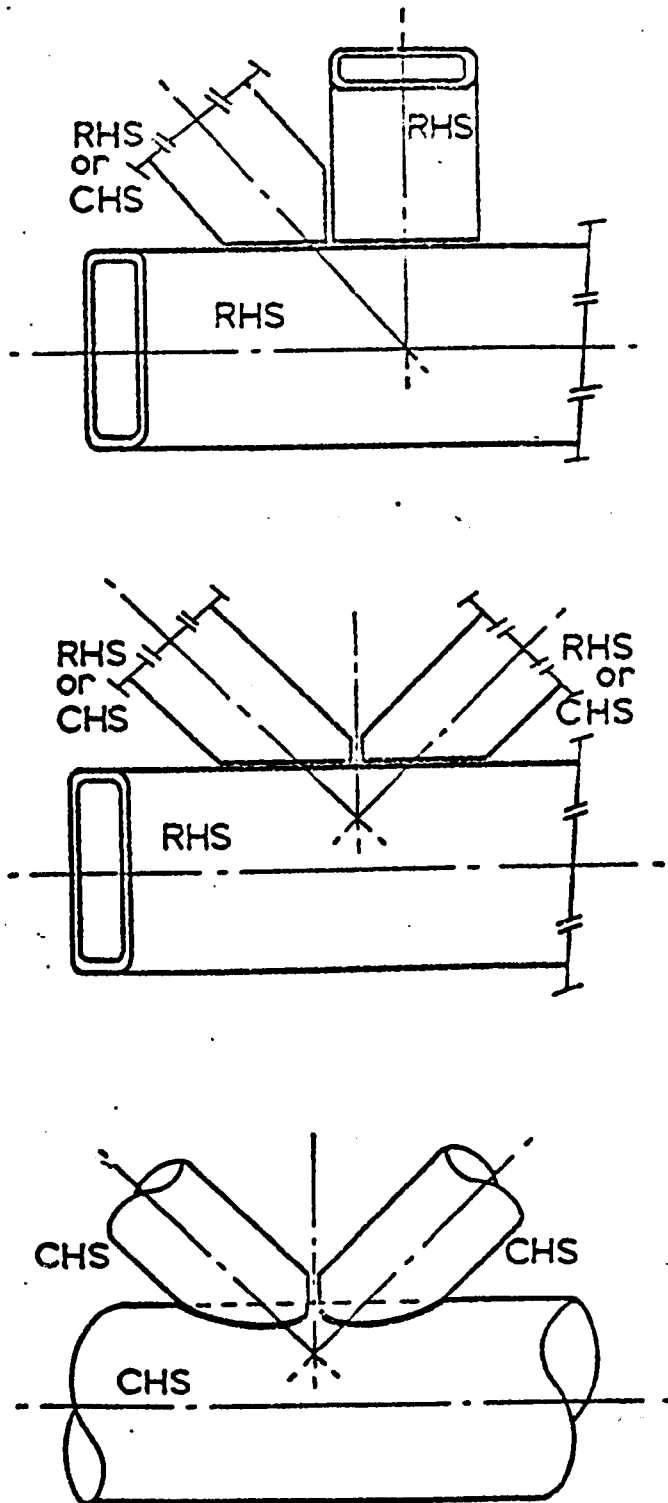
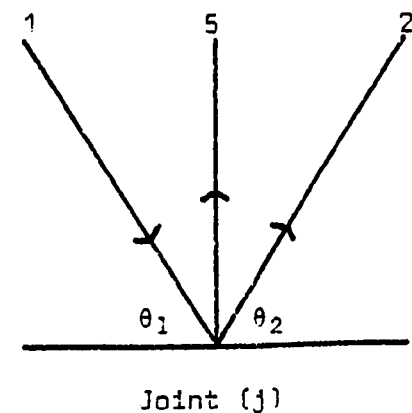
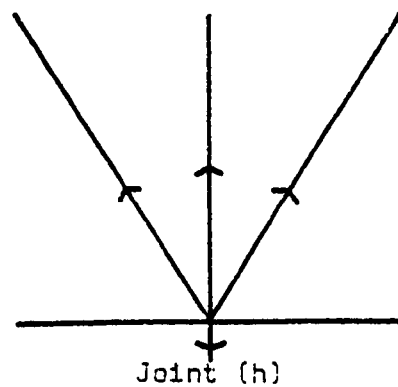
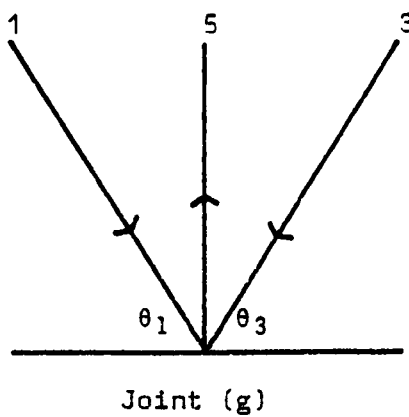
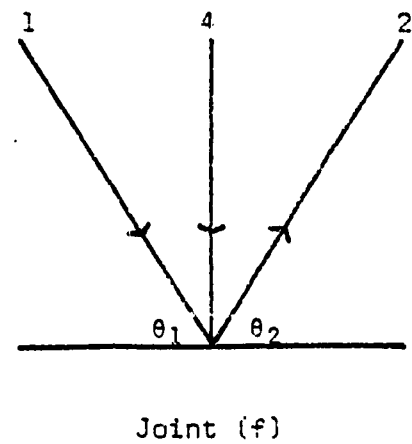
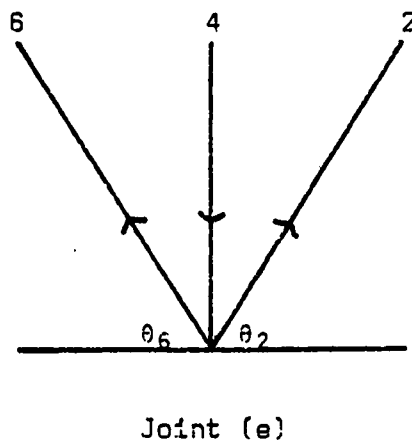
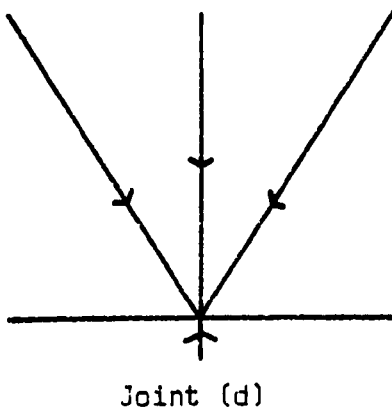
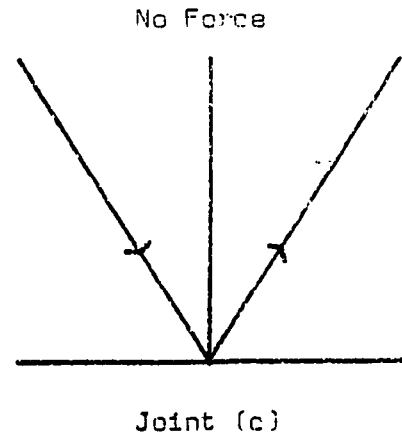
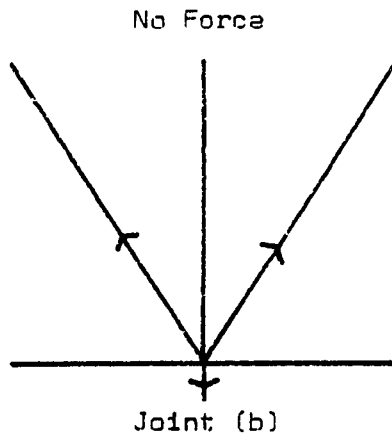
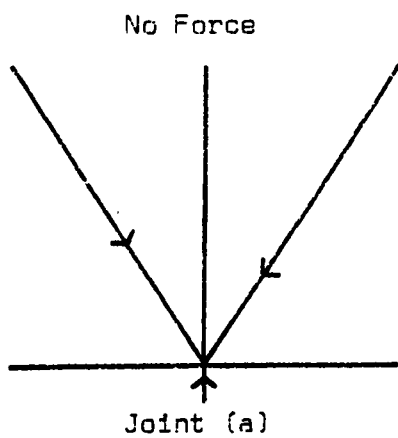


Figure 16 - Welding Conditions for Joints in HSS



$n = 1, 2, 3, 4, 5, 6$ are bracing member numbers.

Figure 17 - Joints with Three Bracing Members

CHAPTER 3

EXISTING METHODS FOR CALCULATING THE STATIC STRENGTH OF T, Y, K AND N-JOINTS IN CHS, WHICH ARE AVAILABLE FOR AXIAL LOADS ONLY

3.1. Introduction

A systematic correlation of all the available experimental results with the results calculated from eighteen existing design formulae, using a statistical analysis to give a basis for discussion of the applicability and value of each formula has been carried out. In all, 245 test results were considered. A summary of the type of tests and geometrical properties of the joints tested is given in Table 1A. In none of the tests has a value of shear yield stress been given. In order to have a common basis for comparison, a value of shear yield stress has been found by dividing the appropriate yield stress by 1.732 (Von Mises criterion, $1.732 = \sqrt{3}$).

The present investigation considers all 18 of the existing proposed design formulae for T, Y, K and N joints. These are:-

Shear Area ²²	
Column Analogy ²³	
Roark (Theoretical) ²⁴	1941
Roark (Empirical) ²⁵	
Kellogg ²⁶	1956
Kurcbane ¹⁸	1964
Naka, Kato and Kanatani ¹⁶	1965
Washio, Togo and Mitsui ²⁰	1969
Canadian Steel Company Code - (based on work by Bouwkamp ¹³)	1971
Reber ⁷	1973
Toprac and Marshall ¹¹	1973
Kato, ¹⁵	1974
American Petroleum Industry Code ^{27*}	1974
American Welding Society Code ²⁸	1974
Det Norske Veritas ²⁹	1974

*since revised 1978.

Visser³⁰

1975

Harlicot, Mouty, Tournay Verification Formula³¹

1976

Harlicot, Mouty, Tournay - Envelope Formula³¹

1976

Some of these design formulae are currently recommended for use in practice.

When dealing with K-joints, the strength of the joint is considered to be due to a combined strength of two Y-joints. In the case of one compression branch member and one tension branch member the theoretical load will generally be based upon the lower Y-joint strength i.e. that of the compression branch member. In the case of a joint with both branch members in compression or tension then the total effect of the two Y-joint mechanisms is added in order to estimate the joint strength.

Effects due to secondary moments have not been directly considered in any of the design formulae. A correction factor which takes account of these moments has been proposed and is described in the conclusions to this chapter. Similarly the bracing effect of overlapping branches in K-joints has not been directly considered in any of the relevant formulae except that account is taken of the shearing mechanism along the welded intersection between the two branch members.

The majority of design formulae has been proposed for restricted parameter ranges (See Table 1B), for example:-

A formula may only apply to T-joints.

A formula may have a recommended range of d_o/t_o or d_1/d_o^* , outside which its use is unconfirmed by tests. The results of this selective analysis are shown in Tables 3-6, pages 105 - 108.

-
- * d_o = diameter of chord tube.
 - d_1 = diameter of branch tube.
 - t_o = thickness of chord tube.

A further analysis was also carried out, in which all of the eighteen existing formulae were used in evaluating all the available T-joint and K-joint tests, irrespective of the recommended parameter limitations. These results are shown in Tables 7-10, pages 109 - 112.

3.2. Existing Methods for Calculating Either the Working Strength or the Ultimate Strength of a Welded Tubular Connection

3.2.1. Shear Area

Historically this method appears to be the earliest method of tubular joint design used in practice. First mentioned by Toprac¹⁰, who refers to Johnson²², "The Welded Tubular Joint Problem in Offshore Oil Structures", in which it is stated that this method does not give a reasonable estimate of the true stress conditions in the joint.

Toprac¹⁰ used the shear area method to calculate predicted loads for his own seven test specimens. From maximum shear stress theory a value of 20k.s.i. (138N/mm²) for shear yield stress was chosen, which was half of the tensile yield stress. His results are presented below, together with those obtained by taking a shear yield stress based on the Von Mises criterion (i.e. tensile yield stress/ $\sqrt{3}$).

TEST	PU MEASURED/PU PREDICTED	
	MAXIMUM SHEAR STRESS THEORY	VON MISES
1	0.96	1.18
2	1.06	1.29
3	0.87	1.03
4	0.83	1.26
5	1.09	0.84
6	0.72	0.98
7	<u>0.86</u>	<u>1.04</u>
	ave = 0.91	ave = 1.09

Toprac concluded from his results that the method was inherently unsafe and, therefore, should be viewed with caution.

The assumed mechanism for the method is one where load acting around the branch tube circumference causes shear failure in the chord wall. Limitations which should arise from this mechanism are due to:-

Variation in parameters of both tubes is ignored (e.g. d_1/d_o , d_o/t_o , t_1/t_o).

Bending and membrane stresses in chord wall are ignored.

It is assumed that failure is by shear in the chord wall only, and the selection of a value for the yield shear stress is arbitrary.

The formula is usually recommended for the ratio of diameter of branch to diameter of chord, $d/D < 0.2$.

The ultimate load for a joint is found from the formula.

$$P_u = f_{yo} \cdot \pi \cdot d_1 \cdot t_o \dots\dots\dots(3.1)$$

where

- P_u = ultimate axial load on the branch tube.
- f_{yo} = yield shear stress.
- d_1 = diameter of branch tube.
- t_o = thickness of chord tube.

allowance may be made for inclination of the branch member i.e.

$$P_u = f_{yo} \cdot \pi \cdot d_1 \cdot t_o / \sin \theta \dots\dots\dots(3.2)$$

where θ is the angle of intersection of the tubes.

The allowable load is then found by dividing the ultimate load by an appropriate safety factor.

The value of shear yield stress is taken as nominal yield stress divided by 1.732. This is the Von Mises shear criterion and has been shown to give the safest results.

3.2.2. Column Analogy or Closed Ring Method²³

This was one of the earliest methods used for determining T- and K-joint strength. A ring consisting of a reasonable length of chord extending symmetrically on each side of the branch tube is considered and analysed by column analogy using the equivalent load system shown in Figure 18. A minimum length of $2.\pi.r_o$ should be taken as the effective length, according to the Japanese research, where r_o = radius of chord tube.

It is found that the ultimate punching shear stress of the joint,

$V_p = F_{yof}(\beta)/0.5\gamma \dots\dots\dots(3.3)$

where

- V_p = ultimate punching shear stress.
- $f(\beta)$ = function of diameter of branch/diameter of chord, See Figure 19 below.
- γ = radius of chord/thickness of chord (r_o/t_o).
- F_{yo} = shear yield stress of chord material.

The ultimate load is then found by comparing stress V_p with the stress acting on the joint given by equation 3.29, page 65.

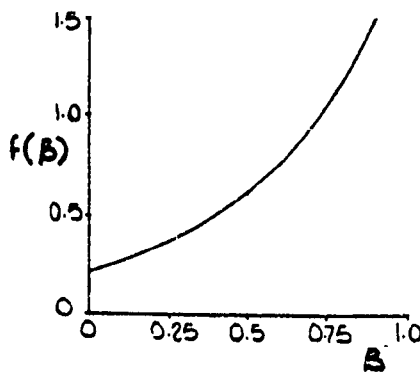
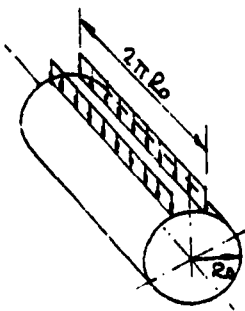


Figure 18 - Equivalent Load System

Figure 19 - $f(\beta)$ Function

As part of an investigation to find a design method for reinforced K-joints, Bouwkamp¹³ has carried out a column analogy using the load system shown in Figure 20.

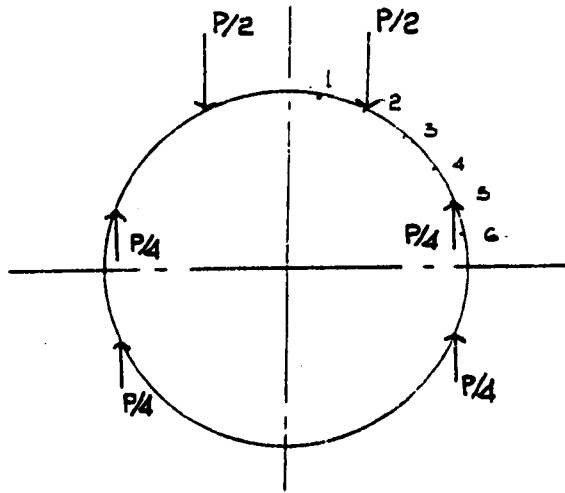


Figure 20 - Load System for Column Analogy by Bouwkamp

It was found that the maximum compression in the outer fibres = $3.3.P$ and occurred at point 1.

The maximum tension in the outer fibres = $2.84.P$ and occurred at point 5.

It is suggested that the method be adapted for bending by converting bending stress to an equivalent axial stress.

The limitations of the method are:-

The length of ring is arbitrarily chosen.

No allowance is made for circumferential resistance to load.

No interaction between the chord and branch tube is considered.

Johnson²² says that the method fails because it does not consider the part of the chord between the two braces, and since the load from one brace is transferred to another brace through the chord

then the part of the chord between the two braces must be designed to carry the load transfer in shear, possibly requiring expensive reinforcement with rings.

3.2.3. Roark Method I - Proposed by R. J. Roark in 1941²⁴

The method originated from experiments to find stresses in hollow sections due to concentrated loads. The concentrated loads were applied equally and opposite to the inside surface of the tubes using a system of levers to apply the load, such that no change in support forces occurred. Strains were measured using extensometers.

Using the formula given by Nadai³²:-

$M_x = [(1 + \mu)/4\pi] . P . \ln (2a/\pi x)$ and dividing through by the section modulus of a strip ($t_o^2/6$) gave:-

$$S_x = KP . \ln (CR/x) / t_o^2 \dots\dots\dots(3.4)$$

where C and K are constants which Roark obtained empirically to give:-

$$S_x = - P/t_o^2 [0.42 . \ln (0.215 R/x)] \dots\dots\dots(3.5)$$

and

$$\text{max. } S_x = \frac{-P}{t_o^2} \left[0.42 \ln (0.215 \frac{r_o}{r_1}) + \frac{6}{4\pi} \right] \dots\dots\dots(3.6)$$

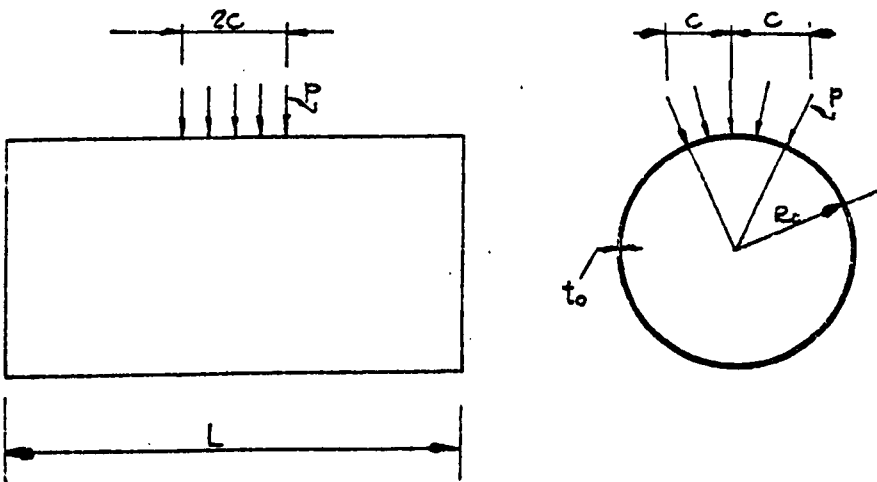
$$\text{Similarly max. } S_y = \frac{-P}{t_o^2} \left[0.42 . \ln (0.215 \frac{r_o}{r_1}) + \frac{6\mu}{4\pi} \right] \dots\dots\dots(3.7)$$

where

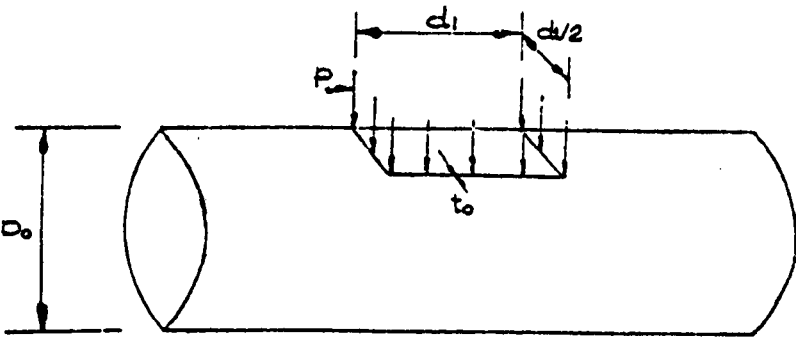
- S_x = circumferential stress.
- S_y = longitudinal stress.
- P = axial load in branch member taken as a line load on the chord member.
- t_o = chord wall thickness.
- r_o = chord radius.
- r_1 = branch radius.
- μ = Poisson's ratio.
- x = chord length.

When $\frac{r_1}{r_o} > 0.05$, which is normally the case, the formulae when combined, reduce to give an expression for the resultant bending stress of:-

$$f_b = \frac{-P}{2t_o^2} \cdot \ln \left[\frac{0.3r_o}{r_1} \right] \dots\dots\dots(3.8)$$



(a) Uniform Load



(b) Square Tube Type

Figure 21 - Assumed Load System for Analysis

The limitations of the method are:-

The effect of interaction of the stiffnesses of the branch tube and chord tube is neglected.

The formulae apply to values of the ratio r_1/r_o around 0.05 while the practical values are usually nearer to 0.5.

The analysis is based on thin shell theory.

3.2.4. Roark Method 2 - Empirical Formula Proposed by Roark²⁵

This formula is presented by Roark in "Formulas for Stress and Strain"²⁵, as a design method for pipes on supports at intervals. For an unstiffened pipe resting in simple saddle supports there are high local stresses, longitudinally and circumferentially. The maximum value of these stresses will not exceed that derived from the formula.

$$P_u = f_{y_o} t_o / K \ln \left[\frac{d_o}{2t_o} \right] \dots\dots\dots(3.9)$$

where

- K = 0.02 - 0.00012 ($2\alpha^0$ - 90^0).
- α = $\sin^{-1} d_1/d_o$.
- P_u = ultimate axial load in the branch tube.
- f_{y_o} = yield stress of chord material.
- t_o = thickness of chord tube.
- d_o = diameter of chord tube.
- d_1 = diameter of branch tube.

This formula has been derived from a study of test results by Hartenberg³³ and Wilson³⁴, and has some limitations on it's use:-

The formula, by implication, applies to T-joints only.

d_o/t_o ratio should be greater than 40.

Loads must be axial.

It is also stated that the maximum value a pipe can sustain as a concentrated load is about 2.25 times the value of load that will produce a maximum stress equal to the yield point of the pipe material.

3.2.5. Kellogg Method - Developed by M. W. Kellogg Co.²⁶

The method was originally developed in order to estimate the effect of concentrated loading on piping. The method makes use of an approximate solution based on the bending of a beam on an elastic foundation. Initially the forces considered were nozzle bending moment and radial thrust. To make the method applicable to joint design the following procedure is adopted:-

The primary load in the branch tube at the joint is computed. This stress is then applied as a line load to the surface of the chord (Figures 22 & 23). The intensity of the line load due to axial forces is increased by a factor of 1.5 and added to the maximum intensity of line load caused by moment.

The total line load is applied, uniformly distributed, around a circular section of the tube (Figure 23).

The design formula is:-

$$f_b = \frac{1.17\sqrt{r_o}}{t_o^{1.5}} (q_m + 1.5q_p) \dots\dots\dots(3.10)$$

$$q_m = M/\pi.r_1^2 \dots\dots\dots(3.11)$$

$$q_p = P/2.\pi.r_1 \dots\dots\dots(3.12)$$

where

- f_b = local longitudinal bending stress in chord (Kips/in²).
- r_o = chord radius (in).
- t_o = chord thickness (in).
- q_p = line load due to axial load (Kips/in).

q_m = line load due to bending moment (Kips/in).
 M = longitudinal moment at the joing (Kip.in).
 P = axial load in branch member (Kips).
 r_1 = mean radius of branch (in).

The value of q_p may be expressed more accurately by dividing P by the actual length of intersection of the branch tube on the chord tube.

The method is acknowledged by the authors as being conservative possibly because stresses and rotations due to circumferential moments in the branch are ignored.

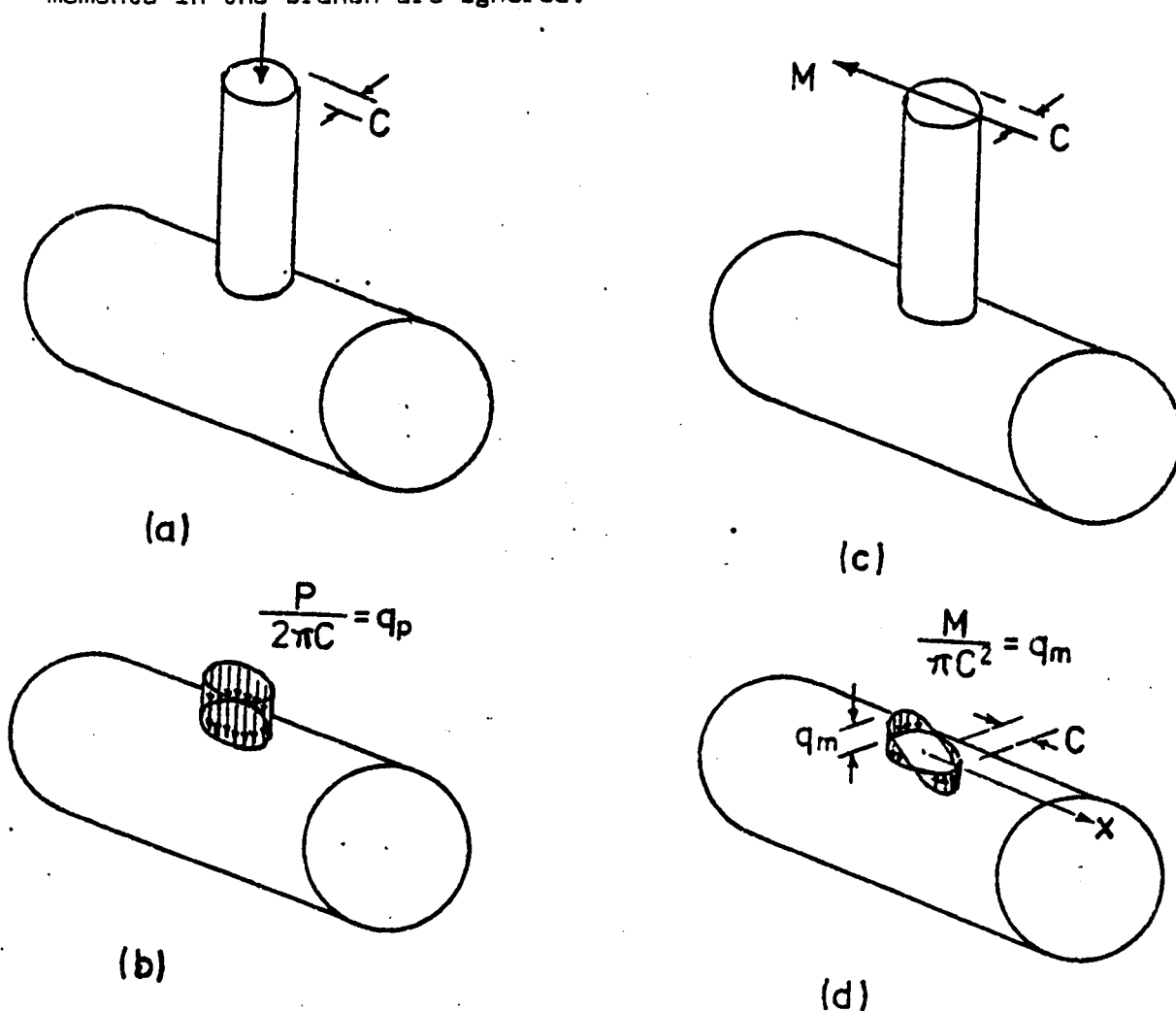


Figure 22 - Loads by Kellogg Method

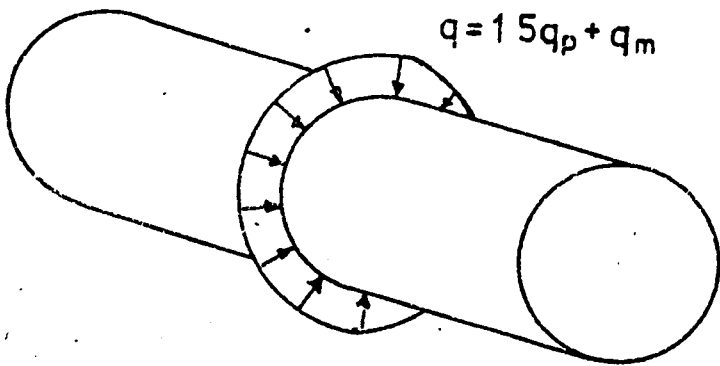


Figure 23 - Kellogg Method for Stresses

If moment loading only is assumed then:-

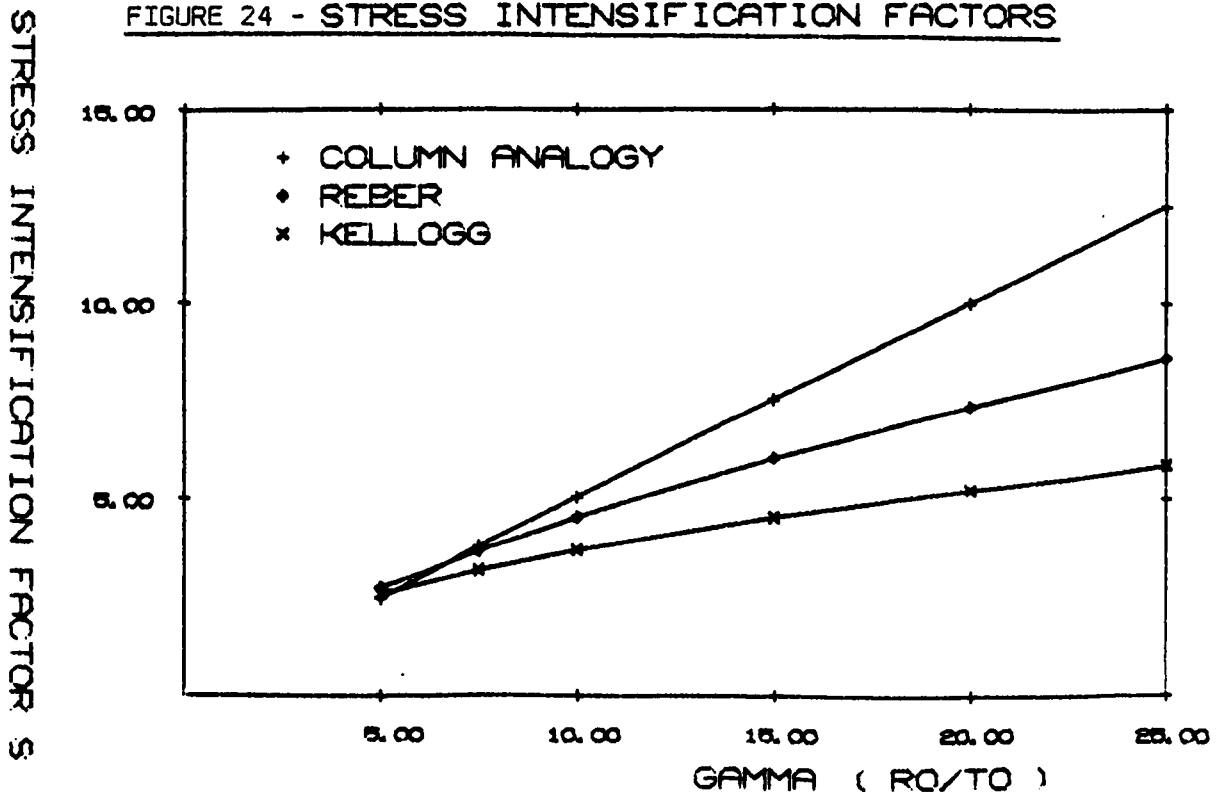
$$f_b = \frac{1.17\sqrt{r_o}}{t_o^{1.5}} \cdot \frac{M}{\pi r_1^2} \dots\dots\dots(3.13)$$

multiplying through by $\frac{t_o}{r_o}$ gives $f_b = 1.17 (r_o/t_o)^{\frac{1}{2}} \cdot M/\pi r_1^2 t_o$

It is of interest to compare the term.

$1.17 (r_o/t_o)^{\frac{1}{2}}$ with $0.9 (r_o/t_o)^{0.7}$ from analysis by Reber and $0.5 (r_o/t_o)$ from column analogy (Figure 24).

FIGURE 24 - STRESS INTENSIFICATION FACTORS



It is suggested that the method may also be used to find the rotation of the joint.

$$\theta = \frac{2.46.M}{E} \left[\frac{r_o}{t_o r_1^2} \right]^{3/2} \dots\dots\dots(3.14)$$

where

- θ = the angle of rotation due to moment M.
- E = Young's modulus of elasticity for the material.

3.2.6. Empirical Formulae Proposed by Kurobane¹⁸

The experimental program carried out by Kurobane has been the most extensive work carried out in the field of tubular joint strength. In all, some 154 tests were carried out on K-joints in hollow steel sections (Test Nos. 38-191, Table 1). The objectives of the test program were:-

To investigate the effect of branch sizes and eccentricities. Those eccentricities chosen were - $d_o/4$, 0 and $d_o/4$ where d_o was the diameter of the chord tube.

To examine the effects of stiffening the chord walls. This was achieved by increasing their thickness to 3.2mm or filling them with concrete.

To examine the effect of changes in intersection angles between members. Compression branch angles were 30, 45, 60 and 90 degrees.

To examine the influence of axial stress in the chord.

To examine the influence of welding conditions, two methods being used:-

- a. automatic flame cut and weld by covered electrode of limetitanium type,
- b. saw cutting process and weld by covered electrode of high titania type.

From the results a relationship is deduced between P_u , the axial load causing failure in the joint, and g , the distance between intersecting lines of tension and compression branches (weld gap), (See Figure 25).

After selecting certain tests i.e. those with 60.5mm diameter x 2.6mm chords which had failed by local deformation, and had compression branches intersecting at 45° , a least squares method was used to derive an experimental equation:-

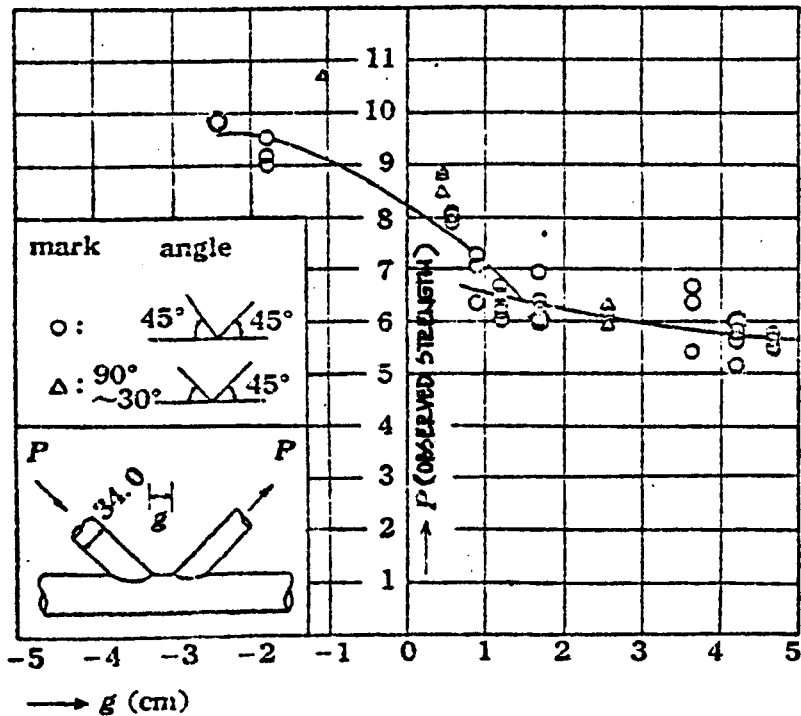


Figure 25 - Correlation Between Observed Strength P and Gap g

$$g \geq 9\text{mm}$$

$$P = \left[8.933 - 4.21 (g/d_o) + 2.89 (g/d_o)^2 \right] \left[0.264 + 1.16 (d_1/d_o) \right] \text{ tons} \dots (3.15)$$

unbiased estimate of standard deviation of P_u is given as 0.195 tons.

$$g \leq 9\text{mm}$$

$$P = \left[0.7999 - 0.469 (g/d_o) - 0.373 (g/d_o)^2 \right] \left[7.908 + 5.94 (d_1/d_o) \right] \text{ tons} \dots (3.16)$$

unbiased estimate of standard deviation of P_u is given as 0.625 tons.

where

g = distance between intersecting lines of tension and compression branches.

$P_u = P/1.414 \sin\theta$, where P = axial load.

P_u = ultimate load of joint.

θ = angle of intersection of branch and chord.

d_o = diameter of chord tube.

d_1 = diameter of compression branch.

The correlation between observed and estimated strength is shown in Figure 26 below.

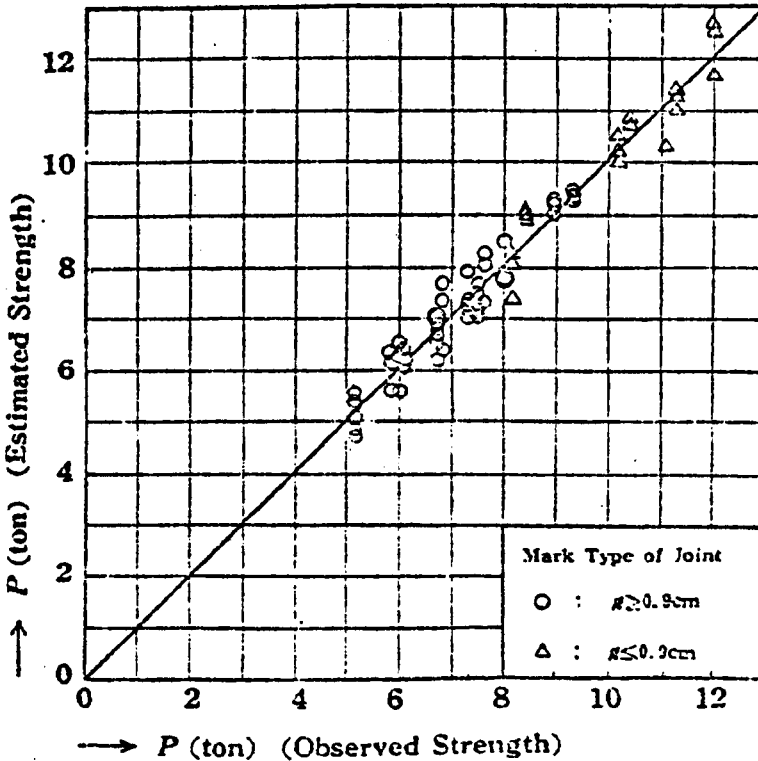


Figure 26 - Correlation Between Observed and Estimated Strength

Efficiency of compression branch is given by:-

$$\eta = P_u/\pi.t_1 (d_1 - t_1) f_{y1} \dots\dots\dots(3.17)$$

where

- P_u = ultimate load estimated from the above empirical equations.
- t₁ = thickness of compression branch.
- d₁ = diameter of compression branch.
- f_{y1} = tensile strength of branch material.

This value η is plotted against d₁/d_o ratio in Figure 27.

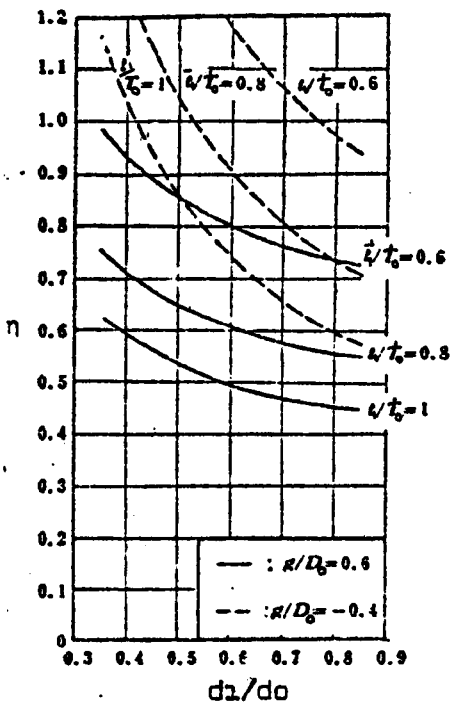


Figure 27 - Efficiency of Compression Branches

Note that η appears to decrease for increasing d₁/d_o and for increasing t₁/t_o.

Strength of a Similar Joint of Different Chord Size and Material

$$P_s = P_{ux} (f_{ys}/5.16) \times (d_{os}/60.5)^2$$

where

P_u = ultimate strength of joint.

P_s = ultimate strength of similar joint.

f_{ys} = tensile strength of similar joint material (tons/cm²)*

d_{os} = diameter of chord tube (mm) in a similar joint.

The modification should not be used when D/T is less than 22.8.

From the study of the effects of axial load in the chord it was found that:-

<u>Type of Axial Load</u>	<u>Effect on Joint Strength</u>
Large compressive	10% reduction
Slight tensile	20% increase
Large tensile	No apparent change

The probable limitations of the method are:-

Formulae apply only to K-joints.

Loads must be axial.

Formulae are based on test results on very small tube sections.

3.2.7. Empirical Formula Proposed by Naka, Kato, Kanatani¹⁶

The investigation consisted of 21 tests (Test Nos. 8-29, Table 1A) on T-joints to study:-

The ratio, diameter of chord/thickness of chord, (d_o/t_o).

The ratio, diameter of branch/thickness of branch, (d_1/t_1).

The ratio, thickness of branch/thickness of chord, (t_1/t_o).

*1N/mm² = 0.01 tons/cm².

The effects of shear spans and support conditions used in the testing procedure.

The differences between T- and cross joints.

The difference between axial tension and axial compression in the branch tubes of T-joints.

Specimen No.	Chord		Branch		d/D	α degrees
	$D \times T$	D/T	$d \times t$	d/t		
C-A-1	139.8×6.5	21.5	139.8×6.5	21.5	0.952	72.2
2			114.3×4.0	28.6	0.818	54.9
3			101.6×4.0	25.4	0.727	46.6
4			76.3×3.2	23.8	0.546	33.1
5			48.6×2.4	20.2	0.348	20.4
C-B-1	139.8×6.5	21.5	139.8×6.5	21.5	0.952	72.2
2			101.6×3.2	31.8	0.727	46.6
3			89.1×3.2	27.8	0.637	39.6
4			48.6×2.3	21.1	0.348	20.4
5			42.7×2.3	18.5	0.306	17.8
6			34.0×2.3	14.8	0.243	14.1
C-D-1	139.8×4.5	31.1	139.8×4.5	31.1	0.957	75.0
2			114.3×4.0	28.6	0.818	54.9
3			101.6×4.0	25.4	0.727	46.6
4			76.3×4.0	19.1	0.546	33.1
5			48.6×2.4	20.2	0.348	20.4
C-C-1	114.3×4.0	28.6	114.3×4.0	28.6	0.951	74.0
2			89.1×3.2	27.8	0.780	51.3
3			76.3×3.2	23.8	0.658	41.9
4			60.5×2.9	20.8	0.529	31.9
5			34.0×2.4	14.2	0.297	17.3

Figure 28 - List of Specimens for Test Program

All specimens reached their ultimate strength as a result of radial deformations at the central part of the chord i.e. local deformation.

Plotting a graph of P ultimate against α where

$\alpha = \sin^{-1} d_1/d_o$, the equation found which gives a best fit to the results in the range $\alpha = \pi/2$ to $\pi/3$ ($d_1/d_o = 0.26$ to 0.87) is:-

$$P_u = (80\alpha/\pi + 2.0).f_{yo}.Z/r_o - \text{branch tube in compression} \dots\dots(3.18)$$

where

$$\alpha = \sin^{-1} (d_1/d_o).$$

$$Z = B_s.t_o^2/6.$$

$$B_s = 1.52 r_o/\sqrt{r_o/t_o}.$$

d_1 = diameter of branch tube.

d_o = diameter of chord tube.

r_o = radius of chord tube.

t_o = thickness of chord tube.

f_{yo} = yield stress of chord tube.

It is established that the average ratio $\frac{P \text{ max tension}}{P \text{ max compression}}$ is 1.5. The above equation, therefore, is multiplied by 1.5 to give $P \text{ max}$ for the branch tube in tension.

$$P \text{ max} = (120\alpha/\pi + 3.0).f_{yo}.Z/r_o - \text{branch tube in tension} \dots\dots(3.19)$$

Summarising the conclusions which apply to joints in steel to 50kips/in² (345N/mm²) and of d_o/t_o ratio 15 to 40, gives:-

d_o/t_o and d_1/d_o may be considered separately when evaluating their effect on joint strength.

The larger d_1/d_o , the higher is the local strength, but for the same load intensity in the branch, a joint with smaller d_1/d_o has higher local strength.

When the shear span exceeds $3d_o$ then end conditions do not affect joint behaviour. However, the stiffening effect of the support still exists. Reduction in shear span leads to an approximately linear decrease in joint strength, more especially in the range $\alpha = \pi/6$ to $\pi/3$ ($d_1/d_o = 0.5$ to 0.87).

Stress concentration increases with α , (d_1/d_o).

Note:-

An attempt has been made to apply the formula to K-joints by dividing the right hand side of the equation for P_u by $\sin\theta$, where θ is the angle of intersection of branch and chord tube, (See Table 2).

3.2.8. Empirical Formula by Washio, Togo²⁰

$$P_u = f_{yo} \left[\frac{d_o}{2} \right]^2 \cdot \left[\frac{d_o}{2t_o} \right]^{-1.5} \cdot \left(1 + 6.52 \frac{d_1}{d_o} \right) \cdot \frac{(1 - 0.26 \cos^2 \theta_c)}{\sin \theta_c} \cdot \left(1.75 - 2.65 \frac{g}{d_o} \right) \cdot f(F_p) \quad \dots\dots\dots (3.20)$$

where

- P_u = ultimate axial load in compression branch.
- f_{yo} = yield stress of chord material.
- d_o = diameter of chord tube.
- t_o = thickness of chord tube.
- d_1 = diameter of compression branch.
- g = gap between braces measured along crown of chord.
- θ_c = angle of intersection of compression branch and chord.
- $f(F_p)$ = 1, in the context of this formula*.

The term $\left(1.75 - 2.65 \frac{g}{d_o} \right)$ is for $0 < g/d_o > 0.23$, and becomes

$\left(1.15 - 0.06 \frac{g}{d_o} \right)$ for $0.23 < g/d_o < 1.8$.

Note:-

The most important reference²⁰ to the experimental work leading to this formula has not been available to date.

This formula has formed the basis of the Det Norske design rules for offshore tubular structures. Extensive manipulation of the present formula has been carried out³¹ by Harlicot, Mouty and Tournay in order to simplify some of the terms.

*It has been suggested³¹ that this term, which allows for the effects of secondary bending stresses in the compression bracing member, be presented as a ratio of axial stress/axial stress plus bending stress, i.e. $f(F_p) = f_a/f_a + f_b$.

3.2.9. Ultimate Strength Method Proposed by J. Blair Reber⁷

The method is based on the results of a computer analysis to find the stresses in joints subject primarily to axial load. Two computer programs are used:-

(i) Scordelis

This program uses Donnell's equation for cylindrical shells (See Figure 29). The chord is assumed to be simply supported at the ends and contains end diaphragms which are perfectly rigid in their own planes. The results of a parameter study carried out are shown in Figure 30, where K is the joint strength factor and hot spot stresses = KP.

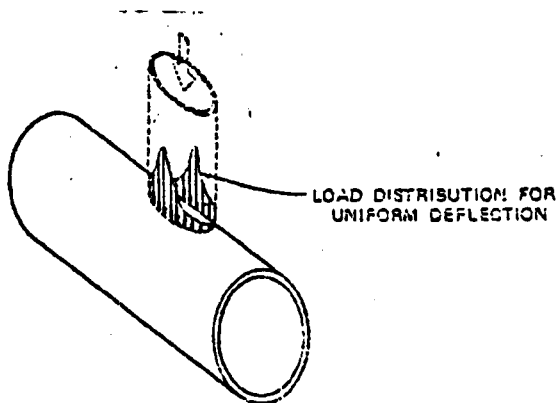


Figure 29 - Analytical Model Used in Scordelis Program

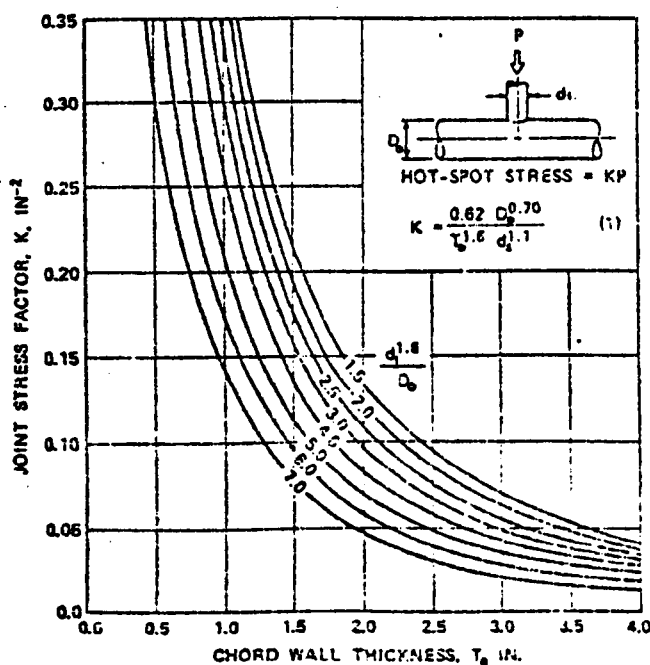


Figure 30 - Curves for Predicting Hot Spot Stresses in T-Joints

A good mathematical approximation to these curves is given by the equation:-

$$K = \frac{0.62 d_o^{0.70}}{t_o^{1.6} d_1^{1.1}} \dots\dots\dots(3.21)$$

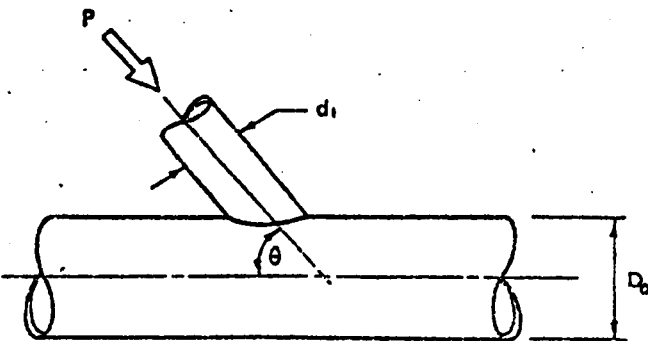
The modification for joint angle is:-

$$\text{maximum stress} = KP.\text{Sin}^{1.5} \theta \dots\dots\dots(3.22)$$

The assumption of a uniform deflection of the chord, which is required by the analysis, becomes less valid as the angle (θ), between the chord and the branch, decreases.

(ii) Clough

Using a program by Clough to analyse a series of K- and Y-joints having similar geometries, a comparison is given with the stresses found from the above equation (See Figures 31 & 32).



$$\text{MAX. STRESS} = KP \sin^{1.5} \theta \qquad (2)$$

$\frac{d_1}{D_o}$	MAX. STRESS, KSI		EQ. (1)
	EQ. (1)	CLOUGH	CLOUGH
0.375	99.3	101.	0.98
0.431	85.0	89.5	0.95
0.498	72.5	74.0	0.98
0.566	63.0	61.4	1.03
0.638	55.3	51.7	1.07
0.693	50.5	42.1	1.20

Figure 31 - Comparison of Hot Spot Stresses in Y-Joints as Computed from Equation 3.22 and by Clough Program

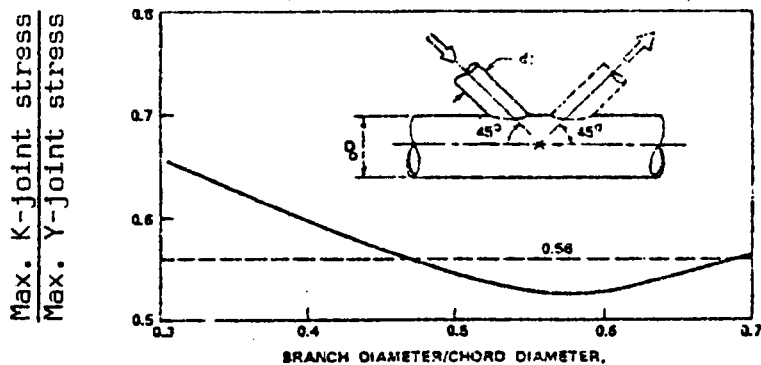


Figure 32 - Relationship Between Maximum K-Joint Stress and Maximum Y-Joint Stress

The hot spot stresses were compared for each type (See Figure 32) and a single value for the ratio of K- to Y-joint stress was chosen as 0.56 i.e. the stress in an average K-joint is about 56% of that in a Y-joint having similar geometry and axial load.

Test Correlations

The ratio of ultimate load, P_u , to the yield load, P_y , is plotted against d_1/d_0 , (See Figure 33(a)).

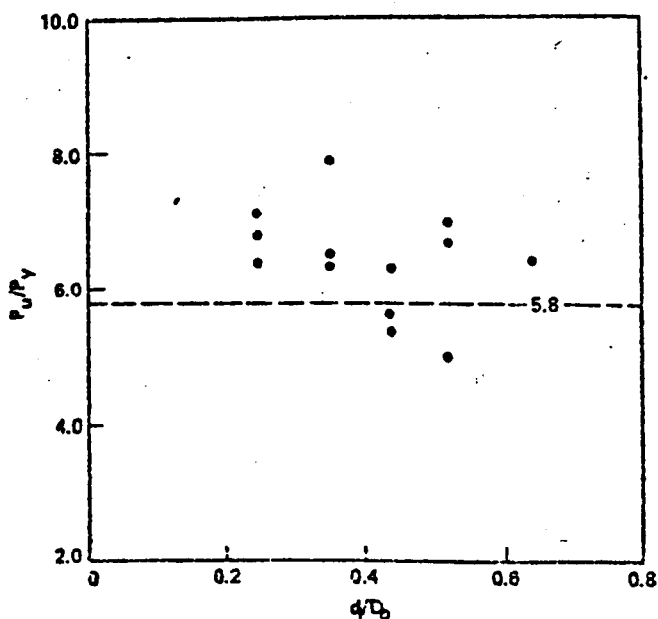


Figure 33(a) - P_u/P_y Versus d_1/d_0 for T-Joints, $F_{y0} = 36-41 \text{ k.s.i.}$ (248- 283N/mm²)

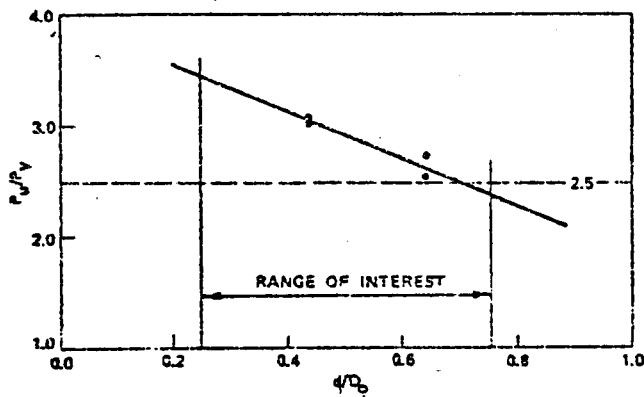


Figure 33(b) - P_u/P_y Versus d_1/d_o for K-Joints; $F_y = 36-41 \text{ k.s.i.}$
($248-283 \text{ N/mm}^2$)

Note:-

The values of P_y used are those found from the Scordelis program, since in practice it is difficult to measure hot spot stresses as they usually occur close to the weld.

For T-joints and Y-joints an average value of P_u/P_y of 5.8 is chosen. A similar graph of P_u/P_y against d_1/d_o is plotted for K-joints and an average value of P_u/P_y of 2.5 is chosen (See Figure 33(b)).

In order to relate P_u/P_y for K- and T-joints it is assumed that P_u/P_y varies with F_y (See Figures 34 & 35).

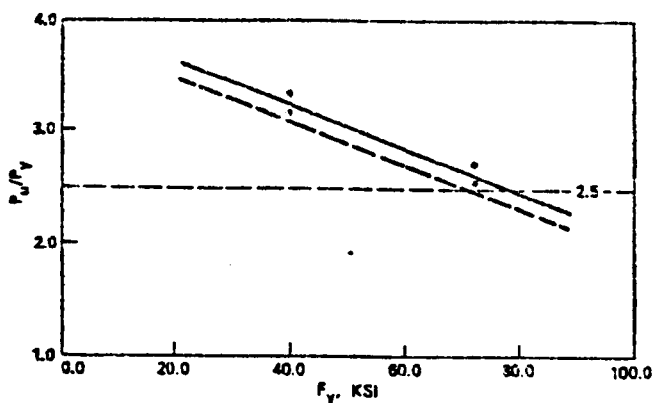


Figure 34 - P_u/P_y Versus F_y for K-Joints; $d_1/d_o = 0.638$

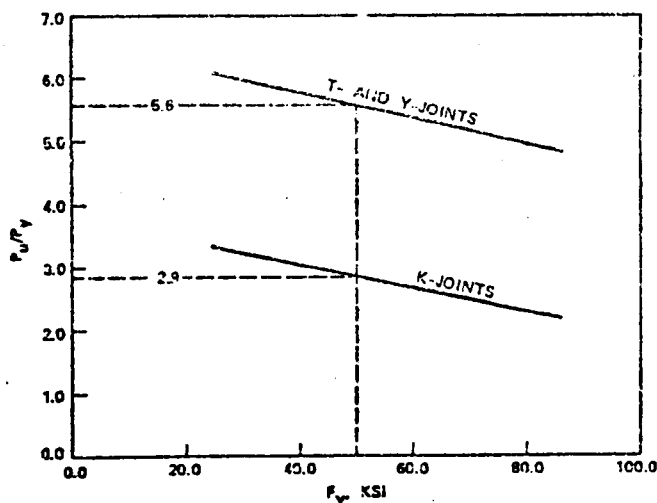


Figure 35 - P_u/P_y Versus F_y for T, Y and K-Joints

The bottom line in Figure 35 is the dotted line from Figure 34 and the top line is the assumed behaviour of T- and Y-joints. This top line is constructed by first assigning it the same slope as the K-joint line (P_u/P_y varying with F_y) and then requiring it to pass through a P_u/P_y value of 5.8 at a yield stress of 40k.s.i. (See Figure 33(a)), (275N/mm^2).

For this design method P_u/P_y values corresponding to a yield stress of 50k.s.i., (345N/mm^2), are chosen as being representative of all yield stresses. The resulting values of P_u/P_y then are:-

5.6 for T- and Y-joints, and
2.9 for K-joints.

In order to relate both by one constant a K-joint is considered as two Y-joints; in this case, as hot spot stress in a K-joint is 0.56 of the hot spot stress in a Y-joint, we have for Y-joint:-

$$\frac{P_u}{P_y/0.56} = 2.9 \quad \text{i.e.} \quad \frac{P_u}{P_y} = 5.2$$

Here 5.2 corresponds to 5.6 obtained previously (Figure 35).

Taking an average of 5.2 and 5.6, we have:-

$$\frac{P_u}{P_Y} = 5.4$$

or expressing this in terms of stresses:-

$$\text{maximum stress} = 5.4f_{y0}$$

$$P_u = \frac{5.4.P_Y}{K.\sin^{1.5}\theta} \dots\dots\dots(3.23)$$

$$K = \frac{0.62d_o^{0.7}}{t_1^{1.5} d_1^{1.1}} \dots\dots\dots(3.24)$$

where

- P_u = axial branch load causing joint failure (kips).
- f_{y0} = chord yield stress (kips/in²)
- θ = angle of intersection of joint members.
- d_o = diameter of chord (in).
- d₁ = diameter of branch considered (in).
- t_o = thickness of chord (in)
- P_Y = branch load causing joint yield (kips) found from Scordelis program.

The assumptions and limitations involved in this analysis are:-

- Joints are non gusseted T, Y and K-joints.
- d₁/d_o is in range 0.25 to 0.75. This means there can be essentially no overlap between branches.
- Joints must be primarily loaded by axial load on the branch tube, rather than by branch end moments. Reber states that this limitation is insignificant because in practice 2/3 of the stress, or more, is caused by axial load.

3.2.10. Empirical Formula Proposed by A. A. Toprac and P. W. Marshall
Based on Studies in Japan¹²

A simplified limit analysis of joints between circular tubes has been reported¹² which derives an expression for theoretical ultimate strength:-

$$V_p = \frac{0.5}{\beta(1-\beta)} \cdot \frac{f_{yo}}{0.5\gamma} \cdot \frac{B_c}{2\pi \cdot r_o} \dots\dots\dots(3.25)$$

where

- V_p = ultimate punching shear stress.
- β = diameter of branch/diameter of chord (d_1/d_o).
- γ = radius of chord/thickness of chord (r_o/t_o).
- r_o = radius of chord.
- f_{yo} = yield stress of chord material.
- B_c = effective length of chord chosen for limit analysis.

When the effective length B_c is taken as equal to the chord circumference* then the last term becomes unity and the equation is similar to that deduced for square tubes using limit analysis, i.e.

$$V_p = \frac{0.25}{\beta(1-\beta)} \cdot \frac{f_{yo}}{0.5\gamma} \dots\dots\dots(3.26)$$

with a term for the basic variation of V_p with f_{yo} and γ , modified by a term for the β effect.

*It is the limiting factor that the round to round joint must be as strong, at least, as a square to square joint which requires that the minimum effective length of chord, B_c , be equal to the chord circumference.

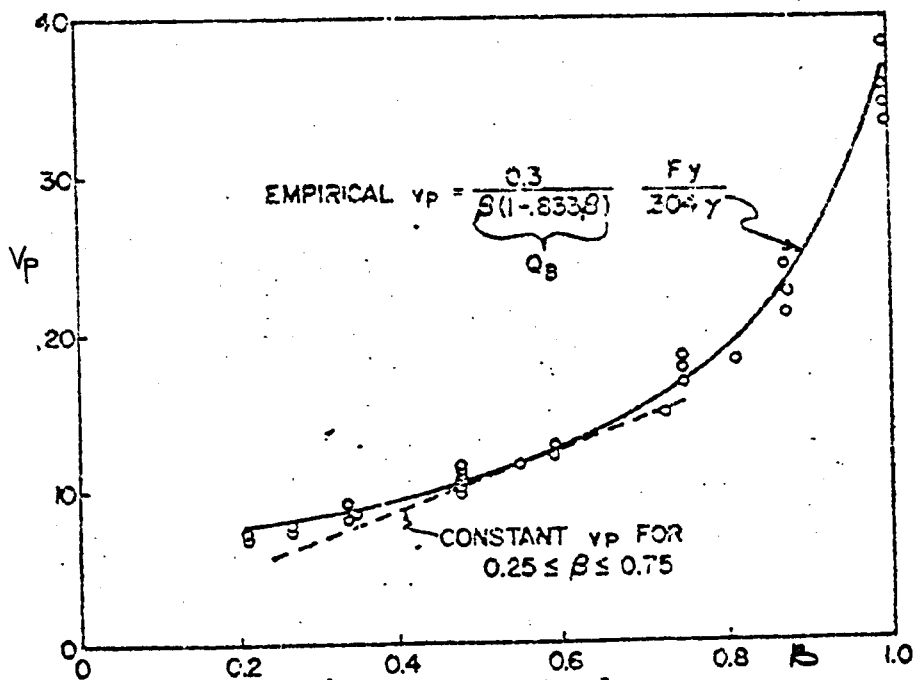


Figure 36 - Japanese Results for Cross Joints

Test data have been used to justify an empirical modification of the expression for ultimate punching shear, leading to Figure 36, and the expression:-

$$V_p = \frac{0.3}{\beta(1-0.833\beta)} \cdot \frac{f_{yo}}{0.304\gamma} \dots\dots\dots(3.27)$$

In this expression the term for the β modification has the following implications:-

- i. a value of 1.0 for β = 0.6,
- ii. increasing joint efficiency for larger β ratios, up to a limiting increase of 1.8 - fold for β = 1.0.

Note that for the mid range of diameter ratios (β from 0.25 to 0.75) the assumption of constant punching shear also provides a reasonable fit to the data of Figure 36, in line with earlier results. For very small β ratios there is little experimental justification for the large increases in joint efficiency predicted by the β-modifier in

the above equation, for example:-

$$\beta = 0.25, \text{ then } \frac{0.3}{\beta(1-0.833\beta)} = 1.5, \text{ i.e. efficiency} = 150\%.$$

It has, therefore, been recommended that a modifier of unity be recommended for values of β less than 0.6. This is consistent with the results for square tubes.

Considering equation 3.27 when β is less than 0.6 gives:-

$$V_p = \frac{f_{yo}}{0.304\gamma} = \frac{f_{yo}}{0.304} \cdot \frac{t_o}{r_o} \dots\dots\dots(3.28)$$

i.e. increasing chord thickness (t_o) increases punching shear,
 increasing chord radius (r_o) decreases punching shear.

The value of V_p found from equation 3.27 should be compared with a stress acting on the joint calculated from the following formula:-

$$V_p = \tau \left[\frac{f_a}{k_a} + \frac{f_b}{k_b} \right] \sin \theta \dots\dots\dots(3.29)$$

where

- τ = thickness of branch tube/thickness of chord tube.
- f_a = axial stress in branch tube.
- f_b = bending stress at joint in branch tube.
- k_a = relative length factor (See Figure 37).
- k_b = relative section factor (See Figure 37).

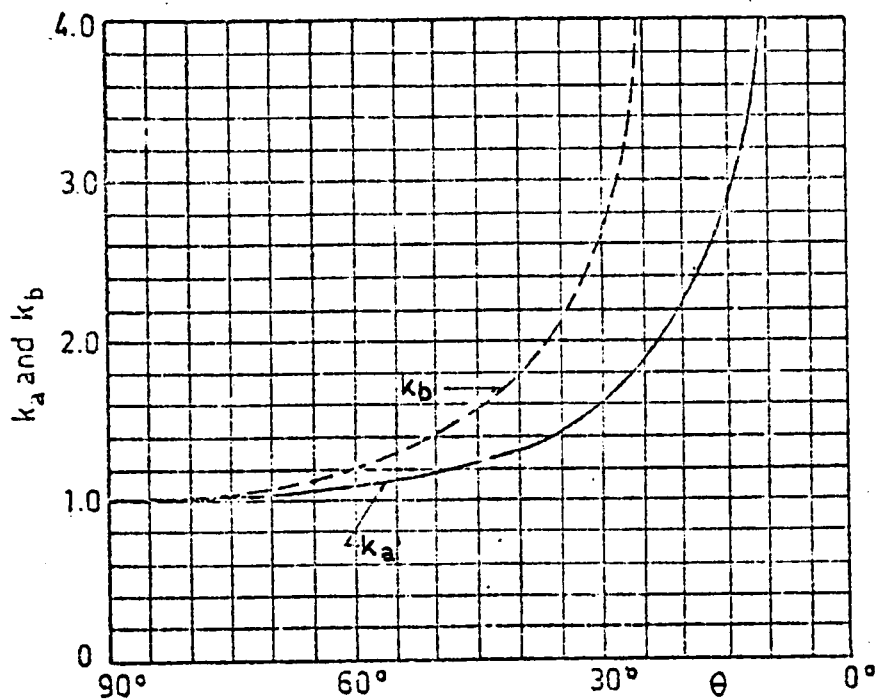


Figure 37 - True Intersection Line Effects

As mentioned previously it is suggested that the best results are obtained for β in the range 0.25 - 0.75.

3.3.11. Design Formulae Proposed by Kato¹⁵

The equations proposed are those found from nearly 200 tests carried out by the Society of Steel Construction in Japan¹⁹.

In this investigation the ultimate load is defined as the peak load soon after yielding (Figure 38(a)). When gradual increase of load is observed after yielding the load at which stable plastic deformation initiates is taken into account for the calculations (Figure 38(b)).

The ultimate load P_{yo} is found as follows:-

The point where the tangent A of that part of the $P - \delta$ curve, where stable plastic deformation occurs, meets the initial tangent gives P_y . (Figure 38(b)).

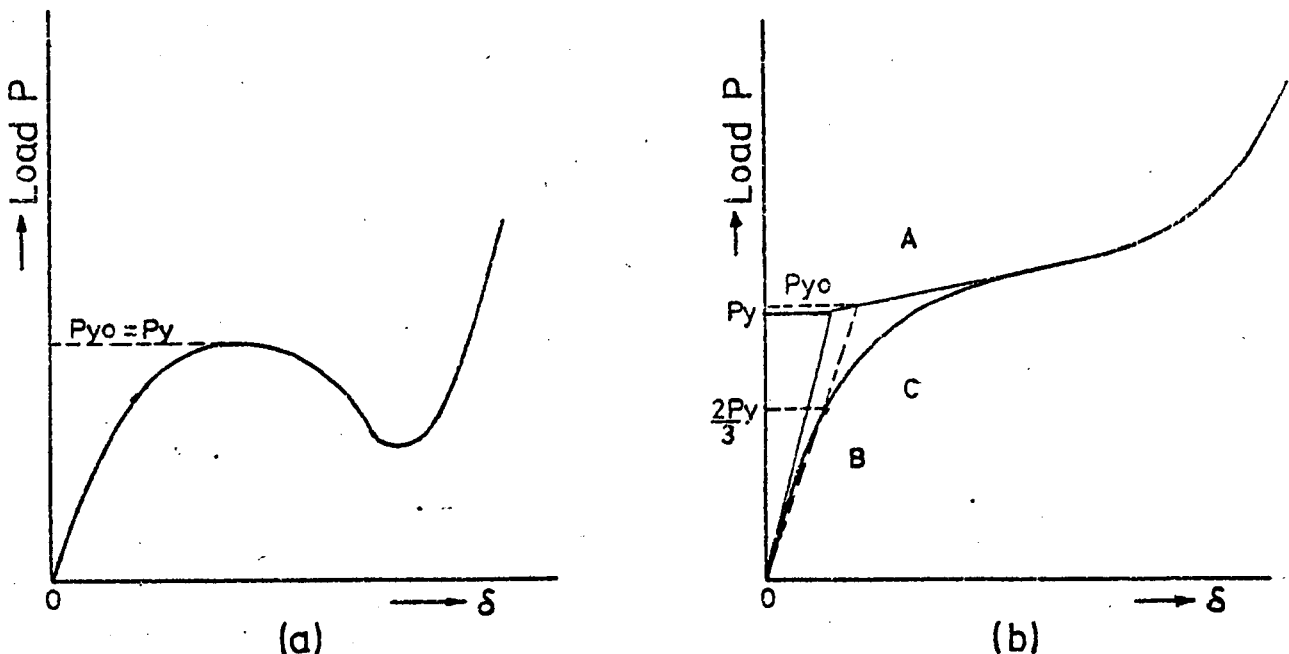


Figure 38 - Definition of Ultimate Load (Yield Load) in Investigations by ISSC

The line going through zero and the point of the curve for $P = \frac{2}{3} P_y$ meets the tangent at a point which gives p_{yo} .

The design equations found are:-

Axial Load

$$P_{yo}/f_{yo} \cdot t_o^2 = 7.3/[1 - 0.833 \cdot d_1/d_o] \dots\dots\dots(3.30)$$

for inclined branch $P_{yo} = P_{yo}/\sin \theta$.

Longitudinal Moment

$$M_{yo}/f_{yo} \cdot t_o^2 = [0.3 (d_o/t_o) + 5] \cdot (d_1/d_o)^2 \cdot d_o \dots\dots\dots(3.31)$$

Circumferential Moment

$$M_{yo}/f_{yo} \cdot t_o^2 = -[0.03 (d_o/t_o) + 6.1] \cdot (d_1/d_o)^2 \cdot d_o \dots\dots\dots(3.32)$$

where

- P_{yo} = ultimate axial load on branch tube.
- M_{yo} = ultimate moment on joint.
- f_{yo} = yield stress of chord material.
- d₁ = diameter of branch tube.
- d_o = diameter of chord tube.
- t_o = thickness of chord tube.

For application of the above formulae the following conditions should be obeyed:-

- d_o/t_o ratio should be in the range 40-100.
- d₁/d_o ratio should be in the range 0.2-0.6.

3.2.12. American Petroleum Industry - Code for the Design of Fixed Offshore Platforms²⁷

Punching shear acting on the chord $V_p = \tau \sin \theta \left[\frac{f_a}{k_a} + \frac{f_b}{k_b} \right] \dots\dots\dots(3.33)$

where

- τ = thickness of branch/thickness of chord.
- θ = angle of intersection of tubes at the joint.
- f_a = stress due to axial load in the branch.
- f_b = stress due to longitudinal moment at the joint.
- k_a = relative length factor (See Figure 37).
- k_b = relative section factor (See Figure 37).

The value of V_p must not be greater than the punching shear capacity calculated from:-

$V_p = Q\beta.Q_f.f_{yo}/0.9\gamma^{0.7} \dots\dots\dots(3.34)$

where

- Qβ = 0.3/ β(1 - 0.833β) for β > 0.6.
- Qβ = 1 for β < 0.6.

β = diameter of branch tube/diameter of chord (d_1/d_0).
 Q_f = $1.22 - 0.5A$ for $A > 0.44$.
 Q_f = 1 for $A < 0.44$.
 A = $(|f_a| + |f_b|)/0.6f_{yo}$.
 f_{yo} = yield stress of tube material (chord).
 γ = radius of chord/thickness of chord (r_o/t_o).

Other recommendations are:-

Brace axial loads and bending moments essential to the integrity of the structure should be included in the calculation of punching shear. For diagonal braces, only the load component perpendicular to the chord wall need be considered and full advantage may be taken of the increased length of the potential failure surface.

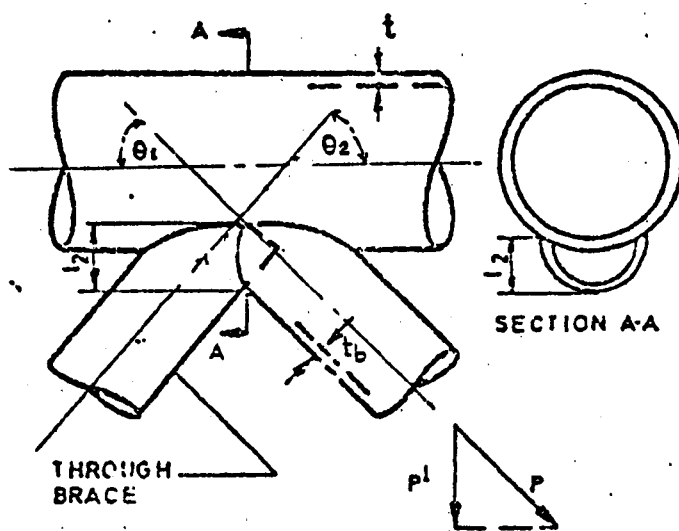


Figure 39 - Detail of Overlapping Joint

It is suggested that:-

The overlap should take about 50% of the acting P^1 .

The brace thickness should never exceed that of the chord.

Moments caused by eccentricity of brace working lines should be considered in the structural analysis.

The brace which is largest or carried the largest load shall have the maximum contact with the chord.

If an increased chord wall thickness is required at the joint, it must be extended past the outside edge of the bracing a minimum of $d_o/4$ or 300mm (whichever is greater).

Where increased brace wall thickness is required, it must extend a minimum of one brace diameter or 600mm (whichever is greater) from the joint.

A joint may be considered nominally concentric (zero eccentricity) if the braces are offset to obtain a minimum of 2 clear inches between them along the chord surface.

Where joints cannot be provided with the minimum of 50mm between braces they must be considered as overlapping and designed as follows:-

$$P^1 = (V_p.t_o.l_1) + (2V_w.tw.l_2) \dots\dots\dots(3.35)$$

where

P^1 = allowable total load component perpendicular to the chord.

t_o = chord thickness.

l_1 = actual length of contact for that portion of the brace in contact with the chord. (Also called U_c).

V_w = allowable shear stress for weld between braces.

tw = lesser of:-

1. weld throat thickness.

ii. thickness of thinner brace (t_b).

l_2 = projected chord length (one side) of the overlapping weld, measured perpendicular to the chord. (Also called U_b).

(See Figure 39).

Formulae for calculating intersection lengths l_1 and l_2 are given on page 40 Appendix B.

3.2.13. American Welding Society²⁸ - Section 10 - Design of
New Structures

The code uses a simplified approach to calculate the punching shear at a joint:-

$$V_p = \frac{P}{t_o \times L} \dots\dots\dots(3.36)$$

and

$$V_p > f_{yo}/0.9.\gamma^{0.7*} \dots\dots\dots(3.37)$$

- P is the axial load in the branch of a T- or K-joint.
- t_o is the thickness of the chord.
- L is the length of intersection of branch and chord tube = 2.π.r.k.
- V_p is the allowable punching shear stress.

where

- $k = x + y + 3 \sqrt{x^2 + y^2} \dots\dots\dots(3.38)$
- $x = 1/(2\pi \sin\theta)$
- $y = \frac{1}{3\pi} \frac{(3 - \beta^2)}{(2 - \beta^2)}$
- β = diameter of branch/diameter of chord.
- r = shortest distance from centre line of branch to the toe of the connecting weld on the main member outside surface (effective radius of intersection).
- f_{yo} = specified minimum yield strength of the main member steel, but not more than 2/3 of the tensile strength.
- γ = radius of chord tube/thickness of chord.
- θ = angle of intersection of tubes at the joint.

The value of k equal to 1 may be used as a conservative approximation.
The value of the punching shear acting, V_p, may also be calculated using the formula given in the API Code, page 68.

*The alternate form of the equation for ultimate punching shear, V_{p(ult)} = f_{yo}/0.5γ^{0.7}, is used in the present investigation.

Uneven Distribution of Load

To prevent progressive failure of the weld and insecure ductile behaviour of the joint, the minimum welds provided in simple, T, Y or K connections shall be capable of developing, at their ultimate breaking strength, the lesser of brace member yield strength or V_p on the main member shear area.

Ultimate breaking strength of fillet welds and partial penetration groove welds shall be computed as:-

2.67 x basic allowable stress for 60 and 70k.s.i. tensile strength, and 2.21 x basic allowable stress for higher strength levels.

Lamellar Tearing

Due to occasional inconsistencies in cross sectional properties, tensile stress in the through thickness direction shall not exceed 20 k.s.i. (138N/mm^2), regardless of specified yield strength.

For best results using this, and all punching shear methods, the following limitations apply:-

Loads should be primarily axial.

Diameter ratio of the tubes should be in the range 0.25-0.75, and preferably less than 0.6.

3.2.14. Canadian Standards Association Std.G40.20, on the Manufacture of Hollow Structural Sections⁴

'K' and 'N' Joints

The code provides joint efficiency graphs based on the research of Bouwkamp¹³. (See Figures 40 & 41).

Joint efficiency = ratio of test failure load to calculated theoretical ultimate load of the tension web member.

It is seen from the Figures that for 100% efficiency minimum t_o/d_o values may be reduced from 0.09 to 0.05 for zero eccentricity joints, and from 0.09 to 0.03 for negative eccentricity joints.

Here t_o = thickness of chord tube and d_o = diameter of chord tube.

Limitations

The method is not valid when the wall of the diagonal tube is thicker than the wall of the main chord.

The method considers the effect of d_o/t_o and d_1/d_o parameters only.

The value of the joint strength appears to depend mainly upon the size of the diagonal and the d_o/t_o ratio of the chord.

T-Joints

For $\beta < 0.2$, a shear area method is recommended:-

$$P_u = S_{sy} \cdot \pi \cdot d_s \cdot t_o \dots\dots\dots (3.39)$$

where

P_u = ultimate axial load in the branch tube.

S_{sy} = shear yield strength.

d_s = distance between toes of welds (Figure 42).

t_o = thickness of chord tube.

β = diameter of branch/diameter of chord.

Basis for Proposal

The results of 34 tests carried out by J. G. Bouwkamp (Test Nos. 192-225, Table 1A).

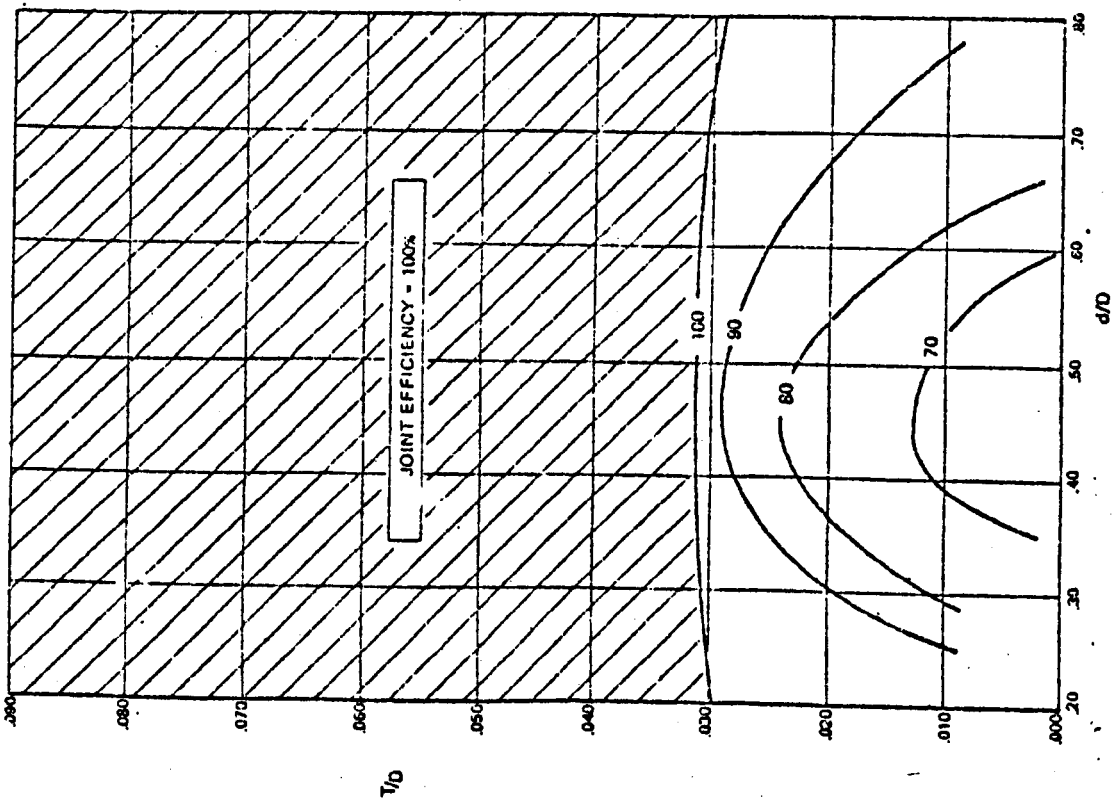


Figure 40 - Joint Efficiency Values for Negative Eccentricity

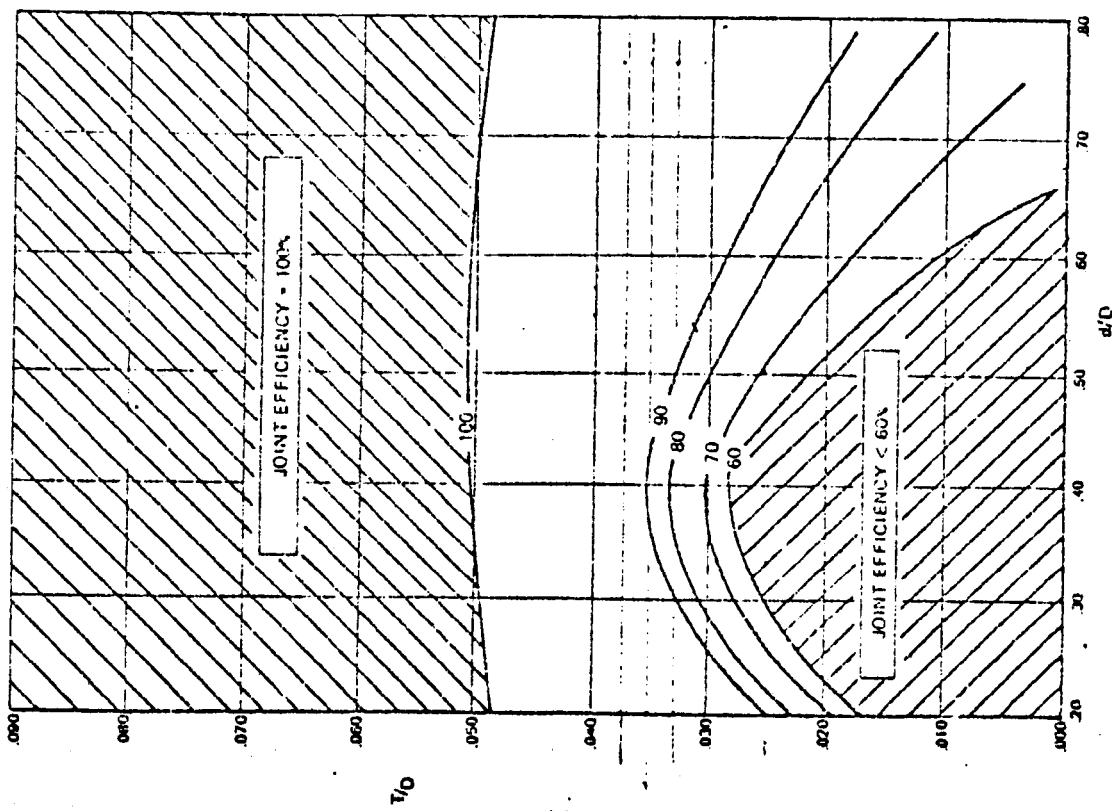


Figure 41 - Joint Efficiency Values for Zero Eccentricity

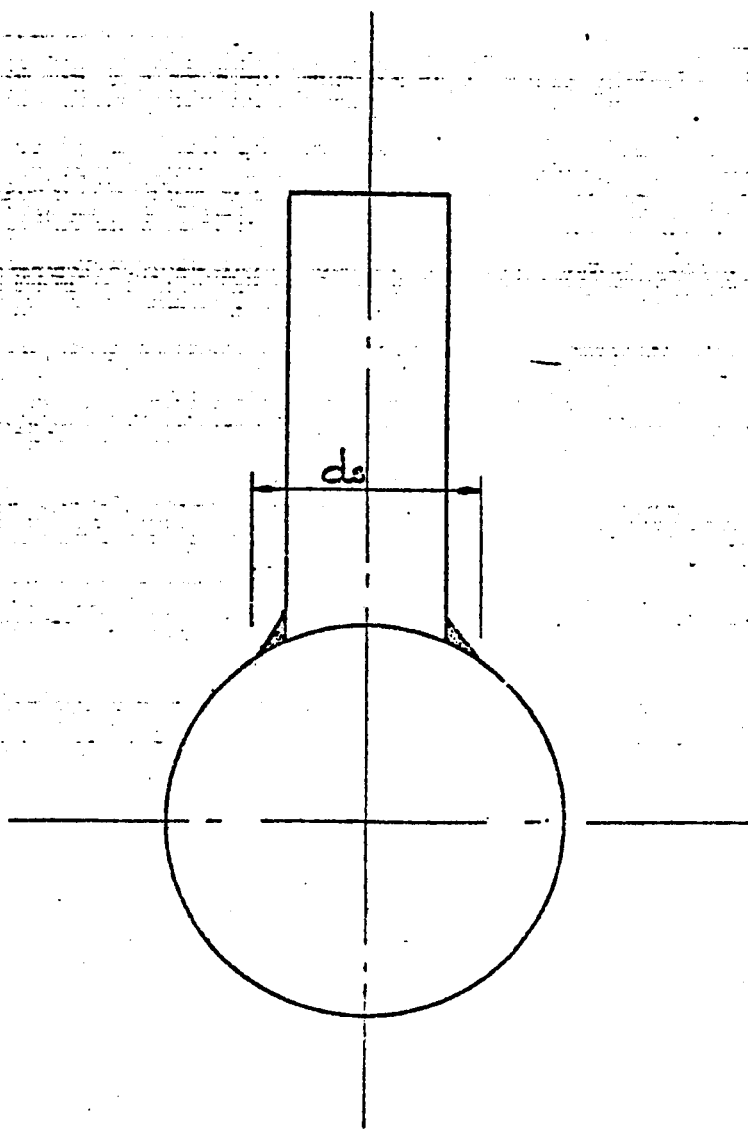


Figure 42 - Section Showing Distance Between Toes of Welds, d_s .

3.2.15. Rules for the Design and Construction and Inspection of Fixed Offshore Structures - Det Norske Veritas 1974

$$\text{Punching shear stress } \tau_p = \frac{t_1}{t_0} \frac{2 \sin^2 \theta}{1 + \sin \theta} (|\sigma_a| + |\sigma_b|) \dots\dots\dots (3.39)$$

and $\tau_p > \text{lesser of } n_p \cdot f_{yo} / \sqrt{3} \text{ or } n_p \cdot \tau_u$

where

- t_1 = thickness of branch tube.
- t_0 = thickness of chord tube.
- θ = angle of intersection of tubes.
- σ_a = stress due to axial load.
- σ_b = stress due to bending load.
- n_p = permissible usage factor
 - functional loads $n_p = 0.5$.
 - environmental loads $n_p = 0.67$.
- f_{yo} = specified minimum upper yield stress of material.
- τ_u = ultimate punching shear stress.
- $\tau_u = \frac{1.2 f_{yo}}{\sqrt{\gamma}}$ for $0.25 < \beta < 0.85$.
 $10.0 < \gamma < 20$
- γ = radius of chord / thickness of chord.

K-Joints

To be treated as two separate Y-joints if, $P_1 \sin \theta_1 \neq P_2 \sin \theta_2$, or $g^* > g_0$ (See Figure 43).

For all overlapping joints the total load component, P^1 , perpendicular to the chord must not be greater than:-

$$\tau_p \cdot t_0 \cdot L_1 + 2 \cdot \tau_w \cdot t_w \cdot L_2 \dots\dots\dots (3.40)$$

*g = Gap between adjacent branch tubes
 Diameter of chord tube

where

L_1 = circumferential length of brace at connection.

L_2 = projected chord length (1 side) of the overlapping weld,
measured perpendicular to the chord.

τ_w = $n_p \cdot f_y / \sqrt{3}$ (see above for definitions).

t_w = lesser of overlapping weld throat thickness, and the
thickness t of the thinner brace.

(See Figure 44).

The Value of Ultimate Punching Shear Stress τ_u is Given Below for the Following Types of Joint:-

T-Joint - Compression in Branch

$$\tau_u = 1.2f_{yo}/\sqrt{\gamma} \quad \begin{matrix} 0.25 \leq \beta \leq 0.85 \\ 10 \leq \gamma \leq 20 \end{matrix}$$

T-Joint - Tension in Branch

$$\tau_u = (0.37 + 0.96\beta) f_{yo}/\sqrt{\gamma\beta} \quad \begin{matrix} 0.2 \leq \beta \leq 1.00 \\ 9 \leq \gamma \leq 30 \end{matrix}$$

Y-Joint - Compression in Branch

$$\tau_u = 2.4 \sin\theta \cdot f_{yo}/(1 + \sin\theta)\sqrt{\gamma} \quad \begin{matrix} 0.25 \leq \beta \leq 0.85 \\ 10 \leq \gamma \leq 20 \\ 30^\circ \leq \theta \leq 90^\circ \end{matrix}$$

Y-Joint - Tension in Branch

$$\tau_u = 1.91 (0.38 + \beta) \sin\theta \cdot f_{yo}/(1 + \sin\theta)\beta\sqrt{\gamma} \quad \begin{matrix} 0.2 \leq \beta \leq 0.85 \\ 10 \leq \gamma \leq 30 \\ 30^\circ \leq \theta \leq 90^\circ \end{matrix}$$

Cruciform Joint - Compression in Opposite Branches

$$\tau_u = 1.18f_{yo}/(1.2 - \beta)\beta\gamma \quad \begin{matrix} 0.25 \leq \beta \leq 1.00 \\ 10 \leq \gamma \leq 25 \end{matrix}$$

N- and K-Joints

$$\begin{aligned} \tau_u &= 1.2f_{yo}/\sqrt{\gamma} \cdot f(\theta_1) \cdot f(\beta_1) \cdot f(g) & 0.25 \leq \beta \leq 0.85 \\ f(\theta_1) &= \sin\theta_1 & 10 \leq \gamma \leq 55 \\ f(\beta_1) &= (1 + 6.1\beta_1)/4.2\beta_1 & 30 \leq \theta \leq 90 \\ f(g) &= (2.4 + 1.8g)/(2.4 + 7g) & 0 \leq g \leq g_o \end{aligned}$$

where β_1 = compression brace diameter/chord diameter

Additional Recommendations

If an increased wall thickness, or special steel, is required in the chord at the joint, it is to be extended past the outside edge of the bracing by a minimum of $d_o/4$ or 300mm (whichever is greater).

Overlapping Joints

For the purposes of this code a joint is considered to be overlapping if there is less than 50mm clear gap, between adjacent braces, along the surface of the chord.

A joint may be considered nominally concentric (zero eccentricity) if the braces are offset along the centre line of the chord in order to achieve the minimum 50mm gap.

The overlap should be preferably proportioned to transfer at least 50% of the allowable total load component perpendicular to the chord.

Brace wall thickness should never exceed that of the chord.

Where braces carry substantially different loads and/or one brace is thicker than the other, the heavier brace should be the through brace and it's full circumference welded to the chord.

Where braces tend to overlap at congested joints the following corrective measures may be made:-

- i. Where primary braces are substantially thicker than the secondary braces, they may be made the through members with the secondary braces designed as overlapping members.
- ii. The chord may be given an enlarged joint section.
- iii. A spherical joint may be used.

iv. Secondary braces causing interference may be offset.

Limitations

The formula are given for certain parameter ranges (see page 79).

Basis of Proposal

A punching shear method. For diagrammatic representation see Figure 44.

3.2.16. Design Formula Proposed by Visser

Solutions for unstiffened tubular joints are obtained using the SATE program (a finite element solution for thin shells).

Originally the work was to check the design of cross-joints, but the solutions are applied to T- and K-joints. The stress concentration factors (S.C.F.) for the joints analysed* are approximated by the following formula:-

$$\text{S.C.F.} = \frac{t_1}{t_o} (10 + 0.3 \frac{r_o}{t_o}) \sin^2 \theta \cdot \left[1.4 - 0.75 \frac{r_1}{r_o} \right] \dots\dots\dots(3.41)$$

where

- t_1 = thickness of branch tube.
- t_o = thickness of chord tube.
- r_o = radius of chord tube.
- r_1 = radius of branch tube.
- θ = angle of intersection of tubes as joint.

The following equations, found in reference⁹, are used:-

$$V_p = \frac{t_1}{t_o} \sin \theta \cdot \frac{f_a}{k_a}$$

$$V_p = Q\beta \cdot Q_f \cdot f_{yo} / 0.9 \gamma^{0.7}$$

*The Author analyses 14 fictitious T, K and X-joints, varying the chord wall thickness only.

re-arranging, $f_a = V_p \cdot t_o \cdot k_a / t_1 \cdot \sin \theta$
 and substituting for V_p , with $Q\beta = 0.3 / (r_1 / t_o (1.0 - 0.833 r_1 / r_o))$
 for $0.5 < r_1 / r_o < 1.0$, gives:-

$$f_a = \left[\frac{t_1}{t_o} 0.9 \left[\frac{r_o}{t_o} \right]^{0.7} \cdot \sin \theta \cdot \frac{r_1}{r_o} \left[1.0 - 0.833 \frac{r_1}{r_o} \right]^{-1} \right] f_{yo} \dots\dots\dots (3.42)$$

where

- f_{yo} = yield stress of chord tube.
- k_a = a function of (See Figure 37).
- $Q\beta$ = load factor ($Q\beta = 1$, for $f_a < 0.25 f_{yo}$).
- γ = radius of chord/thickness of chord.
- f_a = allowable brace stress.

The dimensionless quantity in square brackets is called the punching shear number (P.S.N.).

Stress Concentration Factors in Unstiffened Tubular Joints			
	S.C.F.	Punching Shear No.	S.C.F./P.S.N.
T1	3.3	1.1	3.0
T2	6.6	2.3	2.9
T3	4.0	1.8	2.2
T4	8.0	3.7	2.2
T5	16.0	7.3	2.2
T6	4.8	2.4	2.0
T7	9.6	4.9	2.0
T8	8.0	3.7	2.2
K1	4.0	2.0	2.0
K2	12.0	6.7	1.8
K3	4.0	2.0	2.0
K4	4.0	2.0	2.0
X1	4.2	1.3	3.2
X2	10.4	4.0	2.6

The results of analyses using stress concentration factor (S.C.F.) and punching shear number (P.S.N.) are summarised above. It is

seen from these results that the punching shear number is approximately half of the stress concentration factor.

Summarising gives:-

$$f_a = \frac{(S.C.F.)}{2} f_{yo} \dots\dots\dots(3.43)$$

where S.C.F. = stress concentration factor (Equation 3.41).

It is noted that the analysis was carried out varying only the chord wall thickness parameter. The Author claims that a full study of a braced K-joint would entail considering 13 geometric parameters. Furthermore, he suggests that unstiffened joints are only practical if their S.C.F.'s are less than 10.

Visser did not, in fact, intend that his method be used as a design formula, but it is included in this present study as the stress concentration factor approach is of general interest and becomes more useful in the study of the effects of fatigue loading on joints in C.H.S.

3.2.17. Harlicot, Mouty, Tournary Verification Formulae³¹

Extensive parametric studies have been carried out in order to simplify the Washio, Togo Formula²⁰. Each term in the original equation has been simplified, and the whole equation multiplied by a constant of correlation between the strength predicted by the equation and experimental results. It is not, however, stated which experimental results are considered.

3.2.17.1. Y- and T-Joints

$$P_u \leq 5.32 \text{ to } d_1 f_{yo} \left[\frac{t_o}{d_o} \right]^{0.5} \left[\frac{d_o}{d_1} \right]^{\gamma} \cdot \left[\frac{1+\sin\theta}{2\sin\theta} \right] \left[\frac{\theta I_N}{\theta I_N + \theta I_M} \right]^* \left[1 - 0.23 \frac{f_o}{f_{yo}} + \frac{f_o^2}{f_{yo}^2} \right] \dots\dots\dots(3.44)$$

*This term allows for the effects of secondary bending stress in the branch member only and is not intended for application to joints with primary bending moments applied.

The equation is for tensile and compressive branch members.

$\gamma = 0.2$ for branch in compression.

$\gamma = 0.5$ for branch in tension.

The last term is taken as unity when the chord preload is tensile (i.e. f_o is a tensile stress).

Limitations of the method are:-

$$0.25 \leq \beta \leq 1.0$$

$$10 \leq \frac{d_o}{t_o} \leq 66$$

$$30^\circ \leq \theta \leq 90^\circ$$

3.2.17.2. N- and K-Joints

(i) N- and K-Joints with Gap Between Branch Members

$$P_u \leq \text{equation 3.44} \times \frac{0.17 + g/d_o}{0.1 + g/d_o} \dots\dots\dots(3.45)$$

For joints without secondary bending stress omit the term:-

$$\frac{\theta_{IN}}{\theta_{IN} + \theta_{IM}}$$

For f_o tensile the term $\left[1 - 0.23 \left[\frac{f_o}{f_{yo}} + \frac{f_o^2}{f_{yo}^2} \right] \right]$ is taken as unity

(ii) N- and K-Joints With Overlapping Branch Members

$$P_1 \sin \theta_1 \leq \frac{f_{yo}}{\sqrt{3}} \left[\left[t_o L_1 \frac{\theta_{IN}}{\theta_{IN} + \theta_{IM}} \right] + 2 t_r L_2 \right] \dots\dots\dots(3.46)$$

Limitations are as for equation 3.44 above, both for joints with gap and overlap. Also:-

$$g/d_o \leq 0.66$$

$$P_1 \sin \theta_1 \approx P_2 \sin \theta_2$$

If the last two conditions are not fulfilled then the joint should be designed as separate Y-joints using equation 3.44 above.

3.2.17.3. X-Joints

$$P_u \leq A \cdot \frac{t_o}{1.2 - \beta} \cdot f_{yo} \cdot \frac{1}{\sin \theta_1} \left[1 - 0.23 \left[\frac{f_o}{f_{yo}} + \frac{f_o^2}{f_{yo}^2} \right] \right] \dots\dots\dots (3.47)$$

where

- A = 7.4 for compressive load in branch member.
- A = 11.1 for tensile load in branch member.

The last term is taken as unity when f_o is a tensile stress.

Limitations

- $0.25 \leq \beta \leq 1.00$
- $8 \leq \frac{d_o}{t_o} \leq 66$
- $30^\circ \leq \theta \leq 90^\circ$

3.2.18. Harlicot, Tournay, Mouty Simplified Formulae ("Envelope Formulae")

3.2.18.1. T- and Y-Joints

$$P_u \leq 2.87 \cdot t_o \cdot d_1 \cdot f_{yo} \left[\frac{t_o}{d_o} \right]^\gamma \frac{1 + \sin \theta_1}{2 \sin \theta_2} \dots\dots\dots (3.48)$$

where

- $\gamma = 0.2$ for branch in compression.
- $\gamma = 0.5$ for branch in tension.

3.2.18.2. N- and K-Joints with Gaps

$$P_u \leq B \cdot t_o \cdot d_1 \cdot f_{yo} \left[\frac{t_o}{d_o} \right]^{0.5} \frac{1 + \sin \theta_1}{2 \sin \theta_2} \dots\dots\dots (3.49)$$

where

- B = 3.16 for compression load in chord.
- B = 5.85 for tension load in chord.

Simplifying assumptions that have been in order to produce these envelope formulae are:-

The connection bears no loads outside the joint.

Joint eccentricity is ignored provided that it is less than $d_o/8$.

The effect of d_1/d_o is ignored.

The term g/d_o is taken at it's smallest value i.e. 1.1 for $g/d_o = 0.6$.

The term which allows for chord preload is taken as the extreme values, 1 for tension and 0.54 for compression.

The limitations are as for the general formulae given previously (Pages 83 to 85).

3.2.18.3. X-Joints

No envelope formula has been produced as the general formula is relatively simple to use.

3.3. Summary of Existing Recommendations on T, K, Y and N-Joints

The general recommendations drawn from existing research work are:-

Joint strength increases with increasing diameter ratio.

Joint strength increases with decreasing diameter/thickness ratio in the chord.

Joint strength is generally not significantly affected by the thickness of the branch tube, however an effect is more likely in a joint with overlapping branches than one with separate branches.

The effect of axial load in the chord on the joint strength has been studied and the results and summarised overleaf:-

Author	Type of Joint	Effect of Axial Load in Chord	
		Tension	Compression
Toprac ¹¹	Cross	None shown	27% reduction for full chord utilization
Bouwkamp ¹³	K	None	None
Dutta ³⁵ (quotes Sammet)	Cross	None	None
Dutta ³⁵ (quotes Washio)	K or N	None	20% reduction for 60% chord utilization
Kurobane ¹⁸	K	Small load - 20% increase Large load - none	Large load - 10% reduction

Joint strength may be increased by bracing or sleeving¹¹.

3.3.1. T-Joint Recommendations

Diameter ratio should be in the range 0.25 - 0.75.

If the diameter ratio is less than 0.25 then the simple shear area method gives a good assessment of joint strength.

Loads must be primarily axial.

The diameter ratio optimises at a value of 0.5 for T-joints.

3.3.2. K- and N-Joint Recommendations

$$d_o/t_o > 30 + d_o/40$$

where

d_o = diameter of chord tube (ins).

t_o = thickness of chord tube (ins).

Positive joint eccentricity should be avoided.

Negative joint eccentricity should not exceed $0.25d_o$.

In order to ensure overlapping, the height of intersection H, due to overlap of diagonal members, should not be less than $0.65d_o$. Here d_o is the diameter of chord tube.

Diameter ratio of branch to chord tube should not be less than 0.4.

Thickness ratio of branch to chord tube should not be greater than 1.0.

Inclination of diagonal members should not be less than 30° to ensure proper joint welding.

Loads must be primarily axial.

Buckling stability should be checked if d_o/t_o is greater than $3300/f_y$ or β is greater than 0.25. Here:-

d_o = diameter of chord tube.

t_o = thickness of chord tube.

f_y = yield stress (kip/in²).

β = diameter ratio of branch and main chord.

K-joints should be treated as two separate Y-joints if:-

$$P_1 \sin \theta_1 \neq P_2 \sin \theta_2 \quad \text{or} \quad g > g_o$$

(See Figure 44 Page 78).

Total load component perpendicular to chord must not be greater than $[\tau_p \cdot t_o \cdot L_1 + 2 \cdot \tau_w \cdot t_w \cdot L_2]$

Interconnection of branch tubes in a welded K-joint increases the ability of the joint to transmit loads.

100% efficiency for K-joints may be obtained independently of the diameter ratio, by having a minimum value of chord Thickness/chord diameter ratio.

3.4. Calculation of Ultimate Loads, P_u , and the Ratios, P_u (exptl)/ P_u (calc) Using the Existing Design Formulae

This section gives the results for the ultimate loads calculated from the existing eighteen formula (see pages 37 & 38), also the application of these formulae has been straightforward, with the exception of Bouwkamp's method¹³ (K-joints) used in the Stelco design recommendation⁴. In the latter case no explicit formula exists and some simplification has been introduced when taking a joint efficiency value for given d_o/t_o and d_1/d_o ratios; for example, whenever d_o/t_o is greater than 33 (for negative eccentricity joints) the joint efficiency has been taken as 100%; for values of d_o/t_o equal to 100 and 50 the corresponding values of joint efficiency have been assumed equal to 70% and 80% respectively. The majority of the 206 K-joint tests considered have a d_o/t_o less than 33 and a joint efficiency of 100%, and the theoretical joint strength according to Bouwkamp's method is then equal to the strength of the tension branch member.

The complete test data, showing specimen dimensions, yield stress and experimental failure loads is given in Table 1 (page 1A to 4A), and a summary is given in Table 1A (page 103). All the considered tests have been carried out on T- and K-joints.

The values of failure loads, P_u , calculated for all 245 tests from the existing formulae, taking account of the recommended parameter ranges (see Table 1B, page 104) are given in Appendix A.

The values of failure loads, P_u , calculated for all 245 tests from the existing formulae, regardless of the recommended parameter range, are given in Appendix A.

The corresponding values of the ratios of experimental to calculated failure loads, using the existing formulae, are given in Appendix A. These tables show, in detail, the degree of agreement between the experimental and calculated failure loads for each group of tests, for each of the existing formulae. The values of means and standard deviations of these ratios are given in Tables 3 to 10 respectively (page 105 to 112).

Histograms are given in Figures 45 to 48, based on means of P_u ratios in Tables 3-6, calculated for those tests for which the selected existing formulae are recommended.

3.5. Discussion of the Results Obtained for Each Existing Formula

3.5.1. Shear Area (Tables 1 - 10)

The use of this very basic formula gave some of the better results for T- and K-joints in the present investigation.

The values of means and standard deviations of the ratio P_u (experimental) to P_u (calculated) are given in Table 3. Histograms, based on these P_u ratios, are given in Figure 45. No limitations in parameter ranges are considered.

For T-joint tests, only 2 out of 39 tests had a P_u ratio less than 0.85 (see Table 2), the mean value for all T- tests being 1.08. Table 2 and the histogram in Figure 45 indicate that safe results using this formula may be obtained if a safety factor of between 25% and 50% is introduced.

For K-joint tests, better results were obtained for Kurobane's and Bouwkamp's tests, (Test Nos. 38-225, Tables 2 & 5), than for the Delft tests (Test Nos. 226-243).

It is interesting to note that the formula gave better results for Kurobane's K-joint tests than the Author's own proposed formula.

Originally this method was used for design of T-joints only, having low d_1/d_o ratios. Stelco⁴, for example, recommends the value d_1/d_o less than or equal to 0.2. The results of the present investigation appear to justify the use of this formula for d_1/d_o ratios between 0.2 and 1.0.

It appears that the use of the shear area formula for K-joints under estimates the strength of overlapped (negative eccentricity) joints and over estimates the strength of gap joints (positive eccentricity), (see Tables 2 & 5, Test Nos. 38 - 243).

3.5.2. Column Analogy²³ (Tables 1 - 10)

The method gave very conservative results, with high values of P_u ratios and corresponding standard deviations (Tables 3 & 5). This may be due to the way in which the influence of d_1/d_o and r_o/t_o are introduced in the formula.

It has been found to be unsuitable in the present investigation both for T- and K-joints.

3.5.3. Roark 1²⁴ (Tables 1 - 10)

The method is not applicable to any of the existing tests. However, if used outside the recommended parameter range it gave bad results for all the tests (Table 7). This may be because the formulae were originally derived from thin shell theory.

3.5.4. Roark 2²⁵ (Tables 1 - 10)

The method gave bad results. It is applicable when $d_o/t_o > 40$ and θ , the angle of intersection of branch and chord, is equal to 90° , a requirement suited to thin shell conditions. No advantage was gained from these limitations, their main effect being, to drastically reduce the range of application of the formulae.

3.5.5. Kellogg²⁶ (Tables 1 - 10)

As the original authors predicted, the method is very conservative for all the test results. Standard deviations for all tests were in the range 0.5 to 3.37 except for the Delft tests where it was 0.36. It, generally, gave better results for T-joint tests than for K-joint tests.

No restrictions are imposed on the use of this formula. In view of the unsatisfactory results obtained in this present investigation it's use would lead to very uneconomic designs.

3.5.6. Kurobane¹⁸ (Tables 1 - 10)

This method was proposed for K-joints only, and the formula appears to have been derived on the basis of the Author's 151 tests. Only small diameter tubes were considered, the d_1/d_o and d_o/t_o ratios varying between (0.36 - 0.8) and (15 - 24) respectively (see Table 1). The results were unsafe whenever negative eccentricity occurred in the Author's tests (small diameter tubes). For the larger diameter tubes (Bouwkamp's tests), the results were unsafe for positive and negative eccentricities, as shown below:-

TEST	POSITIVE GAP		NEGATIVE GAP	
	Ave.	Std. Dev.	Ave.	Std. Dev.
Kurobane (38 - 191)	1.15	0.29	0.88	0.25
Bouwkamp (192 - 225)	0.93	0.41	0.96	0.49

It is interesting to note that the 'best fit' line in the graph in Figure 26 appears to have been drawn for only a limited number of tests and not for all the 151 tests.

3.5.7. Naka, Kato & Kanatani¹⁶ (Tables 1 - 10)

This method gave very good results for T-joints, the calculated Pu ratios being always greater than one (Tables 2 and 3). This applied even to the tests outside the recommended range of do/to ratios (see Table 7). Furthermore, the standard deviations are reasonably low when related to the mean values of Pu ratios.

The use of the modified formula for analysing K-joints has led to little success when dealing with small diameter tubes (Kurobane's Tests), and gave unsatisfactory results when applied to larger diameter tubes (Bouwkamp's Tests), (See Table 9).

3.5.8. Washio²⁰ (Tables 1 - 10)

The formula is applicable to K-joints with positive gaps only, for which it gave very satisfactory results.

More conservative results were obtained for smaller diameter K-joints (Kurobane's Tests, Table 5).

Very good results were obtained for the nine Delft K-joint tests.

The limitation of this formula to K-joints with positive gap only, imposes a severe restriction on its application in practice; most of the other joint parameters, however, are taken into consideration.

3.5.9. Reber's Formula⁷ (Tables 1 - 10)

The values of means and standard deviations of Pu (exptl)/Pu (calc) obtained using Reber's formula were found to be conservative (T-joints) or unsafe (K-joints), (See Tables 3 & 5).

The results were found to be more satisfactory in the case of T-joint tests carried out by Naka, Kato and Kanatani¹⁶.

3.5.10. Toprac¹¹ (Tables 1 - 10)

The method gave very conservative results with large standard deviations (Tables 4 & 6).

3.5.11. Kato¹⁵ (Tables 1 - 10)

The method gave very unsatisfactory results, as seen in Tables 4 and 6.

3.5.12. American Petroleum Industry Formula (A.P.I.)²⁷ (Tables 1 - 10)

Comments made for Toprac's formula apply equally here.

3.5.13. American Welding Society Formula²⁸ (Tables 1 - 10)

The use of this formula gave reasonably good results for T-joints with do/to ratios less than 25; and conservative results for do/to ratios larger than 25. In the case of K-joints the results were only satisfactory for small diameter tubes.

The method is based on the shear area formula, in which a modified punching shear stress based on the do/to ratios is used: this is the reason for the lower calculated Pu loads for higher values of the ratio do/to.

3.5.14. Bouwkamp's Formula⁴ (Tables 1 - 10)

The design procedure was originally proposed for K-joints only. It is, therefore, not used for T-joints in the present investigation.

In the case of K-joints the following observations can be made:-

For specimens with smaller diameter tubes (Kurobane's and Delft tests) the use of the formula gave unsafe results, as seen in Table 6 and Figure 47).

For specimens with larger diameter tubes (Bouwkamp's tests) the use of the formula gave much better results.

It is seen from Figures 40 & 41 that the efficiency of the joint is independent of the d_1/d_o ratio when d_o/t_o is smaller than 20 (zero eccentricity) or 33 (negative eccentricity). The higher value of d_o/t_o for negative eccentricity joints is because overlapping increases the strength of a joint.

While the efficiency of the joint depends, generally, on d_o/t_o and d_1/d_o ratios, the strength of the joint depends on the strength of the branch tube in tension. This may seem to be a weakness of the method; it does appear, however, that for small d_o/t_o ratios the strength of the joint is governed by the strength of the tensile branch member.

3.5.15. Det Norske Veritas²⁹ (Tables 1 - 10)

This design method is valid for the range of recommended parameters given in Table 1B, page 104.

The use of the proposed formula for T-joints gave conservative results; the values of the P_u ratio were greater than 1.25 for all 24 tests considered.

The use of the proposed formula for K-joints with positive and negative gaps, gave very good results for small diameter tubes (Kurobane's tests, Table 6).

For larger diameter K-joints (Bouwkamp's tests) the results were conservative.

3.5.16. Visser³⁰ (Tables 1 - 10)

The method gave unsafe results for the whole range of existing T- and K-joint tests (Tables 4 & 6). This may be due to the way in which the formula was derived, the only parameter considered being the chord wall thickness. It was also expected that any attempt to apply the stress concentration factor

approach to joint design formulae would not be successful, since there is no evidence of a relationship between S.C.F. and P_u . Redistribution of stress after initial yield in the joint will preclude any possible relationship.

3.5.17. Harlicot, Mouty, Tournay³¹ (Tables 1 - 10) General Formula

3.5.17.1. T- and Y-Joints

It can be seen in Figure 45 that the accuracy of the proposed formula was not as good as some of the other formulae considered. Two points, however, are of significant interest:-

1. The formula is of the same general form as the N- and K-joint formula of Washio; therefore, it is more suitable to use in practice where engineers are happier with a form of equation they commonly recognise.
- ii. The formula has a higher average ratio of ultimate calculated load to ultimate experimental load and corresponding standard deviation than some of the other formulae but none of the individual ratios is less than one. Considering the relatively small number (37) of test results available, this last fact may be important when considering this formula as a proposed design method.

3.5.17.2. K- and N-Joints

The aim of the French appears to have been to modify the Washio, Togo formula, in order to simplify its use and to show the relationship to the Det Norske Veritas formula. This has, apparently, been done successfully by an in-depth analysis of all the parameter terms involved. However, the modification of the gap function has had an error introduced. This is because some of the experimental data on Kurobane's original graph, which is used for this exercise (Figure 49), has been plotted in the wrong position. The continuous gap function introduced by the

French is, therefore, given an incorrect accuracy, and in fact the original discontinuous function (page 56) is much more correct, although marginally more complicated to use.

Although the average and standard deviation values for the ratio of calculated load to experimental load have been reduced when compared to the Washio, Togo formula, a more reliable and accurate design formula may be achieved by factoring the Washio, Togo formula by a factor of 2.0. This, for example, when comparing the two formula for Kurobane's test results gives:-

FORMULA	AVERAGE $\frac{P_u \text{ (calc)}}{P_u \text{ (exptl)}}$	Std. Deviation
French general	1.10	0.36
Washio, Togo (factored by 2.0)	1.125	0.35

In terms of absolute values the French formula has more than 50% of individual ratio values less than 1, whereas, the factored Washio, Togo formula has less than 30% of individual ratios values less than 1.0.

3.5.18. Harlicot, Mouty, Tournay³¹ (Tables 1 - 10) Envelope Formulae

T-, Y-, K- and N-Joints

The results of T-, Y-, K-, and N-joints using the "envelope" formulae have been found to be very conservative. In view of the greater accuracy obtained using other formulae including the French General Formula it is not considered necessary to use these envelope formulae for joint design.

3.6. Recently Available Experimental and Theoretical Data

Additional test results have recently been published for T, K and X-joint tests^{101,102}, also there have been further proposals for design formulae^{101,102}.

Summarising, these formulae are:-

3.6.1. Pan, Plummer

T or Y-Joint with Axial Load in Branch Member

$$P_u = K.f_{yo}.t_o^2 \left[\frac{d_o}{t_o} \right]^{\frac{1}{2}} \frac{d_1}{d_o} / \sin \theta \quad 0.19 \leq \frac{d_1}{d_o} \leq 0 \quad \dots\dots\dots(3.50)$$

$$30^\circ \leq \theta \leq 30^\circ$$

where

K = 3.1 for compressive axial load in branch.

K = 11.5 for tensile axial load in branch.

Cross (X) Joint with Axial Load in Branch Members

$$P_u = K.f_{yo}.t_o^2 \left[\frac{d_1}{d_o} \right]^{0.64} / \sin \theta \quad 30 \leq \theta \leq 90^\circ \quad \dots\dots\dots(3.51)$$

where

K = 16.31 for compressive axial load and $0.19 \leq \frac{d_1}{d_o} \leq 0.8$.

K = 30 for compressive axial load and $0.8 \leq \frac{d_1}{d_o} \leq 1.0$.

K = 22.75 for tensile axial load and $0.19 \leq \frac{d_1}{d_o} \leq 0.8$.

The formula becomes:-

$$P_u = 41.5 f_{yo}.t_o^2 \left[\frac{d_1}{d_o} \right]^{3.42} / \sin \theta \quad \dots\dots\dots(3.52)$$

for tensile axial load and $0.8 \leq \frac{d_1}{d_o} \leq 1.0$.

Equations 3.50, 3.51 and 3.52 have been found by "correlation" using data from 346 joint tests. No numerical statistical data is given for the degree of correlation achieved but graphs appear to show good correlation between the proposed formula and those of API, Det Norske Veritas and Washio, Togo.

3.6.2. Kurobane, Makino, Mitsui

Cross Joint

$$P_u = \left[\frac{6.57}{1 - 0.81 \left[\frac{d_1}{d_o} \right]} \right] f_{yo}.t_o^2 \dots\dots\dots(3.53)$$

T-Joint

$$P_u = 6.43 \left[1 + 4.6 \left[\frac{d_1}{d_o} \right]^2 \right] f_{yo}.t_o^2 \dots\dots\dots(3.54)$$

T, Y and K-Joint

$$P_u = 7.14 \left[1 + 3.79 \left[\frac{d_1}{d_o} \right]^2 \right] \left[\left(1 + \frac{2}{\pi} \tan^{-1} \left(0.4 - 0.2 \frac{g}{t_o} \right) \right) \right. \\ \left. \left[1 + 0.0392 \cos \theta - 0.187 \cos^2 \theta \right] (1 + 0.254 n - 0.339 n^2) \right] f_{yo}.t_o^2/\sin \theta \dots\dots\dots(3.55)$$

where

$$n = F_o/f_{yo}.A_o$$

A regression method has been used to derive equations 3.53, 3.54 and 3.55. Test results used in the analysis are the same as those presented by Pan and Plummer, but with some inexplicable variation in ultimate loads, due, possibly, to rounding errors in conversion to SI units.

The criterion for the mathematical model was that it should give the best explanation of variation of ultimate strength data for the minimum number of independent variables. (This criterion may be automatically included in regression analysis by using the stepwise regression method, see Chapter 8).

3.6.3. Ultimate Strength of X-Joints

X-joints were not previously considered for critical review because:-

- 1. the only existing formula was then given by Det Norske Veritas,
- ii. very few X-joint test results had been published. Recent developments have, however, made consideration of these joints available.

Formulae now available for calculation of ultimate strengths of X-joints are:-

Tensile Load in Branch Members

- 1. Harlicot, Mouty, Tournay
$$P_u = 5.5 f_{y0} d_1 t_o / \beta (1.2 - \beta) (d_o / 2 t_o) \dots\dots\dots (3.56)$$
- 2. Pan, Plummer (See page 98)
Equation 3.51.

Compressive Load in Branch Members

- 1. Harlicot, Mouty, Tournay
$$P_u = 3.71 f_{y0} d_1 t_o / \beta (1.2 - \beta) (d_o / 2 t_o) \dots\dots\dots (3.57)$$
- 2. Det Norske Veritas
$$P_u = 1.18 f_{y0} d_1 t_o w / \beta (1.2 - \beta) (d_o / 2 t_o) \dots\dots\dots (3.58)$$
- 3. Pan, Plummer
Equation 3.51.
- 4. Kurobane
Equation 3.53.

FORMULA	TYPE OF JOINT	RATIO PU(EXPTL)/PU(CALC)			NO. OF TESTS
		MEAN	STANDARD DEVIATION		
Harlicot, Tournay, Mouty	X-tension	1.45	(0.31)	0.45	32
Pan, Plummer	X-tension	1.72	(0.34)	0.59	32
Harlicot, Tournay, Mouty	X-compression	0.94	(0.08)	0.077	27
Pan, Plummer	X-compression	0.96	(0.19)	0.19	27
Det Norske	X-compression	0.94	(0.08)	0.077	27
Kurobane	X-compression	0.92	(0.09)	0.086	27

Results of a Review of More Recent Joint Strength Formulae and Previously
Considered Formulae, Based on Recently Available Test Results

FORMULA	TYPE OF JOINT	RATIO PU(EXPTL)/PU(CALC)			NO. OF TESTS
		MEAN	STANDARD DEVIATION		
Pan, Plummer	T-joint	1.843	(0.21)	0.385	76
Harlicot, Tournay, Mouty	T-joint	1.25	(0.24)	0.294	76
N.K.K.	T-joint	0.99	(0.2)	0.198	76
A.W.S.	T-joint	1.07	(0.19)	0.207	76
Dutch Code	T-joint	1.38	(0.21)	0.308	76
Kurobane	T-joint	1.06	(0.21)	0.221	76
Harlicot, Tournay, Mouty	K-joint	0.857	(0.266)	0.228	346
Det Norske	K-joint	2.119	(0.49)	1.030	427
Washio, Togo	K-joint	1.006	(0.25)	0.257	322
Kurobane	K-joint	1.065	(0.41)	0.436	427
Dutch Code	K-joint	1.366	(0.27)	0.366	346
Shear Area	K-joint	1.133	(0.47)	0.534	427

The standard deviation given in brackets is for the mean ratio
adjusted to 1.00.

3.6.4. Discussion and Conclusion

X-Joints

i. In Tension

The formula proposed by Harlicot, Tournay and Mouty gave the best results: mean ratio of 1.45 with standard deviation of 0.45.

ii. In Compression

The formula proposed by Harlicot, Tournay and Mouty gave the best results: mean ratio of 0.94 with standard deviation of 0.077.

T-Joints

The formula proposed by Naka, Kato and Kanatani gave a marginally better result than the American Welding Society Formula, but was slightly unsafe with a mean ratio of 0.987 compared with 1.069: standard deviations of the ratio were 0.198 and 0.207 respectively.

K-Joints

The formula proposed by Washio, Togo gave the best result: Mean ratio of 1.006 with standard deviation of 0.26. This formula was applicable to all of the 427 tests.

RESEARCH BY	TEST NOS.	TYPE OF JOINT	CHORD DIA. (do) (mm)	BRANCH DIA. (d1) (mm)	d1/do	do/to	t1/to	YIELD STRESS (N/mm ²)
Toprac	1-7	T	218-406	71-142	0.22-0.64	25-62	0.4-1.04	228
Naka, Kato, Kanatani	8-28	T	114-140	34-140	0.24-1.00	21-47	0.35-1.00	255
Southern Methodist University	29-37	T	219-457	114.3	0.25-0.52	21-59	0.38-1.00	255
Kurobane	38-191	K	60	27-48	0.36-0.8	15-24	0.69-1.30	414
Bouwkamp	192-225	K	168-273	60-168	0.33-0.78	12-85	0.39-1.79	248-414
Delft	226-243	K	114, 114.8	48-114.8	0.42-1.00	20-29	1.0	455-469
Kingston Polytechnic	244, 245	T	114.3	48, 76	0.42, 0.67	21, 23	0.59, 0.80	350

Table 1A - Summary of Tests Analysed

TABLE 1B - RECOMMENDED RANGE OF PARAMETERS

Parameter Formula	d ₁ /d ₀	d ₀ /t ₀	θ ⁰	t ₁ /t ₀	Weld Gap
Shear Area ²²	<0.2				
Col. Analogy ²³	0.25 - 0.75				
Roark 1 ²⁴	<0.1	>40			
Roark 2 ²⁵		>40	90		
Kellogg ²⁶					
Kurobane ¹⁸			<90		
Naka, Kato, Kanatani ¹⁶	0.26 - 0.67	15 - 40	90		
Washio ²⁰					0 ≤ g/D ≤ 0.23 0.23 ≤ g/D ≤ 1.0
Reber ⁷	0.25 - 0.75				
Toprac ¹¹	0.25 - 0.75				
Kato ¹⁵	0.2 - 0.6	40 - 100			
A.P.I. ²⁷	0.25 - 0.75				
A.W.S. ²⁸	0.25 - 0.75				
Stelco ⁴ (Bouwkamp)			<90	<1	
Det Norske ²⁹	T	20 - 40			
	K	20 - 40	30 - 90		
Visser ³⁰					

TABLE 3 - RESULTS OF STATISTICAL ANALYSIS OF $P_{u, test} / P_{u, calc}$ RATIOS - T-JOINTS
USING RECOMMENDED PARAMETER RANGES OF FORMULAE

Test by Formula Proposed by	A.A. Toprac Univ. of Texas (Tests 1-7)		Naka, Kato, Kanatani Univ. of Tokyo (Tests 8-28)		Southern Methodist University (Tests 29-37)		Kingston Poly. (Tests 244, 245)		T-Tests	
	Ave.	Std. Dev.	Ave.	Std. Dev.	Ave.	Std. Dev.	Ave.	Std. Dev.	Ave.	Std. Dev.
Shear Area										
Col. Analogy	12.07 ⁷	3.051	5.70 ²¹	1.206	10.50 ⁹	1.88	5.85 ²	0.375	8.08 ⁵⁷	3.32
Roark 1										
Roark 2	2.79 ⁵	0.351			2.32 ⁴	0.481			2.59 ⁹	0.46
Kellogg	5.22 ⁷	0.847	3.75 ²¹	0.556	5.06 ⁹	0.748	3.75 ²	0.092	4.35 ³⁹	0.95
Kurobane										
Naka, Kato, Kanatani	1.73 ²	0.364	1.29 ²¹	0.171	1.97 ⁵	0.105	1.407 ²	0.028	1.45 ³⁰	0.32
Washio										
Reber	2.25 ⁴	0.165	1.53 ¹⁹	0.225	2.34 ⁹	0.380	1.57 ²	0.012	1.93 ²⁶	0.49

KEY TO TESTS

T-Joints, Tests 1-37, 244 & 245

Number of tests applicable shown in top right-hand corner with average ratio value for each case.

STANDARD DEVIATION calculated using the formula

$$s = \left[\frac{\sum (x_i - \bar{x})^2}{n - 1} \right]^{1/2}$$

where \bar{x} = mean value of ratio.

TABLE 4 - RESULTS OF STATISTICAL ANALYSIS OF Pu_{test}/Pu_{calc} RATIOS - T-JOINTS
USING RECOMMENDED PARAMETER RANGES OF FORMULAE

Test by Formula Proposed by	A.A.Toprac Univ. of Texas (Tests 1-7)		Naka,Kato,Kanetani Univ. of Tokyo (Tests 8-28)		Southern Methodist University (Tests 29-37)		Kingston Poly. (Tests 244, 245)		T-Tests	
	Ave.	Std.Dev.	Ave.	Std.Dev.	Ave.	Std.Dev.	Ave.	Std.Dev.	Ave.	Std.Dev.
Toprac	5.78	1.314	2.77	1.026	4.75	1.030	2.69	0.622	3.92	1.59
Kato	3.16	0.27			2.68	0.548			2.96	0.46
A.P.I.	4.75	0.345	3.01	0.489	4.68	0.710	3.14	0.290	3.86	1.01
A.W.S.	2.53	0.187	1.63	0.261	2.57	0.404	1.67	0.005	2.10	0.56
Stelco (Bouwkamp)										
Det Norske	2.61		1.79	0.235	2.64	0.180	1.89	0.033	2.02	0.44
Visser	0.26	0.307	0.520	0.352	0.600	0.473	0.39	0.108	0.49	0.39
Harlicot,Mouty Tournay, General	2.0	0.3	1.62	0.33	1.96	0.28	0.79	0.07	1.77	0.35
Harlicot,Mouty Tournay,Envelope	4.6	0.74	3.31	0.49	4.47	0.66	1.66	0.03	3.84	0.64

KEY TO TESTS

T-Joints, Tests 1-37, 244 & 245

Number of tests applicable shown in top right-hand corner with average ratio value for each case.

STANDARD DEVIATION calculated using the formula

$$s = \left[\frac{\sum (x_i - \bar{x})^2}{n - 1} \right]^{\frac{1}{2}}$$

where \bar{x} = mean value of ratio.

TABLE 5 - RESULTS OF STATISTICAL ANALYSIS OF P_{u_test}/P_{u_calc} RATIOS - K-JOINTS
USING RECOMMENDED PARAMETER RANGES OF FORMULAE

Test by Formula Proposed by	Kurobane Univ. of Kumamoto (Tests 38-191)		Bouwkamp Univ. of California (Tests 192-225)		Delft Calculated Gap (Tests 226-234)		Delft Measured Gap (Tests 235-243)		K-Tests	
	Ave.	Std.Dev.	Ave.	Std.Dev.	Ave.	Std.Dev.	Ave.	Std.Dev.	Ave.	Std.Dev.
Shear Area										
Col. Analogy	4.64	1.61	7.68	6.20	2.59	0.805			4.97	3.16
Roark 1										
Roark 2										
Kellogg	4.30	1.265	5.89	3.369	2.53	0.360			4.41	1.93
Kurobane	1.05	0.305	0.95	0.460	0.65	0.140	0.59	0.140	1.00	0.35
Naka, Kato Kanatani										
Washio	2.25	0.700	1.60	1.03	1.30	0.071	1.01	0.072	2.03	0.79
Reber	1.09	0.346	1.544	0.991	0.69	0.071			1.14	0.54

KEY TO TESTS

K-Joints, Tests 38-243

Number of tests applicable shown in top right-hand corner with average ratio value for each case.

STANDARD DEVIATION calculated using the formula

$$s = \left[\frac{\sum (x_i - \bar{x})^2}{n - 1} \right]^{1/2}$$

where \bar{x} = mean value of ratio.

TABLE 6 - RESULTS OF STATISTICAL ANALYSIS OF P_{u_test}/P_{u_calc} RATIOS - K-JOINTS
USING RECOMMENDED PARAMETER RANGES OF FORMULAE

Test by Formula Proposed by	Kurobane Univ. of Kumamoto (Tests 38-191)		Bouwkamp Univ. of California (Tests 192-225)		Delft Calculated Gap (Tests 226-234)		Delft Measured Gap (Tests 235-243)		K-Tests	
	Ave.	Std.Dev.	Ave.	Std.Dev.	Ave.	Std.Dev.	Ave.	Std.Dev.	Ave.	Std.Dev.
Toprac	3.14	1.176	3.86	3.368	1.40	0.390			3.16	1.79
Kato										
A.P.I.	2.40	0.799	3.49	2.368	1.55	0.15			2.53	1.28
A.W.S.	1.62	0.499	2.37	1.619	1.03	0.098			1.71	0.86
Stelco (Bouwkamp)	1.08	0.421	1.35	0.379	0.75	0.141			1.10	0.43
Det Norske	1.59	0.45	2.70	1.25	0.84	0.05	0.68	0.06	1.66	0.73
Visser	0.510	0.186	0.770	0.505	0.26	0.036			0.53	0.29
Harlicot,Mouty Tournay, General	1.10	0.36	1.06	0.63	0.72	0.1	0.67	0.11		
Harlicot,Mouty Tournay,Envelope	2.79	0.83	2.78	1.56	1.69	0.24	1.68	0.24		

KEY TO TESTS

K-Joints, Tests 38-243

Number of tests applicable shown in top right-hand corner with average ratio value for each case.

STANDARD DEVIATION calculated using the formula

$$s = \left[\frac{\sum (x_i - \bar{x})^2}{n - 1} \right]^{1/2}$$

where \bar{x} = mean value of ratio.

TABLE 7 - RESULTS OF STATISTICAL ANALYSIS OF P_{u_test}/F_{u_calc} RATIOS - T-JOINTS
 FORMULAE USED OUTSIDE RECOMMENDED PARAMETER RANGES

Test by Formula Proposed by	A.A.Toprac Univ.of Texas (Tests 1-7)		Naka,Kato,Kanatani Univ.of Tokyo (Tests 8-28)		Southern Methodist University (Tests 29-37)		Kingston Poly. (Tests 244, 245)		T-Tests (All tests are consid- ered in this table)	
	Ave.	Std.Dev.	Ave.	Std.Dev.	Ave.	Std.Dev.	Ave.	Std.Dev.	Ave.	Std.Dev.
Shear Area	1.08	0.168	1.04	0.109	1.18	0.295	1.13	0.028	1.06	0.18
Col.Analogy	12.07	3.051	5.70	1.206	10.50	1.882	5.85	0.375	8.08	3.32
Roark 1	0.47	0.293	1.04	0.763	0.32	0.253	0.88	0.521	0.76	0.68
Roark 2	2.56	0.805	1.37	0.507	2.07	0.445	1.26	0.277	1.77	0.73
Kellogs	5.22	0.847	3.75	0.556	5.06	0.748	3.75	0.092	4.35	0.95
Kurobane										
Naka, Kato, Kanatani	1.88	0.269	1.29	0.170	1.85	0.265	1.40	0.028	1.55	0.36
Washio										
Reber	2.48	0.54	1.58	0.240	2.34	0.380	1.57	0.012	1.92	0.53

KEY TO TESTS

T-Joints, Tests 1-37, 244 & 245

Number of tests applicable shown in top right-hand corner with average ratio value for each case.

STANDARD DEVIATION calculated using the formula

$$s = \left[\frac{\sum (x_1 - \bar{x})^2}{n - 1} \right]^{\frac{1}{2}}$$

where \bar{x} = mean value of ratio.

TABLE 8 - RESULTS OF STATISTICAL ANALYSIS OF Pu_{test}/Pu_{calc} RATIOS - T-JOINTS
 FORMULAE ARE USED OUTSIDE RECOMMENDED PARAMETER RANGES

Test by Formula Proposed by	A.A. Toprac Univ. of Texas (Tests 1-7)		Naka, Kato, Kanatani Univ. of Tokyo (Tests 8-28)		Southern Methodist University (Tests 29-37)		Kingston Poly. (Tests 244, 245)		T-Tests (All tests are consid- ered in this table)	
	Ave.	Std. Dev.	Ave.	Std. Dev.	Ave.	Std. Dev.	Ave.	Std. Dev.	Ave.	Std. Dev.
Toprac	4.92	1.638	2.42	0.966	4.75	1.030	5.85	0.375	3.46	1.63
Kato	2.92	0.718	1.60	0.409	2.60	0.393	1.71	0.139	2.10	0.74
A.P.I.	5.10	1.044	2.83	0.586	4.68	0.710	3.14	0.029	3.71	1.25
A.W.S.	2.76	0.561	1.67	0.262	2.57	0.404	1.67	0.005	2.10	0.61
Stelco (Bouwkamp)										
Det Norske	2.62	0.440	1.86	0.274	2.51	0.371	1.90	0.033	1.60	0.70
Visser	0.26	0.307	0.52	0.352	0.60	0.473	0.39	0.108	0.53	0.29

KEY TO TESTS

T-Joints, Tests 1-37, 244 & 245

Number of tests applicable shown in top right-hand corner with average ratio value for each case.

STANDARD DEVIATION calculated using the formula

$$s = \left[\frac{\sum (x_i - \bar{x})^2}{n - 1} \right]^{1/2}$$

where \bar{x} = mean value of ratio.

TABLE 9 - RESULTS OF STATISTICAL ANALYSIS OF $P_{u_{test}}/P_{u_{calc}}$ RATIOS - K-JOINTS
 FORMULAE ARE USED OUTSIDE RECOMMENDED PARAMETER RANGES

Test by Formula Proposed by	Kurobana Univ. of Kumamoto (Tests 38-191)		Bowkemp Univ. of California (Tests 192-225)		Delft Calculated Gap Tests 226-234)		Delft Measured Gap (Tests 235-243)		K-Tests (All tests are consi- dered in this table)	
	Ave.	Std.Dev.	Ave.	Std.Dev.	Ave.	Std.Dev.	Ave.	Std.Dev.	Ave.	Std.Dev.
Shear Area	1.24	0.344	1.49	0.599	0.72	0.114			1.24	0.43
Col. Analogy	4.64	1.615	7.68	6.201	2.59	0.805			4.97	3.16
Roark 1	2.22	0.789	0.87	0.773	0.78	0.330			1.88	0.96
Roark 2	1.62	0.540	2.85	2.615	0.86	0.238			1.77	1.27
Kellogg	4.30	1.265	5.89	3.369	2.53	0.360			4.41	1.93
Kurobana	1.05	0.305	0.95	0.46	0.65	0.14	0.59	0.14	1.00	0.35
Naka, Kato, Kanatani	1.15	0.343	1.55	0.890	0.62	0.165			1.17	0.52
Washio	4.27	6.947	1.66	0.899	1.30	0.107	1.013	0.072	3.56	6.12
Reber	1.08	0.337	1.55	0.962	0.63	0.110			1.12	0.54

KEY TO TESTS

K-Joints, Tests 38-243

Number of tests applicable shown in top right-hand corner with average ratio value for each case.

STANDARD DEVIATION calculated using the formula

$$s = \left[\frac{\sum (x_1 - \bar{x})^2}{n - 1} \right]^{1/2}$$

where \bar{x} = mean value of ratio.

TABLE 10 - RESULTS OF STATISTICAL ANALYSIS OF Pu_{test}/Pu_{calc} RATIOS - K-JOINTS
 FORMULAE ARE USED OUTSIDE RECOMMENDED PARAMETERS

Test by Formula Proposed by	Kurobane Univ. of Kumamoto (Tests 38-191)		Bouwkamp Univ. of California (Tests 192-225)		Delft Calculated Gap (Tests 226-234)		Delft Measured Gap (Tests 235-243)		K-Tests (All tests are consid- ered in this table)	
	Ave.	Std.Dev.	Ave.	Std.Dev.	Ave.	Std.Dev.	Ave.	Std.Dev.	Ave.	Std.Dev.
Toprac	3.05	1.207	3.77	3.284	1.09	0.554			3.00	1.81
Kato	1.50	0.482	2.33	1.826	0.76	0.263			1.58	0.93
A.P.I.	2.37	0.783	3.48	2.999	1.25	0.472			2.46	1.28
A.W.S.	1.61	0.487	2.37	1.569	0.93	0.175			1.68	0.84
Stelco (Bouwkamp)	1.08	0.421	1.35	0.379	0.75	0.141			1.10	0.43
Det Norske	1.51	0.47	1.98	1.27	0.80	0.080	0.66	0.06	1.52	0.47
Visser	0.51	0.186	0.77	0.505	0.26	0.036			0.53	0.29

KEY TO TESTS

K-Joints, Tests 38-243

Number of tests applicable shown in top right-hand corner with average ratio value for each case.

STANDARD DEVIATION calculated using the formula

$$s = \left[\frac{\sum (x_j - \bar{x})^2}{n - 1} \right]^{1/2}$$

where \bar{x} = mean value of ratio.

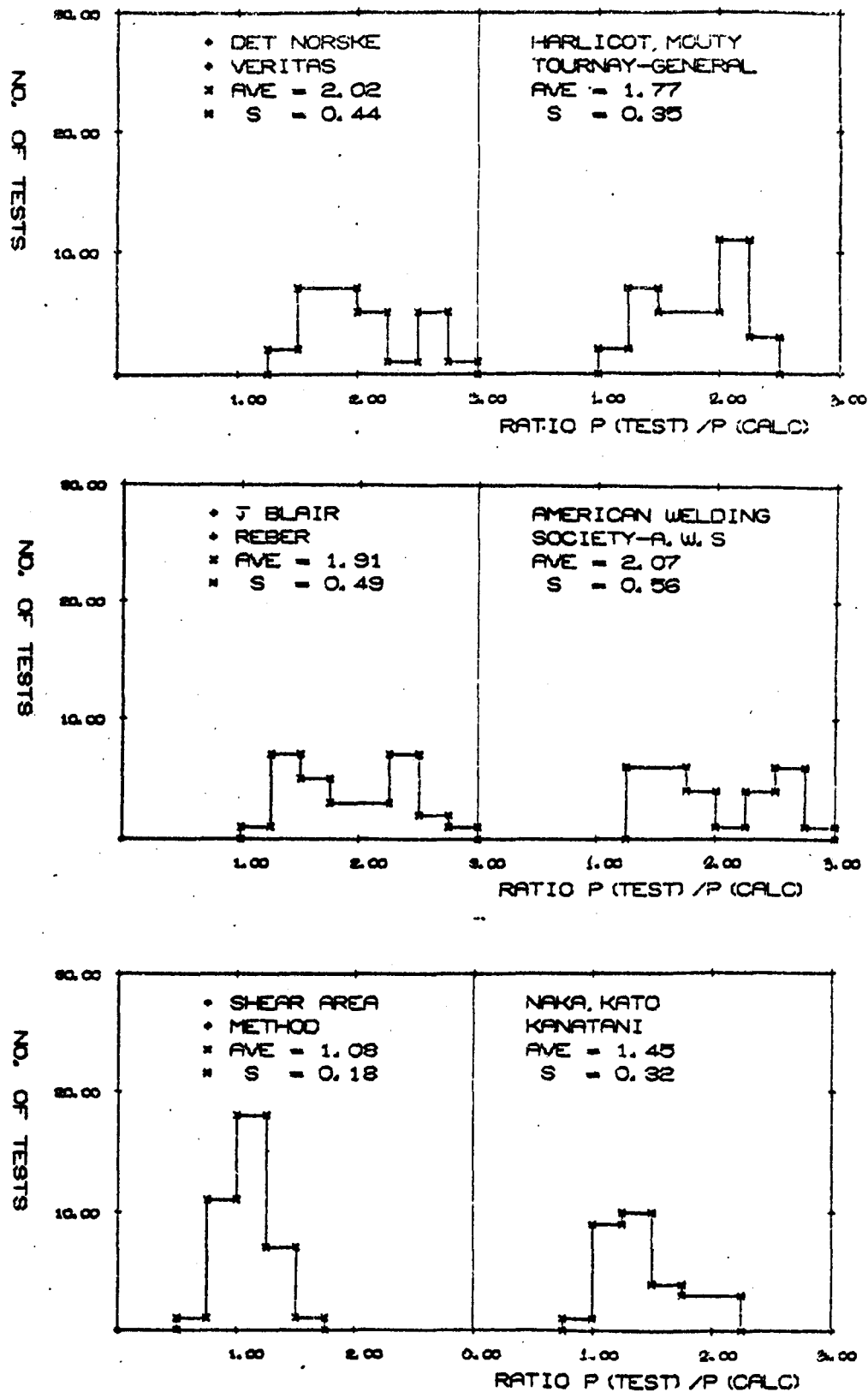


Figure 45. Histograms for T-joint tests

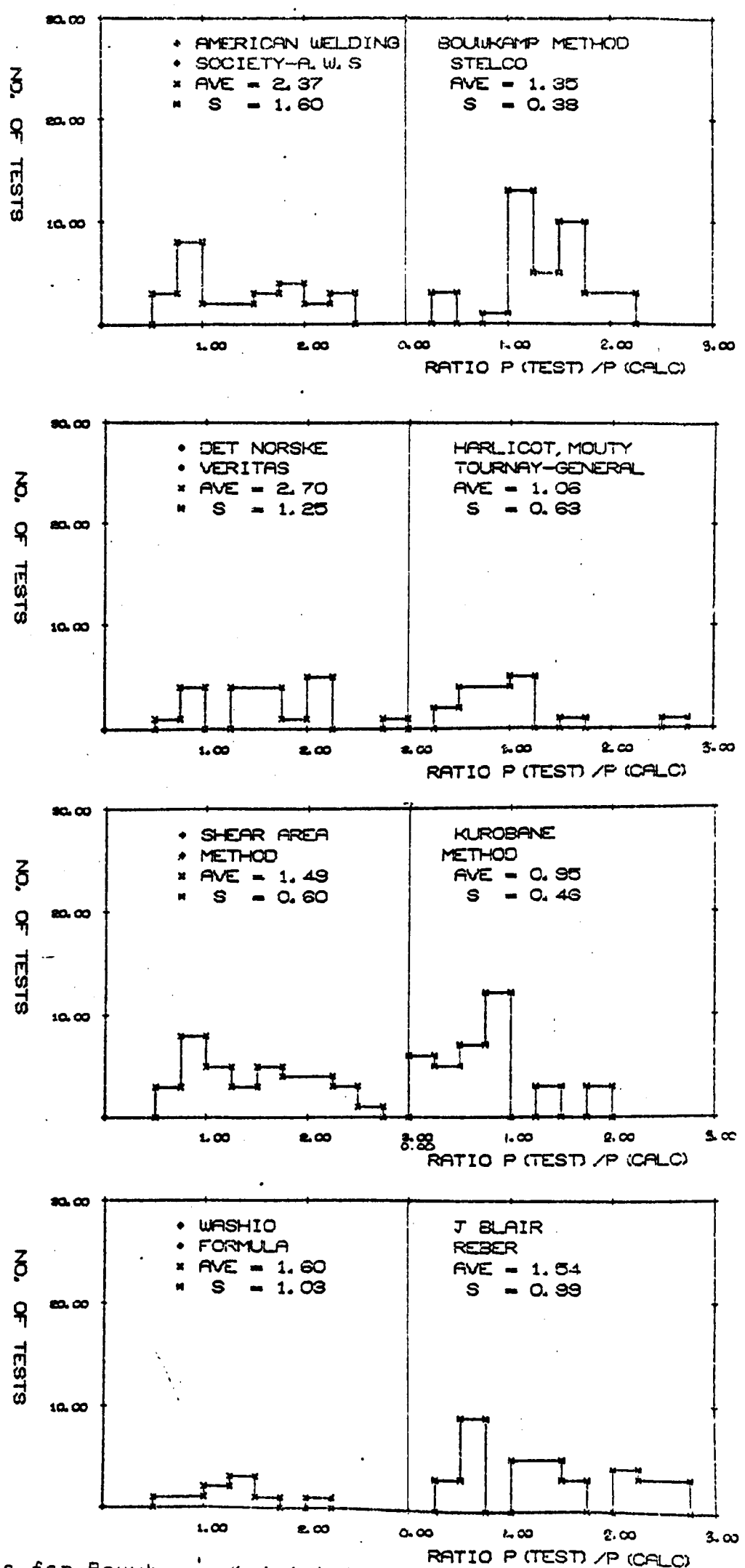


Figure 46. Histograms for Bouwkamp's K-joint tests

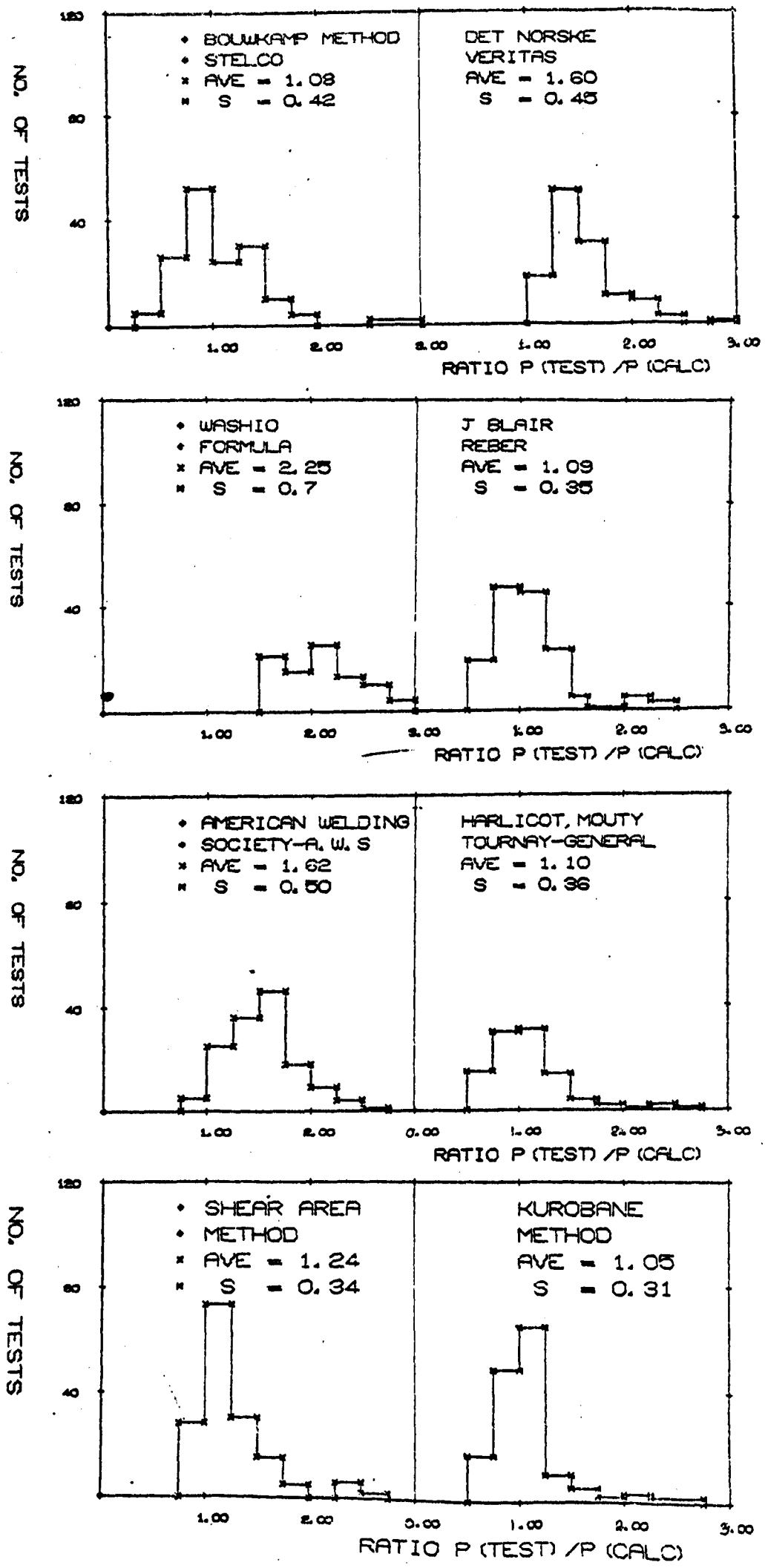


Figure 47. Histograms for Kurobane's K-joint tests

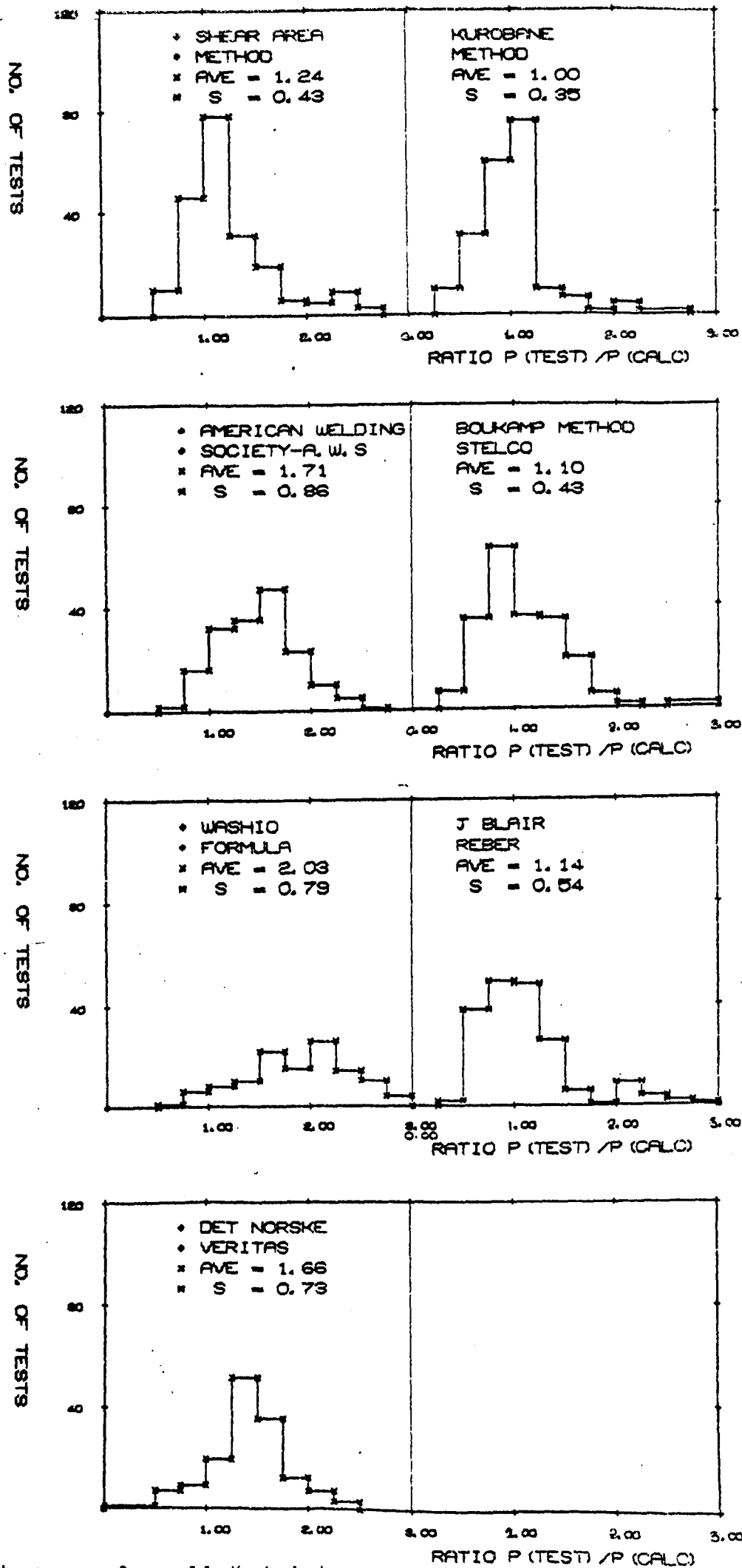


Figure 48. Histograms for all K-joint tests



CHAPTER 4

FINITE ELEMENT METHOD USED IN THE PRESENT INVESTIGATION FOR ANALYSING T-JOINTS*

4.1. Finite Element Computer System

4.1.1. General

The finite element displacement method is an analytical technique that can provide the solution to a wide range of structural and continuous problems. The basic theory is general and has been well established, and matrix notation is convenient for the implementation of the method of digital computing machines. A virtue of the finite element method is the similarity of computer code required for various types of problems; thus a method can form the basis for the development of large general purpose structural analysis systems. The system used for the analysis of the T-joint considered in this present investigation is the LUSAS** system. This has been developed at Imperial College in London by Dr. P. Lyons³⁶. The system has been developed for the linear static analysis of one, two and three-dimensional structures and contains a comprehensive range of elements which permit a wide range of modelling capabilities. The modularity of LUSAS has permitted new facilities to be added easily and quickly.

In addition to the usual facilities provided in finite element computer systems the LUSAS system incorporates some special facilities some of which are described below.

4.1.2. Machine Independence and Requirements

Most of the system has been written in ANSI[†] fortran, which is acceptable to the majority of alternative computer installations. The system requires a minimum central memory equivalent to 25k of 60 bit words, within which a wide range of problems can be solved.

* See Section 4.7. page 164 for notation.

**London University Structural Analysis System.

† American National Standards Institute.

4.1.3. Modular Internal Data Structure and Dynamic Vector Array

The internal data is organised in a modular way by the use of a single dynamic vector array which is divided into a string of data records. The lengths of the data records are determined automatically during execution according to the individual problem requirements, and the positions of the first and last location of each record are recorded in a pointer table. This technique ensures an economical use of the available central memory and enables control information and numerical data to be transferred from one module of subroutines to another using a simple common statement containing the single dynamic vector array. This dynamic array also simplifies the re-start facility, since a simple transfer statement can be used to save the whole core image on secondary storage at any stage in the computation. Also, user control of the array size minimises the amount of central memory required.

4.1.4. Modular Computer System Structure

The system is organised in a modular way by grouping subroutines into overlay modules each of which performs a logically well defined function. The system consists of several of these overlay modules which are stored in a library on permanent disc file and brought in turn into the computer central memory. This overlay procedure allows consecutive modules to occupy the same area of central memory and so reduces the total central memory requirements.

4.1.5. Independent User Options

The user has control over the internal computations of the computer system by the use of several options. For example the type of data processing, amount of data processing, solution order, and type of output can be controlled by the user.

The system is also flexible enough to permit the assimilation of a user's external subroutine into the main program. For example it may be required to introduce a subroutine which permits additional arithmetic to be performed on post solution data.

4.1.6. The Computer System

The computer system is divided into nine primary overlay modules, one of which is optional. Each overlay module, which consists of a group of subroutines that carry out a well defined task, is called, in turn, into the central memory by a simple main program, which remains in core throughout problem execution and contains the single dynamic vector array. The length of the dynamic vector array is determined by two statements in the main program, and is easily adjusted by the user to suit each particular problem. The first four overlays process the data input, the fifth computes the segment lengths of the dynamic vector array required for the problem, the sixth retrieves data and computes the characteristic matrices for each element, the seventh assembles the structure stiffness method and solves the displacements for each load case by the frontal technique³⁷, and the eighth uses these displacements to compute and output the stresses for each element, and the displacements and reactions for the structure. The ninth overlay module is optional and can be supplied by the user to post-process the results according to his or her particular requirements. The sixth overlay module is served by a subset of thirteen secondary overlay modules each of which contains a family of finite element subroutines for each particular structure type.

Simplified flow charts for the overall system and for the primary and secondary overlay modules of LUSAS are given in Figures 50 & 51 and the subdivisions of the dynamic vector during each phase of analysis are shown in Figures 52 to 56.

4.1.7. Data Processors

The data input for LUSAS has been designed to be compact, self-explanatory and in a free format field. A free format subroutine and a data generation subroutine are kept in the central memory during the data processing phase. Thus, the alphanumeric characters in each column of a card are read and assembled into complete numbers or words, allowing flexibility in the mixing of numbers and words in input record formats. Data is input in the normal manner i.e.

Element connectivities (node numbering)
Node co-ordinates
Material properties
Boundary restraints
Loadcases

but with some additional advantages.

Incremental generation is available for use with all data input records³⁸.

Gaps may be left in the numbering of nodes without affecting the requirements of the central memory.

The node numbers of any element can be overwritten by the node numbers of any new element, even if the number of nodes is different.

All data input records can be overwritten by the inclusion of updated information, except in the case of load data where additional load at a node already specified as being loaded, is added to the load previously imposed.

The solution of the structure load deflection equations in LUSAS is carried out by random access frontal solution technique. This solution technique, as with many others, requires that the equations are reduced in certain order to keep the front width (akin to band width), and therefore the total number of arithmetic operations, to a minimum. For the frontal solution this is governed by the order in which the elements are presented. In LUSAS the ordering of elements may be controlled by the user according to any one of the following procedures:-

Solution Order Ascending

This procedure is used when the element numbering is across the narrow direction of the structure and, therefore, in optimum condition.

Solution Order Presented

This procedure is adopted when it is convenient to carry out a solution in the order in which elements are presented or generated.

Solution Order $i, i + k, i + 2k, i + 3k \dots j$

This procedure enables a manual user specification for the order of elemental solution, where i and j are positive integer element numbers, and k is a positive or negative integer, as i, j, k .

As a special case, the series may only consist of i .

4.1.8. Finite Element Library

Finite element types implemented in the LUSAS system include joint elements, spar and beam elements, extensional elements, flexural elements, axi-symmetric elements, extensional-flexural plate elements, doubly curved thin shell elements, doubly curved thick shell elements, and solid three-dimensional elements. The characteristic matrices of nearly all of the standard elements incorporated in the computer system are computed using numerical integration. A detailed description of most of the elements can be found in the text by Zienkiewicz³⁹.

LUSAS also contains several elements (ISOFLEX and ISOBEAM) that have been specially developed for use in the analysis of plates in flexure, and cellular structures. The element selected for the present linear analysis of T-joints was called QSL8 a semi-loof, doubly curved quadrilateral thin shell element (See Section 4.6.2. page 158).

4.1.9. Pre-Solution Processor

The pre-solution processor retrieves data stored in the dynamic vector array and assembles each of the individual element records in turn. Each element record includes arrays of the element node numbers, number of variables at each node, node destinations, support node destinations, node appearance codes, node coordinates,

elastic properties, thermal properties, support values, support codes whether free, restrained or spring, constant body forces, body force potentials, nodal initial stresses and strains, node numbers for each variable, equation numbers, front destinations and variable appearance codes, see Figure 52. This data is then transferred to the appropriate secondary element overlay module where the element stress matrices are computed and written onto tape, the stiffness matrix is computed, and the element load vector due to constant body forces and body force potentials is calculated. Control is then returned to the primary overlay module where the stiffness matrix and element load vectors are modified in accordance with the support conditions. The concentrated loads for nodes making their last appearance are added into the element load vector, and the second element record which contains the solution data, including the element load vector, is transferred to tape followed by the element stiffness matrix.

4.1.10. Random Access Front Processor

The computational procedure of the finite element displacement method requires the solution of the matrix equation:-

$$K\delta = P \dots\dots\dots(4.1)$$

where K is the coefficient or structure stiffness matrix, δ is the vector of unknown displacements, and P is the vector of applied loads. This matrix equation constitutes a set of, perhaps, several thousand simultaneous equations, the coefficient matrix of which is symmetrical, positive-definite and banded about the diagonal. Theoretically the various direct solution algorithms that have been developed to date are similar, but their computer implementation differs significantly. Thus, the principle scientific discipline involved is that of system engineering, and it is in this area that considerable research has been carried out in the quest for efficient equation solvers^{43,44,45,46}.

The algorithm which solves a set of linear algebraic equations with the minimum of arithmetic operations is Gaussian elimination, or one of its closely associated techniques. For symmetric positive-definite equations, Gaussian elimination is guaranteed to be numerically stable irrespective of the order in which the equations are eliminated, and with floating point arithmetic a pivotal search is unnecessary.

Virtually all structure stiffness matrices, as found in the finite element method, are not only banded about the diagonal but exhibit areas of sparsity within this band. The fundamental requirement for the efficient solution of these structure equations is to avoid superfluous arithmetic operations on the zeros. Basically, there are two ways of handling sparsity:-

- i. In the data structure by excluding all zero coefficients from storage.
- ii. In the computations by excluding all operations on zero coefficients.

Each approach has its advantages, but it is not clear which is to be preferred in general.

An elegant solution procedure for avoiding the zero coefficients within the band of a structure stiffness matrix is frontal technique, as developed by Irons³⁷ and Bamford⁴⁷. The computer algorithm is based on Gaussian elimination and takes advantage of both the symmetry and sparsity found in structural stiffness matrices. Large variations of local band width are handled in a compact area of central memory, and numerical operations on zeros are essentially avoided. Consequently, the method is particularly efficient for finite elements with side nodes, or for bifurcated structures, when re-entrant sparseness occurs. The solution proceeds according to the ordering of the elements for which there is an optimum, and the node numbering is irrelevant. In general, element ordering is more natural and straightforward to use than node ordering, especially when a computer system is enhanced with

a reordering option. For these reasons, the frontal technique has been incorporated into the general finite element computer system described here, together with a user specified solution order facility. Irons³⁷ has presented a detailed description and Fortran listing of the frontal technique and it is from this that the present solution routine has been developed.

The principle of the frontal solution is indicated by the Gaussian algorithm itself. The elimination of δ_r for row r of a system of equations leads to a modification of the coefficients in the remaining rows according to:-

$$K_{ij}^* = K_{ij} - \frac{K_{ir}K_{rj}}{K_{rr}} \dots\dots\dots(4.2)$$

$$P_i^* = P_i - \frac{K_{ir}P_r}{K_{rr}} \dots\dots\dots(4.3)$$

where the modifications are only for non-zero admissible pairs i, j . The elimination reduces the matrix K to an upper triangular matrix. The terms K_{ij} for the overall stiffness matrix and P_i for the overall load vector are the sum of the individual element contributions, and need not be fully summed when the above modification is executed. However, it can be seen from the expressions that the terms K_{ir} (which is equal to K_{ri} by symmetry), K_{rj} , K_{rr} and P_r or row r , must be fully summed before δ_r can be eliminated. It, therefore, does not matter in which order the element contributions are added to K_{ij} and P_i , or in which order the δ_r are eliminated provided that row r is fully summed. Also the only variables required in the central memory are the active coefficients of K_{ij} and the active terms of P_i which are to be modified. The coefficients of K_{ij} form a densely populated triangular array which excludes the zeros outside the band and this is often smaller than the corresponding triangle of coefficients required for a band algorithm. These coefficients continually change but the frontal technique avoids disturbing the active variables residing in core by using the rows and columns vacated by recently eliminated equations. Thus, the frontal technique

continuously alternates between the assembly of the element contributions to form the overall stiffness matrix, and the elimination of completed equations. The reduced equations are saved on secondary storage to be retrieved later for the back-substitution phase. The dimension of the triangle of stiffness coefficients is termed the front width, and this changes as the solution proceeds. It is important that the element stiffness matrices and load vectors are introduced into the central memory in an optimum order to keep the front width to a minimum. The maximum area of central memory required for a solution is dependent on the maximum front width.

The back-substitution phase reads the element records and reduced equations from tape in reversed order and calculates the displacements according to:-

$$\delta_n = \frac{P_n^*}{K_{nn}^*} \dots\dots\dots(4.4)$$

and

$$\delta_i = (P_i^* - \sum_{j=i+1}^{j=n} K_{ij}^* \delta_j) / K_{ii}^* \text{ for } i < n \dots\dots\dots(4.5)$$

where n is the total number of unknown displacements.

The housekeeping for the frontal solution procedure can be briefly illustrated by reference to the simple structure shown in Figure 57, which has only one variable at each node.

Element number 1 with variables 1, 2, 6 is introduced into the central memory and its coefficients are assembled into locations in the overall stiffness and load vectors in accordance with its destination vector (1, 2, 3). Since variable 1 appears for the last time it is eliminated and the reduced equation preserved on backing storage. The positions of the active variables remaining in the core are {0, 2, 6}.

Element number 2 with variables 2, 3, 7 is now introduced. Variable 2 already has a place in the second location, variable 3 is new so is given the vacant place in the first equation, and variable 7 is also new so is given a place in the fourth location. The destination vector for element number 2 is, thus, (2, 1, 4). Since variable 3 appears for the last time it is eliminated and the reduced equation preserved on backing storage. The position of active variables remaining in core are {0, 2, 6, 7}.

Finally, element number 3 with variables 2, 7, 6 is introduced and since all of these variables are already active the destinations are obviously (2, 4, 3). All of these variables appear for the last time and accordingly are eliminated.

From the preceding example it can be seen that the maximum size of problem is limited by the amount of central memory available for the overall stiffness and load vector arrays. The random access front processor implemented in LUSAS is organised to provide a maximum amount of storage for these arrays, by segmenting the dynamic vector array for each phase of the solution as shown in Figure 55. The elimination phase for the first solution is critical and the only arrays used in addition to the overall stiffness and load arrays are the arrays for the current active nodes and variables, the array for element record 2 which consists essentially of element loads, and the buffer array which is used for element stiffness matrices and reduced equation coefficients consecutively. The latter action is possible since the element stiffness coefficients are immediately assembled into the overall stiffness matrix as they appear in core, leaving the equation buffer free to receive the next set of reduced equation coefficients. For elements with large stiffness matrices, for example, the 32 node isoparametric solid element with 4656 stiffness coefficients, the buffer length is minimised by fragmenting the stiffness record into several shorter records. With these core saving arrangements up to 95% of the dynamic vector array is available for the overall stiffness matrix and load vectors.

The frontal solution processor implemented can take account of elements with different numbers of variables at each node. This has been achieved by operating with the destination and appearance code for each variable instead of each node of the element. This approach is more efficient in that there is a greater likelihood of finding a vacant position in the front for a single variable than a vacant position for a node with a particular number of variables. Also this approach has greater flexibility and can accommodate, for example, the coupling of individual variables. The implementation of such facilities involves modifications to only the pre-processing routines which must determine the appropriate destination and appearance codes of each variable.

Every tape reading operation after the initial forward elimination process, must access the records in reversed order. The original version of the frontal program required the computer action BACKSPACE-READ-BACKSPACE, but this is costly, both in peripheral and central processing time[†]. In the present program this action was avoided by a simple modification which involves the use of random access disc transfers. The frontal solution procedure requires the tape records to be accessed sequentially by both forward and backward reading. If, during the creation of a series of records, the random access position of each record is stored with the following records, and so on; then the series of records can be read backwards because as each record is read the position on disc of the next record is given. This procedure is completely dynamic because only the exact length of each record, which varies throughout the solution, is transferred to disc. This procedure has the advantage of being straightforward to implement and does not require the use of further valuable central memory locations.

The computational efficiency of the front processor was improved further by the incorporation of a machine code subroutine of the innermost reduction loop.

[†] Of the order of 30x the cost of a READ statement for a CDC6500 computer.

The success of implementing both the random access and machine code subroutine facilities can be judged from the following example. The problem was a shell roof which was idealised with a mixed mesh of beam and shell elements, and required the solution of 1512 equations with a maximum front width of 108. The computer used was a CDC6500 and the total problem costs included data pre-processing, the assembly of the element characteristic matrices, the solution of equations and the output post-processing phases. A comparison of computer costs with and without the machine code and random access facilities are given in Table 11.

The refined diagonal decay criterion for the estimation of round-off damage, as suggested by Irons, was incorporated into the frontal solution. During the forward elimination process the diagonal stiffness terms decrease monotonically but remain positive. If the final pivotal value is small, compared with the proceeding values, ill-conditioning would be suspected. In the program each time a diagonal term is modified during the elimination, its initial value squared is accumulated into an extra overall load vector. The criterion is that ratio of the square root of this sum divided by the final value of the diagonal should not exceed a certain value:-

$$C_{crit} = \frac{\{\sum (K_{ii})^2\}^{\frac{1}{2}}}{K_{ii} (final)} \dots\dots\dots(4.6)$$

If C_{crit} is greater than 10^4 then ill-conditioning is suspected but the solution continues. If C_{crit} is greater than 10^{11} fatal ill-conditioning is assumed, and the solution is terminated. The program prints out the node number and variable which caused the problem to enable the user to, perhaps, correct the fault.

4.1.11. Post-Solution Processor

The post-solution processor retrieves, from tape, the overall solution vector of displacements, and calculates and outputs the element stresses, displacements at each node and reactions to

earth, for each load case. There are several output options available which may be required by the user, including element stresses with respect to the element local coordinates, as opposed to system coordinates, averaged nodal stresses, and force components as opposed to stress components. The output is concise and self-explanatory with many texts.

External user supplied subroutines can be incorporated into the computer system to post-process and output the results in accordance with the user's particular requirements. Since the element records, reduced equations and element results for a problem are stored on disc, it would be possible for the user to update the element load vectors or stiffness matrices and resolve. This would enable simple non-linear or dynamic problems to be tackled.

4.2. Thin Plate Flexure Elements

4.2.1. Introduction

In the finite element analysis of plates with arbitrary boundaries or shells comprised of flat plates, triangular and quadrilateral flexural elements having three variables at the vertices, are commonly used. Elements with this simple nodal configuration have the advantage of being readily incorporated into computer systems which accept only elements with a constant number of variables at each node. They can also be used in conjunction with the standard grillage beam element for the analysis of, for example, a ribbed plate.

Elements with a linear stress response

$M = f(1, x, y) \dots\dots\dots(4.7)$

are known to have a good performance. A conforming plate flexure displacement element, with only the lateral displacement and its

two first derivatives at the vertices, cannot accommodate this linear stress response because there is only sufficient information to define a linear variation of the tangential rotation along each side as opposed to the required quadratic variation. It is possible that a hybrid formulation could succeed, but as an alternative, a higher order element could be created by the introduction of a midside node at which a tangential rotation is specified^{48,49,50}. This additional rotation variable would have the minor disadvantage of producing an element with different numbers of nodal variables, but this is preferable to the use of higher order derivatives, which require special treatment for abrupt changes of plate thickness or properties. If the departure from linearity of the midside tangential rotation is used instead of the absolute value⁵⁰, then such an element can still be used in conjunction with a standard grillage beam element, simply by constraining this variable to zero in the presence of a beam. A midside node can also be used to define curved element boundaries and this gives an improved geometric definition for many structures.

A unified formulation which includes triangular and quadrilateral elements with the aforementioned nodal configurations does not exist. Furthermore, nearly all individual formulations, to date, fail to satisfy the requirements for thin plate flexure elements.

The classical requirements for thin plate flexure elements are that the assumed displacements should be continuous within each element and across the element boundaries, and should provide every state of constant curvature including rigid body motions. Also, the Kirchhoff thin plate theory, in which normals to the middle surface remain straight and normal to the mid-surface during deformation, is required to exclude shear deformations. In the displacement formulation, if these requirements are fulfilled then the principle of minimum potential energy is valid, and convergence to the correct solution is ensured. However, Irons⁵¹ has shown that it is impossible to specify simple polynomial expressions for shape

functions that ensure both displacement (C^0) and slope (C^1) continuity, when only three variables are prescribed at the element vertices. Consequently, earlier attempts to produce satisfactory elements included formulations which either introduced complex functions to satisfy slope continuity, or violated this requirement precipitating precarious convergence characteristics. For example, the fully conforming triangles of Bazeley et al⁵² and Clough and Tocher⁵³, and the fully conforming quadrilaterals of Clough and Felippa⁵⁴ and Veubeke⁵⁵, all require complex computer code, whilst the simple non-conforming triangle also by Bazeley et al has limited convergence properties.

The hybrid method, pioneered by Pian⁶³, avoids the difficulties encountered with the conventional displacement formulations, and some of the more notable work has been carried out by Allman^{49,58}, Severn and Taylor⁵⁹, Wolf⁶⁰, and Torbe and Church⁶¹. However, hybrid elements are prone to spurious mechanisms^{†62,60}, and the formulation is often cumbersome, but it is generally recognised that they are capable of providing accurate solutions⁶³.

In recent years, it has been established that a necessary and sufficient condition for convergence to the correct solution is that an element should pass the patch test^{64,65,66}. This test in itself does not remove the difficulties encountered with the formulation of plate flexure elements, but it does broaden the search to include, for example, non-conforming elements, elements with approximately integrated energy, and elements in which the Kirchhoff requirement for thin plates is imposed discretely. Regrettably there are relatively few simple elements which pass the patch test.

Irons and Razzaque^{67,50} have developed synthetic versions of Allman's triangular elements which are based on an incompatible displacement formulation with smoothed derivatives. These elements pass the patch test and are coded into a shape function subroutine, but the higher order element cannot accommodate curved boundaries.

[†] A perturbation which carries no strain energy.

A radical approach for the formulation of plate flexure elements is to proceed, initially from the basic equations of elasticity and allow shear deformations to occur^{68,69,70,71,61,72†}. The Kirchhoff hypothesis for thin plates is then invoked by applying constraints at discrete points within the element domain, for example, at the nodes, the boundaries, or the Gauss points^{73,74,75,76,77}. Irons and Razzaque^{73,78,48} used this technique to formulate a higher order quadrilateral with a good performance, but this element does not pass the patch test for quadrilateral geometry.

4.2.2. Requirements for Thin Plate Flexure Elements

The requirements for thin plate flexure elements may be summarised as follows:-

- i. The elements should be capable of being used in triangular and quadrilateral form and should be capable of representing tapering thickness and curved boundaries when necessary. In general, quadrilateral elements are preferred requiring less data preparation and computer output and for a given number of variables can give greater accuracy. Triangular elements are occasionally required when the element size is refined in the vicinity of rapidly varying stress fields, or for irregular boundaries.
- ii. The nodal configuration should be simple and permit the standard grillage beam element to be incorporated into an idealization. Second or higher order derivatives should be avoided and low order elements should have a constant number of variables at each node.
- iii. As a mesh of arbitrarily shaped elements is refined, convergence to the correct solution should be ensured. With certain provisos, the existence of fine-mesh convergence for an element can be established by the patch test^{64,65}. The convergence of a mesh comprised of both triangular and quadrilateral elements should also be established.

† Note also the extensive work based on Ahmads' stacked shell element^{79 80 81 82 78 83}

- iv. The equations produced should not be ill-conditioned and fail for certain geometries.
- v. The coarse mesh performance should be such that if an idealization is in error the results are not unreasonable.
- vi. The element(s) should be easy to implement and computationally efficient. A shape function subroutine is easy to implement, and reduced numerical integration invites computational efficiency. Ideally, it should be possible to code a family of elements into a single compact shape function subroutine thus saving a substantial area of computer core.
- vii. The stresses should be available at the nodes to be consistent with the majority of finite element system output schemes. Sometimes stress output at the Gauss points is acceptable if the accuracy is improved⁸⁴.

4.3. Theory for Constrained Thin Plate Elements

The derivation commences with the three dimensional equations of elasticity which include shearing deformations. Thus, the in-plane and lateral displacements u , v and w are specified independently, and are in coordinate directions shown in Figure 59. The Kirchhoff hypothesis for thin plates without shearing deformations is then invoked discretely by applying constraints to the displacement field.

4.3.1. Basic Assumptions

The basic assumptions for a plate including shearing deformations are:-

- i. The deflections are small.
- ii. Lines originally normal to the mid-surface remain straight during the deformations.
- iii. Stresses and strains, normal to the mid-surface, are always negligible.

For thin plates the additional assumption required is:-

- iv. Lines originally normal to the mid-surface remain normal during the deformations, i.e. zero shear strain.

4.3.2. Derivation of the Thin Plate Theory

From the basic assumptions for a plate with transverse shearing deformations, the displacements of any point x, y and z in the plate can be specified as:-

$$\delta = \begin{Bmatrix} u \\ v \\ w \end{Bmatrix} = \begin{Bmatrix} +z\theta_y \\ -z\theta_x \\ w \end{Bmatrix} \dots\dots\dots (4.8)$$

where θ_x and θ_y are the rotations of the normals to the mid-surface with the sign convention of Figure 60.

From this definition of displacements the strain components can be expressed as:-

$$\epsilon = \begin{Bmatrix} \epsilon_n \\ \epsilon_s \end{Bmatrix} = \begin{Bmatrix} \epsilon_x \\ \epsilon_y \\ \gamma_{xy} \\ \gamma_{xz} \\ \gamma_{yz} \end{Bmatrix} = \begin{Bmatrix} \frac{\delta_u}{\delta_x} \\ \frac{\delta_v}{\delta_y} \\ \frac{\delta_u}{\delta_y} + \frac{\delta_v}{\delta_x} \\ \frac{\delta_w}{\delta_x} + \frac{\delta_u}{\delta_z} \\ \frac{\delta_w}{\delta_y} + \frac{\delta_v}{\delta_z} \end{Bmatrix} \dots\dots\dots (4.9)$$

where ϵ_n is the in-plane strain components and ϵ_s the transverse shear strain components.

Combining equations 4.8 and 4.9 for the in-plane components of strain gives:-

$$\epsilon_n = z \left\{ \begin{matrix} \frac{\delta \theta_y}{\delta x} \\ -\frac{\delta \theta_x}{\delta y} \\ \frac{\delta \theta_y}{\delta y} - \frac{\delta \theta_x}{\delta x} \end{matrix} \right\} = z \epsilon_f \dots\dots\dots (4.10)$$

Noting that $\theta_x = \frac{\delta v}{\delta z}$ and $\theta_y = \frac{\delta u}{\delta z}$, the rotational derivatives ϵ_f can be rewritten as:-

$$\epsilon_f = \left\{ \begin{matrix} \frac{\delta^2 u}{\delta x \delta z} \\ \frac{\delta^2 v}{\delta y \delta z} \\ \frac{\delta^2 u}{\delta y \delta z} + \frac{\delta^2 v}{\delta x \delta z} \end{matrix} \right\} \dots\dots\dots(4.11)$$

The displacement field is now constrained to effectively exclude transverse shear strains as required by the Kirchhoff hypothesis, see assumption (iv), by the technique described in a subsequent section. The evaluation of the element stiffness matrix now involves only in-plane stress and strain products. The in-plane stress components σ_n are given by the usual equation:-

$$\sigma_n = D_n \epsilon_n \dots\dots\dots(4.12)$$

where D_n is the conventional membrane modulus matrix where:-

$$D_n = \begin{bmatrix} d_x & d_l & 0 \\ d_l & d_y & \\ 0 & 0 & d_{xy} \end{bmatrix} \dots\dots\dots(4.13)$$

$$\begin{aligned}
 \text{with } d_x &= d_y = \frac{E}{1 - \nu^2} \\
 dl &= \frac{E}{1 - \nu^2} \dots\dots\dots(4.14) \\
 d_{xy} &= \frac{E}{2(1 + \nu)}
 \end{aligned}$$

for an isotropic material, in which E is the elastic modulus and ν Poisson's ratio.

From the variational principle of minimum potential energy the contribution of the internal stresses to the energy functional is the volume integral:-

$$\frac{1}{2} \int_V \epsilon_n^T \sigma_n dv \dots\dots\dots(4.15)$$

Substituting equations 4.10 and 4.12 into this integral, expanding and rearranging gives:-

$$\begin{aligned}
 \frac{1}{2} \int_V \epsilon_n^T \sigma_n dv &= \frac{1}{2} \iiint \epsilon_n^T \sigma_n dx dy dz \\
 &= \frac{1}{2} \iiint z \epsilon_f^T D_n z \epsilon_f dx dy dz \dots\dots\dots(4.16) \\
 &= \frac{1}{2} \iint \epsilon_f^T D_n z^2 dz \epsilon_f dx dy
 \end{aligned}$$

The innermost integral contains the coordinate z which can be integrated explicitly before the integration with respect to x and y. Thus, the energy integral may be rewritten as:-

$$\frac{1}{2} \iint \epsilon_f^T \sigma_f dx dy \dots\dots\dots(4.17)$$

$$\text{where } \sigma_f = D_f \epsilon_f \dots\dots\dots(4.18)$$

$$\text{and } D_f = \int D_n z^2 dz \dots\dots\dots(4.19)$$

so that the final integration may be carried out with respect to x and y only.

The generalised stress vector σ_f represents the conventional flexural stress resultants of thin plate theory:-

$$\sigma_f = \{M_y, M_x, M_{xy}\}^T \dots\dots\dots(4.20)$$

and the generalised strain vector ϵ_f represents the conventional curvatures. Since the transverse shear strains are only constrained to be approximately zero, these strains are more appropriately termed pseudo-curvatures. For approximately zero shear, $\frac{\delta_u}{\delta_z} = \frac{-\delta_w}{\delta_x}$, and $\frac{\delta_v}{\delta_z} = \frac{-\delta_w}{\delta_y}$ equation 4.11 becomes:-

$$\epsilon_f = \left\{ \begin{array}{c} \frac{\delta^2_u}{\delta x.\delta z} \\ \frac{\delta^2_v}{\delta y.\delta z} \\ \frac{\delta^2_u}{\delta y.\delta z} + \frac{\delta^2_v}{\delta x.\delta z} \end{array} \right\} \approx \left\{ \begin{array}{c} \frac{-\delta^2_w}{\delta x^2} \\ \frac{-\delta^2_w}{\delta y^2} \\ \frac{-\delta^2_w}{\delta x.\delta y} \end{array} \right\} \dots\dots\dots(4.21)$$

The integration of equation 4.19 gives the conventional flexural rigidity D_f where:-

$$D_f = \begin{bmatrix} D_x & D_L & 0 \\ D_L & D_y & 0 \\ 0 & 0 & D_{xy} \end{bmatrix} \dots\dots\dots(4.21)$$

For orthotropy with respect to the x and y axes and in the case of an isotropic material reduces to:-

$$\begin{aligned} D_x &= D_y = \frac{Et^3}{12(1 - \nu^2)} \\ D_L &= \frac{Et^3}{12(1 - \nu^2)} \dots\dots\dots(4.23) \\ D_{xy} &= \frac{Gt^3}{12} = \frac{Et^3}{24(1 + \nu)} \end{aligned}$$

where t is the plate thickness and G the membrane shearing modulus

The formulation now follows the standard displacement method³⁹. The displacement field can be expressed in terms of a set of discrete nodal displacement δ^e by use of suitable shape functions N .

$$\delta = N \delta^e \dots\dots\dots(4.24)$$

suitable constraints are applied to exclude shear strains and from equation 4.21 the flexural strains are defined as:-

$$\epsilon_f = B \delta^e \dots\dots\dots(4.25)$$

Where B is the strain matrix which also contains shear constraints.

The element stiffness matrix can be derived from equations 4.17 and 4.25 by virtual work principles as:-

$$K^e = \iint B^T . D . B \, dx . dy \dots\dots\dots(4.26)$$

where D is the flexural modulus matrix equation 4.13 with the suffix removed for convenience.

4.3.3. Unconstrained Displacement Fields

The unconstrained nodal configurations and co-ordinate systems are shown in Figure 59. The discrete nodal displacements for the i th node are chosen as the mid-surface displacement w_1 and the two rotations of the normal θ_{x1} and θ_{y1} .

By employing suitable shape functions \bar{N}_i , the global displacement field can be written as:-

$$\delta = \sum_{i=1}^n \bar{N}_i \delta_i \dots\dots\dots(4.27)$$

where n is the total number of nodes. For variable thickness elements, defined by nodal thickness t_1 , the displacements at a point ξ, η and distance z above the mid-surface, can be given by expanding equation 4.27 as:-

$$\begin{Bmatrix} u \\ v \\ w \end{Bmatrix} = \sum_{i=1}^n \begin{bmatrix} 0 & 0 & \frac{z}{t} N_i t_i \\ 0 & -\frac{z}{t} N_i t_i & 0 \\ N_i & 0 & 0 \end{bmatrix} \begin{Bmatrix} w \\ \theta_x \\ \theta_y \end{Bmatrix}_i \dots\dots\dots(4.28)$$

where for midside and central nodes the discrete nodal displacements are changed as:-

$$\begin{Bmatrix} w \\ \theta_x \\ \theta_y \end{Bmatrix}_i \rightarrow \begin{Bmatrix} \Delta w \\ \Delta \theta_x \\ \Delta \theta_y \end{Bmatrix}_i \dots\dots\dots(4.29)$$

The symbol Δ refers to the departure from linearity of the value with respect to the values at the corner nodes. The departures from linearity are:-

$$\Delta \delta_j = \delta_j - \frac{1}{(l-m+1)} \sum_{i=l}^m \delta_i \dots\dots\dots(4.30)$$

where l to m refers to the two corner nodes at the extremities of the side of the midside node j, or all corner nodes for the central node j.

4.3.4. Hierarchical Shape Functions

Hierarchical shape functions take account of the variables specified as the departure from linearity. For the triangle the shape functions are conveniently defined in area coordinates L at each node i as:-

$$\begin{aligned} N_1 &= L_1 && \text{for } i = 1,2,3 \\ N_1 &= 4L_{1-3} L_{j-3} && \text{for } i = 4,5,6 \text{ and } j = 5,6,3 \dots\dots\dots(4.31) \\ N_1 &= 27L_1 L_2 L_3 && \text{for } i = 7 \end{aligned}$$

The area coordinates can be defined in terms of the natural coordinates as:-

$$\begin{aligned} L_1 &= \xi \\ L_2 &= \eta \\ L_3 &= 1 - \xi - \eta \end{aligned} \dots\dots\dots(4.32)$$

For the quadrilateral elements the hierarchical shape functions are defined in natural coordinates as:-

$$\begin{aligned} N_1 &= \frac{1}{4} (1+\xi_0) (1+\eta_0) && \text{for } i = 1,4 \\ N_1 &= \frac{1}{2} (1-\xi^2) (1+\eta_0) && \text{for } i = 5 \text{ and } 7 \hspace{1cm} \dots\dots\dots(4.33) \\ N_1 &= \frac{1}{2} (1+\xi_0) (1-\eta^2) && \text{for } i = 5 \text{ and } 8 \\ N_1 &= (1-\xi^2) (1-\eta^2) && \text{for } i = 9 \end{aligned}$$

where

$$\xi_0 = \xi \xi_1 \text{ and } \eta_0 = \eta \eta_1$$

With the definition of the functions N_i established, equations 4.27 and 4.28 define a unique variation of the displacements within the element and over any external face and full C^0 continuity between adjacent elements is maintained.

4.3.5. Hierarchical Mapping and the Jacobian Matrix

It is now necessary to establish the relationship between the Cartesian and natural curvilinear coordinate systems. The x and y coordinates and thickness t at a point $\zeta\eta$ on the mid-surface can be given in a special form as:-

$$\begin{bmatrix} x \\ y \\ t \end{bmatrix} = \sum_{i=1}^n N_i \begin{bmatrix} x \\ y \\ t \end{bmatrix}_i \hspace{1cm} \dots\dots\dots(4.34)$$

where the hierarchical shape functions N are in terms of the natural ζ,η coordinates and the summation is taken over n nodes on the element periphery which are sufficient to define the element geometry. When midside nodes are required the nodal coordinates $\{x,y,t\}_i^T$ become the departures from linearity $\{\Delta x, \Delta y, \Delta t\}_i^T$ which are calculated simply as:-

$$\begin{Bmatrix} \Delta x \\ \Delta y \\ \Delta t \end{Bmatrix}_i = \begin{Bmatrix} x \\ y \\ t \end{Bmatrix}_i - \frac{1}{2} \begin{Bmatrix} x \\ y \\ t \end{Bmatrix}_l - \frac{1}{2} \begin{Bmatrix} x \\ y \\ t \end{Bmatrix}_m \dots\dots\dots (4.35)$$

where i is now a midside node and l and m are the adjacent corner nodes.

This special form of coordinate transformation, referred to here as hierarchical mapping, permits the same shape functions to be adopted for the definition of the displacement field as for the geometry. Furthermore, the same shape functions apply for the geometry of both the straight edged elements defined by corner nodes only, and the curvilinear elements defined by corner and midside nodes. This approach saves computer time compared with an alternative subparametric formulation³⁹ which would require the computation of two sets of shape functions.

The shape functions are in terms of the natural ξ, η coordinates and, therefore, it is now necessary to establish the analytical process for calculating the strain derivatives of equation 4.21 which are expressed in Cartesian x, y coordinates.

Since the thickness of these elements is variable, and the mid-surface planar, then the geometry is a special case of a three-dimensional solid element. The transformation relationship can, therefore, be expected to contain zero products which could be avoided in the numerical process with an explicit derivation, and to be similar to the two-dimensional relationship. For comparison both the two-dimensional and special three-dimensional transformation relationships will now be derived.

From the chain rule the relationship between the natural and Cartesian derivatives in two-dimensions can be written in matrix notation as:-

$$\begin{Bmatrix} \frac{\delta}{\delta \xi} \\ \frac{\delta}{\delta \eta} \end{Bmatrix} = \begin{Bmatrix} \frac{\delta x}{\delta \xi} & \frac{\delta y}{\delta \xi} & \frac{\delta}{\delta x} \\ \frac{\delta x}{\delta \eta} & \frac{\delta y}{\delta \eta} & \frac{\delta}{\delta y} \end{Bmatrix} = (J) \begin{Bmatrix} \frac{\delta}{\delta x} \\ \frac{\delta}{\delta y} \end{Bmatrix} \dots\dots\dots(4.36)$$

where J is defined as the Jacobian matrix. The components of J can be found numerically for any position ξ, η within the element from equation 4.34 as:-

$$(J) = \sum_{i=1}^n \begin{Bmatrix} \frac{\delta N_i}{\delta \xi} & \frac{\delta N_i}{\delta \eta} \end{Bmatrix} \begin{Bmatrix} x_i & 0 \\ 0 & y_i \end{Bmatrix} \dots\dots\dots(4.37)$$

where x_i, y_i are the x and y coordinates for corner node i or the Δx and Δy coordinates for midside node i. The summation is only for nodes on the element periphery.

Inverting the Jacobian in equation 4.36 gives the two-dimensional transformation relationship explicitly as:-

$$\begin{Bmatrix} \frac{\delta}{\delta x} \\ \frac{\delta}{\delta y} \end{Bmatrix} = \frac{1}{\det(J)} \begin{Bmatrix} \frac{\delta y}{\delta \eta} & -\frac{\delta y}{\delta \xi} & \frac{\delta}{\delta \xi} \\ \frac{\delta x}{\delta \eta} & \frac{\delta x}{\delta \xi} & \frac{\delta}{\delta \eta} \end{Bmatrix} = \begin{Bmatrix} \frac{\delta \xi}{\delta x} & \frac{\delta \eta}{\delta x} \\ \frac{\delta \xi}{\delta y} & \frac{\delta \eta}{\delta y} \end{Bmatrix} \begin{Bmatrix} \frac{\delta}{\delta \xi} \\ \frac{\delta}{\delta \eta} \end{Bmatrix} \dots\dots(4.38)$$

where $\det(J) = \frac{\delta x}{\delta \xi} \frac{\delta y}{\delta \eta} - \frac{\delta x}{\delta \eta} \frac{\delta y}{\delta \xi}$

For the three-dimensional transformation relationship the natural coordinate ζ is introduced for convenience. The z coordinate at any point ξ, η, ζ is now given by:-

$$z = \frac{t}{2} \zeta \dots\dots\dots(4.39)$$

where the thickness to of the element at the same point is given

numerically by equation 4.34. From the chain rule in matrix notation:-

$$\begin{bmatrix} \frac{\delta}{\delta \xi} \\ \frac{\delta}{\delta \eta} \\ \frac{\delta}{\delta \zeta} \end{bmatrix} = \begin{bmatrix} \frac{\delta x}{\delta \xi} & \frac{\delta y}{\delta \xi} & \frac{\delta z}{\delta \xi} \\ \frac{\delta x}{\delta \eta} & \frac{\delta y}{\delta \eta} & \frac{\delta z}{\delta \eta} \\ \frac{\delta x}{\delta \zeta} & \frac{\delta y}{\delta \zeta} & \frac{\delta z}{\delta \zeta} \end{bmatrix} \begin{bmatrix} \frac{\delta}{\delta x} \\ \frac{\delta}{\delta y} \\ \frac{\delta}{\delta z} \end{bmatrix} = (J) \begin{bmatrix} \frac{\delta}{\delta x} \\ \frac{\delta}{\delta y} \\ \frac{\delta}{\delta z} \end{bmatrix} \dots\dots\dots(4.40)$$

Inverting the Jacobian gives:-

$$(J)^{-1} = \frac{1}{\det(J)} \begin{bmatrix} \frac{\delta y}{\delta \eta} \frac{\delta z}{\delta \zeta} - \frac{\delta y}{\delta \zeta} \frac{\delta z}{\delta \eta} & \frac{\delta y}{\delta \zeta} \frac{\delta z}{\delta \xi} - \frac{\delta y}{\delta \xi} \frac{\delta z}{\delta \zeta} & \frac{\delta y}{\delta \xi} \frac{\delta z}{\delta \eta} - \frac{\delta y}{\delta \eta} \frac{\delta z}{\delta \xi} \\ \frac{\delta x}{\delta \zeta} \frac{\delta z}{\delta \eta} - \frac{\delta x}{\delta \eta} \frac{\delta z}{\delta \zeta} & \frac{\delta x}{\delta \xi} \frac{\delta z}{\delta \zeta} - \frac{\delta x}{\delta \zeta} \frac{\delta z}{\delta \xi} & \frac{\delta x}{\delta \eta} \frac{\delta z}{\delta \xi} - \frac{\delta x}{\delta \xi} \frac{\delta z}{\delta \eta} \\ \frac{\delta x}{\delta \eta} \frac{\delta y}{\delta \zeta} - \frac{\delta x}{\delta \zeta} \frac{\delta y}{\delta \eta} & \frac{\delta x}{\delta \zeta} \frac{\delta y}{\delta \xi} - \frac{\delta x}{\delta \xi} \frac{\delta y}{\delta \zeta} & \frac{\delta x}{\delta \xi} \frac{\delta y}{\delta \eta} - \frac{\delta x}{\delta \eta} \frac{\delta y}{\delta \xi} \end{bmatrix} \dots\dots\dots(4.41)$$

A geometrical interpretation of the Jacobian is that the rows of J constitute three vectors which are tangential to the coordinate curve ξ , η , ζ at the point of intersection and are known as the covariant base vectors; the columns of J^{-1} constitute three vectors which are normal to the coordinate surfaces $\xi = \text{constant}$, $\eta = \text{constant}$ and $\zeta = \text{constant}$ and are known as contravariant base vectors.

Mathematically the relationship between the Jacobian J and its inverse can be written as:-

$$(J) = \begin{bmatrix} \rightarrow J_\xi \\ \rightarrow J_\eta \\ \rightarrow J_\zeta \end{bmatrix} \dots\dots\dots(4.42)$$

and

$$\begin{aligned}
 &= (J)^{-1} = \frac{1}{\det(J)} \left[\vec{J}_\eta * \vec{J}_\zeta, \vec{J}_\zeta * \vec{J}_\xi, \vec{J}_\xi * \vec{J}_\eta \right] \dots\dots\dots(4.43) \\
 &= \begin{bmatrix} \vec{J}_\xi & \vec{J}_\eta & \vec{J}_\zeta \end{bmatrix}
 \end{aligned}$$

where \vec{J}_ξ etc., are the covariant and contravariant base vectors respectively, and the symbol * signifies a vector cross-product.

Since x and y are functions of ξ and η only, the derivatives $\frac{\delta x}{\delta \zeta}$ and $\frac{\delta y}{\delta \zeta}$ must be zero, and the inverse Jacobian can be simplified to:-

$$(J)^{-1} = \frac{1}{\det} (J) \begin{bmatrix} \frac{\delta y}{\delta \eta} \frac{\delta z}{\delta \zeta} - \frac{\delta y}{\delta \xi} \frac{\delta z}{\delta \zeta} & \frac{\delta y}{\delta \xi} \frac{\delta z}{\delta \eta} - \frac{\delta y}{\delta \eta} \frac{\delta z}{\delta \xi} \\ - \frac{\delta x}{\delta \eta} \frac{\delta z}{\delta \zeta} & \frac{\delta x}{\delta \xi} \frac{\delta z}{\delta \zeta} & \frac{\delta x}{\delta \eta} \frac{\delta z}{\delta \xi} - \frac{\delta x}{\delta \xi} \frac{\delta z}{\delta \eta} \\ 0 & 0 & \frac{\delta x}{\delta \xi} \frac{\delta y}{\delta \eta} - \frac{\delta x}{\delta \eta} \frac{\delta y}{\delta \xi} \end{bmatrix} \dots\dots\dots(4.44)$$

where $\det (J) = \frac{\delta z}{\delta \zeta} \left(\frac{\delta x}{\delta \xi} \frac{\delta y}{\delta \eta} - \frac{\delta x}{\delta \eta} \frac{\delta y}{\delta \xi} \right).$

On inspection, it can be seen that the first 2 x 2 partition is identical to the inverted two-dimensional Jacobian, equation 4.37.

Noting from equation 4.39 that $\frac{\delta z}{\delta \zeta} = \frac{t}{2}$ and from equation 4.44 that $\frac{\delta z}{\delta x} = \frac{\zeta}{2} \frac{dt}{dx} = \frac{z}{t} \frac{\delta t}{\delta x}$ etc., and substituting these expressions into equation 4.44 gives:-

$$(J)^{-1} = \begin{bmatrix} \frac{1}{\det (J)} \frac{\delta y}{\delta \eta} - \frac{1}{\det (J)} \frac{\delta y}{\delta \xi} - \frac{2z}{t^2} \frac{\delta t}{\delta x} \\ - \frac{1}{\det (J)} \frac{\delta x}{\delta \eta} & \frac{1}{\det (J)} \frac{\delta x}{\delta \xi} - \frac{2z}{t^2} \frac{\delta t}{\delta y} \\ 0 & 0 & \frac{t}{2} \end{bmatrix} \dots\dots\dots(4.45)$$

where the first 2 x 2 partition is identical to J^{-1} for the two-dimensional Jacobian. Noting that equation 4.45 gives $\frac{\delta}{\delta z} = \frac{t}{2} \frac{\delta}{\delta \zeta}$, the final relationship for the Cartesian x and y

$$\begin{Bmatrix} \frac{\delta}{\delta x} \\ \frac{\delta}{\delta y} \end{Bmatrix} = \begin{bmatrix} \frac{1}{\det(J)} \frac{\delta}{\delta \eta} & -\frac{1}{\det(J)} \frac{\delta y}{\delta \xi} & -\frac{z}{t} \frac{\delta t}{\delta x} \\ -\frac{1}{\det(J)} \frac{\delta x}{\delta \eta} & \frac{1}{\det(J)} \frac{\delta x}{\delta \xi} & -\frac{z}{t} \frac{\delta t}{\delta y} \end{bmatrix} \begin{Bmatrix} \frac{\delta}{\delta \xi} \\ \frac{\delta}{\delta \eta} \\ \frac{\delta}{\delta z} \end{Bmatrix} \dots\dots\dots(4.46)$$

The physical interpretation of equation 4.46 is that for variable thickness an in-plane strain component, for example $\epsilon_x = \frac{\delta u}{\delta x}$, includes a small strain contribution from the change of u over the thickness. When the plate is constant thickness this contribution vanishes.

For numerical convenient equations 4.34 and 4.37 can be combined and expanded to include the necessary components to creat the transformation relationship of equation 4.46 as:-

$$\begin{bmatrix} x & y & t \\ \frac{\delta x}{\delta \xi} & \frac{\delta y}{\delta \xi} & \frac{\delta t}{\delta \xi} \\ \frac{\delta x}{\delta \eta} & \frac{\delta y}{\delta \eta} & \frac{\delta t}{\delta \eta} \end{bmatrix} = \sum_{i=1}^n \begin{bmatrix} N_i & N_i & N_i \\ \frac{\delta N_i}{\delta \xi} & \frac{\delta N_i}{\delta \xi} & \frac{\delta N_i}{\delta \xi} \\ \frac{\delta N_i}{\delta \eta} & \frac{\delta N_i}{\delta \eta} & \frac{\delta N_i}{\delta \eta} \end{bmatrix} \begin{bmatrix} x_i & 0 & 0 \\ 0 & y_i & 0 \\ 0 & 0 & t_i \end{bmatrix} \dots\dots\dots(4.47)$$

where as before the i nodal values are summed over the nodes on the periphery and midside nodes are present the nodal coordinates become the departures from linearity.

4.3.6. Strain-Displacement Relations

It is now possible to derive the relationship between the flexural strains and the discrete nodal displacements. The transformation relationship, equation 4.46, can be regarded as the standard two-dimensional transformation with a variable thickness correction. Thus the flexural strain components, equation 4.11, can be written

in the form:-

$$\begin{bmatrix} \frac{\delta^2 u}{\delta x \delta z} & \frac{\delta^2 v}{\delta x \delta z} \\ \frac{\delta^2 u}{\delta y \delta z} & \frac{\delta^2 v}{\delta y \delta z} \end{bmatrix}_{3D} = \frac{\delta}{\delta z} \left\{ \begin{bmatrix} \frac{\delta u}{\delta x} & \frac{\delta v}{\delta x} \\ \frac{\delta u}{\delta y} & \frac{\delta v}{\delta y} \end{bmatrix} - \frac{z}{t} \begin{bmatrix} \frac{\delta t}{\delta x} \\ \frac{\delta t}{\delta y} \end{bmatrix} \left[\frac{\delta u}{\delta z}, \frac{\delta v}{\delta z} \right] \right\}_{2D} \dots (4.48)$$

where all the derivatives to the right involve only the two-dimensional transformation. Since the displacement field will be constrained to have approximately zero shear strains, the second derivatives in z can be dealt with by noting that $\frac{\delta u}{\delta z} = \frac{\delta w}{\delta x}$ and $\frac{\delta v}{\delta z} = -\frac{\delta w}{\delta y}$ equation 4.48 now becomes:-

$$\begin{bmatrix} \frac{\delta^2 u}{\delta x \delta z} & \frac{\delta^2 v}{\delta x \delta z} \\ \frac{\delta^2 u}{\delta y \delta z} & \frac{\delta^2 v}{\delta y \delta z} \end{bmatrix} = \left\{ \begin{bmatrix} \frac{\delta^2 u}{\delta x \delta z} & \frac{\delta^2 v}{\delta x \delta z} \\ \frac{\delta^2 u}{\delta y \delta z} & \frac{\delta^2 v}{\delta y \delta z} \end{bmatrix} + \frac{1}{t} \begin{bmatrix} \frac{\delta t}{\delta x} \\ \frac{\delta t}{\delta y} \end{bmatrix} \left[\frac{\delta w}{\delta x}, \frac{\delta w}{\delta y} \right] \right\} \dots (4.49)$$

The plate flexure strain displacement relationship can now be written from equations 4.21, 4.28, 4.46 and 4.49 as:-

$$\epsilon_f = \begin{bmatrix} \frac{\delta^2 u}{\delta x \delta z} \\ \frac{\delta^2 v}{\delta y \delta z} \\ \frac{\delta^2 u}{\delta y \delta z} + \frac{\delta^2 v}{\delta x \delta z} \end{bmatrix} = \sum_{i=1}^n \begin{bmatrix} \frac{1}{t} \frac{\delta t}{\delta x} \frac{\delta N_i}{\delta x} & 0 & \frac{t_i}{t} \frac{\delta N_i}{\delta x} \\ \frac{1}{t} \frac{\delta t}{\delta y} \frac{\delta N_i}{\delta y} & -\frac{t_i}{t} \frac{\delta N_i}{\delta y} & 0 \\ \frac{1}{t} \frac{\delta t}{\delta y} \frac{\delta N_i}{\delta x} & -\frac{t_i}{t} \frac{\delta N_i}{\delta x} & \frac{t_i}{t} \frac{\delta N_i}{\delta y} \\ \frac{1}{t} \frac{\delta t}{\delta x} \frac{\delta N_i}{\delta y} & \frac{t_i}{t} \frac{\delta N_i}{\delta y} & -\frac{t_i}{t} \frac{\delta N_i}{\delta x} \end{bmatrix} \begin{bmatrix} w \\ \theta_x \\ \theta_y \end{bmatrix} \dots (4.50)$$

where the summation is taken over all nodes n and derivatives are found from the standard two-dimensional relations. In matrix form

equation 4.50 becomes:-

$$\epsilon_f = \begin{bmatrix} B_1 & \dots & B_1 & \dots & B_n \end{bmatrix} \begin{Bmatrix} \delta_1 \\ \delta_1 \\ \delta_n \end{Bmatrix} \dots\dots\dots(4.51)$$

or $\epsilon_f = B\delta^e \dots\dots\dots(4.52)$

where B_1 is the submatrix relating the flexural strains at any point ξ, η to the displacement components of node 1.

4.3.7. Shape Function Array

It is now possible to relate all the displacements and derivatives, at any point within the element, to the discrete nodal displacements. Using equations 4.28 and 4.50 gives:-

$$\begin{Bmatrix} w \\ \frac{\delta u}{\delta z} \\ \frac{\delta v}{\delta z} \\ \frac{\delta w}{\delta x} \\ \frac{\delta w}{\delta y} \\ \frac{\delta^2 u}{\delta x \delta z} \\ \frac{\delta^2 v}{\delta y \delta z} \\ \frac{\delta^2 u}{\delta y \delta z} + \frac{\delta^2 v}{\delta x \delta z} \end{Bmatrix} = \sum_{i=1}^n \begin{bmatrix} N_1 & 0 & 0 \\ 0 & 0 & \frac{1}{t} N_1 t_1 \\ 0 & -\frac{1}{t} N_1 t_1 & 0 \\ \frac{\delta N_1}{\delta x} & 0 & 0 \\ \frac{\delta N_1}{\delta y} & 0 & 0 \\ \frac{1}{t} \frac{\delta t}{\delta x} \frac{\delta N_1}{\delta x} & 0 & \frac{t_1}{t} \frac{\delta N_1}{\delta x} \\ \frac{1}{t} \frac{\delta t}{\delta y} \frac{\delta N_1}{\delta y} & -\frac{t_1}{t} \frac{\delta N_1}{\delta y} & 0 \\ \frac{1}{t} \frac{\delta t}{\delta y} \frac{\delta N_1}{\delta x} & -\frac{t_1}{t} \frac{\delta N_1}{\delta x} & \frac{t_1}{t} \frac{\delta N_1}{\delta y} \\ + \frac{1}{t} \frac{\delta t}{\delta x} \frac{\delta N_1}{\delta y} \end{bmatrix} \begin{Bmatrix} w \\ \theta_x \\ \theta_y \end{Bmatrix} \dots\dots\dots(4.53)$$

or more concisely $\delta^* = w\delta^e \dots\dots\dots(4.54)$

The use of a shape function array is numerically convenient since on extracting the appropriate rows any element matrix can easily be formed. However, the shape function array has yet to be constrained to preclude shear strains.

4.3.8. Kinematic Constraints

The unconstrained nodal variables for the triangular and quadrilateral elements, Figure 58 are now reduced to the constrained nodal configurations, Figure 59, by the application of sets of independent shear constraints. The 20 unconstrained variables for ISOFLEX 6 and ISOFLEX 3 triangles require 8 and 11 constraints respectively, and the 27 unconstrained variables for the ISOFLEX 8 and ISOFLEX 4 quadrilaterals require 11 and 15 constraints respectively. If these constraints were enforced so that the shear strains were exactly zero throughout an element domain that the Kirchhoff requirement for thin plates would be satisfied exactly. However, the constraints adopted here are enforced so that the shear strains are zero at discrete points within an element domain, but since an element gains only a small quantity of shear strain energy the Kirchhoff requirement is effectively satisfied. Furthermore, the unconstrained variables and applied kinematic constraints are such that the elements pass the patch test for arbitrary triangular and quadrilateral element geometry.

1. The midside translation and rotation - 2 constraints along each edge.

It can be verified that a planar beam element can be formulated in a similar manner to the technique proposed in this chapter by specifying unconstrained nodal variables at three nodes as $(w, \frac{\delta u}{\delta z})$ $i = 1, 3$ with quadratic variations of $w = f(x^2)$ and $\frac{\delta u}{\delta z} = f(x^2)$. If the two variables at the central node are eliminated by constraining the shears to be zero at the two Gauss points, and the integration for the element stiffness is carried out using the two point Gauss rule, then the resulting element stiffness matrix is identical to that given by the standard formulation based on a variation of $w = f(x^3)$ with explicit integration.

For the ISOFLEX elements the transverse tangential shear strain γ_t is constrained to zero at the two Gauss points on each edge of the element. If each edge is imagined to be a narrow beam then these constraint positions are ideal in accordance with the optimum constraint positions for the corresponding beam element. Furthermore, boundary constraints have the advantage of being identical for two adjacent elements even though the computation is repeated. The direction of the tangent at each Gauss point for curvilinear or straight element boundaries is given by the covariant base vectors $J\xi$ or $J\eta$, equation 4.42.

ii. The two rotations at the centre - 2 constraints.

The work done during a rigid body displacement of an element is zero requiring the shear forces in the x and y directions to be zero. These shear forces can be found by integrating the shear stresses over the element area and since stresses are proportional to strains this reduces to the following integrations:-

$$\int \gamma_{xz} \, dA = 0 \quad \dots\dots\dots(4.55)$$

$$\int \gamma_{yz} \, dA = 0 \quad \dots\dots\dots(4.56)$$

These integrations are computed numerically.

iii. The central lateral deflection - 1 constraint.

From vertical equilibrium:-

$$\int \nabla \gamma \, dA = \int \left(\frac{\delta \gamma_{xz}}{\delta x} + \frac{\delta \gamma_{yz}}{\delta y} \right) dA = 0 \quad \dots\dots\dots(4.57)$$

and Green's theorem can be used to give a transformed version which avoids second derivatives⁷⁵ as:-

$$\int \delta \gamma_n \, ds = 0 \quad \dots\dots\dots(4.58)$$

where γ_n is the normal shear strain and ds is around the periphery.

This integral is computed using the two point Gauss rule along each edge of the element. This constraint applies to the quadrilateral elements only since the addition of a central lateral displacement variable to the triangular elements did not affect their performance. For the quadrilateral element to pass the patch test it is an inescapable requirement that it should respond with w as a quadratic in x and y ⁷⁴⁻⁷⁶. A quadrilateral element has $x = f(1, \xi, \eta, \xi\eta)$ and on expanding $w = x^2$, the term $\xi^2 \eta^2$ appears. This term is provided here by the central variable for w which uses the bubble function $(1 - \xi^2)(1 - \eta^2)$.

iv. Midside rotation - 1 constraint on each edge.

For the lower order elements the tangential rotations are enforced to be linear along each edge of the element simply by excluding the midside tangential rotation $\Delta\theta_t$, the departure from linearity, from the element computations.

Extracting the appropriate rows from the shape function array, equation 4.53, transforming the edge shears and integrating the shears over the area and around the periphery gives for the quadrilaterals, for example:-

$$\begin{bmatrix} Y_{t1} \\ \vdots \\ Y_{t8(6)} \\ \int Y_{xz} dA \\ \int Y_{yz} dA \\ \int Y_n ds \end{bmatrix} \begin{bmatrix} 0 \\ \vdots \\ 0 \end{bmatrix} \begin{bmatrix} M_A \\ 11 \times 16 \\ (8 \times 12) \end{bmatrix} \begin{bmatrix} M_B \\ 11 \times 11 \\ (8 \times 8) \end{bmatrix} \begin{bmatrix} \delta_A \\ \delta_B \end{bmatrix} \dots\dots\dots(4.59)$$

where δ_A are the variables for the required nodal configuration and δ_B are the unwanted variables, and the array sizes in brackets refer

to the triangles. After transforming the columns of M for the tangential and normal rotations at the midsides the variables δ_A and δ_B are:-

$$\begin{pmatrix} \delta_A & \delta_B \end{pmatrix}^T = (W, \theta_x, \theta_y, \Delta\theta_{tj}, \dots, \Delta W, \Delta\theta_n)_j, \dots, \Delta\theta_{xk}, \Delta\theta_{yk}, \Delta W_k) \dots\dots\dots(4.60)$$

where i refers to corner nodes, j refers to midside nodes and k refers to the central node.

From equation 4.59 the unwanted variables can be expressed in terms of the wanted variables as:-

$$\delta_B = -M_B^{-1} M_A \delta_A \dots\dots\dots(4.61)$$

Rearranging the columns of the unconstrained shape function array, equation 4.53, to coincide with the wanted and unwanted nodal variables, and introducing the above expression gives:-

$$(\delta^*) = \begin{bmatrix} W_A & -W_B M_B^{-1} M_A \end{bmatrix} (\delta_A) \dots\dots\dots(4.62)$$

or

$$\delta^* = W_C \delta^e \dots\dots\dots(4.63)$$

where $W_C = W_A - W_B M_B^{-1} M_A$ and is the constrained shape function array which gives the displacements and strain variables at any point ξ, η within the element in terms of required element variables δ^e .

The inversion of the matrix M_B followed by a matrix multiplication for the product $M_B^{-1} M_A$ can be avoided and solved collectively by a scheme suggested by Faddeeva⁸⁶. The product is equivalent to the

solution of n systems of a special form:-

$$\begin{bmatrix} M_B & -M_A \\ -I & 0 \end{bmatrix} \dots\dots\dots(4.64)$$

where I is the square n by n unit matrix which is the same size as M_B. By annulling all the rows in the lower left corner, and by the addition of suitable linear combinations of the first n rows, the product M_B⁻¹ M_A is obtained in the lower right corner. This can be accomplished by the ordinary forward elimination of the Gauss process.

4.3.9. Numerically Integrated Stiffness Matrix

Introducing the standard expression:-

$$dx \; dy \; = \; |J| \; d\xi \; d\eta \; \dots\dots\dots(4.65)$$

and noting that B is a function of ξ, η equation 4.26 can be rewritten in the form:-

$$K^e \; = \; \int_{-1}^1 \int_{-1}^1 B^T D \; B |J| \; d\xi . d\eta \; \dots\dots\dots(4.66)$$

or in submatrix form:-

$$K_{ij}^e \; = \; \int_{-1}^1 \int_{-1}^1 B_i^T \; D \; B_j |J| \; d\xi . d\eta \; \dots\dots\dots(4.67)$$

Where K_{ij}^e is a typical submatrix linking nodes i and j. When evaluating the triple product B_i^T D B_j advantage should be taken of the sparsity of B and D, thus saving many unnecessary matrix manipulations.

The integration of the stiffness coefficients is carried out numerically, and equation 4.67 is replaced by a weighted summation

of the values at certain points in the element:-

$$K^e = \sum_{i=1}^n W_p \left[f(\xi_p, \eta_p) \right] \dots\dots\dots(4.68)$$

where $\left[f(\xi_p, \eta_p) \right] = B^T D B \left| J \right|$ is evaluated at the appropriate sampling points ξ_p, η_p and W_p is the corresponding weight coefficient at this point.

4.3.10. Nodal and Distributed Loading

As with other finite element displacement models, the force-displacement relationship takes the form:-

$$F^e = K^e \delta^e + \bar{F}^e \dots\dots\dots(4.69)$$

where \bar{F}^e represents a set of unique nodal forces required to maintain equilibrium at $\delta^e = 0$. Those forces may be associated with external surface tractions, body forces and initial strains. In the present context we will consider only the following constituents:-

$$\bar{F}^e = \bar{F}_1^e + \bar{F}_2^e \dots\dots\dots(4.70)$$

where \bar{F}_1^e, \bar{F}_2^e are the consistent nodal forces associated with concentrated nodal loads and distributed pressures respectively.

The vector \bar{F}^e will consist of three force components for corner nodes and one for a midside node. Thus, for example:-

$$\bar{F}^e = \begin{Bmatrix} \bar{F}_1^e \\ \bar{F}_1^e \\ \bar{F}_n^e \end{Bmatrix} \quad \text{with } \bar{F}_1 = \begin{Bmatrix} P_{x1} \\ M_{x1} \\ M_{y1} \end{Bmatrix} \quad \text{for corner nodes} \dots\dots\dots(4.71)$$

$$\quad \quad \quad \text{or } \bar{F}_1 = \begin{Bmatrix} \Delta M_{x1} \end{Bmatrix} \quad \text{for midside nodes}$$

where ΔM_x is associated with the departure from linearity of the tangential rotation $\Delta \theta_T$, but since this has no physical significance it will, in general, be neglected.

The consistent nodal forces \bar{F}_2^8 due to a distributed pressure q over the area of an element can be determined simply as:-

$$\bar{F}^8 = - \int_A W^T q \, dA \quad \dots\dots\dots(4.72)$$

where dA is the infinitesimal surface area $dx dy$, and W here refers to the first row of the shape function array for the lateral deflection. The integration is carried out numerically and concurrently with the stiffness integration. In general q will vary over the surface of an element and must, therefore, be interpolated from the values specified at the nodes as:-

$$q = \sum_{i=1}^n N_i q_i \quad \dots\dots\dots(4.73)$$

where N_i here refers to the standard shape functions for an element with n nodes as opposed to the hierarchical shape functions mentioned previously.

4.4. Reduced Numerical Integration and Spurious Mechanisms

The reduced numerical integration rules adopted here permit an economical evaluation of the element integrals, and the resulting stiffness matrix gives an improved structural response over the correct order of integration.[†] The reduced numerical integration employed here is the three-point rule for the triangles and the four-point rule for the quadrilaterals³⁹, (i.e. 2 x 2 Gauss points). However, to prevent spurious mechanisms the stiffness of the higher order quadrilateral is integrated by a five-point rule suggested by Irons⁷⁶ as:-

$$\int_1^1 \int_1^1 f(\xi, \eta) d\xi d\eta = 0.2f(0,0) + 0.95 \sum_1^4 (\pm 0.59234888, \pm 0.59234888) \dots\dots\dots(4.75)$$

[†] For Gaussian integration in one dimension n points gives exact values for the integral of a polynomial of degree $2n-1$.

where $b = (1 - \frac{1}{4}a)$ and $B = (3b)^{-\frac{1}{2}}$, and with $a = 0.2$ becomes:-

$$\int_{-1}^1 \int_{-1}^1 f(\xi, \eta) d\xi d\eta = 0.2f(0,0) + 0.95 \sum_{i=1}^4 (\pm 0.59234888, \pm 0.59234888) \dots (4.75)$$

Ideally the stiffness matrix for an element should have a rank of: (the number of nodal variables - (the number of rigid body notions available))⁷⁴. The ISOFLEX plate flexure elements, therefore, require a rank of:-

- 9 - 3 = 6 for ISOFLEX 3
- 12 - 3 = 9 for ISOFLEX 6
- 12 - 3 = 9 for ISOFLEX 4
- 16 - 3 = 13 for ISOFLEX 8

Since each integration point can contribute, at most, 3 (the rank of the modulus matrix) the integration rules mentioned previously, should provide adequate rank thus avoiding spurious mechanisms.

4.5. Stress Smoothing

Since reduced numerical integration has been adopted for the evaluation of the element integrals it is natural to expect these integration points to be the most appropriate stations for sampling the stresses. These points have the added attraction of enabling the element stress matrices to be evaluated concurrently with the stiffness matrix, thus avoiding further entries to the shape function subroutine and increasing the computational efficiency. For the higher order quadrilateral, for numerical convenience, the stresses are sampled at the four corner points of the five-point rule.

Although the integration points give the most accurate stresses, nodal values may be more convenient. These nodal values are

obtained by a linear and bilinear extrapolation of the values at the integration points, and is equivalent to a least squares best fit of the nodal values.

The three integration points for the triangles, or the four integration points for the quadrilateral are used to construct a fictitious triangular or quadrilateral element subdomain. Since the stresses are assumed to vary linearly or bilinearly, the smoothed stresses, both inside and outside, of the fictitious element subdomain are given as:-

$$\bar{\sigma} = \sum_{i=1}^n N_i \sigma_i \dots\dots\dots(4.76)$$

where $\bar{\sigma}$ is the smoothed stress at, for example a node of the element, N_i are the linear or bilinear shape functions, and σ_i are the stress values at the n vertices of the fictitious element.

4.6. Semi-Loof Element

4.6.1. General

Until recently most general thin shell elements have not given satisfactory solutions when used to analyse problems with, either, complicated geometries or loading systems. Sharp corners and junctions between curved surfaces are examples of the problems met, particularly in shell structures.

A recently developed element by Irons⁴⁰ appears to have distinct advantages in overcoming these and other problems. The element is non-conforming and it's use is, therefore, confirmed by the use of the patch test⁴¹. It adopts isoparametric concepts for geometrical and generalised displacement definitions, and the present version QSL8 used in LUSAS is an eight noded parabolic model. Each node has three associated displacement components and C¹ continuity is provided by the introduction of normal rotation variables at discrete points (Loof nodes) on the element boundary.

Shear constraints are used at the Loof nodes to eliminate certain nodal variables. Loof nodes are points located at the Gaussian integration positions along the element edges. Since the element does not permit lateral shear it is restricted to thin shell situations. Variations in thickness in individual elements can be readily handled and thickness discontinuity between adjacent elements is permitted. Experience⁴² in static situations has shown that the element is efficient and accurate, even with relatively coarse meshes.

4.6.2. The Element

A quadrilateral Semi-Loof shell element is shown in Figure 61. Figure 61 also shows the coordinate system and nodal variables for this element. Three types of node are defined:-

1. Corner and midside nodes at which three global displacement components (u^i, v^i, w^i) are taken as node parameters.
2. Loof nodes which are located at the Gaussian quadrature positions for two-point integration along the element sides. These nodes are, therefore, positioned at a distance $0.289 (1/2 \sqrt{3})$ times the side length from the centre. The nodal parameters of a Loof node, j , are taken as the two rotations σ^j_{YZ} which are respectively normal and parallel to the element edge and are expressed with respect to a local coordinate system defined by the orthogonal unit vector systems $(\hat{X}, \hat{Y}, \hat{Z})$.
3. The central node at which the nodal parameters are chosen to be the three local displacement components and the two rotations about the isoparametric curvilinear axes ξ and η .

These are arranged as follows:-

$$\begin{aligned}
 \{\delta^e\} &= (u^1, v^1, w^1, \dots, u^9, v^9, w^9) \\
 \{\sigma^e_{XZ}\} &= (\sigma^1_{XZ}, \dots, \sigma^9_{XZ})^T \\
 \{\sigma^e_{YZ}\} &= (\sigma^1_{YZ}, \dots, \sigma^9_{YZ})^T
 \end{aligned}$$

The 45 degrees of freedom are condensed to 32 by prescribing constraints on the shear behaviour of the element. Generation of local coordinate system (\hat{X} , \hat{Y} , \hat{Z}) at any point P(x, y, z) is carried out as follows:-

Compute unit normal vector \hat{Z} from the vector product:-

$$\overline{Z} = \frac{\delta \overline{P}}{\delta \xi} \times \frac{\delta \overline{P}}{\delta \eta} \dots\dots\dots(4.77)$$

One of the in-plane directions is chosen to be the local ξ direction and is computed from:-

$$\overline{X} = \frac{\delta \overline{P}}{\delta \xi} \dots\dots\dots(4.78)$$

The orthogonal set is completed by using the normalised form of equation 4.77 and equation 4.78 to give:-

$$\hat{Y} = \hat{X} \times \hat{Z}$$

If the global displacements of point P(x, y, z) are denoted by (d) = {u, v, w}^T then these values are interpolated by using the shape functions (N) such that:-

$$(d) = (N) (\delta^e) \dots\dots\dots(4.79)$$

Displacement components of \hat{X} , \hat{Y} , and \hat{Z} are denoted by U, V and W respectively and are projects of (d) on the unit base vectors, and are given by the scaler products:-

$$U = (X)^T (d) = (X)^T (N) (\delta^e) \dots\dots\dots(4.80)$$

$$V = (Y)^T (d) = (Y)^T (N) (\delta^e) \dots\dots\dots(4.81)$$

$$W = (Z)^T (d) = (Z)^T (N) (\delta^e) \dots\dots\dots(4.82)$$

4.6.3. In-Plane Behaviour

To calculate the geometric matrix derivatives of U and V with respect to the local directions X and Y, i.e.

$$\frac{\delta U}{\delta X} = (X)^T \begin{bmatrix} \delta N \\ \delta X \end{bmatrix} (\delta^e) \dots\dots\dots (4.83)$$

where $\frac{\delta N}{\delta X}$ is a (3 x 9) matrix whose components are given by:-

$$\begin{Bmatrix} \frac{\delta N^1}{\delta X} \\ \frac{\delta N^1}{\delta Y} \end{Bmatrix} = \begin{bmatrix} \hat{X}.\bar{\xi} & \hat{X}.\bar{\eta} \\ \hat{Y}.\bar{\xi} & \hat{Y}.\bar{\eta} \end{bmatrix}^{-T} \begin{Bmatrix} \frac{\delta N^1}{\delta \xi} \\ \frac{\delta N^1}{\delta \eta} \end{Bmatrix}$$

where $\bar{\xi}$ and $\bar{\eta}$ are respectively $\delta \bar{P} / \delta \xi$ and $\delta \bar{P} / \delta \eta$. Similar expressions hold for $\frac{\delta U}{\delta Y}$, $\frac{\delta V}{\delta X}$ and $\frac{\delta V}{\delta Y}$.

4.6.4. Out Of Plane Behaviour

The out of plane derivatives $\frac{\delta U}{\delta Z}$ and $\frac{\delta V}{\delta Z}$ require to be derived.

$$\frac{\delta U}{\delta Z} = \left\{ \frac{\delta U}{\delta Z} \right\}^L + \left\{ \frac{\delta U}{\delta Z} \right\}^N \dots\dots\dots (4.84)$$

where the first term is the contribution from the rotations at the Loof and central nodes, and the second term is the contribution from the displacements of the corner, midside and central nodes.

To evaluate $\left\{ \frac{\delta U}{\delta Z} \right\}^L$ a thickness vector \bar{T}^j is defined at each loof node and central node, j.

$$\bar{T}^j = t^j \hat{Z}^j$$

where t^j is the shell thickness at node j.

The rotation shared by adjacent elements is given by the vector $\vec{R}^j = \vec{T}^j \times \vec{Y}^j$ and the slope along the element edge, at node j, is given by $\vec{S}^j = t^j \hat{Y}^j$

These vectors \vec{R}^j , \vec{S}^j and \vec{T}^j are shown in Figure 61. Using these vectors the term $\left\{ \frac{\delta U}{\delta Z} \right\}^L$ can be expressed as:-

$$\left\{ \frac{\delta U}{\delta Z} \right\}^L = \sum_{j=1}^9 \left[(\vec{R}^j)^T (X) \frac{L^j}{t} \sigma^j_{XZ} + (\vec{S}^j)^T (X) \frac{L^j}{t} \sigma^j_{YZ} \right] \dots\dots\dots(4.85)$$

where L^j represents the shape functions for the Loof and central nodes.

A similar expression exists for $\left\{ \frac{\delta V}{\delta Z} \right\}^L$

To evaluate $\left\{ \frac{\delta U}{\delta Z} \right\}^N$ the thickness vector at any point P can be interpolated as:-

$$\vec{T} = \sum_{j=1}^9 L^j \vec{T}^j$$

This vector \vec{T} is not necessarily normal to the mid-surface which implies that the points (say A and B) on the two surfaces (inner and outer) are not orthogonally opposite.

In the plane XZ:-

$$\left\{ \frac{\delta U}{\delta Z} \right\}^N_{XZ} = \frac{u_B - u_A}{t} = \frac{T_x}{t} \frac{\delta U}{\delta X} \dots\dots\dots(4.86)$$

where t is the shell thickness at the point considered, and T_x is the component of \vec{T} along the local X axis.

The component from the YZ plane is similar and must be added

therefore,

$$\left\{ \frac{\delta U}{\delta Z} \right\}^N = \frac{1}{t} \left[T_X (X)^T \left\{ \frac{\delta N}{\delta X} \right\} + T_Y (X)^T \left\{ \frac{\delta N}{\delta Y} \right\} \right] (\delta^e) \dots\dots\dots(4.87)$$

The expression for $\left\{ \frac{\delta V}{\delta Z} \right\}^N$ is similar.

4.6.5. Shear Constraints

The degrees of freedom corresponding to the displacements (u, v, w) of the central node are combined to give a deflection normal to the element, the in-plane components being discarded.

Further variable elimination is made by imposing eleven shear constraints on the element. The shears constrained to zero are at the Loof nodes, along the boundary, and over the element area.

There are then 32 remaining degrees of freedom which are:-

24 displacement components, with respect to global axes, at the corner and midside nodes.

8 rotations relative to the element edge at each loof node (i.e. σ_{XZ}).

The eleven constraint equations can be written in matrix form:-

$$\left[\begin{array}{c|c} C_A & C_B \end{array} \right] \begin{Bmatrix} P_A \\ P_B \end{Bmatrix} = 0 \dots\dots\dots(4.88)$$

where (P_A) represents the 32 degrees of freedom to be retained, and (P_B) denotes those 11 the be eliminated.

(C) is a (11 x 43) constraint matrix.

The local displacement components and their derivatives are assembled as follows:-

$$\begin{aligned} (G) &= \left\{ U, V, W, \frac{\delta U}{\delta X}, \frac{\delta U}{\delta Y}, \frac{\delta V}{\delta X}, \frac{\delta V}{\delta Y}, \frac{\delta U}{\delta Z}, \frac{\delta V}{\delta Z} \right\}^T \\ &= \left[\begin{array}{c|c} S_A & S_B \end{array} \right] \left\{ \begin{array}{c} P_A \\ P_B \end{array} \right\} \dots\dots\dots(4.89) \end{aligned}$$

where submatrices S_A and S_B are composed of the shape functions or their local axes derivatives.

Using the constraints conditions of equation 4.88 gives equation 4.89 as:-

$$(G) = \left[\begin{array}{c} S_A \\ S_B \end{array} \right] - \left[\begin{array}{c} S_B \end{array} \right] \left[\begin{array}{c} C_B \end{array} \right]^{-1} \left[\begin{array}{c} C_A \end{array} \right] (P_A) \dots\dots\dots(4.90)$$

This is the final shape function array used in the evaluation of the geometric and mass matrices.

For computational coding convenience only the degrees of freedom corresponding to the two Loof nodes along an element side are associated with the midside node lying along that edge. Consequently, for practical purposes each midside node is assumed to have five nodal variables (3 displacements and 2 rotations) while each corner node has only three degrees of freedom (3 displacements).

4.7. Notation for Finite Element System (LUSAS)

Notation for finite element methods has become universally standardised. To avoid changing any of this notation in the context of the present work a separate notation is given for this chapter, 4, only.

B	strain matrix
C_{crit}	diagonal decay criterion
D_n	extensional modulus matrix
D_f	flexural rigidity matrix
E	modulus of elasticity for an isotropic material
e	eccentricity of a plate measured from the plane of the plate to the reference plane
F^e	element nodal force vector
I	unit matrix
J	the Jacobian matrix
\vec{J}	vector of covariant base vectors
\bar{J}	vector of contravariant base vectors
K	structure stiffness matrix
K^e	element stiffness matrix
L	area coordinates for a triangle
M	flexural moment components

M_x, M_y flexural moments per unit width perpendicular to the x and y axes, respectively

M_{xy} twisting moment per unit length perpendicular to the x axis

M_A, M_B constraint matrices referring to the wanted and unwanted variables respectively

M_{xi}, M_{yi} nodal moments about the x and y axes respectively

N shape functions

P vector of applied nodal loads

q distributed pressure acting on the surface of an element

\bar{R} rotation vector

\bar{S} slope vector

\bar{T} thickness vector

t thickness of plate

u, v, w global displacement components at a point

W shape function array

W_A, W_B partitions of the shape function array which refer to the wanted and unwanted variables respectively

W_C constrained shape function array

γ_{xy} shearing component of strain in the xy plane

γ_{xz}, γ_{yz} transverse shear strain components in the xz and yz planes respectively

δ vector of global displacements

δ vector of global displacements for an element

δ_A, δ_B element displacements associated with the wanted and unwanted variables

δ^* vectors of displacements and derivatives at any point within an element

ϵ strain vector

ϵ_x, ϵ_y normal components of strain in the x and y directions respectively

ϵ_y extensional strain components

ϵ_s transverse shear strain components

ϵ_f flexural strain components (curvatures)

ζ natural coordinate in the zeta direction

η natural coordinate in the eta direction

θ_x, θ_y rotations of normals to the mid-surface about the x and y axes respectively

θ_z rotation about the z axis

ν Poisson's ratio

ξ natural coordinate in the xi direction

σ stress vector

σ_x, σ_y normal components of stress in the x and y directions respectively

σ_n extensional stress components

σ_f flexural stress components (moments)

$\tilde{\sigma}$ smoothed stress components

σ_B bending stress

τ shearing stress

Type of code for innermost reduction loop, and tape reading action		Standard Fortran, & BACKSPACE-READ-BACKSPACE	Machine code, & random access disc	Percentage saving
Central processing time (secs)	Forward elimination	164	122	27
	Backsubstitution	19	11	40
	Total for problem	287	236	18
Total problem cost (central processing time + I/O)		59.3	44.7	25

Table 11. Comparison of computing costs for the solution of a problem with and without the machine code and random access facilities.

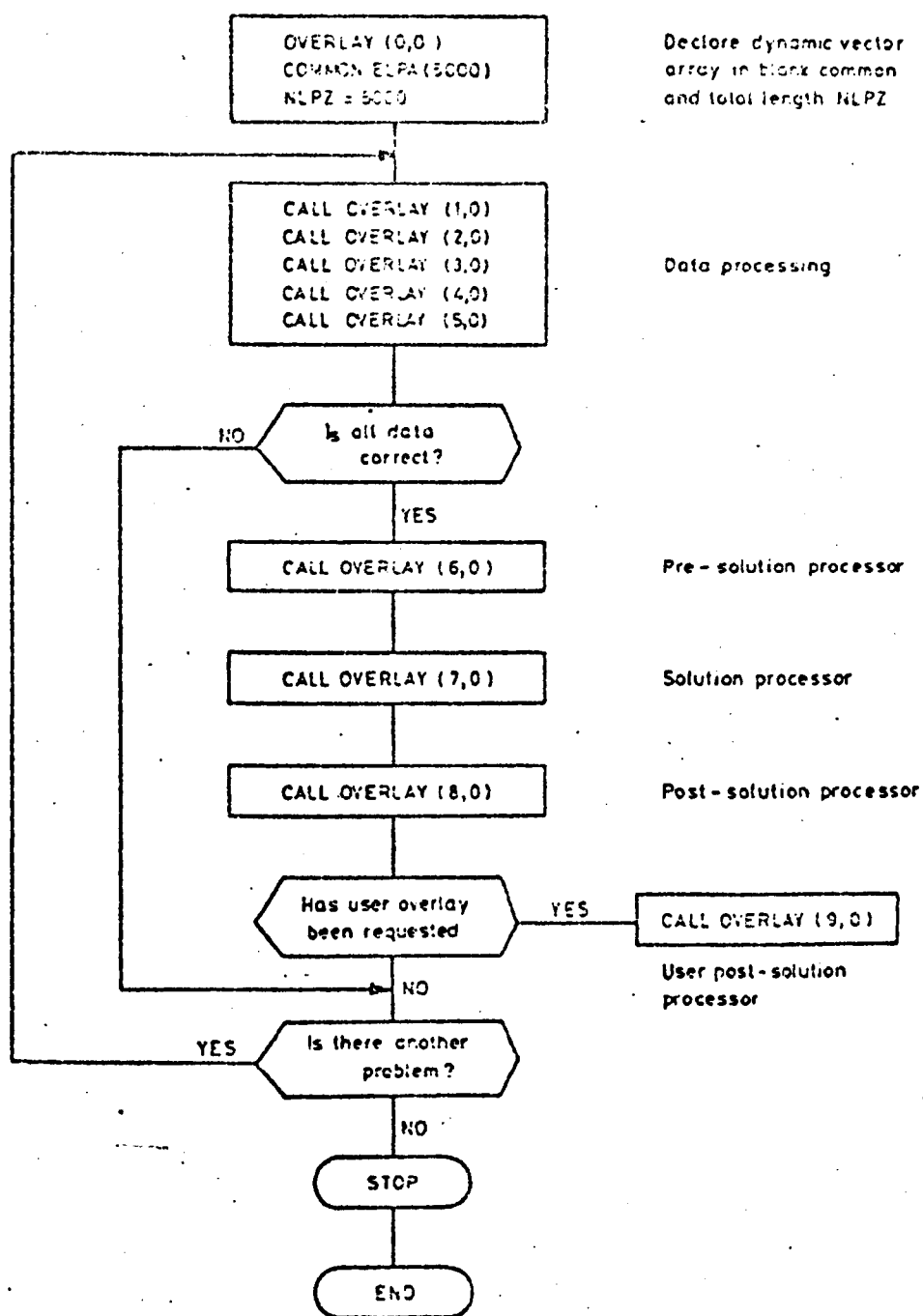


Figure 50. Flow diagram of main program overlay of LUSAS.

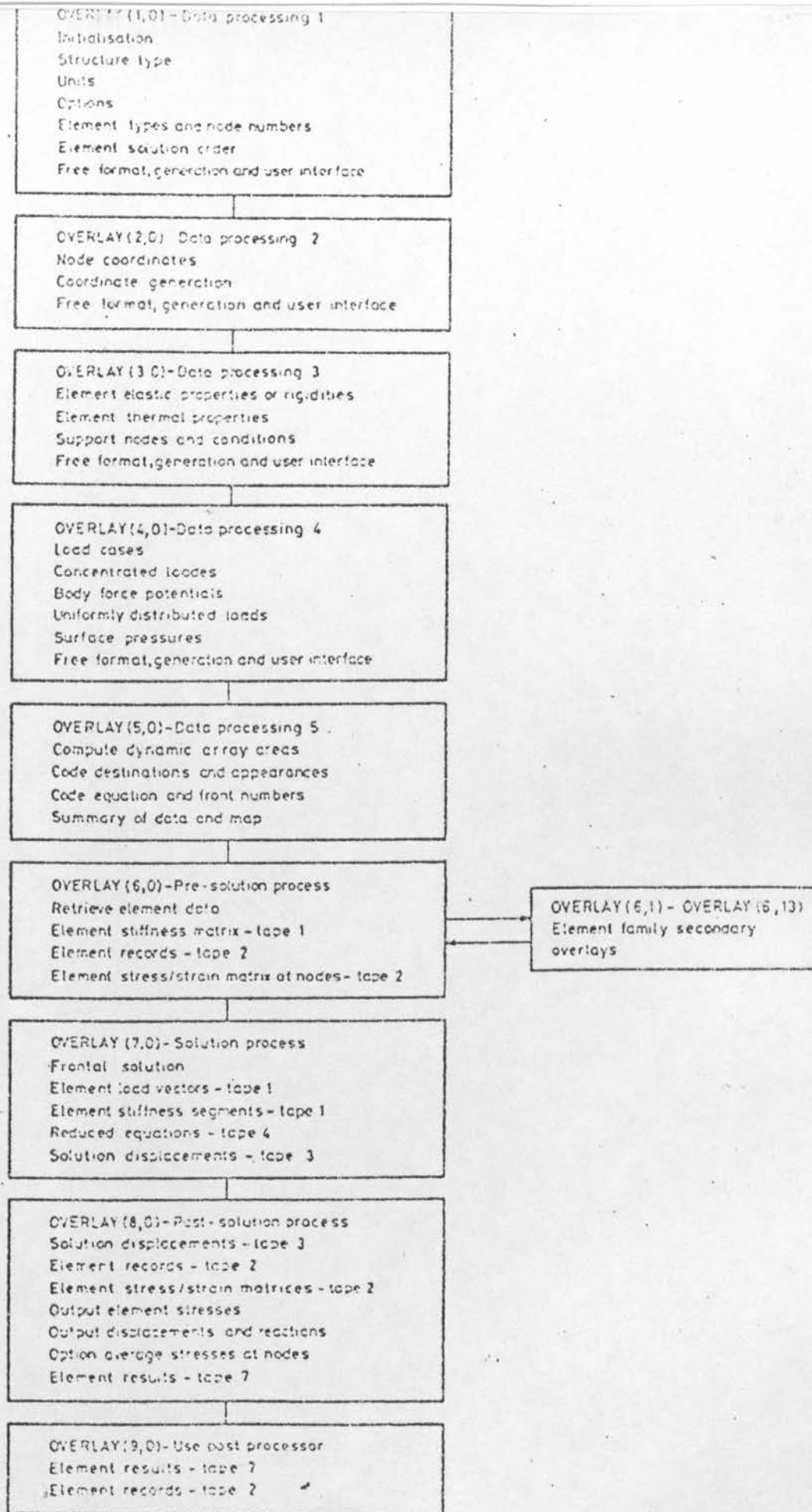


Figure 51. Primary and secondary overlay structure of LUSAS.

[illegible][illegible]

Element variables record 1	LNODES Element node numbers	NODVAR Element nodal variables	LNODS Element node destinations	LSPTDS Element support node destinations	LNODAP Element node appearance codes	ELXYZ Element coordinates	ELPR Element elastic properties	ELTHPR Element thermal properties	ELSUCO Element support values
L1	L2	L3	L4	L5	L6	L7	L8	L9	L10
LSUCO Element support codes	CBF Element constant body forces	BFP Element body force potentials	STRSI Element nodal initial stresses/strains	KG Element global stiffness matrix	RDC Element rotated basis direction cosines	STRSIG Element Gauss point initial stresses/strains	MG Element global mass matrix		
L11	L12	L13	L14	L15	L16	L17			
LNODV Element nodes for each variable	LDISV Element equation numbers	LFNTV Element front destinations	LNSTRS Element variable appearance codes	ELRHS Element load cases					
L21	L22	L23	L24	L25					
Element variables record 2									
M1	M2								

- 171 -

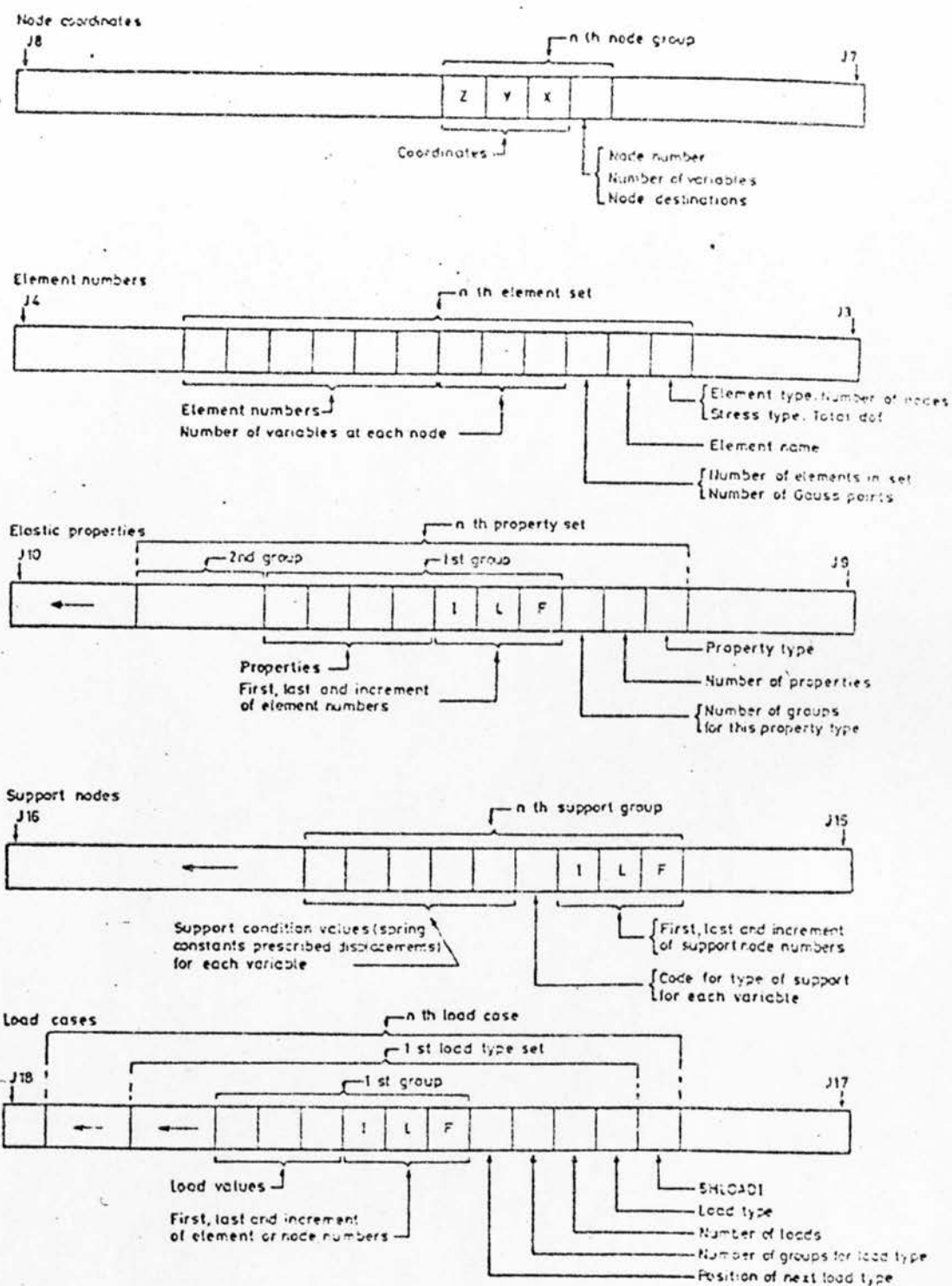
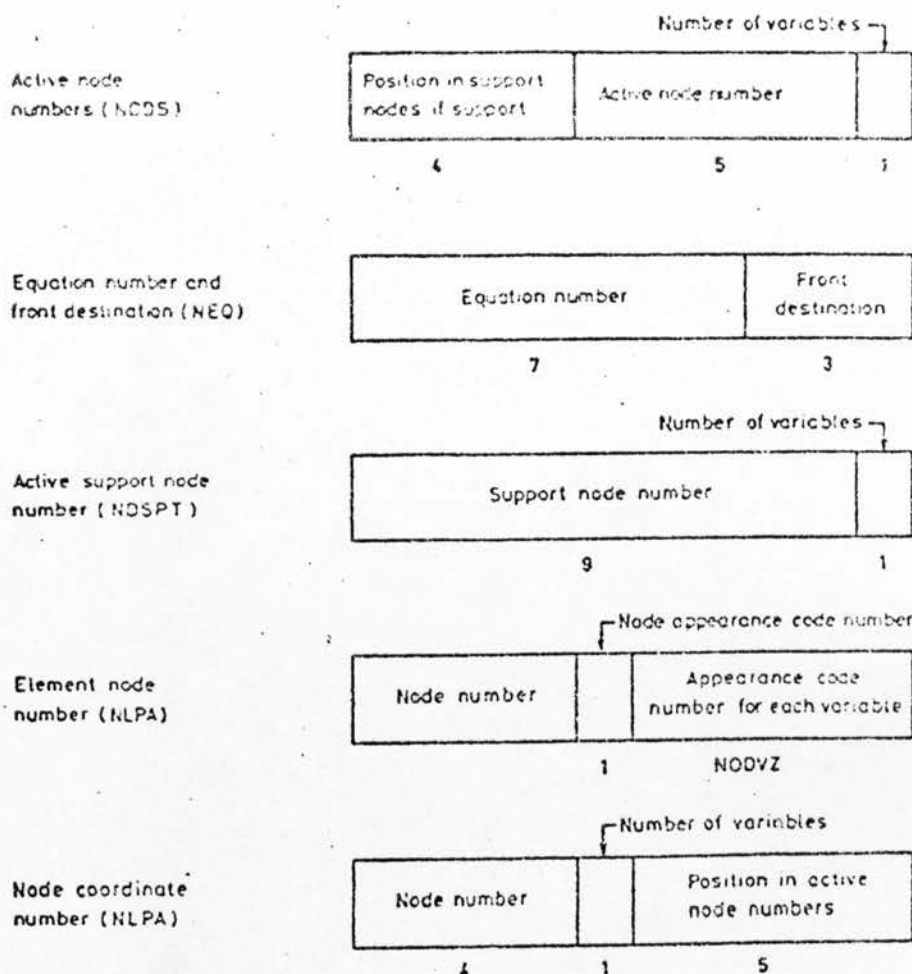


Figure 53. Data structure for arrays during data processing.



Node and variable appearance code numbers

Inactive	= 0
Intermediate appearance	= 1
Last appearance	= 2
First and last appearance	= 3
First of several appearances	= 4

Figure 54. Computer word structure for various arrays after integer compaction at end of data processing.

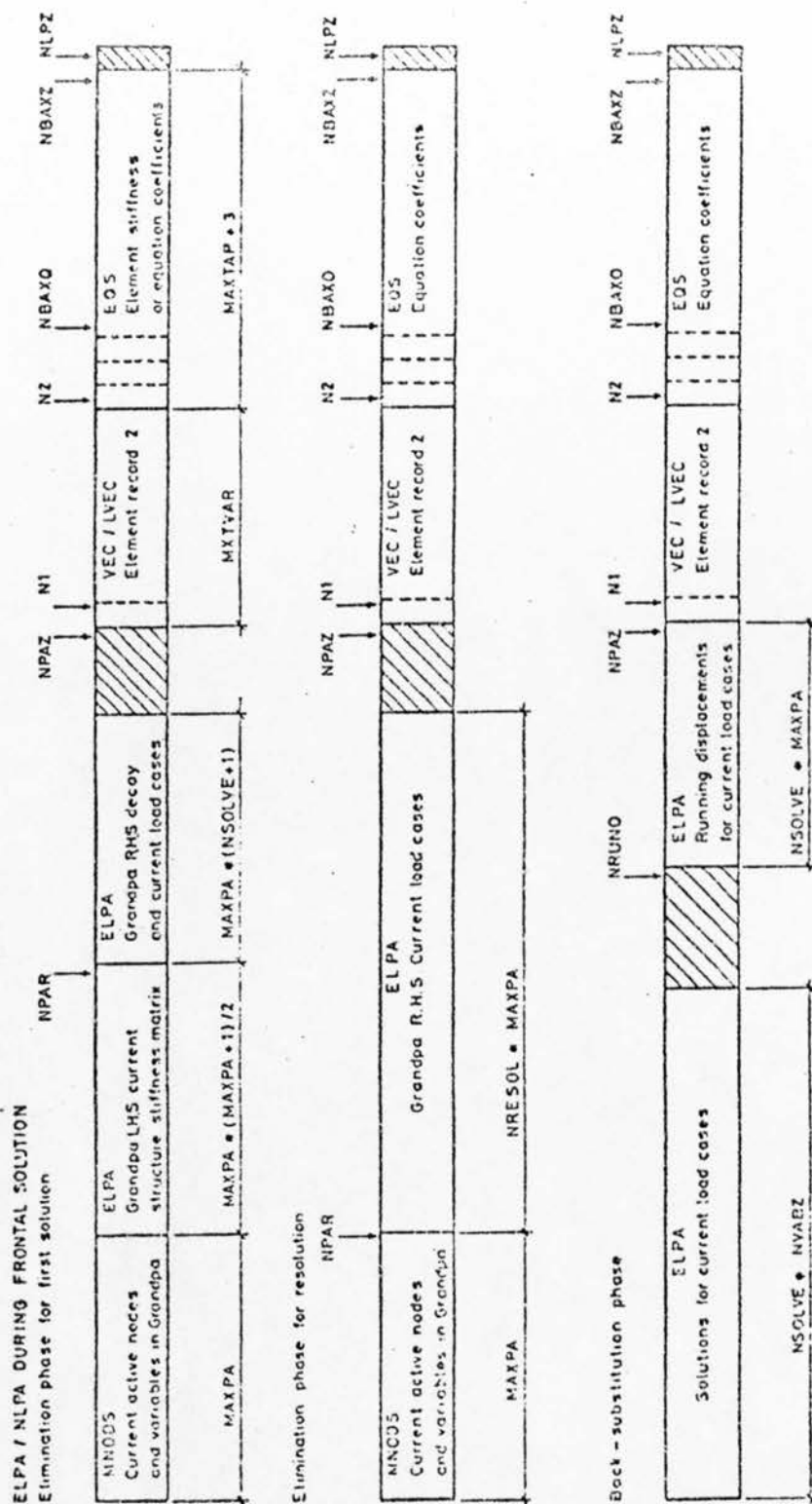
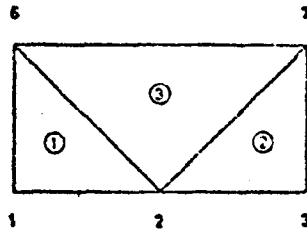


Figure 55. Dynamic vector array during frontal solution.

	11 (M2)	12	13	14	15	16	17	18	19	20	21
Individual element record 1	Individual element record 2	DISP Elemnt displs	STRESS Elemnt nodal stresses/strains	STRSG Elemnt Gauss pt. stresses/strains	SG Elemnt stress matrix	NODS Active node numbers	NDSPT Active support node numbers	RMSG Global solution displ vector	RHS Solution displ vector	REACT Reactions at support nodes	AVGSD Average stresses at nodes
LSGMAX	NORMAX	NDS5 * MYLNDZ	NDS5 * MXGP	NSG	NACNDZ	NACSPT	NODVZ * NACNDZ	NVABZ	NODVZ * NACSPT	IND * LACNDZ	

LGSMAX	=	maximum length of combined individual element records
MXTVAR	=	maximum length of element record 2
NACINDZ	=	total number of active nodes (nodes with variables)
NDOUVZ	=	maximum number of variables at a node
NACSP1	=	total number of active support nodes
NAXFA	=	maximum number of variables that appear in the solution front
NSOLVE	=	number of load cases to be processed during first solution phase
NIKISQ	=	number of load cases that can be processed during resolution or back substitution phase
NIKATAP	=	maximum size of buffered element stiffness records or equation coefficients
NVABZ	=	total number of equations for problem
NDSMAX	=	maximum number of variables for an element
NDS5	=	total number of stresses and strains at a point
MXINDZ	=	maximum number of element nodes
MXGP	=	maximum number of Gauss points for an element
NSG	=	maximum size of element stress matrix
ND	=	maximum number of stresses at a point

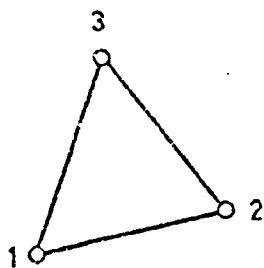
- 175 -



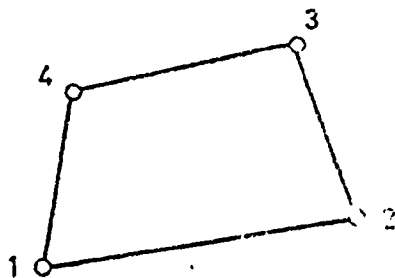
Element number	Element variables	Element destination vector	Position of variables in current overall stiffness matrix
1	1 2 6	1 2 3	1 ^e 2 6
2	2 3 7	2 1 4	3 ^e 2 6 7
3	2 7 6	2 4 3	2 ^e 6 ^e 7 ^e

◆ Element contributions complete, variable eliminated

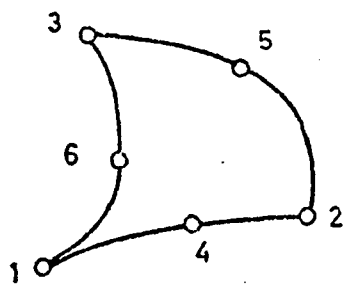
Figure 57. Simple example of housekeeping in the frontal solution procedure.



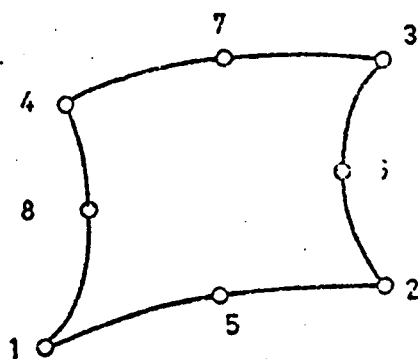
ISOFLEX 3.



ISOFLEX 4.



ISOFLEX 6.



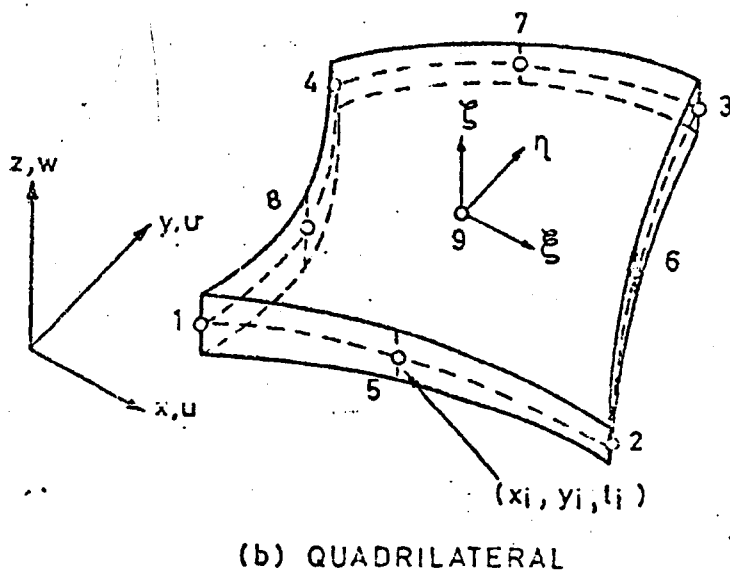
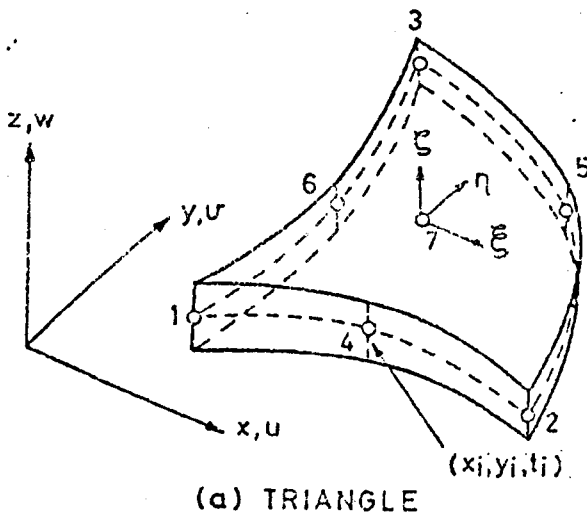
ISOFLEX 8.

Nodal variables

$$\delta_i = \begin{Bmatrix} w \\ \theta_x \\ \theta_y \end{Bmatrix}_i = \begin{Bmatrix} w \\ \frac{\partial w}{\partial y} \\ -\frac{\partial w}{\partial x} \end{Bmatrix}_i \quad \text{for corner nodes}$$

$$\delta_i = \{\Delta\theta_T\}_i \quad \text{for midside nodes}$$

Figure 58. The ISOFLEX family and nodal configurations.



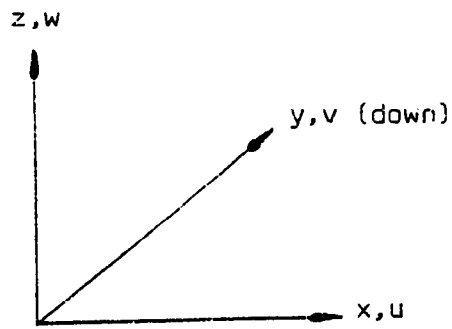
Nodal variables

$$\delta_i = \begin{Bmatrix} w \\ \theta_x \\ \theta_y \end{Bmatrix}_i \quad \text{for corner nodes}$$

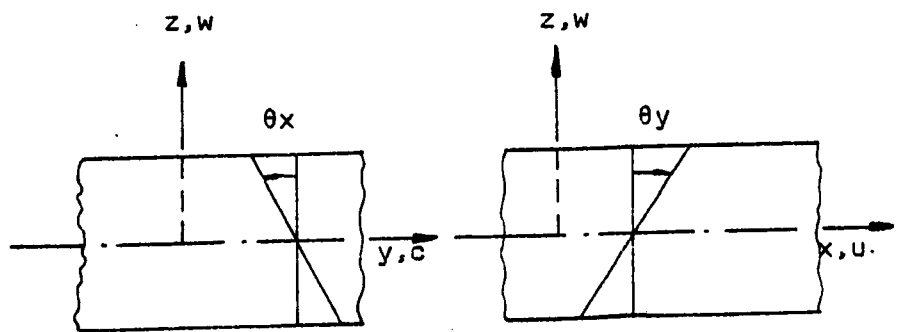
$$\delta_i = \begin{Bmatrix} \Delta w \\ \Delta \theta_x \\ \Delta \theta_y \end{Bmatrix}_i \quad \text{for midside nodes and central node of quadrilateral}$$

$$\delta_i = \begin{Bmatrix} \Delta \theta_x \\ \Delta \theta_y \end{Bmatrix} \quad \text{for central node of triangle}$$

Figure 59. Unconstrained element nodal configurations and co-ordinate systems.



(i) Right-handed cartesian co-ordinates



(ii) Positive θ_x and θ_y (right-hand-screw rule)

Figure 60 - Global Co-ordinate System and Sign Convention

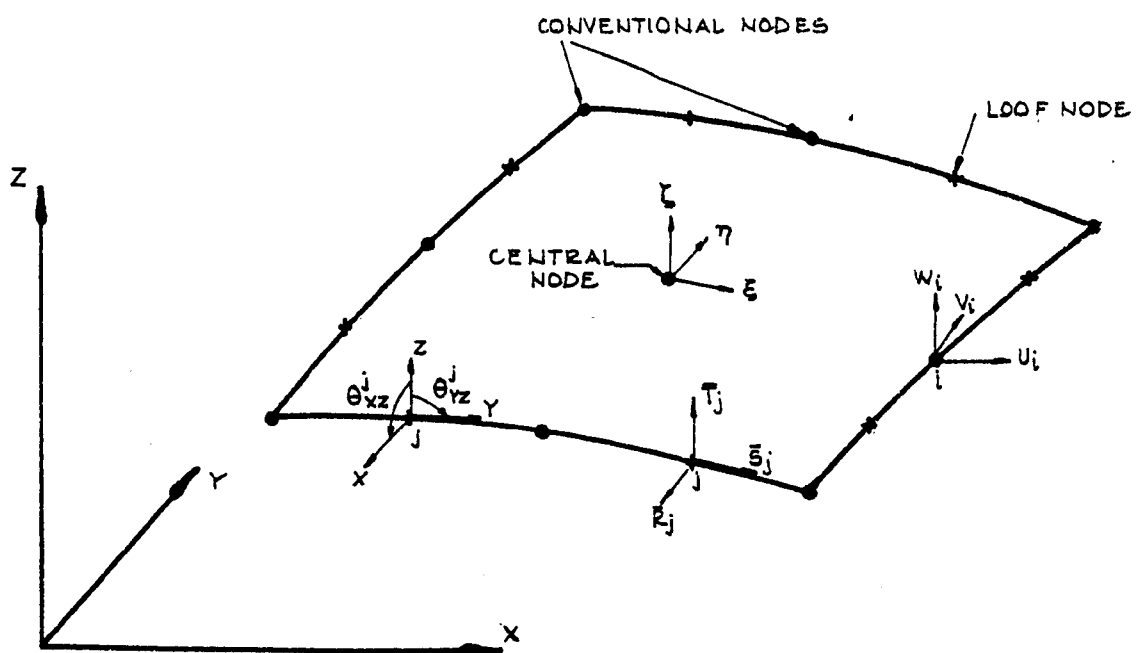


Figure 61. Node configurations of the SEMILOOF element.

CHAPTER 5

RESULTS OF FINITE ELEMENT ANALYSIS OF T-JOINTS WHICH WERE TESTED IN THE PRESENT INVESTIGATION FOR AXIAL AND BENDING LOADS

5.1. Finite Element Analysis

A range of T-joints in CHS has been analysed using the Lusas finite element system. The range of parameters studied has been:-

Beta (d_1/d_o) = 0.42, 0.53, 0.67, 0.77, 1.0

Gamma (d_o/t_o) = 18, 23, 32

This range of parameters corresponds to the range of T-joints tested as part of the experimental investigation described in Section 6.4.

Load systems applied have been:-

Axial load applied to the branch tube.

Bending load, applied as a lateral load to the branch tube.

Fairly coarse meshes were used (Figures 62-64) partly as a point of principle, also because the element (QSL8) was quite sophisticated. A mesh generation routine developed by Javadi⁸⁵ at Imperial College was used in order to simplify data generation. Half of the T-joint only was analysed for bending load and a quarter only for axial load. The use, therefore, of symmetry gave a considerable reduction in problem size.

In order to keep the results general and increase their range application the following decisions were taken:-

1. Stresses were plotted only for given lines of interest on the T-joint structure. These lines are clearly defined and are commonly chosen as being of interest. They are:-
 - a. Branch edge
 - b. Branch centre line

- c. Chord crown
 - d. Chord circumference
 - e. Intersection line of chord and branch (See Figure 65)
- ii. These lines of interest have been reduced to dimensionless form by expressing distances to the plotted values as a ratio of the length of the line. The lines are, therefore all 100 long and distances to plotted points are plotted as percentages of 100.

This is possible since the finite element method takes no account of size factor in the joint analysis i.e. a geometrically similar but much larger joint would have the same stress distribution for a unit load.

- iii. Stresses plotted are for unit axial load and unit moment applied to the joint.

i.e. 1kN axial load
1kNm moment

Stresses output are in N/mm^2 .

The unit moment load was applied as a lateral load on the branch member at a fixed distance from the joint i.e. its free end. This, unfortunately, makes the moment load case uniquely applicable to the experimental tests carried out in the present test since in the analysis the effects of shear at the joint due to the lateral load will vary depending upon the distance from the joint at which the lateral load is applied.

5.2. Results of Finite Element Analysis of T-Joints

Stress distributions for a range of diameter ratios (β) and diameter to thickness ratios (γ) are plotted and shown in Figures 66-93.

The stresses given are in N/mm^2 and are for unit axial load (kN) and unit moment (kNm). Positions of stresses are plotted as non-dimensional axes varying from 0 to 100% of the line which is being studied.

For certain discrete points of interest - so called 'hot-spots' - the variation of stress within the joint parameters is plotted (Figures 94 & 95).

A major problem with presentation of this type of analysis is the enormous volume of data generated. For example, in the present investigation using a doubly curved shell element the data output for each element is:-

Membrane stress and strain.

Flexural stress and strain.

Top surface stress and strain.

Bottom surface stress and strain.

These stresses and strains are given for:-

Component in local Y plane.

Component in local X plane.

Component in local XY plane.

Maximum principal component.

Minimum principal component.

For the present investigation the stresses plotted are the maximum and minimum principal for the top and bottom surfaces.

At present there is no facility available for fully or even partially interactive graphics to be used for this type of analysis. The program developed at Kingston to plot the stresses shown uses standard plotting routines incorporated into a larger general system which reads data which has been manually extracted from the LUSAS output.

Work is continuing in this field and a full system of, at least, partially interactive graphics will soon be available. It will then be realistically possible to plot any, or all, of the data output from the analysis and this will be a major help in understanding, fully, joint behaviour under elastic loads.

In the present investigation the results given are of general interest and may later be the basis of a tabulated series of design charts which can be used to check local stress intensity when the engineer is assessing a system of joints for a proposed Vierendeel frame.

5.3. Conclusions

Valid discussion of Finite element results is difficult when comparing the results of theoretical elastic analysis and experimental ultimate load tests. Lyons has shown³⁶ that using the semi-loop shell element, even in relatively coarse meshes, gives convergence to the correct solution. Comparison between theoretical strains and measured strains is shown to be good.

The results of the present elastic analysis, which involved the variation of the parameters d_1/d_o and d_o/t_o , give a graphical representation of the stress distributions along lines of interest on the T-joint surfaces, inner and outer. There are no inconsistencies in the results obtained, and therefore, when plotted to a suitable scale the graphs may be used to obtain the stresses and strains at points of interest.

The general conclusions are thus:-

The magnitudes of the principal stresses and their points of application vary significantly with changing joint parameters d_1/d_o and d_o/t_o (figures 66 to 93).

Graphs of the major and minor principal top and bottom surface stresses have been plotted for axial load (figures 86 to 88) and bending load (figures 89 to 93). These stresses have been plotted for unit load and unit moment respectively and for dimensionless joint geometry.

Regions of high stress ("hot spots") occur in the vicinity of the intersection line between branch and chord member. These "hot spot" stresses are greater for moment load than for axial load, since under axial load there is a more even distribution of stress around the chord circumference.

Stress concentration factor, the relation between nominal (average) axial stress in the branch tube, and maximum stress in the joint, has been found to vary from 2.0 to 5.0 depending mainly on the parameter d_1/d_o rather than the parameter d_o/t_o i.e. the stress concentration factor decreases as d_1/d_o increases.

Axial load was found to cause a "hot spot" stress at point D (figure 94) i.e. the lowest point on the intersection line.

Moment load was found to cause a "hot spot" stress at points A and B (figure 95), particularly point B on the chord crown close to the intersection.

The degree of interaction of these two separate "hot spots", when they combine, depends upon the d_1/d_o ratio of the joint (see Chapter 7.3). This interaction is of interest not only for static joint strength but also for the study of the fatigue strength of this type of joint.

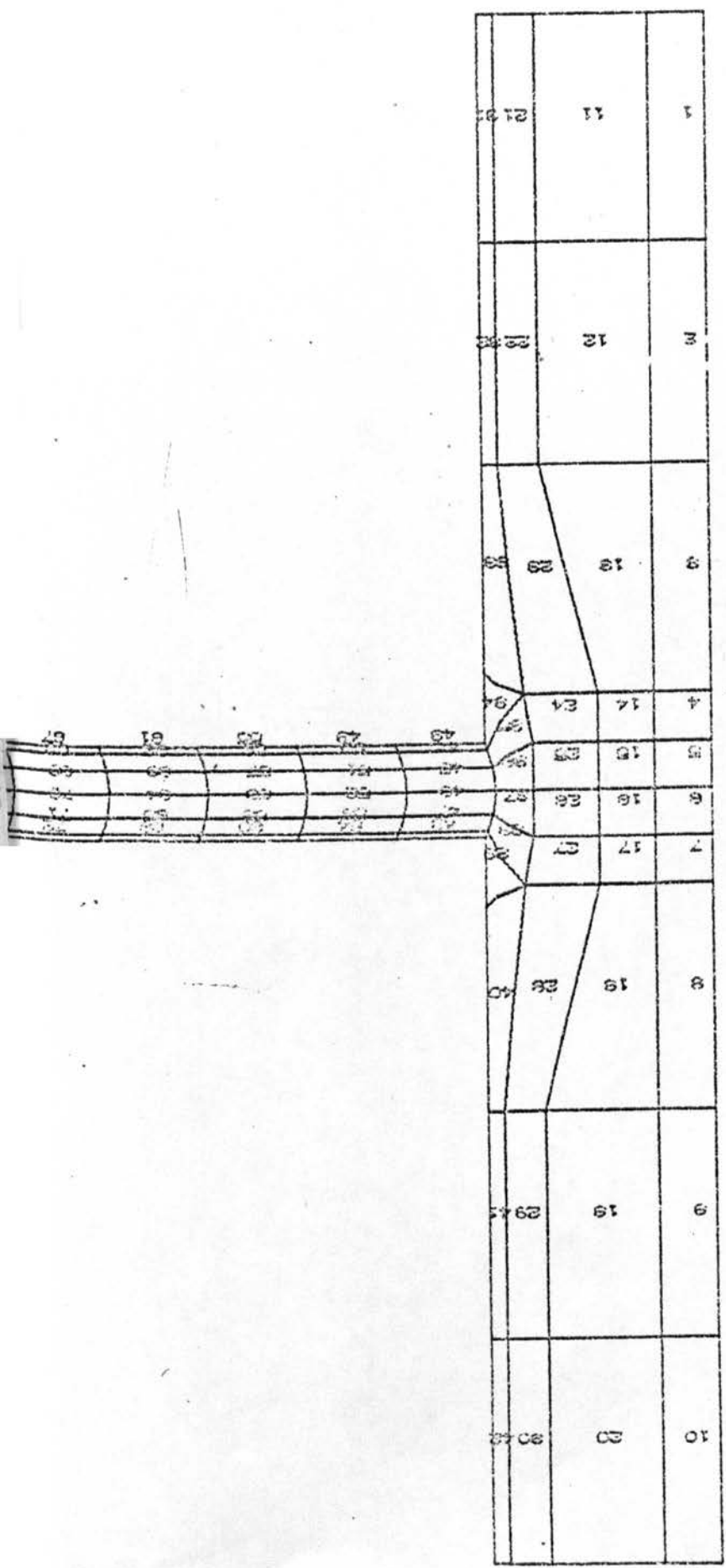


Figure 62. Finite element mesh for $\beta = 0.42$ - solution using semiloof shell elements.

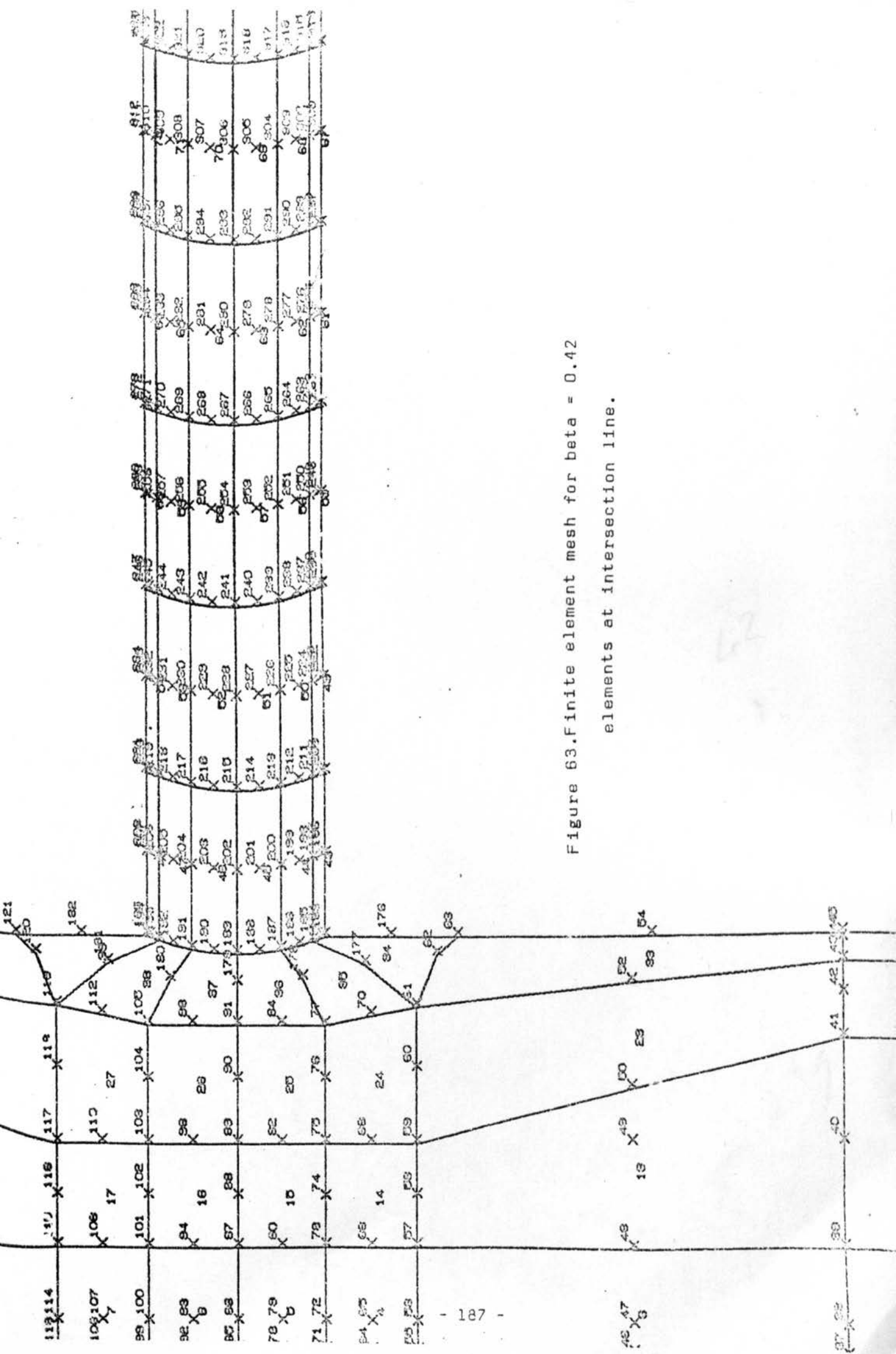


Figure 63. Finite element mesh for $\beta = 0.42$
elements at intersection line.

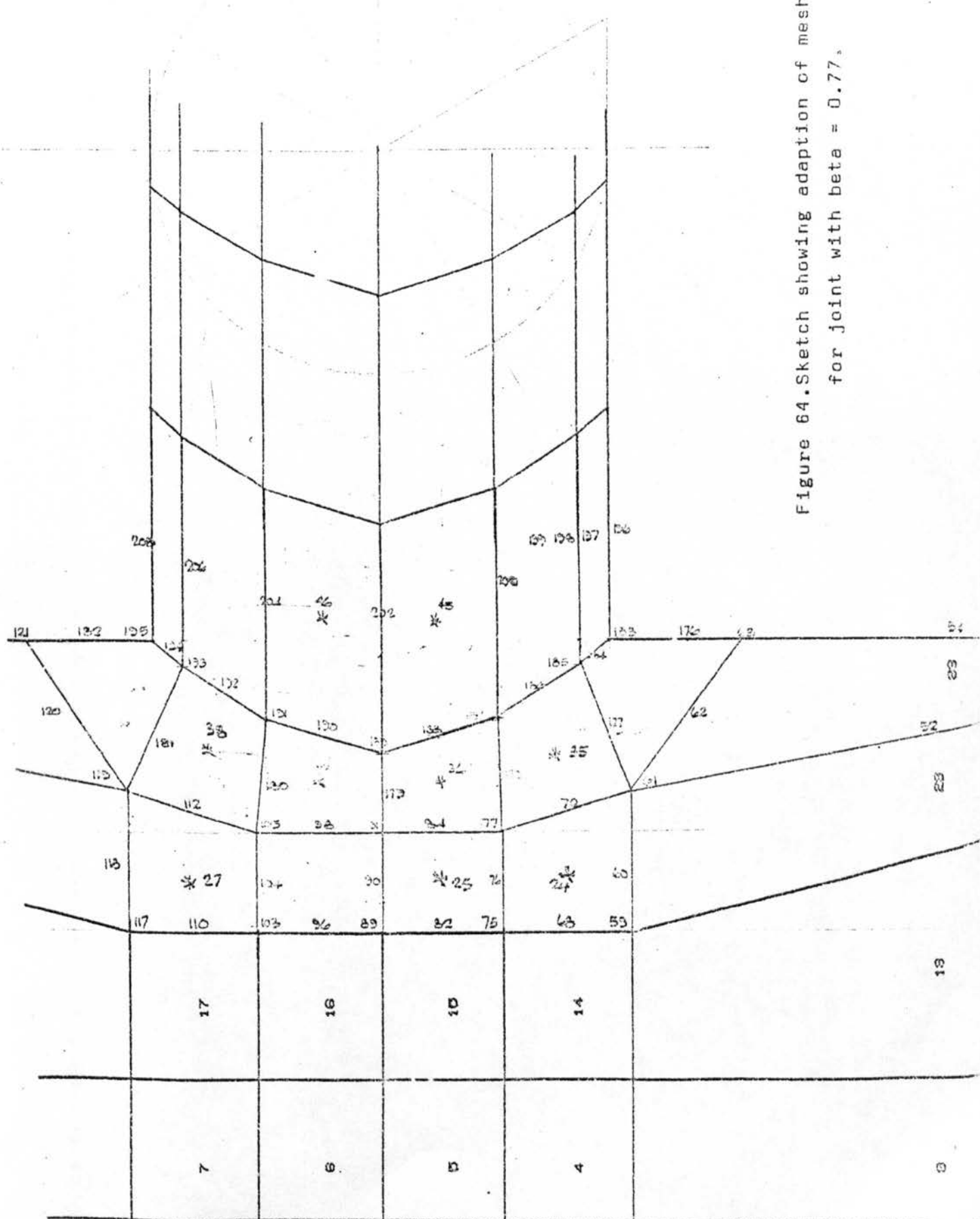


Figure 64. Sketch showing adaption of mesh for joint with $\beta = 0.77$.

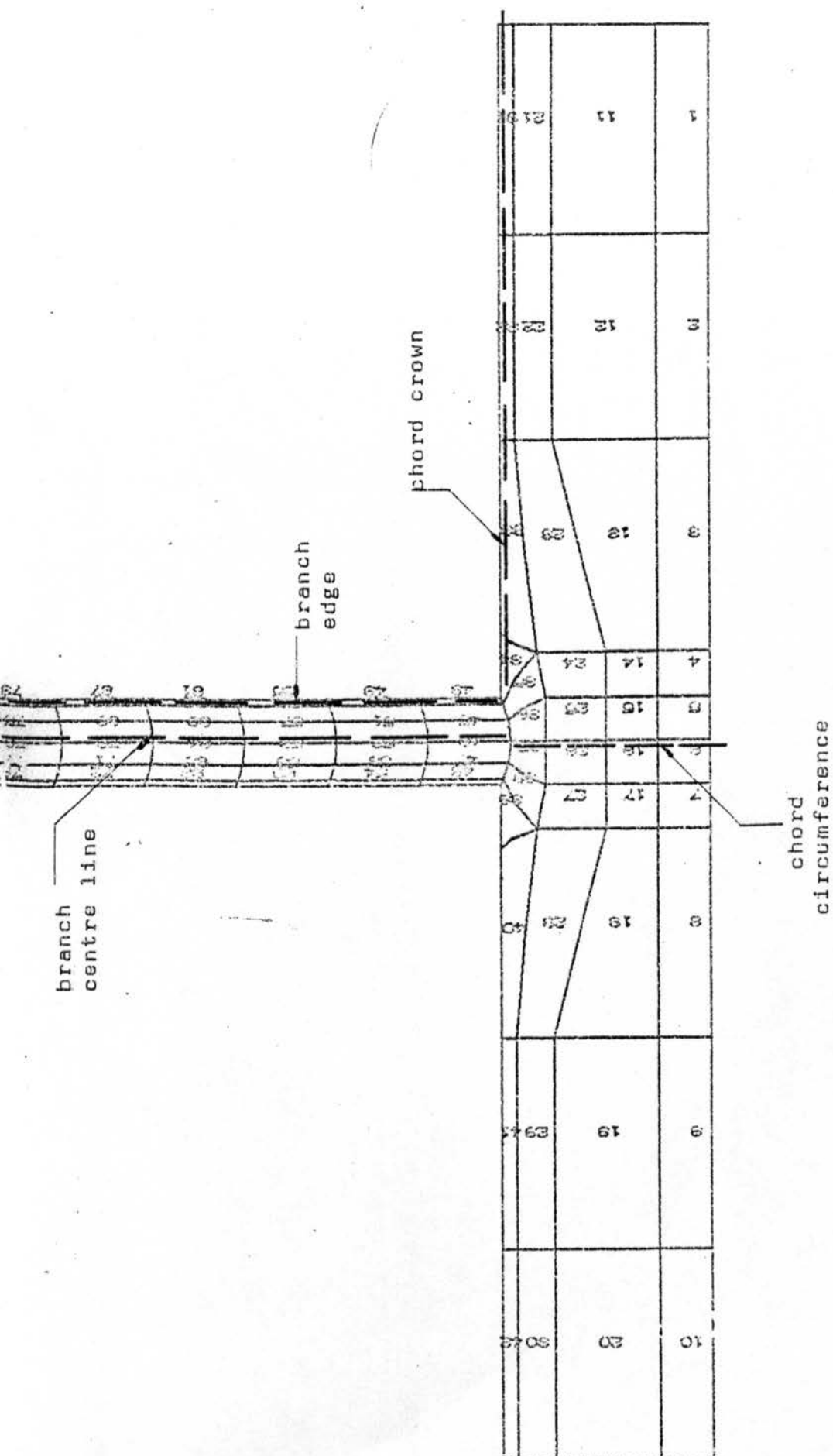
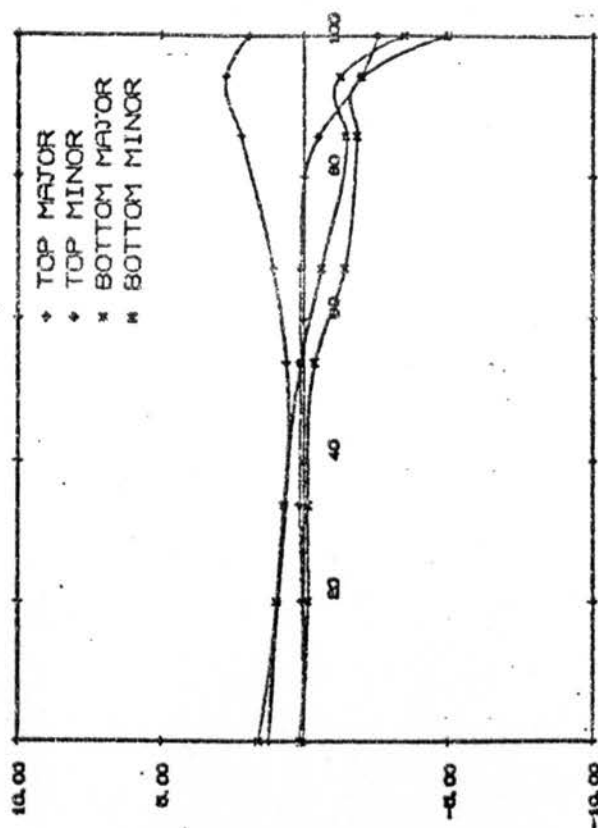


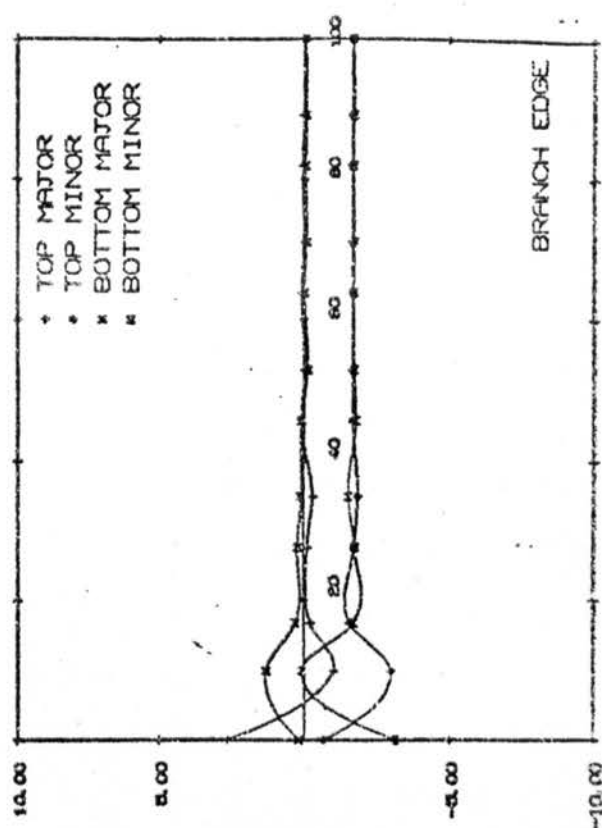
Figure 65. "Lines of interest" along which stresses have been plotted in Figures 66 - 93.

BETA = 0.42 D/T = 13



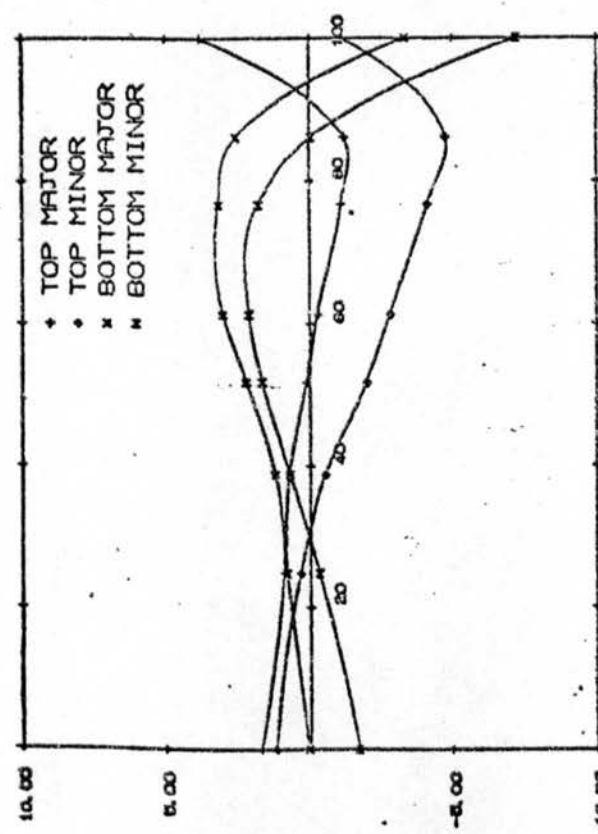
CHORD CROWN

BETA = 0.42 D/T = 18



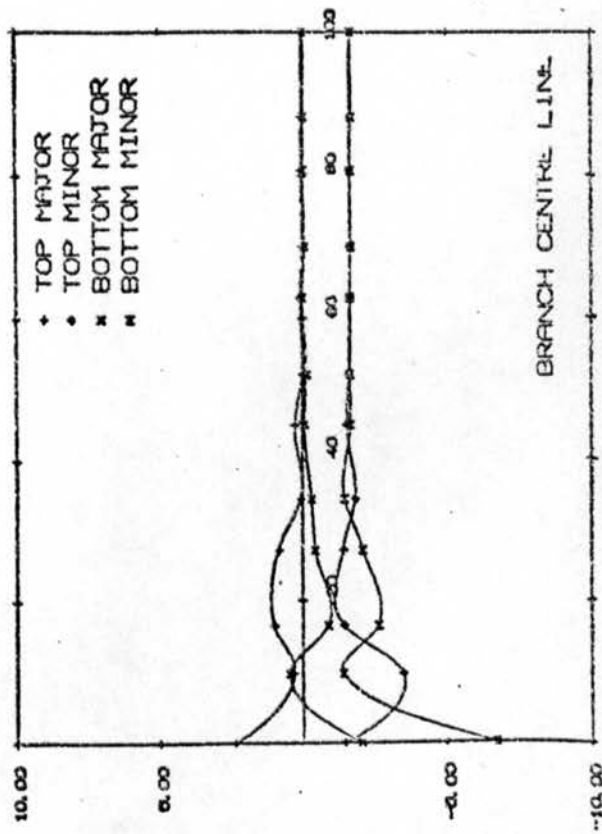
BRANCH EDGE

BETA = 0.42 D/T = 18



CHORD CIRCUMFERENCE

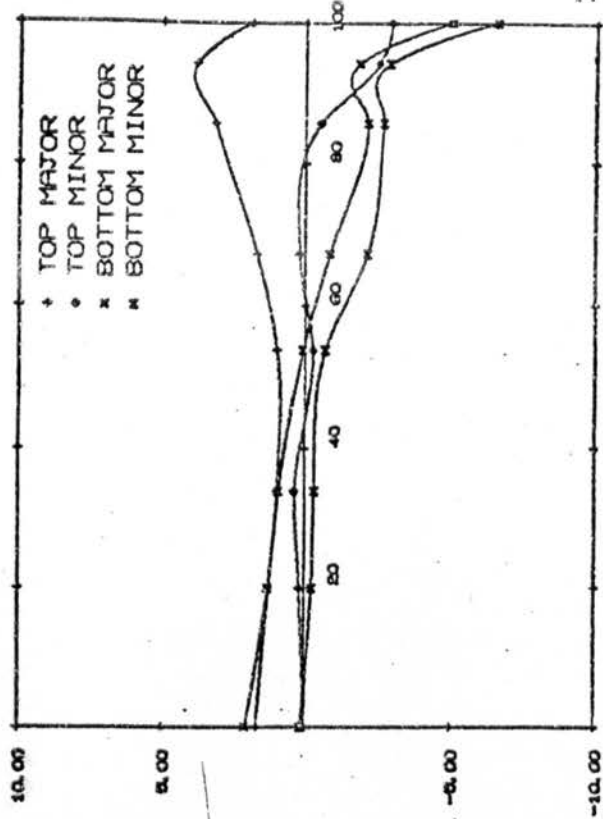
BETA = 0.42 D/T = 18



BRANCH CENTRE LINE

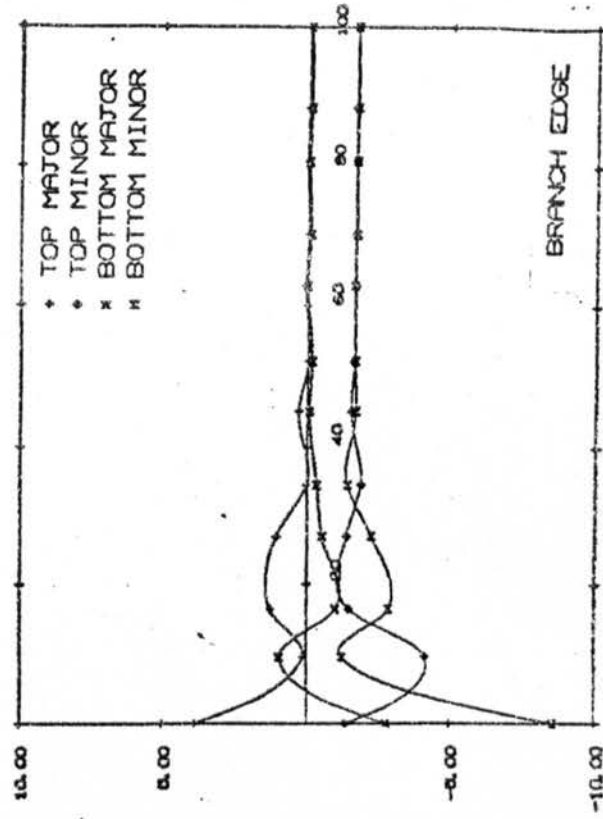
Figure 66. Stresses for unit axial load

BETA = 0.42 D/T = 23



CHORD CROWN

BETA = 0.42 D/T = 23

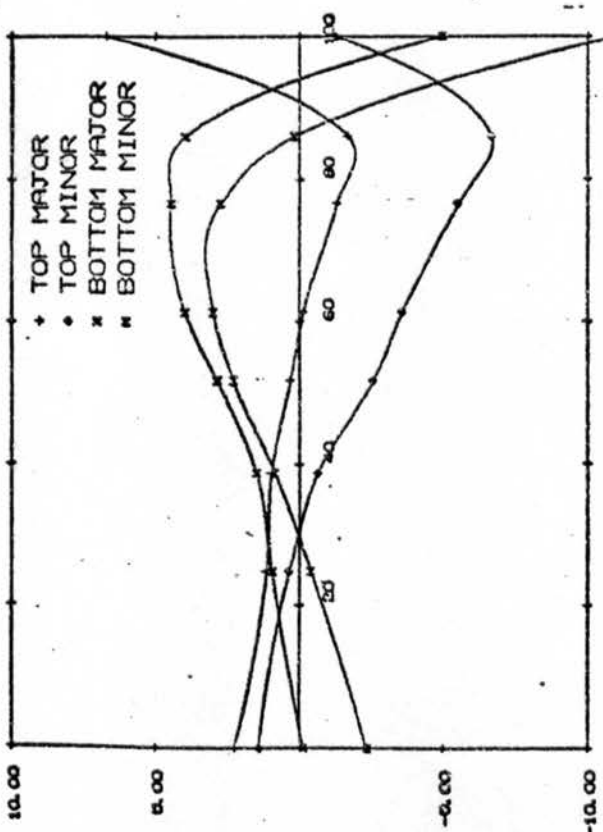


BRANCH EDGE

MAJOR AND MINOR PRINCIPAL STRESSES

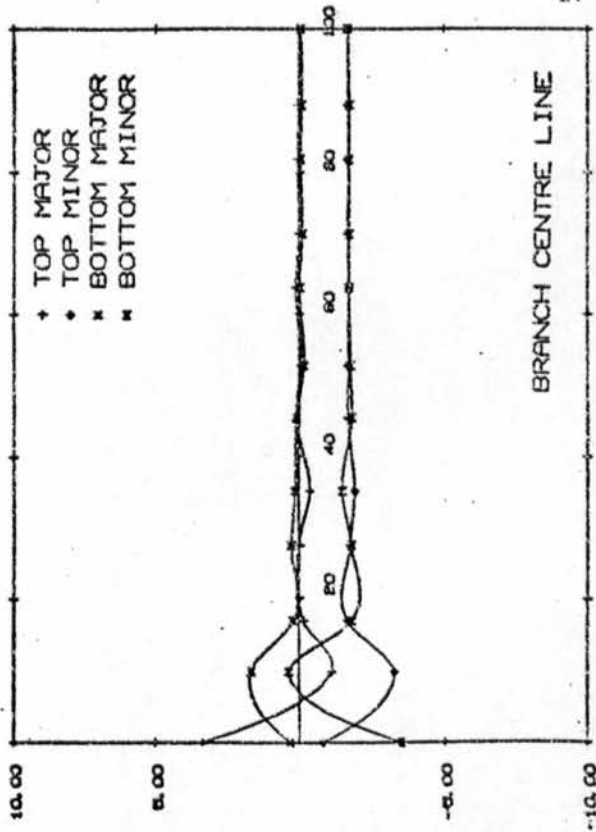
MAJOR AND MINOR PRINCIPAL STRESSES

BETA = 0.42 D/T = 23



CHORD CIRCUMFERENCE

BETA = 0.42 D/T = 23



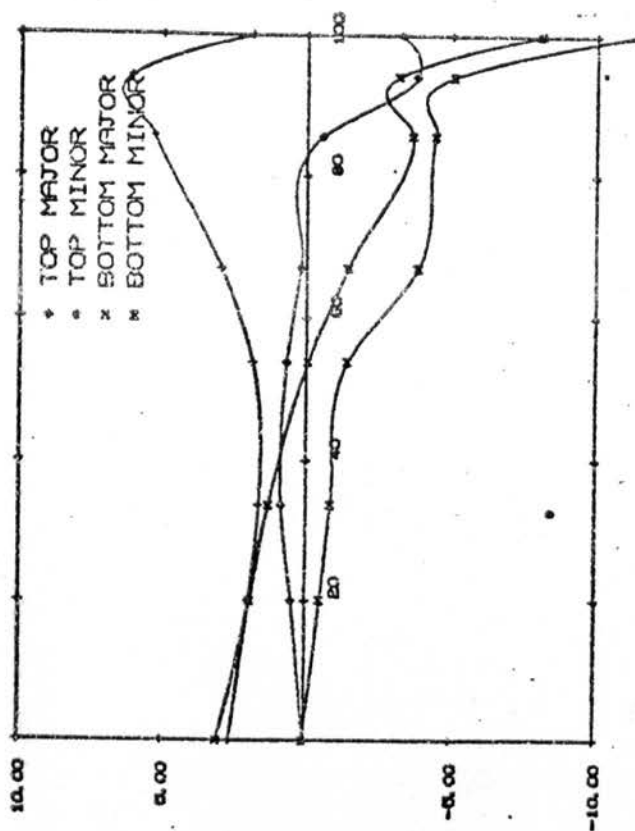
BRANCH CENTRE LINE

MAJOR AND MINOR PRINCIPAL STRESSES

MAJOR AND MINOR PRINCIPAL STRESSES

Figure 67. Stresses for unit axial load

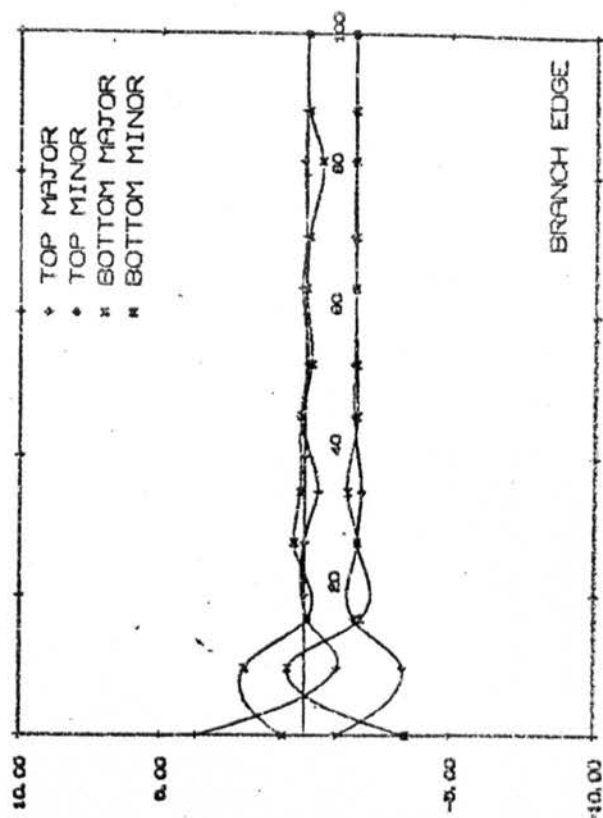
BETA = 0.42 D/T = 32



MAJOR AND MINOR PRINCIPAL STRESSES

CHORD CROWN

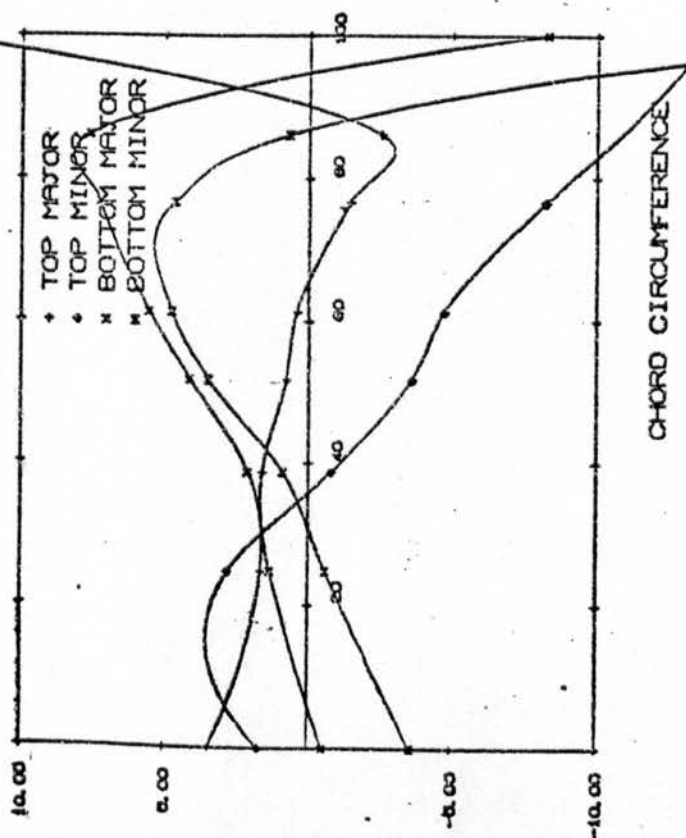
BETA = 0.42 D/T = 32



MAJOR AND MINOR PRINCIPAL STRESSES

BRANCH EDGE

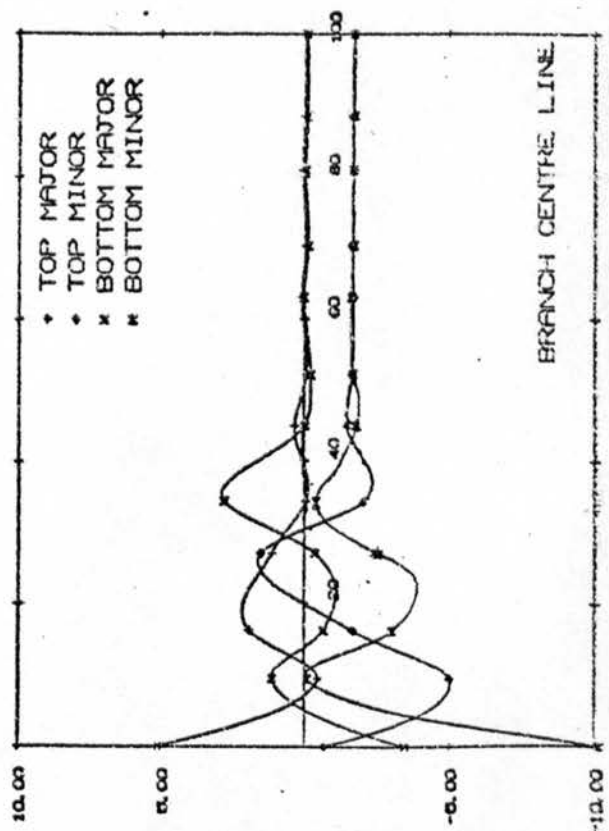
BETA = 0.42 D/T = 32



MAJOR AND MINOR PRINCIPAL STRESSES

CHORD CIRCUMFERENCE

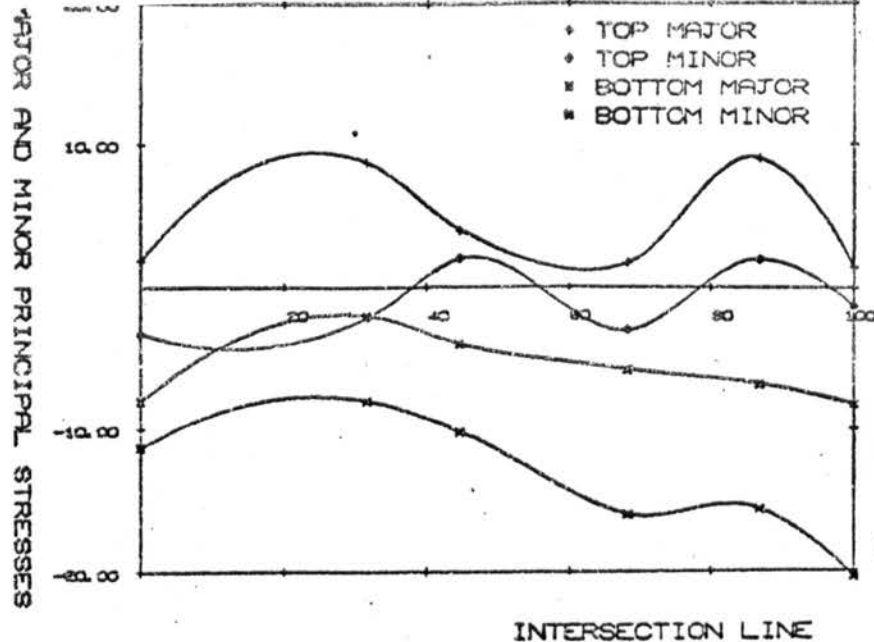
BETA = 0.42 D/T = 32



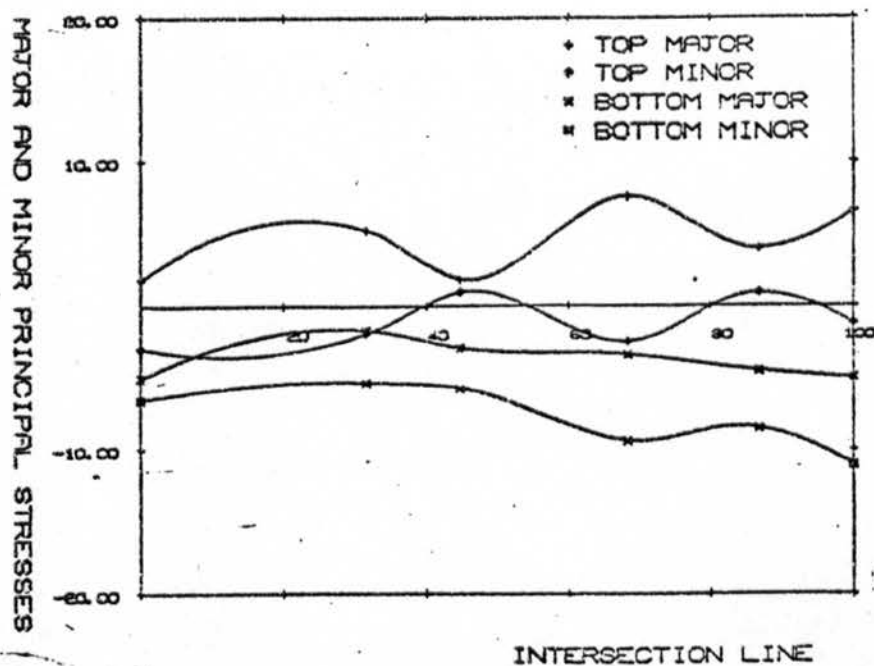
MAJOR AND MINOR PRINCIPAL STRESSES

BRANCH CENTRE LINE

Figure 68. Stresses for unit axial load.



BETA = 0.42 D/T = 23



BETA = 0.42 D/T = 18

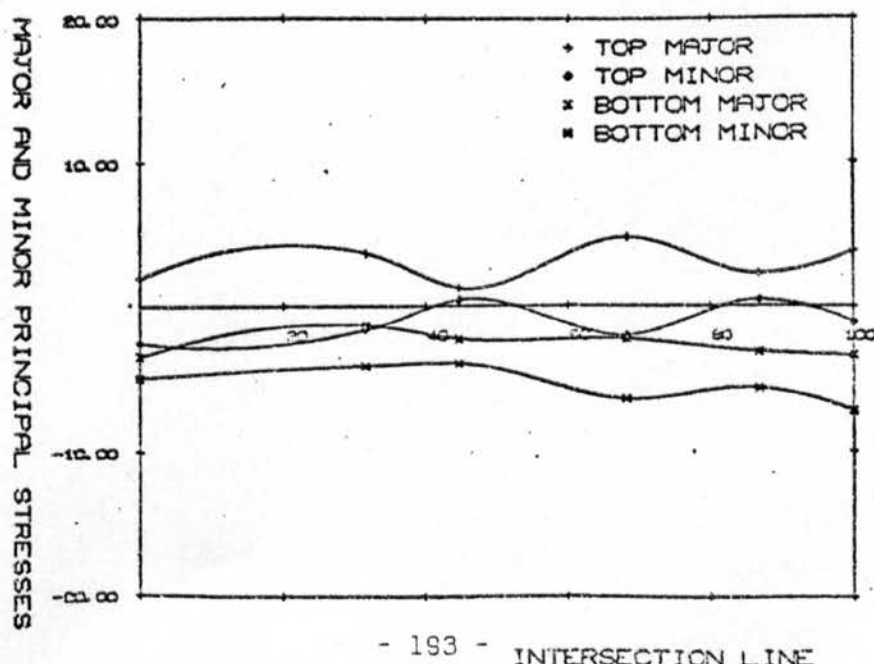
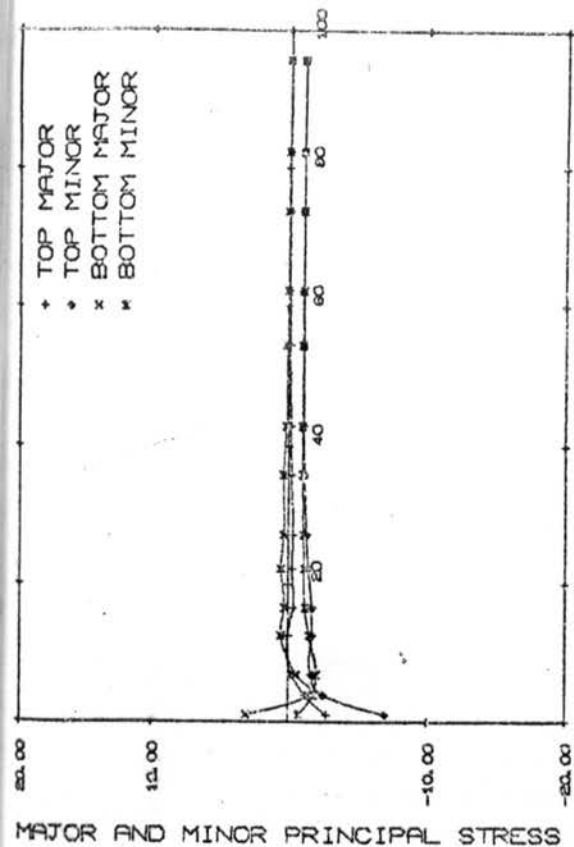
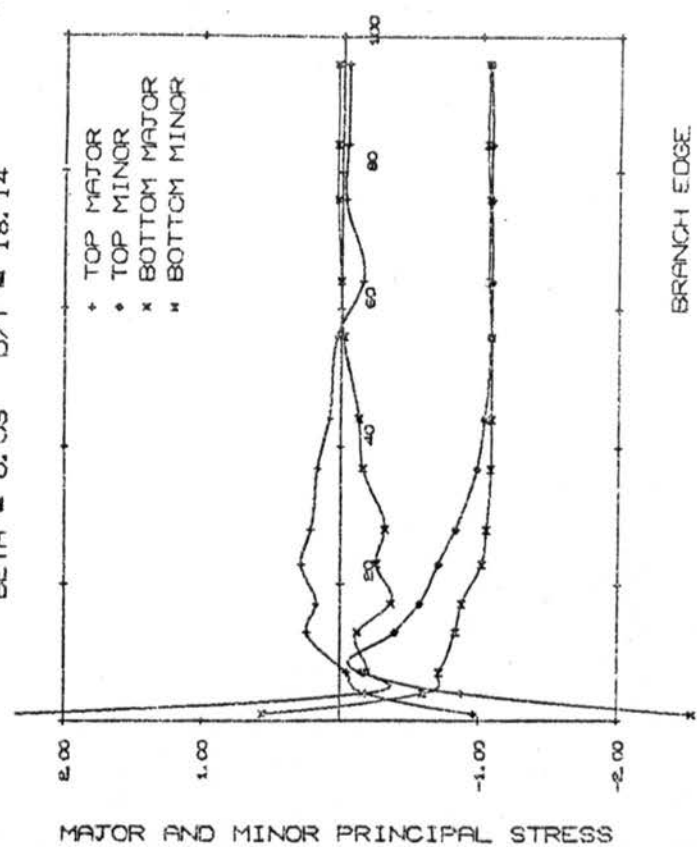


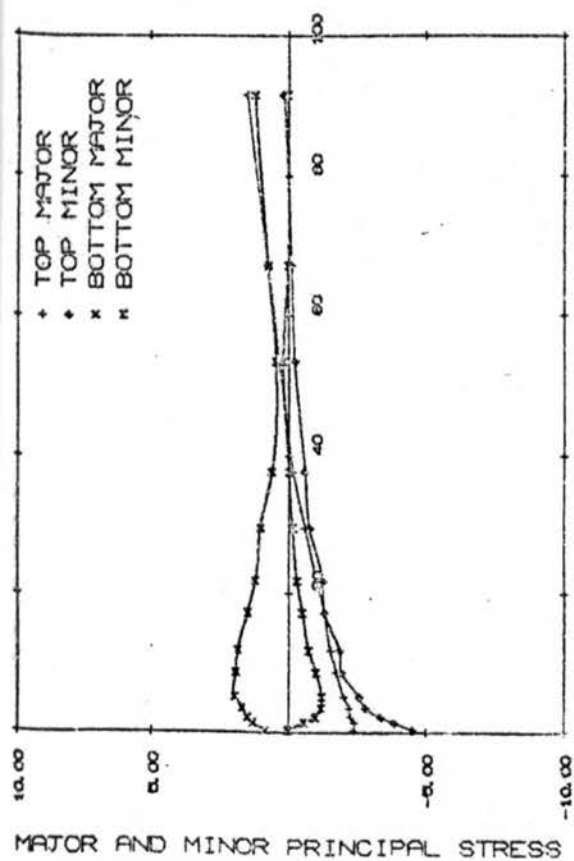
Figure 69. Stresses for unit axial load



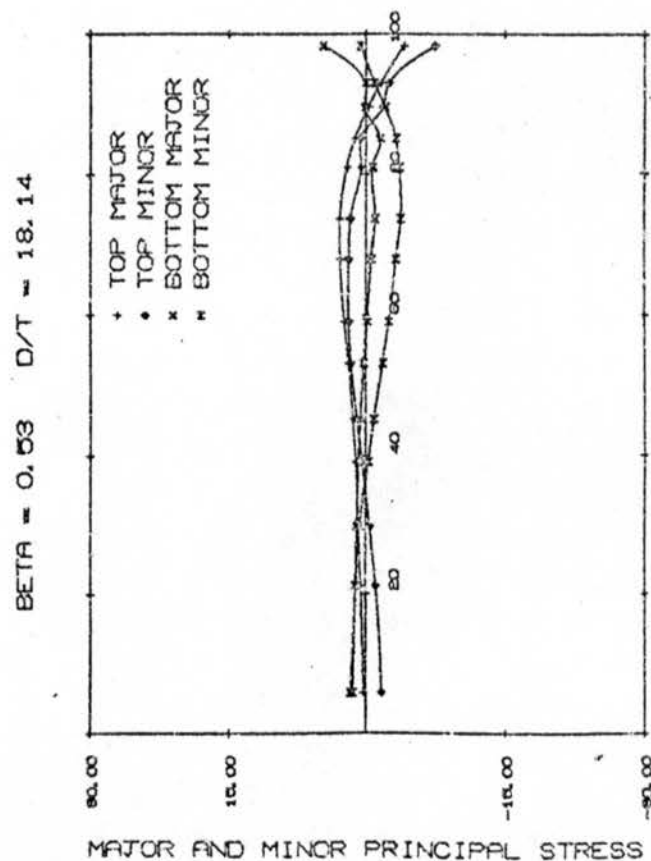
BRANCH CENTRE LINE



BRANCH EDGE

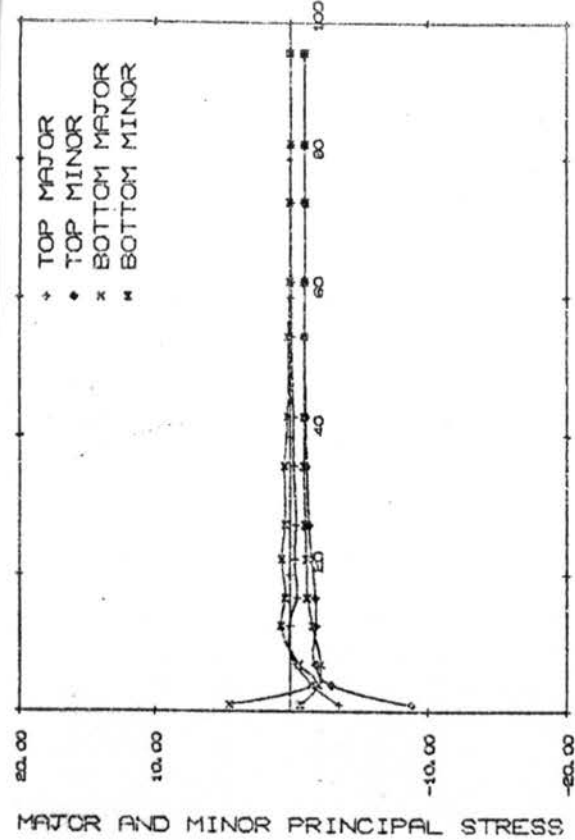


CHORD CROWN

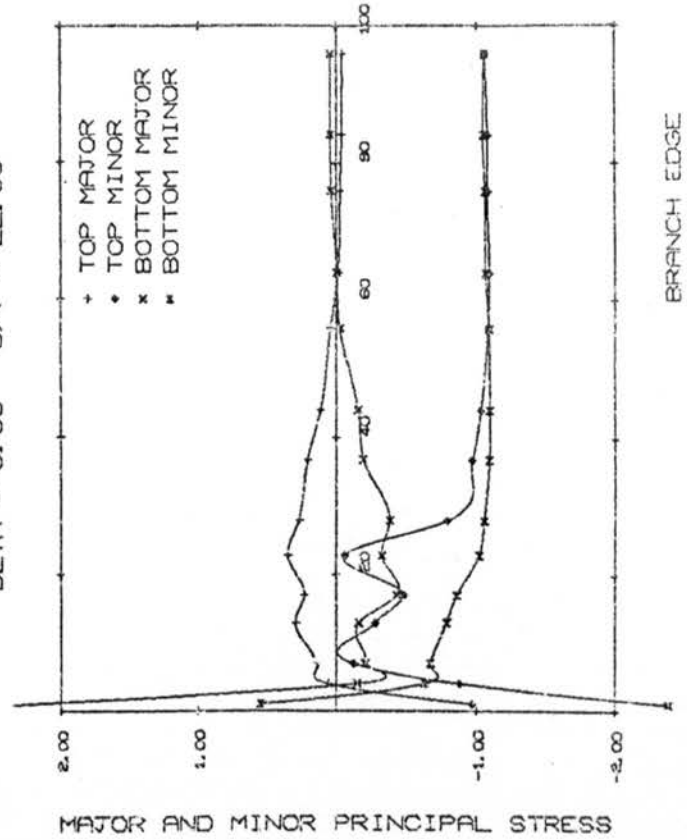


CHORD CIRCUMFERENCE

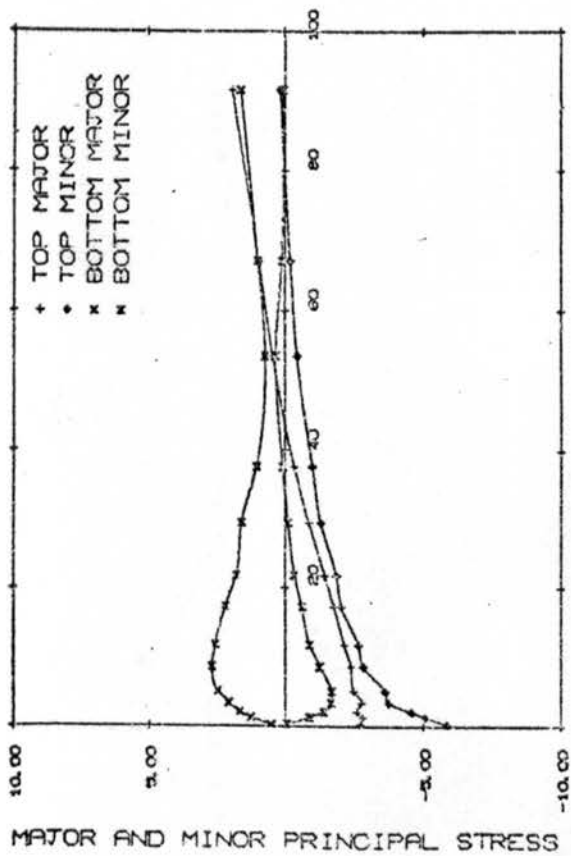
Figure 70. Stresses for unit axial load,



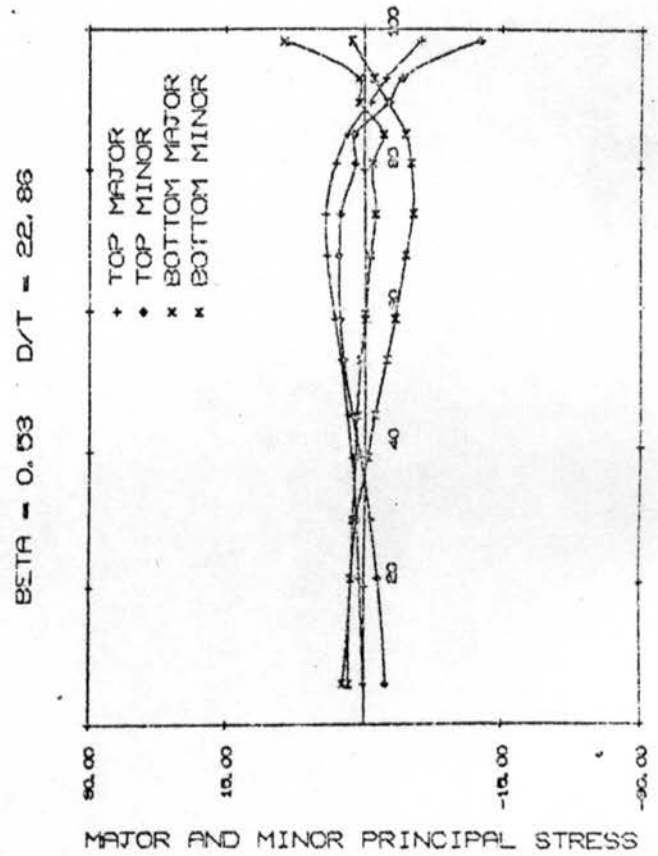
BRANCH CENTRE LINE



BRANCH EDGE

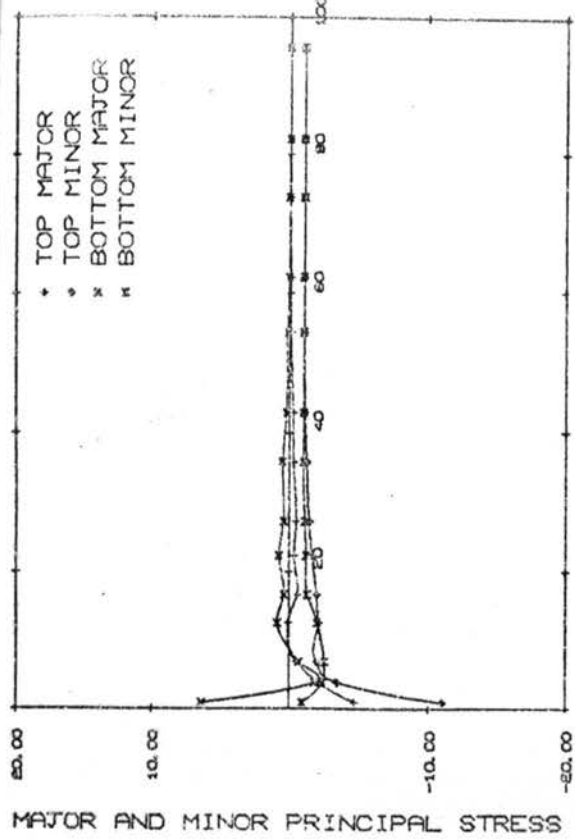


CHORD CROWN

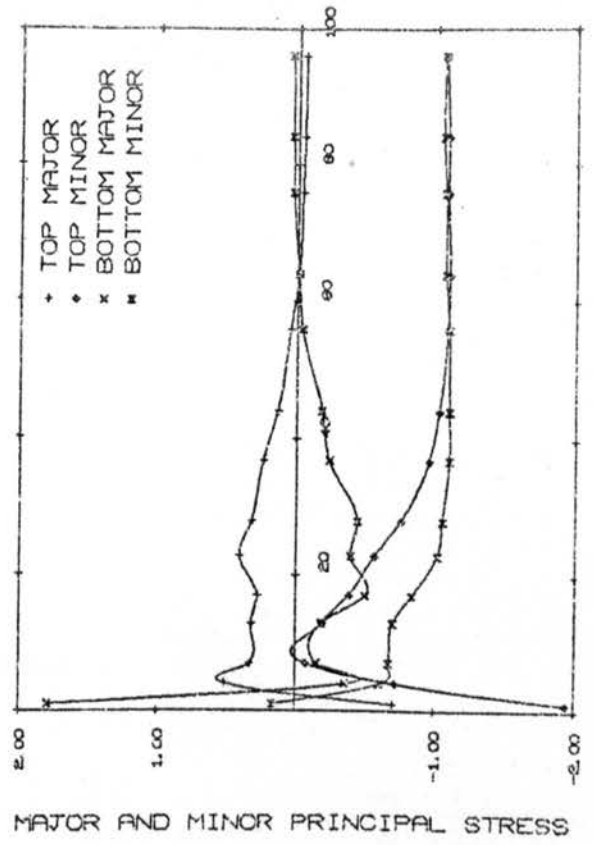


CHORD CIRCUMFERENCE

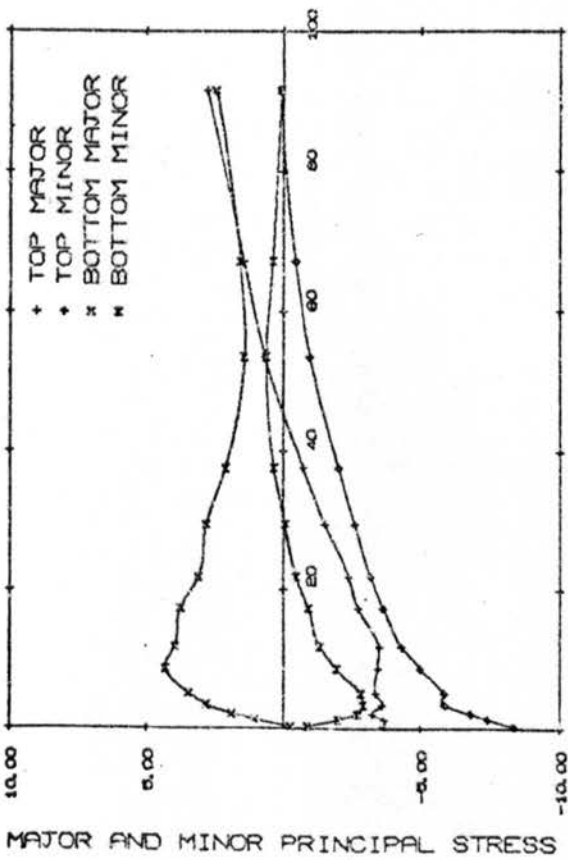
Figure 71. Stresses for unit axial load.



BRANCH CENTRE LINE

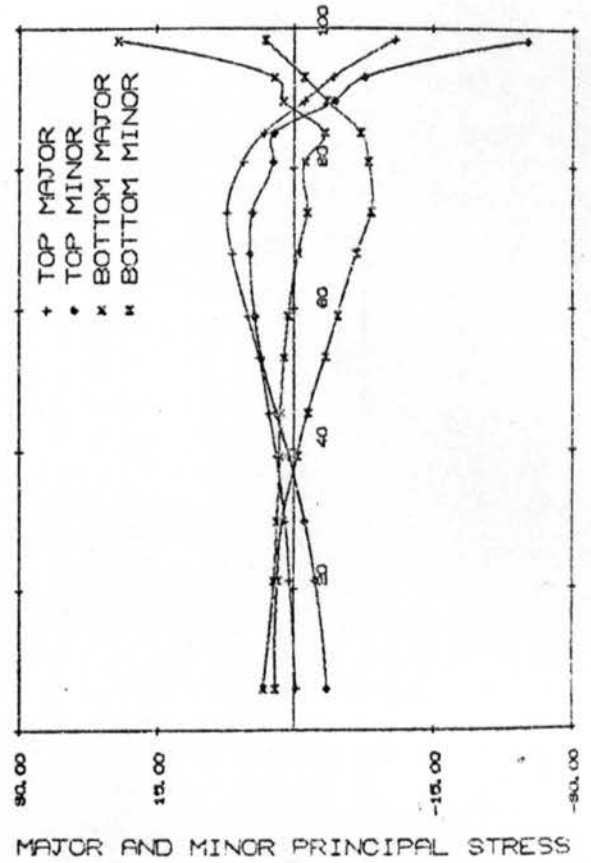


BRANCH EDGE



CHORD CROWN

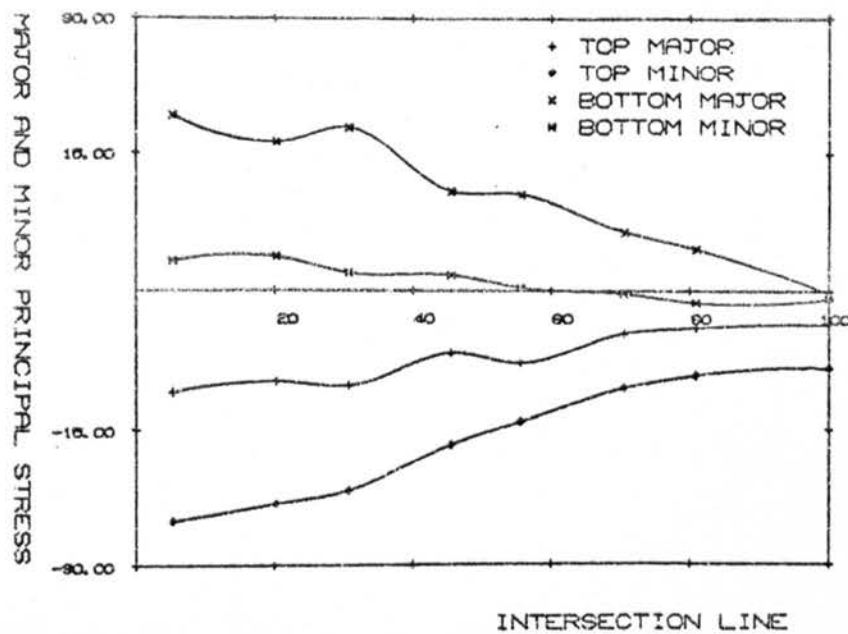
BETA = 0.53 D/T = 31.75



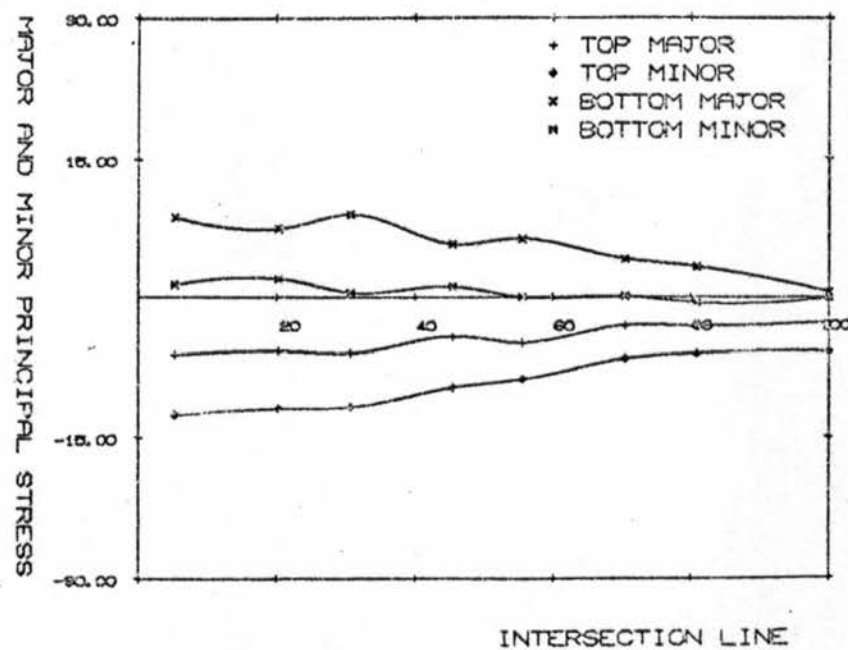
CHORD CIRCUMFERENCE

Figure 72. Stresses for unit axial load.

BETA = 0.53 D/T = 31.75



BETA = 0.53 D/T = 22.86



BETA = 0.53 D/T = 18.14

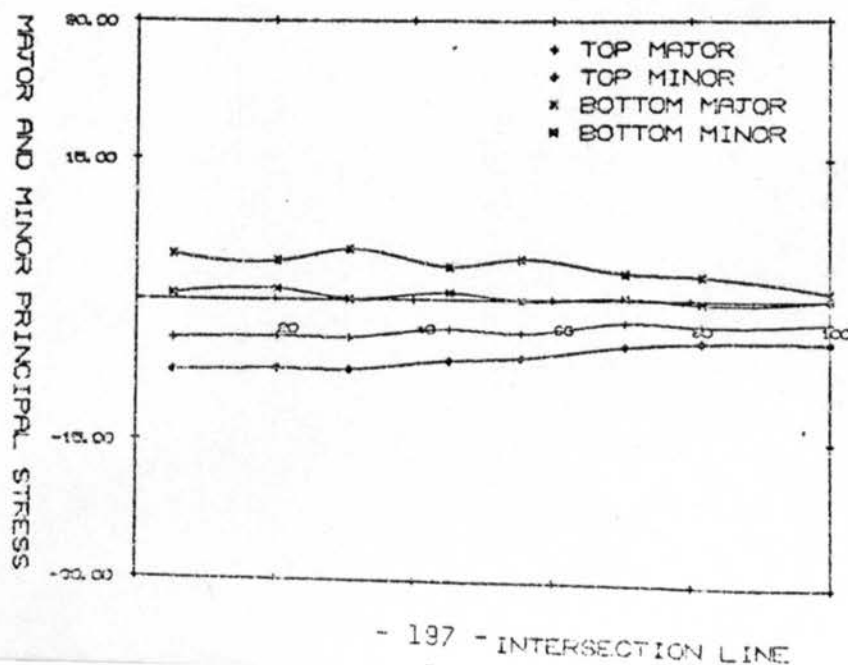


Figure 73. Stresses for unit axial load.

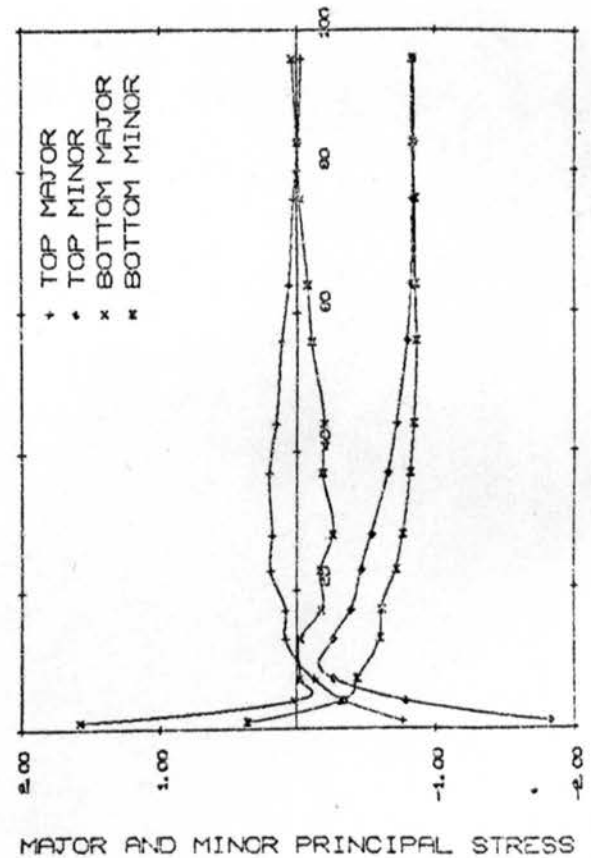
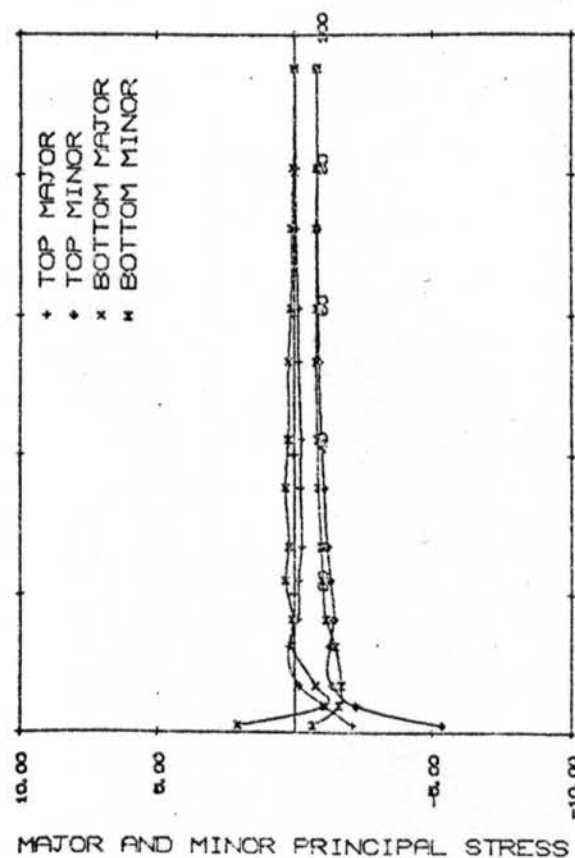
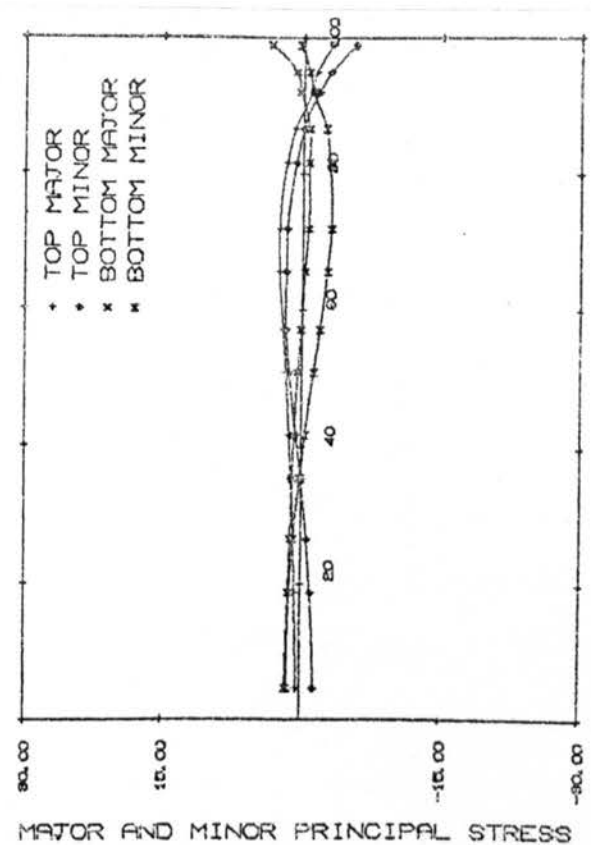
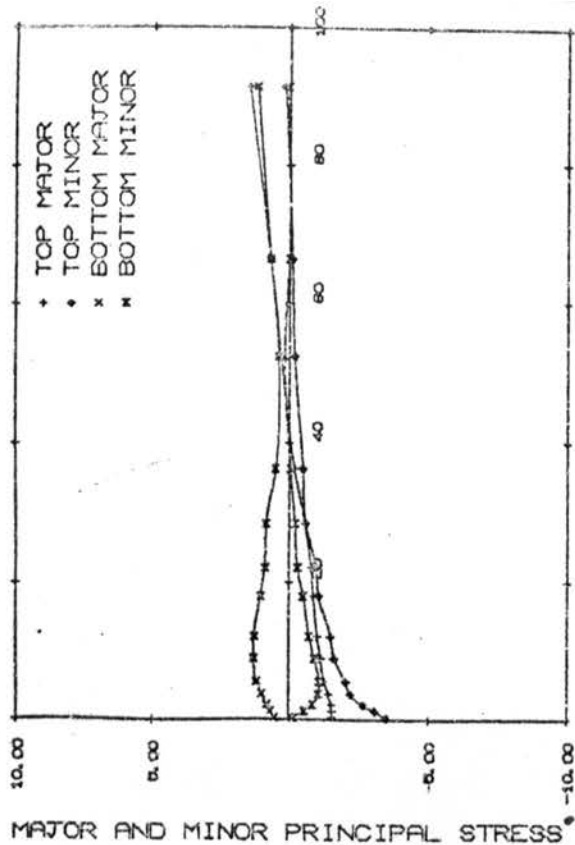
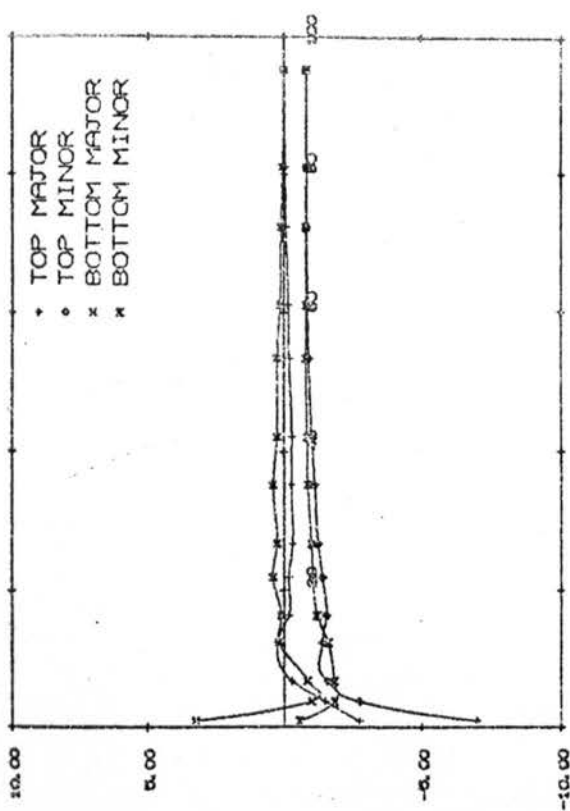
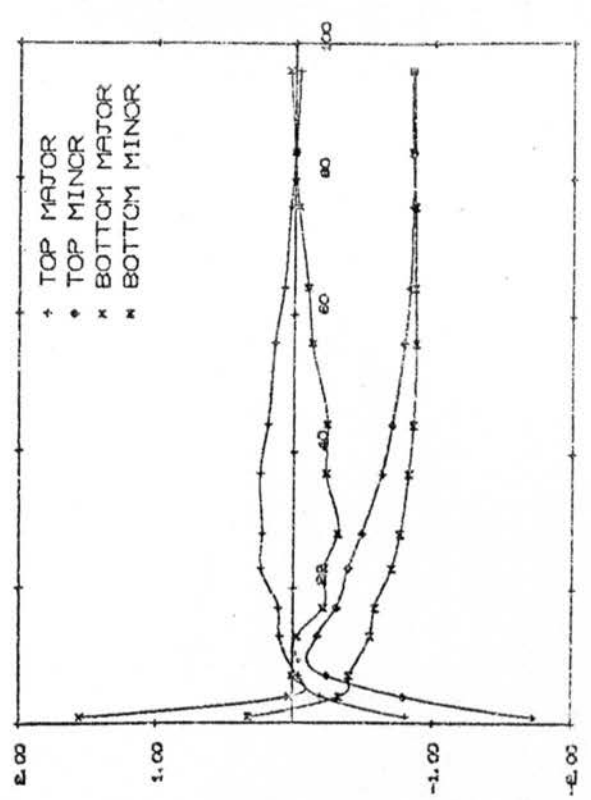


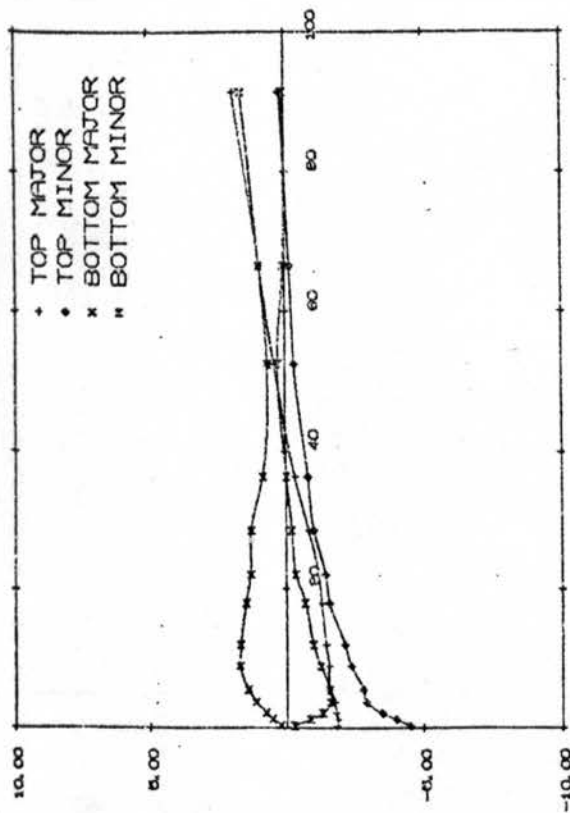
Figure 74. Stresses for unit axial load.



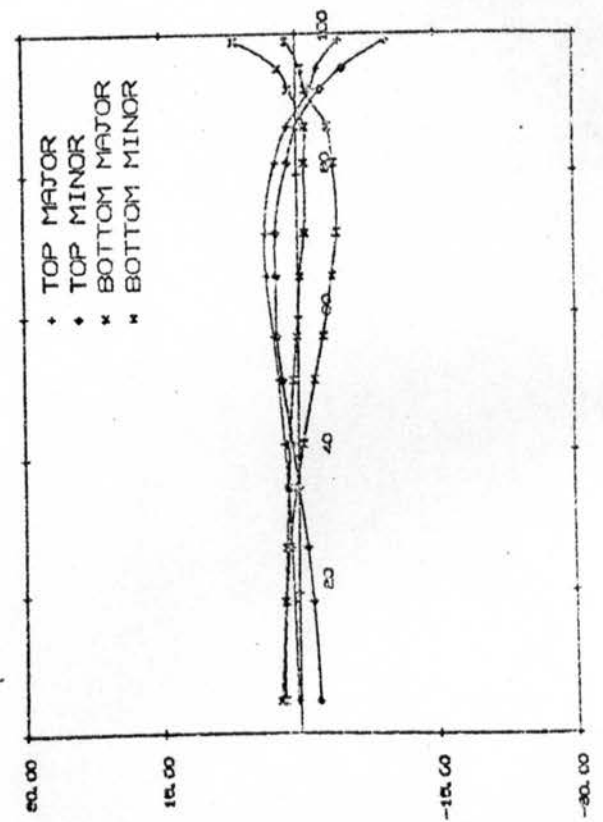
BRANCH CENTRE LINE



BRANCH EDGE

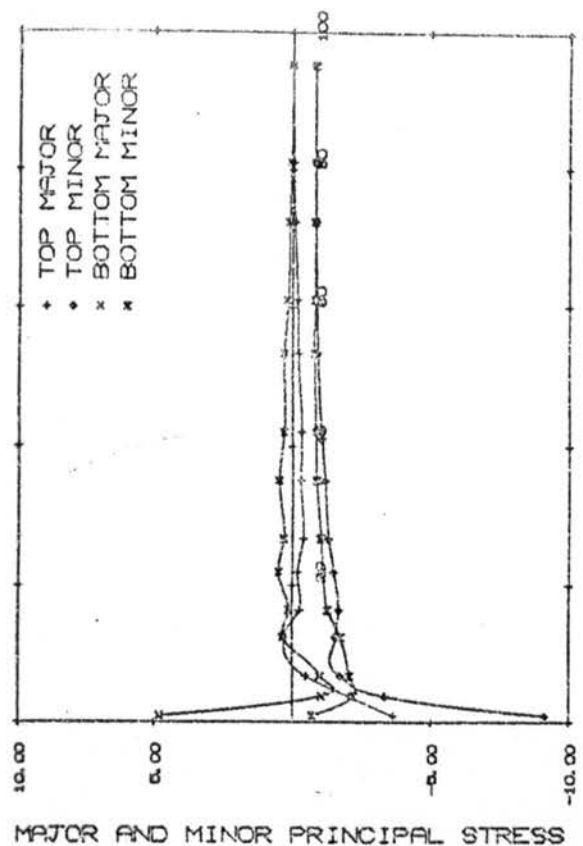


CHORD CROWN

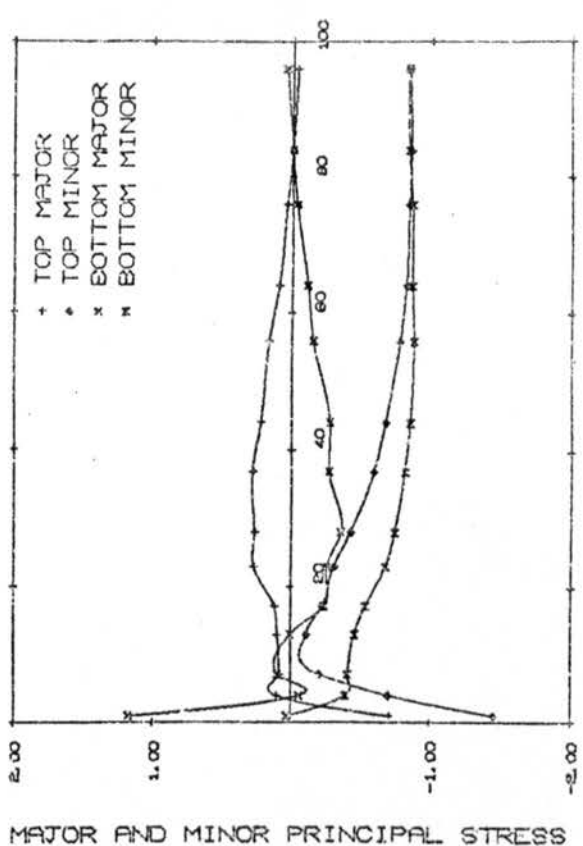


CHORD CIRCUMFERENCE

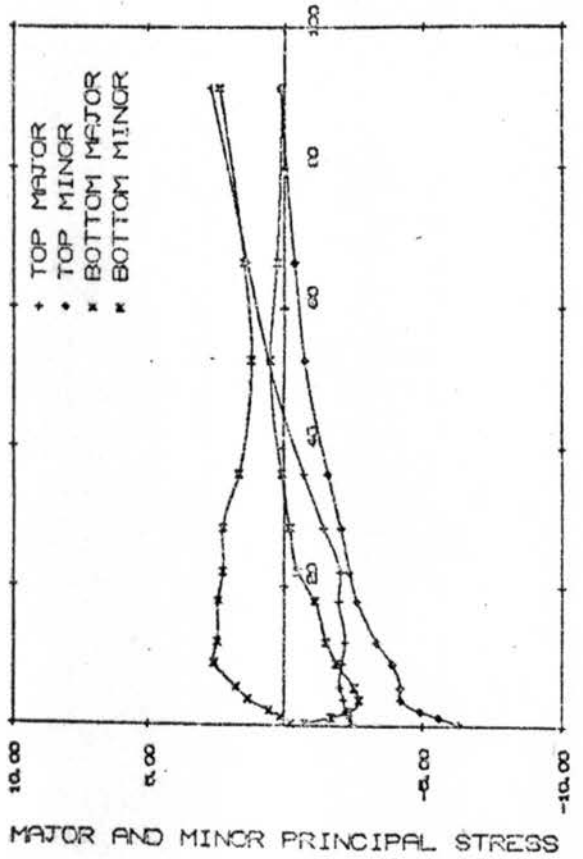
Figure 75. Stresses for unit axial load.



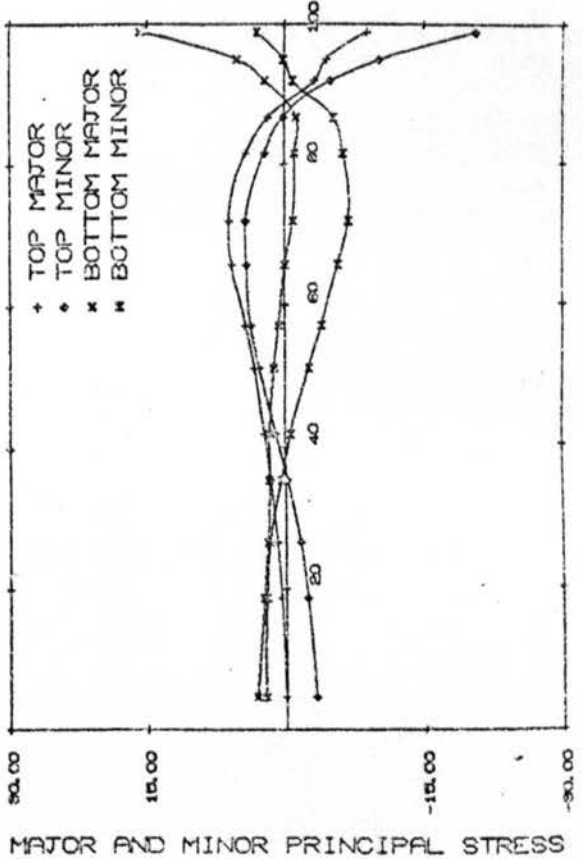
BRANCH CENTRE LINE



BRANCH EDGE



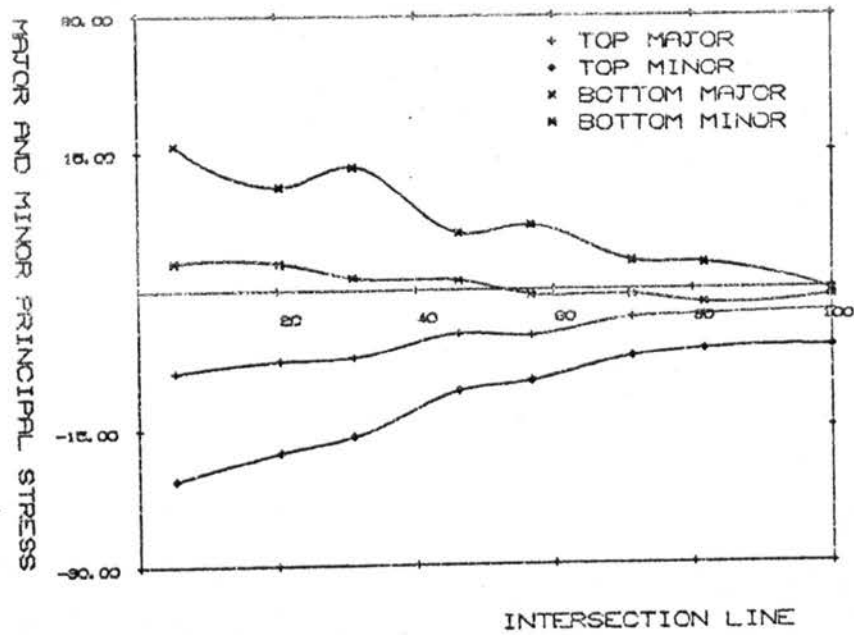
CHORD CROWN



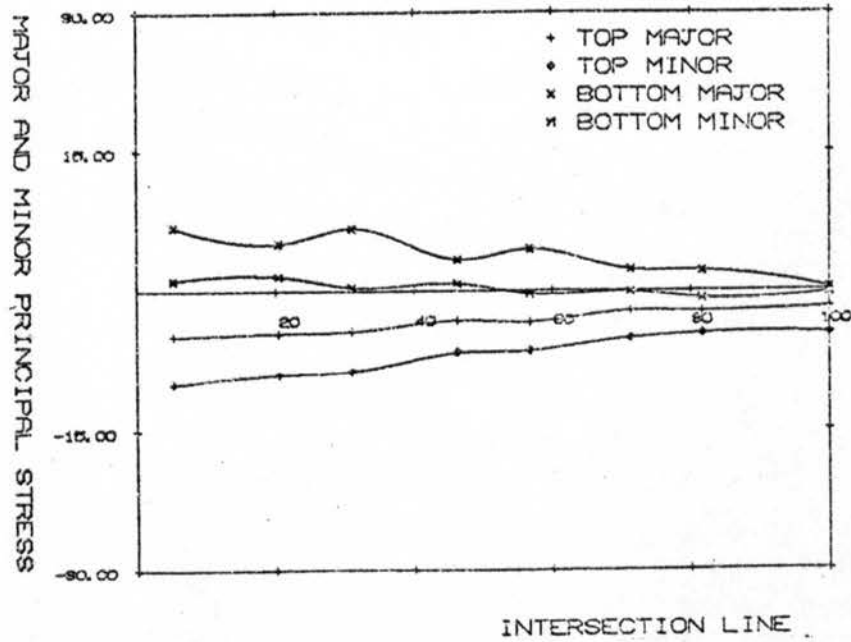
CHORD CIRCUMFERENCE

Figure 76. Stresses for unit axial load.

$$\text{BETA} = 0.67 \quad D/T = 31.75$$



$$\text{BETA} = 0.67 \quad D/T = 22.86$$



$$\text{BETA} = 0.67 \quad D/T = 18.14$$

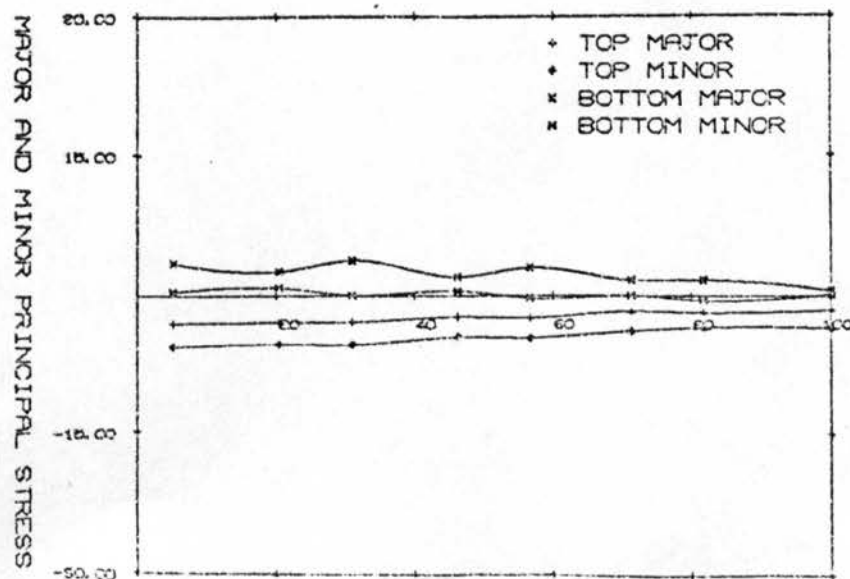
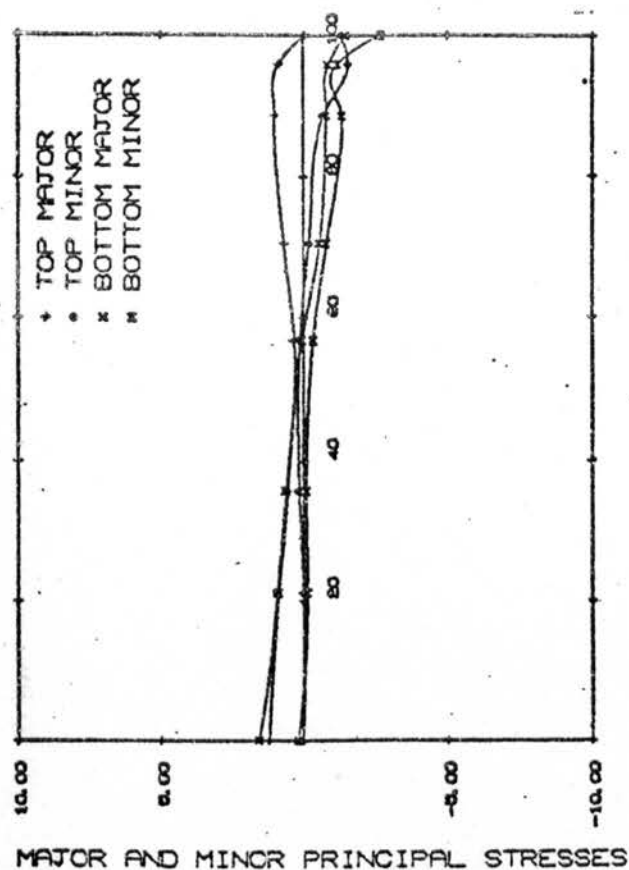
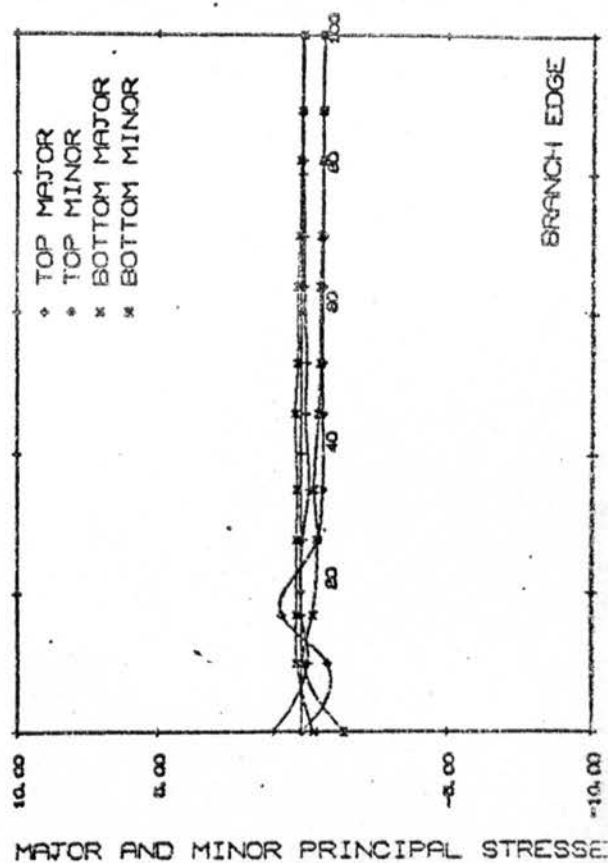


Figure 77. Stresses for unit axial load.

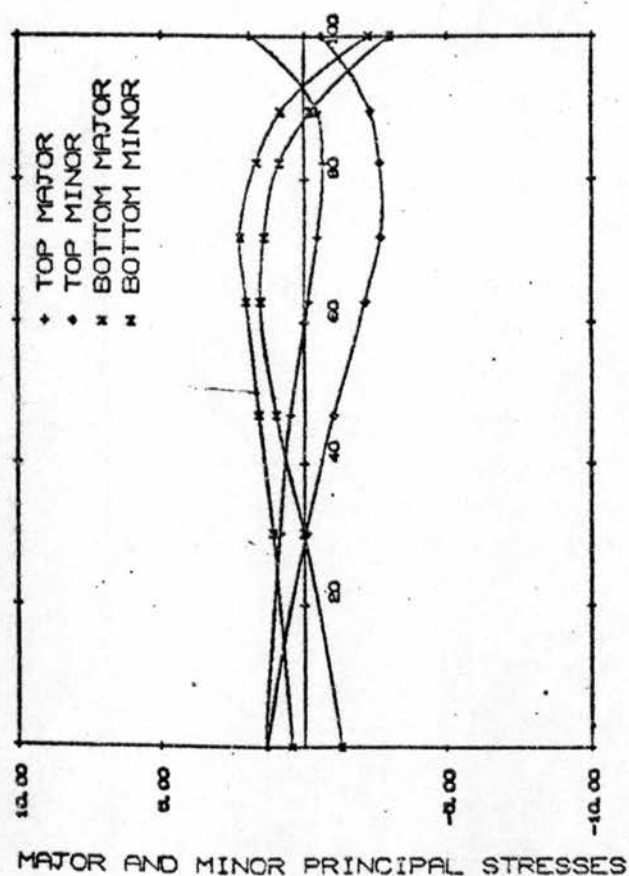
BETA = 0.77 D/T = 18



BETA = 0.77 D/T = 18



BETA = 0.77 D/T = 18



BETA = 0.77 D/T = 18

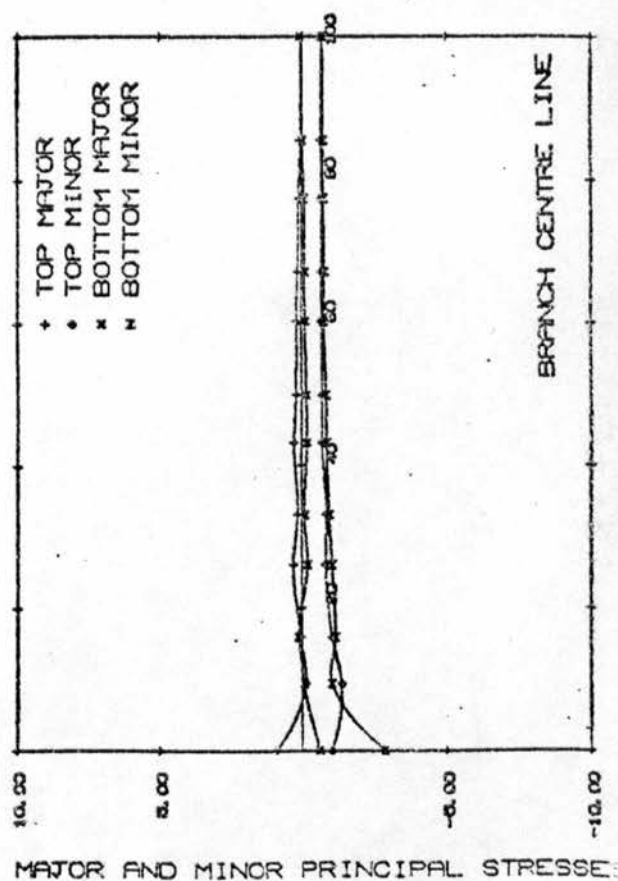
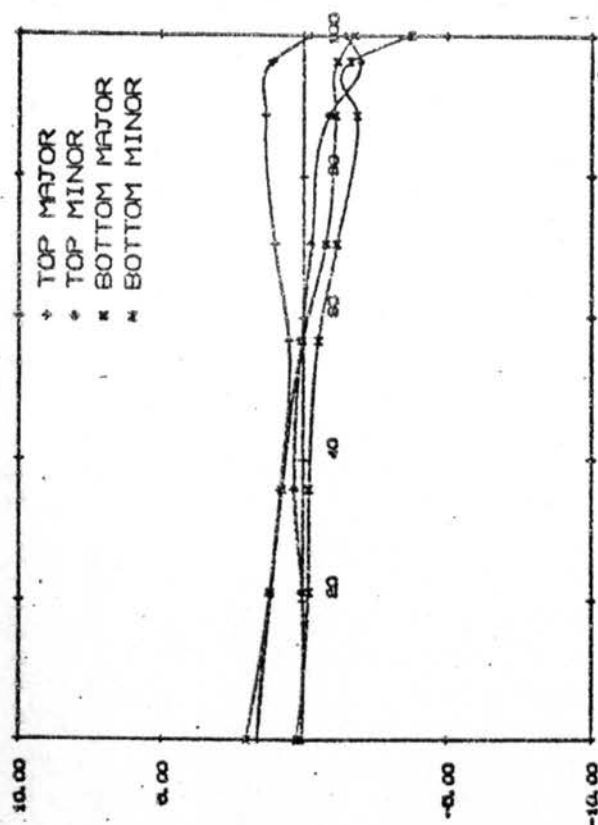


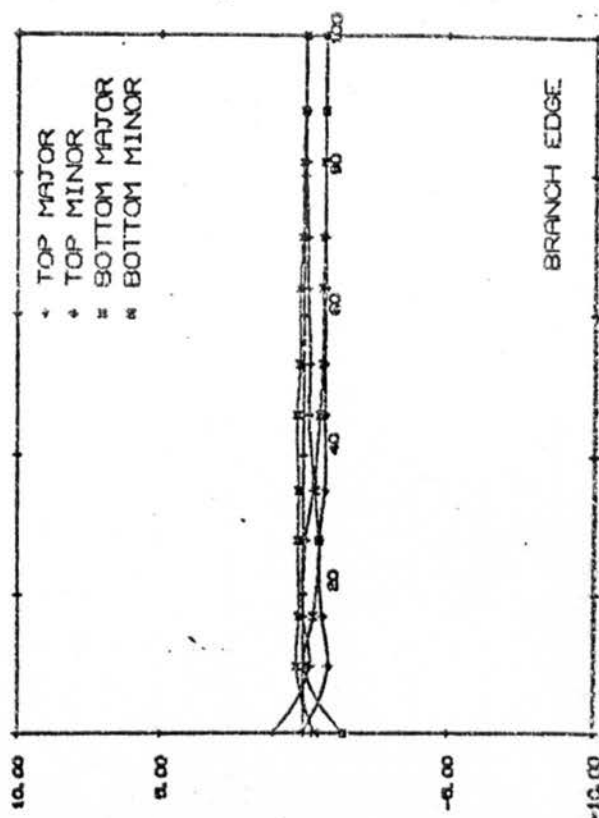
Figure 78. Stresses for unit axial load.

BETA = 0.77 D/T = 23



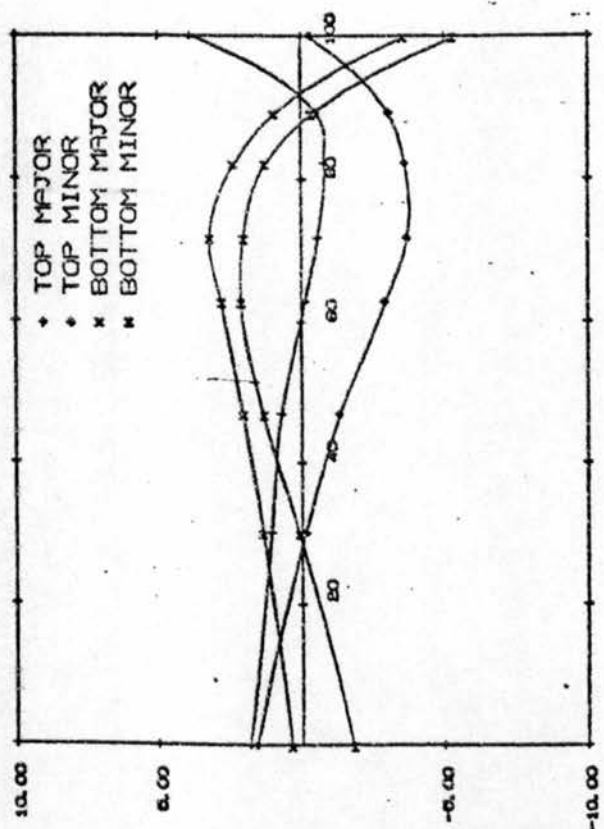
CHORD CROWN

BETA = 0.77 D/T = 23



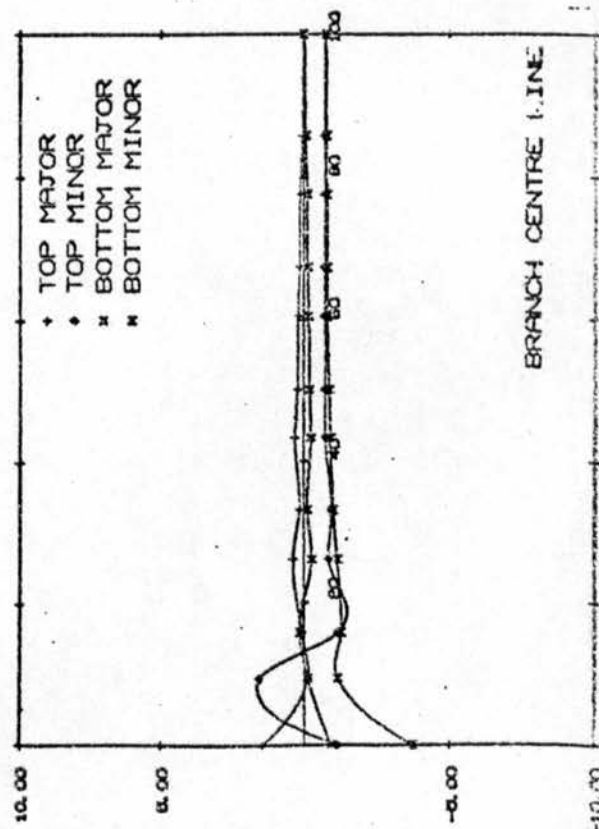
BRANCH EDGE

BETA = 0.77 D/T = 23



CHORD CIRCUMFERENCE

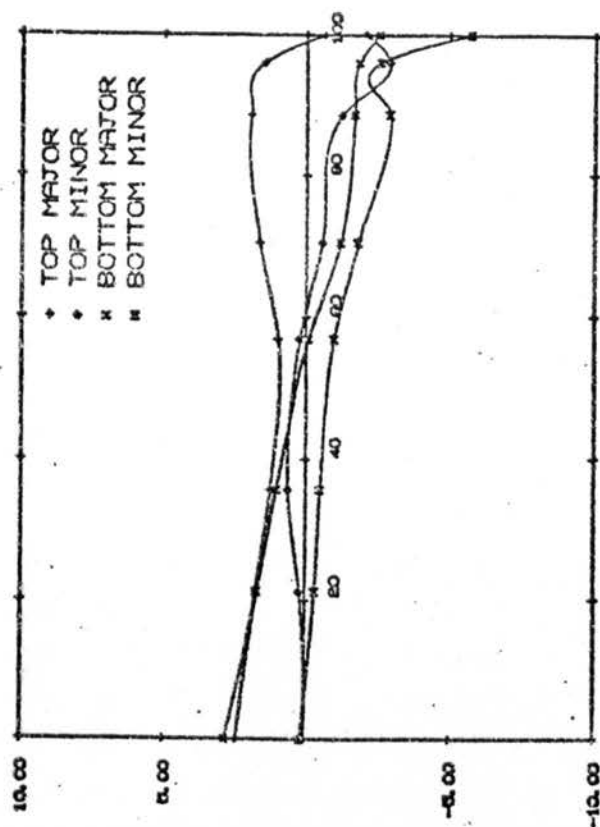
BETA = 0.77 D/T = 23



BRANCH CENTRE LINE

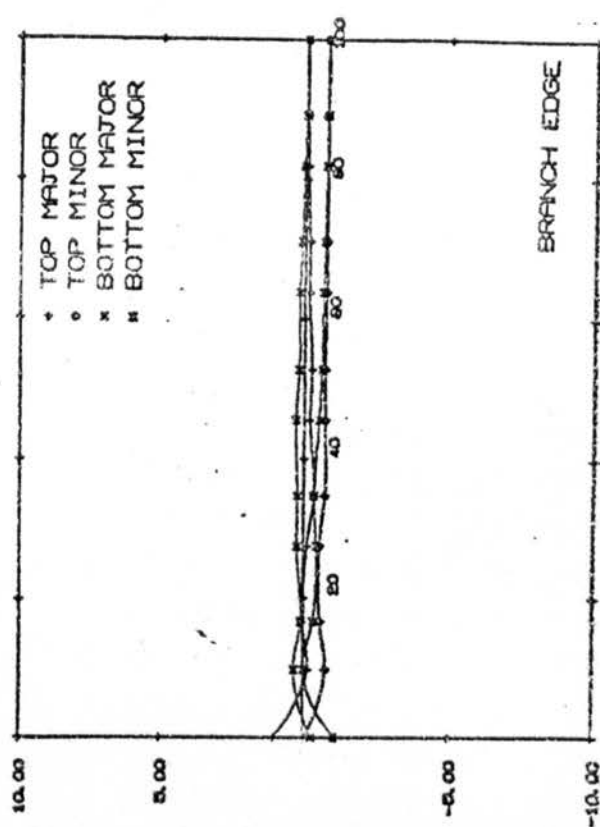
Figure 79. Stresses for unit axial load.

BETA = 0.77 D/T = 32



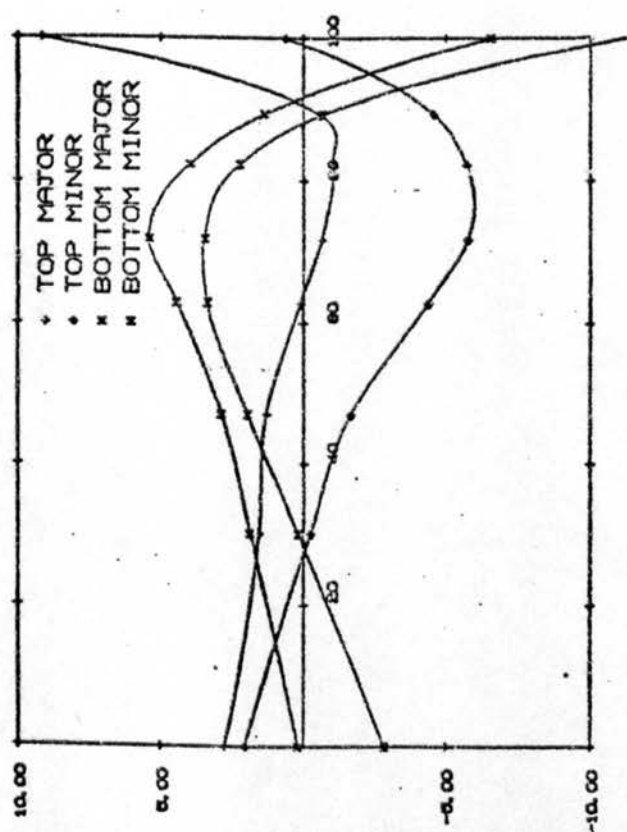
CHORD CROWN

BETA = 0.77 D/T = 32



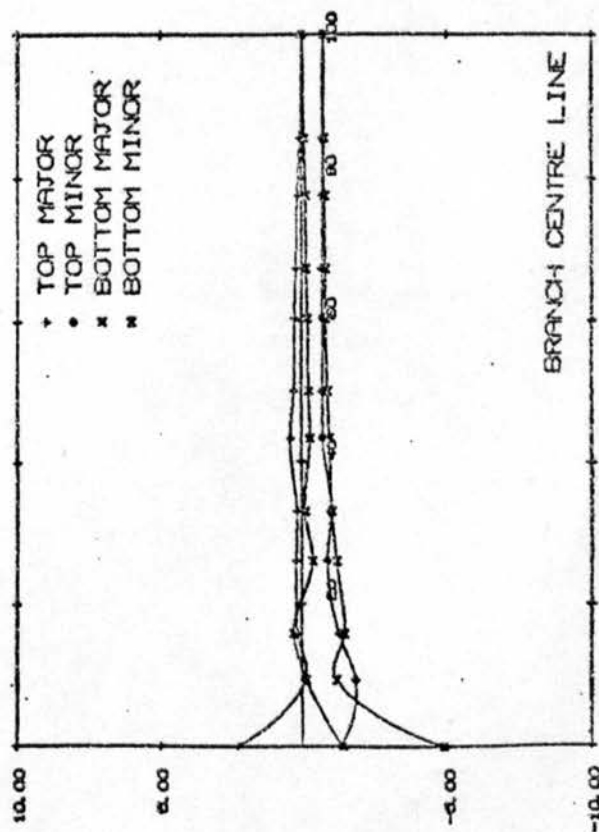
BRANCH EDGE

BETA = 0.77 D/T = 32



CHORD CIRCUMFERENCE

BETA = 0.77 D/T = 32



BRANCH CENTRE LINE

Figure 80. Stresses for unit axial load.

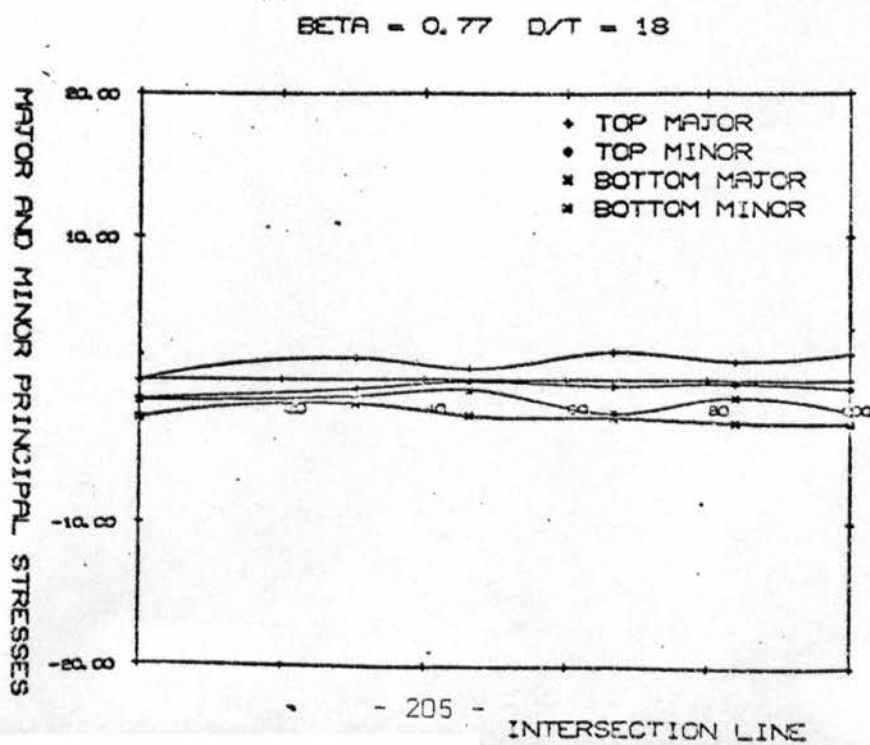
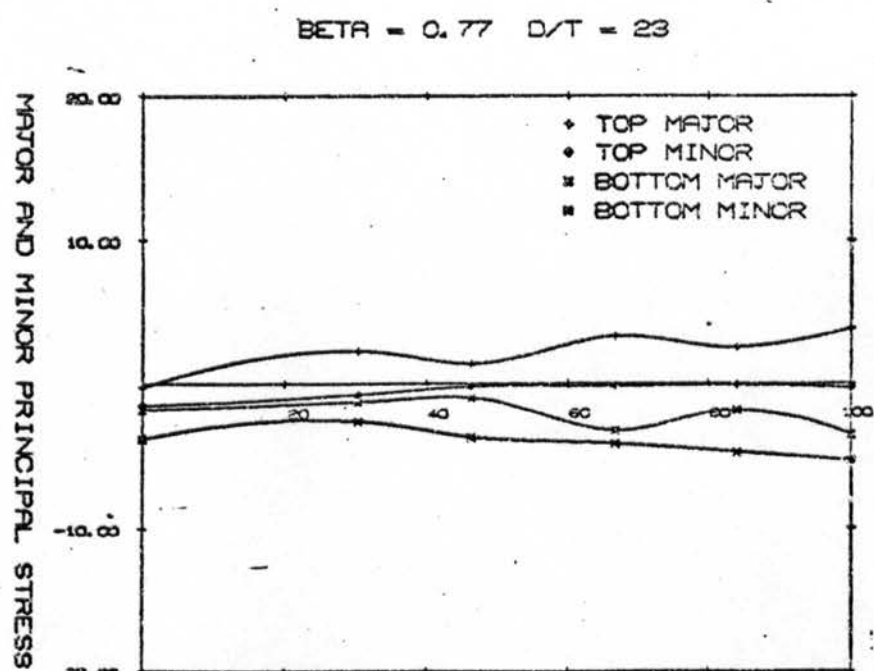
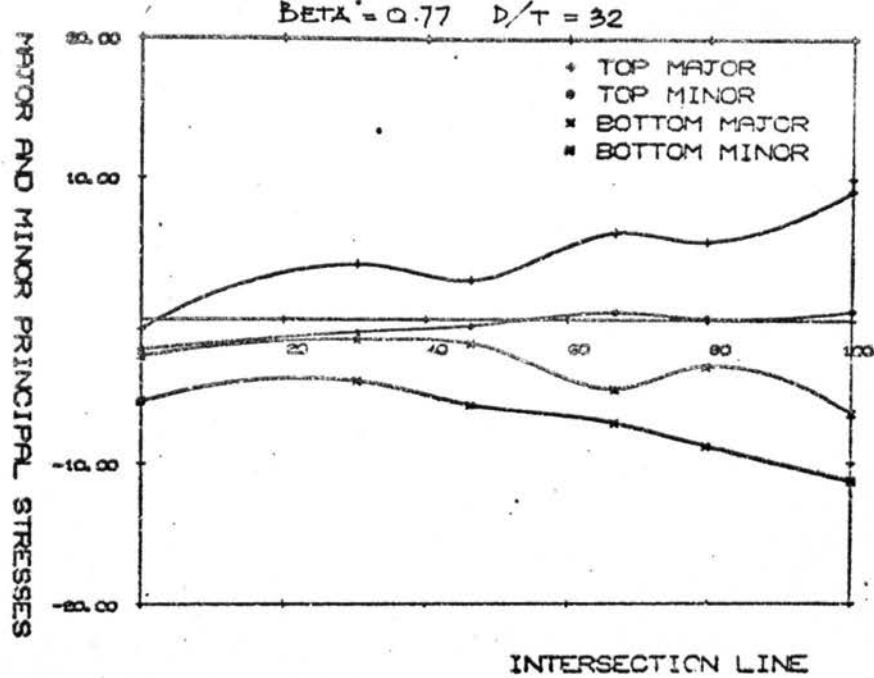
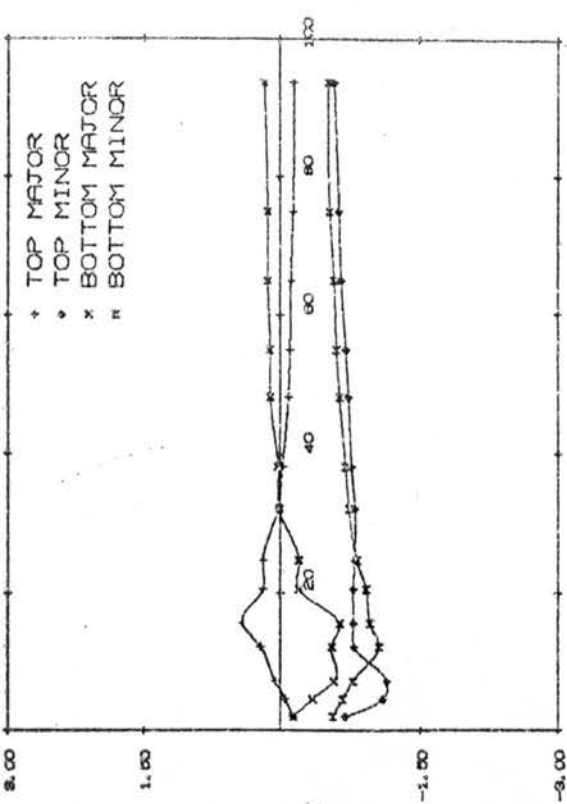
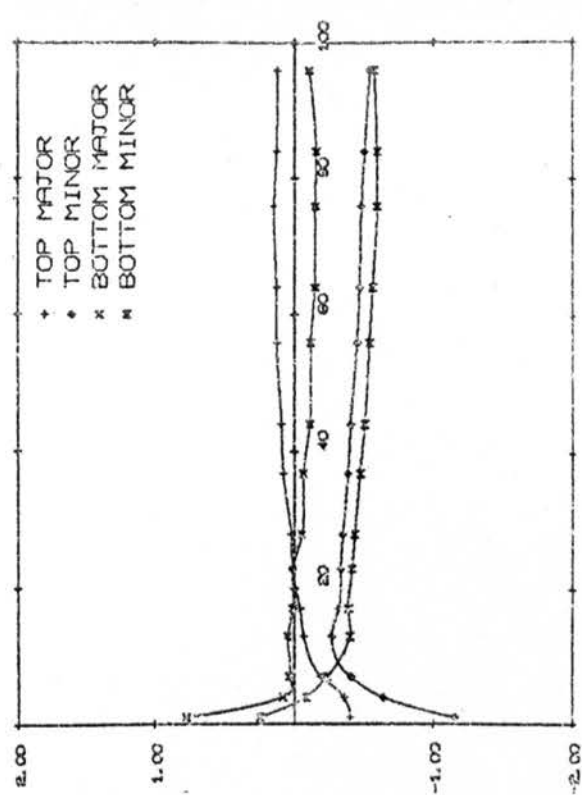


Figure 81. Stresses for unit axial load.



BRANCH CENTRE LINE

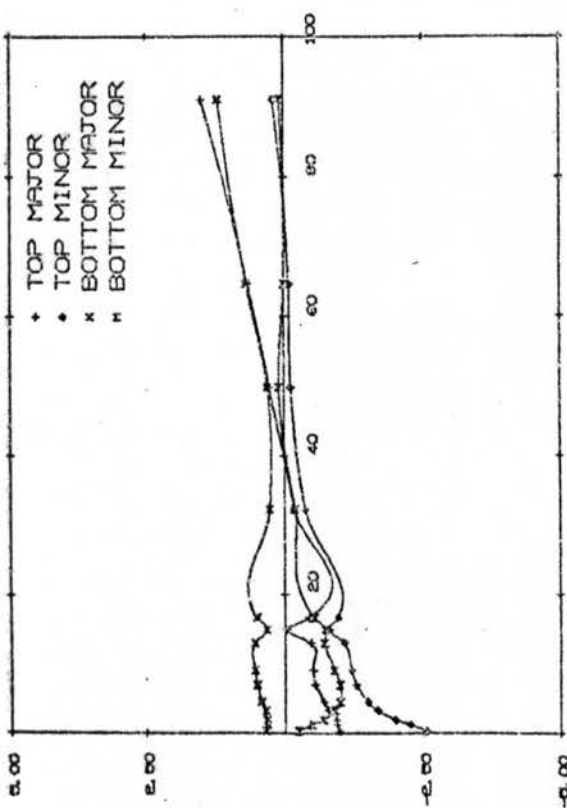
BETA = 1.00 D/T = 18.14



BRANCH EDGE

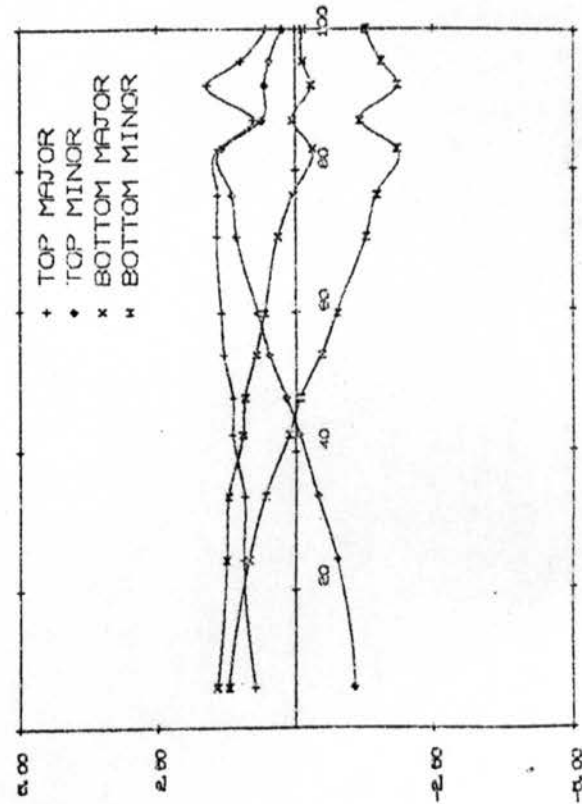
MAJOR AND MINOR PRINCIPAL STRESS

MAJOR AND MINOR PRINCIPAL STRESS



CHORD CROWN

BETA = 1.00 D/T = 18.14

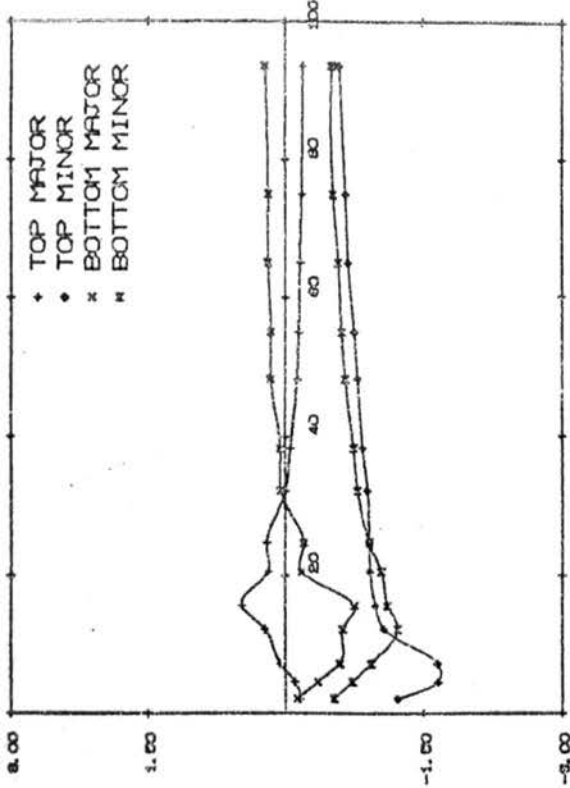


CHORD CIRCUMFERENCE

MAJOR AND MINOR PRINCIPAL STRESS

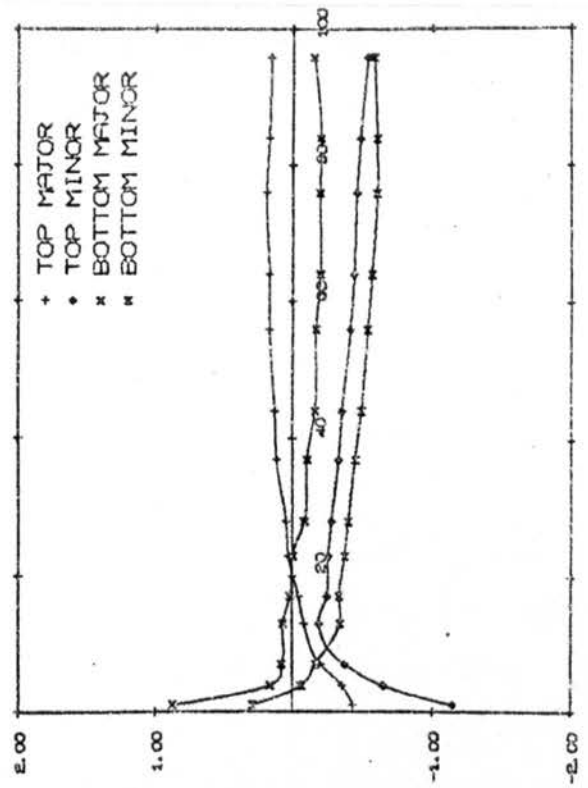
MAJOR AND MINOR PRINCIPAL STRESS

Figure 82. Stresses for unit axial load.



BRANCH CENTRE LINE

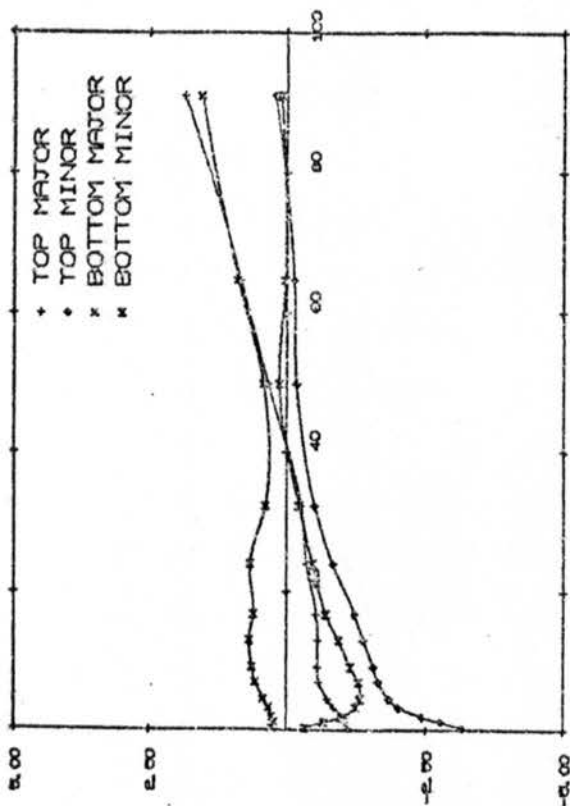
BETA = 1.00 D/T = 22.86



BRANCH EDGE

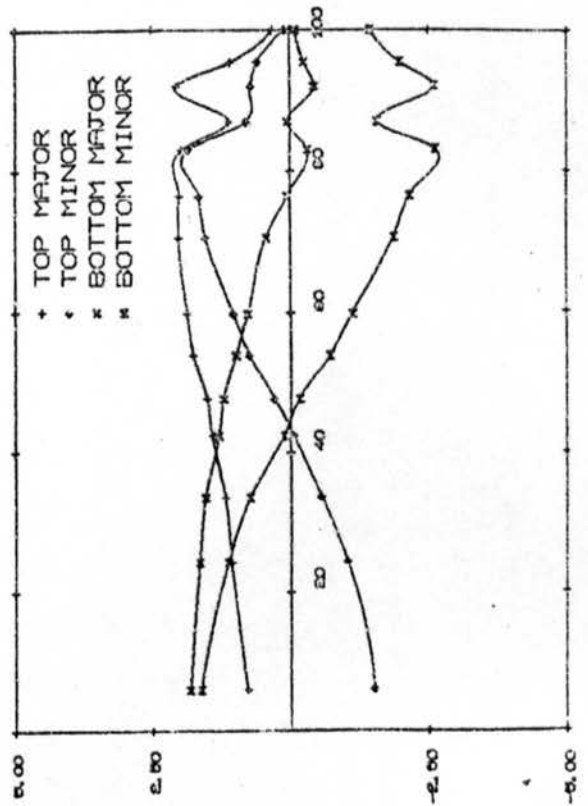
MAJOR AND MINOR PRINCIPAL STRESS

MAJOR AND MINOR PRINCIPAL STRESS



CHORD CROWN

BETA = 1.00 D/T = 22.86

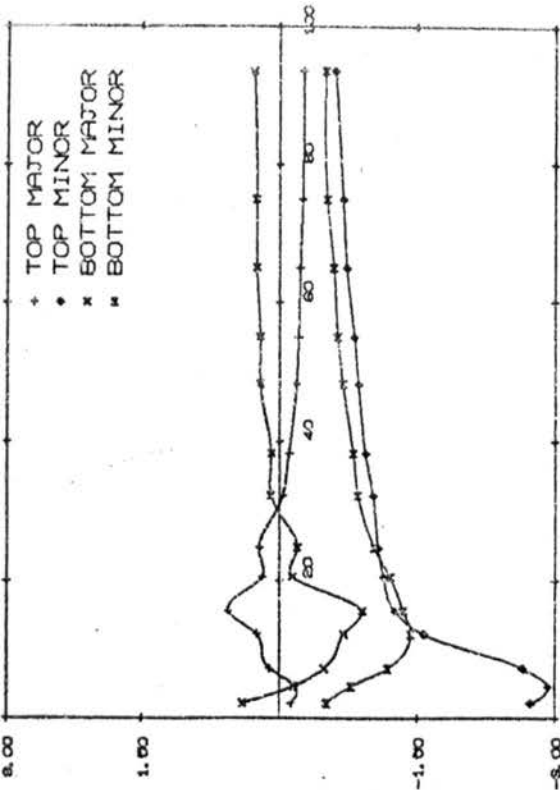


CHORD CIRCUMFERENCE

MAJOR AND MINOR PRINCIPAL STRESS

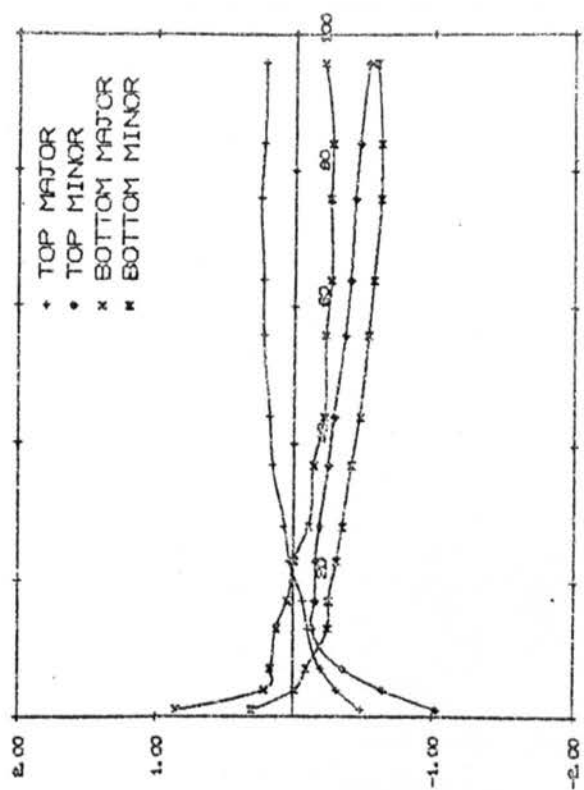
MAJOR AND MINOR PRINCIPAL STRESS

Figure 83. Stresses for unit axial load.



BRANCH CENTRE LINE

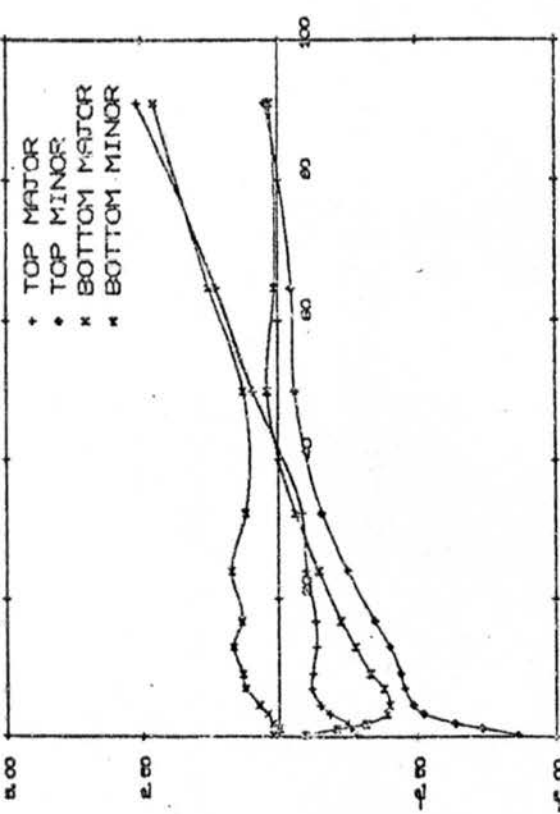
BETA = 1.00 D/T = 31.75



BRANCH EDGE

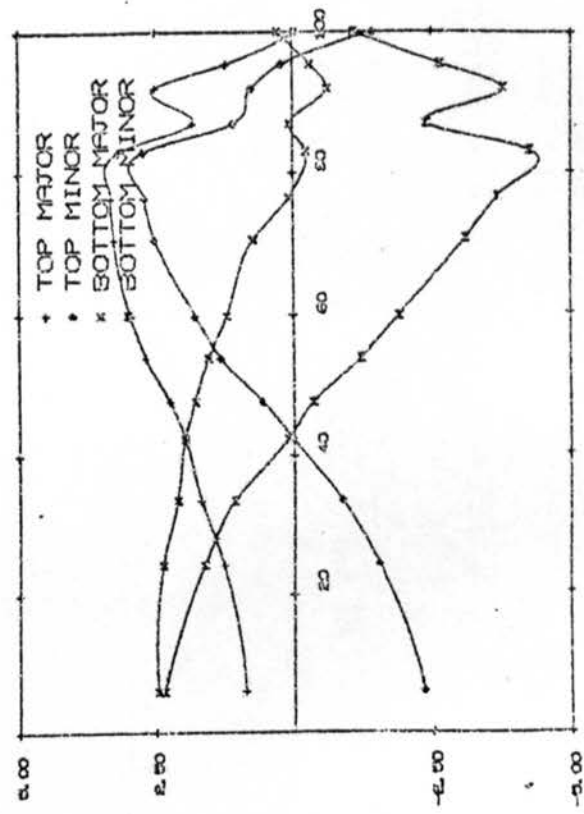
MAJOR AND MINOR PRINCIPAL STRESS

MAJOR AND MINOR PRINCIPAL STRESS



CHORD CROWN

BETA = 1.00 D/T = 31.75



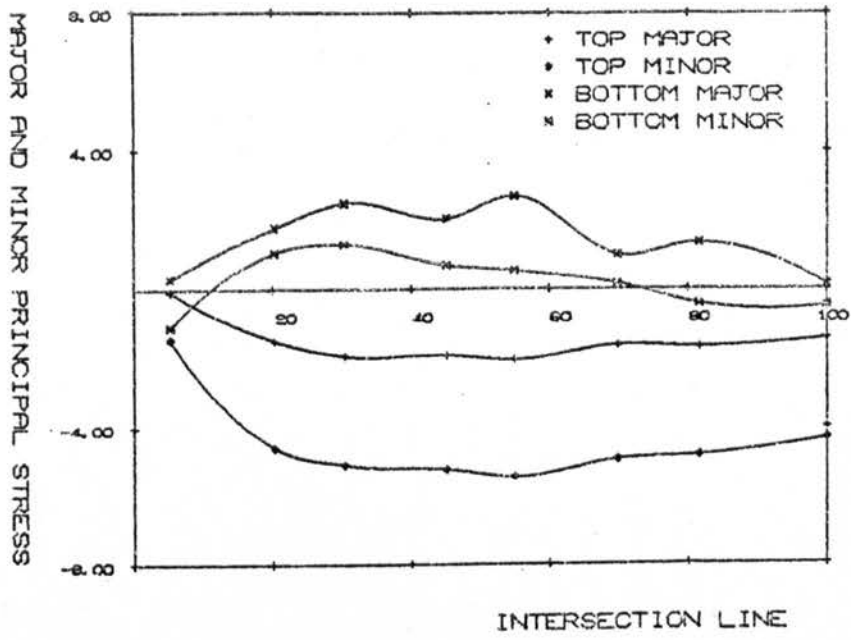
CHORD CIRCUMFERENCE

MAJOR AND MINOR PRINCIPAL STRESS

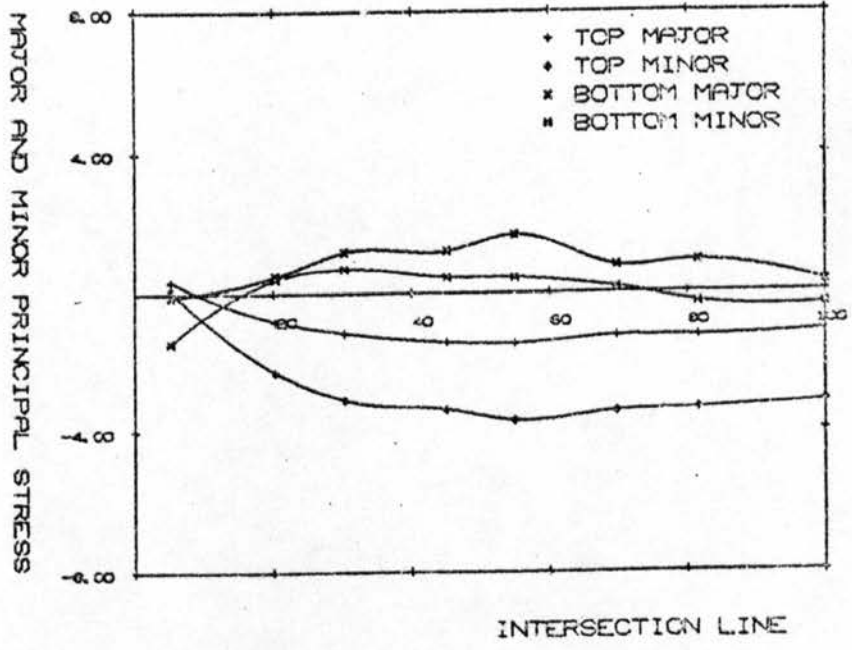
MAJOR AND MINOR PRINCIPAL STRESS

Figure 84. Stresses for unit axial load.

BETA = 1.00 D/T = 31.75



BETA = 1.00 D/T = 22.86



BETA = 1.00 D/T = 18.14

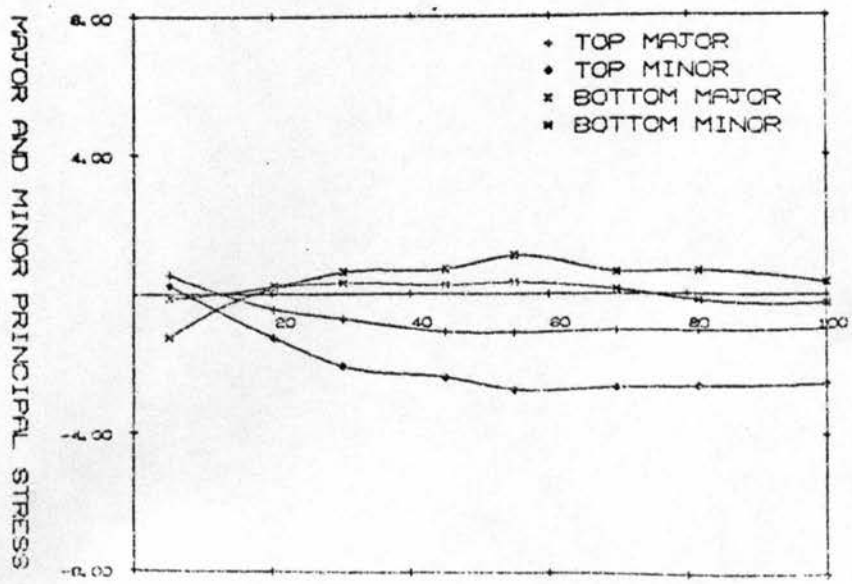
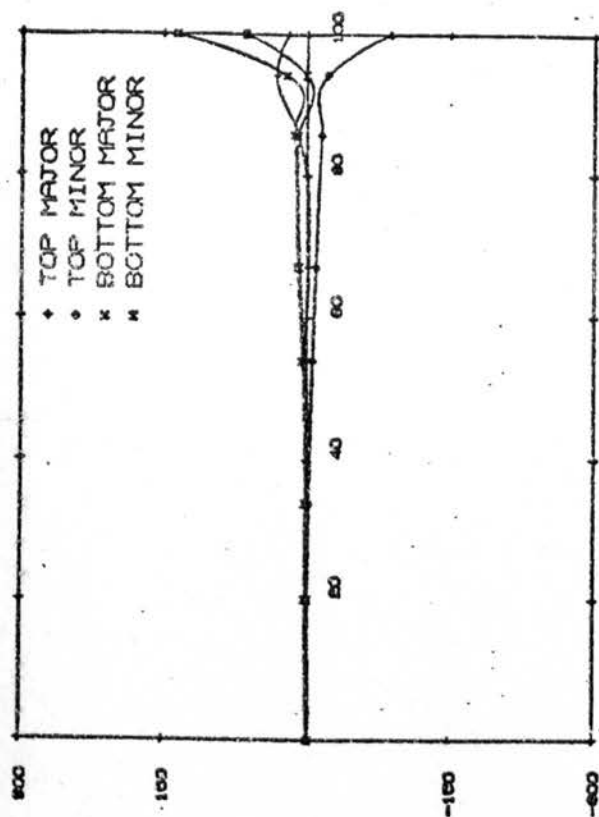


Figure 85. Stresses for unit axial load.

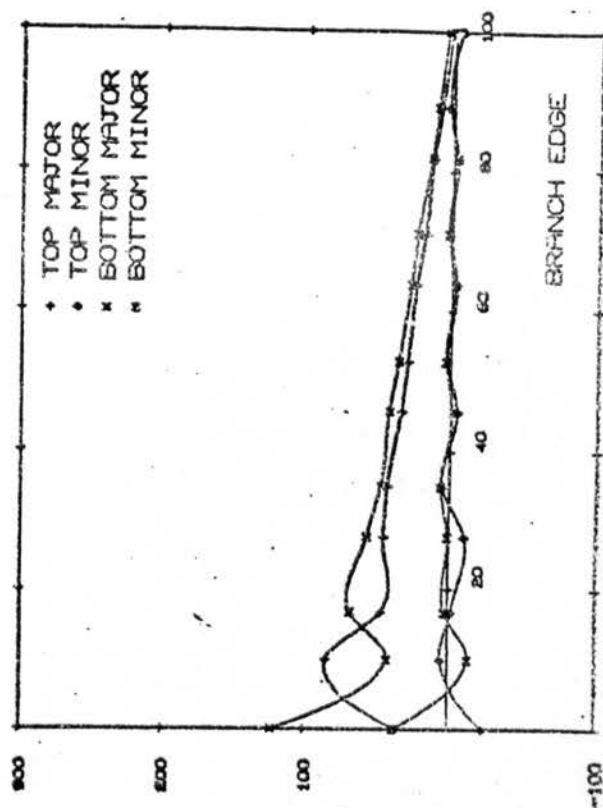
BETA = 0.42 D/T = 18



MAJOR AND MINOR PRINCIPAL STRESSES

CHORD CROWN

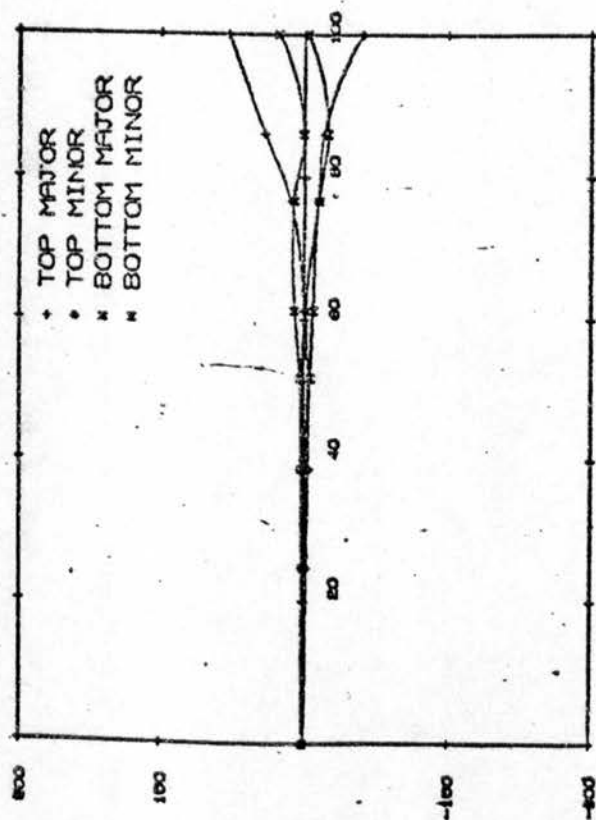
BETA = 0.42 D/T = 18



MAJOR AND MINOR PRINCIPAL STRESSES

BRANCH EDGE

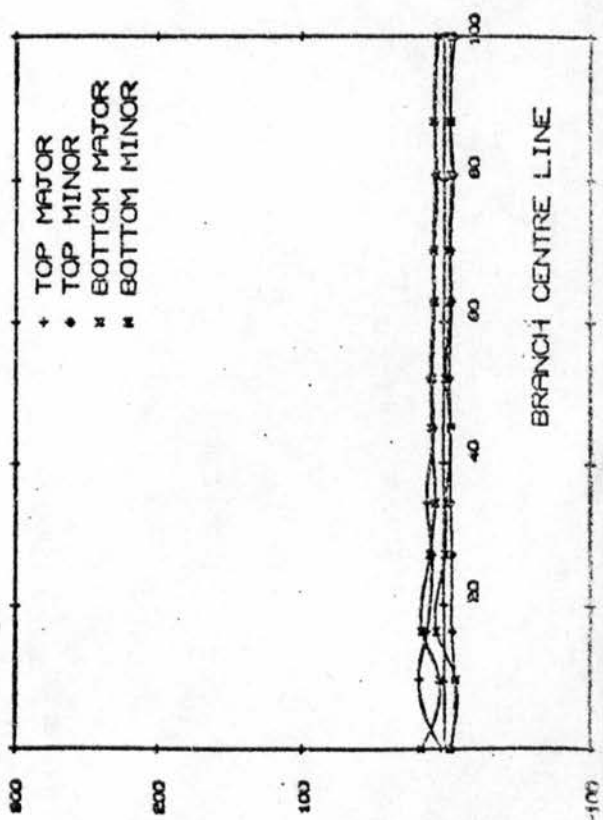
BETA = 0.42 D/T = 18



MAJOR AND MINOR PRINCIPAL STRESSES

CHORD CIRCUMFERENCE

BETA = 0.42 D/T = 18

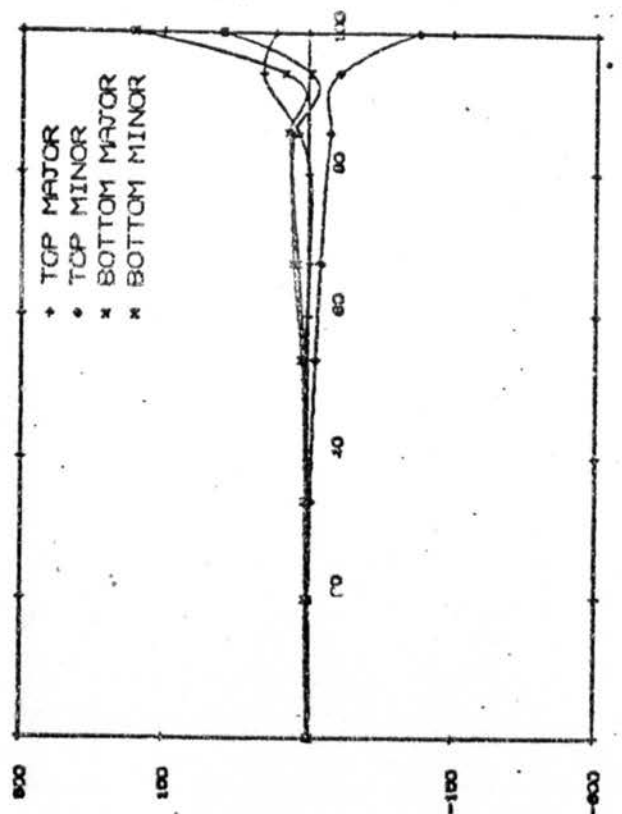


MAJOR AND MINOR PRINCIPAL STRESSES

BRANCH CENTRE LINE

Figure 86. Stresses for unit bending load.
(1 kNm)

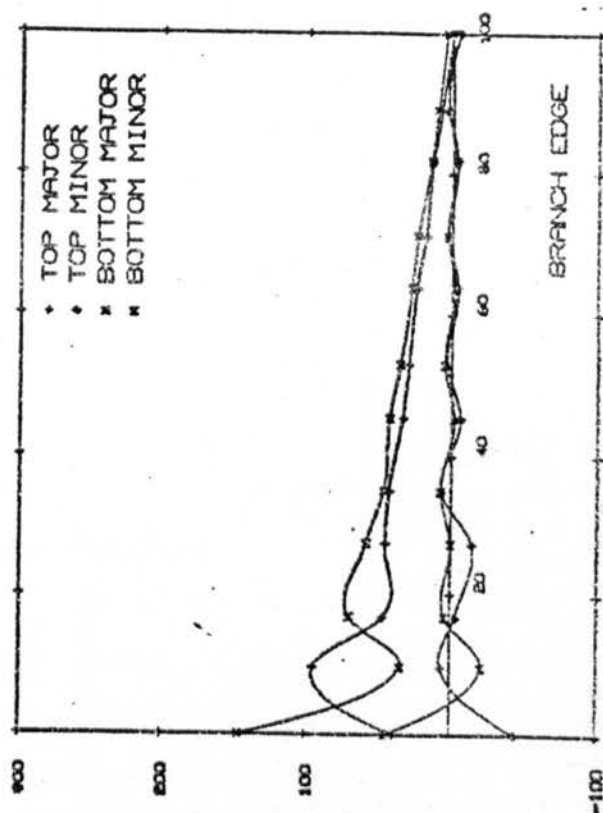
BETA = 0.42 D/T = 23



MAJOR AND MINOR PRINCIPAL STRESSES

CHORD CROWN

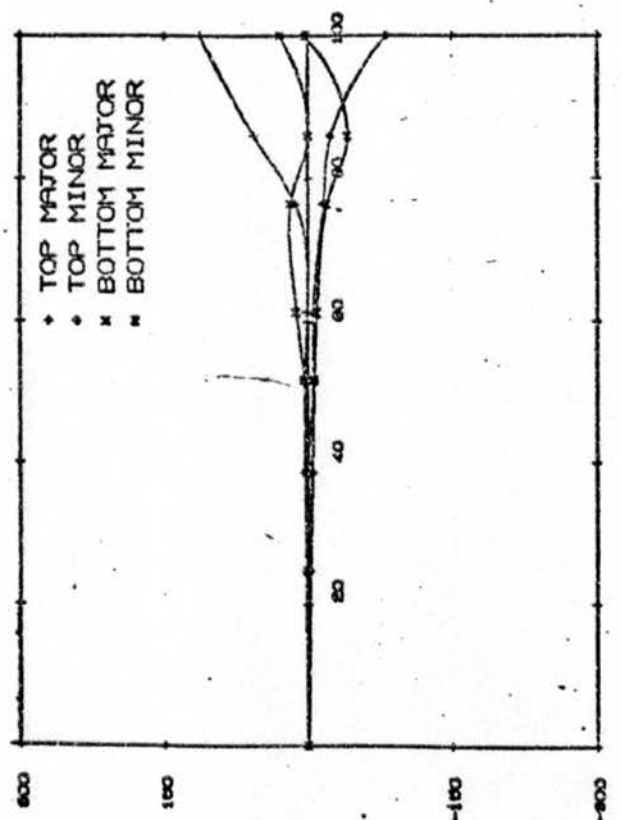
BETA = 0.42 D/T = 23



MAJOR AND MINOR PRINCIPAL STRESSES

BRANCH EDGE

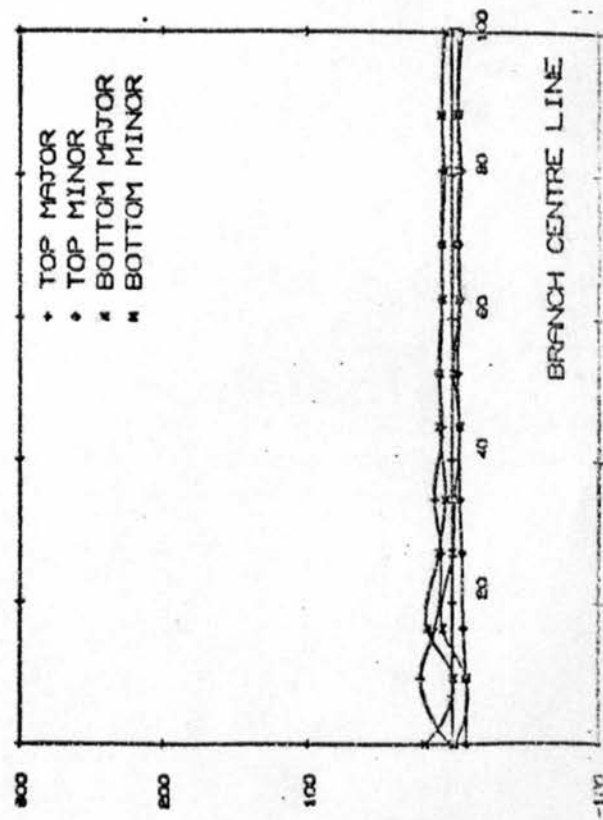
BETA = 0.42 D/T = 23



MAJOR AND MINOR PRINCIPAL STRESSES

CHORD CIRCUMFERENCE

BETA = 0.42 D/T = 23

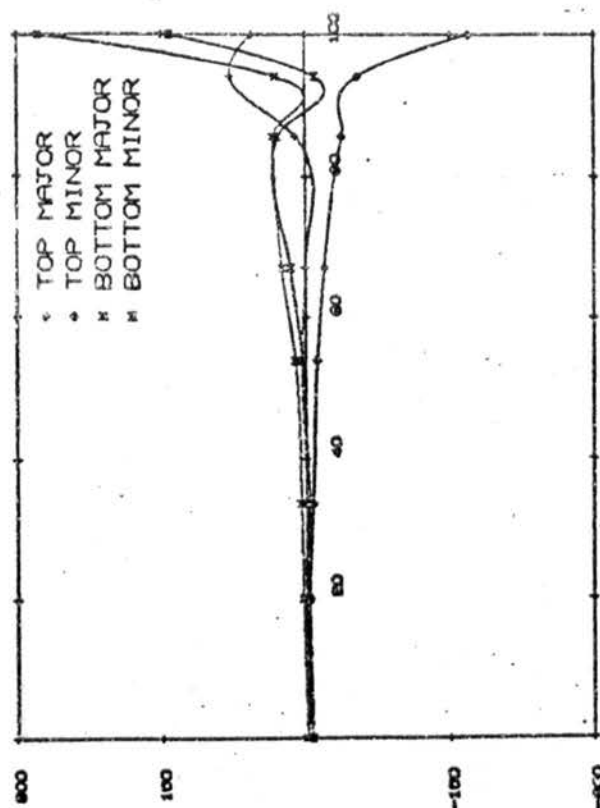


MAJOR AND MINOR PRINCIPAL STRESSES

BRANCH CENTRE LINE

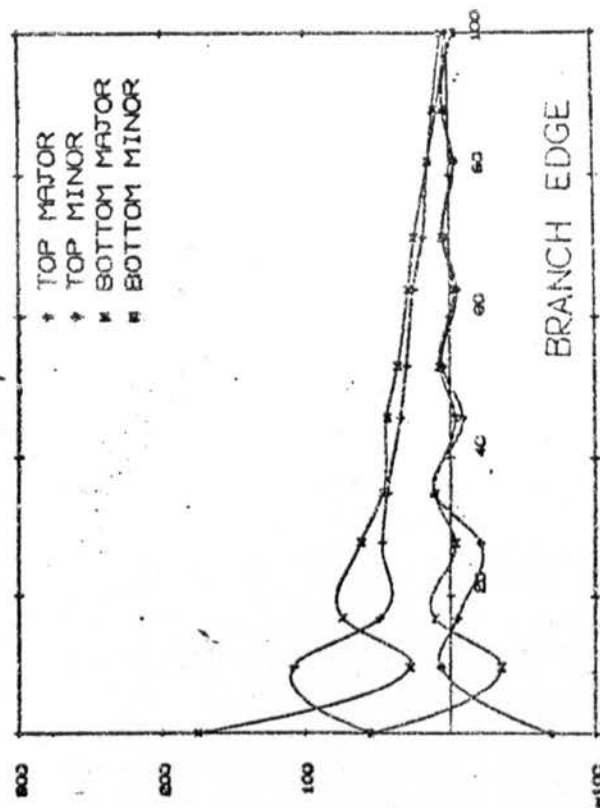
Figure 87. Stresses for unit bending load (1 kNm)

BETA = 0.42 D/T = 32



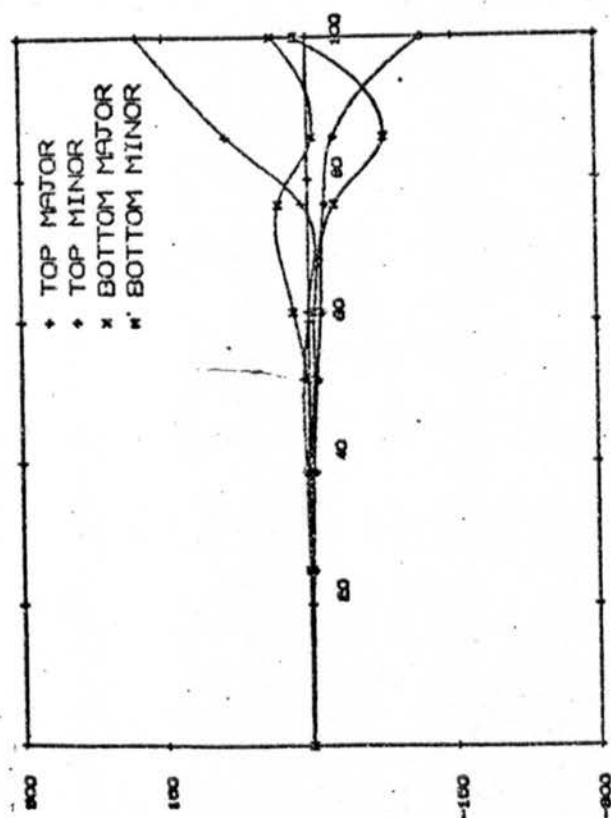
CHORD CROWN

BETA = 0.42 D/T = 32



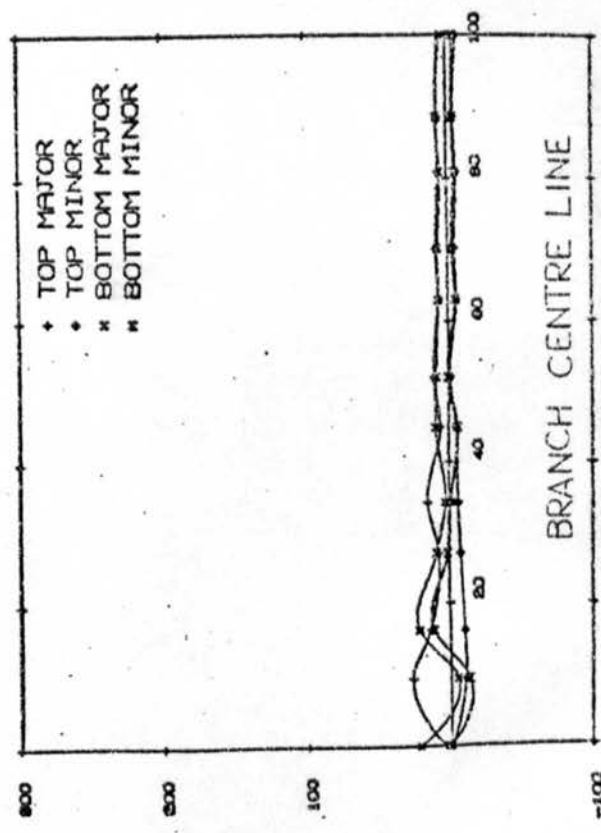
BRANCH EDGE

BETA = 0.42 D/T = 32



CHORD CIRCUMFERENCE

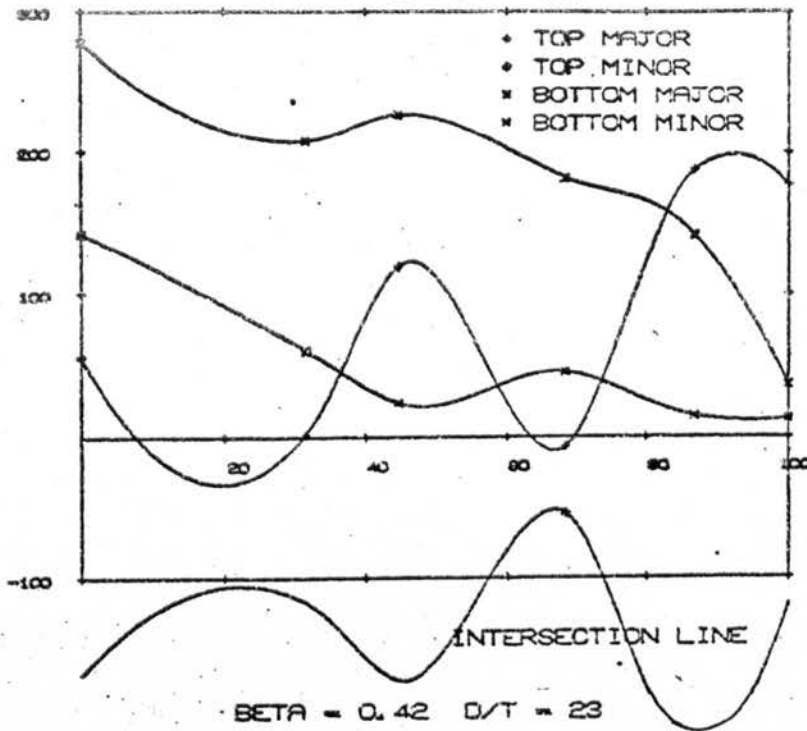
BETA = 0.42 D/T = 32



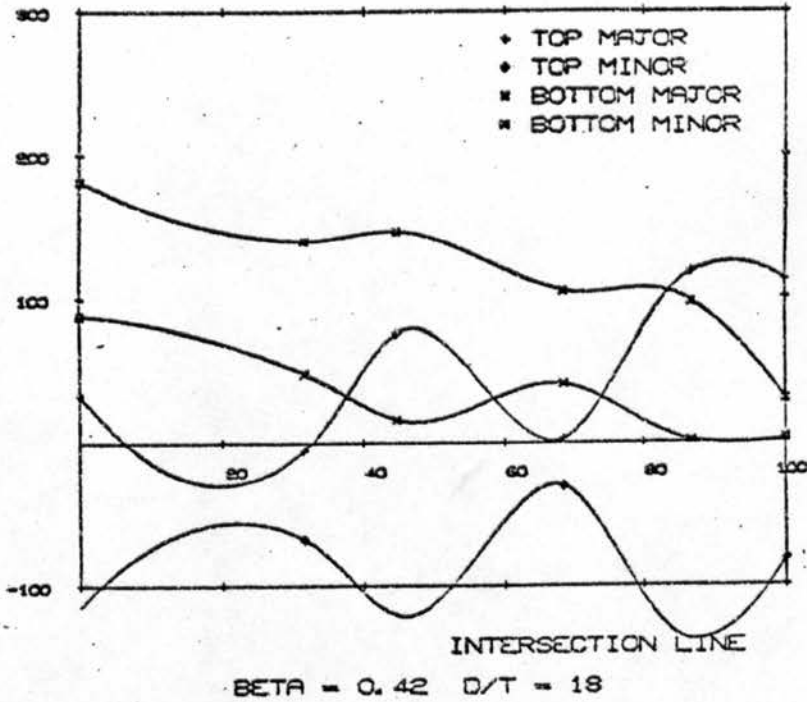
BRANCH CENTRE LINE

Figure 88. Stresses for unit bending load (1 kNm).

MAJOR AND MINOR PRINCIPAL STRESSES



MAJOR AND MINOR PRINCIPAL STRESSES



MAJOR AND MINOR PRINCIPAL STRESSES

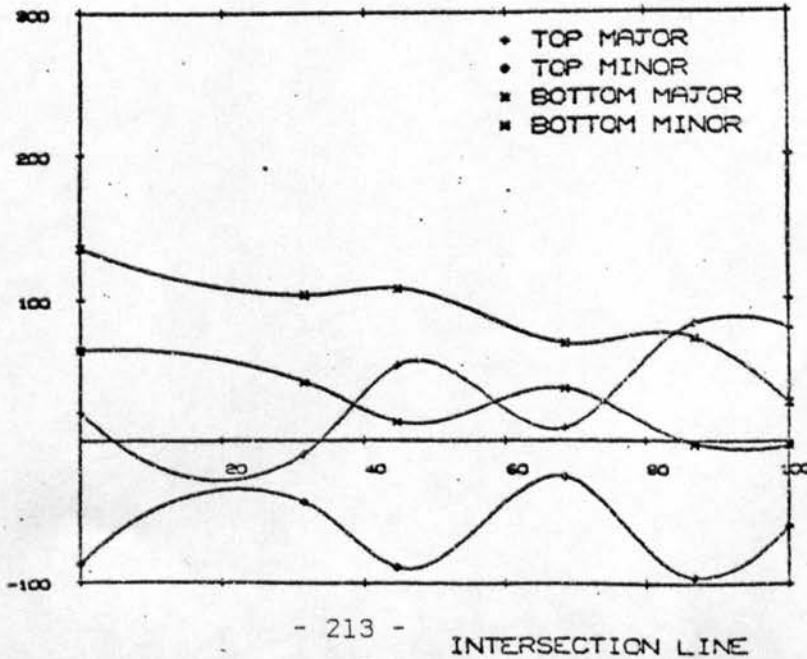
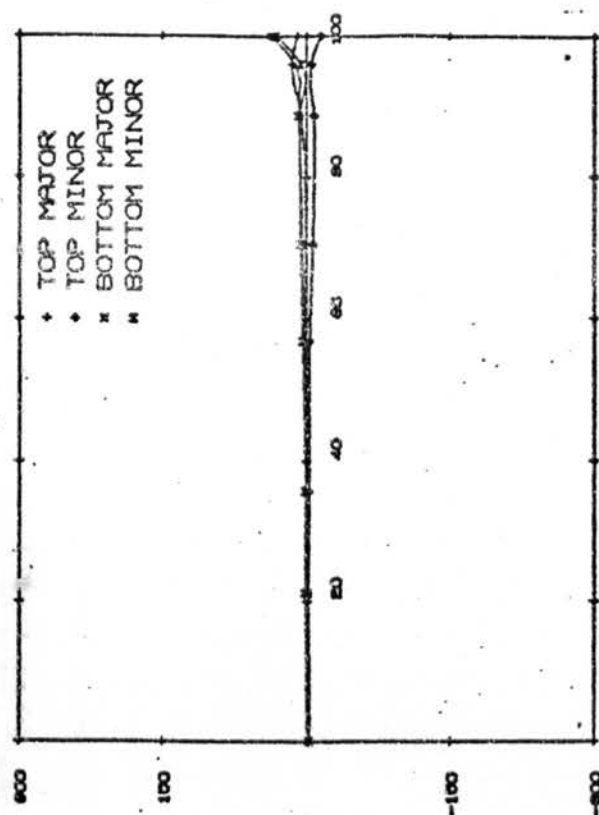


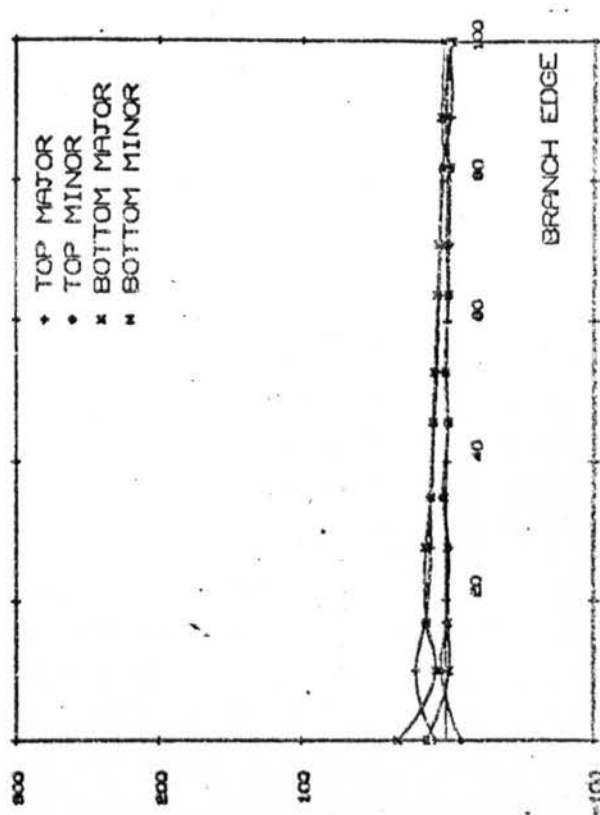
Figure 89. Stresses for unit bending load (1 kNm).

BETA = 0.77 D/T = 18



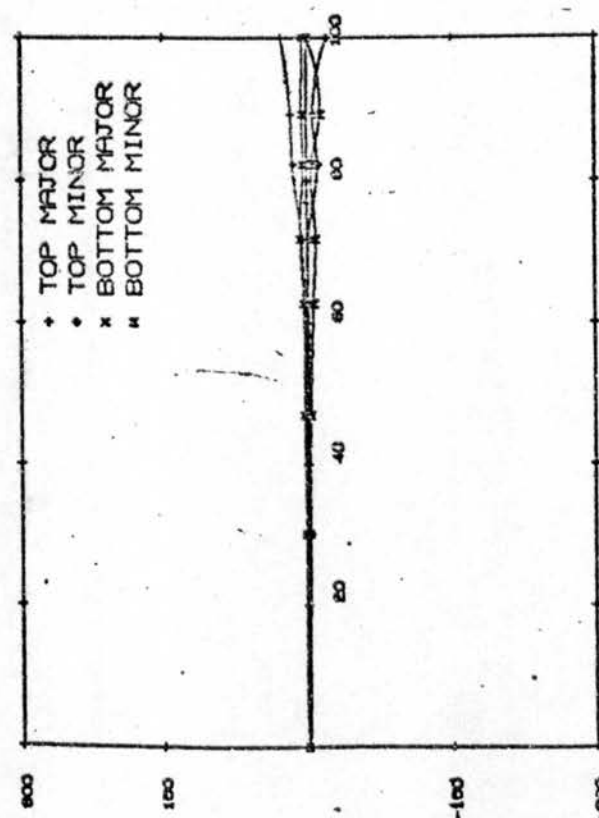
CHORD CROWN

BETA = 0.77 D/T = 18



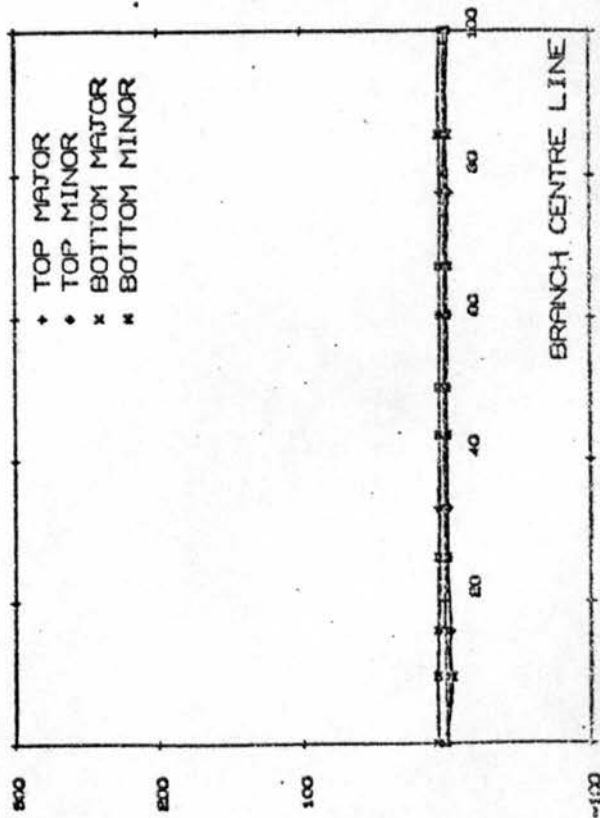
BRANCH EDGE

BETA = 0.77 D/T = 18



CHORD CIRCUMFERENCE

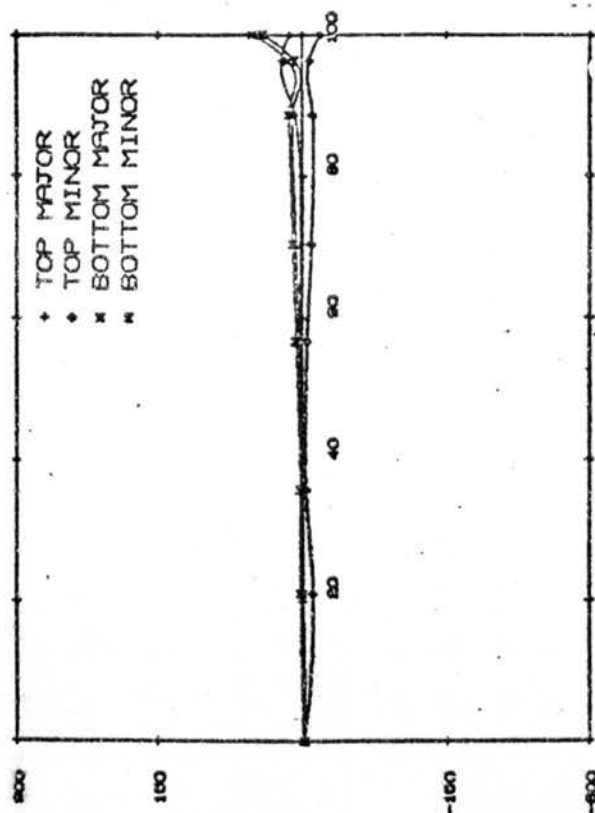
BETA = 0.77 D/T = 18



BRANCH CENTRE LINE

Figure 90. Stresses for unit bending load (1 kNm).

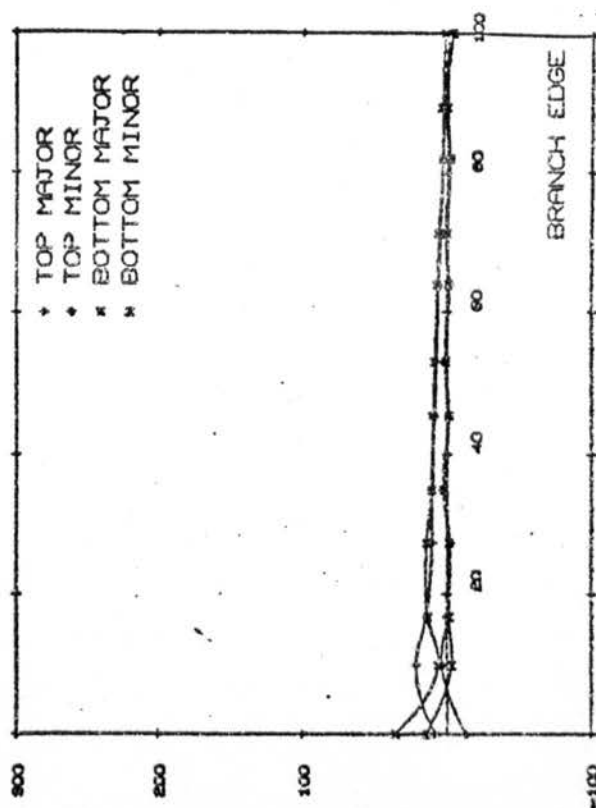
BETA = 0.77 D/T = 23



CHORD CROWN

MAJOR AND MINOR PRINCIPAL STRESSES

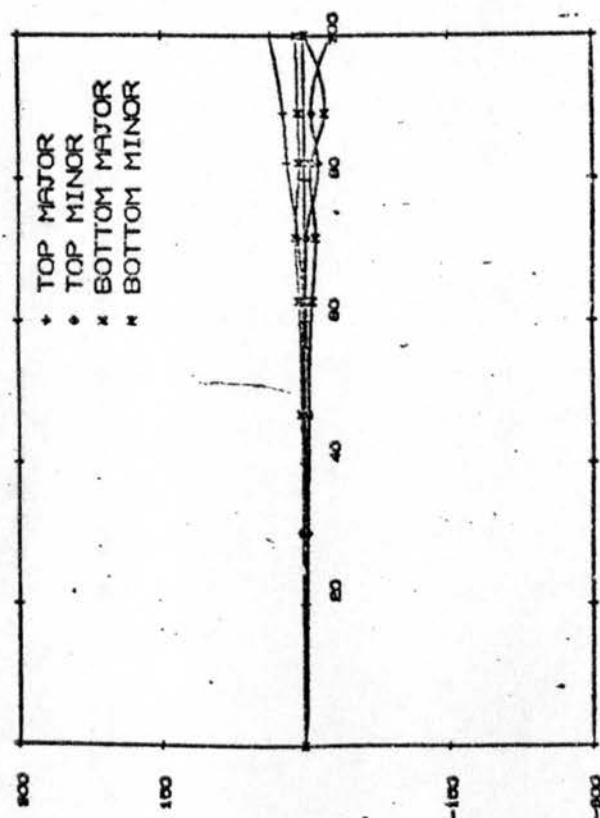
BETA = 0.77 D/T = 23



BRANCH EDGE

MAJOR AND MINOR PRINCIPAL STRESSES

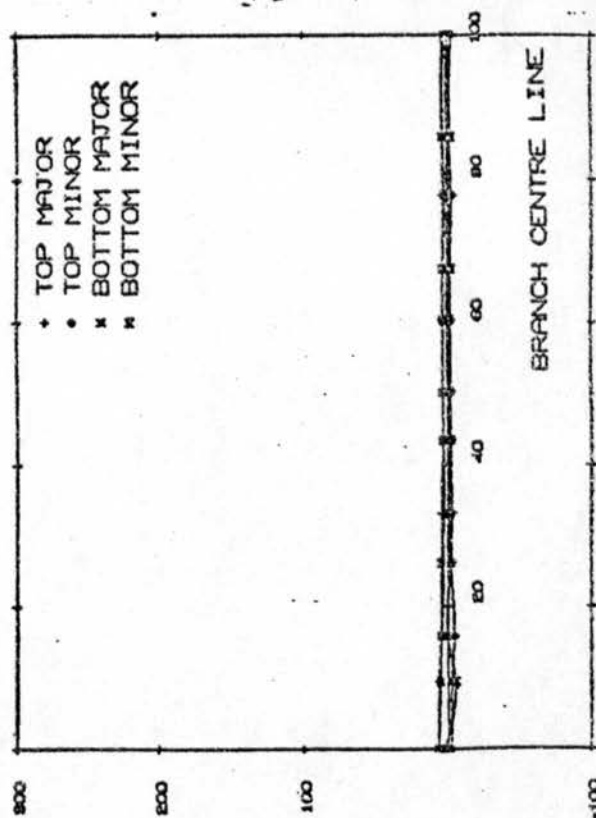
BETA = 0.77 D/T = 23



CHORD CIRCUMFERENCE

MAJOR AND MINOR PRINCIPAL STRESSES

BETA = 0.77 D/T = 23

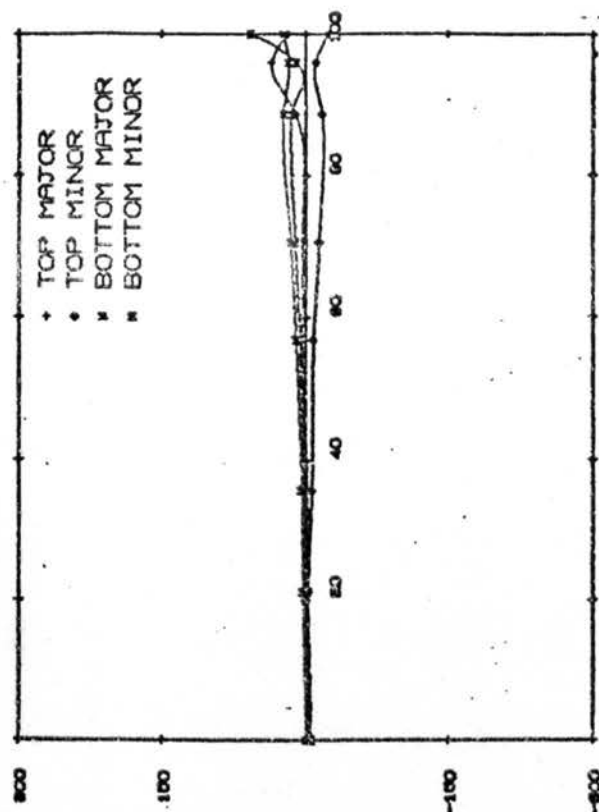


BRANCH CENTRE LINE

MAJOR AND MINOR PRINCIPAL STRESSES

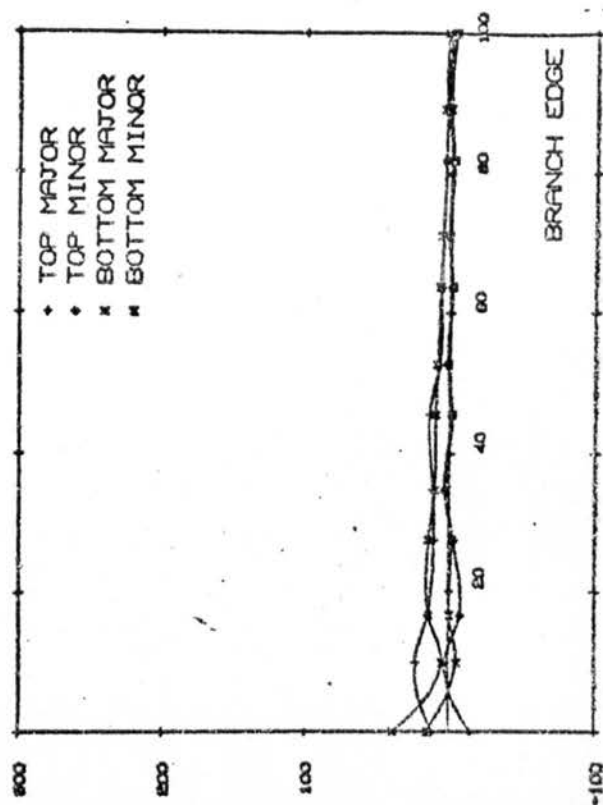
Figure 91. Stresses for unit bending load (1 kNm).

BETA = 0.77 D/T = 32



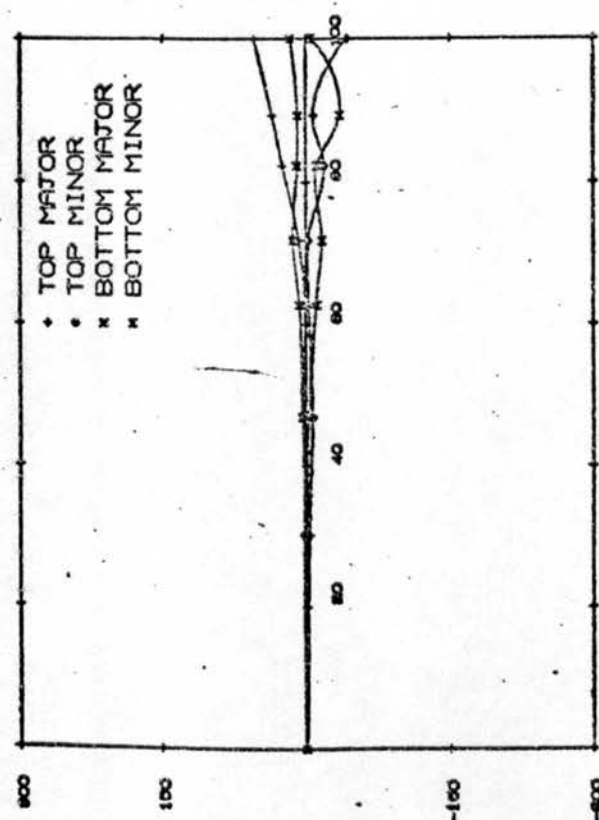
CHORD CROWN

BETA = 0.77 D/T = 32



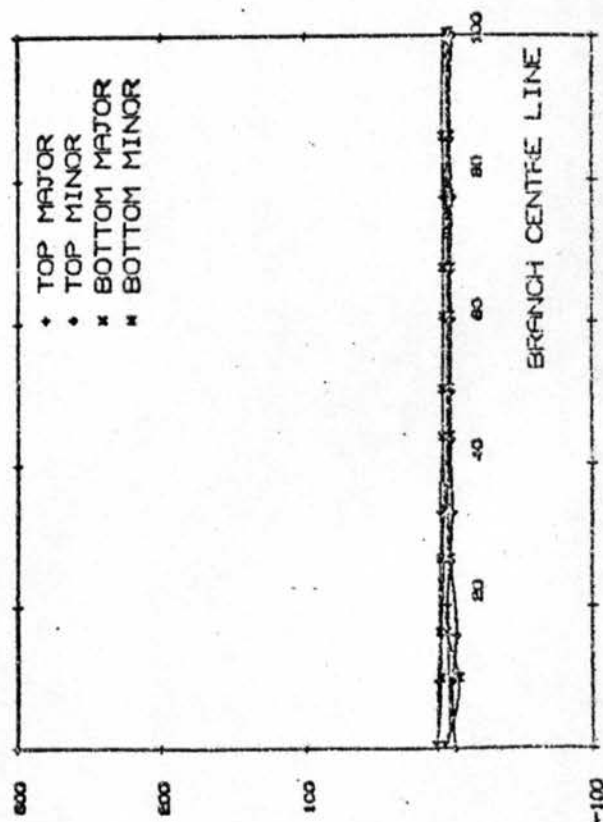
BRANCH EDGE

BETA = 0.77 D/T = 32



CHORD CIRCUMFERENCE

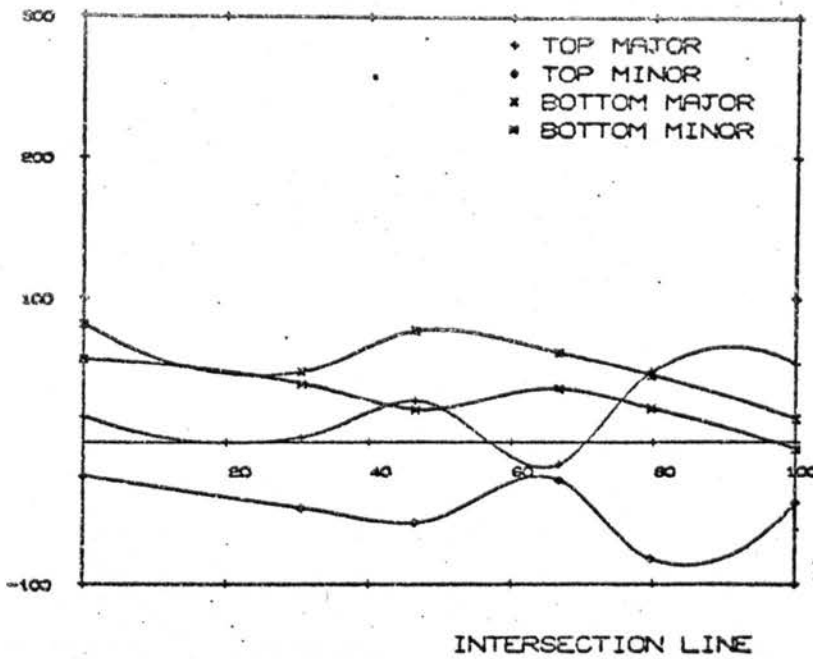
BETA = 0.77 D/T = 32



BRANCH CENTRE LINE

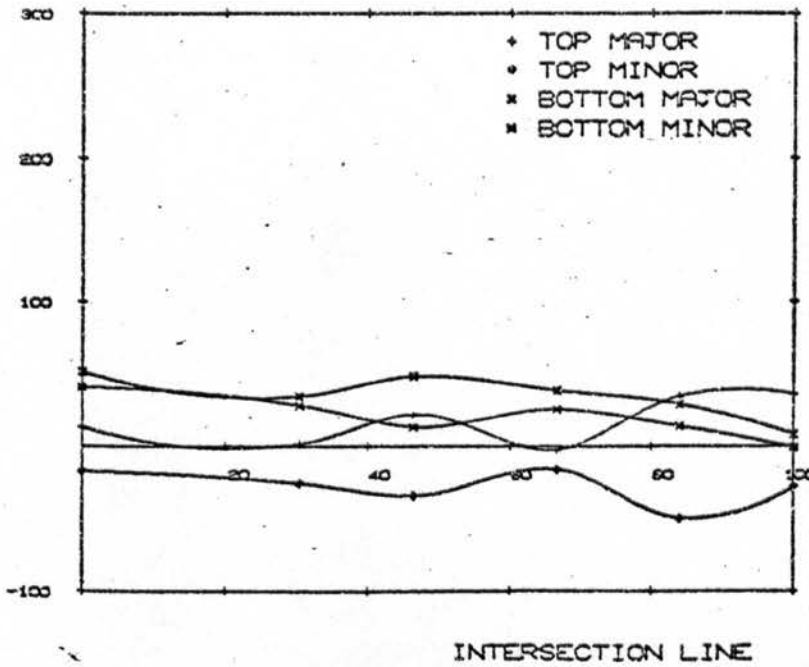
Figure 92. Stresses for unit bending load (1 kNm).

MAJOR AND MINOR PRINCIPAL STRESSES



BETA = 0.77 D/T = 23

MAJOR AND MINOR PRINCIPAL STRESSES



BETA = 0.77 D/T = 18

MAJOR AND MINOR PRINCIPAL STRESSES

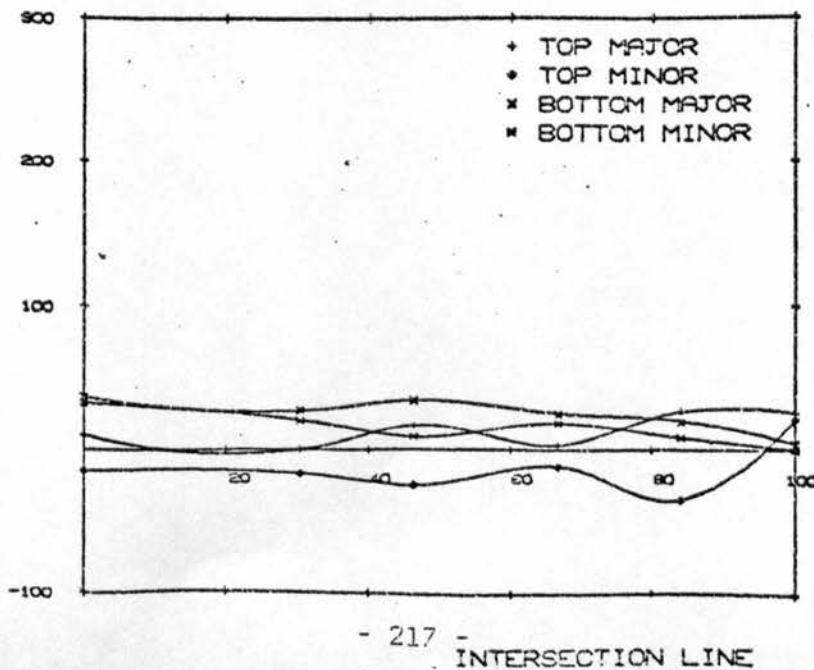
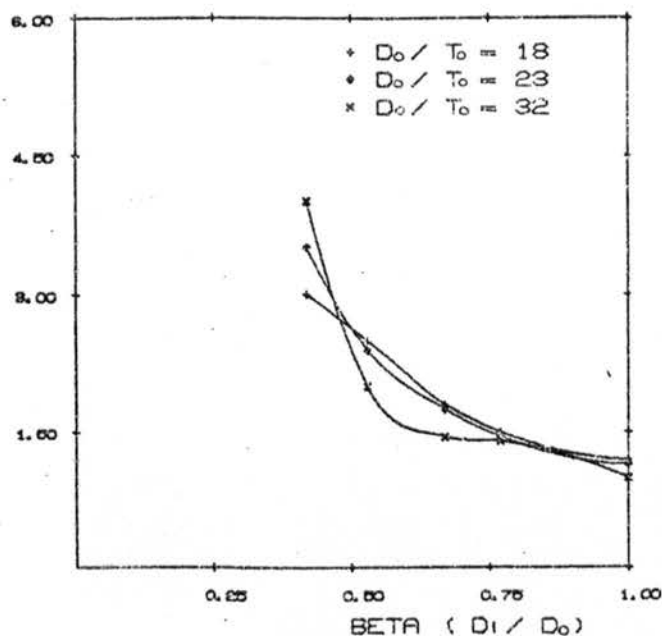
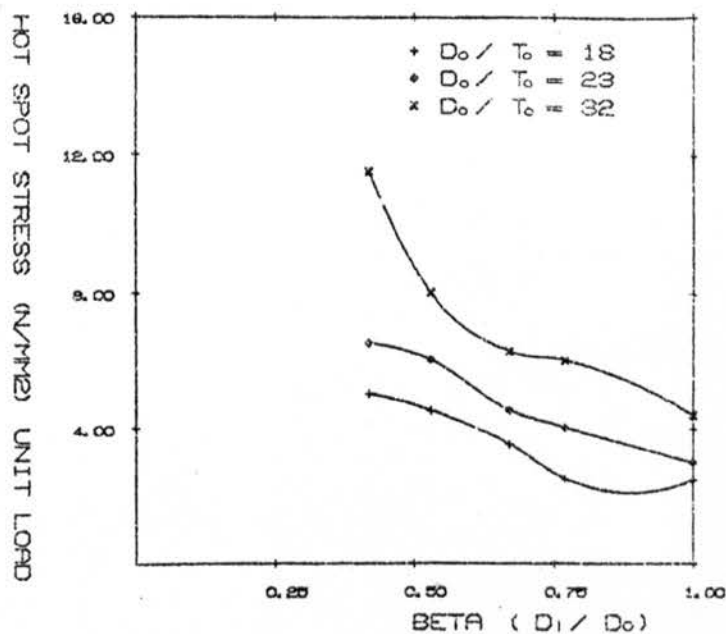


Figure 93. Stresses for unit bending load (1 kNm).

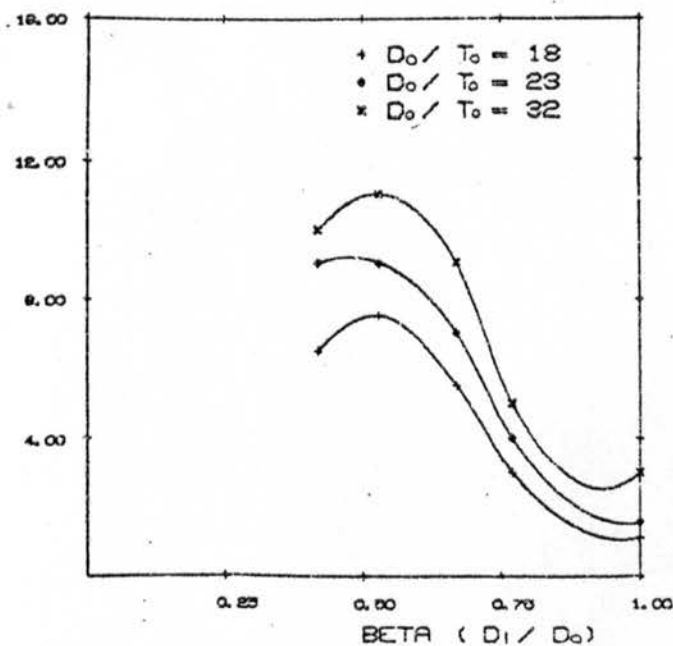
HOT SPOT STRESS AT POINT A



HOT SPOT STRESS AT POINT B



HOT SPOT STRESS AT POINT C



HOT SPOT STRESS AT POINT D

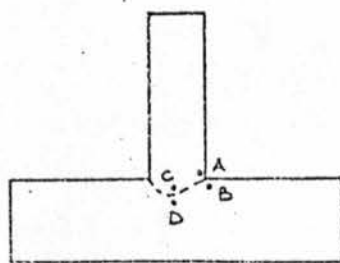
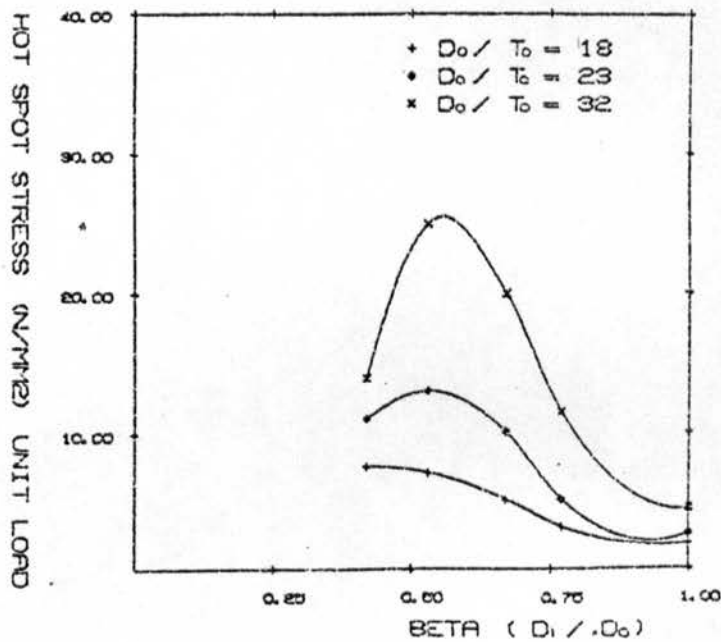
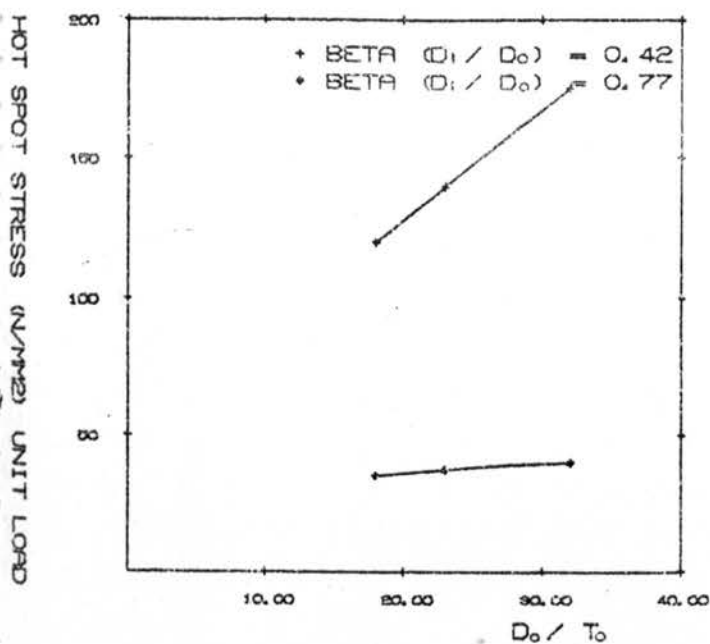
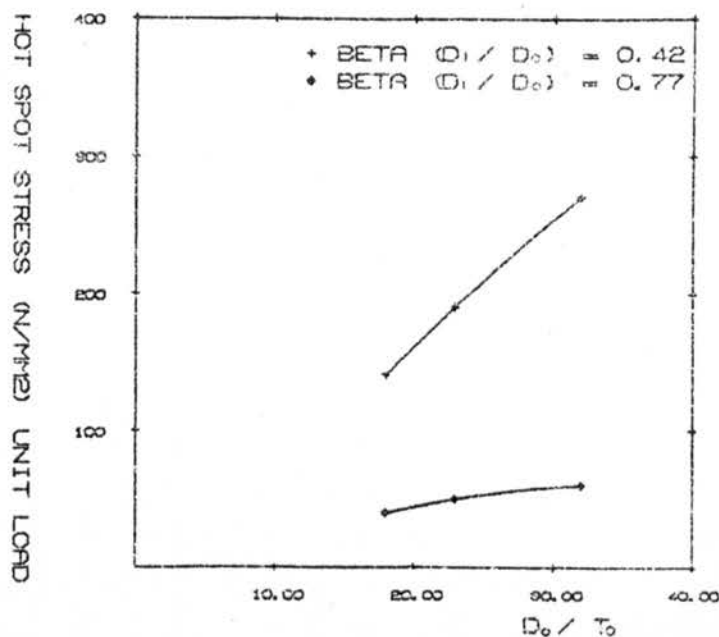


Figure 94. Hot spot stresses for axial load on joint.

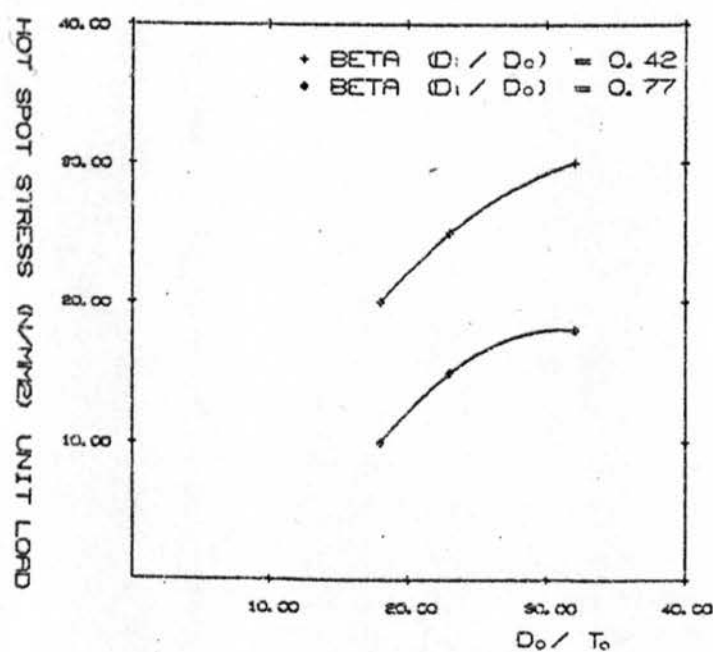
HOT SPOT STRESS AT POINT A



HOT SPOT STRESS AT POINT B



HOT SPOT STRESS AT POINT C



HOT SPOT STRESS AT POINT D

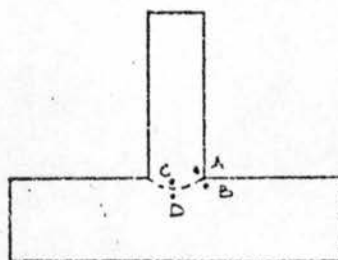
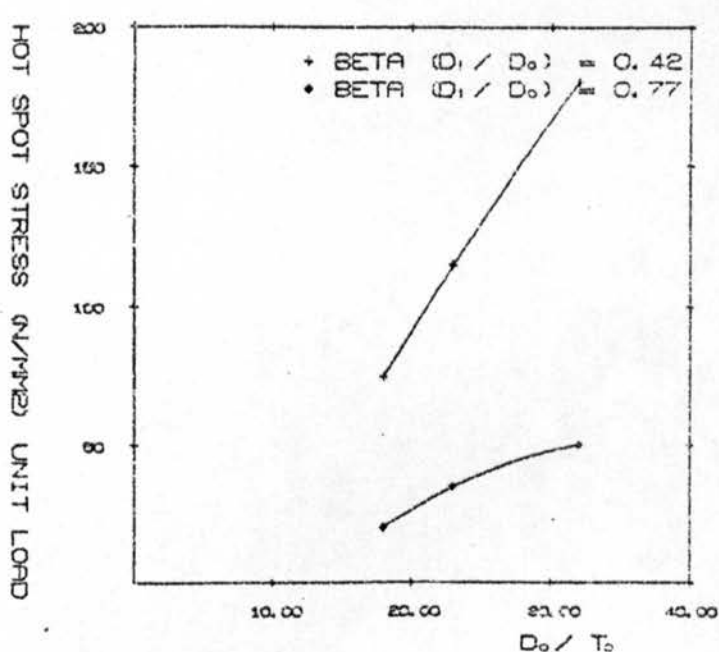


Figure 95. Hot spot stresses for bending load on joint.

CHAPTER 6

EXPERIMENTAL PROCEDURE FOR THE PRESENT INVESTIGATION

6.1. General

In 1896 the Belgian Engineer, Prof. Arthur Vierendeel, proposed the form of girder that now carries his name, in which the applied loads are transmitted by the bending of the members and the stiffness of the joints, (Figure 97), rather than by the axial tensile and compressive forces of the conventional truss. The Vierendeel girder is a statically indeterminate structure. However symmetrical Vierendeel girders can be satisfactorily designed statically by assuming points of contraflexure at the centre of each member¹⁰⁴. The resulting shear and end load distributions are shown in Figure 98 and the bending moment distribution in Figure 99.

For cases not suitable to this treatment and for the calculation of deflections, standard plane frame computer programs can be used to carry out the required analysis. Having determined the member forces, members can be sized according to the requirements of BS 449¹⁰⁵ or BS 153 for members subject to combined bending and axial load. There has been, however, no experimental work up to the present to either confirm or deny this method of design, especially in the field of Vierendeel frames with circular hollow section members. For this reason the present investigation has been carried out at Kingston Polytechnic in conjunction with the Research Centre of the British Steel Corporation's Tubes Division at Corby. Specifically, the aim of the research has been to investigate the ultimate strength of welded T-joints in circular hollow sections. The load cases considered have been:-

1. Compressive axial load in the branch member.
11. Lateral load in the branch member, causing a primary bending moment in the joint at the branch/chord interface.

iii. A combination of the two loads effects described above in (i) and (ii). The interaction between the two types of load case has been studied.

The strength of any type of joint in C.H.S. is governed by several joint parameters, many of which are common to the joint strength of R.H.S. members. As described in Chapter 3 several parameter studies have been carried out by other investigators, considering axial load only, and it is generally believed that any design formula to predict joint strength would be of the general form:-

$$P_1 = f(d_1/d_o, t_1/t_o, d_o/t_o) f_{y_o}$$

with additional factors for:-

Effect of branch member inclination.

Effect of axial load in chord member.

Effect of stresses due to secondary moments induced by joint eccentricity or initial lack of straightness of members.

In the present experimental investigation all three of the main joint strength parameters have been varied, although the actual chord diameter has been kept constant in order to simplify the experimental procedure for this series of tests.

The parameter ranges studied have been:-

d_1/d_o : 0.42, 0.53, 0.67, 0.77, 1.0

d_o/t_o : 18, 21, 23, 32

t_1/t_o : 0.63, 0.74, 0.79, 0.8, 1.0, 1.1, 1.38

The last parameter listed above, i.e. the thickness of branch member to thickness of chord member ratio, has not been studied explicitly. However, because of the availability of tube thicknesses in certain diameters a variation in t_1/t_o ratios has occurred which has been studied.

6.2. Welding

In the present study it was decided that the weld between the branch member and the chord member should be eliminated as a joint strength parameter. This was achieved by developing a full strength fillet or fillet-butt weld at this junction. The welding was carried out under carefully controlled conditions at the British Steel Corporation's Tubes Division, and as a result there have been no weld failures in the present series of tests. Whether the weld is a fillet weld or a fillet butt weld depends upon the diameter ratio of the joint.

Figure 100 shows two bracings, of the same size, meeting main members of different sizes. In both cases welding conditions at the crown of the main chord are the same, so for similar loads in the members identical fillets would be used.

At the flanks, however, conditions differ. The curvature of the large main chord continues to give good fillet weld conditions. The curvature of the smaller main chord necessitates the provision of a butt weld. The change from one form of weld to the other must be continuous and smooth.

For calculating weld sizes, both types are considered as fillet welds. The fillet-butt preparation is used where the diameter of the bracing is one third or more of the diameter of the main chord member, i.e. d_1/d_0 greater than 0.33.

6.3. Strength of Fillet Welds

The safe working load (S.W.L.) for a fillet weld in tension or compression is a product of:-

The allowable working stress, 0.7 of the nominal or specified fillet size ("L" in Figures 101 & 102) and the length of the weld.

The allowable working stresses derived from BS 449 clauses 53c and 53d are:-

Steel to BS 15 or BS 968 using electrodes to BS 639 - Part 2.

Steel to BS 968 using electrodes to BS 639 - Part 4.

Very little research has been carried out to investigate the effects of weld strengths on joints in C.H.S. Kurobane¹⁹ has stated that in his research program, where various profiling and welding techniques were used, it was noted that no failures occurred due to cracks in the welds or in the heat affected regions close to the welds.

6.4. Present Program

The present program of theoretical and experimental work has been supported by the British Steel Corporation, Tubes Division at Corby, Northants, England. Recently there has been a trend towards using tubular steel in various structures, as illustrated earlier, and this has required a greater knowledge of structure and joint behaviour. Very little experimental work on circular hollow sections (C.H.S.) has been carried out in the United Kingdom and Kingston Polytechnic was fortunate to be given the present program. The project has been carried out in conjunction with the Research Centre at Corby and in co-operation with C.I.D.E.C.T., the International Committee for the study of joints in circular hollow sections.

The problem of joint strength in C.H.S. sections is quite complex, covering very many types, sizes and configuration of joints; for example there are T, Y, K and N-joints (See Figure 13a) and also other joints with more than two bracing members. Various countries have their own standard diameters of tube and multitudes of tube thicknesses. Finally, there are various different types of load

which may be applied at any joint. Loads may be axial, shear or bending or any combination of these loads. Also, bending loads may be moments in the plane of the joint (longitudinal) or perpendicular to the plane of the joint (circumferential).

The present research program has studied the strength of welded T-joints in circular hollow steel sections under axial load (P), longitudinal moment (M), and combinations of axial load and longitudinal moment. The sections studied have all been typical British Steel Corporation commercial sections, manufactured in grade 43C steel. The chord or main tube diameter has been kept constant, and by varying its thickness and also the diameter and thickness of the bracing member it has been possible to carry out tests covering the following joint geometric parameters:-

1. chord diameter - 114.3mm
- chord thickness - 3.6mm
- 5.0mm
- 5.4mm
- 6.3mm

giving chord diameter to chord thickness ratios d_o/t_o of 32, 23, 21 and 18, respectively.

2. chord diameter - 114.3mm
- brace diameter - 48.3mm
- 60.3mm
- 76.1mm
- 88.9mm
- 114.3mm

giving brace diameter to chord diameter ratios d_1/d_o of 0.42, 0.53, 0.66, 0.77 and 1.00, respectively.

3. chord thickness - 3.6mm
5.0mm
5.4mm
6.3mm

brace thicknesses - 4.0mm
5.0mm

giving brace thickness to chord thickness ratios t_1/t_o of between 0.63 and 1.4.

At the outset of the research program it was decided that the type of welding would be kept the same for all joints, and it was of 10mm fillet weld. In this way the weld condition was eliminated as a joint parameter in the present study. This assumption was later confirmed by the fact that in all the tests for ultimate joint strength the welded joints held despite some very large member rotations.

Loads studied have been axial load applied to the joint through the bracing member, and longitudinal moment applied to the joint as a lateral load perpendicular to the bracing member. Tests have been carried out for pure axial load, pure bending load (including the associated shear load at the joint), and for combinations of axial and bending loads. The latter tests were carried out in order to study the interactive effects of these two loads.

Pure longitudinal moment loads on circular hollow steel sections had not been studied experimentally previously. Similarly the experimental interactive tests had not been studied previously except for 2 tests carried out in Japan ¹⁹.

Instrumentation for the tests consisted of deflection gauges, electrical resistance strain gauges, a digital datalogger, hydraulic jack load cells and in some tests brittle lacquer paint on the joints to give a visual demonstration of stress pattern.

6.5. Experimental Apparatus

6.5.1. Testing Rig (See Figure 103)

A rig was designed and constructed in order to carry out the isolated T-joint tests. A plane frame configuration was chosen because of the simplicity of construction, and because it was a statically determinate structure. Construction was in the horizontal plane to utilise the strong floor which was present in the testing laboratory. One side of the square structure was constructed in such a way that it could be finely adjusted for position, to take up discrepancies in test specimen length. This side member could also be moved further back in position to enable a bigger specimen to be tested, or to permit the insertion of a jack to give axial load in the specimen chord member.

All members were of composite construction, consisting of a central section of 203.2 x 101.6 x 5.85 hollow box to which 152.4 x 76.2 x 12 angles were bolted top and bottom to act as flanges. The angles were bolted right through the box section with $\frac{3}{4}$ " diameter bolts at centres, to ensure composite action in resistance to bending. The two larger side members were fixed to the strong floor using 1" diameter holding down bolts which, using bolt spacers (detail B Figure 106), also lifted the rig clear of the floor. The fixed end member had $\frac{1}{2}$ " mild steel plates welded to each end with $\frac{1}{4}$ " fillet weld. The plates were drilled for fixing this member to the side members (detail A Figure 108) using $\frac{3}{4}$ " diameter bolts. The fixed end member was also bolted to the floor on a spaced holding down bolt (detail B Figure 106). The moveable end member also had $\frac{1}{2}$ " mild steel plates welded to each end. These were drilled for fixing the member to the side members using $\frac{3}{4}$ " diameter bolts. These holes were elongated in order to permit some fine adjustment in position which might be caused by small variations in the length of test specimens. The side members had several sets of fixing holes along their length which gave a variety of fixing positions for the moveable end member.

The test specimen was bolted, using $\frac{3}{4}$ " diameter bolts, between the fixed end member and the moveable end member. Test specimens had $\frac{1}{2}$ " mild steel plates welded to the ends of the chord in order to facilitate this operation (see Figure 109). It was found, in later experiments using very high loads, that some additional clamping of these plates to the end members was required to prevent damage to the rig.

In the present test series loads were applied by jacking off the rig members onto the test specimen (detail C Figure 107). Of the methods available for applying loads this appeared to be the most satisfactory, but several problems were encountered.

- i. Rotation of the brace member under lateral load (for moment) caused difficulties in maintaining perpendicular application of the load, either laterally for moment load or vertically for axial load. This problem was overcome by constructing a special device for applying the loads at the end of the brace member (detail D Figure 110). This device slotted inside the brace member and enabled ball and socket joints to be used on the ends of the jacks. These joints were also used at the rear of the jacks to enable the jacks to follow the line of rotation of the brace. The insert part of the load applying device was machined to give an individual fit for each brace tube of each specimen tested. This ensured a tight fit and even distribution of load around the brace circumference.
- ii. Initial imperfections in the centering of the brace tube and the chord tube sometimes meant that the jack, when located in the centre of the brace tube was pushing slightly out of plane. This became more serious as the deflection increased in the non-elastic loading range. The problem was more pronounced in the moment loading sequence and was overcome by restraining the jacking assembly within the plane of the rig (detail E Figure 111).

- iii. Under very high axial loads it was necessary to place a large thick steel plate behind the axial jack to prevent local distortion of the face of the main rig side member.
- iv. Difficulties arose during the tests on joints with combined loadings. The problem has been to apply simultaneously, an axial load and a bending moment to a T-joint. It has always been convenient to think of these loads as being external loads applied to the branch member.

The two loads were simultaneously applied to study their effect on the joint and their interaction relationship.

It was first thought that both loads could be increased together and, in fact, three tests were carried out in this way. It was noted, however, that as the axial load P was increased the moment load decreased at some point during the testing, and further increase of the moment load simply caused a large branch deflection sideways with a resulting eccentricity of axial load leading to a premature joint failure.

It was, therefore, decided that further investigation of this point of fall off in applied moment was required. Fixed moments were applied and axial loads increased in increments while deflections, strains and magnitudes of loads applied were measured.

Furthermore, in order to estimate the secondary moments, at failure, due to eccentricity of the axial load two assumptions were made:-

- a. That the branch tube, when deflecting sideways did so as shown in the sketch below (i.e. due to a plastic hinge at the joint, a rigid body movement occurs).
- b. That the angle of deflection θ was small.

To justify these assumptions the following checks have been made:-

1. To confirm assumption (a)

The branch tubes of joints which have been tested to failure have been checked and are found to be straight with no measurable curvature.

A new sample joint ($\beta = 0.42$, $t = 5.0$, $d = 48$, $T = 5.4$, $D = 114.3$) has been tested and the deflection of the branch tube under bending load has been plotted. It is seen that even for very small moments ($M = 3\%$ of M_u) there is a measurable deflection at a point 38mm along the branch from the weld toe, (see Figure 112).

2. To confirm assumption (b)

The measured angle of deflection has been found to have a maximum value of 1° (0.02 rad) in the elastic load range ($\cos \theta = 0.9998$, $\sin \theta = 0.02$).

A theoretical branch deflection profile has been plotted assuming that it acts as a fixed ended cantilever. These theoretical deflections are always found to be much less than those found in tests because the branch tube has rotational flexibility at the joint which, as it increases under increasing axial load, causes a rigid body movement of the branch as the moment (M) tends towards the ultimate moment (M_u).

A further problem, when considering secondary moments, can occur when the axial load is applied. If it is assumed that the bending load (P_B) has been applied first, then the branch tube may assume the deflected position shown in Figure 113(a).

The axial load P_A can, therefore, be applied in either of the three ways shown in Figure 113(b).

- P_{A1} - if this loading condition occurs then the branch deflection would increase and the bending load (P_B) would decrease, which could easily be checked by the readings on the horizontal jack load cell and the dial gauge,
- P_{A2} - the ideal case; no eccentricity, P_A acts as a pure axial load; both the load cell and the dial gauge would show no change,
- P_{A3} - in this case the branch deflection would decrease and the load cell registering bending load would show an increase. This has not happened, however, in any of the tests (at least not to any significant level).

Therefore, in all tests, in order to eliminate as far as possible the errors due to secondary moments, the axial load jack was positioned in such a way that the branch tube showed no secondary deflection (δe) when the axial load was applied.

It is seen from graphs of axial load against sideways deflection that this situation has been achieved in all the tests carried out so far, Figure 113(c). Where (δe) is the secondary deflection due to eccentricity of the axial load.

It is seen that δe increases sharply at an axial load (P') which corresponds to:-

- a. the point where axial deformation of the branch becomes non linear.
- b. the point where applied bending moment decreases.

This is due to the formation of a plastic hinge in the chord wall at the joint and resulting loss in rotational stiffness.

Conclusions

- i. The system of applying loads has some shortcomings, but errors have been allowed for in the testing procedure, and are considered to be minimal.
- ii. T-joint branch deflections under moment load appear to be linear, as the stress level increases and rigid body rotation occurs.
- iii. It is possible to eliminate significant secondary moments from the testing procedure by re-positioning the axial load jack.
- iv. At joint failure under combined loading, i.e. when the joint can no longer sustain its maximum value of combined axial and moment loading (taken as the loading at which the applied moment decreases) the maximum eccentric moments may be of an order of 4-6% of the ultimate moment, (eccentric moment = $P' \times (\delta_o + \delta_e)$; see previous figure), (113(c)).
- v. Joints subject to combined loading appear to undergo a loss of moment resistance when the axial load is high enough for a plastic hinge to be formed at the joint.

The formation of this plastic hinge was first noted by A. A. Toprac and is recently confirmed by the French report (Harlicot, Mouty, Tournay) for the C.I.D.E.C.T. working group on C.H.S. joints.

- vi. It is possible to relate the fall-off in applied moment at the joint to the sideways deflection and axial deflection of the branch tube. Values for P' corresponding to fixed values of M/μ can, therefore, be found in three ways, measuring:-
 - a. the reading on the load cell of the jack giving moment load,
 - b. axial deflection of the branch tube, relative to the deflected chord tube,
 - c. sideways deflection of the branch tube.

Computer Model of Testing Rig (See Figures 114-116)

Theoretical analysis of the rig was carried out using a plane frame computer analysis program LC29 (a standard I.C.L. program). Loads are input at joints or between joints whereupon they must be converted to moments and equivalent joint loads. Joints may be inserted at any point in the structure for ease of data preparation. To prevent rotation of the structure at least two joints must be fixed in directions X and Y. In the actual rig fixing occurred at all the floor mounting positions, and for analysis three conditions were chosen for preventing this rotation:-

- | | | | |
|------|-----------------------|---|-------------------------------|
| i. | Fixing at two joints |) | |
| ii. | Fixing at four joints |) | i.e. displacements in X and Y |
| iii. | Fixing at six joints |) | were set to zero. |

The computer output lists deformations, translational and rotational, shear forces, and bending moments at the joints and member ends respectively.

Several trial analyses were carried out and it was found that the results from the conditions listed in (i) above gave the broadest representation of test rig behaviour.

General Testing Rig Philosophy

It is anticipated that the present plane frame structure of the testing rig will be modified at some time in the future to convert it to a three-dimensional structure. This would enable a greater variety of joints to be tested and would also mean that out of plane loading cases could be considered.

This modification would be relatively simple, requiring only the addition of further modular frame members. For complex joints the system of applying loads would require special consideration.

6.5.2. Load Application

Loads were applied using Enerpac manually operated hydraulic jacks, which were monitored using Mayes electrical resistance load cells. These were calibrated from 50kN to 500kN depending upon the size of jack being used in a particular test.

As mentioned previously, in order to permit the branch tube to deflect a special connection was designed and made which allowed rotation at the jack head (Figure 110). Similar devices were fixed to the front and rear of the axial jack to permit rotation during tests under combined loading. The connection was made to insert into the tube to prevent local buckling of the tube end under loads.

6.5.3. Instrumentation

Deflections were measured using Mercer deflection gauges (gauge constant was always 0.01mm).

Strains were measured using electrical resistance strain (E.R.S.) gauges. Two types were used:-

10mm long, 120 Ω resistance gauge factor 2.07

30mm long, 120 Ω resistance gauge factor 2.12

These were glued to the test specimen either in positions which gave general strain distribution, or in positions of particular interest, e.g. anticipated "hot spots" for stresses.

Strains were monitored using a Dynamco datalogger model D6. This comprises a digital voltmeter with ancillary equipment which enables measurements of strain and displacement to be made on up to 100 input channels continuously, or at predetermined time intervals. In addition to a visual display, the output incorporates a teletype and tape punch for obtaining a hard copy of the voltages recorded. After each load increment the datalogger scanned all the gauge channels and recorded the voltages across them. This data was then output through the teletype on paper tape copy.

A simple computer program has been written, called LOG1, which read in this data, along with gauge constants and base voltage data. The changes in voltage as the load increased were then converted to changes in resistance. Since the change in resistance of this type of strain gauge was a function of the increase in length of the wire in the gauge then the amount of strain on the specimen sample was directly obtained. This information was printed out and has been plotted (Figures 180 to 210, Appendix B).

6.5.4. Test Specimens (See Figure 109)

As previously noted, all specimens were of the type shown in Figure 109. The chord diameter was kept constant and the variables were:-

chord thickness
branch diameter
branch thickness

Table 12 summarises the tests carried out during the present research program.

All specimens were Grade 43C steel fabricated and supplied by the British Steel Corporation, Tubes Division, at Corby. For material properties see Table 13. The values of yield stress and ultimate tensile stress are average values for the specimen derived from three random tensile tests carried out on coupons cut from the specimens which were tested for moment only.*

*In most of the axially loaded tests the chords of the test specimens were deformed and it was difficult to obtain good coupon specimens.

TABLE 12 - DETAILS OF TEST SPECIMENS

TEST	CHORD		BRACE		D/T _o	d/D _o	t ₁ /T _o	TYPE OF LOAD
	DIA	TH.	DIA.	TH.				
A/1	114.3	3.6	48.3	4.0	32	0.42	1.1	Pu
A/2	114.3	3.6	48.3	4.0	32	0.42	1.1	Mu
A/3	114.3	3.6	48.3	4.0	32	0.42	1.1	0.27,0.4,0.6, M/Mu 0.8
B/1	114.3	5.0	48.3	4.0	23	0.42	0.8	Pu
B/2	114.3	5.0	48.3	4.0	23	0.42	0.8	Mu
B/3	114.3	5.0	48.3	4.0	23	0.42	0.8	0.15,.25,0.5, M/Mu 0.75,0.85
C/1	114.3	5.4	48.3	4.0	21	0.42	0.74	Pu
C/2	114.3	5.4	48.3	4.0	21	0.42	0.74	Mu
C/3	114.3	5.4	48.3	4.0	21	0.42	0.74	0.25,0.5,0.75 M/Mu
D/1	114.3	6.3	48.3	4.0	18	0.42	0.63	Pu
D/2	114.3	6.3	48.3	4.0	18	0.42	0.63	Mu
D/3	114.3	6.3	48.3	4.0	18	0.42	0.63	0.25,0.5,0.75 M/Mu
E/1	114.3	3.6	60.3	5.0	32	0.53	1.39	Pu
E/2	114.3	3.6	60.3	5.0	32	0.53	1.39	Mu
E/3	114.3	3.6	60.3	5.0	32	0.53	1.39	0.23,0.46,0.77 M/Mu
F/1	114.3	5.0	60.3	5.0	23	0.53	1.0	Pu
F/2	114.3	5.0	60.3	5.0	23	0.53	1.0	Mu
F/3	114.3	5.0	60.3	5.0	23	0.53	1.0	0.25,0.5,0.75 M/Mu
G/1	114.3	6.3	60.3	5.0	18	0.53	0.79	Pu
G/2	114.3	6.3	60.3	5.0	18	0.53	0.79	Mu
G/3	114.3	6.3	60.3	5.0	18	0.53	0.79	0.23,0.46, M/Mu 0.69,0.86
H/1	114.3	3.6	76.1	4.5	32	0.66	1.25	Pu
H/2	114.3	3.6	76.1	4.5	32	0.66	1.25	Mu
H/3	114.3	3.6	76.1	4.5	32	0.66	1.25	0.2,0.5,0.66, M/Mu 0.8
J/1	114.3	5.0	76.1	4.5	23	0.66	0.9	Pu
J/2	114.3	5.0	76.1	4.5	23	0.66	0.9	Mu
J/3	114.3	5.0	76.1	4.5	23	0.66	0.9	0.18,0.3,0.5, M/Mu 0.9,0.98

TABLE 12 Cont'd

TEST	CHORD		BRACE		D_o/T_o	d/D_o	t/T_o	TYPE OF LOAD
	DIA	TH.	DIA.	TH.				
K/1	114.3	5.4	76.1	4.5	21	0.66	0.83	Pu
K/2	114.3	5.4	76.1	4.5	21	0.66	0.83	Mu
K/3	114.3	5.4	76.1	4.5	21	0.66	0.83	0.15,0.25,0.5, M/Mu 0.75
L/1	114.3	6.3	76.1	5.0	18	0.66	0.71	Pu
L/2	114.3	6.3	76.1	5.0	18	0.66	0.71	Mu
L/3	114.3	6.3	76.1	5.0	18	0.66	0.71	0.25,0.5,0.66, M/Mu 0.82
M/1	114.3	3.6	88.9	5.0	32	0.77	1.39	Pu
M/2	114.3	3.6	88.9	5.0	32	0.77	1.39	Mu
M/3	114.3	3.6	88.9	5.0	32	0.77	1.39	0.27,0.53, M/Mu 0.70,0.76,0.87
N/1	114.3	5.4	88.9	5.0	21	0.77	0.93	Pu
N/2	114.3	5.4	88.9	5.0	21	0.77	0.93	Mu
N/3	114.3	5.4	88.9	5.0	21	0.77	0.93	0.15,0.25,0.4, M/Mu 0.5,0.6,0.75, 0.85
P/1	114.3	6.3	88.9	5.0	18	0.77	0.79	Pu
P/2	114.3	6.3	88.9	5.0	18	0.77	0.79	Mu
P/3	114.3	6.3	88.9	5.0	18	0.77	0.79	0.24,0.36, M/Mu 0.45,0.61,0.82
Q/1	114.3	3.6	114.3	5.0	32	1.0	1.39	Pu
Q/2	114.3	3.6	114.3	5.0	32	1.0	1.39	Mu
Q/3	114.3	3.6	114.3	5.0	32	1.0	1.39	0.31,0.52,0.85 M/Mu
R/1	114.3	5.0	114.3	5.0	23	1.0	1.0	Pu
R/2	114.3	5.0	114.3	5.0	23	1.0	1.0	Mu
R/3	114.3	5.0	114.3	5.0	23	1.0	1.0	0.26,0.52,0.63 M/Mu 0.82
S/1	114.3	6.3	114.3	5.0	18	1.0	0.79	Pu
S/2	114.3	6.3	114.3	5.0	18	1.0	0.79	Mu
S/3	114.3	6.3	114.3	5.0	18	1.0	0.79	0.2,0.42,0.62 M/Mu 0.78

TABLE 13 - TENSILE COUPON TEST RESULTS

TEST	THICKNESS mm	YIELD STRESS N/mm ²	PERCENTAGE ELONGATION	ULTIMATE TENSILE STRESS N/mm ²
A/2	3.6	347	27%	497
B/2	5.0	329	29%	480
C/2	5.4	333	26%	489
D/2	6.3	352	26%	512
E/2	3.6	388	25%	507
F/2	5.0	320	26%	471
G/2	6.3	349	27%	515
H/2	3.6	356	27%	492
J/2	5.0	330	28%	453
K/2	5.4	342	31%	499
L/2	6.3	362	26%	498
M/2	3.6	347	26%	489
N/2	5.4	345	28%	498
P/2	6.3	361	26%	504
Q/2	3.6	341	28%	497
R/2	5.0	335	24%	478
S/2	6.3	359	25%	506

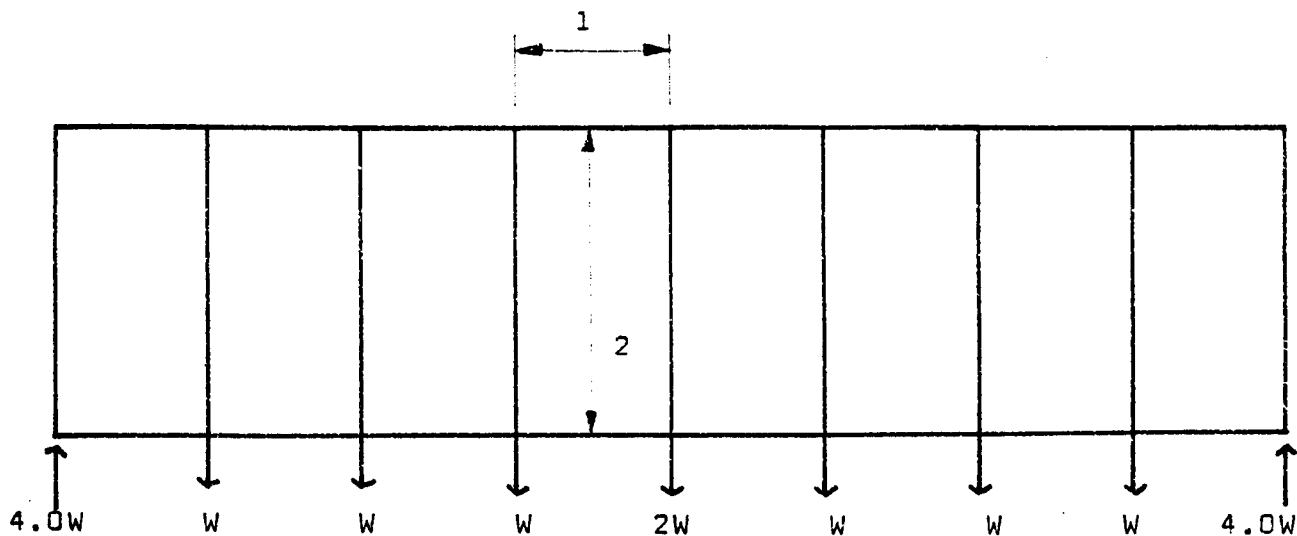


Figure 97. Simply supported Vierendeel girder

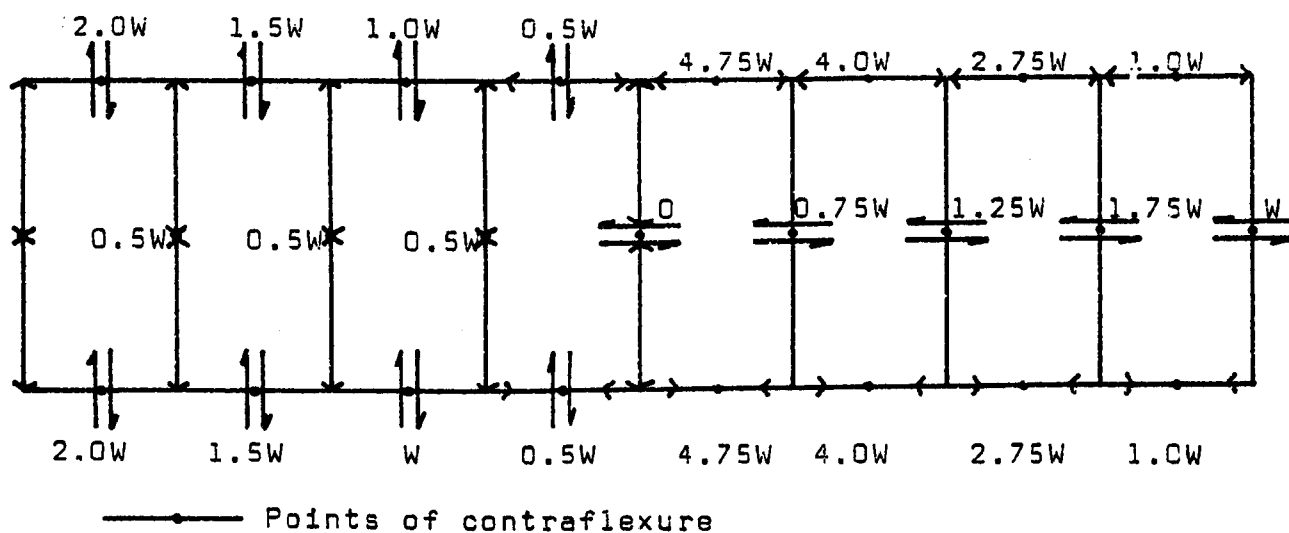


Figure 98. Shear force and end load distribution.

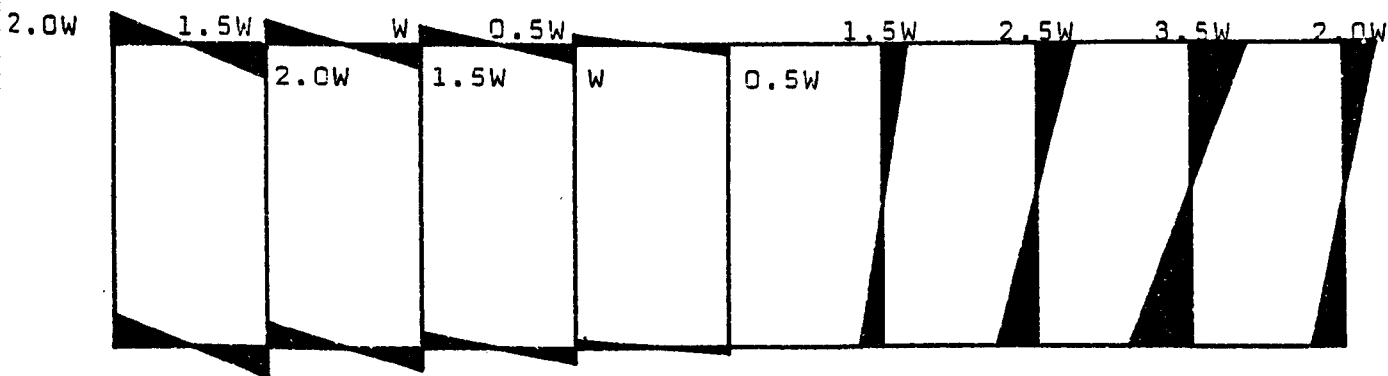


Figure 99. Bending moment distribution.

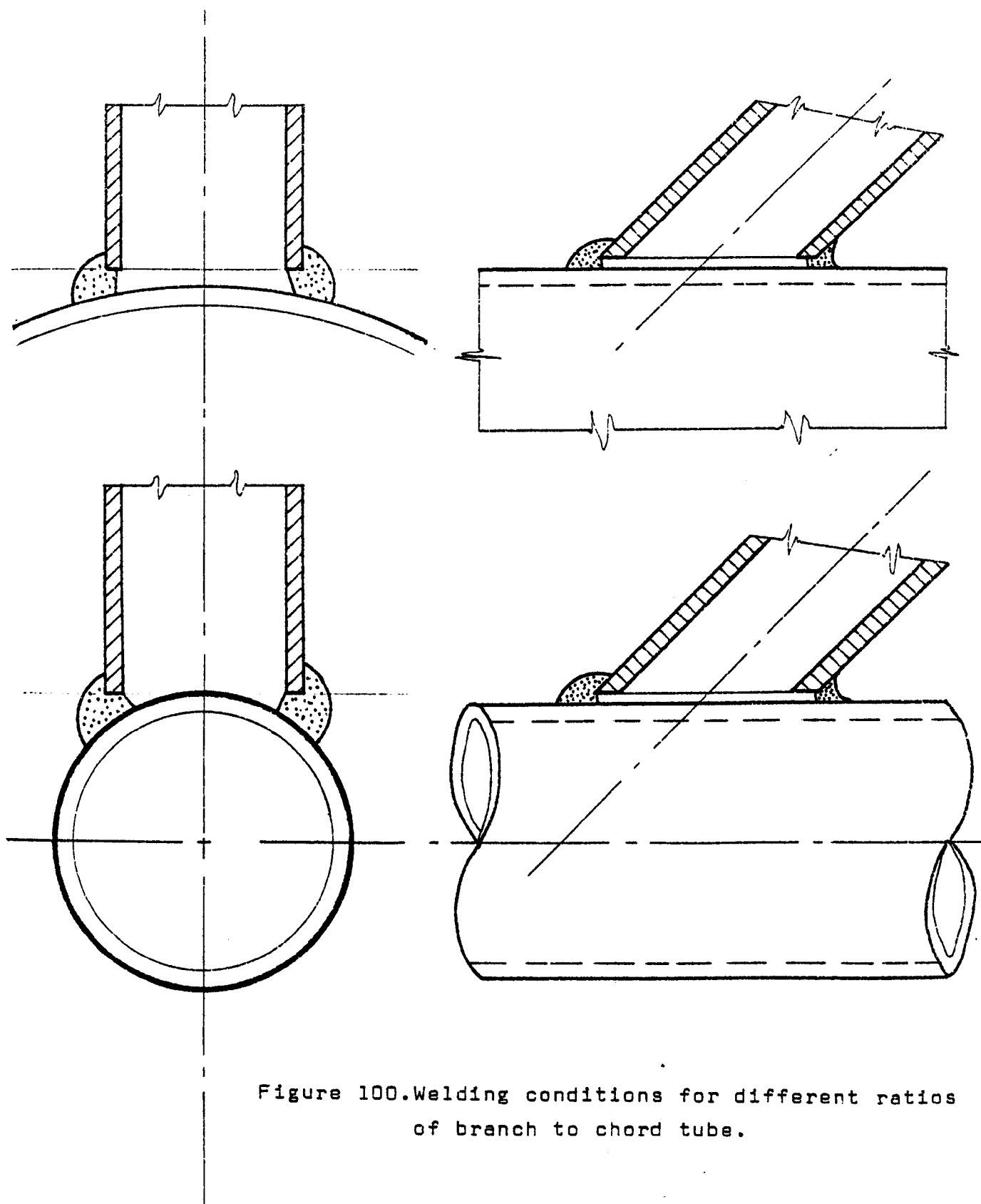


Figure 100. Welding conditions for different ratios of branch to chord tube.

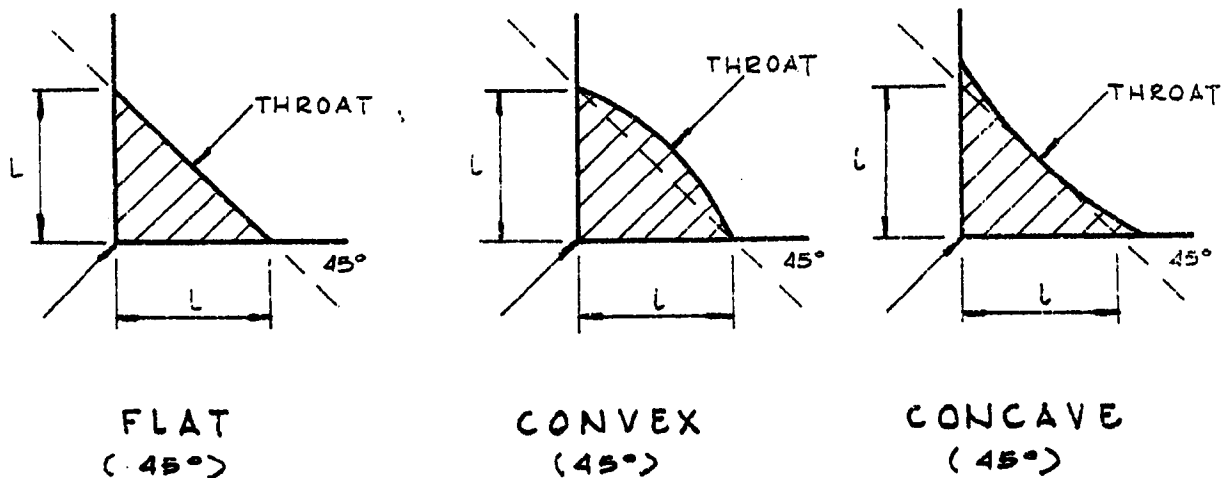


Figure 101. Fillet welds at right angles.

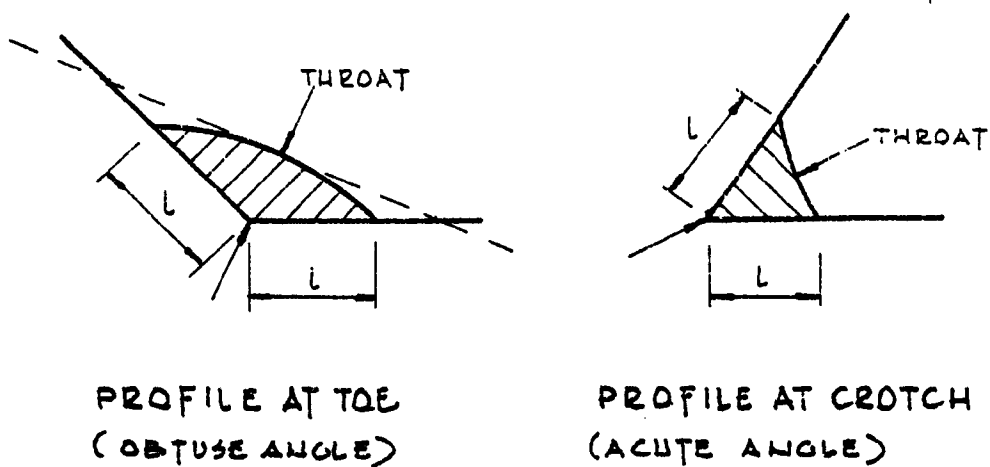


Figure 102. Fillet welds at acute and obtuse angles.

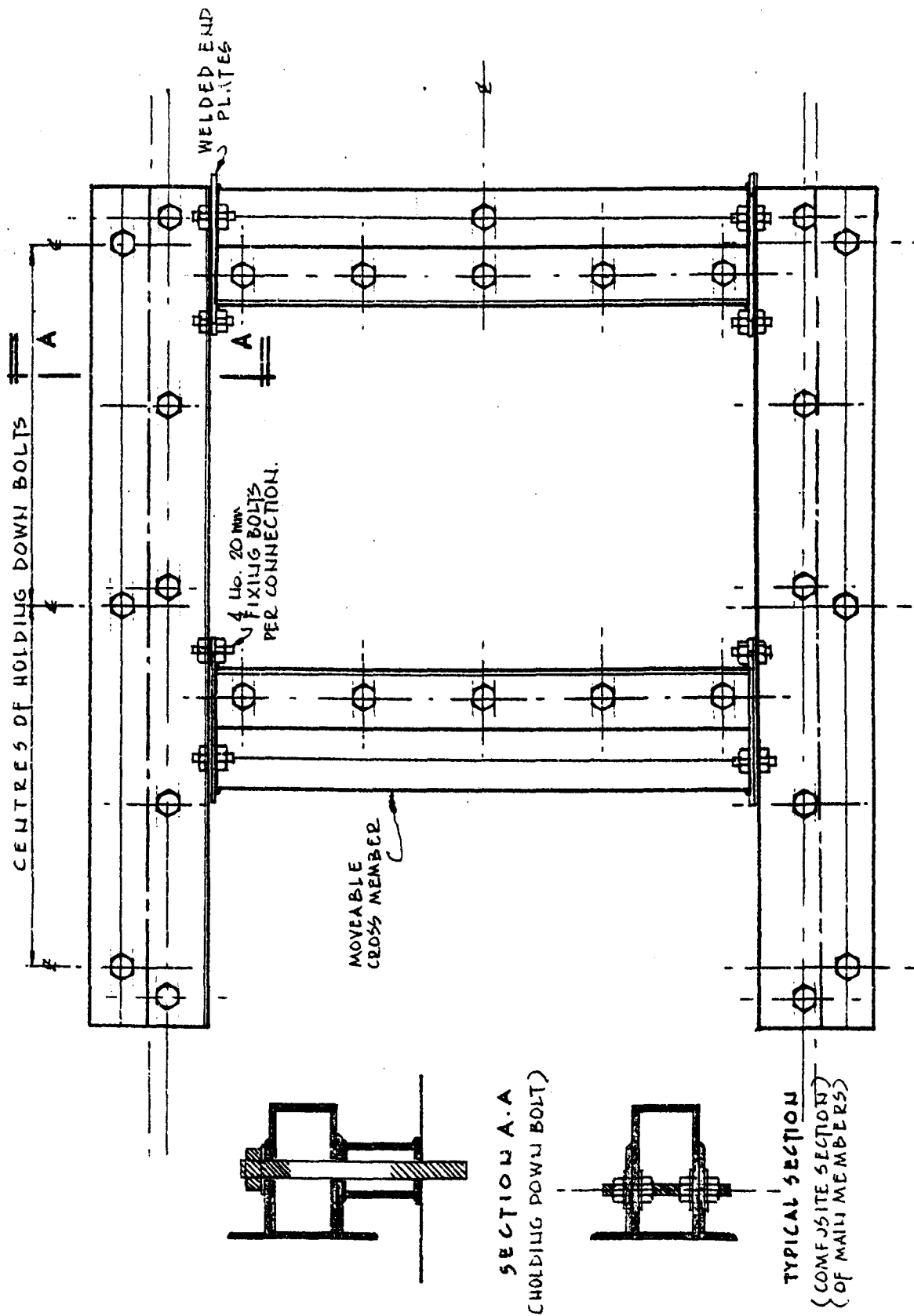


Figure 103. Testing Rig

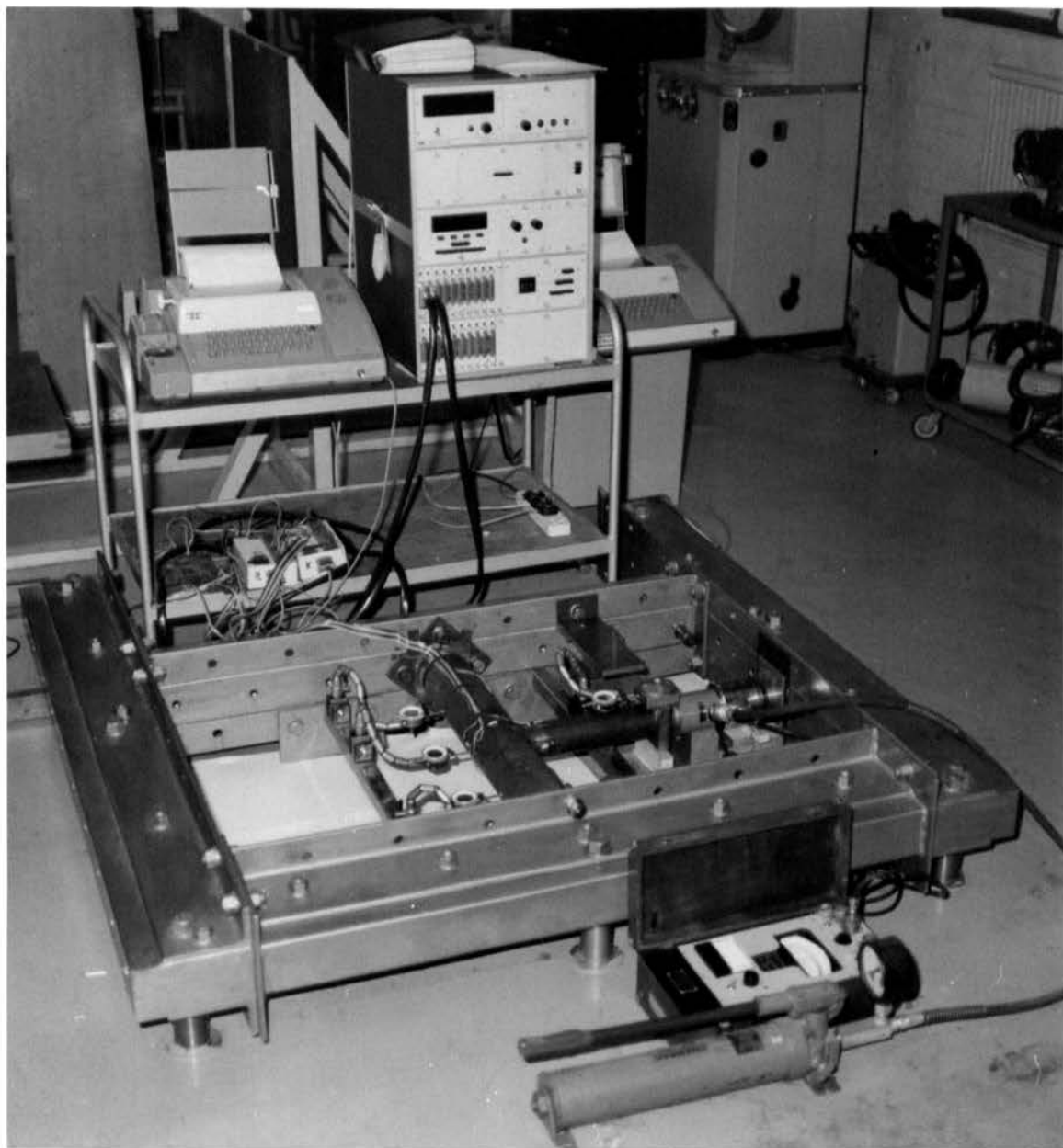


Figure 104 - General View of Testing Rig

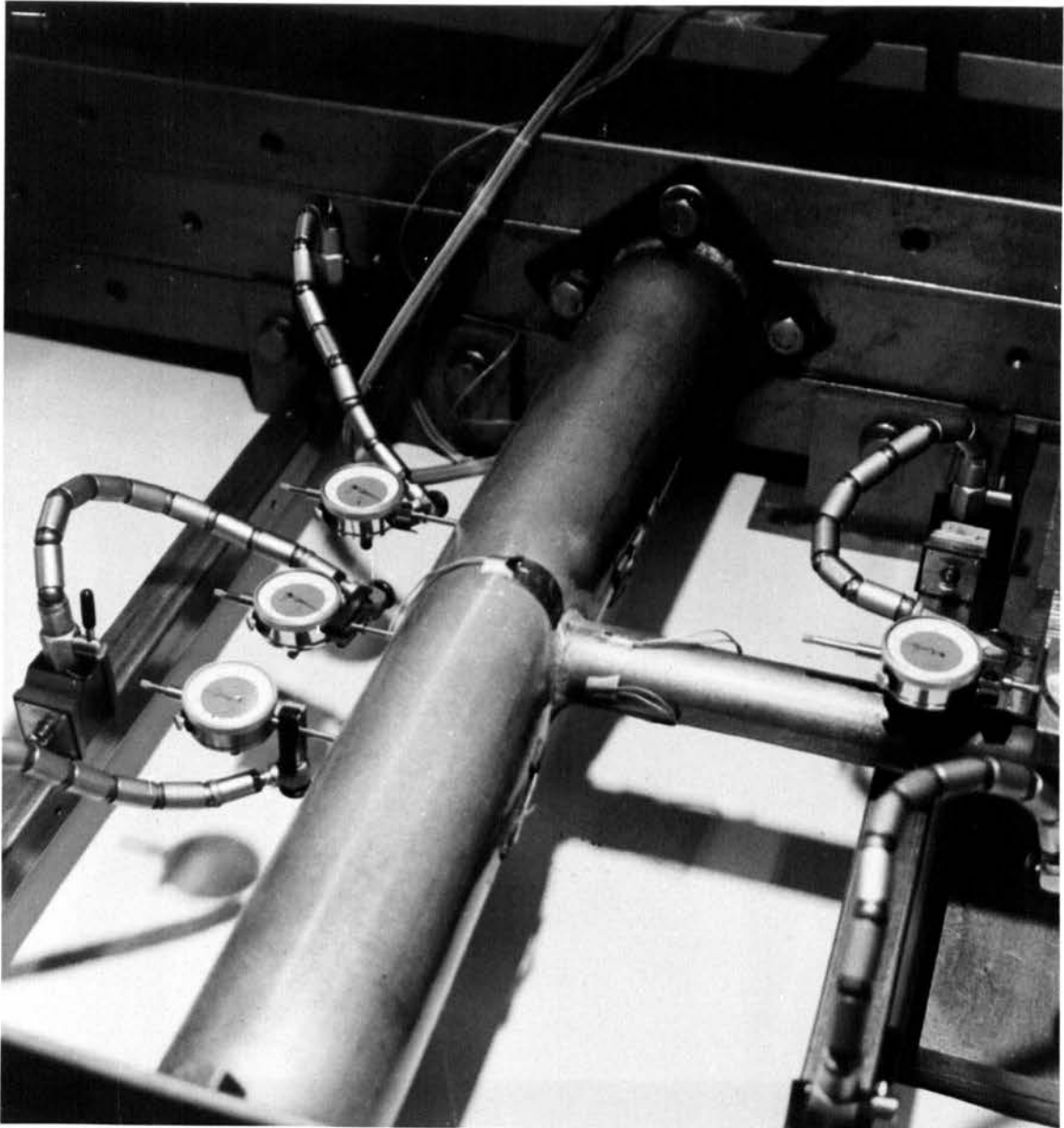


Figure 105 - T-Joint Under Axial Load ($\text{Beta} = 0.42$)

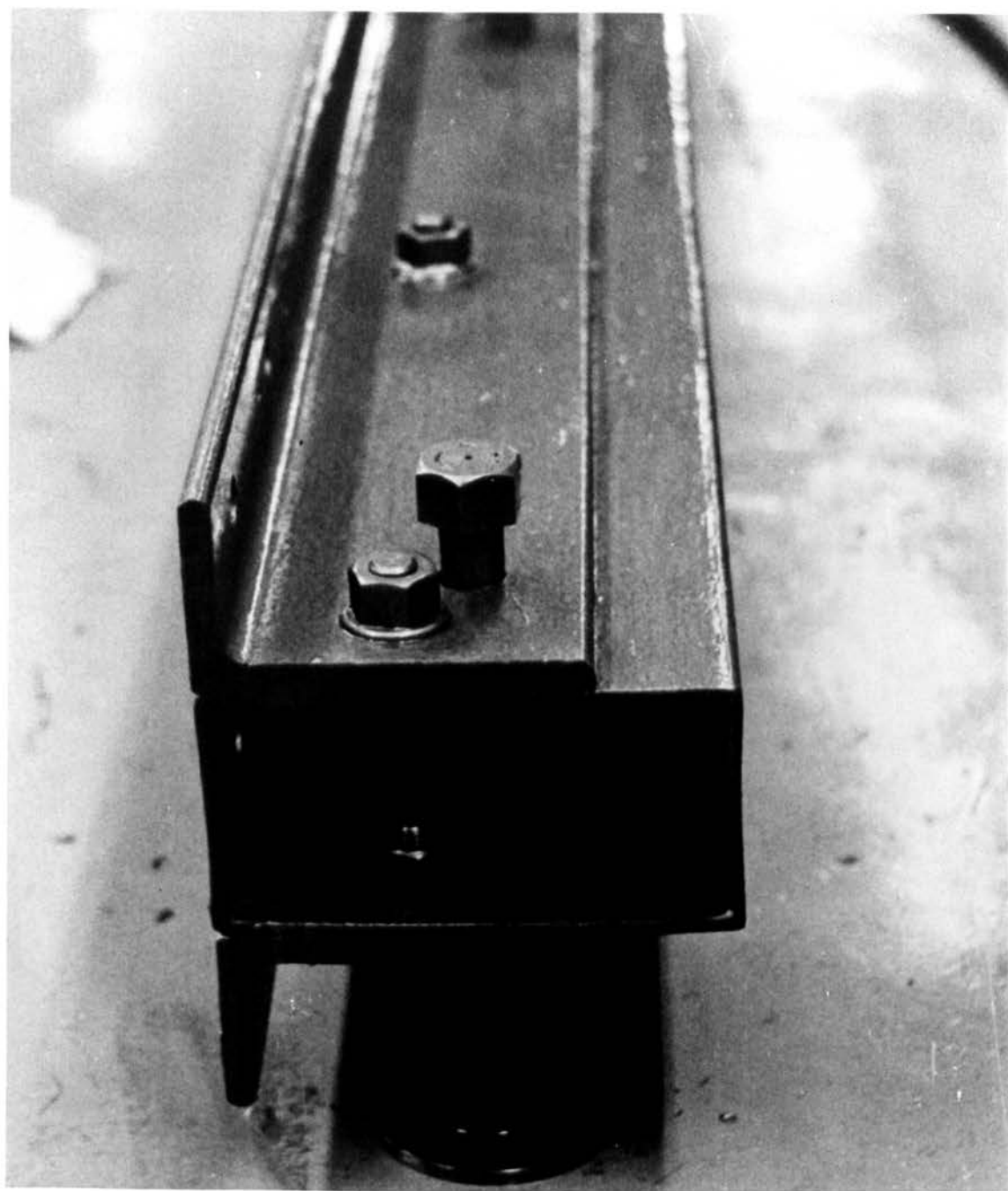


Figure 106 - Detail B - Holding Down Bolt

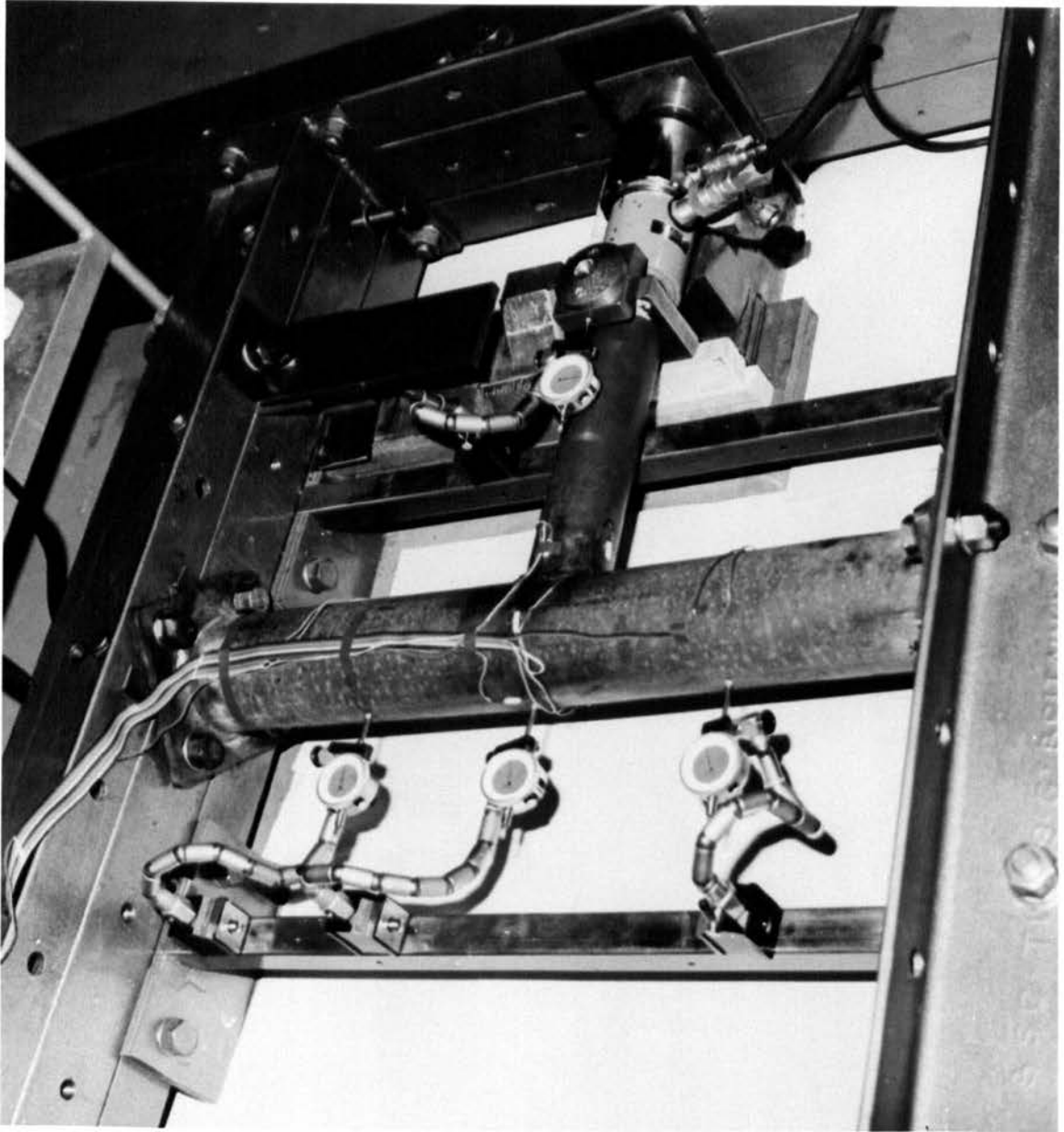


Figure 107 - T-Joint Under Axial Load ($\text{Beta} = 0.66$)

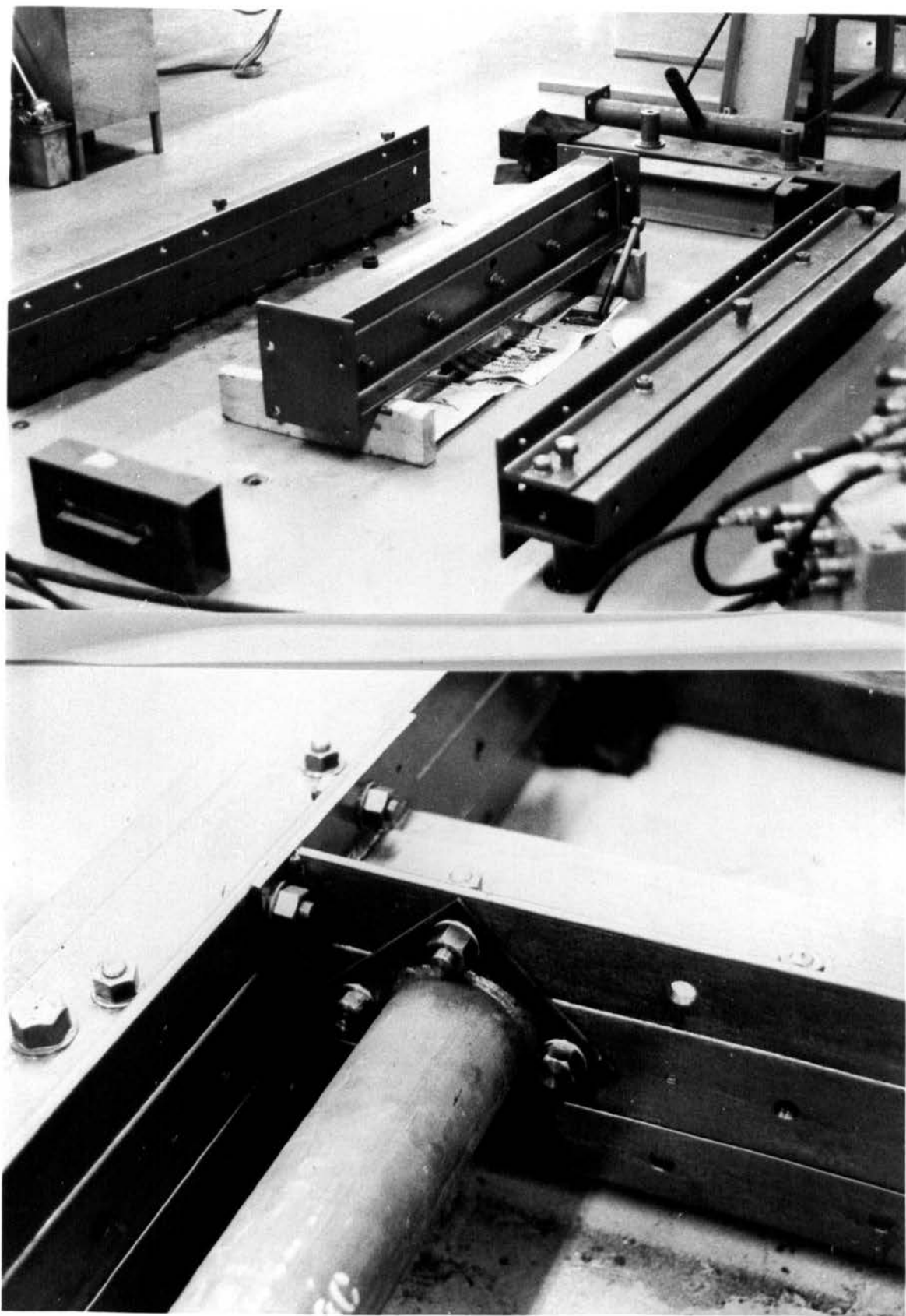


Figure 108 - Detail A - Bolted Connections

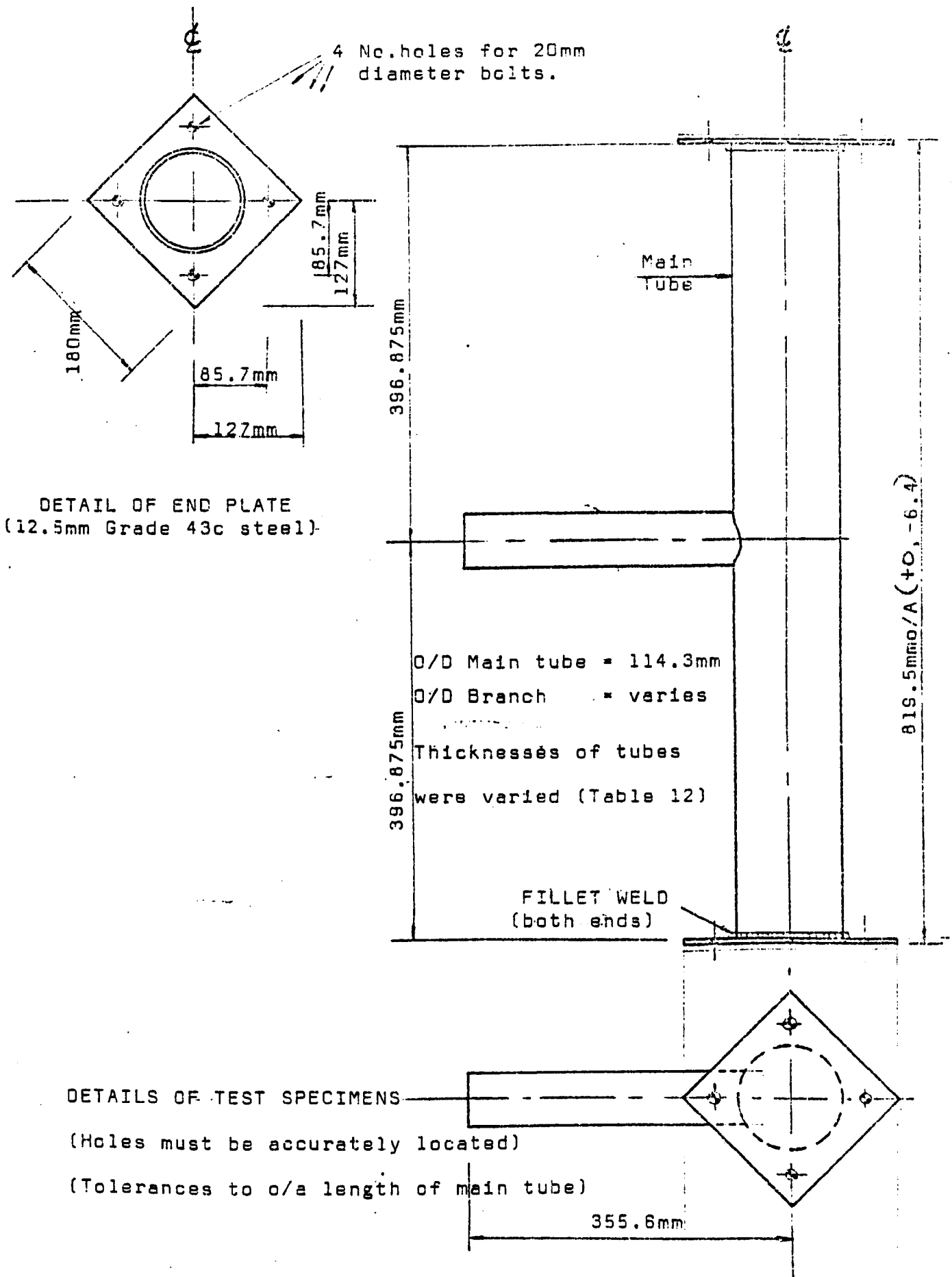


Figure 109. Details of test specimens for current test program.

MULTI-HEAD SWIVELLING DEVICE for
applying load to joint through
the branch tube.

(The branch tube insert is changeable
to permit various sample sizes to be
tested.)

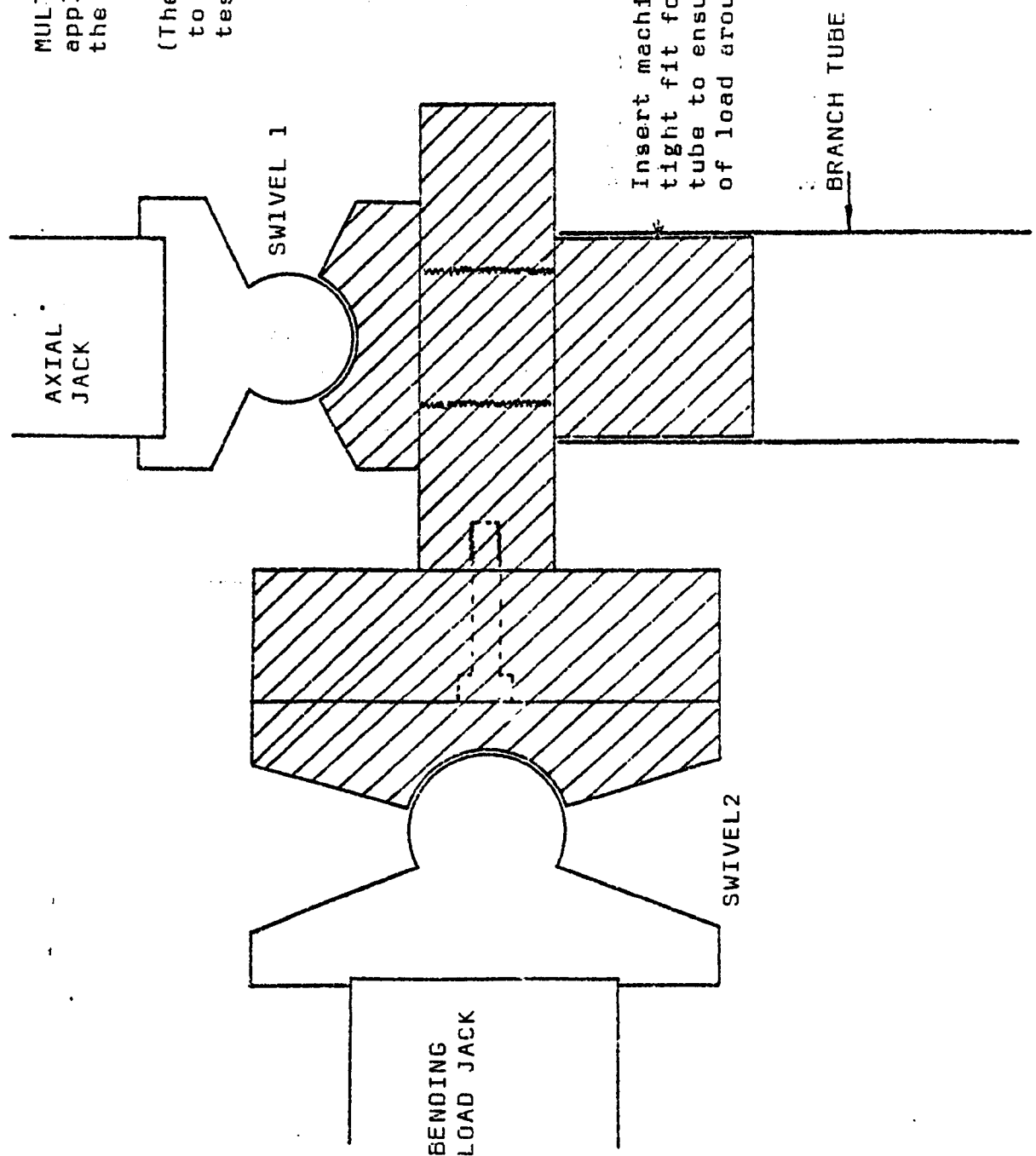


Figure 110. Device for applying load to test specimens. (Detail D)

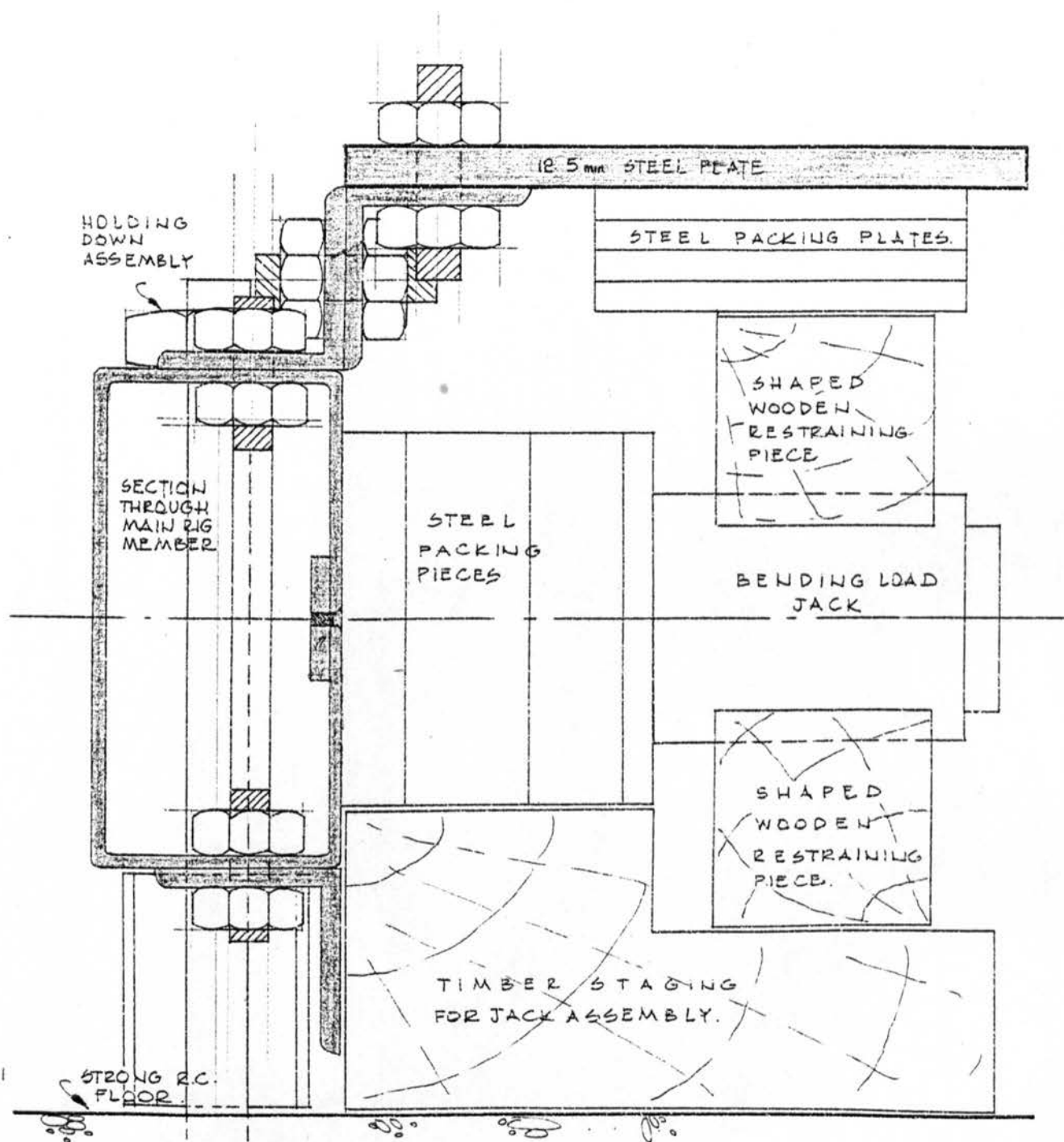


Figure 111. Device to restrain the bending load jack within its plane of action during the testing procedure.

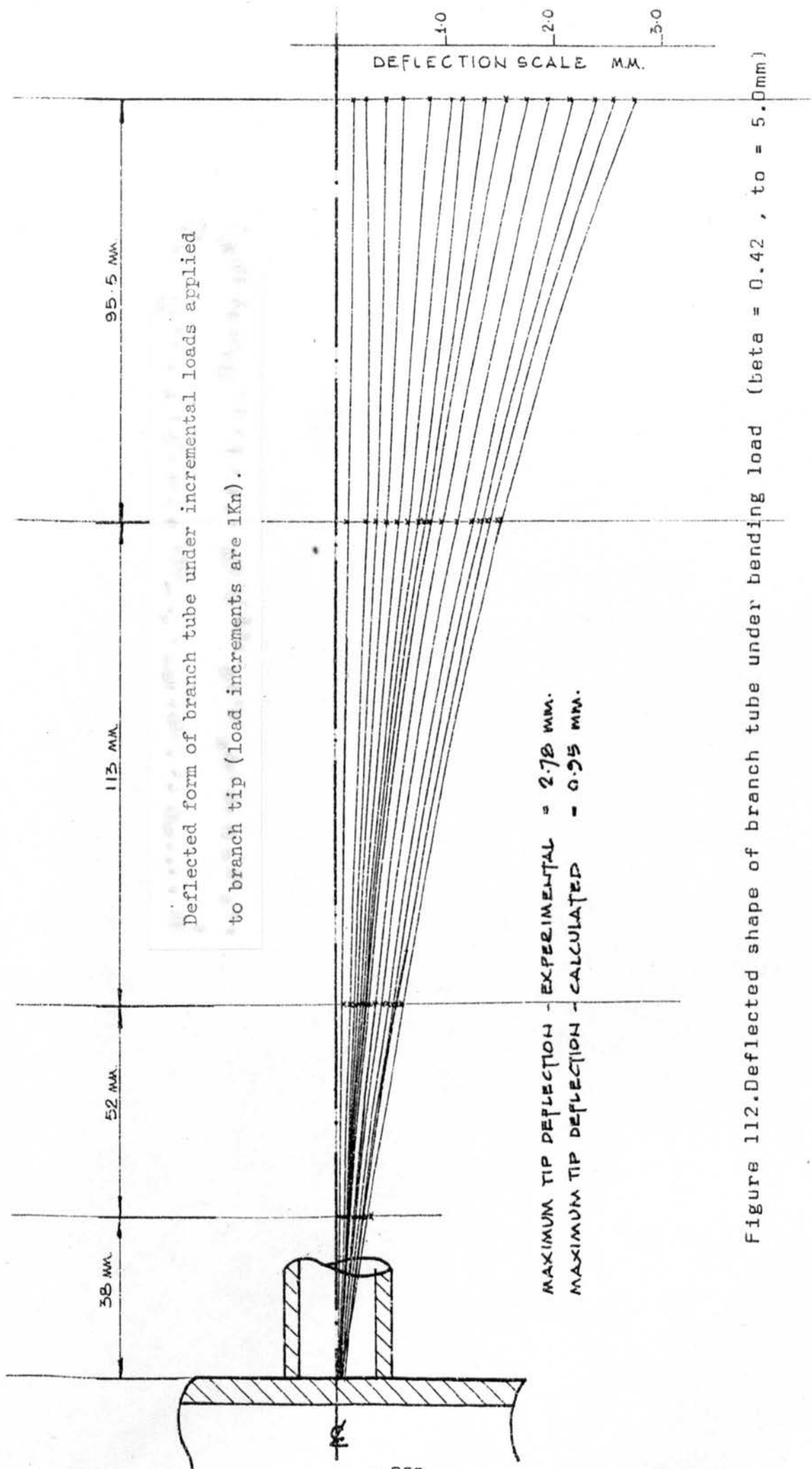


Figure 112. Deflected shape of branch tube under bending load ($\beta = 0.42$, $t_o = 5.0 \text{ mm}$)

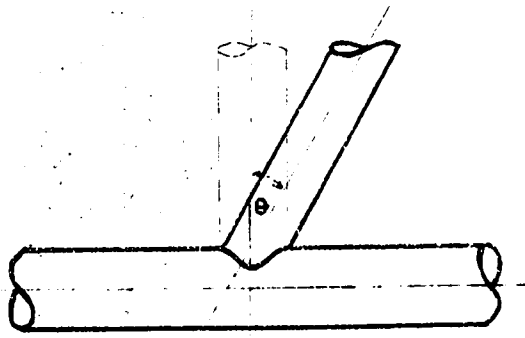


Figure 113(a)

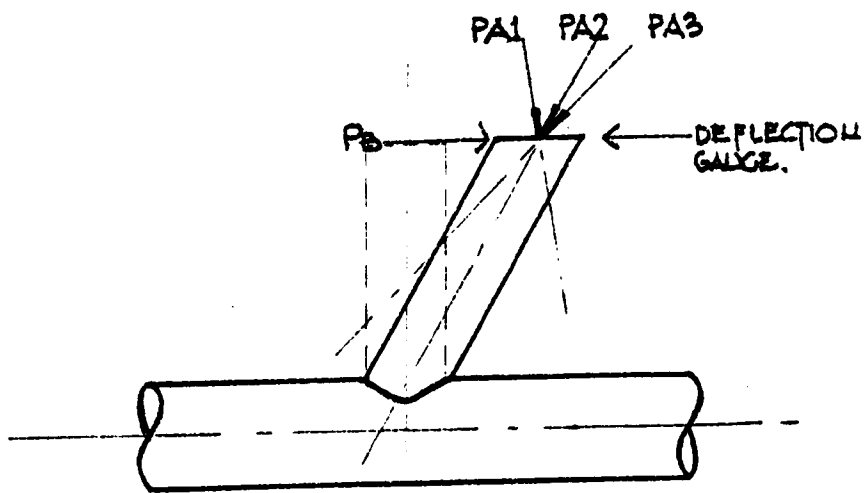


Figure 113(b)

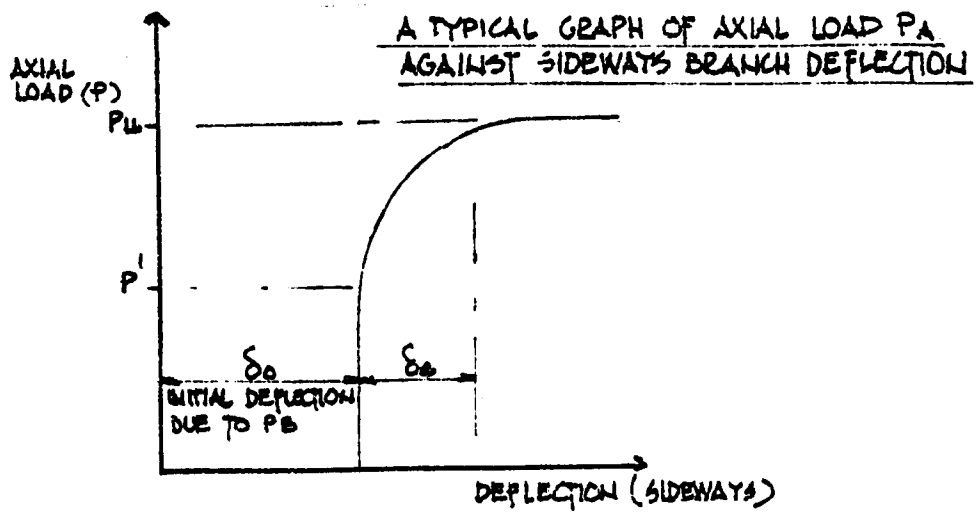
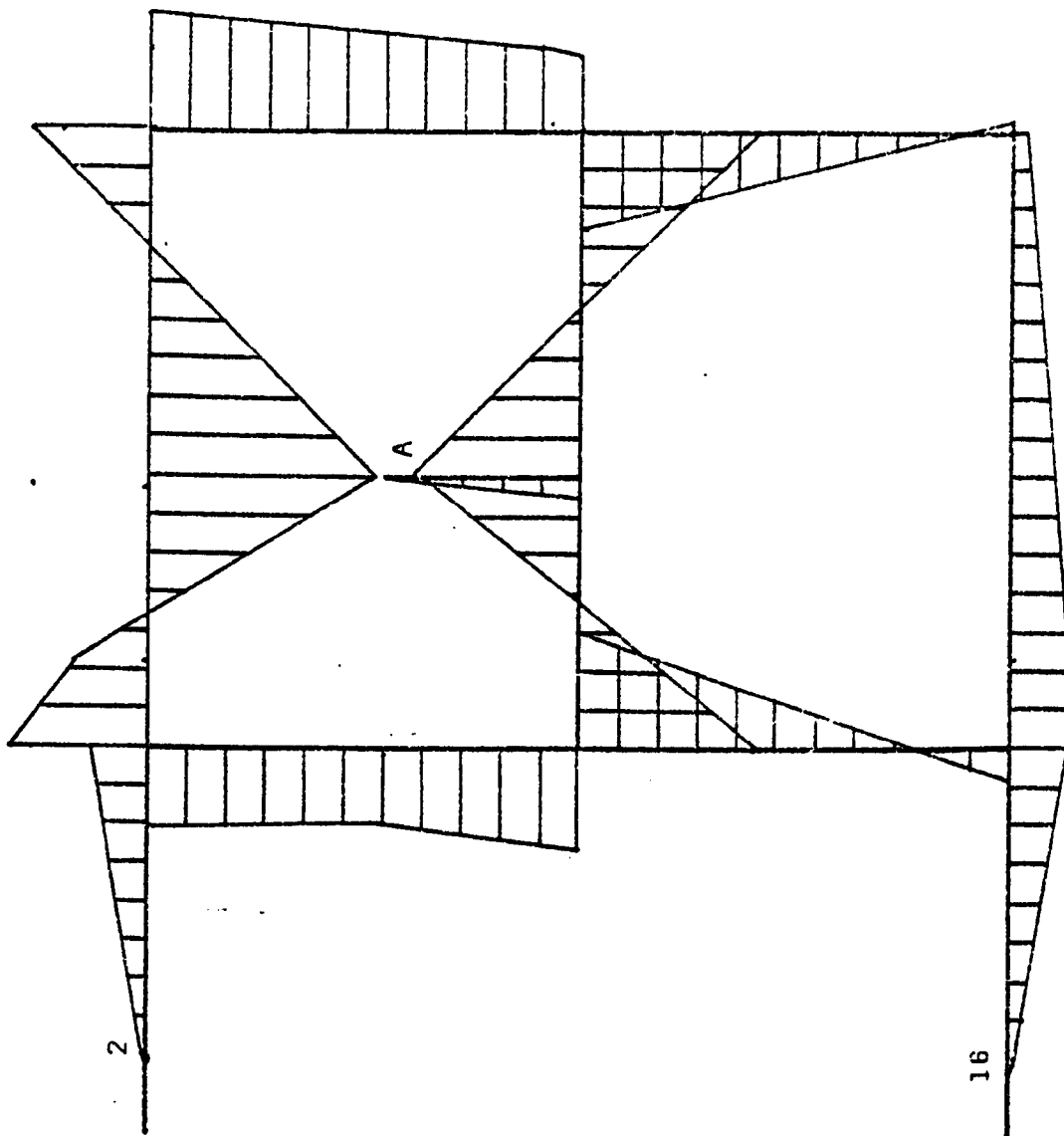


Figure 113(c)



Maximum moment
21 kNm at point A
giving a maximum
stress of approx.
34 N/mm² in the rig
main member.

Corresponding
deflections are
negligible at this
level of loading.

Figure 115. Bending moment diagram for test rig subject to maximum expected
experimental load. (zero displacements at joints 2 and 16 only).

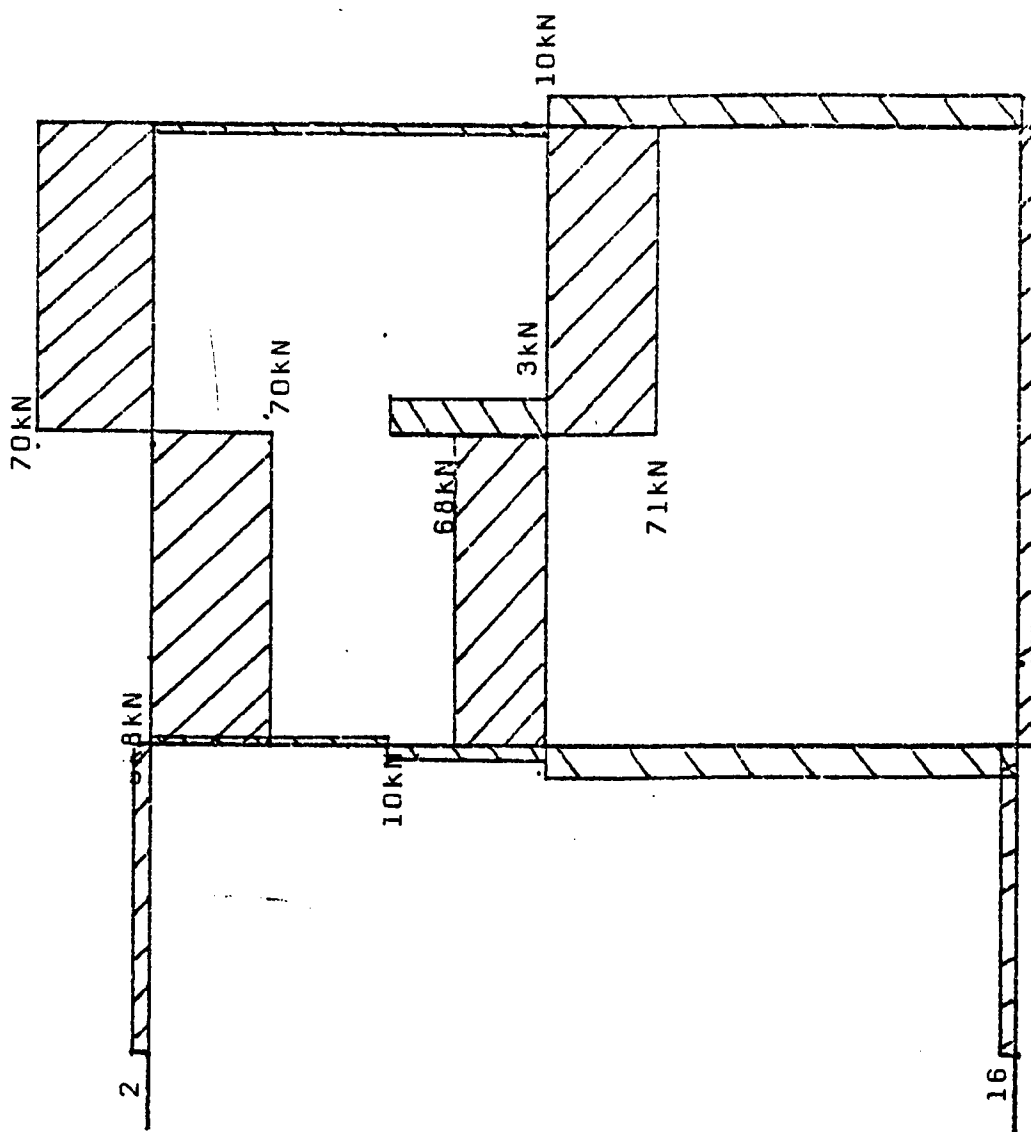


Figure 116. Shear force diagram for test rig subject to maximum expected experimental load (zero displacements at joints 2 and 16 only).

CHAPTER 7

PRESENT EXPERIMENTAL INVESTIGATION OF T-JOINTS UNDER AXIAL LOAD, BENDING LOAD, AND COMBINED AXIAL AND BENDING LOAD - RESULTS AND DISCUSSION

7.1. T-Joints Subject to Axial Load Only Applied to Branch Member

Joints tested were:-

beta (d_1/d_o)	d/to
0.42	18, 21, 23, 32
0.53	18, 23, 32
0.66	18, 21, 23, 32
0.77	18, 21, 32
1.0	18, 23, 32

7.1.1. Beta (d_1/d_o) = 0.42 (Figures 117,127,128,131,159,161,162)

The results of the ultimate axial load tests for beta = 0.42 were:-

do/to	Pu (kN)
32	58
23	100
21	110
18	120

The load deflection graphs for the branch tip (Figure 117) show that for the three lower do/to ratios the deflection mechanism is similar. For do/to = 32 the initial deflection behaviour is similar, but a sudden initial yield at an axial load of 52kN is followed fairly quickly by the total yield of the joint at 58kN. For this do/to ratio the ratio of bending stress in the chord due to the imposed axial load in the branch to the ultimate theoretical bending stress in the chord was approximately 45%, compared with 60% for the joints with lower do/to ratios. This

indicates an early buckling yield in the chord and might have been expected with this higher d_o/t_o ratio.

The ratio of P ultimate for the joint to P ultimate for the branch member was seen to vary from 30% for $d_o/t_o = 32$ to 65% for $d_o/t_o = 18$, (Figure 162). Again, this might be expected from consideration of joint stiffnesses. No strain gauge profiles were taken for the axial load tests for this beta ratio.

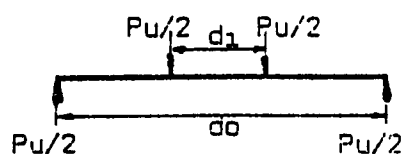
The theoretical ultimate axial load has been calculated assuming a simple punching shear mechanism, and the results are shown below:-

d_o/t_o	$P_u(\text{experimental})/P_u(\text{calculated})$
18	0.82 (0.85)
21	0.67 (0.92)
23	0.65 (0.89)
32	0.52 (0.71)

A yield stress of 350N/mm^2 has been taken.

The second set of ratios given above in brackets, is for P_u calculated using the characteristic yield strength of 255N/mm^2 , for the joint material. It may be concluded, from the table above, that if the mode of failure does approximate to a punching shear mechanism for d_o/t_o values around 21, then it becomes less likely to be this mode of failure for the higher d_o/t_o ratio.

Consideration of a very simple bending mechanism based upon the model



gives the following result:-

do/to	Bending Stress in Chord Wall Under Branch Member (N/mm ²)
18	208
21	302
23	346 punching shear stress
32	538

It conclusion it may be stated that for d_1/d_o equal to 0.42 the variation in do/to has not had a significant effect upon joint behaviour, except for the joint which had a very thin chord section corresponding to a do/to ratio of 32.

7.1.2. Beta ($d_1/d_o = 0.53$ (Figures 118,127,128,131,159,161,162)

The results of the ultimate axial load tests for beta = 0.53 were:-

do/to	Pu(kN)
18	168
23	120
32	70

The load deflection graphs for the branch tip (Figure 118) show a marked similarity for all three do/to ratios. A peculiarity of the tip deflection for the joint with the stiffest chord member (do/to = 18) is that up to a load of approximately 110kN the deflection was greater per unit load than that of the joint with do/to = 23. This is probably due to a slight variation in the rate of load application, or possibly some imperfection in the specimen itself.*

*This point is discussed further in Chapter 6, describing the experimental procedure.

For $d_1/d_o = 0.53$, the ratio of bending stress in the chord due to the imposed axial load in the branch to the ultimate theoretical bending stress in the chord varied from 90% for $d_o/t_o = 18$ to 60% for $d_o/t_o = 32$. Again, this demonstrates the effect of stiffness in the chord, and also indicates that punching shear is the most likely mechanism of failure for this d_1/d_o ratio.

The ratio of P ultimate for the joint to P ultimate for the branch member varied from 25% for $d_o/t_o = 32$ to 55% for $d_o/t_o = 18$ (Figure 162). The effect of increasing beta has been to reduce in each case (d_o/t_o) the value of this ratio. This is probably as much a function of the rapidly increasing value of P ultimate for the branch as it is of the experimental results. One might have expected, however, that as beta increased the area for transforming the axial load into the chord increased correspondingly and, therefore, more of the ultimate axial load capacity of the branch member would be mobilised. This is not seen to be the case.

The theoretical ultimate axial load has been calculated assuming a simple punching shear mechanism and the results are shown below:-

d_o/t_o	$P_u(\text{experimental})/P_u(\text{calculated})$
18	0.70 (0.96)
23	0.63 (0.86)
32	0.5 (0.70)

A yield stress of 350N/mm^2 has been taken. The second set of ratios given above are for P_u calculated using the characteristic yield strength of 255N/mm^2 for the joint material.

Considering the same simple bending mechanism as before ($\beta = 0.42$) gives the following result:-

d_o/t_o	Bending Stress in Chord Wall Under Branch Member (N/mm^2)
18	238.0
23	340.0
32	531.0

For this beta ratio (0.53) it may be concluded that the effect of d_o/t_o on joint behaviour has been quite linear in that joint strength has increased as a simple function of t_o and branch diameter d_1 . The effect of the higher d_o/t_o ratio of 32 has been less pronounced than was seen for $\beta = 0.42$. No strain gauge profiles were taken for axial load tests for this beta ratio.

7.1.3. Beta (d_1/d_o) = 0.67 (Figures 119,127,128,131,159,161,162)

The results of the ultimate axial load tests for $\beta = 0.67$ were:-

d_o/t_o	P_u (kN)
32	94.5
23	160.0
21	177.5
18	180.0

The load deflection graphs for the branch tip (Figure 119) are similar to those for $\beta = 0.42$. The joints with the three lower d_o/t_o ratios have very similar load deflection behaviour, but the joint with higher d_o/t_o ratio of 32 has a much lower load deflection form. This is because, for the same chord section as previous beta ratios, the axial load in the branch member has become relatively large, and, although some of the extra load has been re-distributed, the chord has buckled locally.

The ratio of bending stress in the chord due to the axial load in the branch tube to the ultimate theoretical bending stress in the chord (Figure 162) varies from 100% for $d_o/t_o = 18$ to 80% for $d_o/t_o = 32$. This may explain why the ultimate axial loads in the lower d_o/t_o ratio joints are quite close at 160kN, 177.5kN, and 180kN, i.e. the chord begins to fail due

to two mechanisms:-

- i. local joint failure of a punching shear type,
- ii. local chord failure due to bending in the chord.

This may be the reason for the difficulty in finding formulae which accurately predict the ultimate axial load capacity of T-joints in large circular hollow sections, and also relate the results of isolated joint tests to full girder strengths.

The ratio of P ultimate for the joint to P ultimate for the branch member varies from 25% for $d_o/t_o = 32$ to 45% for $d_o/t_o = 18$.

The theoretical ultimate axial load has been calculated assuming a simple punching shear mechanism and the results are shown below:-

d_o/t_o	$P_u(\text{experimental})/P_u(\text{calculated})$
18	0.59 (0.81)
21	0.68 (0.94)
23	0.66 (0.91)
32	0.54 (0.75)

A yield stress of 350N/mm^2 has been taken.

These results indicate that for $d_o/t_o = 21$ and 23 the punching shear mechanism is feasible but loses some validity for $d_o/t_o = 18$ where chord failure in bending contributes to total failure of the joint, and for $d_o/t_o = 32$ where local buckling failure in the chord contributes to total failure of the joint.

Consideration of the simple bending mechanism shown in the section for $\beta = 0.42$ gives the following results:-

do/to	Bending Stress in Chord Under Branch Member (N/mm ²)
18	180.0
21	282.0
23	320.0
32	508.0

For this beta ratio (0.67) it may be concluded that there are two contributing effects to joint strength:-

- i. do/to when it was higher i.e. 32,
- ii. the effect of bending of the chord member.

7.1.4. Beta (d_r/d_o) = 0.77 (Figures 120,127,128,131,159,161,162)

The results of the ultimate axial load tests for beta = 0.77 were:-

do/to	Pu(kN)
32	110
21	227
18	235

The load deflection graphs for the branch tip (Figure 120) show a close similarity of joint behaviour for do/to = 18 and 21 while the joint with do/to = 32 has a relatively low load and corresponding deflection. This is probably due to interference in joint strength from the bending of the chord member, and can be seen in Figure 159 where the ratio of bending stress in the chord due to the axial load in the branch member to the ultimate theoretical bending stress in chord is approximately 100% for all do/to ratios of this beta ratio.

The ratio of P ultimate for the joint to P ultimate for the branch member varies from 25% for do/to = 32 to 50% for do/to = 18. This is similar to the result for beta = 0.67 and becomes a more significant effect as beta is now increasing towards unity.

The theoretical ultimate axial load for the joint has been calculated assuming a simple punching shear mechanism and the results are shown below:-

do/to	Pu(experimental)/Pu(theoretical)
18	0.66 (0.91)
21	0.75 (1.02)
32	0.54 (0.74)

A yield stress of 350N/mm^2 has been taken. The values of the ratio in brackets are for theoretical loads calculated using a characteristic yield stress of 255N/mm^2 for the chord material.

The low values obtained assuming a punching shear mechanism indicate that it is probably not the most contributory factor in joint failure for this beta ratio.

Consideration of the simple bending mechanism, as before, gives the following results:-

do/to	Bending Stress in Chord Under Branch Member (N/mm^2)
18	156.0
21	240.0
32	393.0

In conclusion it may be stated that for this beta ratio (0.77) failure of the joint is due to failure of the chord from:-

- i. bending of the chord member,
- ii. large deflection failure of the chord walls under the branch member.

This was the only ultimate axial load test for which strain profiles were measured (Figures 203(a)&(b)). The pattern of strain distribution is as might be expected with high stresses at points on the intersection line of branch and chord member.

It is interesting to note the high strain occurring under the chord due to bending of the chord member. At failure this strain corresponds to a stress in excess of 1200N/mm^2 , which is similar to the stress level around the intersection of branch and chord member. These values compare favourably with the predicted stresses from finite element analysis. What is interesting is that, although it is accepted that plastic re-distribution of stress must occur in the vicinity of the joints, the in situ strain gauges still show very high strain levels.

7.1.5. Beta (d_i/d_o) = 1.0 (Figures 121,127,128,131,159,161,162)

The results of the ultimate axial load tests for beta = 1.0 were:-

d_o/t_o	$P_u(\text{kN})$
32	165
23	240
18	270

Figure 121 shows the load deflection graphs for this beta ratio. The deflection graphs for d_o/t_o = 18 and 23 are fairly close, with the deflection graph for d_o/t_o = 32 not very much lower. This indicates that much more axial load, relatively, can be transferred into the chord for this beta ratio. The ratio of bending stress in the chord due to axial load in the branch member to ultimate theoretical bending stress for the chord (Figure 159) varies from 1.0 to 1.2. This might be expected, since transfer of the load into the chord is direct and not influence primarily by chord wall thickness.

The ratio of ultimate axial joint strength to ultimate branch member strength is fairly consistently between 25% and 45%. Although this is similar to previous high beta ratios considered the consistency for d_o/t_o ratios of 23, 21 and 18 is significant and may mean a more predictable mode of behaviour.

Assuming a simple punching shear mechanism the following results were calculated:-

d_o/t_o	$P_u(\text{experimental})/P_u(\text{theoretical})$
32	0.63 (0.87)
23	0.66 (0.91)
18	0.59 (0.81)

As before, a yield stress of 350N/mm^2 was assumed. The values in brackets are for the ratio calculated using a characteristic yield stress of 255N/mm^2 for the chord material. Since the values are low it is apparent that punching shear is not the failure mechanism.

During the tests it was observed that for all the d_o/t_o ratios in this group that chord bending was a strong influence. It was noted, however, that all the joints appeared to fail finally due to a combination of this chord bending and plastic deformation of the chord caused by the increasing axial load in the chord.

7.1.6. General Conclusions

For the ultimate axial load tests the following observations are made:-

- i. The mechanism of failure changes from punching shear failure to chord bending failure with plastic deformation as the beta ratio increases from 0.42 to 1.0.
- ii. The parameter d_o/t_o has little effect on joint strength directly for values of 18, 21 and 23.

iii. Values of the ratio of stress in the chord at the joint due to bending to chord ultimate bending stress increase to exceed unity as the d_1/d_o ratio increases. This observation may not be very significant since computer analysis⁸⁵ indicates that, in fact, theoretical local stresses in the joints may well be in excess of 1000N/mm^2 . Re-distribution of stress, which occurs, will certainly distort any simple analysis of the level of stress in and around the joint.

7.2. T-Joints Subject to Bending Moment Due to Lateral Load Applied to the Branch Member

7.2.1. Beta (d_1/d_o) = 0.42 (Figures 122,129,130,160)

The results of the ultimate moment load tests for beta = 0.42 were:-

d_o/t_o	$M_u(\text{kNm})$
32	2.24
23	2.08
21	2.35
18	2.98

These results show an anomaly for $d_o/t_o = 23$ where the ultimate moment is less than that for $d_o/t_o = 32$. This result is also supported by the load deflection graphs for this beta ratio (Figure 122). Figure 160 shows the relationship between d_1/d_o and the ratio of ultimate experimental moment for the joint to ultimate experimental moment for the joint to ultimate theoretical moment for the branch member. Here it is noted that for d_o/t_o ratios of 32, 23, and 21 the value of the ratio is approximately 80%, while for $d_o/t_o = 18$ the value of the ratio is 110%.

The joint with the stiffer chord $d_o/t_o = 18$ has enabled a greater percentage of the branch member moment capacity to be utilised. It was observed during the ultimate moment tests for this beta ratio (0.42) that:-

d_o/t_o

- 32 - the chord wall close to the branch member deformed very slightly, as did the branch member itself.
- 23) - failure appeared to initiate as a compressive buckling
- 21) in the wall of the branch member close to the branch/chord intersection.
- 18 - no appreciable deformation occurred in the chord wall, and very little observable deformation occurred in the branch wall.

The values of ultimate moments for this beta ratio are relatively small and minor variations and small in section properties, either geometrical or material might make an apparently significant difference to the ultimate moment. Loads were applied evenly and steadily in order that any effects due to variation in rate of load application were eliminated.

Strain gauge profiles were taken for one test in this series when $d_o/t_o = 23$ (Figures 180 & 181).

It is seen that the regions of high strain are along the branch edges, in compression and in tension, and in the corresponding locations on the chord crown close to the intersection of branch and chord. It is apparent from the strain distribution recorded that there is quite significant local effect at the point of application of the lateral load. This, however, is assumed to be local and have no effect on behaviour actually at the joint. This is confirmed by the restoration of normal strain distribution further down the branch member towards the joint.

Total failure of the joint was caused by a compression failure close to the intersection of the branch edge and the chord crown.

7.2.2. Beta (d_1/d_o) = 0.53 (Figures 123,129,130,160)

The results of the ultimate moment load tests for beta = 0.53 were:-

do/to	Mu(kNM)
32	3.87
23	5.66
18	5.22

The results above shown an anomaly for do/to = 18. Figure 123 however, shows that the anomaly may, in fact, be for do/to = 23 i.e. the ultimate moment is much higher than the trend on the graph indicates. Similarly the ultimate moment for do/to = 18 is less than might have been expected.

The load deflection graph for branch tip deflection (Figure 123 shows that the results for do/to = 18 and 23 are very similar and it may be that, as seen in Figure 160, when the ratio of ultimate joint moment to ultimate branch member moment is 100% or close to it, then there is a levelling off process for moment capacity given that the chord has a stiffness such that wall deformation is adequately resisted. Again, from Figure 160 it is seen that this process appears to converge as beta increases.

It was observed during the ultimate moment tests for this beta ratio (0.53) that:-

do/to

- 18, 23 - little deformation of the branch member was noted. A small compressive buckling was seen in the chord crown very close to the weld.
- 32 - no branch deformation was noted. Considerable wall buckling was seen to occur in the chord crown close to the weld.

The values of the ultimate moment loads for this beta ratio were significantly large enough to be able to discount any experimental error in either their individual magnitude or in overall values, e.g. for $d_o/t_o = 23$, load increments of 2kN from zero to failure at 19kN were taken, in the lateral load to cause moment failure.

Strain gauge profiles were taken for one test in this series when $d_o/t_o = 23$ (Figures 190, 191).

The strain gauges indicate that again the regions of high strain were the branch edges and the chord crown closer to the intersection of the branch and chord. Strains prior to failure in excess of 2000 being registered.

It is noticeable that significant chord strains under the branch tube are also seen to occur, as well as an increase in strain along the chord crown. This has been indicated by finite element analysis and is probably caused by re-distribution of stress outwards from the joint, where analysis predicts it to be very high, along the chord tube. It is not caused by bending of the chord member since during the experiment deflections of the chord were found to be negligible.

7.2.3. Beta (d_r/d_o) = 0.67 (Figures 124, 129, 130, 160)

The results of the ultimate moment load tests for beta = 0.67 were:-

d_o/t_o	M_u (kNm)
32	4.47
23	7.45
21	9.70
18	9.09

Figure 124, the load-deflection graphs for this beta value of 0.67 again shown the anomaly for $d_o/t_o = 21$ and 18 where the moment for the joint with the larger d_o/t_o ratio chord has,

unexpectedly, a higher ultimate moment. Figure 160 confirms that for these two do/to ratios the ratio of ultimate joint moment to theoretical ultimate branch moment is approximately 100%. As discussed previously, the "levelling off" effect may be operating here, where, once the chord has sufficient stiffness, the branch can develop it's full moment capacity.

It was observed, during the ultimate moment tests for this beta ratio (0.67), that for all values of do/to tested 18, 21, 23 and 32 the mode of failure was similar, i.e. buckling of the chord wall under the branch tube which allowed the formation of a plastic hinge and subsequent rotation of the branch member.

The difference between the highest ultimate moment: (do/to = 21) and the lowest ultimate moment (do/to = 32) which occurs for this beta (0.67) is the largest recorded during the present experimental investigation. It suggests that there is a complex interaction between the effects of beta (d_1/d_o) and do/to in which small variations, in do/to, in the range where the chord wall might become flexible, have a considerable effect upon the joint strength.

7.2.4. Beta (d_1/d_o) = 0.77 (Figures 125,129,130,160)

The results of the ultimate moment load tests for beta = 0.77 were:-

do/to	Mu (KNM)
32	7.02
21	12.81
18	12.74

The results for do/to = 21 and 18 are very similar as was seen in the previous beta ratio i.e. 0.67. The load deflection graphs (Figure 125) appear to show a difference between 43 and 49 for the bending loads. The branch members for these tests, however,

were different lengths (260mm and 298mm), and the ultimate moments were, in fact, very similar. The test on the joint with $d_o/t_o = 32$ shows a low value as was seen in previous tests. Visually there was very little difference in the modes of failure for all three d_o/t_o values in this series. All three failed due to the formation of a plastic hinge close to the branch member in the chord crown.

Strain gauge profiles were taken for one test in this series when $d_o/t_o = 21$ (Figure 200).

During the range of elastic loading the region of highest strain on the branch member is the tension edge close to the branch/chord intersection. There is a corresponding, but not as high, strain on the compression edge of the branch section. Once the joint becomes plastic the gauges on the branch centre line close to the intersection line show very high strains, as do all the gauges close to the intersection line on the chord member. These sudden very large increases in strain during plastic behaviour are spectacular and demonstrate the degree of redistribution occurring. They are totally arbitrary, however, and serve only to illustrate the degree of non-linearity involved in material behaviour outside the elastic range.

7.2.5. Beta (d_i/d_o) = 1.0 (Figures 126,129,130,160)

The results of the ultimate moment load tests for beta = 1.0 were:-

d_o/t_o	M_u (kNm)
32	12.5
23	18.98
18	19.80

The trend of the results for this series of tests is very similar to that for the previous series with $\beta = 0.77$. Figure 160 shows that the ratio of ultimate joint moment to theoretical ultimate branch moment is approximately 90% for d_o/t_o ratios of 18 and 23. Figure 126, the load deflection graphs for the branch tip, also shows a marked similarity for the joints with these d_o/t_o ratios. The joint with $d_o/t_o = 32$ developed only 50% of the theoretical branch ultimate moment. This was similar to the result for the same joint with $\beta = 0.77$ and was because the branch was, relatively, extremely stiff and caused large deformation of the top of the chord section (chord crown), in the vicinity of the joint, as rotation occurred.

7.2.6. General Conclusions

- i. Ultimate moment capacity increases as β increases.
- ii. For stiff chord members, d_o/t_o less than 23, and for the range of β ratios studied, ultimate joint moment capacity was close to the full theoretical ultimate moment capacity of the branch member.
- iii. For low β ratios (0.42, 0.53) compressive buckling failure of the branch member occurred.
- iv. For all the joints tested the effect of moment on the joint was localised and caused negligible deflection of the chord member.
- v. In a T-joint with an adequately reinforced chord section at the joint, the moment capacity of the joint will be related directly to the moment capacity of the branch member.

7.3. T-Joints Subject to a Combination of Axial Load and Bending Moment

7.3.1. General

The combination of axial load and bending moment was applied using the method described in section 6.5. Ultimate axial loads were always much greater numerically than ultimate moments because of the nature of this type of joint. It was, therefore, important, during combined loading tests, to ensure that eccentricity of loading, particularly axial loading, was eliminated.

It was not sufficient, in fact, to measure and note eccentricity of axial loading but to eliminate it completely if possible. In some cases because of the nature of the materials, problems with lack of straightness, variations in section thickness, and initial eccentricity of the joints due to construction methods, this was not possible. Errors arising from these problems all had the same effect which was to cause an additional moment during the testing procedure which acted either with the applied moment or against it, depending upon the sign of the eccentricity. Some of the final moment ratios i.e. moment applied/ultimate moment were, therefore, modified to allow for these discrepancies. For this reason, although fixed moment ratios were initially applied, the final ratios plotted sometimes had apparently obscure values. Careful consideration has been given to the possibility and magnitude of errors which might have occurred during the combined loading tests and it is concluded that secondary moments of significant magnitude did not occur.

It was noted during the combined loading tests that prior to joint failure, i.e. the point where the joint could not longer sustain the imposed moment and axial load, the largest values of deflection of the branch member did not normally exceed 1° of arc. For the T-joints tested in the current series this deflection gave an eccentricity of 5.2mm, assuming that by some oversight the jack had not been aligned with the branch member prior to applying the axial load.

The lateral load applied to the branch tube to give a bending moment at the joint was not corrected to allow for deflection of the branch tube since the effect was minimal i.e. 0.015% for a deflection angle of 1° , up to 1.5% for a deflection angle of 10° .

7.3.2. Interaction Tests for Combined Axial and Moment Loading

The ratios of applied moment to ultimate moment $\frac{M}{M_u}$ and applied axial load to ultimate axial load $\frac{P}{P_u}$ have been plotted in Figures 149 to 153. All the graphs for all beta ratios and do/to ratios tend toward the 45° line of complete interaction. Individual graphs, however, have different features.

7.3.3. Beta (d_i/d_o) = 0.42 (Figures 132-135, 149)

For all do/to ratios the interaction graphs fall close to, but mainly below the 45° line drawn from $P/P_u = 1.0$ to $M/M_u = 1.0$. Numerically this means that for a given level of stress, say 1 unit, at the joint the sum of the stress due to the axial and bending loads is less than 1.0. This may be because for this beta ratio there were two distinct parts of the joint affected by the different load cases i.e.

The branch wall near the joint for moment loading.

The chord wall near the joint for axial loading.

Since these regions were separate it might be expected that interaction would be inhibited to some extent. Joint failure under moment load was due to buckling of the branch member in the compression face. Additional stress from axial load in the branch accelerated this wall buckling, in compression, and resulted in joint failure before full interaction was achieved.

7.3.4. Beta (d_i/d_o) = 0.53 (Figures 136-138, 150)

For all do/to ratios the graphs show complete interaction between axial and moment loading

The graphs of axial load plotted against bending load (Figures 136-138) show a more stable relationship for this d_1/d_o ratio compared with that for the lower d_1/d_o ratio of 0.42. This is because the magnitude of the bending load is such that the minor joint eccentricities discussed previously in Chapter 6 have become less significant.

7.3.5. (d_1/d_o) = 0.67 (Figures 139-142, 151)

For all d_o/t_o ratios the graphs show complete interaction between axial and moment load. Traditionally it has been recommended that the most efficient value of beta should lie in the range 0.5 to 0.7 and this recommendation is confirmed by the consistency of the interaction results for this and the previous d_1/d_o series.

The interaction graphs (Figures 139 to 142) again show a stable relationship between axial and bending load for this d_1/d_o ratio. The two lowest M/μ graphs for $d_o/t_o = 21$, (Figures 140, 151) show a small increase in bending load for increasing axial load until interaction occurred and the moment load began to decrease. This was the result of initial eccentricity of axial load which has been taken into account in the plotting of the interaction graph in Figure 151 for this d_o/t_o ratio.

7.3.6. (d_1/d_o) = 0.77 (Figures 143-145, 152)

The graphs show interaction for d_o/t_o ratios of 21 and 32 and for higher M/μ ratios for $d_o/t_o = 18$. For lower M/μ ratios and $d_o/t_o = 18$ the graph falls some way below the line of interaction. In practical terms this means that for a given applied moment the axial load that can be achieved is less than would have been expected. This also occurs for $d_1/d_o = 1.0$, and is discussed below.

7.3.7. (d_1/d_o) = 1.0 (Figures 146-149, 153)

For values of M/μ less than 0.5 the graphs all fall below the interaction line and for values of M/μ greater than 0.5 the graphs tend towards falling on or above the interaction line.

The phenomenon seen for low moment values also occurred for $d_o/t_o = 18$ in the previous d_1/d_o series (0.77). Evaluation of the significance of the variation in results on a purely numerical basis would require several more tests to be carried out. It is safe, however, to assume a trend of results and try to explain it. In this case for low applied moments the point of combined stress intensity (hot spot stress) occurs in an intermediate position on the chord circumference, where because the squashing action of the branch member acts on a curved surface weak in local bending, premature failure takes place. As the applied moment is increased the hot spot moves to its more conventional site under combined loading which is in the chord crown on the compression side of the branch member. Full interaction is then possible since the chord is now able to resist the total forces applied, i.e. squashing and bending due to axial load, and bending due to moment load, with its full sectional area in a direction normal to the resultant stress.

It was noted in Section 7.1 that joint strength for this d_1/d_o ratio may have been influenced by the local bending in the chord, and that the ratio of stress from this bending to ultimate stress in the chord tends to unity as axial load in the joint approaches ultimate. When small moments are applied their effect may, therefore, be "hidden" by the magnitude of the chord stress due to bending and the chord stress due to the increasing applied axial load in the branch member.

7.3.8. Analysis of the Relationship Between Ultimate Bending Stress (f_{bu}) and Ultimate Axial Stress (f_{ba}), and the Applied Axial Stress (f_a)

It is difficult in practice to define the numerical values of ultimate axial and bending stresses since using normal steel design techniques allowable stresses only may be found. The relationship between the allowable stresses and the ultimate stresses will only give an approximate guide to the ultimate stress which might be expected. It is more satisfactory to

deduce a relationship which will then take account of the specific test result.

i.e.

$$M_u = s.fbu \quad s = A \frac{d_1}{4}$$

$$\frac{M_u}{P_u} = \frac{s.fbu}{A.fau} = \frac{A}{A} \frac{d_1}{4} \frac{fbu}{fau}$$

$$\frac{fbu}{fau} = \frac{4}{d_1} \frac{M_u}{P_u}$$

If there is no moment at all then fbu/fau equals zero and the load is purely axial i.e. $f_a = fau$, or $f_a/fau = 1.0$.

These relationships are plotted in Figures 154 to 155, for varying beta (d_1/d_o) and in Figures 156 to 158, for varying d_o/t_o .

Figures 161 and 163 show the mean values of the ratio fbu/fau plotted against d_o/t_o and d_1/d_o respectively. The graph of mean values of fbu/fau plotted against d_1/d_o shows a grouping around an average value of approximately 2.6. For the range of d_1/d_o from 0.67 to 1.0 the average ratio fbu/fau was 2.62.

Akiyama, in an, as yet, untranslated paper describing two tests involving moment loads, quotes a value of fbu/fau of 3.22 for a T-joint with $d_1/d_o = 0.53$. In the present series of tests the mean value of fbu/fau for this d_1/d_o ratio was 2.95. For the mid range of d_o/t_o (i.e. 23) the value of fbu/fau was 3.125, which compares well with 3.22.

The value of this ratio gives a numerical indication of the "reserve" or excess bending stress available at ultimate load as compared with the axial stress, and is a function of the branch diameter.

The tables of values calculated is given below:-

Beta (d_1/d_o)	d_o/t_o	f_{bu}/f_{au}
0.42	18	2.06
	21	1.56
	23	1.95
	32	3.20
0.53	18	2.06
	23	3.13
	32	3.67
0.67	18	2.65
	21	2.87
	23	2.45
	32	2.49
0.77	18	2.44
	21	2.54
	32	2.87
1.0	18	2.57
	23	2.65
	32	2.77

7.3.9. General Conclusions

- i. Full interaction between axial load and moment in T-joints is shown to occur, i.e.

$$\frac{M}{M_u} + \frac{P}{P_u} = 1.0$$

- ii. This interaction is more complete when beta (d_1/d_o) is in the range 0.5 - 0.75
- iii. Interaction does not appear to be affected by the parameter d_o/t_o .

- iv. The decrease in moment capacity M after P has been exceeded in the equation above is non linear and in some cases is seen to be disproportionately rapid. It is important that this point be given consideration in proposed design recommendations for combined loading cases.
- v. Moment load considerations will dominate in the combined loading systems found in Vierendeel trusses.

TABLE 14 - TEST RESULTS

d_i/D_o	D_i/D_o	TEST NO.	ULTIMATE AXIAL LOAD P_u (kN)	ULTIMATE MOMENT M_u (kNm)	M/M_u	P/P_u
0.42	32	A/1	58	2.24		
0.42	32	A/2				
0.42	32	A/3			0.27	0.69
0.42	32	A/4			0.4	0.6
0.42	32	A/5			0.6	0.39
0.42	32	A/6			0.8	0.22
0.42	23	B/1	100	2.08		
0.42	23	B/2				
0.42	23	B/3			0.15	0.08
0.42	23	B/4			0.25	0.68
0.42	23	B/5			0.5	0.49
0.42	23	B/6			0.75	0.2
0.42	23	B/7			0.85	0.11
0.42	21	C/1	110	2.35		
0.42	21	C/2				
0.42	21	C/3			0.25	0.64
0.42	21	C/4			0.5	0.45
0.42	21	C/5			0.75	0.18
0.42	18	D/1	120	2.96		
0.42	18	D/2				
0.42	18	D/3			0.25	0.75
0.42	18	D/4			0.5	0.48
0.42	18	D/5			0.75	0.23
0.53	32	E/1	70	3.87		
0.53	32	E/2				
0.53	32	E/3			0.23	0.79
0.53	32	E/4			0.46	0.50
0.53	32	E/5			0.77	0.21
0.53	23	F/1	120	5.66		
0.53	23	F/2				
0.53	23	F/3			0.25	0.75
0.53	23	F/4			0.5	0.5
0.53	23	F/5			0.75	0.28

TABLE 14 Cont'd

d/D	D/T	TEST NO.	ULTIMATE AXIAL LOAD P _u (kN)	ULTIMATE MOMENT M _u (kNm)	M/M _u	P/P _u
0.53	23	F/6	168	5.22	0.85	0.20
0.53	18	G/1				
0.53	18	G/2				
0.53	18	G/3			0.22	0.78
0.53	18	G/4			0.46	0.51
0.53	18	G/5			0.70	0.29
0.53	18	G/6	94.5	4.47	0.86	0.15
0.66	32	H/1				
0.66	32	H/2				
0.66	32	H/3			0.2	0.79
0.66	32	H/4			0.5	0.53
0.66	32	H/5			0.66	0.32
0.66	32	H/6	160	7.45	0.8	0.21
0.66	23	J/1				
0.66	23	J/2				
0.66	23	J/3			0.18	0.79
0.66	23	J/4			0.25	0.67
0.66	23	J/5			0.5	0.53
0.66	23	J/6			0.9	0.09
0.66	23	J/7	177.5	9.70	0.98	0.03
0.86	21	K/1				
0.66	21	K/2				
0.66	21	K/3			0.15	0.76
0.66	21	K/4			0.25	0.66
0.66	21	K/5			0.5	0.5
0.66	21	K/6	180	9.09	0.75	0.33
0.66	18	L/1				
0.66	18	L/2				
0.66	18	L/3			0.25	0.76
0.66	18	L/4			0.5	0.46
0.66	18	L/5			0.66	0.33
0.66	18	L/6			0.82	0.19

TABLE 14 Cont'd

d/D_o	D_o/T_o	TEST NO.	ULTIMATE AXIAL LOAD P_u (kN)	ULTIMATE MOMENT M_u (kNm)	M/M_u	P/P_u
0.77	32	M/1	110			
0.77	32	M/2		7.02		
0.77	32	M/3			0.27	0.72
0.77	32	M/4			0.53	0.5
0.77	32	M/5			0.7	0.32
0.77	32	M/6			0.76	0.29
0.77	32	M/7			0.87	0.14
0.77	21	N/1	227			
0.77	21	N/2		12.81		
0.77	21	N/3			0.15	0.85
0.77	21	N/4			0.25	0.75
0.77	21	N/5			0.4	0.81
0.77	21	N/6			0.5	0.52
0.77	21	N/7			0.6	0.39
0.77	21	N/8			0.75	0.26
0.77	21	N/9			0.85	0.15
0.77	18	P/1	235			
0.77	18	P/2		12.74		
0.77	18	P/3			0.24	0.6
0.77	18	P/4			0.36	0.55
0.77	18	P/5			0.45	0.51
0.77	18	P/6			0.61	0.42
0.77	18	P/7			0.82	0.15
1.0	32	Q/1	165			
1.0	32	Q/2		12.5		
1.0	32	Q/3			0.31	0.64
1.0	32	Q/4			0.52	0.52
1.0	32	Q/5			0.85	0.25
1.0	23	R/1	240			
1.0	23	R/2		18.98		
1.0	23	R/3			0.28	0.63

TABLE 14 Cont'd

d/D_o	D_o/T_o	TEST NO.	ULTIMATE AXIAL LOAD P_u (kN)	ULTIMATE MOMENT M_u (kNm)	M/M_u	P/P_u
1.0	23	R/4	270	19.80	0.54	0.44
1.0	23	R/5			0.64	0.31
1.0	23	R/6			0.82	0.20
1.0	18	S/1				
1.0	18	S/2				
1.0	18	S/3			0.20	0.67
1.0	18	S/4			0.42	0.50
1.0	18	S/5			0.62	0.41
1.0	18	S/6			0.78	0.22

LOAD DEFLECTION GRAPHS FOR BETA = 0.42

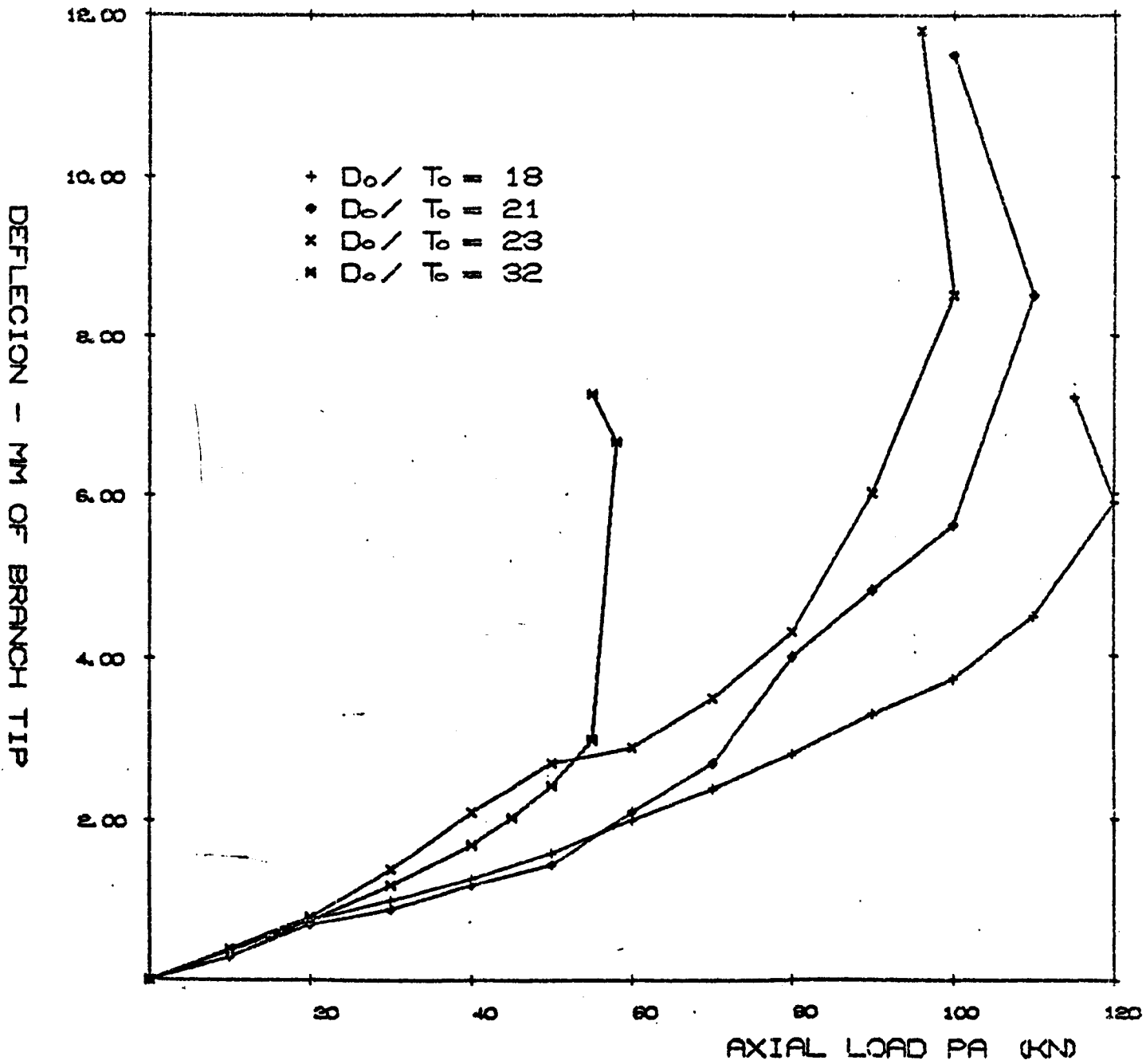


Figure 117. Load deflection graphs for beta = 0.42

LOAD DEFLECTION GRAPHS FOR BETA = 0.53

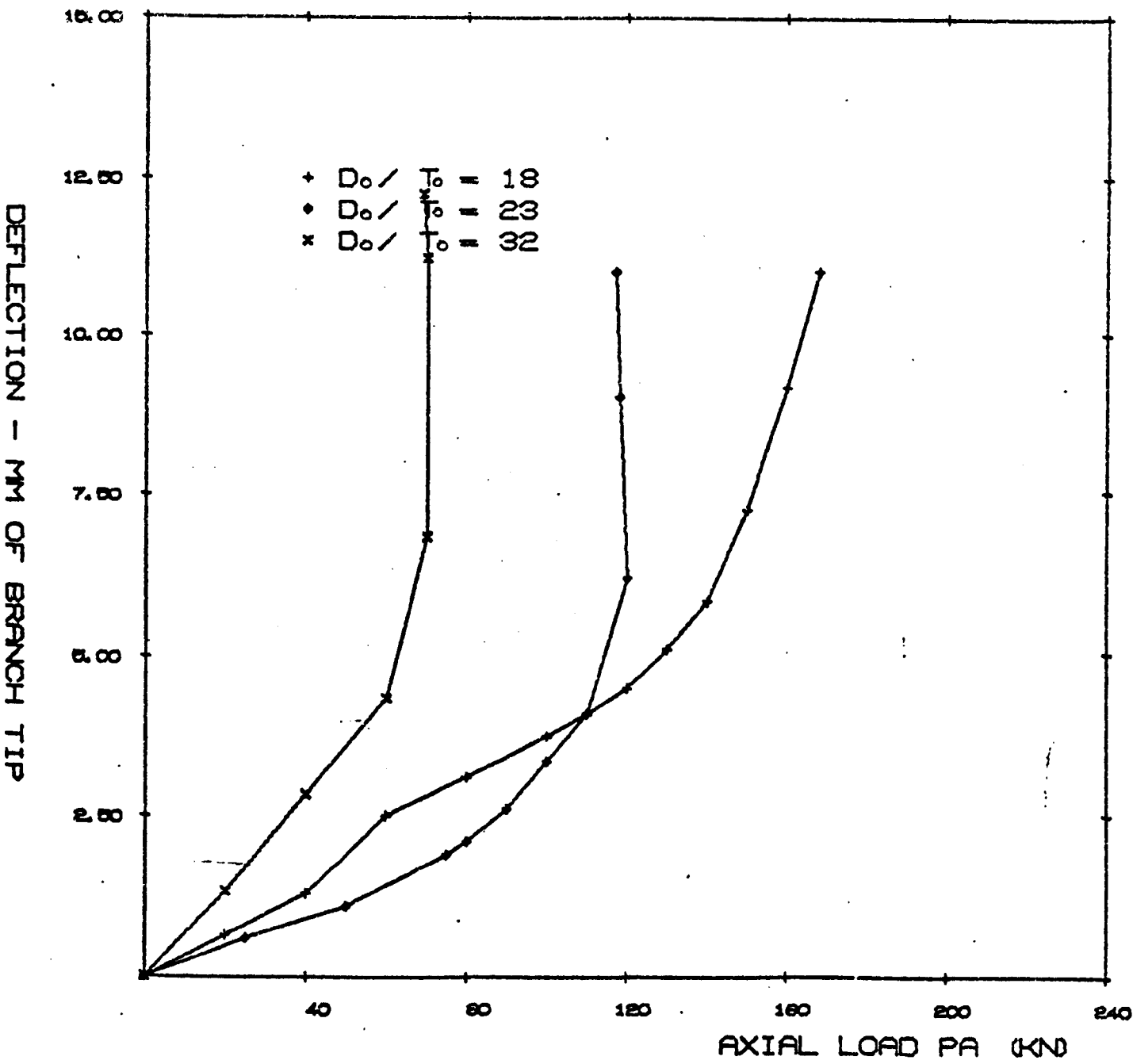


Figure 118. Load deflection graphs for beta = 0.53.

LOAD DEFLECTION GRAPHS FOR BETA = 0.66

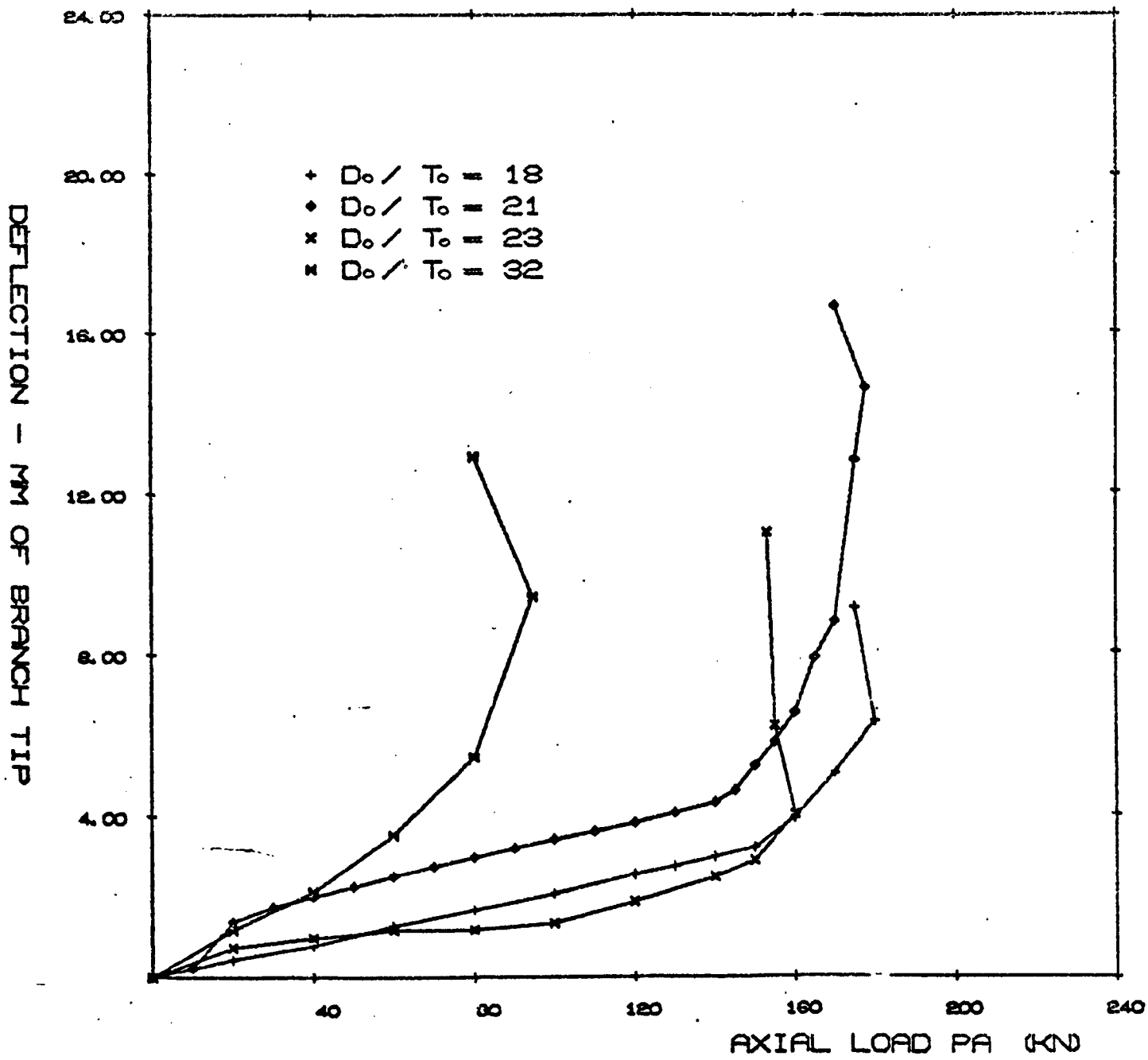


Figure 119, Load deflection graphs for beta = 0.66.

LOAD DEFLECTION GRAPHS FOR BETA = 0.77

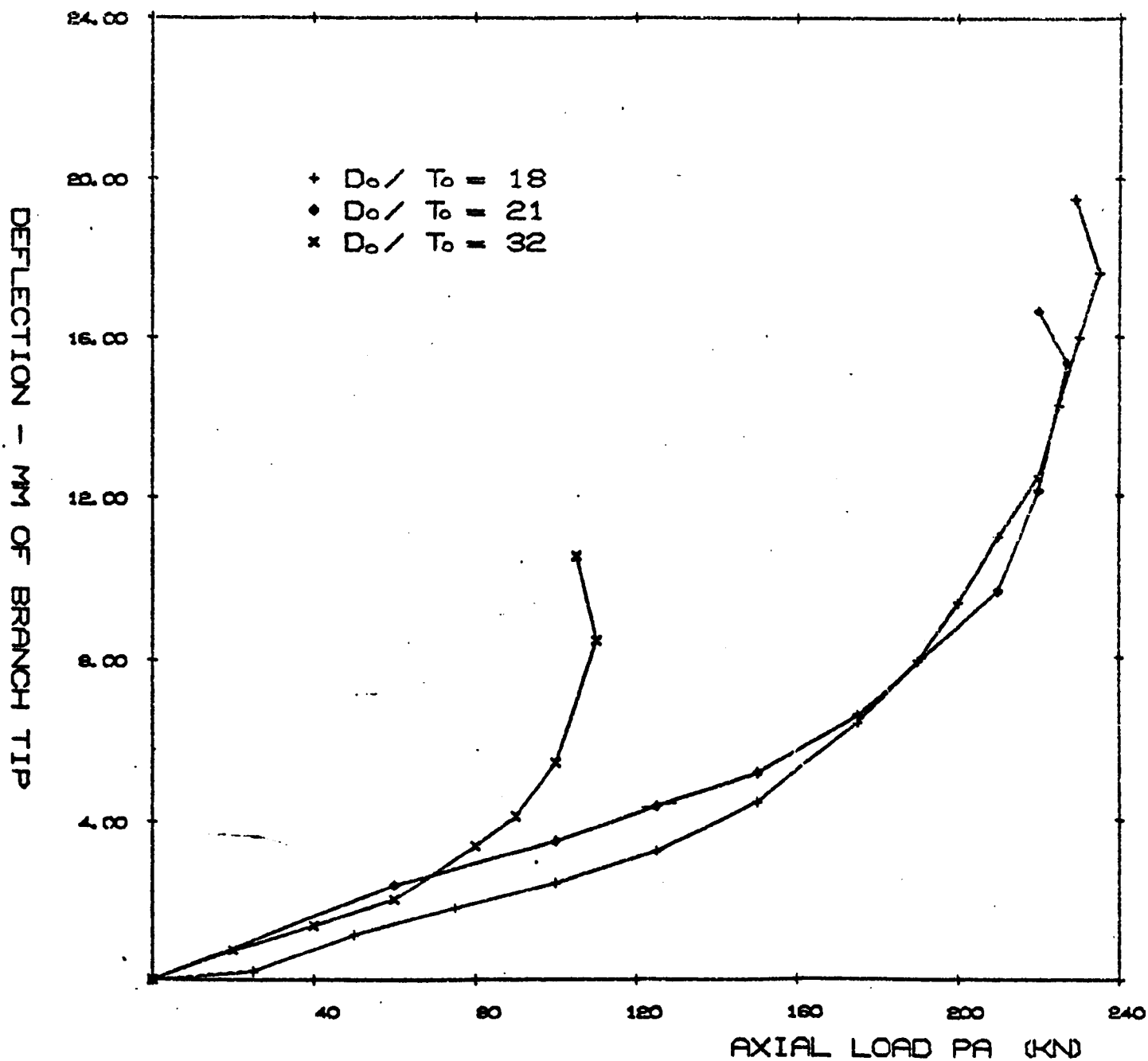


Figure 120. Load deflection graphs for beta = 0.77.

LOAD DEFLECTION GRAPHS FOR BETA = 1.0

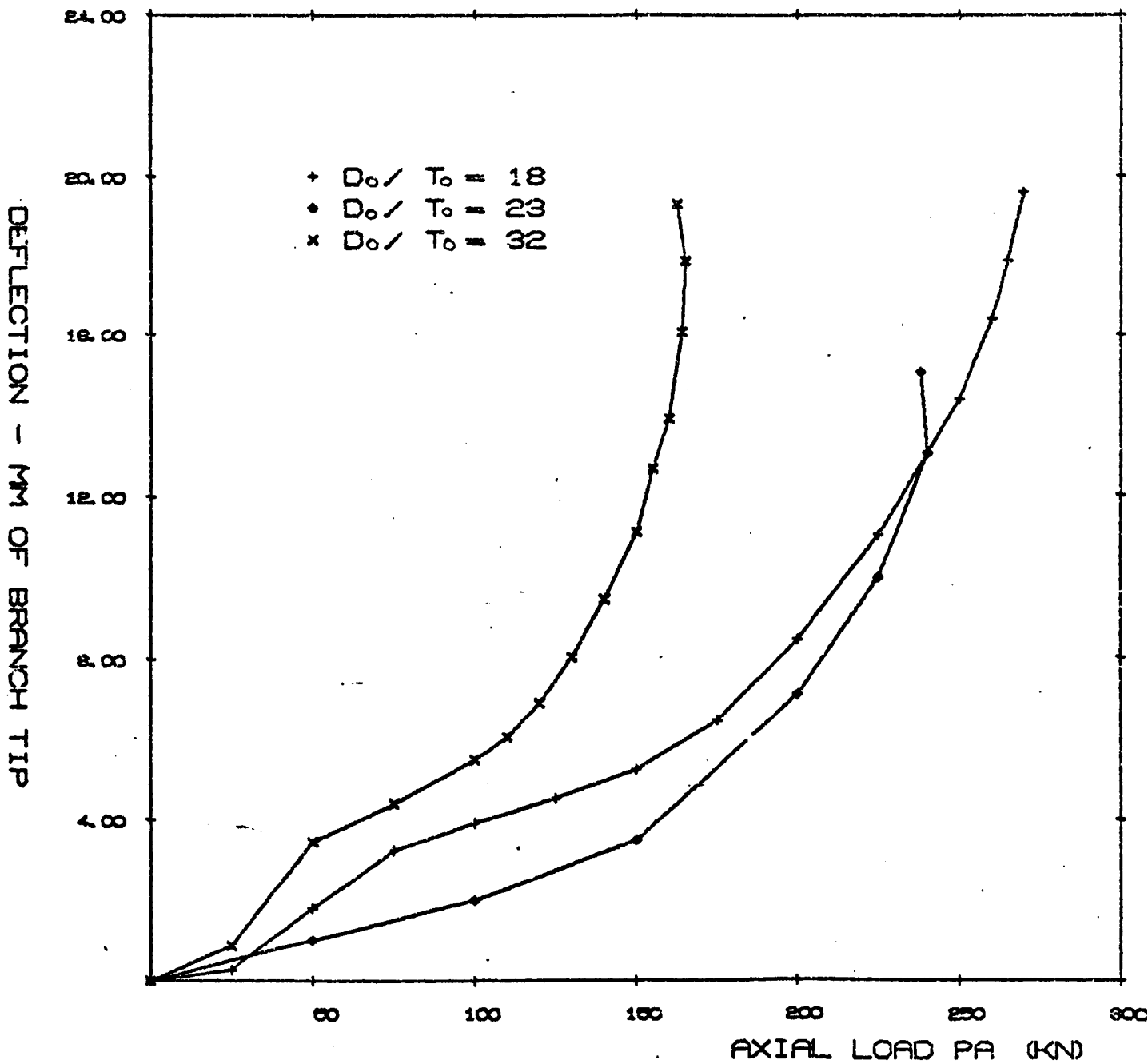


Figure 121. Load deflection graphs for beta = 1.0.

LOAD DEFLECTION GRAPHS FOR BETA = 0.42

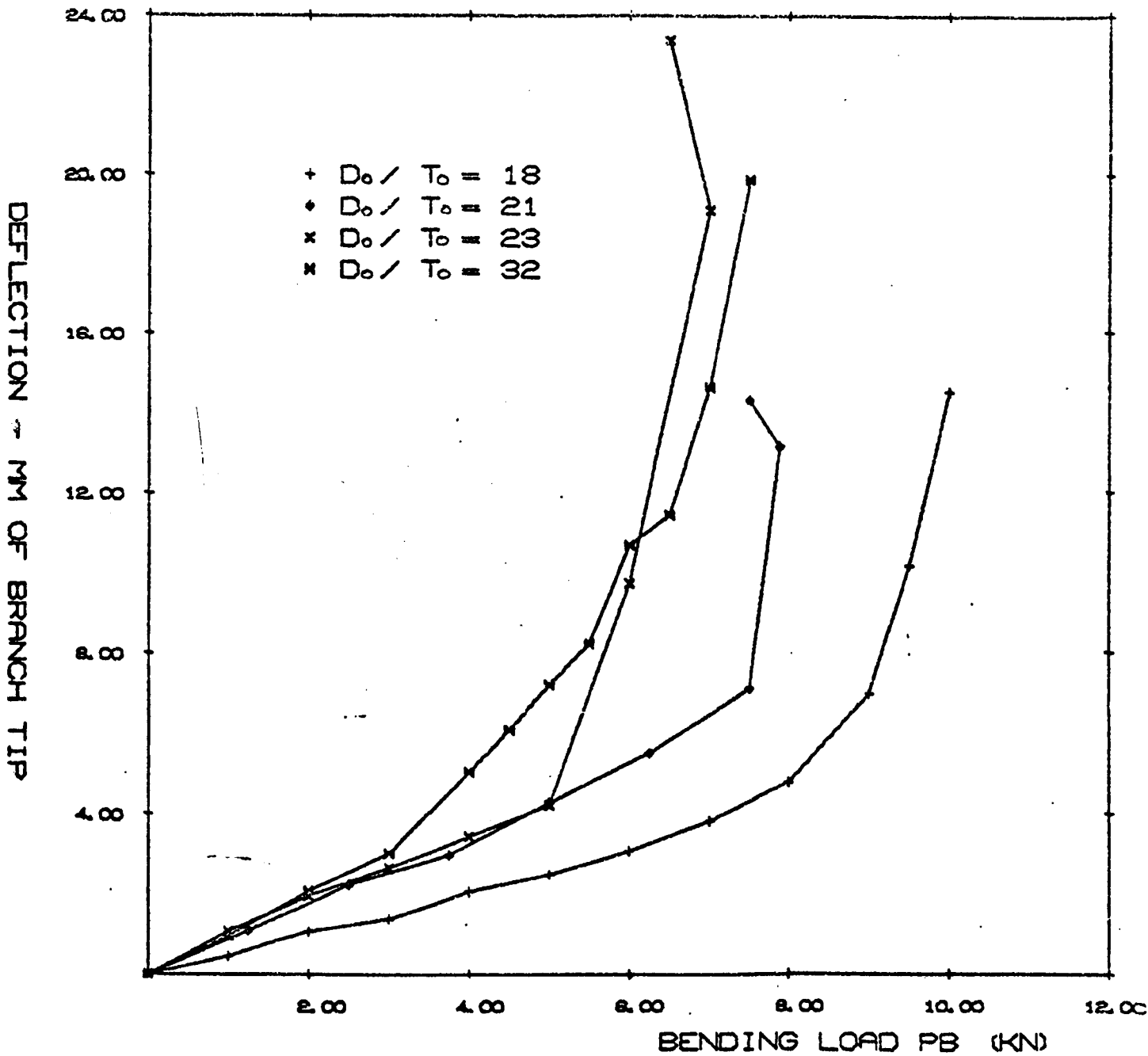


Figure 122. Load deflection graphs for beta = 0.42.

LOAD DEFLECTION GRAPHS FOR BETA = 0.53

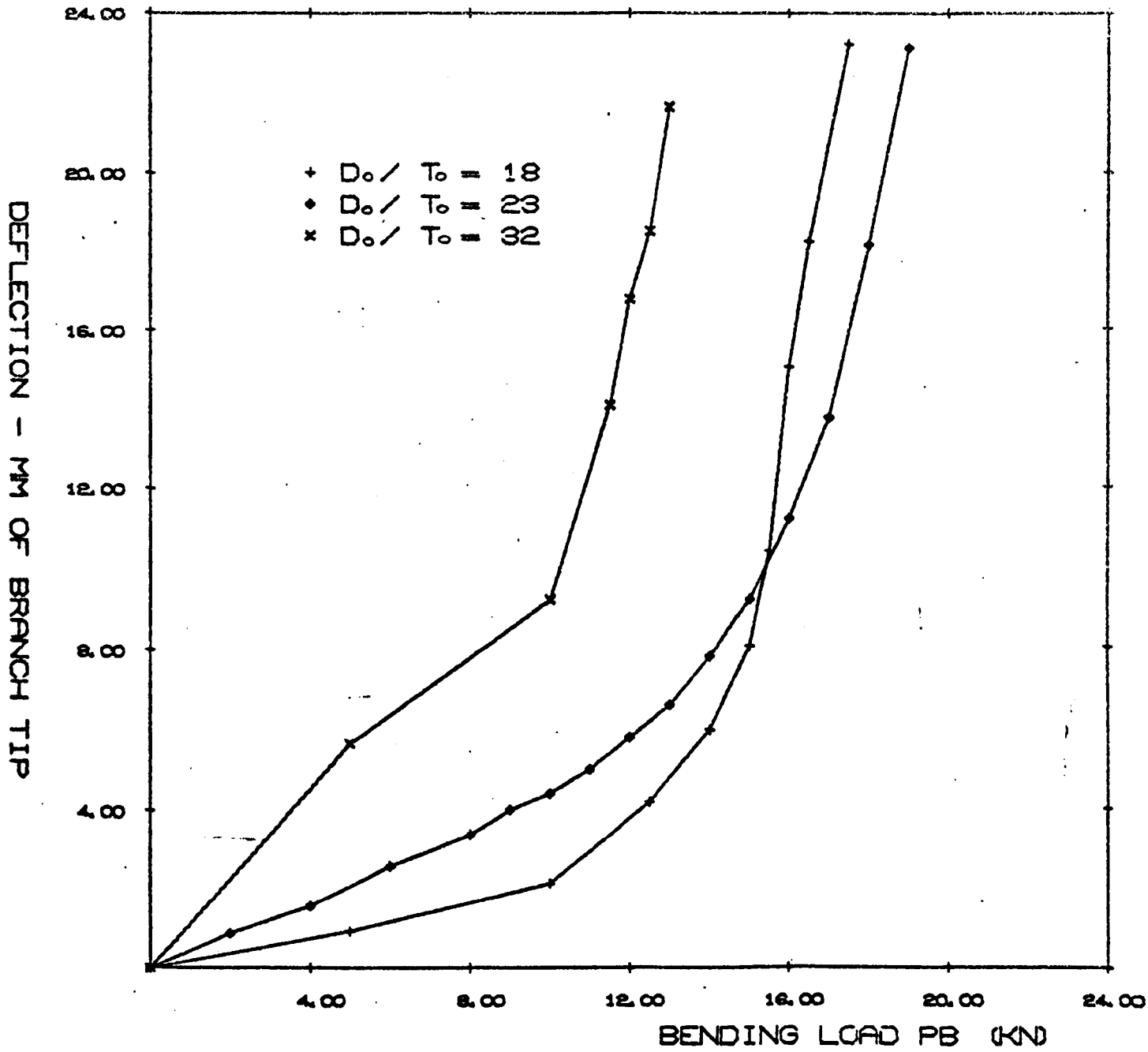


Figure 123. Load deflection graphs for beta = 0.53.

LOAD DEFLECTION GRAPHS FOR BETA = 0.67

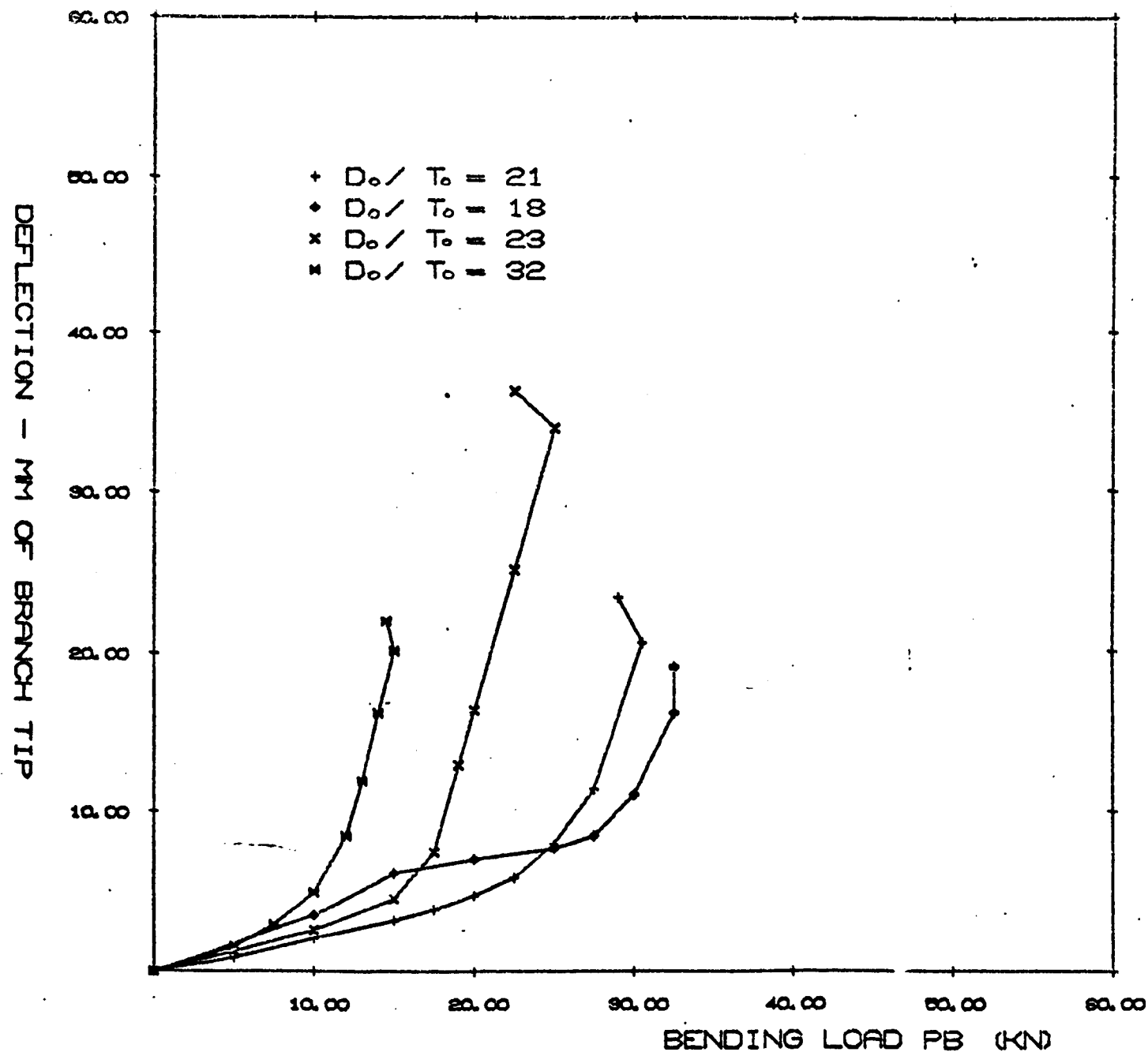


Figure 124. Load deflection graphs for beta = 0.66.

LOAD DEFLECTION GRAPHS FOR BETA = 0.77

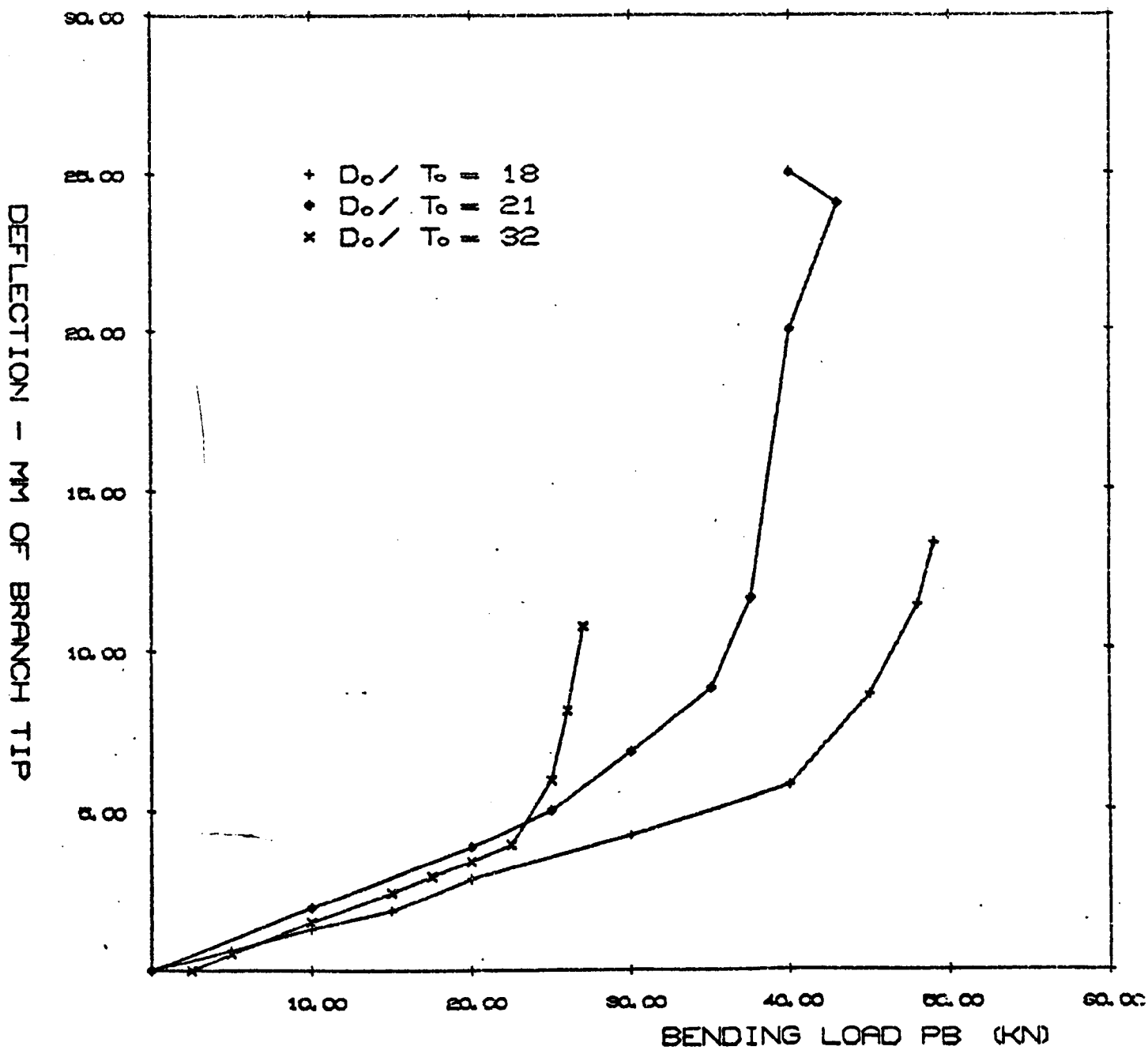


Figure 125. Load deflection graphs for beta = 0.77.

LOAD DEFLECTION GRAPHS FOR BETA = 1.0

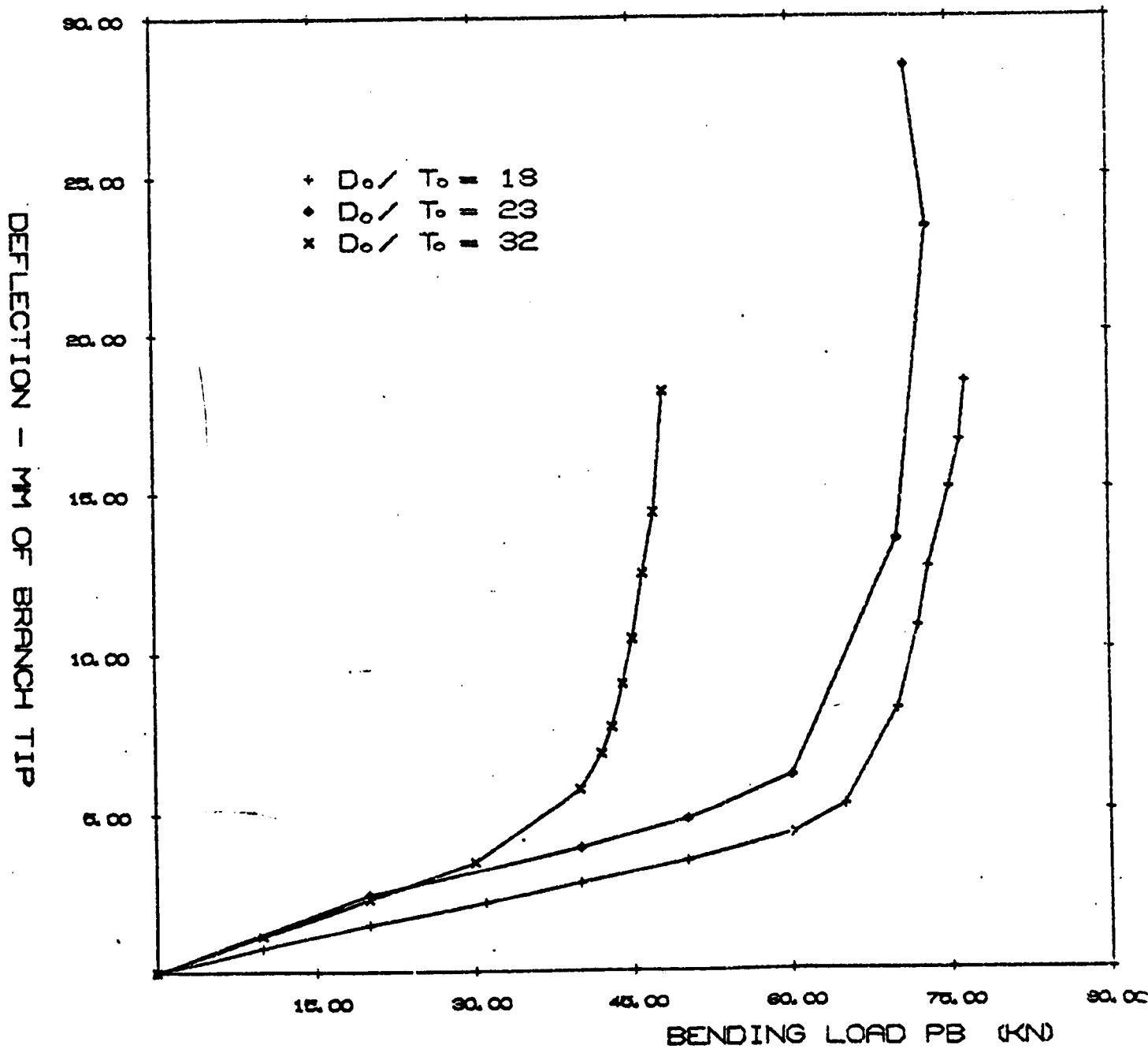


Figure 126. Load deflection graphs for beta = 1.0.

FIGURE 127 ULTIMATE AXIAL LOAD .V. BETA

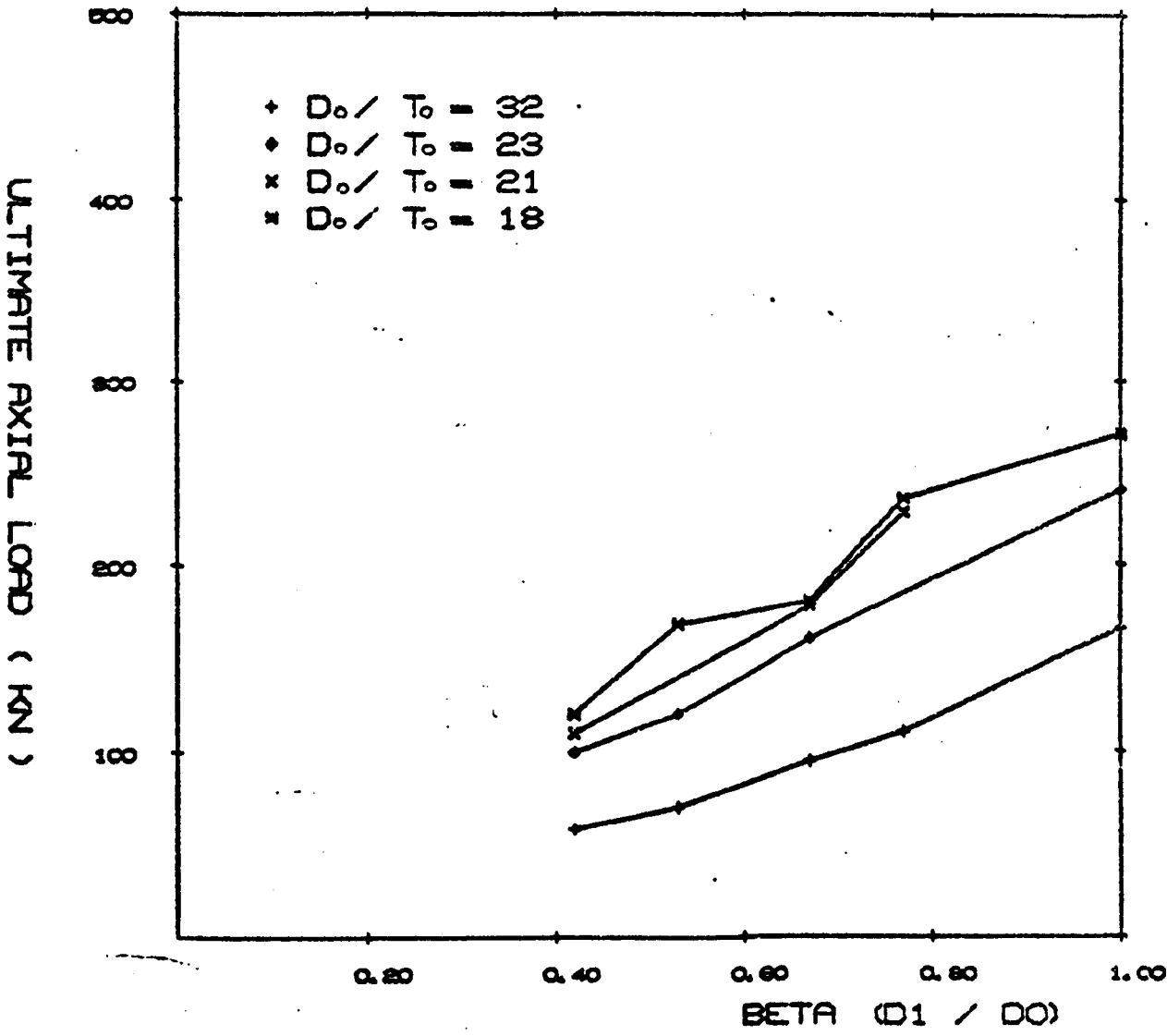


FIGURE 128 ULTIMATE AXIAL LOAD .V. D / T

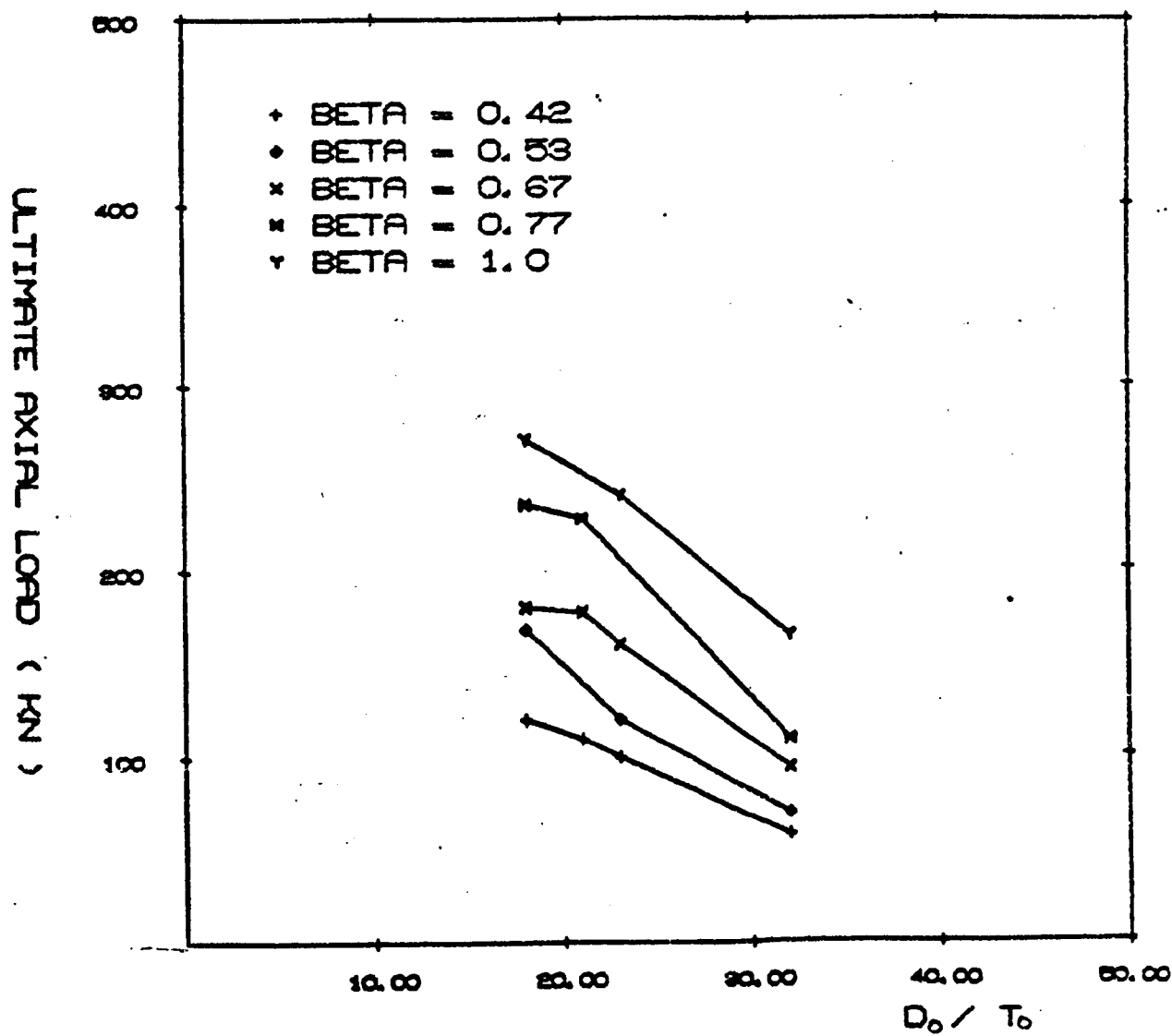


FIGURE 129 ULTIMATE MOMENT .V. D_o / T_o

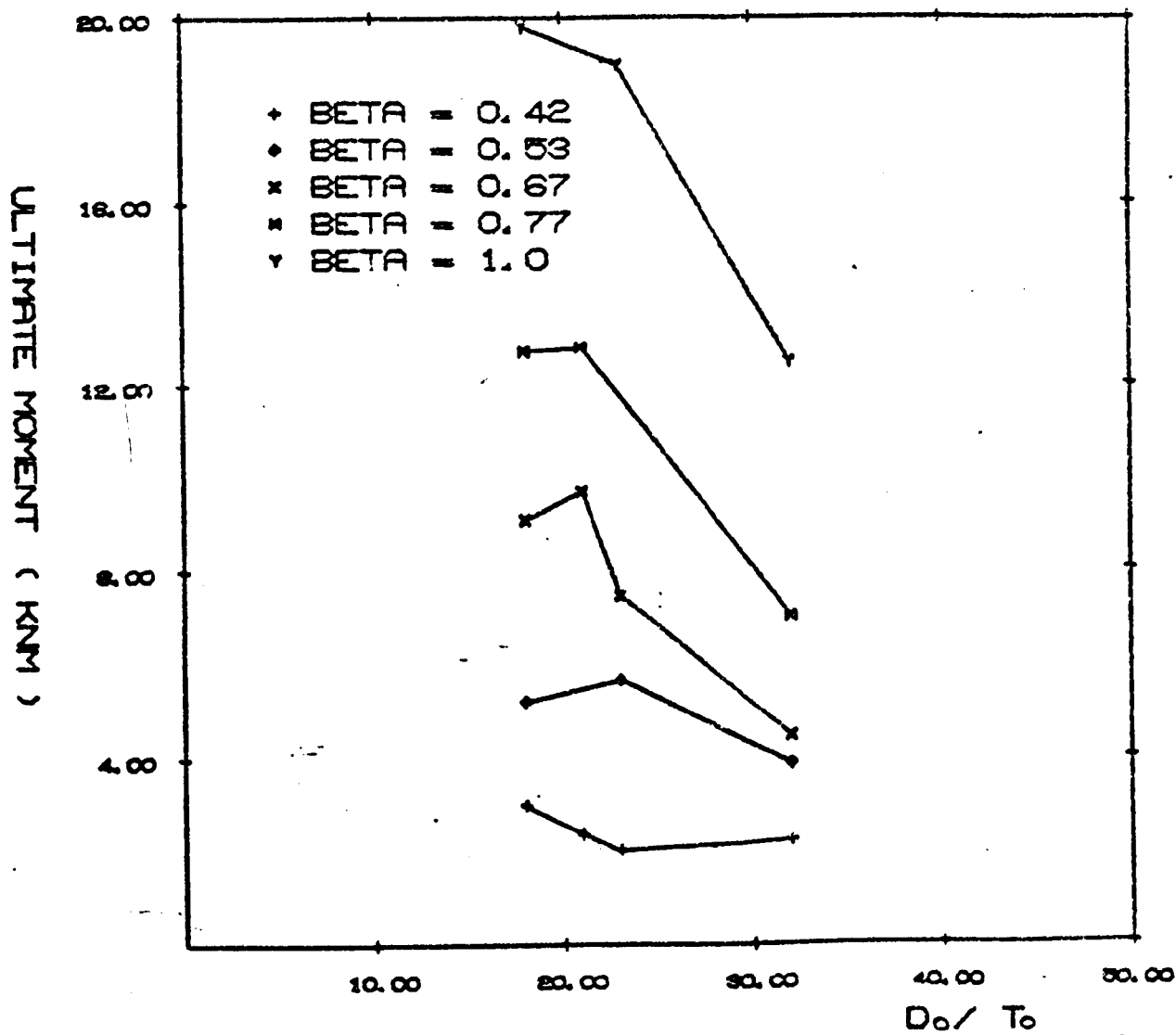


FIGURE 130 ULTIMATE MOMENT .V. BETA

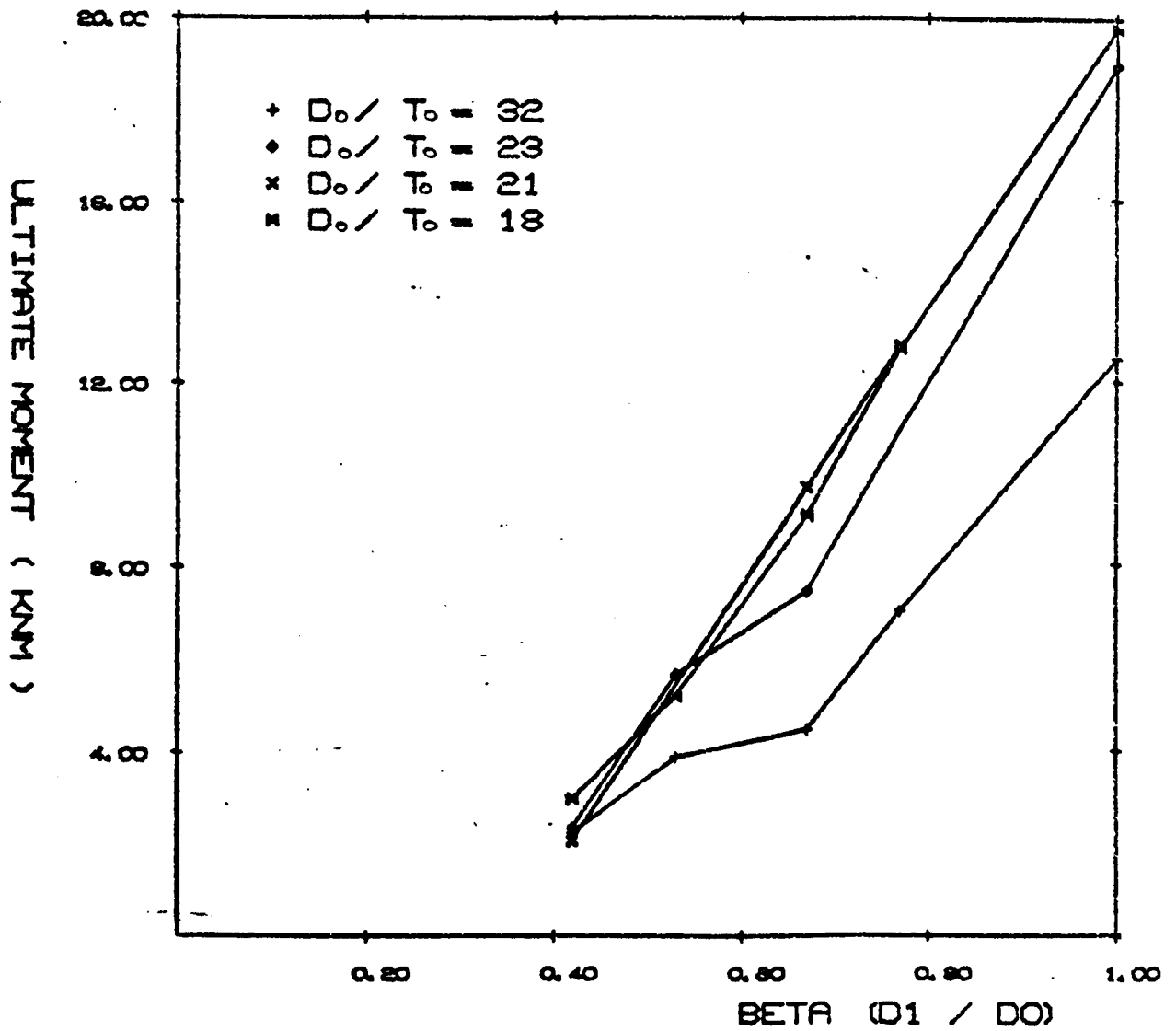


FIGURE 131 JOINT FORCE .V. BETA

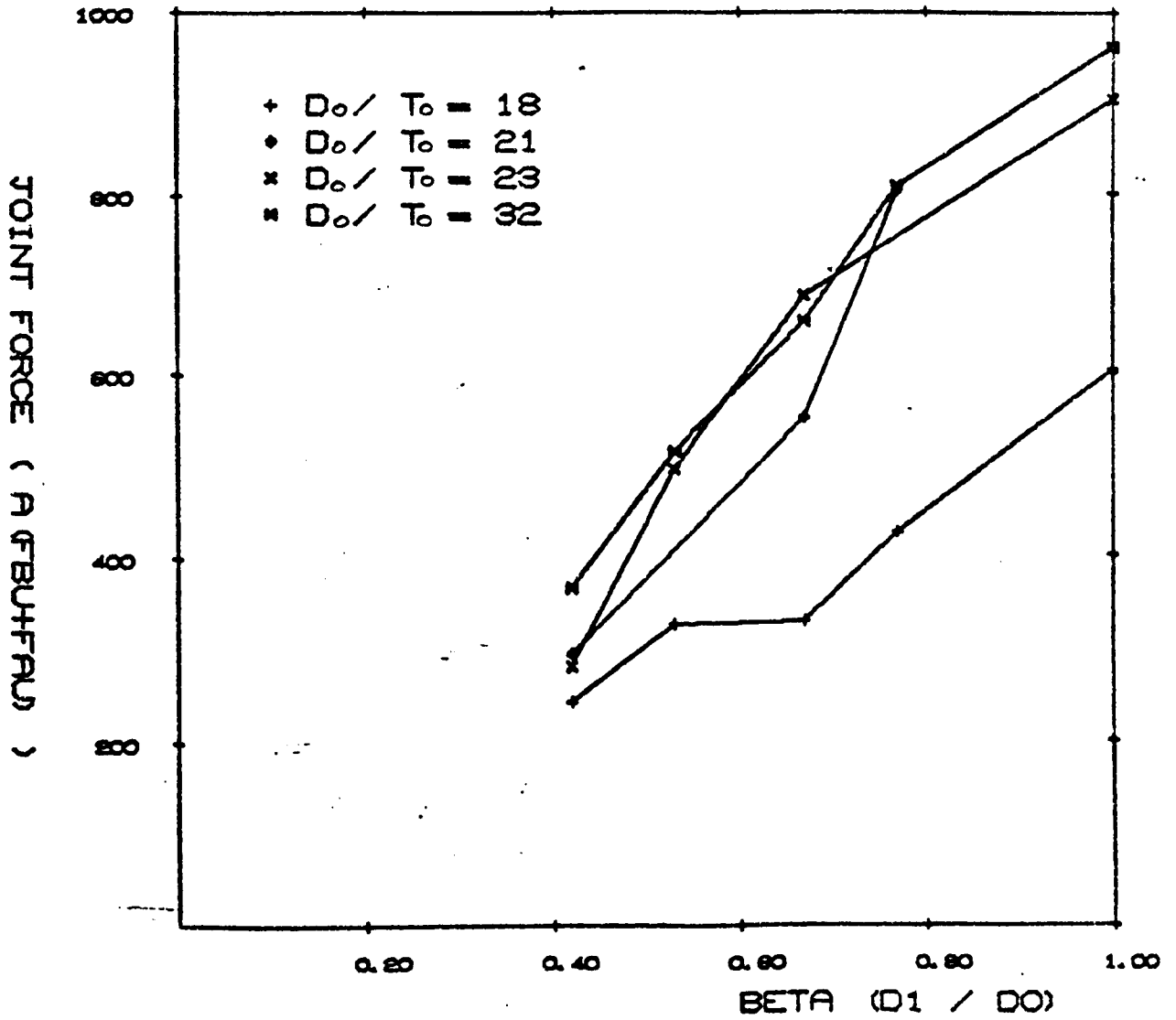


FIGURE 132 BENDING LOAD V. AXIAL LOAD FOR BETA = 0.42

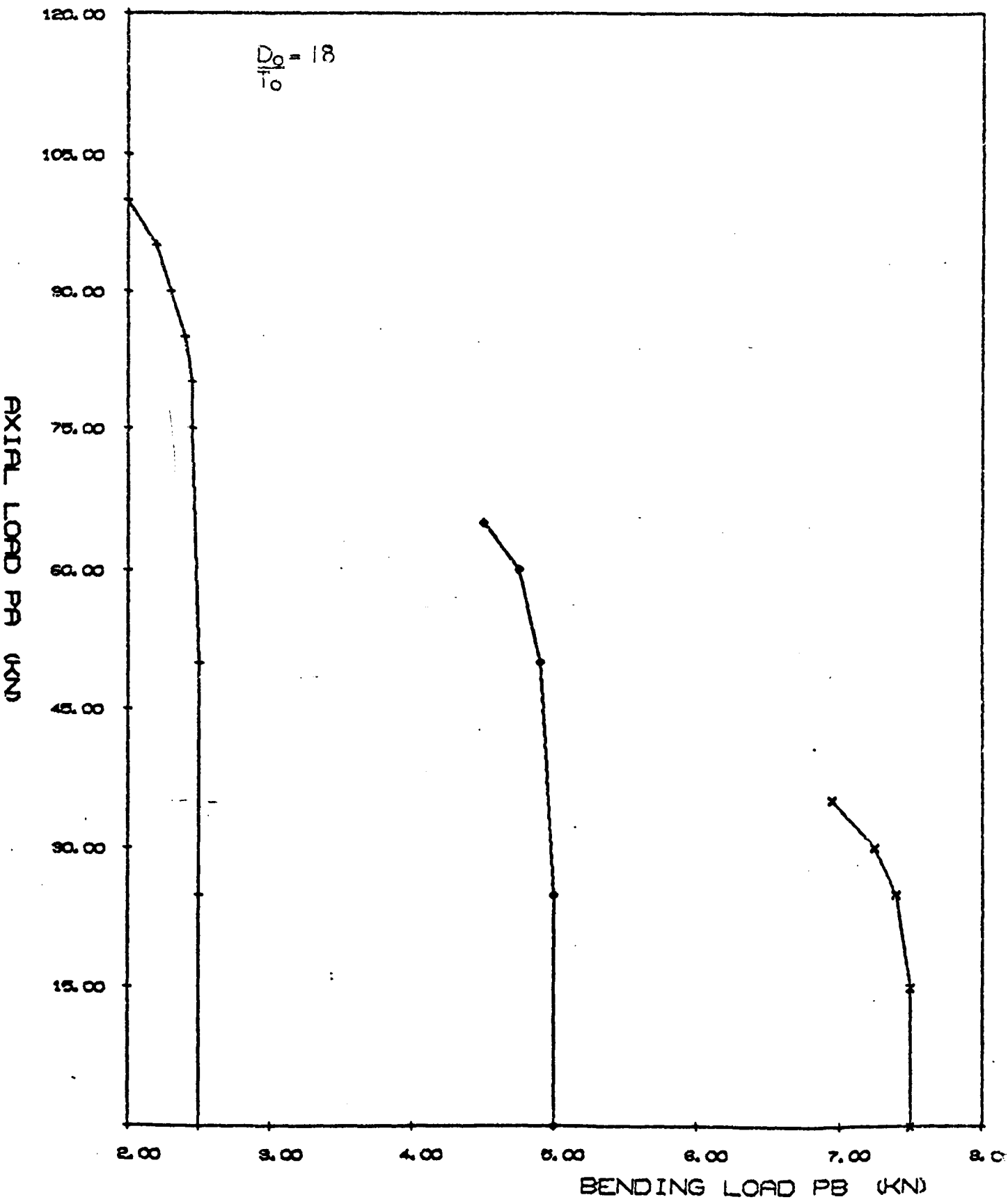


FIGURE 133 BENDING LOAD V. AXIAL LOAD FOR BETA = 0.42

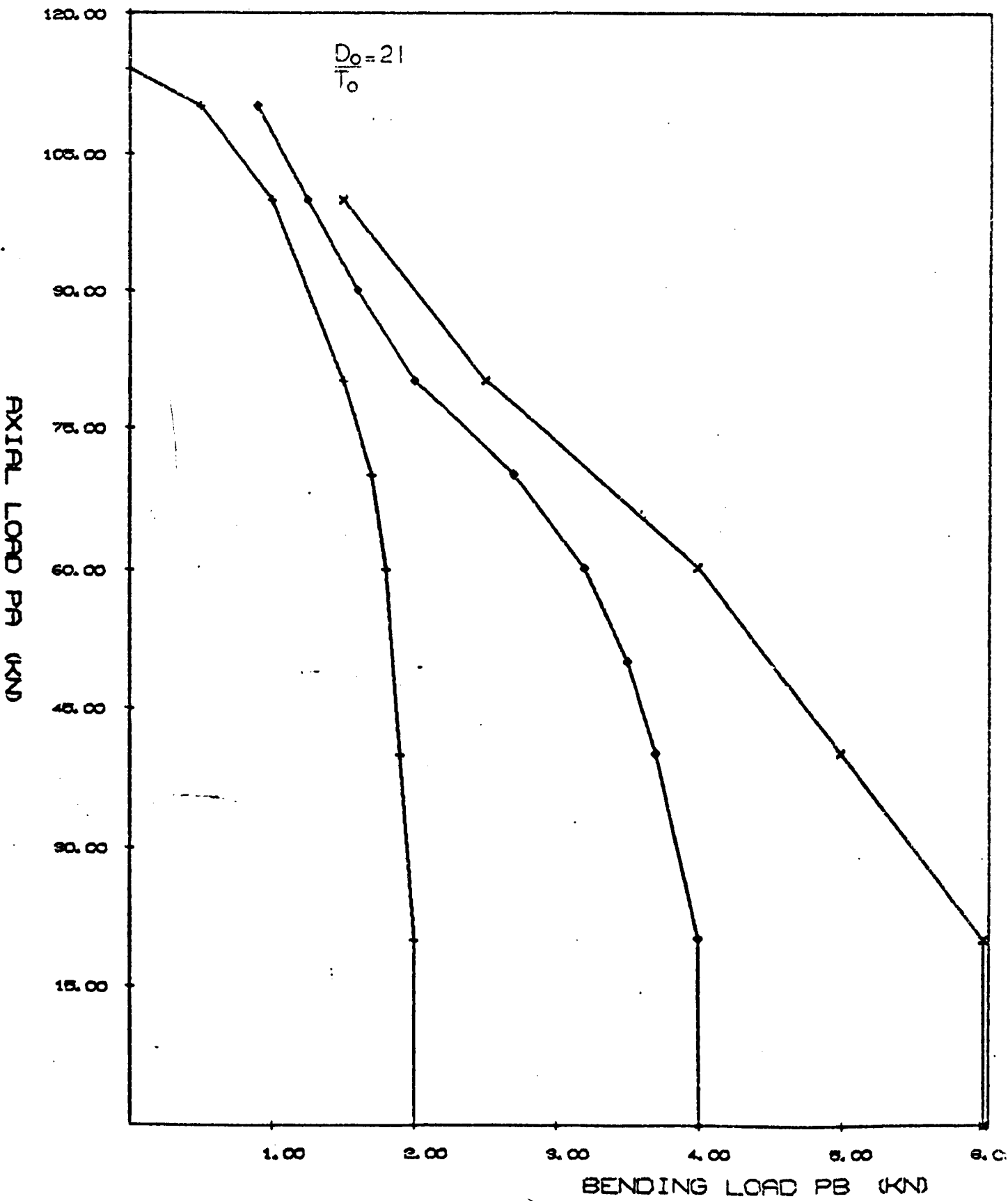


FIGURE 134 BENDING LOAD V. AXIAL LOAD FOR BETA = 0.42

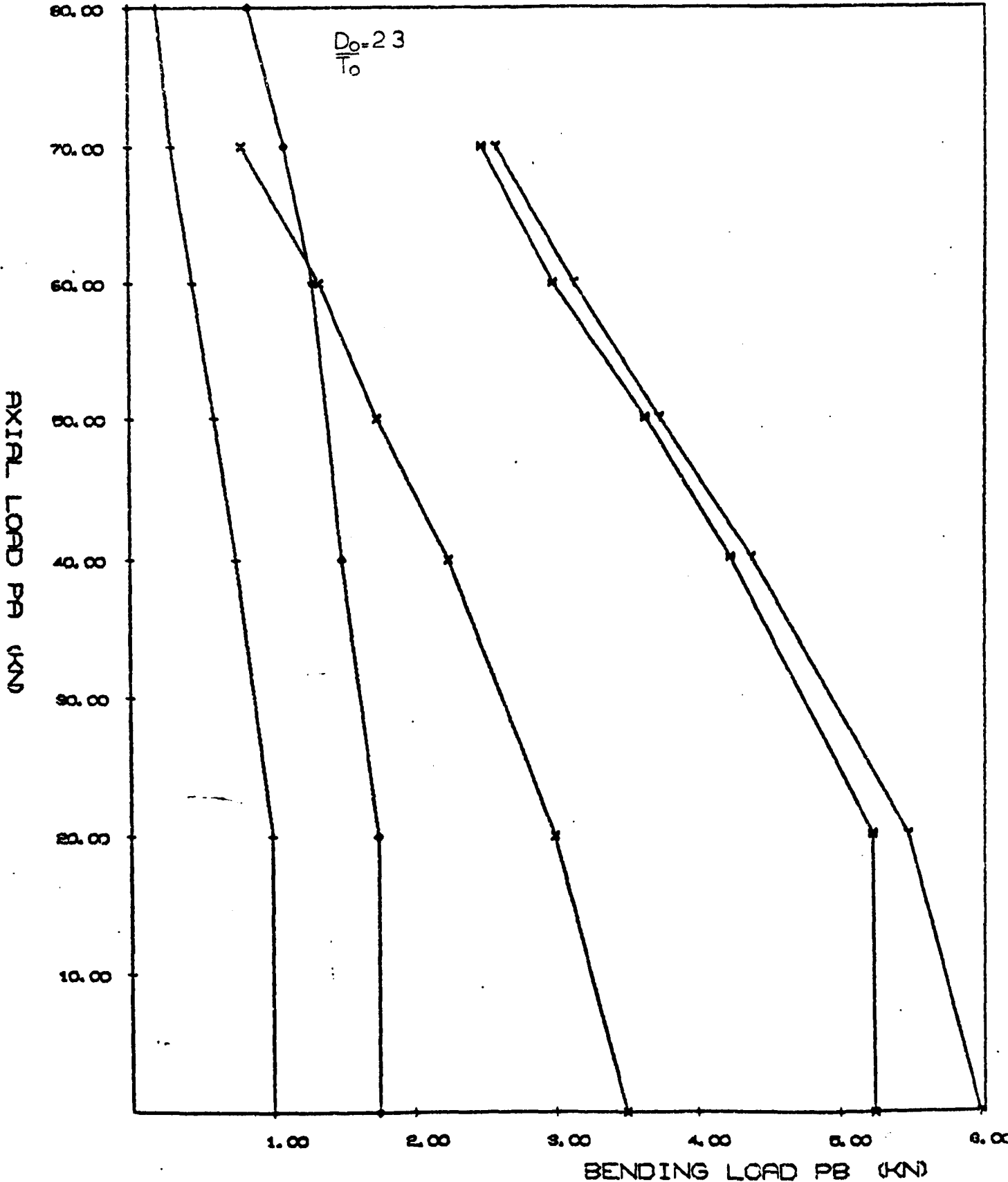


FIGURE 135 BENDING LOAD V. AXIAL LOAD FOR BETA = 0.42

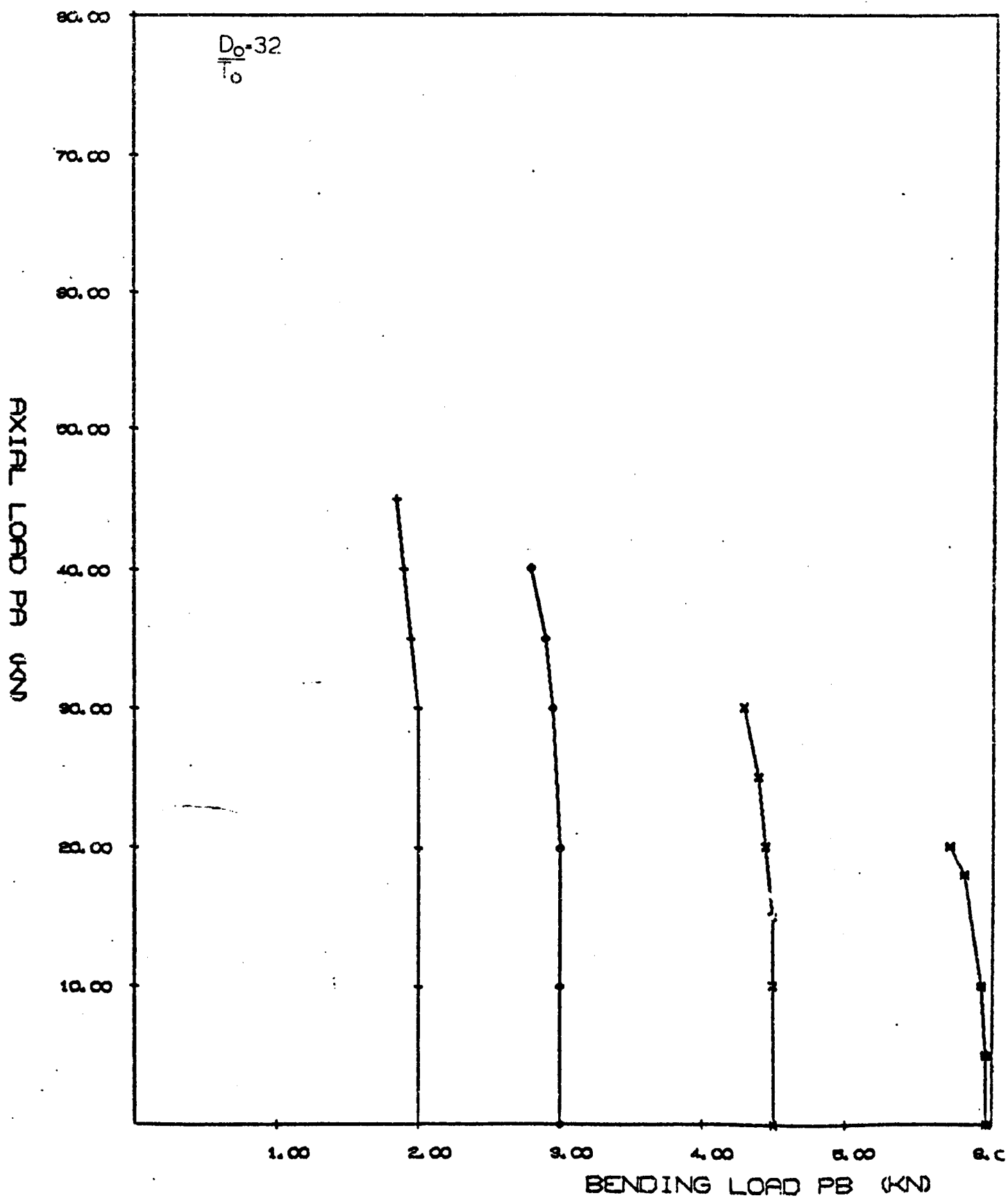


FIGURE 136 BENDING LOAD V. AXIAL LOAD FOR BETA = 0.53

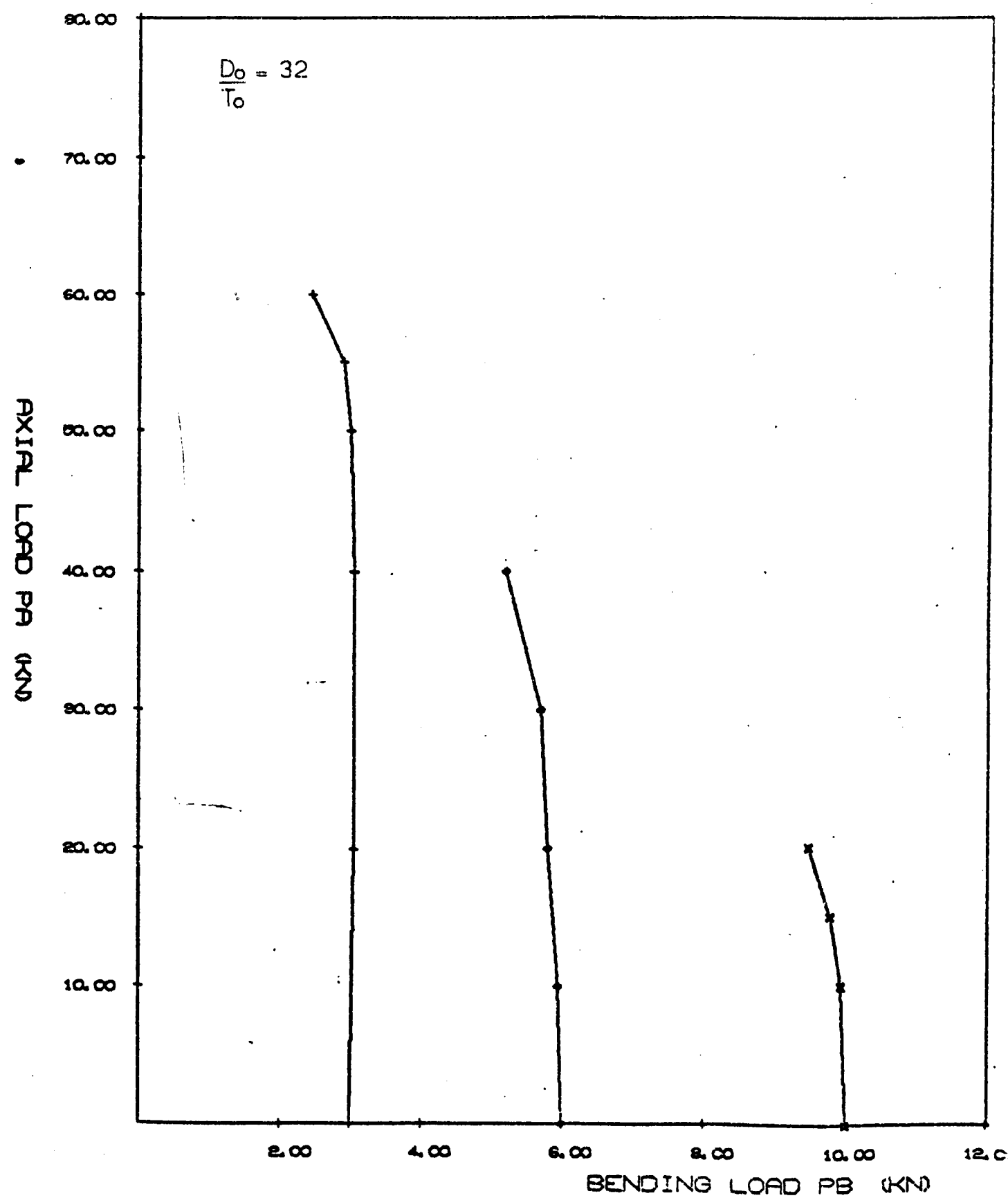


FIGURE 137 BENDING LOAD V. AXIAL FOR BETA = 0.53

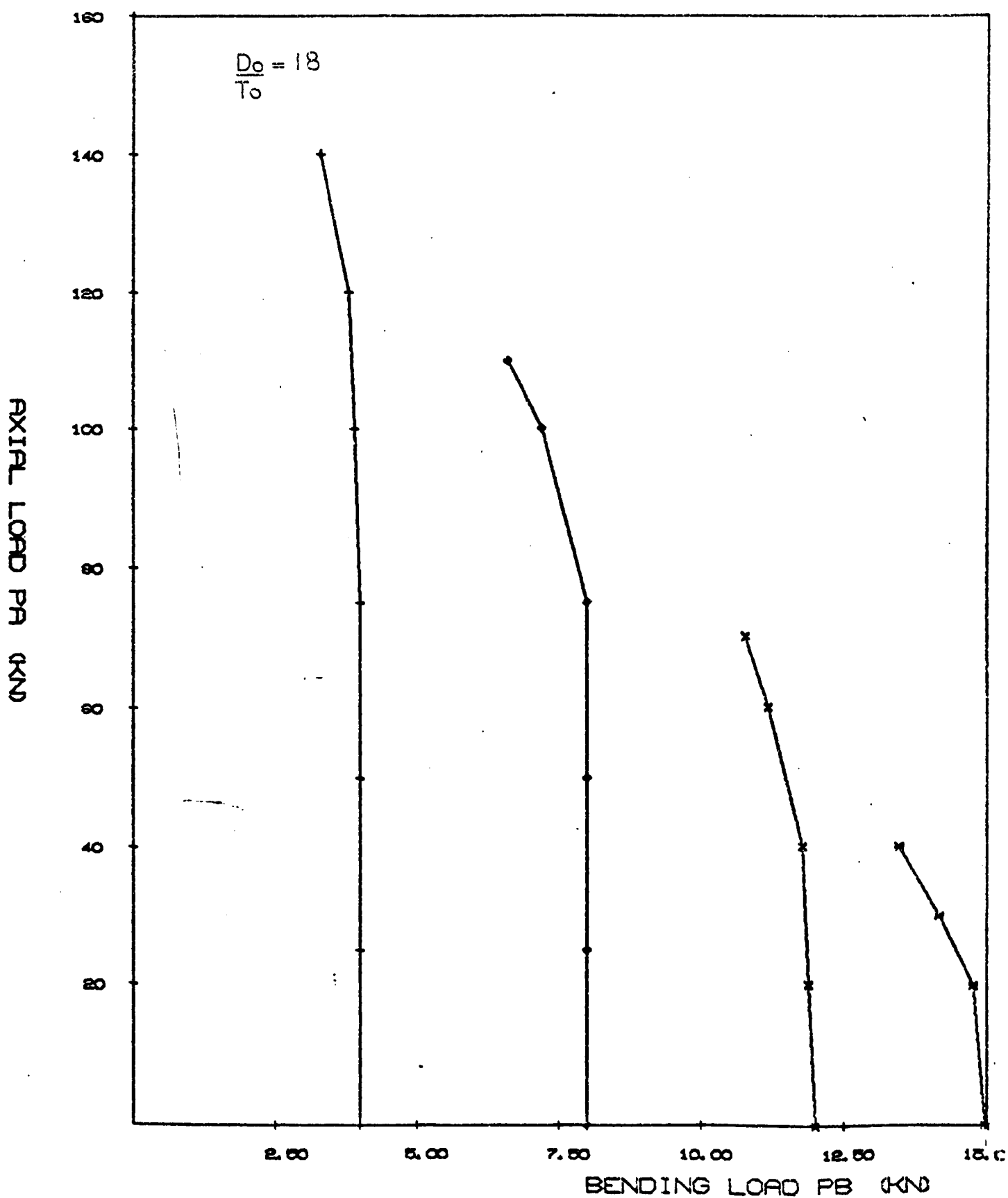


FIGURE 138 BENDING LOAD V. AXIAL LOAD FOR BETA = 0.53

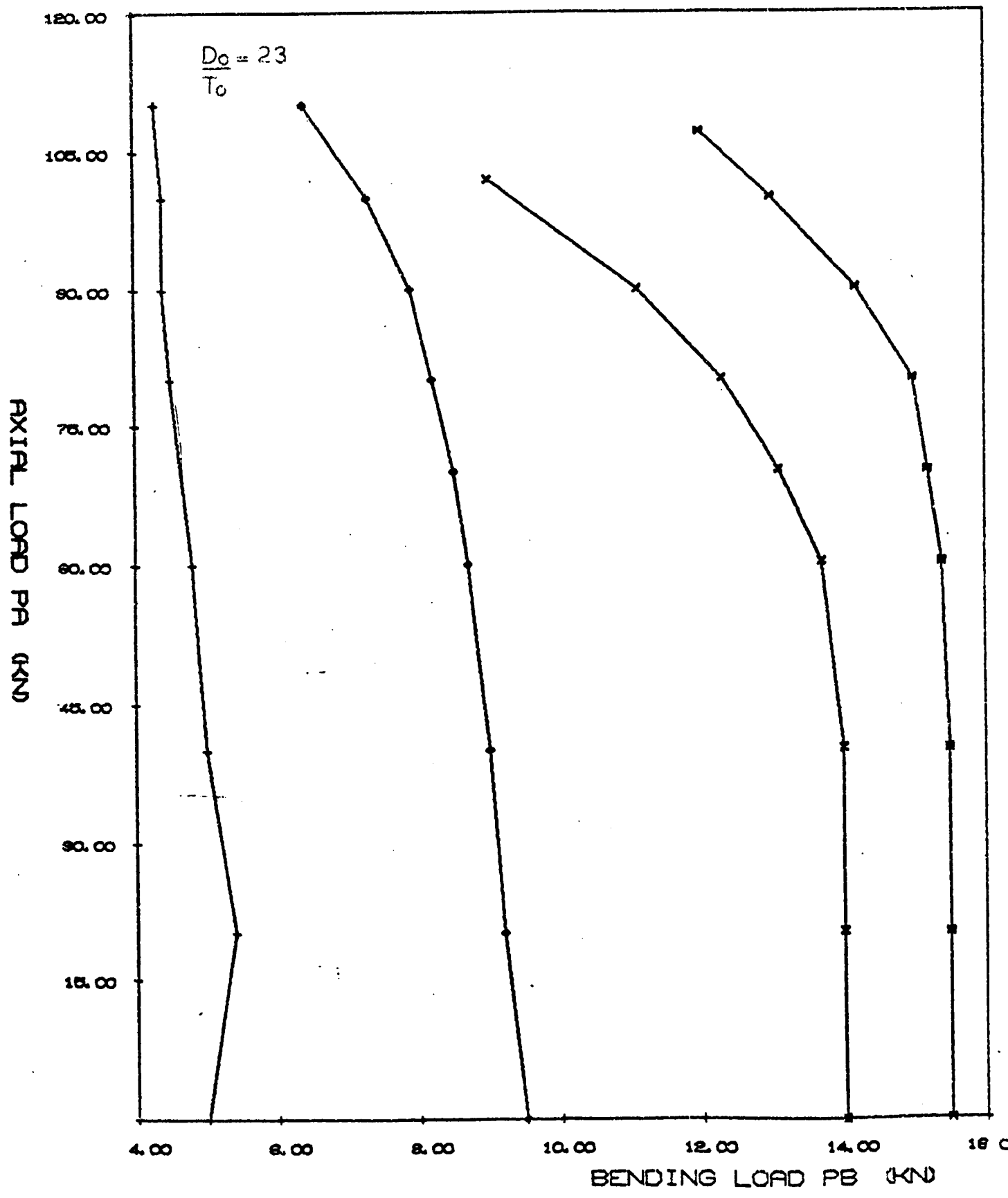


FIGURE 139 BENDING LOAD V. AXIAL LOAD FOR BETA = 0.66'

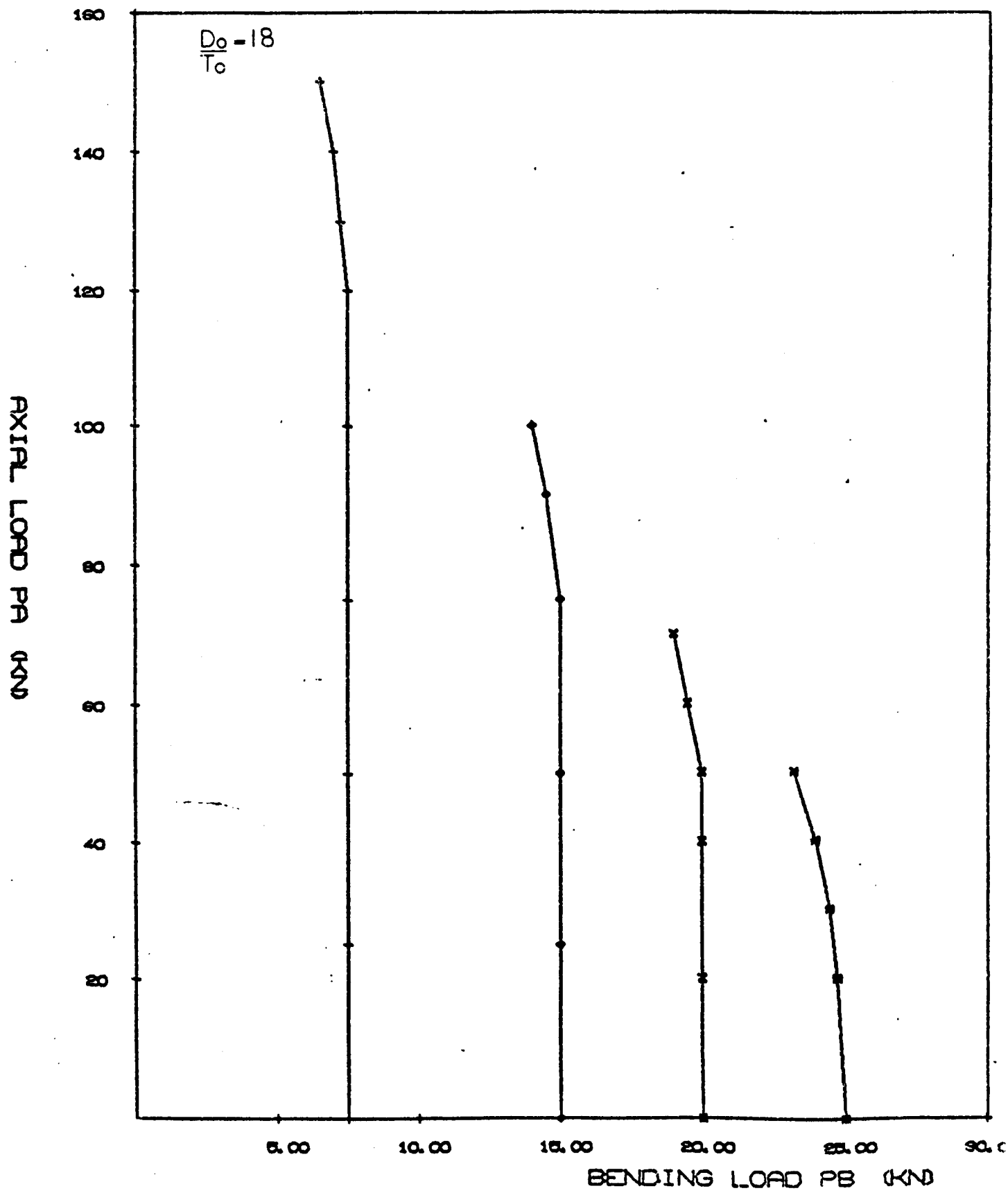


FIGURE 140 BENDING LOAD V. AXIAL LOAD FOR BETA = 0.66'

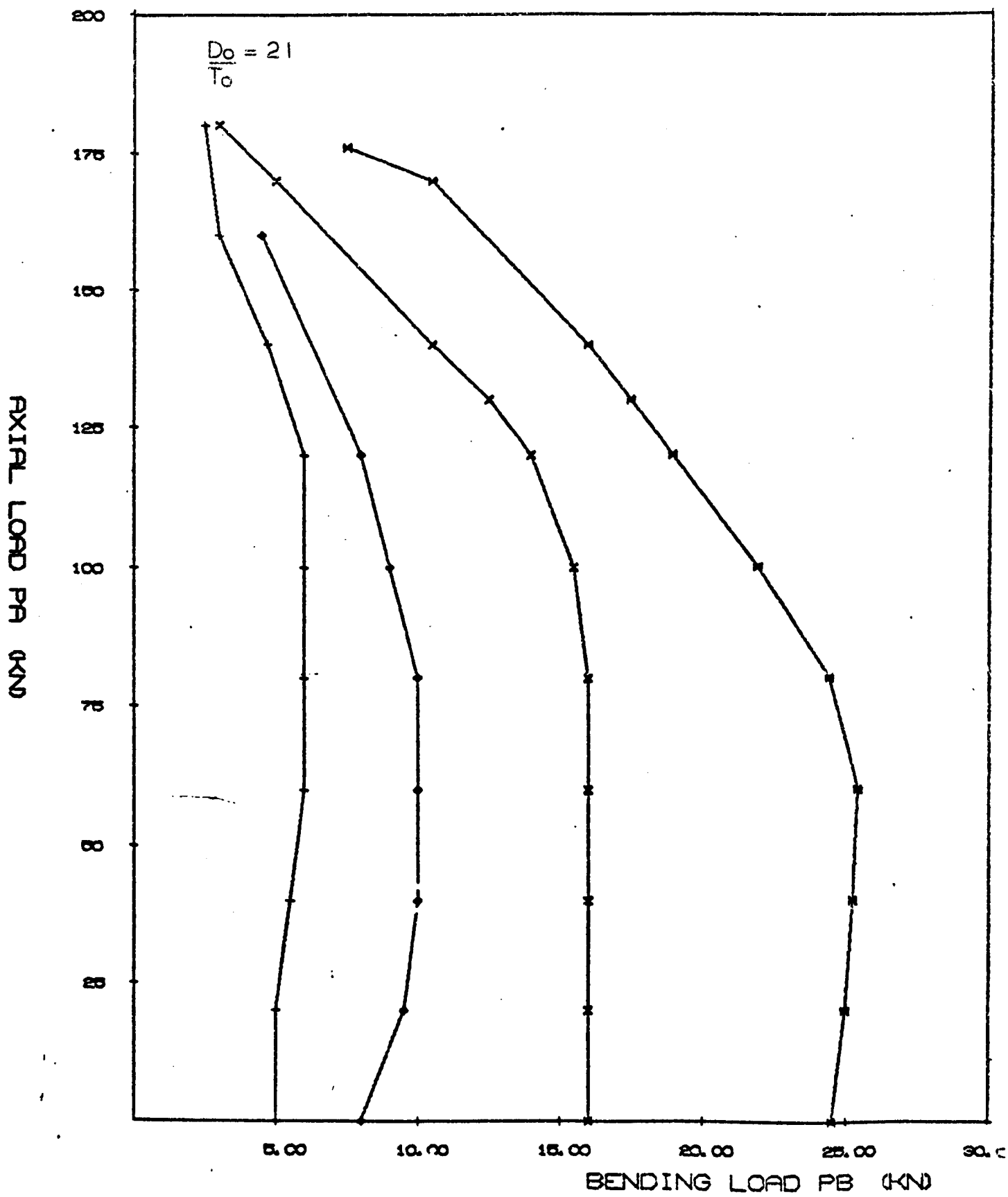


FIGURE 141 BENDING LOAD V. AXIAL LOAD FOR BETA = 0.66'

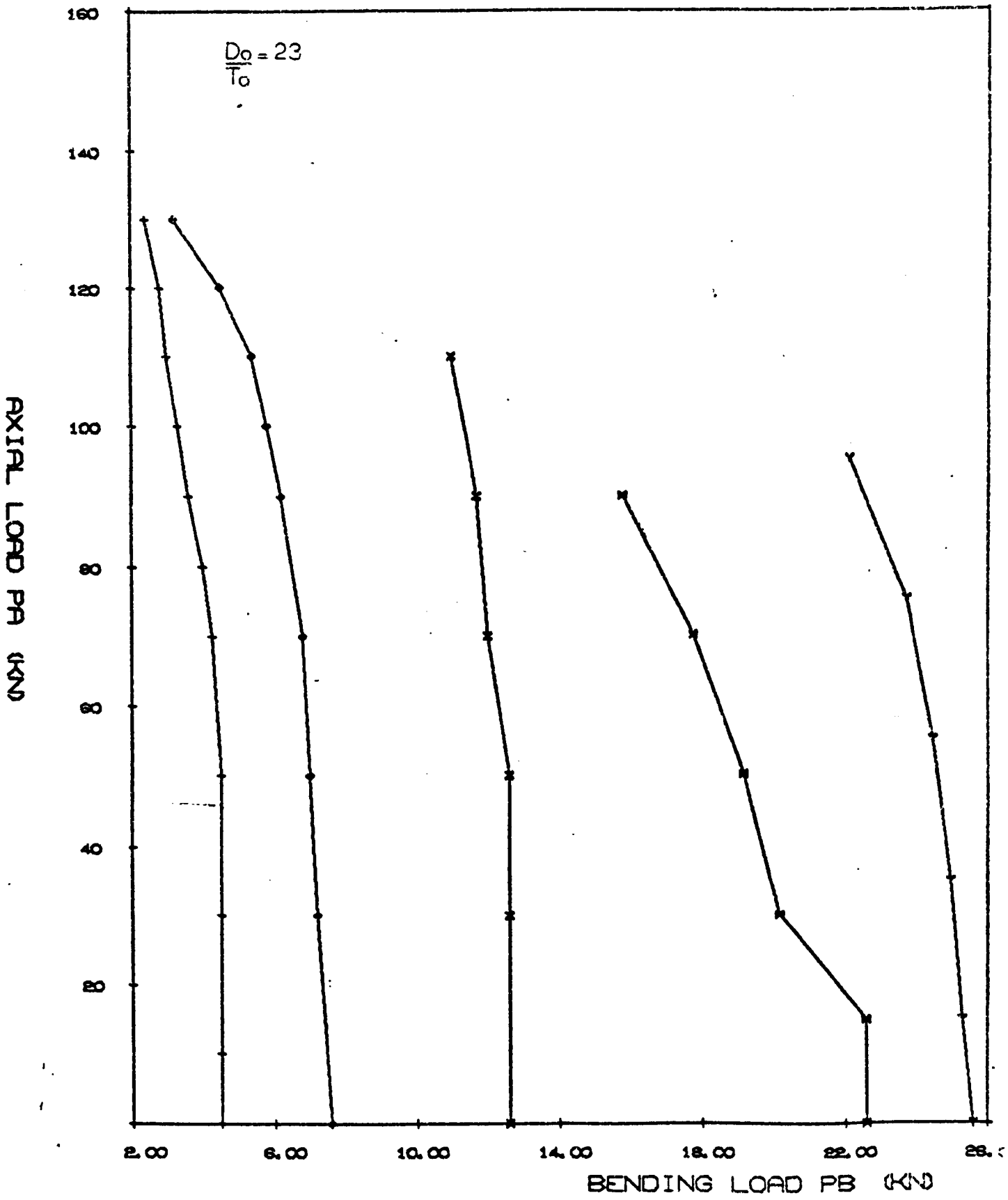


FIGURE 142 BENDING LOAD V. AXIAL LOAD FOR BETA = 0.66'

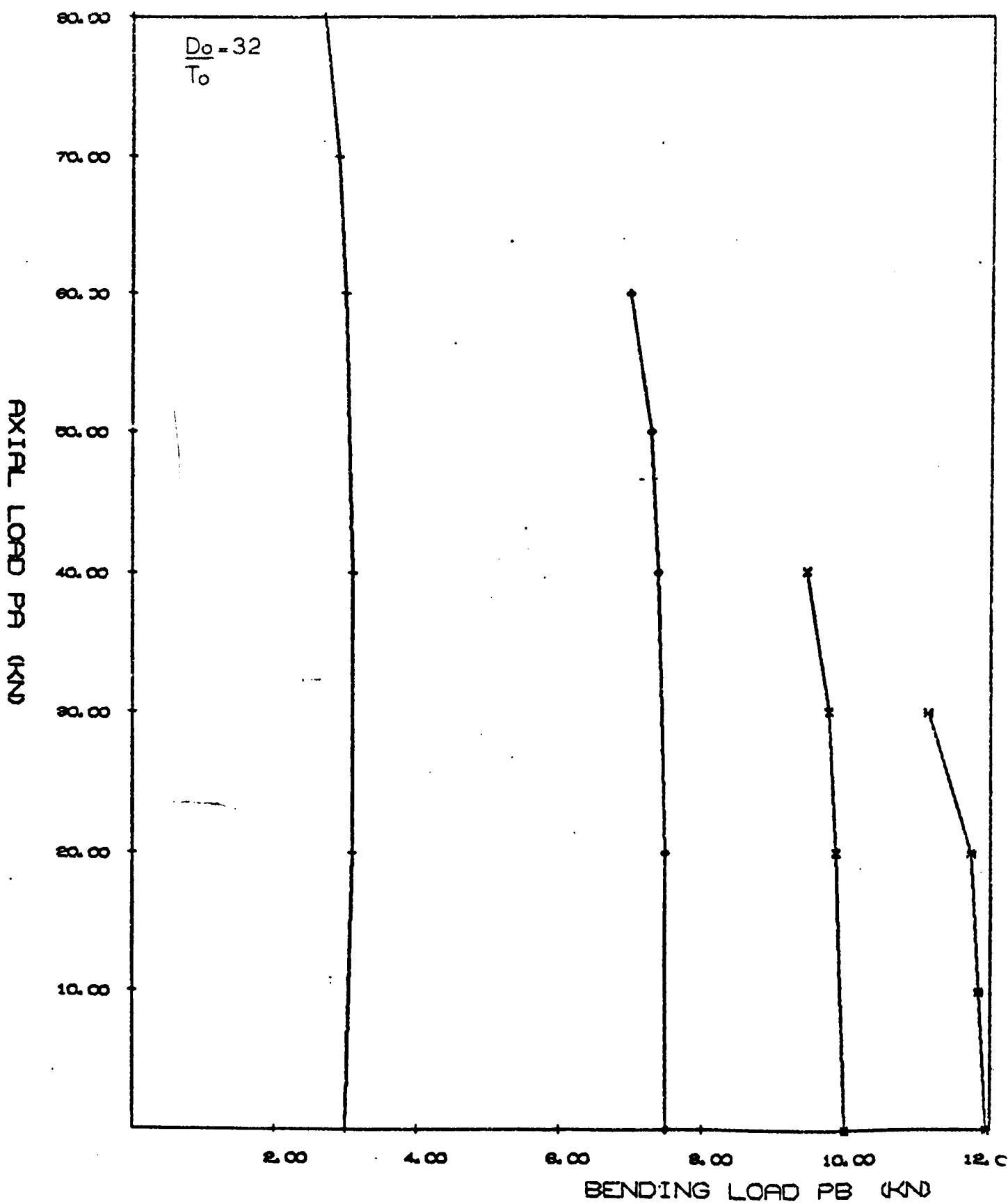


FIGURE 143 BENDING LOAD V. AXIAL LOAD FOR BETA = 0.77

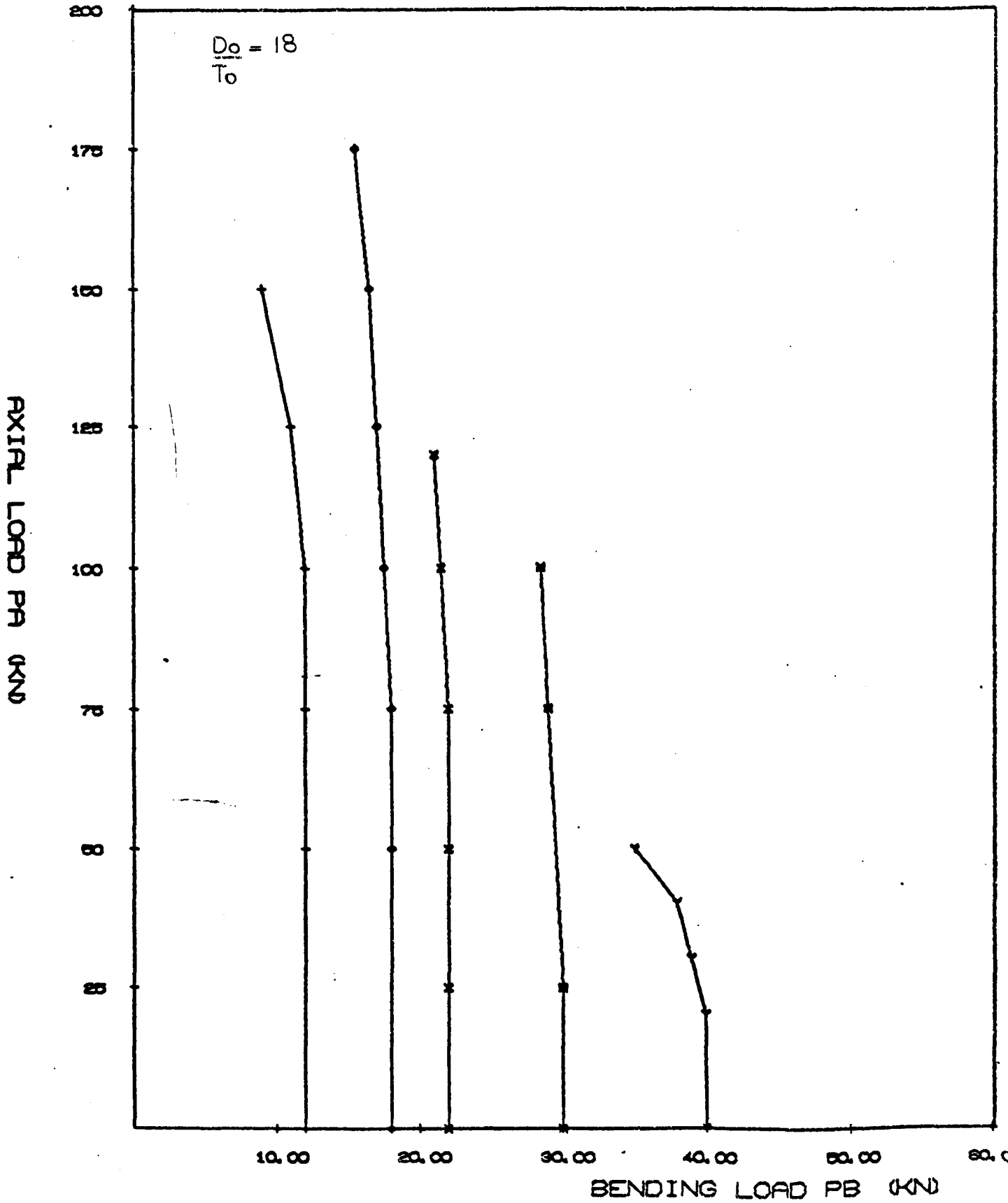


FIGURE 144 BENDING LOAD V. AXIAL LOAD FOR BETA = 0.77

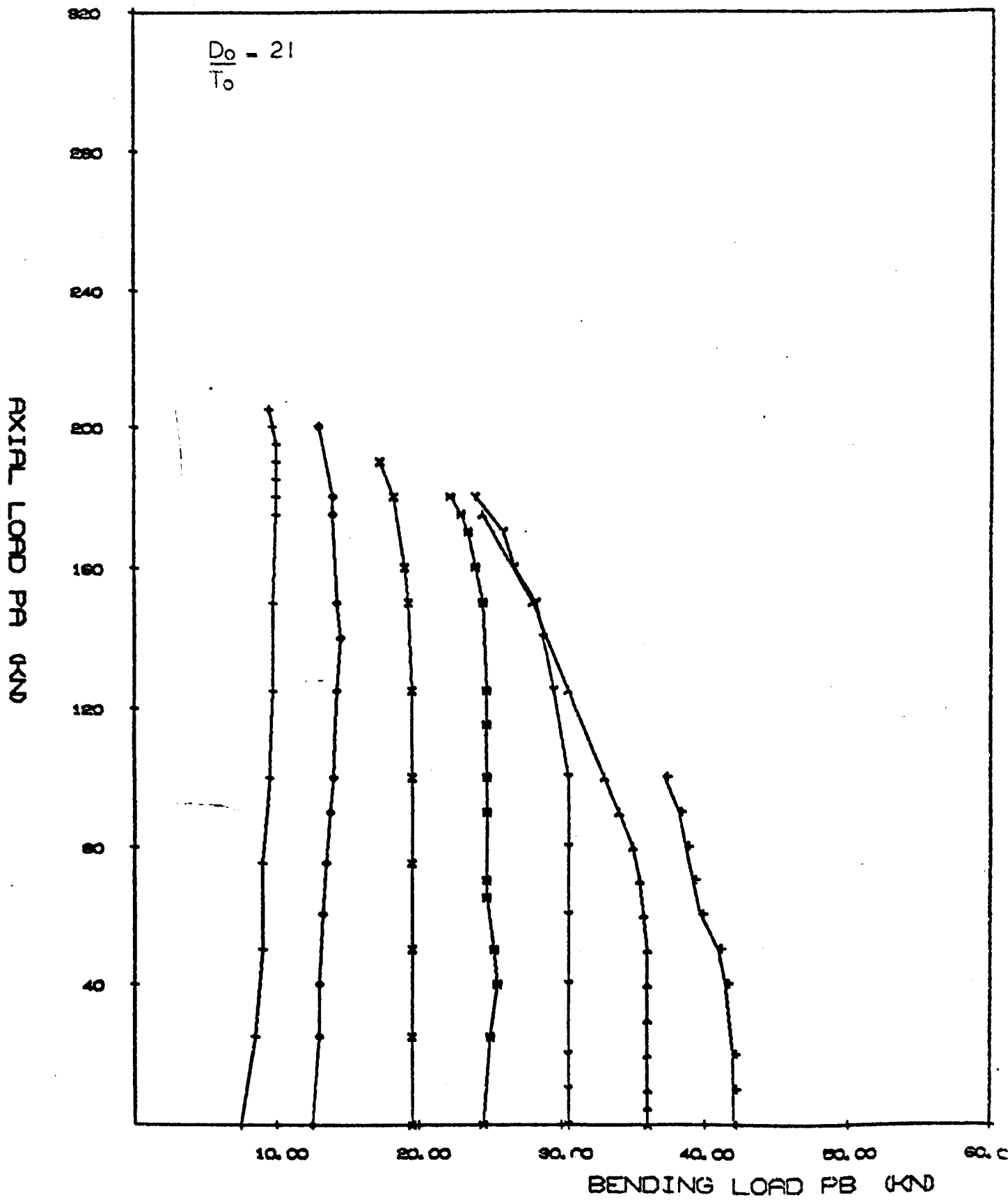


FIGURE 145 BENDING LOAD V. AXIAL LOAD FOR BETA = 0.77

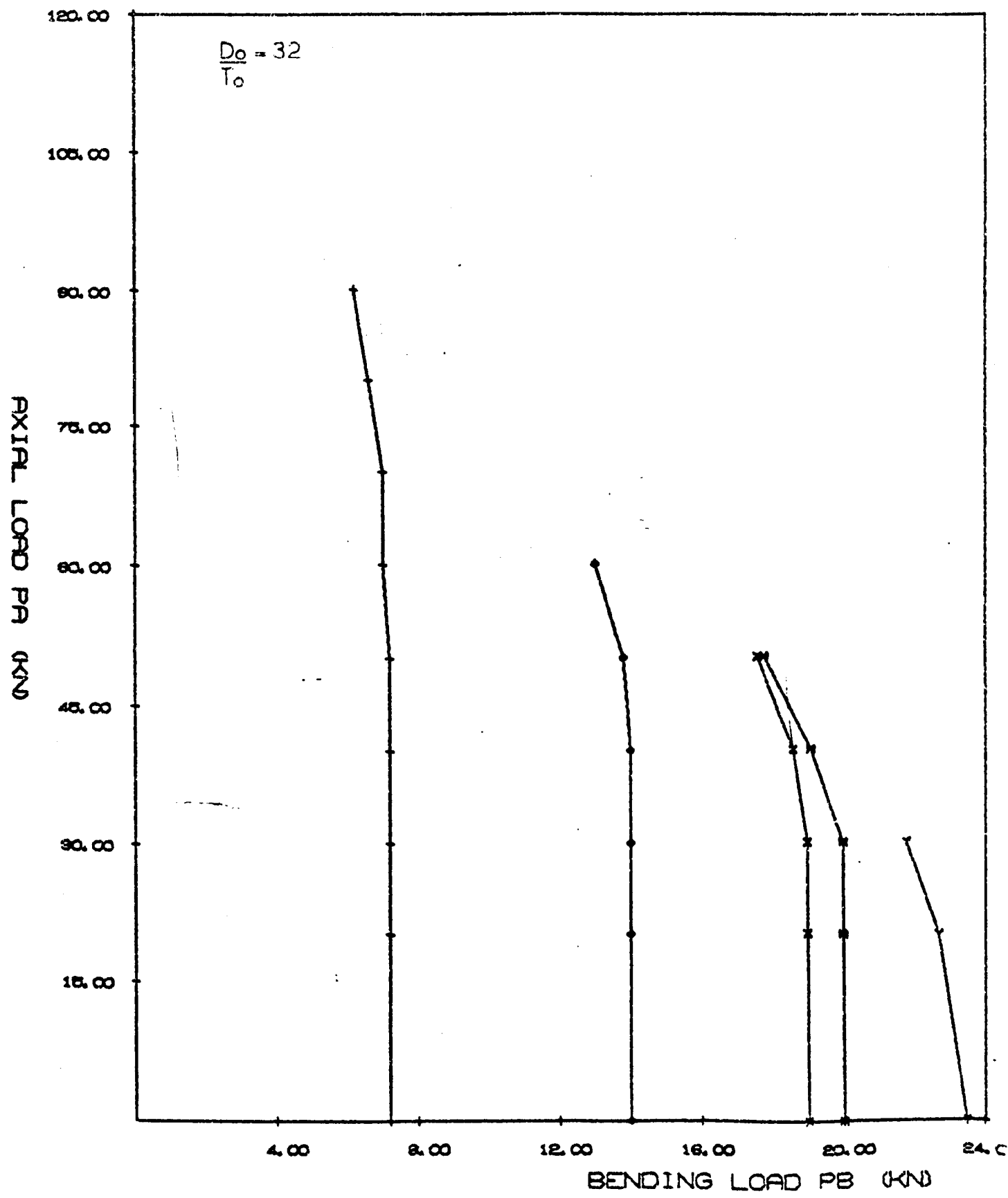


FIGURE 146 BENDING LOAD V. AXIAL LOAD FOR BETA = 1.0

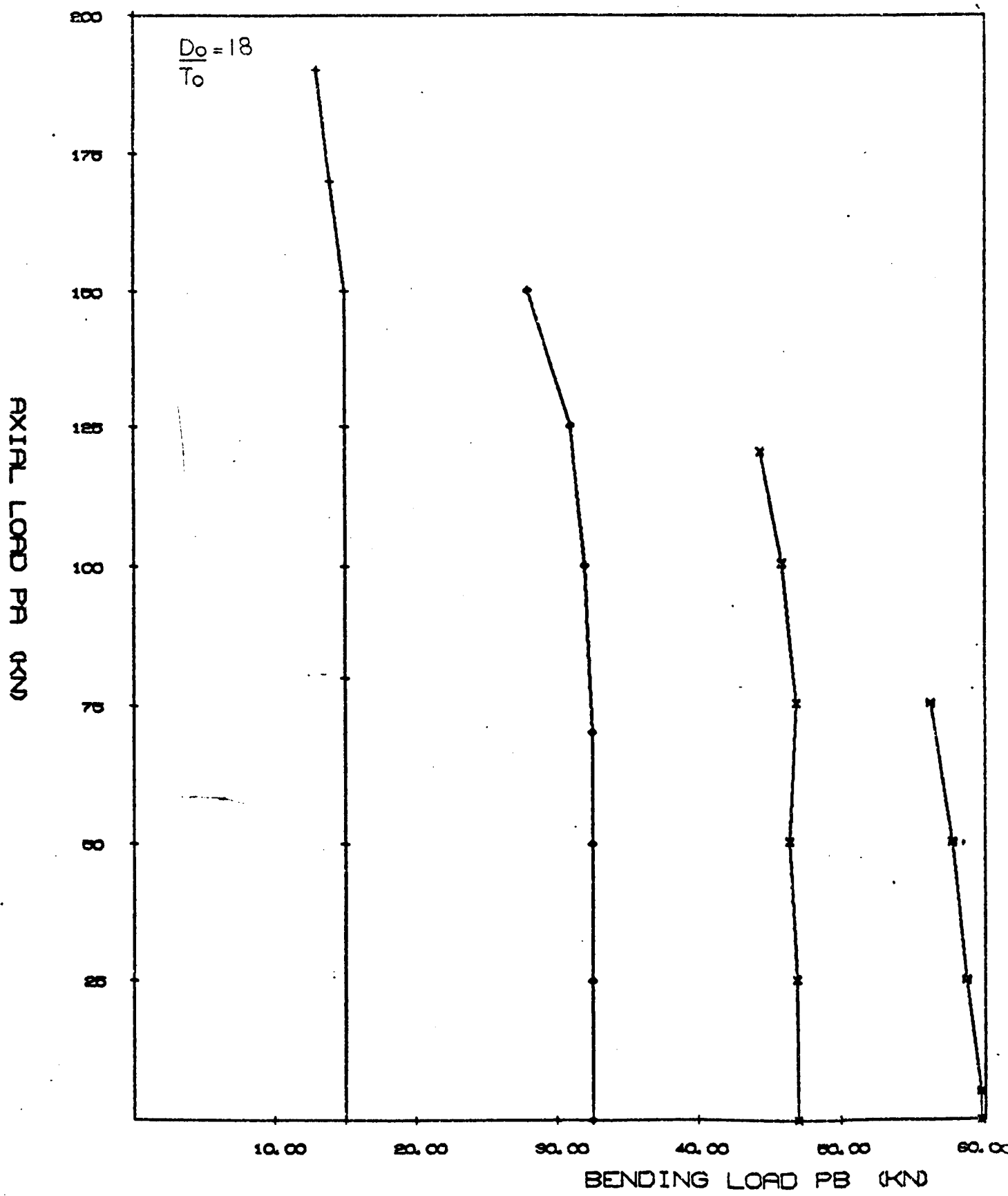


FIGURE 147 BENDING LOAD V. AXIAL LOAD FOR BETA = 1.0

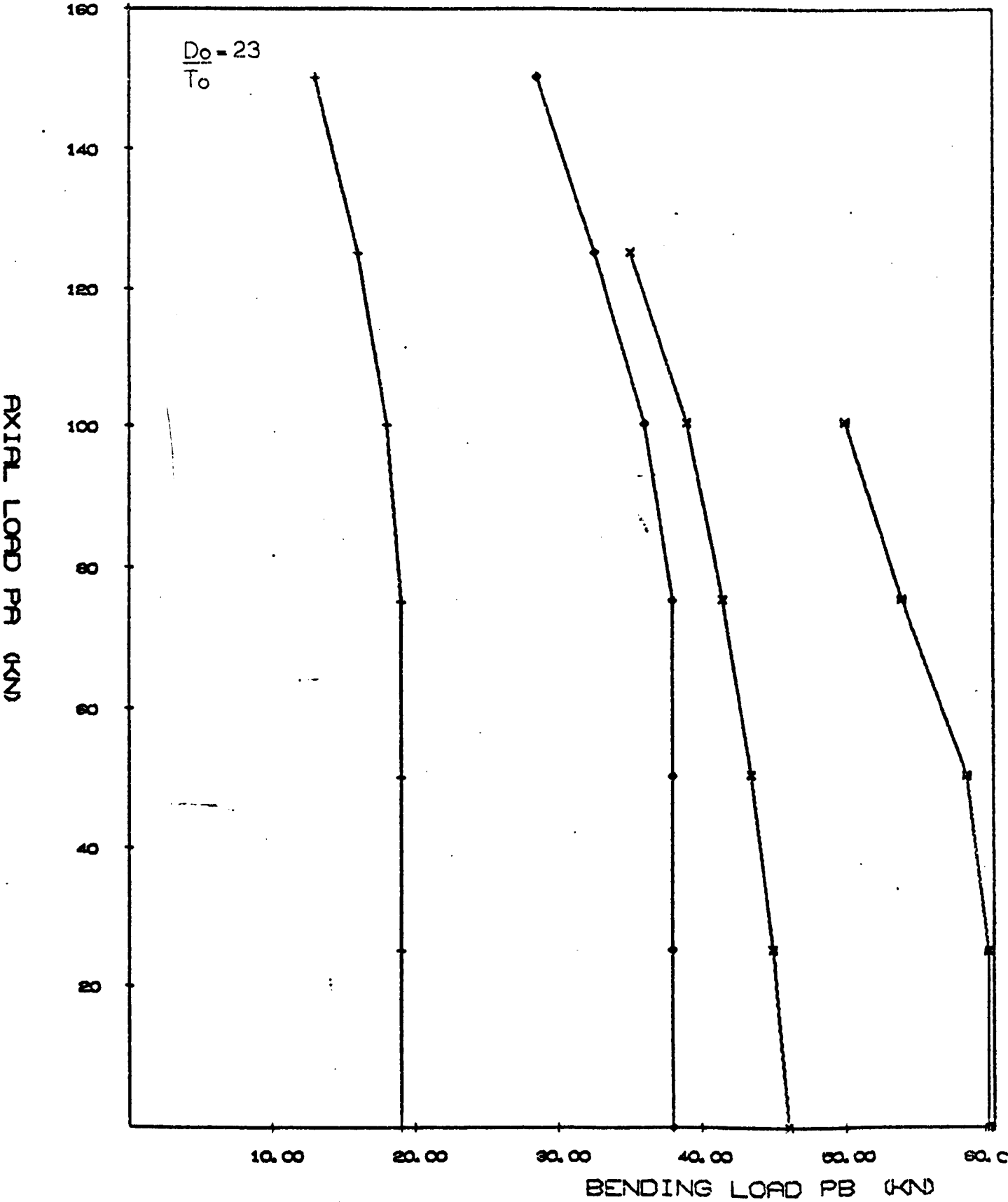


FIGURE 148 BENDING LOAD V. AXIAL LOAD FOR BETA = 1.0

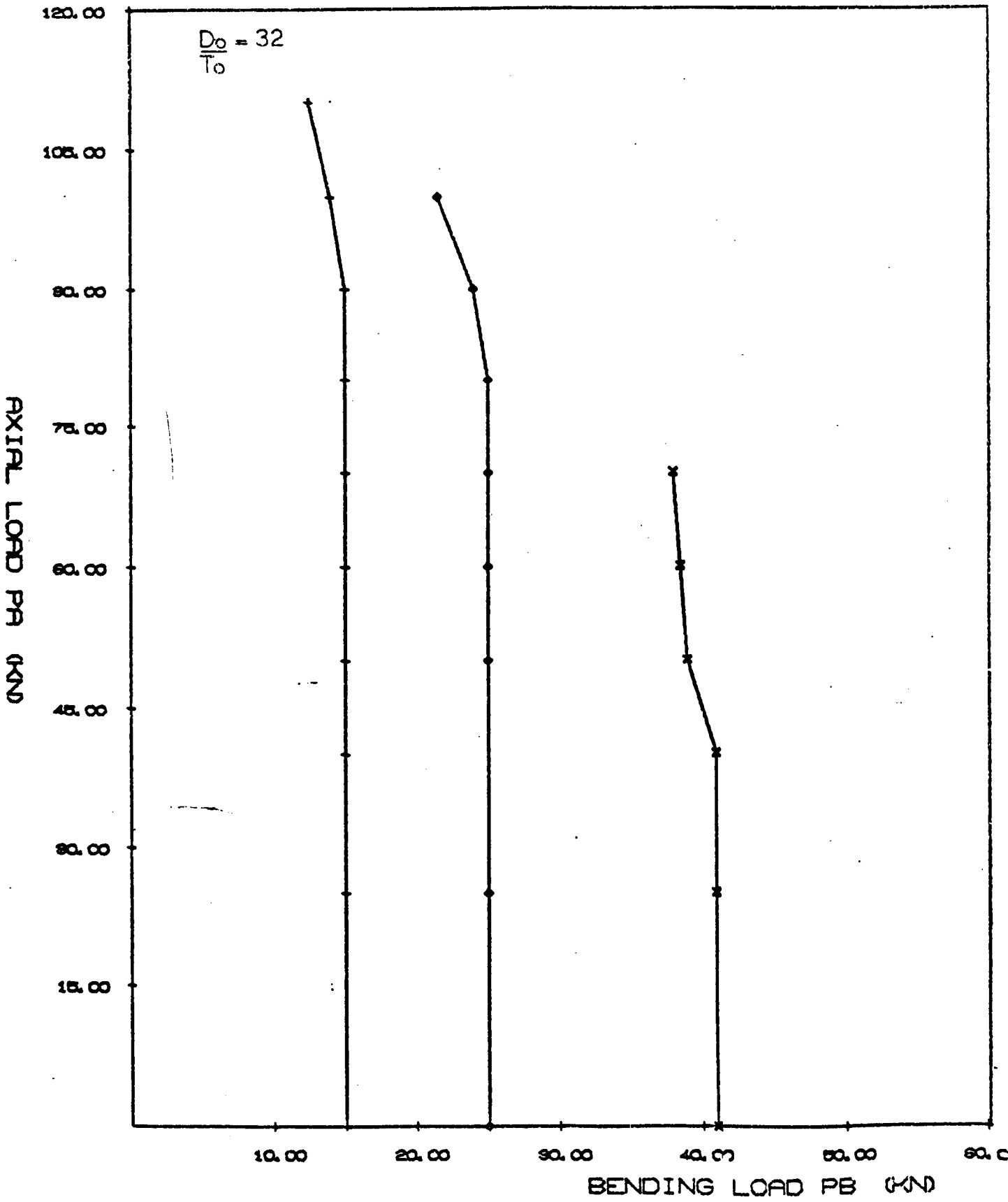


FIGURE 149

INTERACTION GRAPHS FOR BETA = 0.42

APPLIED AXIAL LOAD / ULTIMATE AXIAL LOAD, P/P_U

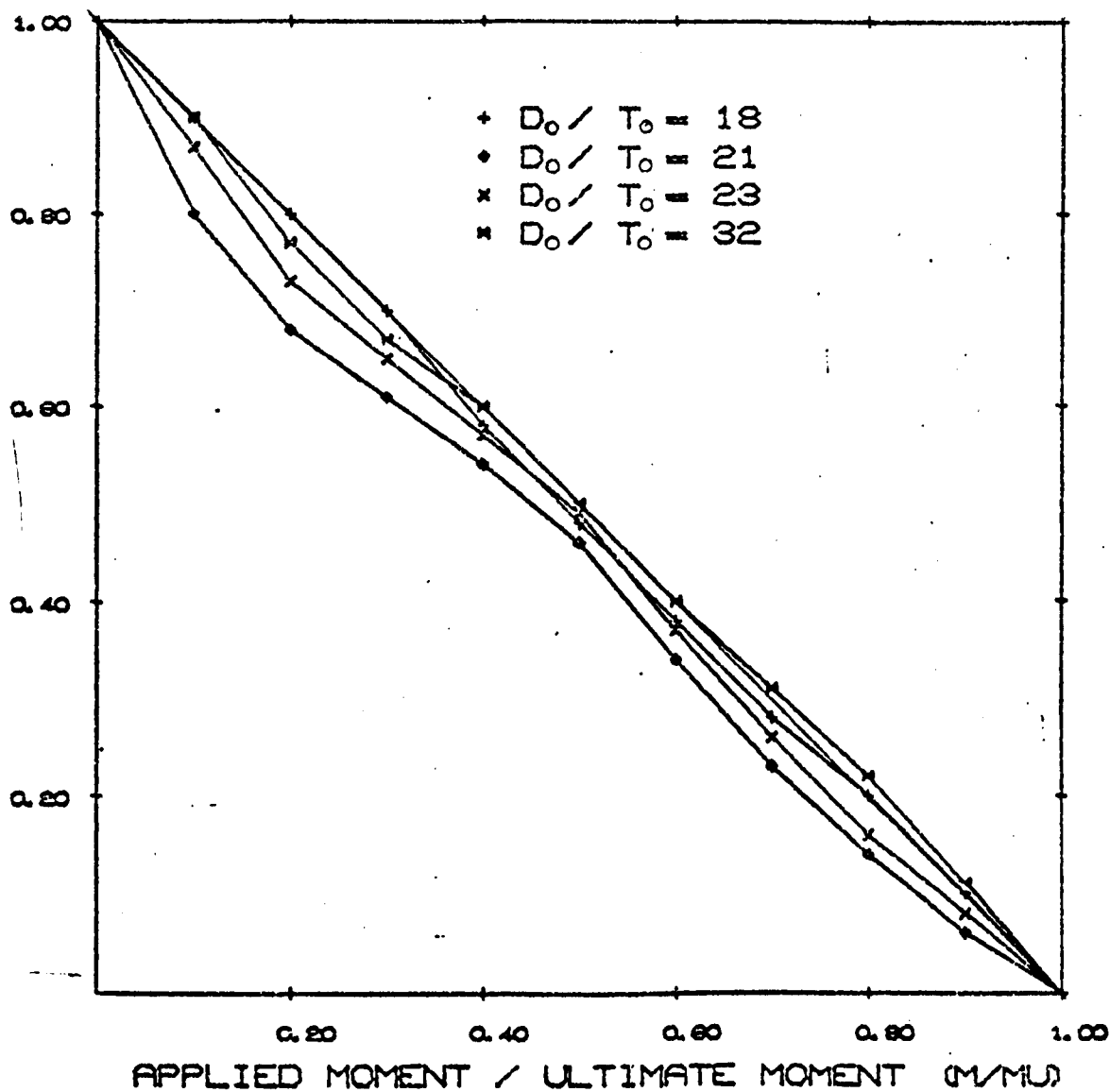


FIGURE 150 INTERACTION GRAPHS FOR BETA = 0.53

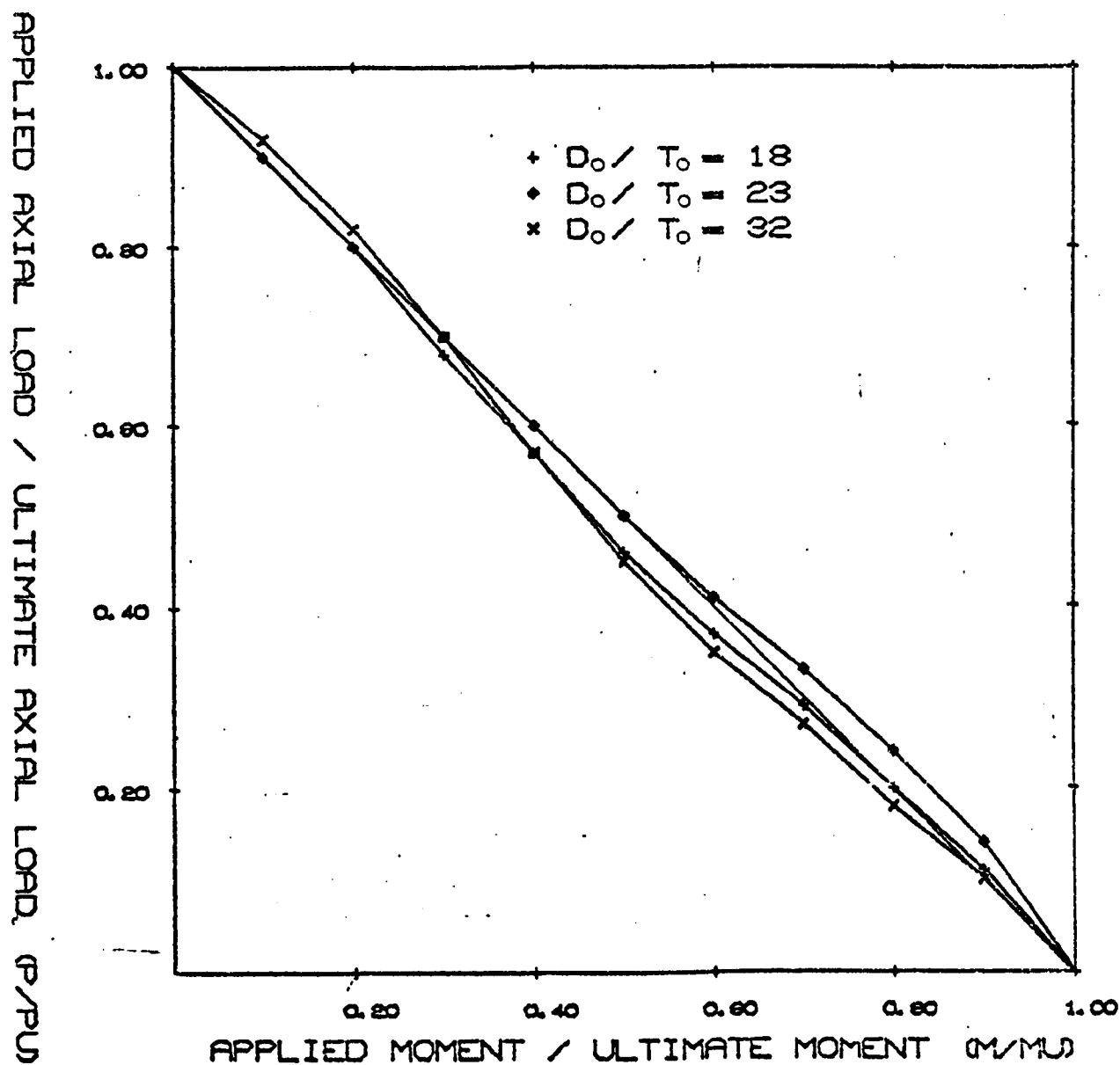


FIGURE 151 INTERACTION GRAPHS FOR BETA = 0.67

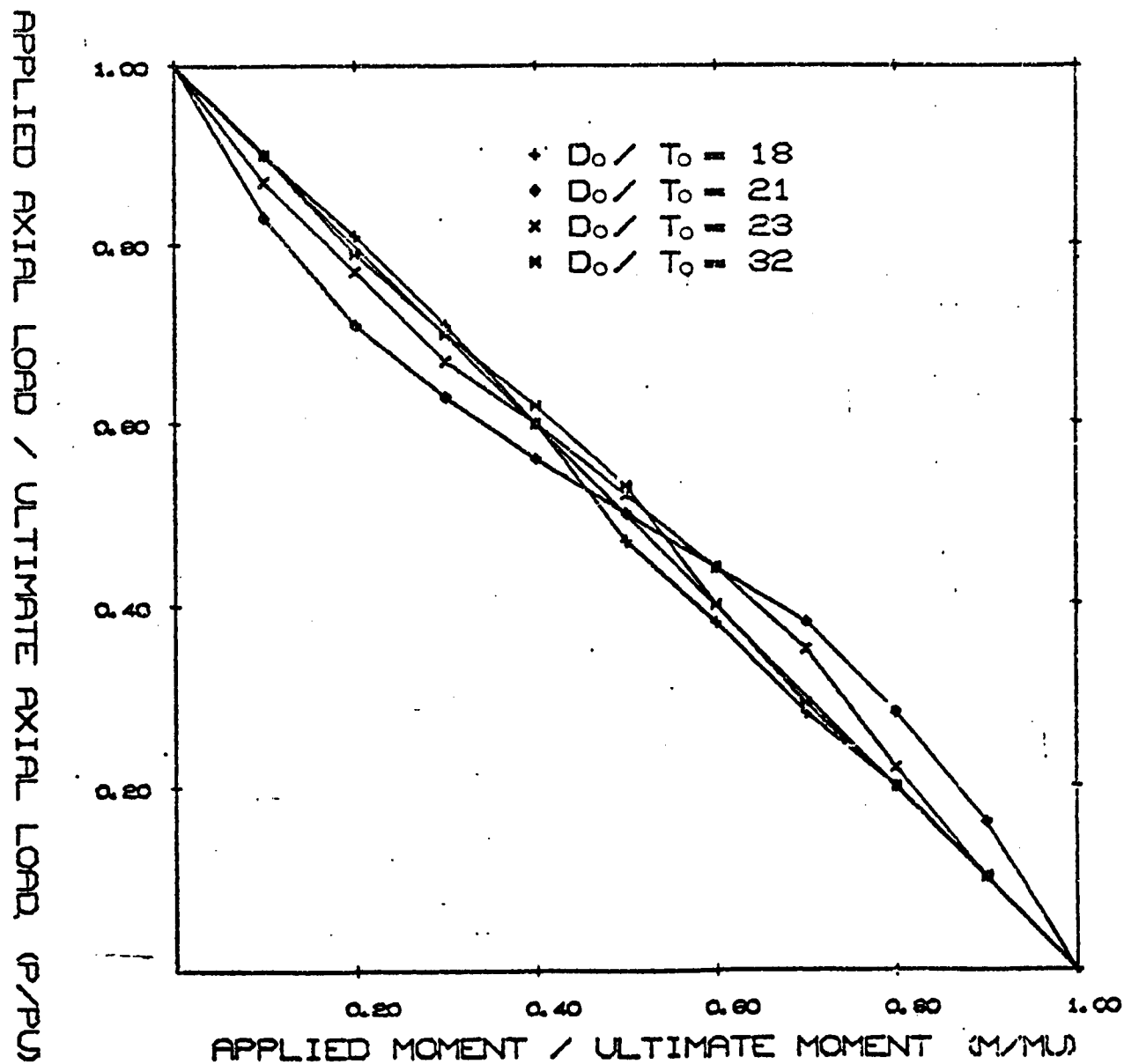


FIGURE 152 INTERACTION GRAPHS FOR BETA = 0.77

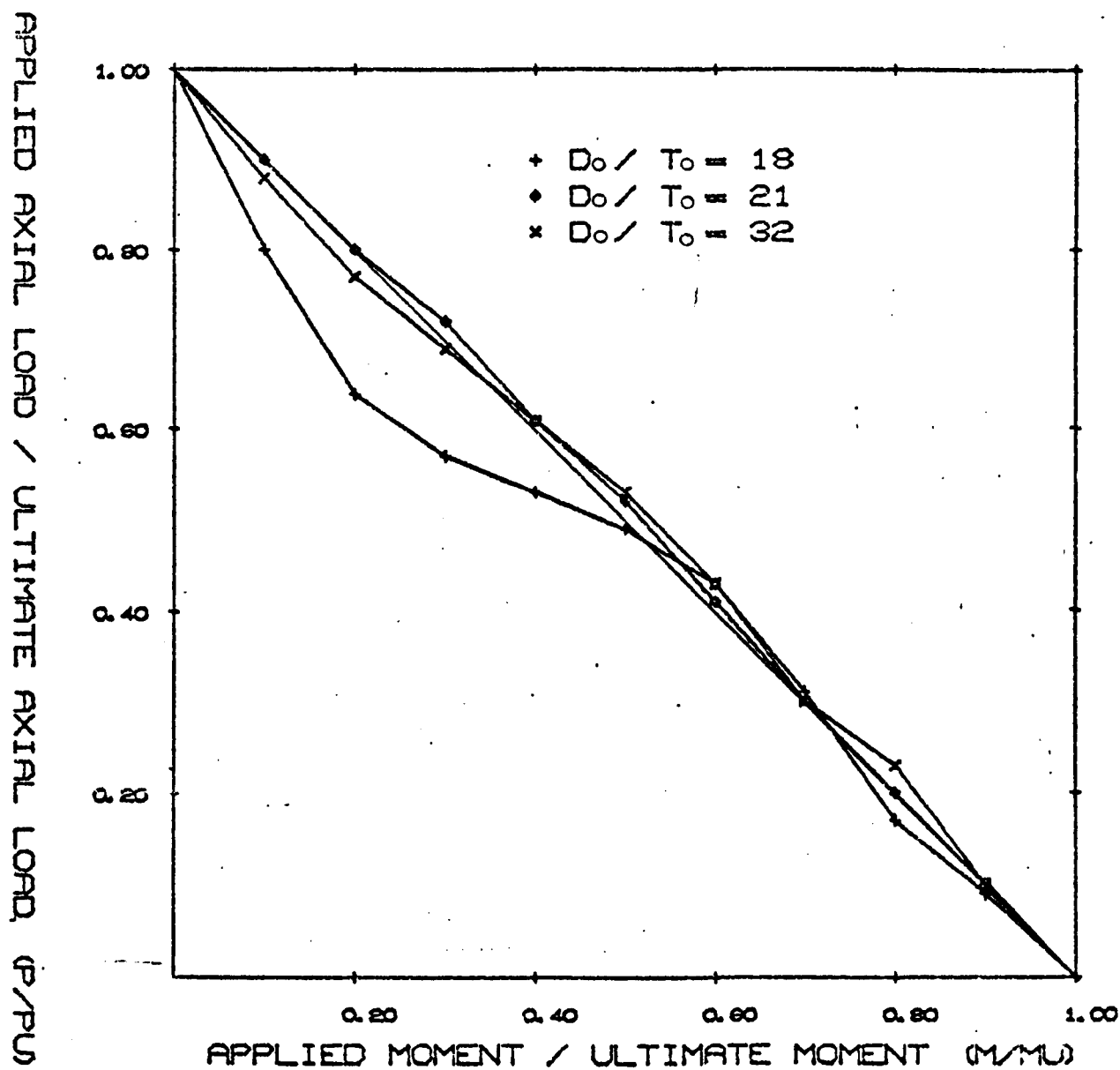
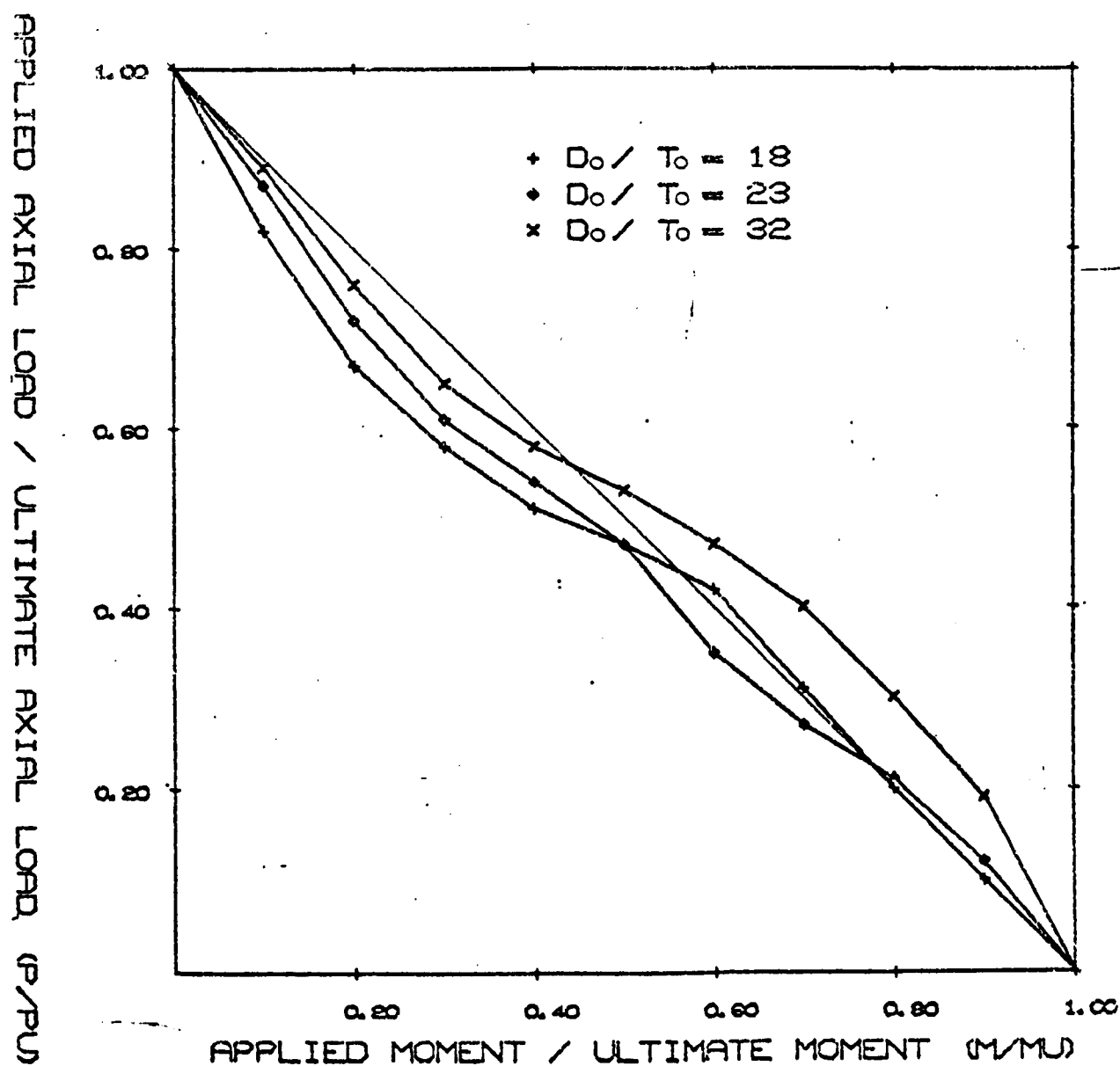
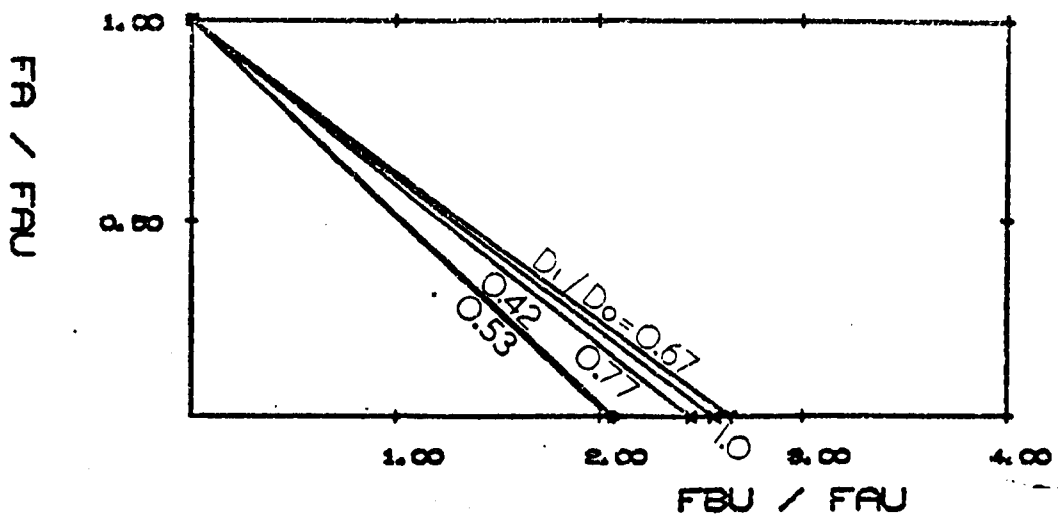


FIGURE 153 INTERACTION GRAPHS FOR BETA = 1.0



$D_o/T_o = 18$ CHORD = 114.3[±]6.3



$D_o/T_o = 21$ CHORD = 114.3[±]5.4

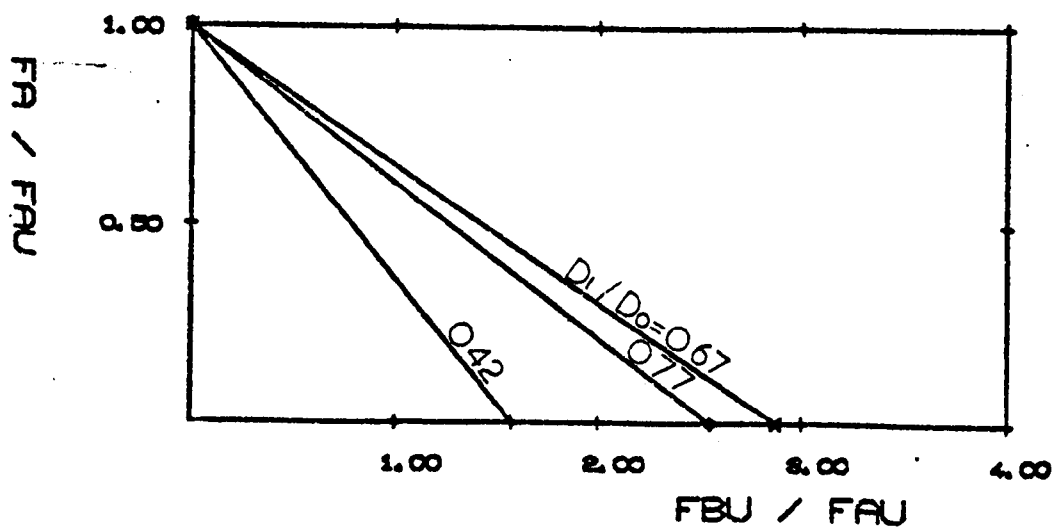
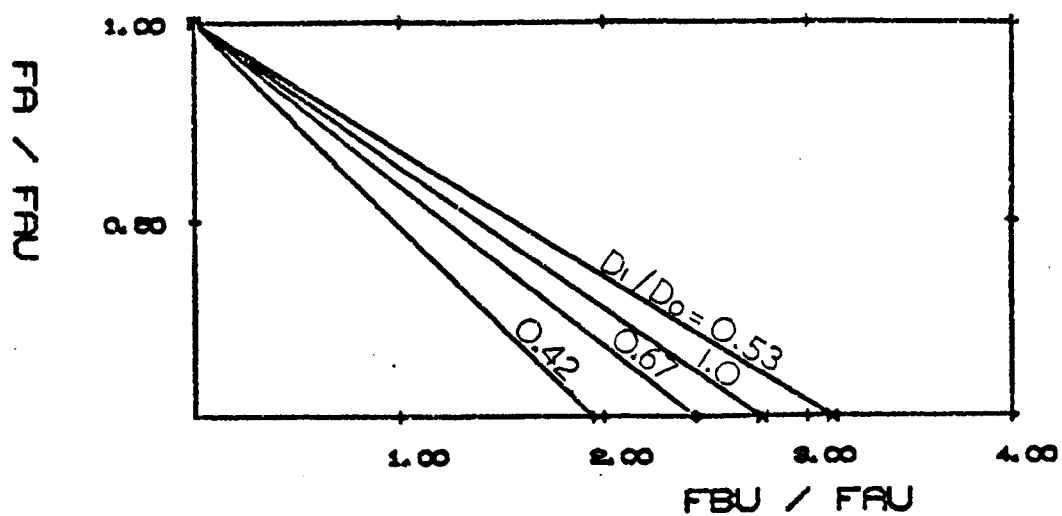


Figure 154. Graphs of f_{bu}/f_{au} for $d_o/t_o = 18$ and 21.

$D_o/T_o = 23$ CHORD = 114.3×5.0



$D_o/T_o = 32$ CHORD = 114.3×3.6

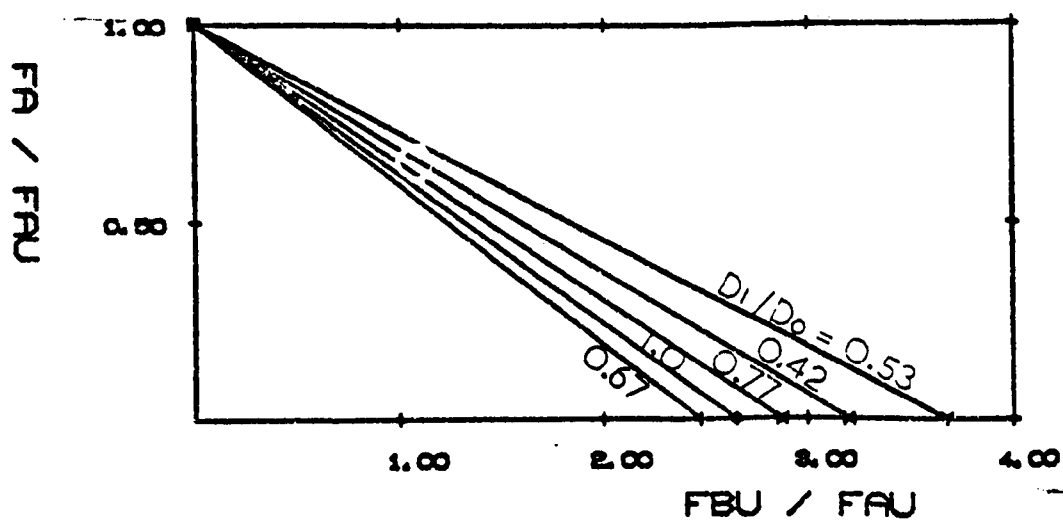
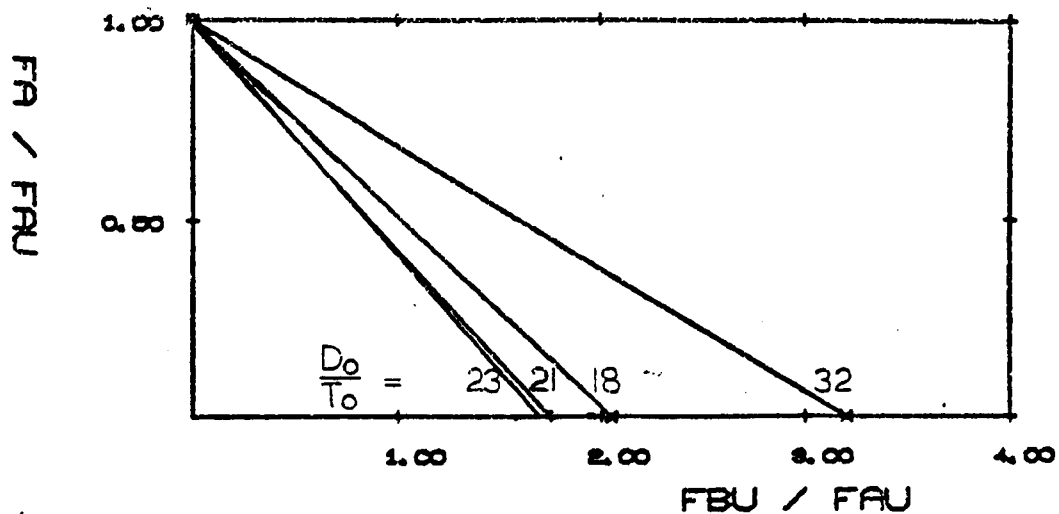


Figure 155. Graphs of f_{bu}/f_{au} for $d_o/t_o = 23$ and 32 .

BETA = 0.42 BRANCH = 48.3° ± 5.0



BETA = 0.53 BRANCH = 60.3° ± 5.0

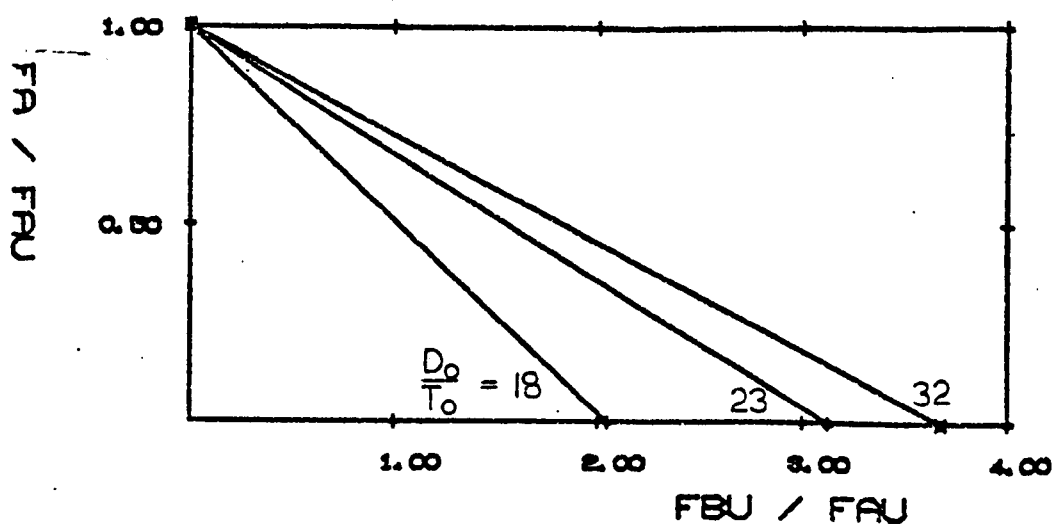
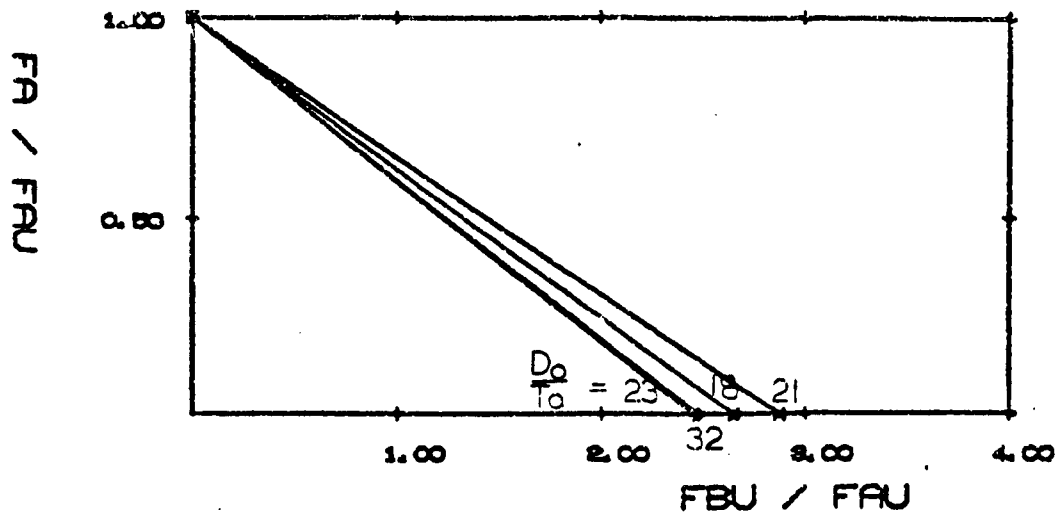


Figure 156. Graphs of f_{bu}/f_{au} for $d_1/d_o = 0.42$ and 0.53 .

BETA = 0.67 BRANCH = 76.1° ± 5.0



BETA = 0.77 BRANCH = 88.9° ± 5.0

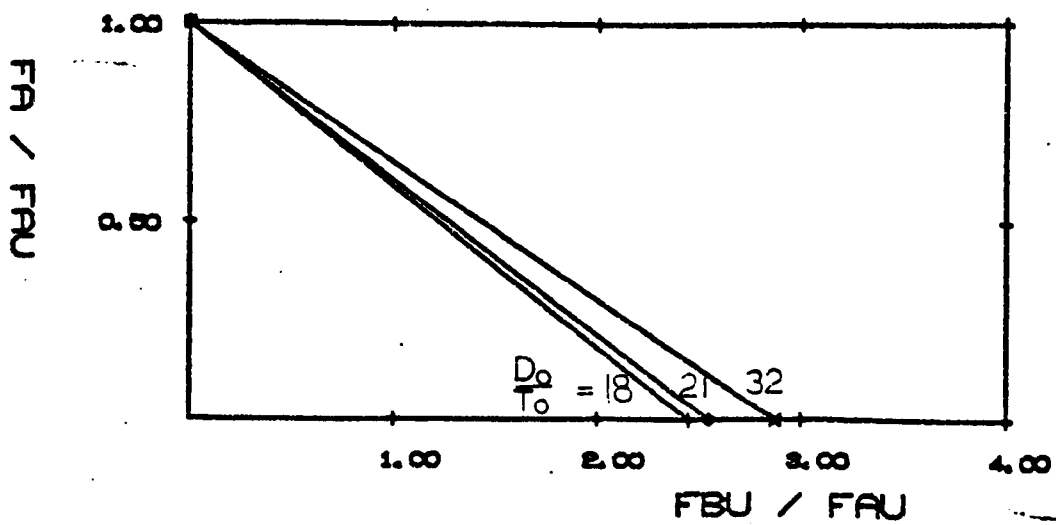


Figure 157. Graphs of f_{bu}/f_{au} for $d_1/d_0 = 0.67$ and 0.77 .

BETA = 1.0 BRANCH = 114.3° 5.0

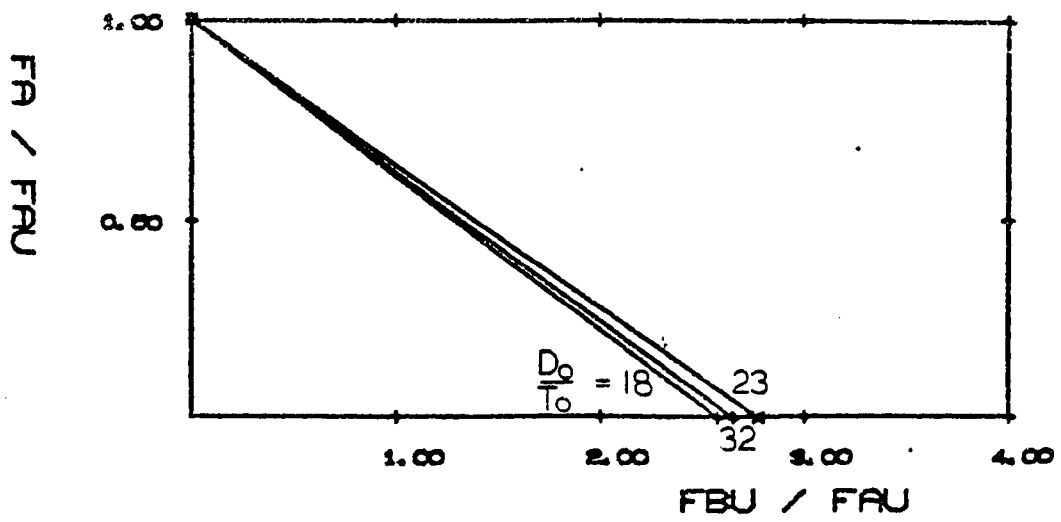


Figure 158. Graph of f_{bu}/f_{au} for $d_1/d_o = 1.0$.

FB / FBU FOR VARIED BETA . V. D_o/T_o

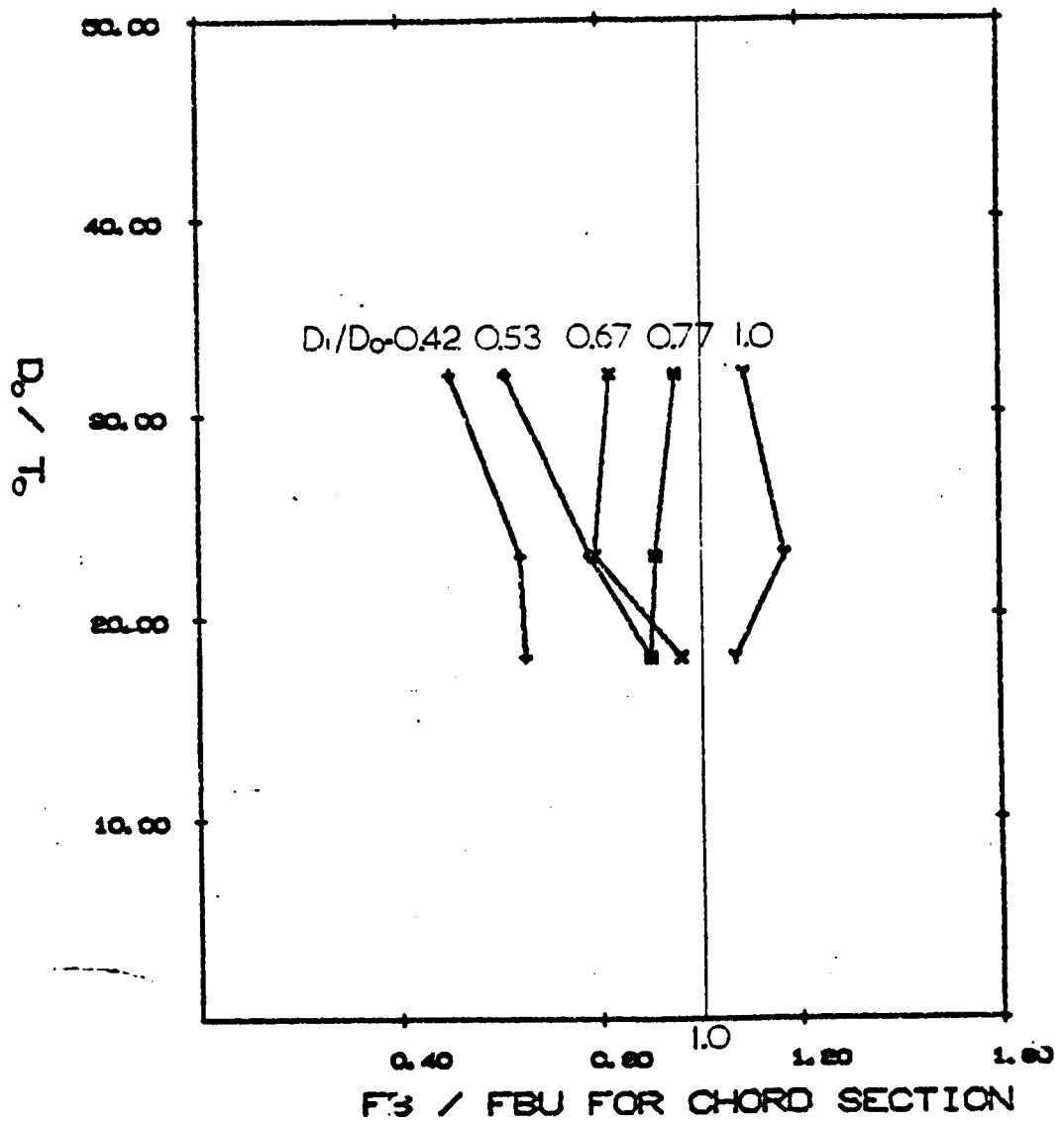


Figure 159. F_{bu}/f_{au} v d_o/t_o .

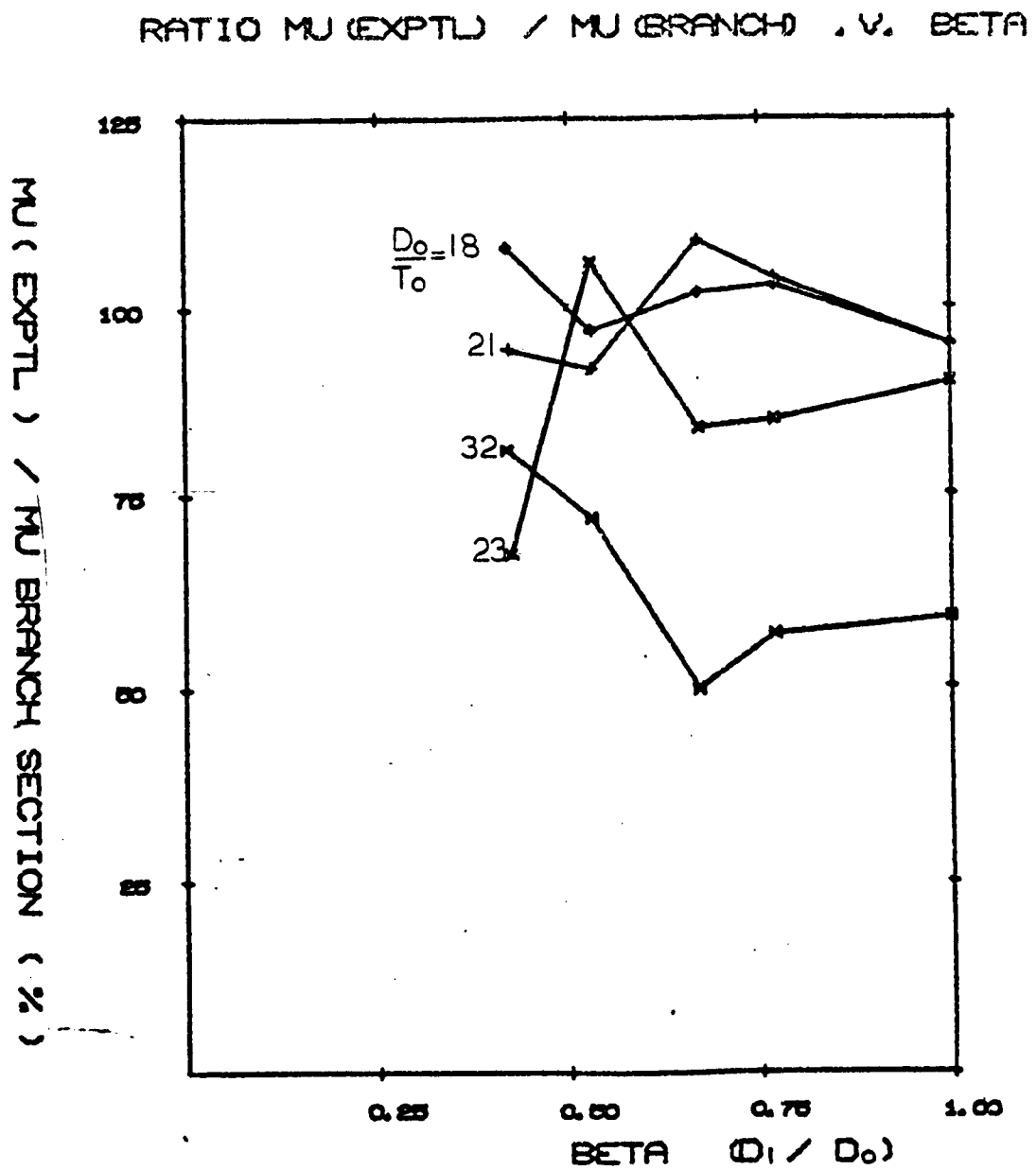


Figure 160. $\mu(\text{exptl})/\mu(\text{branch})$ v d_1/d_0 .

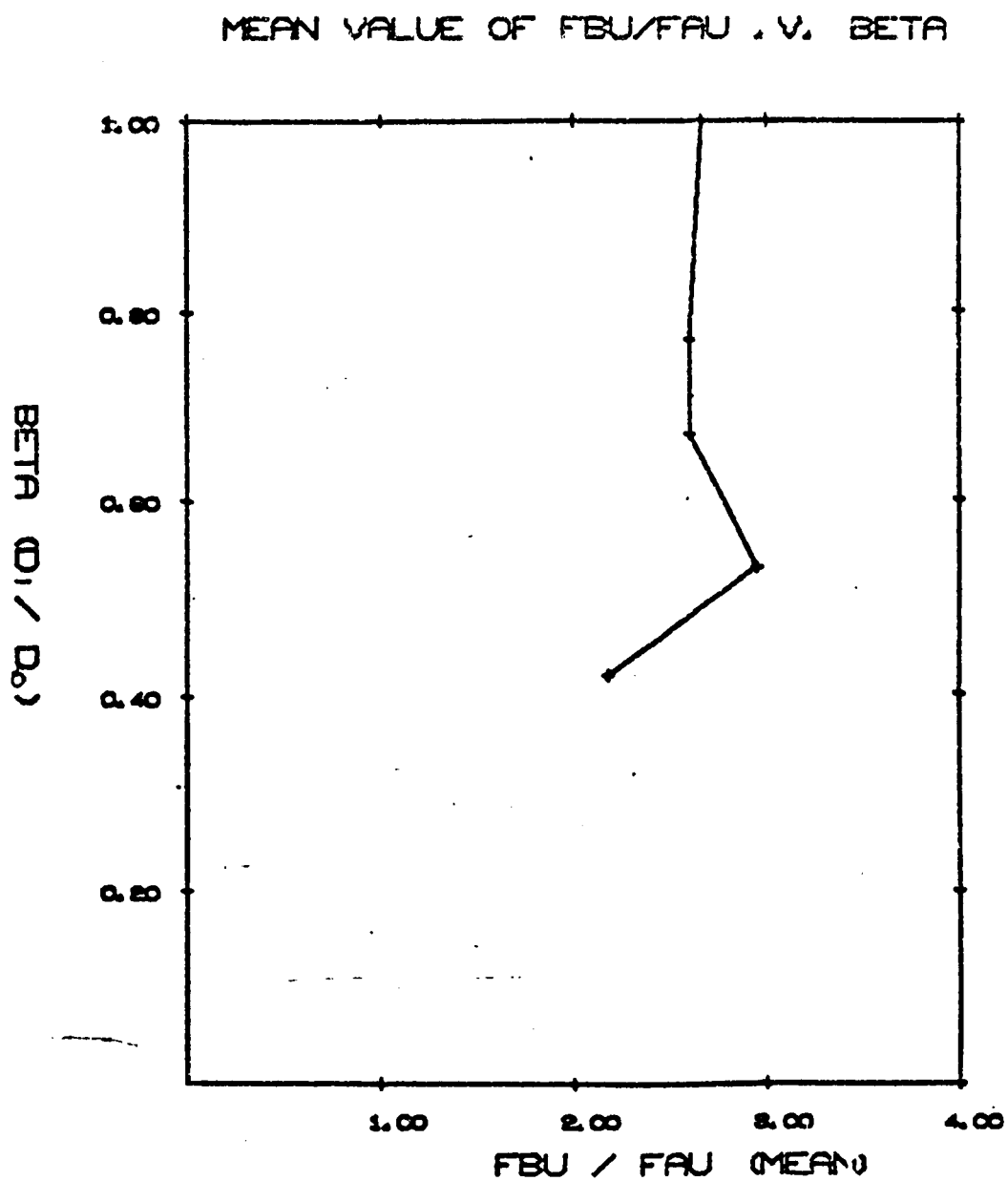


Figure 161. Mean value of f_{bu}/f_{au} v d_1/d_0 .

RATIO PU (EXPTL) / PU (BRANCH) . V. BETA

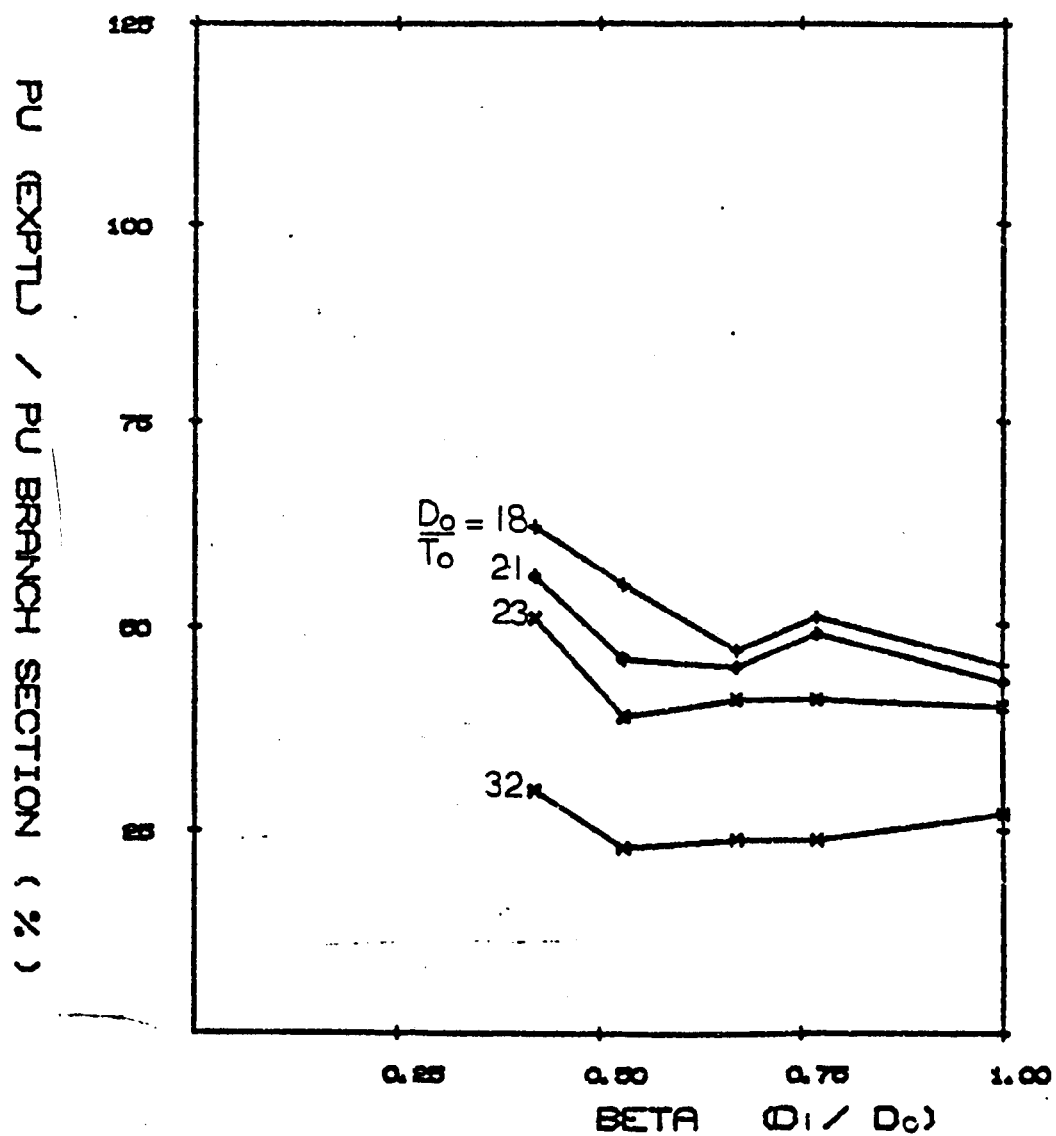


Figure 162. Pu(exptl)/Pu(branch) v d_1/d_0 .

MEAN VALUE OF FBU/FAU . V. D_0 / T_0

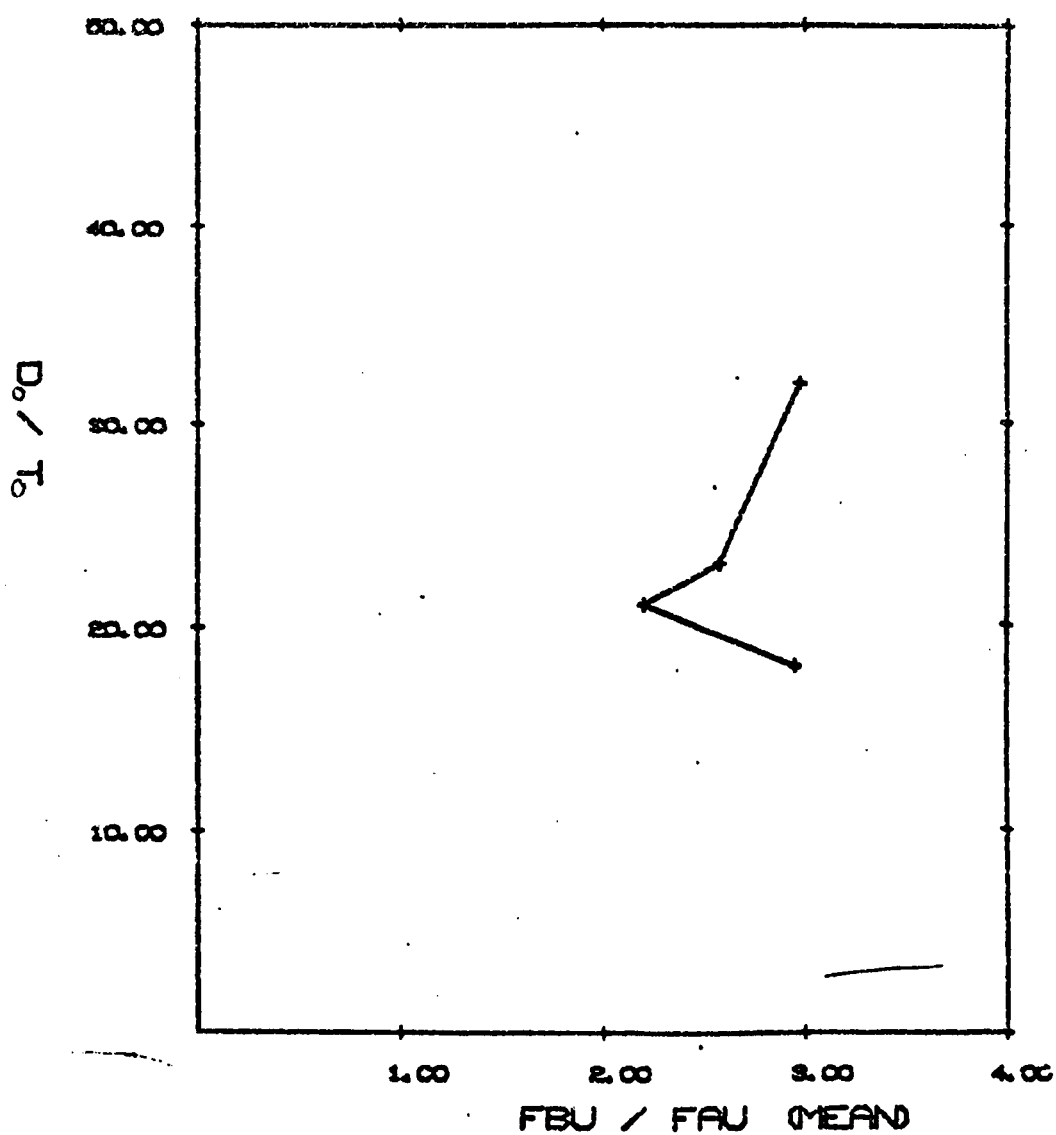


Figure 163. Mean value of fbu/fau v do/to.

FB / FBU FOR VARIED D/T . V. BETA

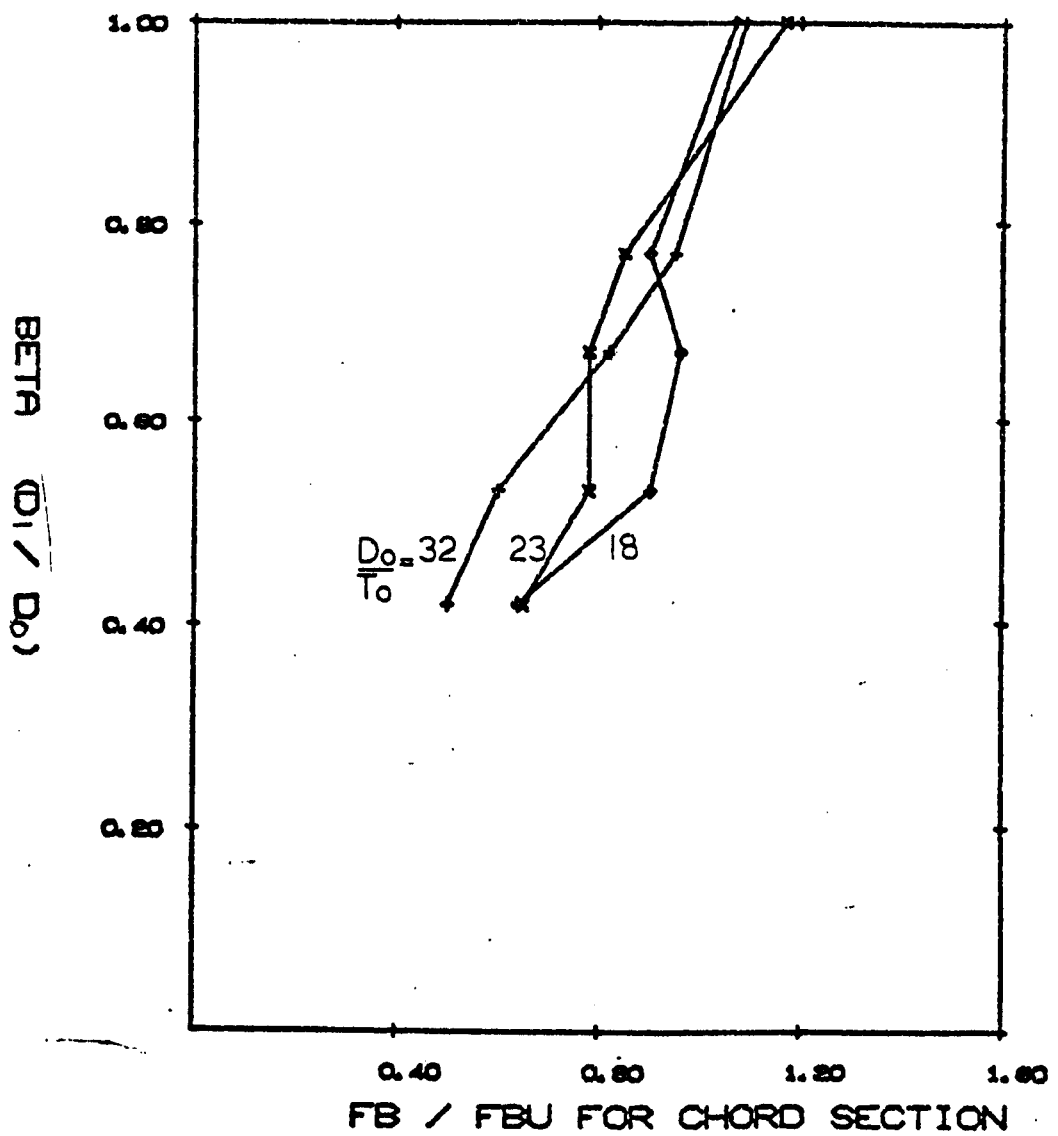


Figure 164.Fb/fbu(chord section) v d1/do.

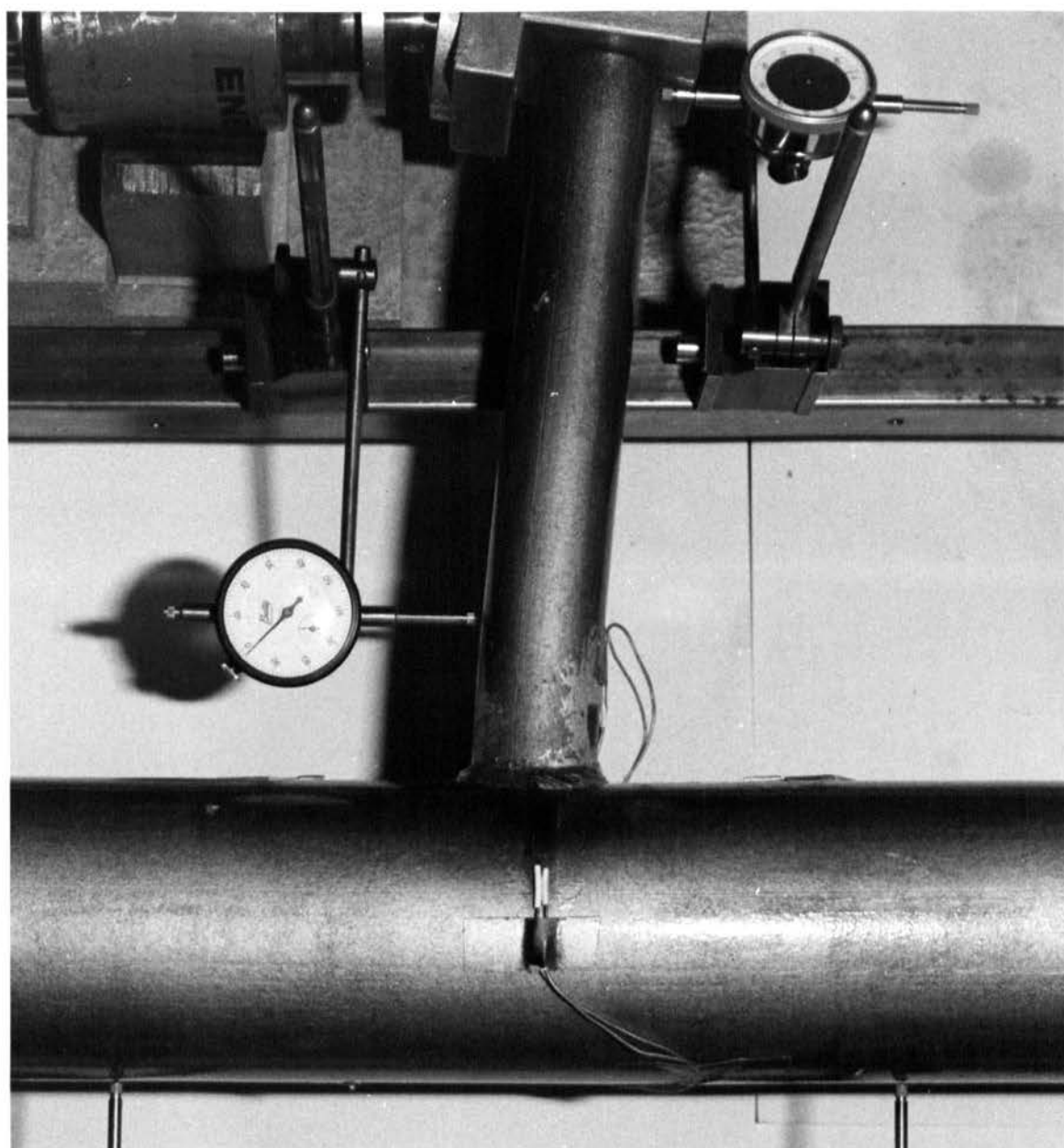


Figure 166 - T-Joint Under Bending Load ($\beta = 0.42$)

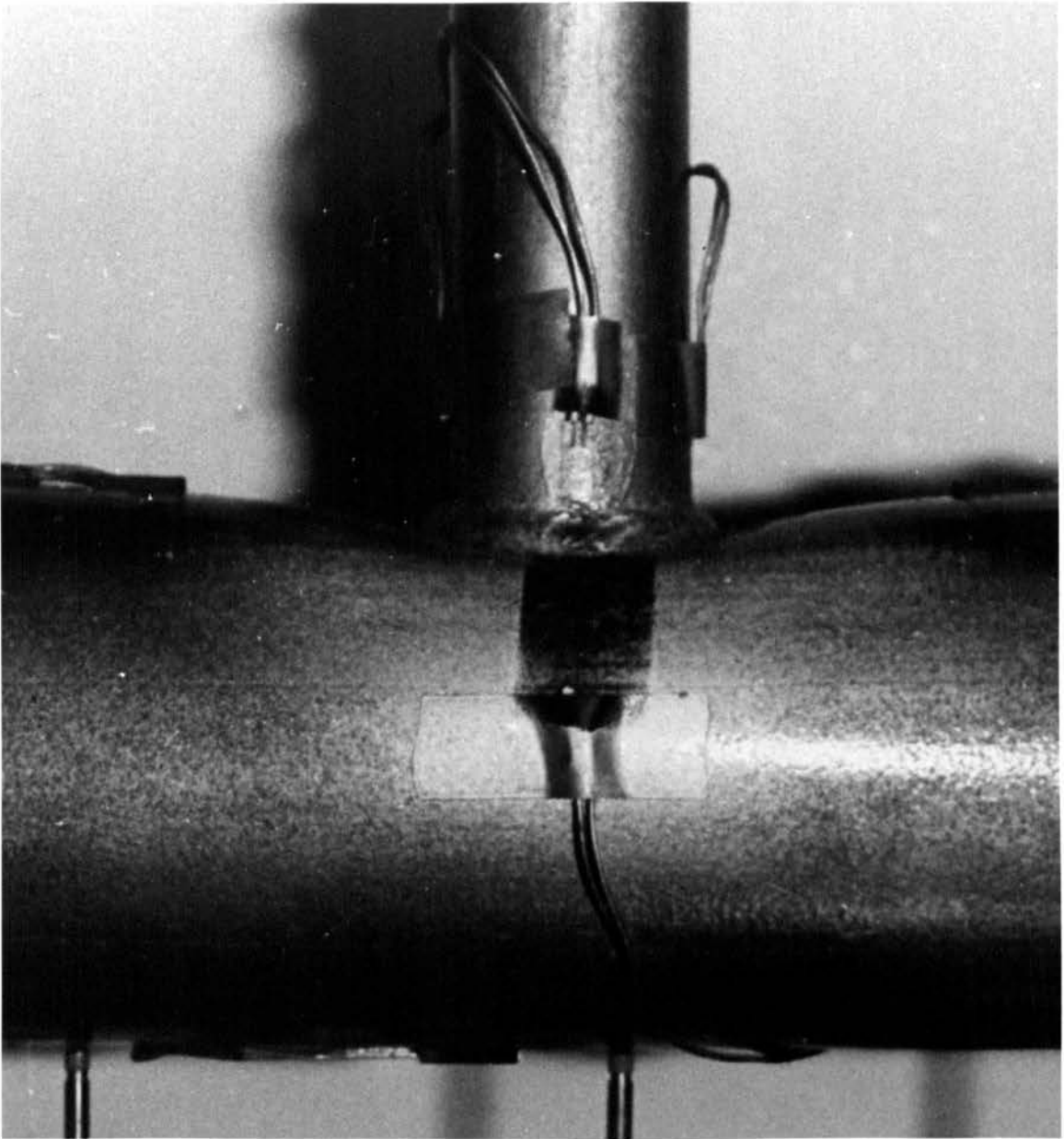


Figure 167 - T-Joint Under Axial Load ($\text{Beta} = 0.42$)



Figure 168 - Sections Through T-Joints ($\text{Beta} = 0.42$) Subject to, Left to Right, Bending Load, Axial Load, Combined Load

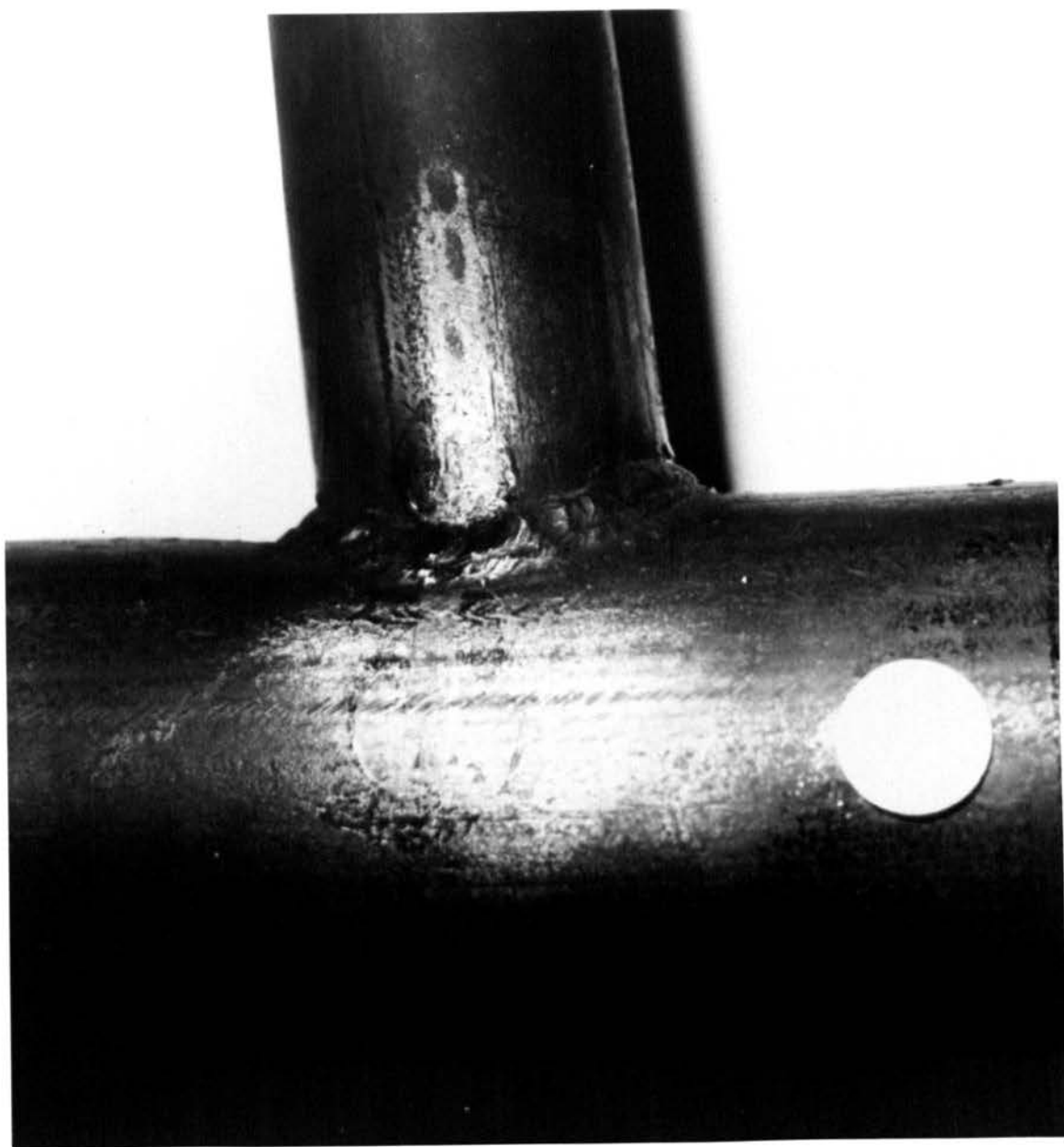


Figure 169 - T-Joint Under Combined Load ($\text{Beta} = 0.66$)

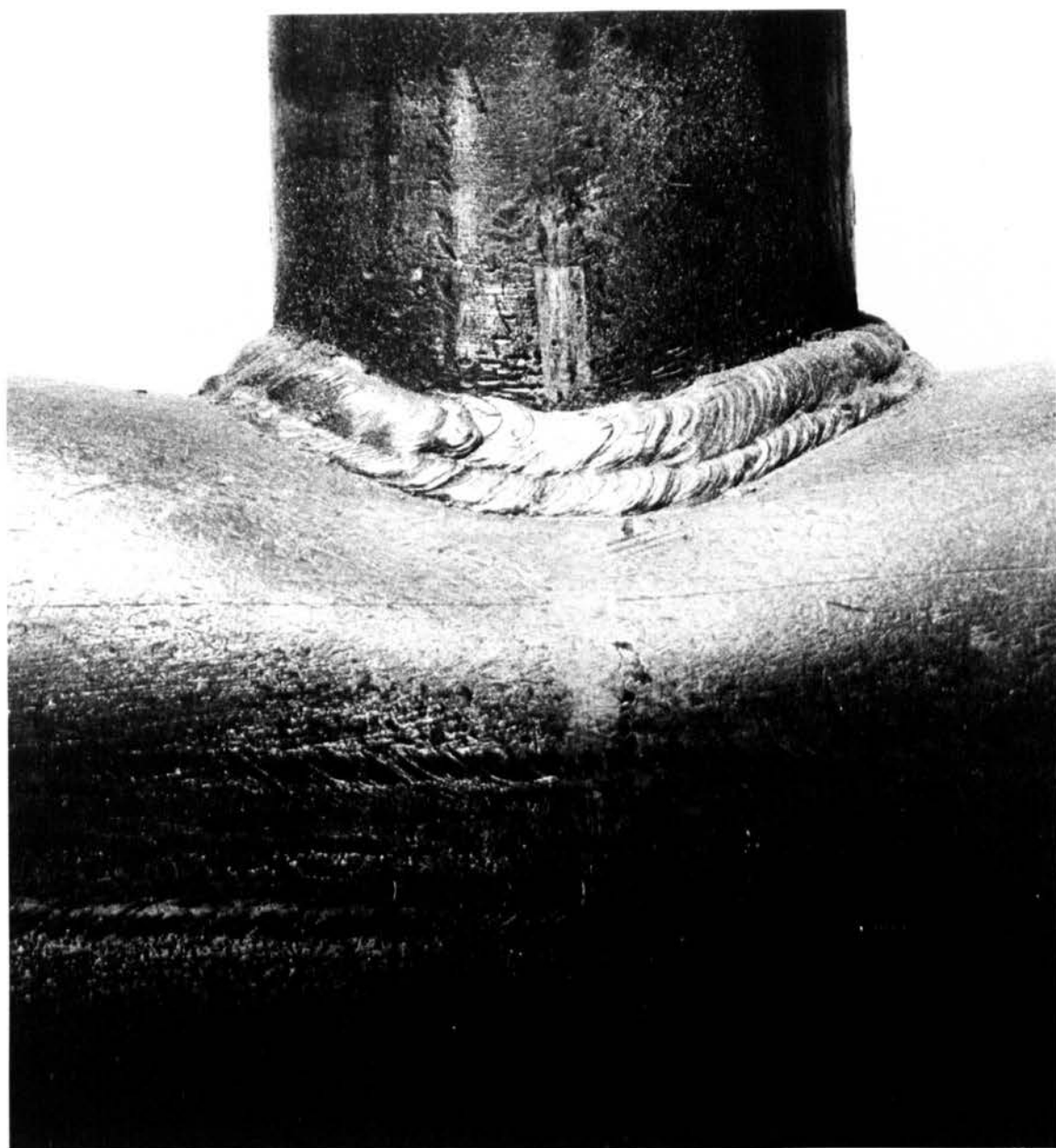


Figure 170 - T-Joint Under Axial Load ($\text{Beta} = 0.77$)

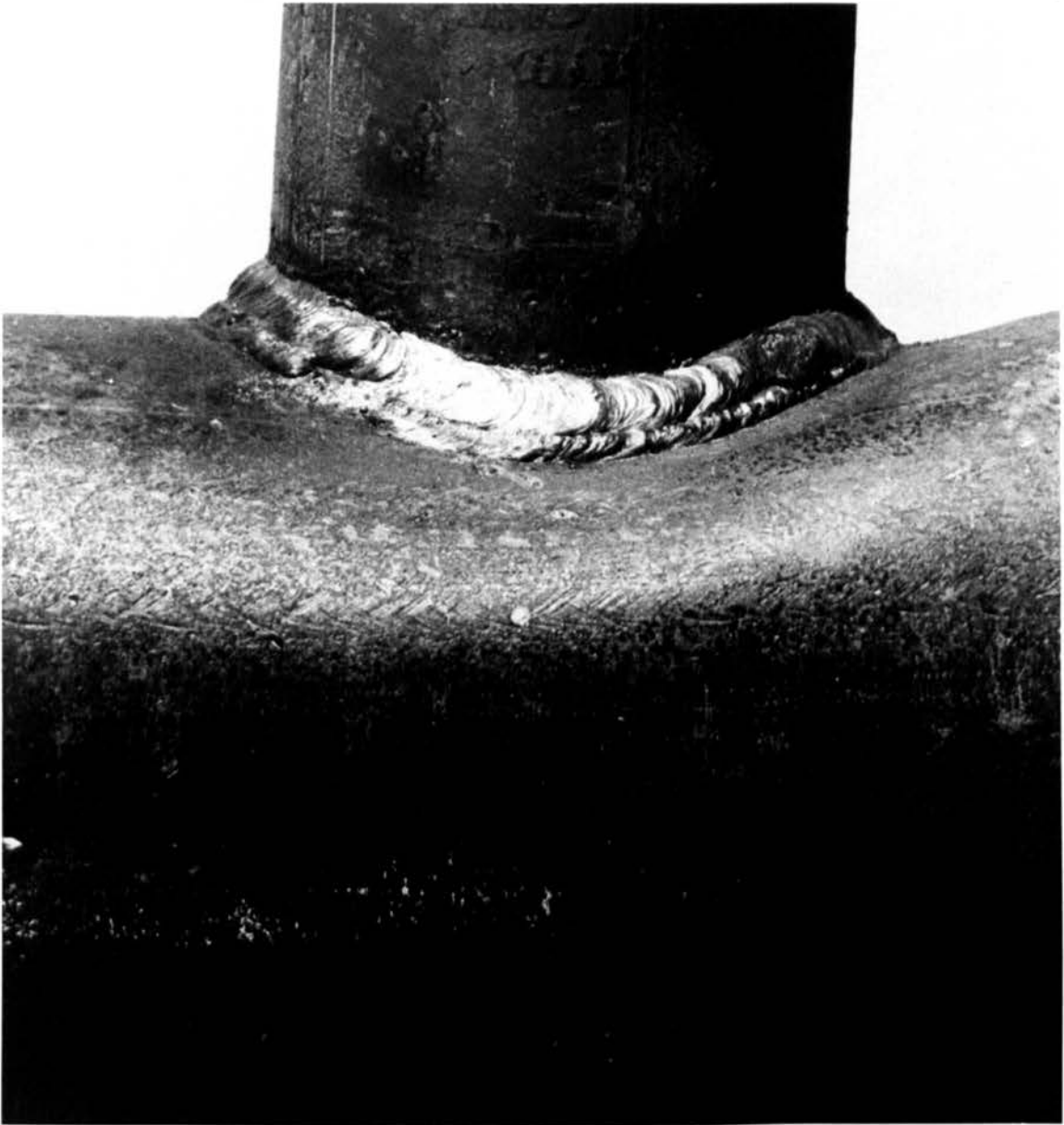


Figure 171 - T-Joint Under Bending Load ($\text{Beta} = 0.77$)



Figure 172 - T-Joints Subject to Axial Load ($\beta = 0.42 - 1.0$)
 $d_o/t_o = 32$, $d_o/t_o = 18$

CHAPTER 8

MULTIPLE REGRESSION FOR ANALYSIS OF THE ULTIMATE LOAD TESTS ON T-JOINTS

8.1. Definitions

8.1.1. Linear Regression

Linear regression is the fitting of the best least squares model to a set of data. A first order linear model may be of the form:-

$$Y = \beta_0 + \beta_1 X_1 + \beta_2 X_2 + \beta_n X_n + E \quad \dots\dots\dots(8.1)$$

where

Y is the dependant variable.

$X_1, X_2, X_3, \dots, X_n$ are the independant variables

$\beta_0, \beta_1, \beta_2, \dots, \beta_n$ are the parameters of the model.

E is the residual error in the calculated value of Y.

Here linear means linearity in the model parameters β_0, β_1 etc.

The use of the term multiple implies that it is anticipated that the dependant variable Y is a function of more than one independant variable, X.

8.1.2. Correlation

If X and Y were both random variables following some unknown bivariate distribution, then the correlation coefficient (ρ) between X and Y may be defined as:-

$$\rho_{XY} = \frac{\text{covariance}(X,Y)}{(\sqrt{V(X)} \cdot \sqrt{V(Y)})} \quad \dots\dots\dots(8.2.)$$

where if $f(X,Y)$ is the continuous joint probability distribution of X and Y then,

$$\text{Covariance } (X, Y) = \int_{-\infty}^{\infty} \int_{-\infty}^{\infty} (Y - E(Y))(X - E(X))f(X, Y)dX.dY \dots\dots(8.3)$$

$$\text{and } V(Y) = \int_{-\infty}^{\infty} (Y - E(Y))^2 f(X, Y) dY \dots\dots\dots(8.4)$$

$$\text{where } E(Y) = \int_{-\infty}^{\infty} Y.f(X, Y) dY \dots\dots\dots(8.5)$$

$V(X)$ and $E(X)$ are similarly defined.

It can be shown that $-1 \leq \rho_{XY} \leq 1$. The value ρ_{XY} is a measure of the association between random variables X and Y .

If $\rho_{XY} = 1$, then X and Y are perfectly positively correlated and the possible values of X and Y all lie on a straight line with a positive slope in the $X Y$ plane.

If $\rho_{XY} = -1$, then X and Y are perfectly negatively correlated and the possible values of X and Y all lie on a straight line with a negative slope in the $X Y$ plane.

If $\rho_{XY} = 0$, the variables may be said to be uncorrelated, that is, unassociated with each other.

If a factor $1/n - 1$ is placed in front of ρ_{XY} then r_{XY} has the form of ρ_{XY} with variances and covariances replaced by sample values, i.e.

$$r_{xy} = \frac{\sum_{i=1}^n (X_i - \bar{X})(Y_i - \bar{Y})}{(\sum_{i=1}^n (X_i - \bar{X})^2)^{\frac{1}{2}} (\sum_{i=1}^n (Y_i - \bar{Y})^2)^{\frac{1}{2}}} \dots\dots\dots(8.6)$$

The fact that r_{XY} is non-zero implies only that there is a relationship between values of X and Y and is not a measure of that relationship: r_{xy} is called the sample correlation coefficient between X and Y and is an empirical estimate of ρ_{XY} .

8.1.3. Correlation and Regression

Given the relationship:-

$$Y = \beta_0 + \beta_1 X + E \dots\dots\dots(8.7)$$

then the sum of squares of deviations from the true line is given by:-

$$S = \sum_{i=1}^n E_i^2 = \sum_{i=1}^n (Y_i - \beta_0 - \beta_1 X_i)^2 \dots\dots\dots(8.8)$$

and the values of b_1 and b_0 , which, when substituted for β_1 and β_0 give a minimum value for S , are given by:-

$$b_0 = \bar{Y} - b_1 \bar{X} \dots\dots\dots(8.9)$$

$$b_1 = \frac{\sum(X_i - \bar{X})(Y_i - \bar{Y})}{\sum(X_i - \bar{X})^2} \dots\dots\dots(8.10)$$

Comparing this equation with equation 8.6 it is seen that:-

$$b_1 = \left[\frac{\sum(Y_i - \bar{Y})^2}{\sum(X_i - \bar{X})^2} \right]^{\frac{1}{2}} r_{XY} \text{ for } i = 1, n \dots\dots\dots(8.11)$$

i.e. b_1 is a scaled version of r_{XY} , scaled by the ratio of the range of values of Y_i divided by the range of values of X_i , i.e.

$$(n - 1)S_Y^2 = \sum(Y_i - \bar{Y})^2 \dots\dots\dots(8.12)$$

$$(n - 1)S_X^2 = \sum(X_i - \bar{X})^2 \dots\dots\dots(8.13)$$

then

$$b_1 = \frac{S_Y}{S_X} r_{XY} \dots\dots\dots(8.14)$$

Therefore, b_1 and r_{XY} are related but give different interpretations.

Correlation k_{XY} measures association between X and Y , while b_1 measures the size of the change in Y which can be predicted when there is a unit change in X .

In the present example the values of partial correlation were:-

$$\left. \begin{array}{l} r_{1Y \cdot 2} = 0.63 \\ r_{3Y \cdot 2} = 0.000182 \end{array} \right\} \text{Section 8.2.4.2.}$$

The value of r relating to variable X_1 suggests a possible association with X_2 and Y .

The value of r relating to variable X_3 suggests that it is unlikely that there is an association with X_2 and Y .

8.2. Methods of Multiple Regression

There are several methods of carrying out multiple regression:-

- i. Full multiple regression.
- ii. Backward elimination procedure.
- iii. Forward selection procedure.
- iv. Stepwise regression procedure; this method is discussed in some detail, as it is most suitable for computer solution.

8.2.1. Full Multiple Regression

If a set of data is analysed assuming the model

$$Y = \beta_0 + \beta_1 X_1 + \beta_2 X_2 + E \dots\dots\dots (8.14)$$

and data is of the form:-

$$\begin{array}{ccc}
 Y_1 & X_{11} & X_{21} \\
 Y_2 & X_{12} & X_{22} \\
 Y_3 & X_{13} & X_{23} \\
 Y_4 & X_{14} & X_{24} \\
 \vdots & \vdots & \vdots \\
 Y_n & X_{1n} & X_{2n}
 \end{array}$$

$$i.e. [Y] = [\beta][X] + [E] \dots\dots\dots(8.15)$$

then it can be shown that the least squares estimates of β_0 , β_1 and β_2 are given by:-

$$b = [X^T X]^{-1} X^T Y^T \dots\dots\dots(8.16)$$

where b is the vector of estimates of the elements of $[\beta]$, provided that $X^T X$ is non-singular.

Although this method takes account of all independent variables there is not enough flexibility to allow for the effects of interaction between variables, of the effect of dropping or including variables at any stage in the regression. The method is also slow, unwieldy and totally impractical unless a large computer is available.

8.2.2. Backward Elimination Procedure

This method is an improvement on full regression, since it considers only the "best" regression containing a certain number of variables. The method is:-

1. A full regression equation is computed.
2. The partial F-test value (see page 348) is calculated for every variable as though it had just entered as the last variable in the regression equation.

3. The lowest F-test value is compared with a pre-selected significance level of F.
- 4a. If F is less than the pre-selected value, remove the variable and rework the regression from stage 2.
- 4b. If F is greater than the pre-selected value, adopt the regression equation as calculated.

8.2.3. Forward Selection Procedure

This method involves insertion of variables in turn until the regression equation is satisfactory. The order of insertion is determined by using the partial correlation coefficient on a measure of variables not yet in the regression. The basic procedure is:-

1. Select the X most correlated with Y, (say X_2), and find the first order, linear regression equation $\hat{Y} = f(X_2)$.
2. Find the partial correlation coefficients for remaining X variables and Y after making allowance for X_2 .
3. Find the largest of these coefficients (say X_1) and perform another regression to give $\hat{Y} = f(X_2, X_1)$.
4. Continue until all "significant" variables are in regression.

After X_1, X_2, X_3, X_n are in the regressions the partial correlation coefficients are the correlations between:-

- a. The residuals from the regression $\hat{Y} = f(X_1 X_2 \dots X_n)$, and
- b. The residuals from a regression $\hat{X}_j = f_j(X_1 X_2 \dots X_n) (j > n)$

As soon as the partial F-value relating to the most recently entered variable becomes non-significant the process is terminated.

8.2.4. Stepwise Regression Procedure

8.2.4.1. Introduction

This is an improved version of the forward selection procedure. The improvement involves the re-examination of all variables at each stage in the regression. A variable which may have been the single best variable to enter at an early stage may later become insignificant because of its relationship with other variables in regression. In order to check this, the partial F-criterion for each variable in the regression at any stage of calculation is evaluated and compared with a pre-selected percentage point of the appropriate F distribution. This provides a judgement on the contribution made by each variable as though it had been the most recent variable entered. The process continues until no more variables are admitted or rejected from the equation. The method lends itself to computation and has been shown to give satisfactory results.

8.2.4.2. General Procedure for Computational Method

Assuming a set of data of the form:-

$$Y = f(X_1, X_2, X_3)$$

The correlation matrix is constructed from the raw data. For this example four sets of assumed results are used, i.e.

X_1	X_2	X_3	Y
7	26	60	80
7	29	52	74
11	56	20	105
11	31	47	88

Calculate the corrected sum of squares and cross product matrix. The matrix of uncorrected sum of squares and uncorrected sums of

cross products is:-

	X ₁	X ₂	X ₃	Y	
totals	36	142	179	347	

$$X^1 X = \begin{bmatrix} 340 & 1342 & 1521 & 3201 \\ - & 5614 & 5645 & 12834 \\ - & - & 8913 & 14884 \\ - & - & - & 30645 \end{bmatrix} \dots\dots\dots(8.17)$$

After correction for means, the corrected sum of squares and cross products matrix is obtained.

The correction algorithm is:-

$$x_i x_j = \Sigma X_i X_j - \frac{(\Sigma X_i)(\Sigma X_j)}{n} \dots\dots\dots(8.18)$$

e.g. $\Sigma x_1 x_2 = 1342 - \frac{36 \times 142}{4} = 64$

$$X_c^1 X_c = \begin{bmatrix} 16 & 64 & -90 & 78 \\ & 573 & -709 & 516 \\ & & 903 & -644 \\ & & & 542 \end{bmatrix} \dots\dots\dots(8.19)$$

Using the $X_c^1 X_c$ matrix calculate the correlation coefficients of the correlation matrix. The algorithm for the coefficients is:-

$$r_{ij} = \frac{\Sigma x_i x_j}{\sqrt{(\Sigma x_i^2)(\Sigma x_j^2)}} \dots\dots\dots(8.20)$$

e.g. $r_{12} = \frac{64}{\sqrt{16 \times 373}} = 0.67$

Assemble the correlation matrix R. For this data there are, k = 3, independant variables, therefore, R is a 3 x 3 matrix.

$$R = \begin{bmatrix} 1.0 & 0.67 & -0.75 \\ & 1.0 & -0.99 \\ & & 1.0 \end{bmatrix} \dots\dots\dots(8.21)$$

The correlation matrix R is augmented to form the A matrix:-

$$A = \left[\begin{array}{c|c|c} R(k \times k) & T^1(k \times 1) & I(k \times k) \\ \hline T(1 \times k) & S(1 \times 1) & O(1 \times k) \\ \hline -I(k \times k) & O(k \times 1) & O(k \times k) \end{array} \right] \dots\dots\dots(8.22)$$

The A matrix is of the form $A = (2k + 1) \times (2K + 1)$

$R(k \times k)$ = correlation matrix for the k independant variables.

$T(1 \times k)$ = correlation vector of the k independant variables
with the response Y, i.e. the values Y_{iY} for $i = 1, 3$.

$T^1(k \times 1)$ = transpose of T.

$S(1 \times 1)$ = correlation of the response with itself.(=1).

$I(k \times k)$ = identity matrix.

$-I(k \times k)$ = negative identity matrix.

The A matrix is, therefore:-

$$A = \left[\begin{array}{ccc|ccc} 1 & 0.67 & -0.75 & 0.84 & 1 & 0 & 0 \\ 0.67 & 1 & -0.99 & 0.93 & 0 & 1 & 0 \\ -0.75 & -0.99 & 1 & -0.92 & 0 & 0 & 1 \\ \hline 0.84 & 0.93 & -0.92 & 1 & 0 & 0 & 0 \\ \hline -1 & 0 & 0 & 0 & 0 & 0 & 0 \\ 0 & -1 & 0 & 0 & 0 & 0 & 0 \\ 0 & 0 & -1 & 0 & 0 & 0 & 0 \end{array} \right]$$

8.2.4.3. Stepwise Procedure

The method performs a regression with several variables as a series of straight line regressions. The A matrix is adjusted at each stage to effect this process. At each stage appropriate entries in the matrix provide the regression coefficients and entries for the analysis of variance table in coded units. The entries can also provide the F-values for two series of tests, one for the entry of a variable into the regression equation, and one for the deletion of a variable from the regression equation. The appropriate F-distribution percentage points can be employed at each stage for tests. It is simpler, however, to choose fixed values that do not depend on the degrees of freedom, which change as the regression proceeds. The critical value of F for entry is normally the same as the critical value of F for deletion.

Step 1

Selection of First Variable to Enter Regression

Calculate a set of statistics, V_i , where

$$V_i = r_{iY} r_{iY}/r_{ii} \dots\dots\dots(8.23)$$

$$\text{i.e. } V_i = A_{i, k+1} \overline{A_{k+1, i}}/A_{ii}$$

for $i = 1, 2, \dots, k$.

For the data $V_1 = 0.7056$

$V_2 = 0.8649$

$V_3 = 0.8464$

Since V_2 is the maximum, variable X_2 is the first to be considered.

Next, it must be determined if X_2 should be entered at all, by applying the standard F test; at later stages the sequential F test may be used, allowance being made for variables already in regression. For this example the critical F-value for entry and

and exit is arbitrarily set at say, 3.5 so that it is unnecessary to consult an F-table at each stage.

If X_j is the first variable entered into regression, the analysis of variance table, in terms of correlation, takes the following form:-

Source of Variation	df	Sum of Squares (SS)	Mean Square (MS)
Total (Corrected)	$n - 1$	$r_{YY}^2 = 1$	
Regression	1	r_{jY}^2	r_{jY}^2
Residual	$n - 2$	$r_{YY}^2 - r_{jY}^2$	$(r_{YY}^2 - r_{jY}^2)/n - 2$

Here $r_{Y2}^2 = V_2 = 0.8649$, we have:-

Source	df	(SS)	(MS)	F
Total corrected	3	1.0000		
Regression (X_1)	1	0.8649	0.8649	11.26
Residual	2	0.1536	0.0768	

Since 11.26 exceeds the selected critical value 3.5, variable X_2 is entered into regression.

It can be shown that, at any stage of the procedure, the test ratio for entry of the next variable takes the general form:-

$$F = \phi.V_{\max}/(r_{YY}^2 - V_{\max}) \dots\dots\dots(8.24)$$

i.e. here $F = 2 \times 0.8649/0.1536 = 11.26$

Adjustment of Correlation Matrix A

The matrix A must be adjusted for the entrance of X_2 into regression. Since variable 2 is the variable to be entered, row 2 in the A matrix is divided by A_{22} .

i.e. If we let the adjusted A matrix be B then:-

$$B_{11} = \frac{A_{11}}{A_{11}}, B_{12} = \frac{A_{12}}{A_{11}} \text{ etc. } \dots\dots\dots(8.25)$$

The rest of the elements in the B matrix are obtained by applying the following algorithm.

$$B_{ij} = A_{ij} - \frac{A_{iL} A_{Lj}}{A_{LL}} \dots\dots\dots(8.26)$$

where L identifies the variable just entered.

Here L = 2, therefore:-

$$\begin{aligned} B_{11} &= A_{11} - \frac{A_{12} A_{21}}{A_{22}} = 1.0 - \frac{0.67 \times 0.67}{1} \\ &= 0.5511 \end{aligned}$$

$$\begin{aligned} B_{12} &= A_{12} - \frac{A_{12} A_{22}}{A_{22}} = 0.67 - \frac{0.67 \times 1}{1} \\ &= 0 \end{aligned}$$

$$\begin{aligned} B_{77} &= A_{77} - \frac{A_{72} A_{27}}{A_{22}} = 0 - \frac{0 \times 0}{1} \\ &= 0 \end{aligned}$$

the B matrix is, therefore:-

$$B = \begin{bmatrix} 0.55 & 0 & -0.087 & 0.217 & 1 & -0.67 & 0 \\ 0.67 & 1 & -0.99 & 0.93 & 0 & 1 & 0 \\ -0.087 & 0 & 0.0199 & 0.0007 & 0 & 0.99 & 1.0 \\ 0.217 & 0 & 0.0007 & 0.1351 & 0 & -0.93 & 0 \\ -1.0 & 0 & 0 & 0 & 0 & 0 & 0 \\ 0.67 & 0 & -0.99 & 0.93 & 0 & 1.0 & 0 \\ 0 & 0 & -1.0 & 0 & 0 & 0 & 0 \end{bmatrix}$$

Summary of Information After Step 1

From matrix B the following information is found:-

ANALYSIS OF VARIANCE TABLE						
		SUM OF SQUARES		MEAN SQUARE		
SOURCE OF VARIATION	df	CORRELATION	ORIGINAL UNITS	CORRELATION	ORIGINAL UNITS	F
Total (Corrected)	3	1	542			
Regression (X ₂)	1	0.8649	469	0.8649	469	11.26
Residual	2	0.1351	73	0.0676	S ² =36.5	

$$S^2 = 73/2 = 36.5$$

Corrected sum of squares is used as a conversion factor from correlation form to original units.

Variable entered is X₂.

Sequential F-test for entrance = 11.26 (calculated before entry).

Percentage variation explained = 0.8649 × 100 = 86.5%.

Standard deviation of residuals = $\sqrt{36.5}$ = 6.04

Standardised b coefficient for X₂ (variable admitted) = B₂₄ = 0.93

decoded b coefficient for X_2

$$b_2 = B_{24} \frac{\sqrt{\sum X_4^2}}{\sqrt{\sum X_2^2}} = B_{24} \times \frac{S_4}{S_2}$$

$$= 0.93 \times \frac{\sqrt{542}}{\sqrt{573}} = 0.90$$

standard error in decoded b coefficient for X_1 .

$$S \sqrt{\frac{B_{22}}{\sum X_2^2}} = \sqrt{\frac{36.5 \times 1}{573}} = 0.25$$

Step 2

Test for the elimination of variables already in the regression.
This test is unnecessary at this stage since only variable X_2 is in the regression.

Selection of Next Variable to Enter Regression

Matrix B is used to find Vmax for the variables not in regression:-

$$V_1 = \frac{B_{14} B_{41}}{B_{11}} = \frac{0.217 \times 0.217}{0.55} = 0.086$$

$$V_3 = \frac{B_{34} B_{43}}{B_{33}} = \frac{0.0007 \times 0.0007}{0.0199} = 0.0000246$$

$$V_{\max} = V_1 = 0.086$$

$$\begin{aligned} \text{F-value for entry of } X_1 &= V_1 \phi / B_{44} - V_{\max} \\ &= 0.086 \times 1/0.1351 - 0.086 \\ &= 1.75 \end{aligned}$$

Since this is less than the chosen F-value X_1 is rejected.

The F-test for X_3 may for entry next be carried out:-

$$\begin{aligned} \text{F-value for entry of } X_3 &= 0.0000246 \times 1/0.1351 = 0.0000246 \\ &= 0.000182 \end{aligned}$$

The variable X_3 is, therefore, rejected.

Had either variable X_1 or X_3 been accepted into the regression the procedure would have been as before. That is, set up the C matrix where the elements are found using the algorithms:-

$$C_{Lj} = \frac{B_{Lj}}{B_{LL}} \text{ for the variable } L \text{ entering the regression}$$

and

$$C_{ij} = B_{ij} - \frac{B_{iL} \times B_{Lj}}{B_{LL}} \text{ for all the other elements where } L$$

is the variable being added.

Calculation of Constant Terms

The constant term for the regression equation at each step is calculated from:-

$$\text{Constant} = \bar{Y} - \sum b_i \bar{X}_i \dots\dots\dots(8.27)$$

where i covers the range of variables in regression.

For this example, i = 2 only.

$$\begin{aligned} \text{Constant} &= 86.75 - 0.9 \times 35.5 \\ &= 54.8 \end{aligned}$$

The final regression equation chosen by this stepwise procedure is:-

$$\hat{Y} = 0.9X_1 + 54.8 \dots\dots\dots(8.28)$$

Using this equation to calculate \hat{Y} for the example being considered gives:-

OBSERVED Y	CALCULATED \hat{Y}	RESIDUAL ($\hat{Y} - Y$)
80	78.2	-1.8
74	80.9	6.9
105	105.2	0.2
88	82.7	-5.3

The square of the correlation coefficient of the variables not in regression with response Y may be calculated as follows:-

$$r^2_{1Y.jk} = \frac{a^2_{1Y}}{A_{11} a_{YY}} \dots\dots\dots(8.29)$$

where a_{ij} denotes the matrix entry, and kj etc., are variables already in regression.

Here, after X_2 was included then:-

$$r^2_{1Y.2} = \frac{B^2_{1Y}}{B_{11} B_{YY}} = \frac{(0.217)^2}{0.55 \times 0.1351} = 0.63$$

$$r^2_{3Y.2} = \frac{B^2_{3Y}}{B_{33} B_{YY}} = \frac{(0.0007)^2}{0.0199 \times 0.1351} = 0.00182$$

These are the correlations respectively of variables X_1 and X_3 with Y after the regression has been adjusted for the presence of X_2 .

8.2.5. Stepwise Multiple Regression:- A Computer Program

A computer program has been written incorporating the stepwise procedure. The program has been used to carry out regression analysis of:-

- i. Experimental results by others
- ii. Experimental results from the present investigation.

Examples of the output are shown on pages 355-361 and the results are discussed in Chapter 9, page 362.

The program gives the user several run time options, including:-

1. Printing of covariance and correlation matrices.
2. Full regression or stepwise regression.
3. Selection of significance levels for stepwise regression.
4. Option of having a constant term.
5. Optional listing of table of residuals of regression.

A listing of the computer program, which is written in standard Fortran is given in Appendix B.

DELETED 00
 12.12.01 REGR DAVE
 TYPE INDEPENDENT VARIABLES BETA, GAMMA, TOR*
 TYPE DEPENDENT VARIABLE AXIAL*
 STEPWISE REQUIRED.
 TYPE YES OR NO NO
 CONSTANT REQUIRED.
 TYPE YES OR NO YES
 RESIDUALS REQUIRED.
 TYPE YES OR NO NO
 FULL MULTIPLE REGRESSION

DEPENDENT VARIABLE IS AXIAL

VARIABLE	COEFFICIENT	STD. ERROR	F-VALUE
CONSTANT	-2.34133	1.8575	1.59
BETA	34.04709	2.5938	172.30
GAMMA	0.06742	0.0299	5.09
TOR	-1.30209	2.0635	0.76

ANALYSIS OF VARIANCE TABLE			
VARIATION	SUM SQUARES	D.F.	MEAN SQUARE
REGRESS	3331.2572	3	1110.4191
RESIDUAL	978.8756	72	13.5955
TOTAL	4310.1329	75	F = 81.68

MULTIPLE CORRELATION = 0.7728897
 DURBIN-WATSON D-STATISTIC = 1.5252

DELETED 00
 12.15.50 REGR DAVE
 TYPE INDEPENDENT VARIABLES BETA, GAMMA, TOR*
 TYPE DEPENDENT VARIABLE AXIAL*

STEPWISE REQUIRED.
 TYPE YES OR NO YES
 F-LEVEL
 TYPE 1,5 OR 1010
 CONSTANT REQUIRED.
 TYPE YES OR NO WAITING
 YES
 RESIDUALS REQUIRED.
 TYPE YES OR NO NO
 STEPWISE REGRESSION

LEVEL OF SIGNIFICANCE 10%

DEPENDENT VARIABLE IS AXIAL

BETA BROUGHT INTO REGRESSION

VARIABLE	COEFFICIENT	STD.ERROR	F-VALUE
CONSTANT	0.14857	1.1817	0.02
BETA	30.90360	2.0382	229.88

ANALYSIS OF VARIANCE TABLE			
VARIATION	SUM SQUARES	D.F.	MEAN SQUARE
REGRESS	3260.5549	1	3260.5549
RESIDUAL	1049.5780	74	14.1835
TOTAL	4310.1329	75	F = 229.88

MULTIPLE CORRELATION = 0.7564859
GAMMA BROUGHT INTO REGRESSION

VARIABLE	COEFFICIENT	STD.ERROR	F-VALUE
CONSTANT	-2.74974	1.7947	2.35
BETA	32.84416	2.1943	224.03
GAMMA	0.05410	0.0256	4.45

ANALYSIS OF VARIANCE TABLE			
VARIATION	SUM SQUARES	D.F.	MEAN SQUARE
REGRESS	3320.8878	2	1660.4439
RESIDUAL	989.2450	73	13.5513
TOTAL	4310.1329	75	F = 122.53

MULTIPLE CORRELATION = 0.7704839
REMAINING VARIABLES ARE INSIGNIFICANT
DURBIN-WATSON D-STATISTIC= 1.3916

DELETED 00

12.22.28 WAITING

12.23.48 WAITING

12.24.50 LOGOUT

CONNECTED FOR 49 MINS

MILL TIME USED 55 SECS - 356 -

DELETED 00
 11.58.18 WAITING
 11.59.35 REGR MOM1
 TYPE INDEPENDENT VARIABLES BETA, GAMMA, TOR*
 TYPE DEPENDENT VARIABLE MOMENT*
 STEPWISE REQUIRED.
 TYPE YES OR NO YES
 F-LEVEL
 TYPE 1, 5 OR 10 10
 CONSTANT REQUIRED.
 TYPE YES OR NO YES
 RESIDUALS REQUIRED.
 TYPE YES OR NO YES
 STEPWISE REGRESSION

LEVEL OF SIGNIFICANCE 10%

DEPENDENT VARIABLE IS MOMENT

BETA BROUGHT INTO REGRESSION

VARIABLE	COEFFICIENT	STD. ERROR	F-VALUE
CONSTANT	-20.31796	8.4758	5.75
BETA	45.73462	10.4534	19.14

ANALYSIS OF VARIANCE TABLE	SUM SQUARES	D.F.	MEAN SQUARE
REGRESS	398.0210	1	398.0210
RESIDUAL	166.3486	8	20.7936
TOTAL	564.3696	9	F = 19.14

MULTIPLE CORRELATION = 0.7052489
 GAMMA BROUGHT INTO REGRESSION

VARIABLE	COEFFICIENT	STD. ERROR	F-VALUE
CONSTANT	-40.83810	7.5552	29.22
BETA	44.24694	6.4479	47.09
GAMMA	2.65065	0.7058	14.11

ANALYSIS OF VARIANCE TABLE

VARIATION	SUM SQUARES	D.F.	MEAN SQUARE
REGRESS	509.1982	2	254.5991
PESIDUAL	55.1714	7	7.8816

TOTAL 564.3696 9 F = 32.30

MULTIPLE COPRELATION = 0.9022425

REMAINING VARIABLES ARE INSIGNIFICANT

TABLE OF RESIDUALS

OPSERVATION	Y(ACTUAL)	Y(ESTIMATED)	Y(ACT)-Y(EST)
1	11.83	15.31	-3.48
2	10.22	10.20	0.02
3	11.41	8.93	2.48
4	7.86	6.99	0.87
5	18.58	19.74	-1.16
6	15.07	13.35	1.72
7	11.01	11.42	-0.41
8	33.09	29.92	3.17
9	26.05	24.80	1.25
10	17.12	21.59	-4.47

DURBIN-WATSON D-STATISTIC= 1.5795

11.40.32 REGR PHD
 CONDENSING
 TYPE NUMBER OF VARIABLES 4
 TYPE VARIABLE NAMES Y, X1, X2, X3*
 DELETED 00
 TABLE OF MEANS AND STANDARD DEVIATIONS

VARIABLE	MEAN	STD. DEVIATION
Y	86.75	13.45
X1	9.00	2.31
X2	35.50	13.82
X3	44.75	17.35

NUMBER OF OBSERVATIONS = 4

COVARIANCE MATRIX REQUIRED.
 TYPE YES OR NO YES
 CORRELATION MATRIX REQUIRED.
 TYPE YES OR NO YES
 MATRIX OF VARIANCES AND COVARIANCES

	Y	X1	X2	X3
Y	180.92			
X1	26.00	5.33		
X2	171.83	21.33	191.00	
X3	-214.75	-30.00	-236.50	300.92

CORRELATION MATRIX

	Y	X1	X2	X3
Y	1.00			
X1	0.84	1.00		
X2	0.92	0.67	1.00	
X3	-0.92	-0.75	-0.99	1.00

DELETED 00
 11.40.32 REGR PHD
 TYPE INDEPENDENT VARIABLES X1, X2, X3*
 TYPE DEPENDENT VARIABLE Y*
 STEPWISE REQUIRED.
 TYPE YES OR NO NO
 CONSTANT REQUIRED.
 TYPE YES OR NO YES
 RESIDUALS REQUIRED.
 TYPE YES OR NO YES
 FULL MULTIPLE REGRESSION

DEPENDENT VARIABLE IS Y

VARIABLE	COEFFICIENT	STD. ERROR	F-VALUE
CONSTANT	-116.96849	0.0000	10 10 10 10 10 10 10
X1	4.35924	0.0000	10 10 10 10 10 10 10
X2	2.50420	0.0000	10 10 10 10 10 10 10

X3

1.68908

0.0000

10 10 10 10 10 10 10

ANALYSIS OF VARIANCE TABLE
VARIATION SUM SQUARES

D.F.

MEAN SQUARE

REGRESS

542.7500

3

180.9167

RESIDUAL

0.0000

0

10 10 10 10 10 10 10 10 10 10

TOTAL

542.7500

3

F = 10 10 10 10 10 10 10

MULTIPLE CORRELATION = 1.0000000

TABLE OF RESIDUALS

OBSERVATION	Y(ACTUAL)	Y(ESTIMATED)	Y(ACT)-Y(EST)
1	80.00	80.00	0.00
2	74.00	74.00	-0.00
3	105.00	105.00	-0.00
4	88.00	88.00	-0.00

DURBIN-WATSON D-STATISTIC= 1.1818

DELETED 00

11.43.55 REGR PHD

TYPE INDEPENDENT VARIABLES X1, X2, X3*

TYPE DEPENDENT VARIABLE*

STEPWISE REQUIRED.

TYPE YES OR NOYES

F-LEVEL

TYPE 1, 5 OR 105

CONSTANT REQUIRED.

TYPE YES OR NOYES

RESIDUALS REQUIRED.

TYPE YES OR NOYES

STEPWISE REGRESSION

LEVEL OF SIGNIFICANCE 5%

DEPENDENT VARIABLE IS Y

REMAINING VARIABLES ARE INSIGNIFICANT

TABLE OF RESIDUALS

OBSERVATION	Y(ACTUAL)	Y(ESTIMATED)	Y(ACT)-Y(EST)
1	80.00	0.00	80.00
2	74.00	0.00	74.00
3	105.00	0.00	105.00
4	88.00	0.00	88.00

DURBIN-WATSON D-STATISTIC= 0.0420

DELETED 00

11.45.52 REGR PHD

TYPE INDEPENDENT VARIABLES X1, X2, X3*

TYPE DEPENDENT VARIABLE*

STEPWISE REQUIRED.

TYPE YES OR NOYES

F-LEVEL

TYPE 1,5 OR 1010
 CONSTANT REQUIRED.
 TYPE YES OR NOYES
 RESIDUALS REQUIRED.
 TYPE YES OR NOYES
 STEPWISE REGRESSION

LEVEL OF SIGNIFICANCE 10%

DEPENDENT VARIABLE IS Y

X2 BROUGHT INTO REGRESSION

VARIABLE	COEFFICIENT	STD.ERROR	F-VALUE
CONSTANT	54.81239	9.8350	31.06
X2	0.89965	0.2625	11.74

ANALYSIS OF VARIANCE TABLE			
VARIATION	SUM SQUARES	D.F.	MEAN SQUARE
REGRESS	463,7701	1	463,7701
RESIDUAL	78,9799	2	39,4900
TOTAL	542,7500	3	F = 11.74

MULTIPLE CORRELATION = 0.8544819
 REMAINING VARIABLES ARE INSIGNIFICANT
 TABLE OF RESIDUALS

ORSPERVATION	Y(ACTUAL)	Y(ESTIMATED)	Y(ACT)-Y(EST)
1	80.00	78.20	1.80
2	74.00	80.90	-6.90
3	105.00	105.19	-0.19
4	88.00	82.70	5.30

DURPIN-WATSON D-STATISTIC= 1.9099

CHAPTER 9

REGRESSION ANALYSIS APPLIED TO THE RESULTS OF ULTIMATE LOAD TESTS ON T-JOINTS UNDER AXIAL AND MOMENT LOADS, CARRIED OUT IN THE PRESENT INVESTIGATION

9.1. Ultimate Axial Load (P_u)

9.1.1. Analysis of Test Results

Observations of experimental joint behaviour, and the results of tests for ultimate axial load, indicate that the ultimate load P_u is a function of several joint parameters:-

1. β = d_1/d_o
2. γ = d_o/t_o
3. σ = material yield strength
4. θ = joint angle, should the analysis be applied to Y-joints
5. L/d_o = ratio of chord diameter to chord length in the test specimen
6. τ = t_1/t_o
7. t_o = chord thickness

i.e. an equation would be of the form:-

$$P_u = f(\beta, \gamma, \sigma, \theta, L/d_o, \tau, t_o), \text{ or}$$

$$P_u = f(1), f(2), f(3), f(4), f(5), f(6), f(7)$$

In order to simplify the analysis some of the above terms may be taken out of the equation:-

$f(3)$, the yield stress of the material is a constant factor and should not be considered an independent variable.

$f(4)$, the joint angle, is a geometric function, of the type $1/\sin\theta$. For the purpose of this investigation it has been ignored.

f(5), ratio of chord diameter to chord length. It has been shown that provided the distance from the joint to the support is greater than twice the chord diameter, then this ratio has no effect on joint strength. For the purpose of this report the factor f(5), therefore, becomes unity.

f(7), the chord thickness, t_o , is a constant parameter for a given joint and has been taken outside the formula and squared to give the dimensionless group:-

$$P_u / F_y \cdot t_o^2$$

The proposed formula will, therefore, be of the form:-

$$\frac{P_u}{F_y \cdot t_o^2} = f\left(\frac{d_1}{d_o}, \frac{t_1}{t_o}, \frac{d_o}{t_o}\right) \dots\dots\dots (9.1)$$

The form of the equation has been investigated further by using multiple linear regression, based on a least squares method of curve fitting, (see Chapter 8).

The equation then takes the form:-

$$\frac{P_u}{F_y \cdot t_o^2} = A_o + A_1 X_1 + A_2 X_2 \dots\dots A_n X_n \dots\dots\dots (9.2)$$

It has been shown (Figures 127, 128) that for axial load the variation of P_u with the parameters d_1/d_o , d_o/t_o and t_1/t_o approximates to a linear relationship.

Two options were used to analyse the data:-

1. Stepwise regression - each of the independant variables is brought into the analysis in turn and the significance of their contribution is considered.
11. Full regression - all the independant variables are used in the analysis.

9.1.2. Results

(i) Stepwise Regression

- a. Considering beta d_1/d_o only the regression equation obtained gives:-

$$P_u = F_y.t_o^2 \left[40 \frac{d_1}{d_o} - 2.2 \right] \dots\dots\dots(9.3)$$

- b. Considering beta d_1/d_o and d_o/t_o the regression equation obtained gives:-

$$P_u = F_y.t_o^2 \left[40 \frac{d_1}{d_o} + 0.7 \frac{d_o}{t_o} - 18.55 \right] \dots\dots\dots(9.4)$$

- c. The inclusion of the variable t_1/t_o was found to be insignificant at the 10% level of analysis carried out.

Equations 9.3 and 9.4 were used to calculate the ratios of experimental axial load to calculated ultimate axial load. The results obtained are shown in Table 15.

The mean values of the ratio $P_u(\text{exptl})/P_u(\text{calc})$ are:-

Equation 9.3 mean = 1.001 Std. Dev. = 0.17

Equation 9.4 mean = 1.019 Std. Dev. = 0.11

(ii) Full Regression

The analysis considered the variables beta (d_1/d_o), d_o/t_o and t_1/t_o , and the regression equation obtained was:-

$$P_u = F_y.t_o^2 \left[40 \frac{d_1}{d_o} + 0.74 \frac{d_o}{t_o} - 0.9 \frac{t_1}{t_o} - 18.8 \right] \dots\dots\dots(9.5)$$

TABLE 15 - RATIO OF ULTIMATE EXPERIMENTAL AXIAL LOAD
CALCULATED ULTIMATE AXIAL USING REGRESSION EQUATIONS

Test	Pu(exptl)/Pu(calc)		
	Equation (9.3)	Equation (9.4)	Equation (9.5)
A/1	1.2	0.86	0.85
B/1	1.07	1.12	1.09
C/1	1.01	1.17	1.15
D/1	0.81	1.13	1.11
E/1	1.11	0.86	0.85
F/1	0.99	1.03	1.02
G/1	0.88	1.12	1.11
H/1	1.17	0.95	0.95
J/1	1.02	1.06	1.05
K/1	0.97	1.07	1.05
L/1	0.72	0.87	0.86
M/1	1.16	0.98	0.97
N/1	1.07	1.16	1.14
P/1	0.81	0.96	0.94
Q/1	1.32	1.16	1.15
R/1	1.00	1.03	1.01
S/1	0.71	0.80	0.79
Mean value	1.001	1.019	1.005
Standard deviation	0.17	0.11	0.12

The equation was used to calculate the ratios of $P_u(\text{expt1})/P_u(\text{calc})$ and the results obtained are shown in Table 15. The value of the mean and standard deviation for the ratio $P_u(\text{expt1})/P_u(\text{calc})$ found from equation 9.5 are 1.005 and 0.12 respectively.

9.1.3. Discussion

Equation 9.3 which considers only the beta (d_1/d_o) variable gives the most accurate mean, but with a high standard deviation. Equation 9.4 gives a higher mean, with a smaller standard deviation. The full regression equation 9.5 gives an accurate mean, with a small standard deviation of 0.12. This value compares favourably with the maximum accuracy that has been achieved by using other design formulae (see Chapter 3).

The results from the regression indicate that the relationship between ultimate axial load and the parameter d_o/t_o is not linear and has an increasing effect upon the results as beta (d_1/d_o) increases. Further analysis assuming a polynomial regression model would give a more accurate equation for joints with high beta ratios and low d_o/t_o ratios.

i.e. assuming the model:-

$$\frac{P_u}{F_y.t_o^2} = A_0 + A_1(\text{beta})^m + A_2(d_o/t_o)^n + A_3(t_1/t_o)^p \dots\dots\dots(9.6)$$

It is probable, however, that because of the nature of the joints being analysed, the resultant equation would be very complicated, difficult to use, and give little improvement in result.

The equation proposed for ultimate axial load calculation was, therefore, of the form:-

$$P_u = F_y.t_o^2 \left[40 \frac{d_1}{d_o} + 0.74 \frac{d_o}{t_o} - 0.9 \frac{t_1}{t_o} - 19 \right]$$

This equation has then been used to calculate the ultimate axial loads for T-joint axial load tests carried out by others: Figure 174. Again the ratio of $P_u(\text{exptl})/P_u(\text{calc})$ has been found for each of the tests considered.

Initially all 76 tests were analysed and the mean value for the ratio of experimental to calculated load was found to be 0.944 with a standard deviation of 0.313. It was noted, however, that the equation, and therefore the results, were sensitive to the do/to ratios of the joints. The analysis was repeated omitting those tests with do/to ratios exceeding 45. The remaining 61 tests gave a mean value for the ratio of 1.083 with a standard deviation of 0.17. For this type of joint with do/to less than 45 the result compares well with, and is better than, any of the existing formulae reviewed in Chapter 3. Although, in practice do/to seldom exceeds values of 35-40 there is a need to have a formula which will cover the range of larger values. This may be achieved by either:-

- (i) Carrying out a regression analysis which includes all the joints in a full range of do/to.
- (ii) Modifying the formula proposed for do/to less than 45 by an empirical factor.
- (iii) Treating this range of do/to as a special case and carrying out a separate regression analysis.

The wide range of the variable do/to prohibits the regression of all the results since the standard deviation obtained has been found to be unacceptably large, (greater than 40%).

Modification of the proposed formula would require two modification factors, one for do/to and one for d_1/d_o .

Proposal of a different formula for d_o/t_o greater than 40 is not immediately appealing since it means that there are two different formulae for T-joint axial load design. It may, however, be beneficial to have two formulae for different d_o/t_o ratio ranges because it will draw the designers attention to the fact that he is working in a range where knowledge is still limited. Very little evidence exists for tests on joints with large d_o/t_o ratios and the fact that all of it has been considered, exclusively, in the regression analysis gives confidence to the design of the joint.

In order to give a fair comparison two further regressions were carried out:-

1. Regression on all 76 tests results.
- ii. Regression on the 15 test results with d_o/t_o greater than 45.

Two further equations were, therefore, found:-

$$P_u = F_y.t_o^2 \left[34 \frac{d_1}{d_o} + 0.07 \frac{d_o}{t_o} - 1.8 \frac{t_1}{t_o} - 2.5 \right] \dots\dots\dots(9.7)$$

based on all 76 tests results, and,

$$P_u = F_y.t_o^2 \left[11 \frac{d_1}{d_o} - 0.1 \frac{d_o}{t_o} + 15.0 \right] \dots\dots\dots(9.8)$$

based on 15 tests with d_o/t_o greater than 45.

These two formulae were then used to calculate the ratios of experimental load to calculated load. The results obtained were:-

EQUATION	NO.OF TESTS	MEAN RATIO	STANDARD DEVIATION
9.5	61	1.083	0.17
9.7	76	1.015	0.21
9.8	15	1.017	0.16

Formula 9.5 has been included for comparison. Histograms for these three formulae are shown in Figure 177.

The formula based on regression of all 76 test results has a good normal distribution of results, but with the median value falling between 0.9 and 1.0.

The formula based on regression of the ultimate axial load tests carried out in the present investigation and used for the 61 test results has it's median value between 1.0 and 1.1 with most results greater than 1.0.

The formula based on regression of the 15 test results with d_o/t_o greater than 45.0 has it's median value between 0.9 and 1.0. However, eight of the values for the ratio of experimental to calculated load are greater than 1.0.

9.1.4. Conclusions and Proposed Formulae for Calculating Ultimate Axial Loads in T-Joints

a. The proposed equations for calculating the ultimate axial load for welded T-joints are:-

$$1. \quad P_u = F_y.t_o^2 \left[40 \frac{d_1}{d_o} + 0.74 \frac{d_o}{t_o} - 0.9 \frac{t_1}{t_o} - 19.0 \right]$$

for d_o/t_o less than 45.0.

$$11. \quad P_u = F_y.t_o^2 \left[11 \frac{d_1}{d_o} - 0.1 \frac{d_o}{t_o} + 15.0 \right]$$

for d_o/t_o greater than 45.0.

- b. All existing formulae, whether empirical or theoretical become less reliable as d_o/t_o increases and becomes greater than 50.
- c. The parameter $\frac{t_1}{t_o}$ has less influence on joint strength than other joint parameters and this influence becomes insignificant when the parameter d_o/t_o is greater than 45.0.

9.2. Ultimate Moment Load (M_u)

9.2.1. Analysis of Test Results

Observation of experimental joint behaviour and the results of tests for ultimate moment load indicate that the ultimate moment is a function of the same basic joint parameters as is the ultimate axial load, (page 362).

For moment loads the proposed formula is considered to be of the form:-

$$\frac{M_u}{F_y.d_o.t_o^2} = f \left[\frac{d_1}{d_o}, \frac{d_o}{t_o}, \frac{t_1}{t_o} \right] \dots\dots\dots(9.9)$$

M_u being divided by the term $F_y.d_o.T_o^2$ to give a dimensionless group on the left hand side of the equation. Figure 130 shows that an assumption of linear variation of ultimate moment with d_1/d_o would be valid for d_o/t_o 18-23, but would become less valid for $d_o/t_o = 32$.

Figure 129 shows that the assumption of linear variation of ultimate moment with d_o/t_o is an approximation. In addition, the relationship between d_o/t_o and the ultimate moment is not

unique, but varies with the d_1/d_o ratio from having negligible influence for $\beta = 0.42$, to having considerable influence for $\beta = 1.0$.

The form of the equation 9.9 has been investigated further by using multiple linear regression, based on test results from the present investigation. The regression has been assumed to be linear, but in order to study the effect of d_o/t_o on the equation, the relationship that $\mu \propto (d_o/t_o)^{0.66}$ has been calculated for $\beta = 0.67$ to 1.0 , based on the results shown in Figure 129. Stepwise regression was carried out.

9.2.2. Results

i. Linear Relationships

Including β only:-

$$\frac{\mu}{F_y.d_o.t_o^2} = \left[37 \frac{d_1}{d_o} - 12.6 \right] \dots\dots\dots(9.10)$$

Including β and d_o/t_o :-

$$\frac{\mu}{F_y.d_o.t_o^2} = \left[36 \frac{d_1}{d_o} + 0.5 \frac{d_o}{t_o} - 24.0 \right] \dots\dots\dots(9.11)$$

Including β , d_o/t_o and t_1/t_o :-

$$\frac{\mu}{F_y.d_o.t_o^2} = \left[38 \frac{d_1}{d_o} + 0.7 \frac{d_o}{t_o} - 6.3 \frac{t_1}{t_o} - 25.0 \right] \dots\dots\dots(9.12)$$

ii. Non-Linear Relationship of μ with d_o/t_o

$$\frac{\mu}{F_y.d_o.t_o^2} = \left[44 \frac{d_1}{d_o} + 2.7 \left[\frac{d_o}{t_o} \right]^{0.66} - 41.0 \right] \dots\dots\dots(9.13)$$

for this analysis the effect of the parameter t_1/t_o was found to be insignificant in the regression.

The four equations found were used to calculate the ratios of ultimate experimental moment to calculated ultimate moment, for the test results. The results of these calculations are shown in Table 16, together with the mean and standard deviation for the ratios calculated from each equation.

9.2.3. Discussion

All the equations give good values for the mean ratio, but the standard deviations vary. The standard deviation of 0.35 for equation 9.10 is too high and must be disregarded, since it is apparent that an equation containing only the variable β is not suitable.

Equations 9.11 and 9.12 give very similar results with equation 9.2 having a slightly smaller standard deviation. Equation 9.13, in which the variable d_o/t_o was raised to the power 0.66 gives a good mean with the lowest standard deviation at 0.15. The equation, however, has not been applied to joints with $\beta = 0.42$ and 0.53.

In Table 16 it is seen that for test no. D/2 equations 9.11 and 9.12 gave very conservative results. This is because the equation is sensitive to small values of d_1/d_o and d_o/t_o occurring simultaneously. The values obtained have been ignored in calculating the means and standard deviations and this point will be commented upon later as a restriction on the applicability of the formula.

The final formula is multiplied by a factor of 255/350, the ratio of characteristic yield strength to yield strength of the material used in the tests since the 255N/mm^2 value was the one upon which the regression analysis was based.

TABLE 16 - RATIOS OF ULTIMATE EXPERIMENTAL MOMENT
CALCULATED ULTIMATE MOMENT FROM REGRESSION EQUATIONS

Test	Mu(exptl)/Mu(calc)			
	Equation (9.10)	Equation (9.11)	Equation (9.12)	Equation (9.13)
A/2	2.01	0.83	0.77	-
B/2	1.09	1.23	1.09	-
C/2	0.83	1.51	1.33	-
D/2	0.88	21.5	8.29	-
E/2	1.46	0.93	1.01	-
F/2	1.10	1.18	1.32	-
G/2	0.64	1.10	1.29	-
H/2	0.97	0.73	0.76	0.77
J/2	0.83	0.87	0.91	1.00
K/2	0.93	1.07	1.11	1.28
L/2	0.64	0.86	0.89	1.13
M/2	1.16	0.94	0.96	0.94
N/2	0.94	1.05	1.07	1.13
P/2	0.69	0.86	0.87	0.97
Q/2	1.35	1.18	1.18	1.11
R/2	1.07	1.10	1.09	1.06
S/2	0.70	0.82	0.80	0.80
Mean value	1.02	1.02	1.03	1.02
Standard deviation	0.35	0.20	0.18	0.15

9.2.4. Conclusions and Proposed Formula for Calculating Ultimate Moments in T-Joints

- i. The proposed equation for calculating the ultimate in-plane moment loads for welded T-joints is:-

$$M_u = F_y \cdot d_o \cdot t_o^2 \left[27 \frac{d_1}{d_o} + 0.5 \frac{d_o}{t_o} - 4 \frac{t_1}{t_o} - 18 \right]$$

- ii. The proposed equation is very conservative for small d_1/d_o values (less than 0.5) with small d_o/t_o values (less than 20). For this type of joint i.e. small beta and small d_o/t_o ratio the approximation that:-

$M_u = 0.75 \times$ theoretical ultimate moment of branch member may be used.

- iii. Further analysis of the test data using a polynomial regression model (9.1.3) may give a slightly more improved result, but would probably complicate the design equation considerably.

P (TEST) . V. P (CALC) FROM EQN. 9.5

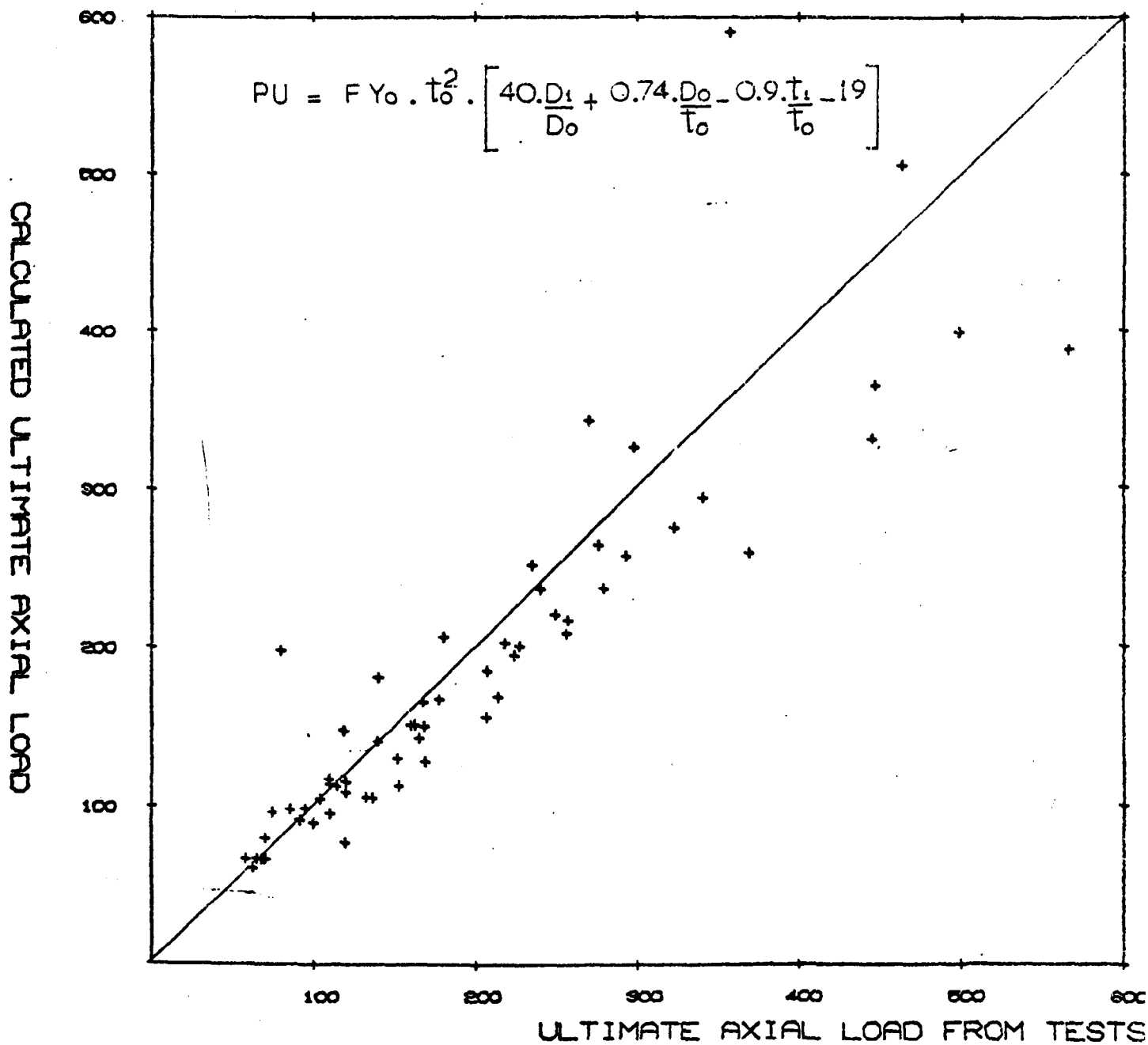


Figure 173. P_U (test) v P_U calculated from equation 9.5

P (TEST) . V. P (CALC) FROM EQN. 9.7

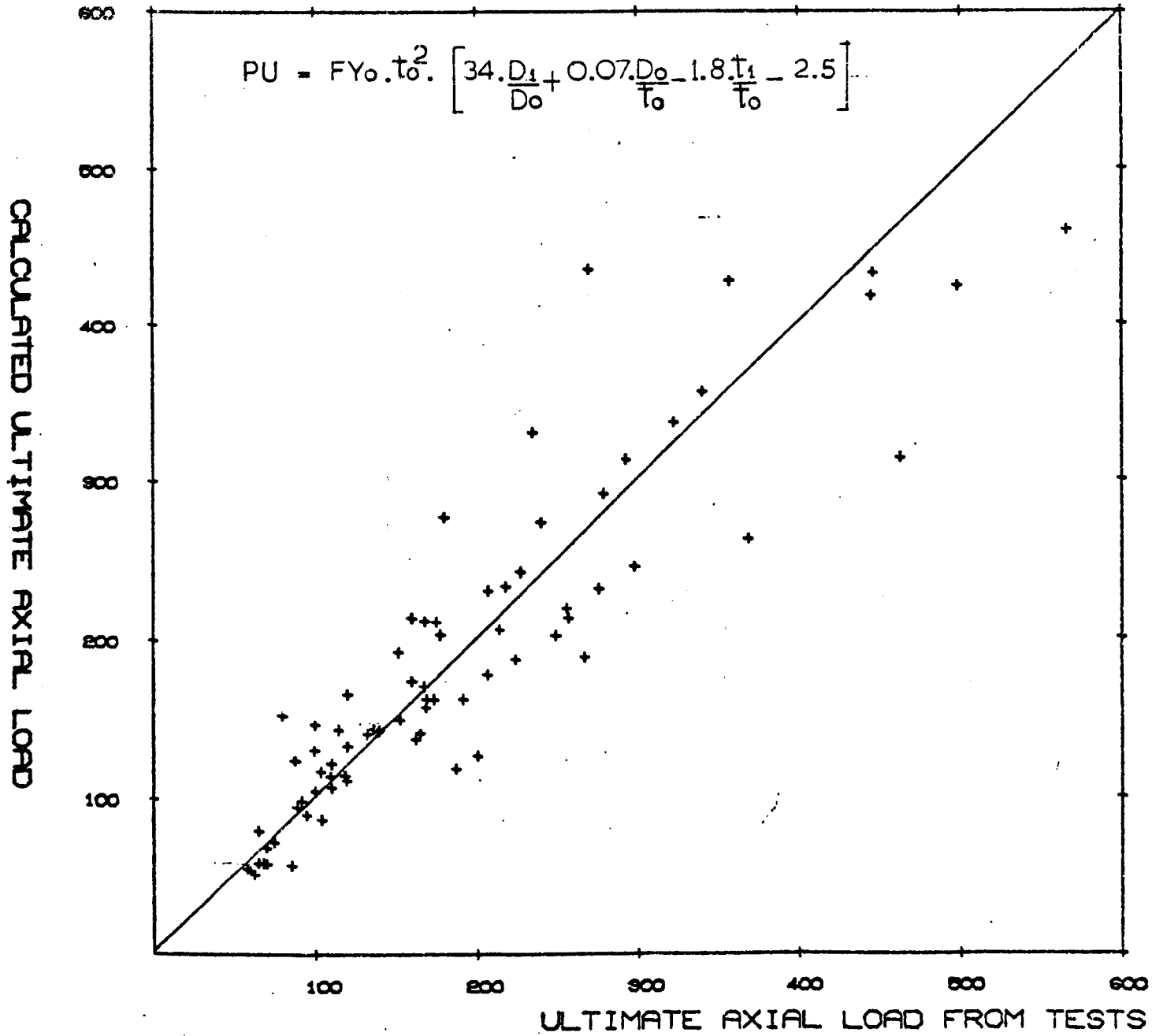


Figure 174. $P_U(\text{test})$ v P_U calculated from equation 9.7.

P (TEST) . V. P (CALC) FROM EQN. 9.8

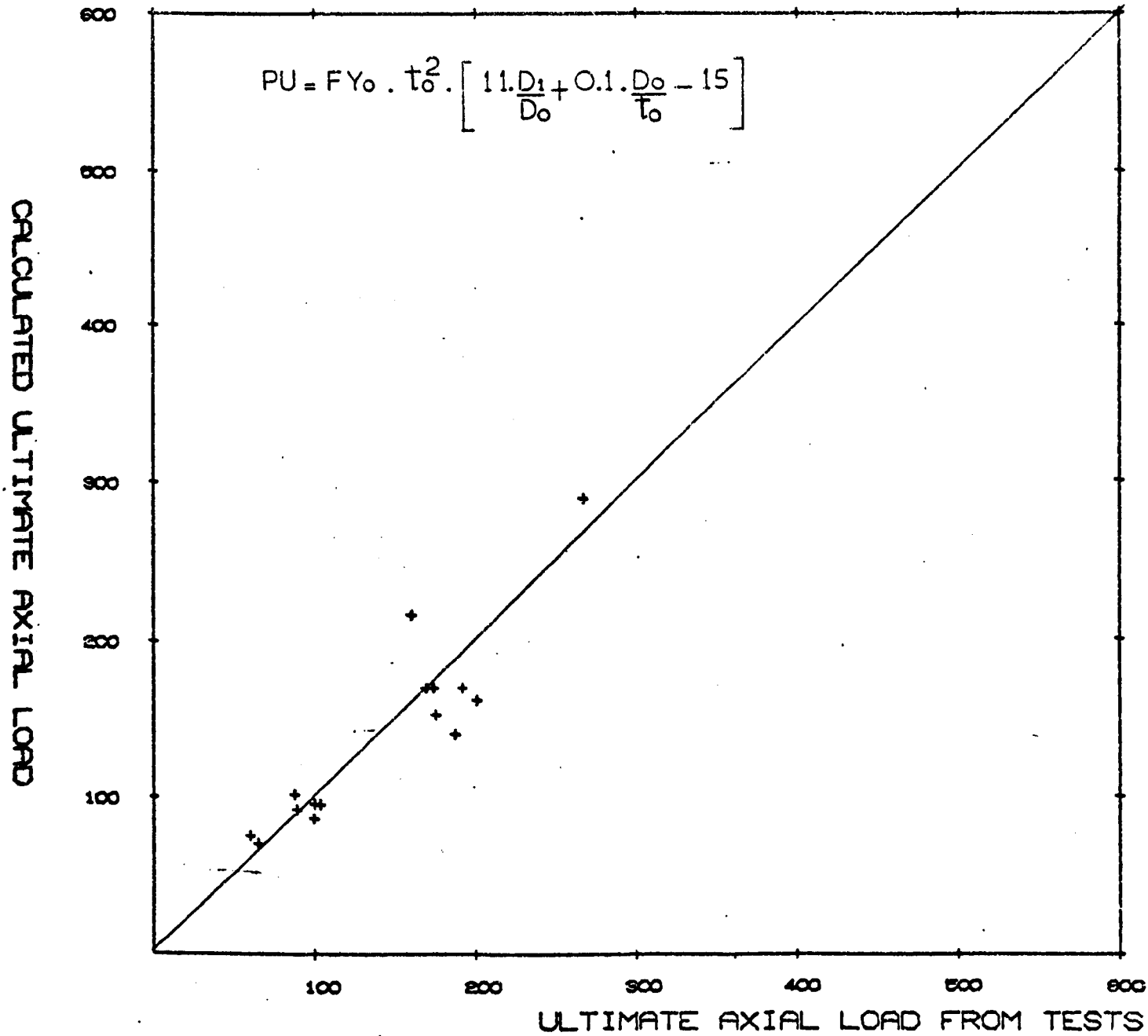


Figure 175. P_u (test) v P_u calculated from equation 9.8.

M (TEST) . V. M (CALC) FROM EQN. 9.12

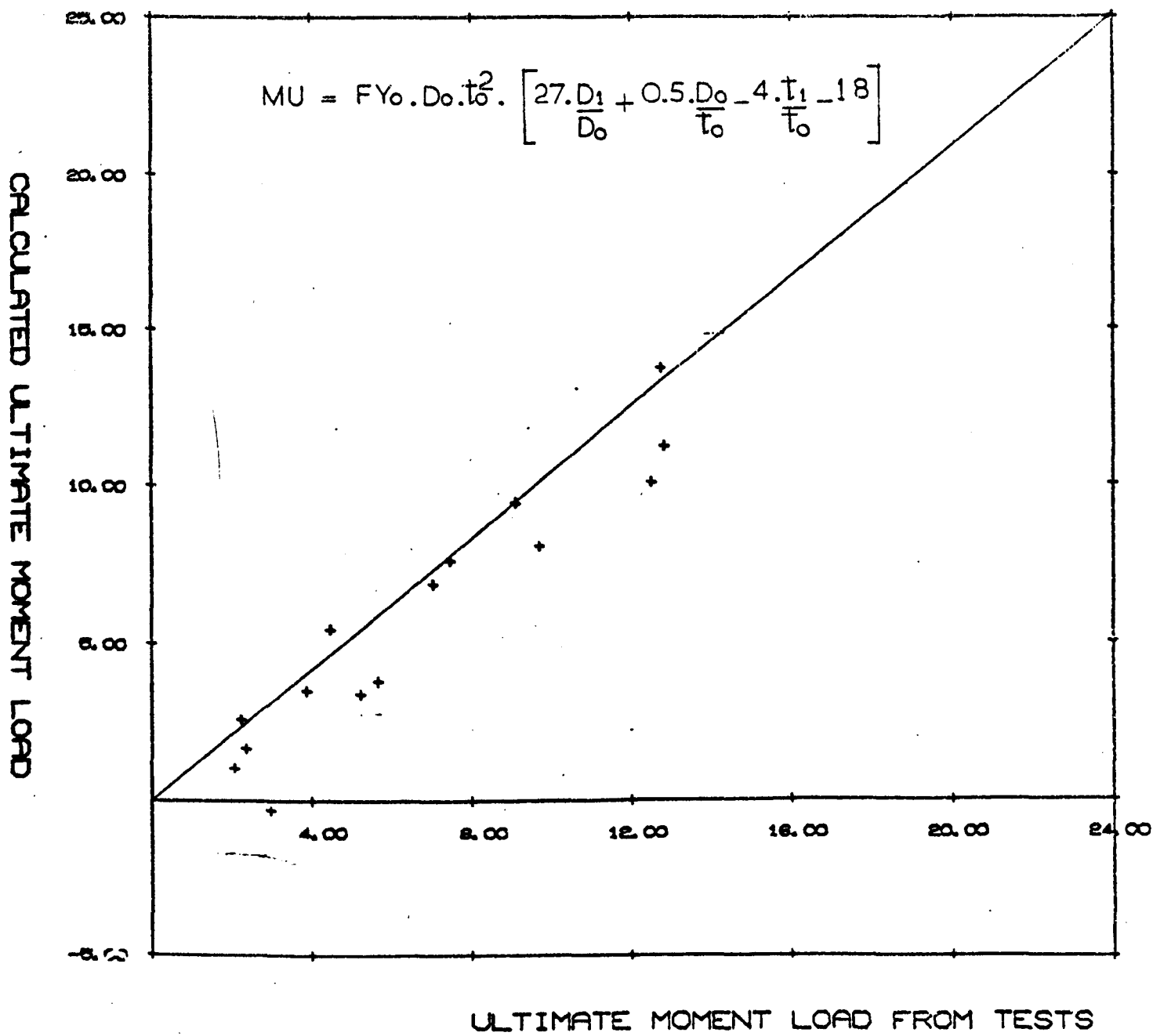


Figure 176. Pu(test) v Pu calculated from equation 9.12.

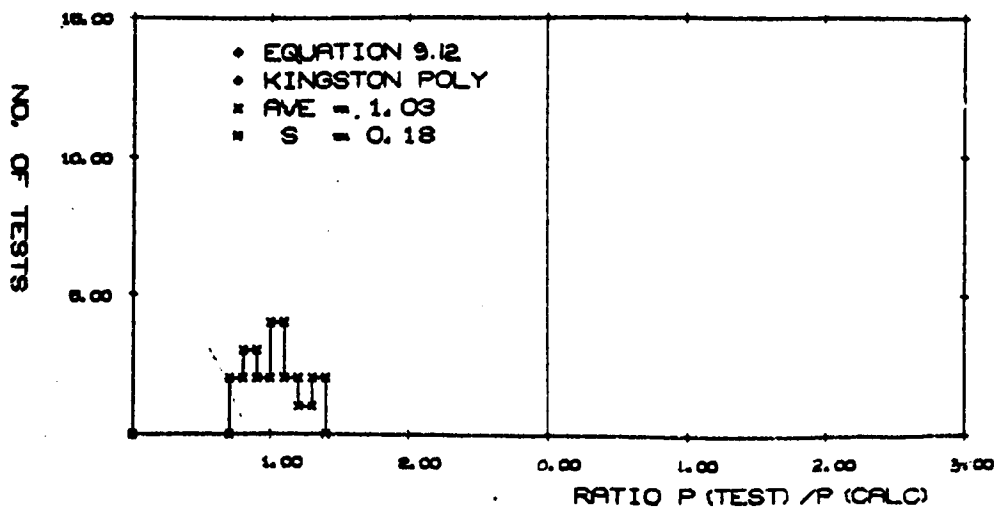
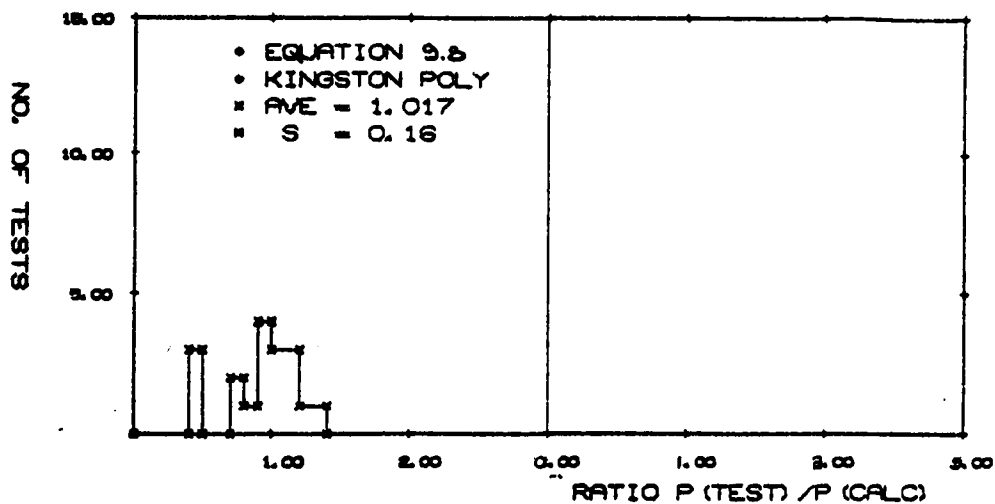
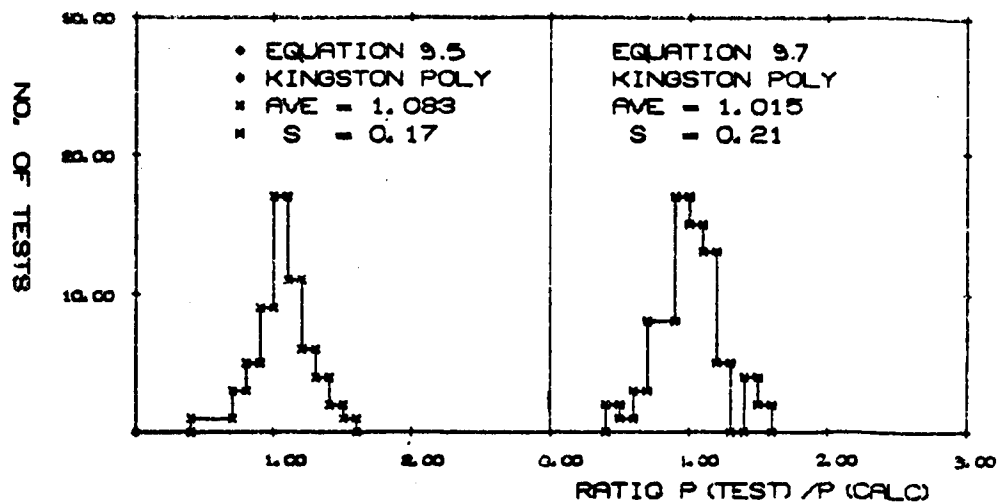


Figure 177. Histograms for equations 9.5, 9.7, 9.8, 9.12 applied to t-joint tests.

CHAPTER 10

FINAL CONCLUSIONS

10.1. Equations Proposed From The Present Experimental Study (Chapter 9)

T-Joints

10.1.1. Ultimate Axial Load (Pu) - (Sections 7.1 and 9.1)

$$P_u = f_{y0}.t_o^2 \left[40 \frac{d_1}{d_o} + 0.74 \frac{d_o}{t_o} - 0.9 \frac{t_1}{t_o} - 19.0 \right] \dots\dots\dots(10.1)$$

$$\text{for } d_1/d_o = 0.4 - 1.0$$

$$d_o/t_o = 15 - 45$$

$$P_u = f_{y0}.t_o^2 \left[11 \frac{d_1}{d_o} - 0.1 \frac{d_o}{t_o} + 15.0 \right] \dots\dots\dots(10.2)$$

$$\text{for } d_1/d_o = 0.4 - 1.0$$

$$d_o/t_o > 45$$

10.1.2. Ultimate Moment Load (Mu) - (Sections 7.2 and 9.2)

$$M_u = f_{y0}.d_o.t_o^2 \left[27 \frac{d_1}{d_o} + 0.5 \frac{d_o}{t_o} - 4 \frac{t_1}{t_o} - 18.0 \right] \dots\dots\dots(10.3)$$

$$\text{for } d_1/d_o = 0.5 - 1.0$$

$$d_o/t_o > 20$$

$$M_u = 0.75 \times \text{ultimate moment of brace member } (S_1.f_{y1})$$

$$\text{for } d_1/d_o < 0.5$$

$$d_o/t_o < 20$$

10.1.3. Combined Axial and Moment Load (Sections 7.3 and 9.3)

$$\frac{M}{M_u} + \frac{P}{P_u} = 1.0 \dots\dots\dots(10.4)$$

$$\text{for } d_1/d_o = 0.25 - 1.0$$

$$d_o/t_o = 15 - 40$$

10.2. Equations Proposed From Statistical Review (Chapter 3)

10.2.1. K-Joints

(i) With Gap

$$P_u = f_{yo} \cdot \left[\frac{d_o}{2} \right]^2 \cdot \left[\frac{d_o}{2t_o} \right]^{-1.5} \cdot \left(1 + 6.52 \frac{d_1}{d_o} \right) (1 - 0.26 \cos^2 \theta) f(g/d_o) \dots (10.5)$$

$$f(g/d_o) = 1.75 - 2.65 g/d_o \quad 0 \leq g/d_o \leq 0.23$$

$$f(g/d_o) = 1.15 - 0.06 g/d_o \quad 0.23 \leq g/d_o \leq 1.0$$

Limitations are: $10 \leq d_o/t_o \leq 50$; $0.25 \leq d_1/d_o \leq 0.85$

(ii) With Overlap

(a) $0.25 \leq d_1/d_o \leq 0.85$

$$P_u = \frac{f_{yo}}{\sqrt{3}} \cdot [t_o \cdot U_c + 2 \cdot t_1 \cdot U_b] \dots (10.6)$$

(See Appendix B page 40 for lengths U_b and U_c).

Limitations are: $10 \leq d_o/t_o \leq 50$.

(b) $0.85 \leq d_1/d_o \leq 1.0$

$$P_u = \frac{f_{yo} \cdot \pi \cdot d_1 \cdot t_o}{\sqrt{3}} \dots (10.7)$$

Limitations are: $10 \leq d_o/t_o \leq 50$

10.2.2. X-Joints

Braces in Compression or Tension

$$P_u = K f_{yo} \cdot d_1 \cdot t_o / \left[\frac{d_1}{d_o} \cdot \left(1.2 - \frac{d_1}{d_o} \right) \frac{d_o}{2t_o} \right] \dots (10.8)$$

$K = 3.71$ for compression in braces.

$K = 5.5$ for tension in braces.

Limitations are: $0.25 \leq d_1/d_o \leq 0.85$; $10 \leq d_o/t_o \leq 50$.

10.3. General.

10.3.1. T-Joints

(i) Axial Load

Joint strength under axial load is a function of the parameters d_1/d_o and d_o/t_o . For d_1/d_o greater than 0.5 the mode of failure is normally plastic deformation of the chord wall. The parameter t_1/t_o does not significantly affect the ultimate axial strength of the joint.

The formula deduced from the present experimental investigation gave a better result when applied to all T-joint test results than any of the formulae reviewed in Chapter 3.

(ii) Bending Load

Joint strength under bending load was a function of the parameters d_1/d_o , d_o/t_o and t_1/t_o . When d_o/t_o is less than 20 then the joint strength is independent of the parameter d_o/t_o and is a function only of the branch member geometry.

The formula deduced from the present experimental investigation was the only formula based on test results presented at this moment in time.

(iii) Combined Axial and Moment Loading

When a T-joint is subjected to combined axial and bending loading the dominant load is the axial load. Any eccentricity of axial load causes failure in the joint due to excessive applied moment.

For the parameter range of joints tested the relationship between M/M_u and P/P_u was found to approximate to unity.

Points of high stress under combined loading change position according to the proportions of axial and bending load applied e.g. high axial load and low moment load may cause a hot spot stress at a different point to a high moment load and low axial load. This phenomenon is seen to occur for higher values of d_1/d_o .

When the combination of axial load and moment was such that the joint failed to sustain both loads the moment carrying capacity decreased non-linearly, as rotation occurred at the joint.

10.3.2. K-Joints

(i) Gapped Joints

A large number of existing test results are available for K-joints. Analysis of the various proposed formulae for gapped K-joints shows that the formula of Washio, Togo, later modified by Harlicot, Mouty and Tournay gave the best results.

(ii) Overlapped Joints

Very little experimental evidence exists for the strength of overlapped K-joints. The formula proposed as a result of the present study (Chapter 3) is a lower bound solution and does not represent the expected failure mechanism for some joint parameters.

10.3.3. X-Joints

The formula proposed by Det Norske Veritas* gave the best results for all the existing X-joint tests.

*This formula is identical to that proposed by Harlicot, Mouty and Tournay, when simplified.

CHAPTER 11

RECOMMENDATIONS FOR FURTHER RESEARCH

11.1. Analytical Work

(i) Further development of computer aided data presentation is required. This should be fully interfaced and would enable complete presentation of, for example, the results of finite element analyses. This type of system is urgently required since at present most methods require a degree of manual involvement.

(ii) Expansion of the present elastic finite element analysis of T-joints to include K, N and X joints would be a natural progression. Presentation of the results in chart or tabular form would enable the steel designer to locate areas of high stress in joints and perhaps implement measures to avoid them or contain them.

(iii) Inelastic finite element analysis of joints is required in order that theoretical correlation with ultimate load tests can be attempted. This work is continuing, at present, at Imperial College and Kingston Polytechnic.

(iv) Since the amount of theoretical work being carried out on joints has recently increased it may be of interest to attempt an analysis using yield line methods. This method has been applied to joints in R.H.S., with some success, at Nottingham University.

(v) Further numerical analysis of existing test results and more recent test results as they become available may be carried out to confirm the applicability of the existing formulae for certain parameter ranges.

11.2. Experimental Work

11.2.1. T-Joints

(i) Further ultimate longitudinal moment tests are required for joints with small d_1/d_o ratios, in order to confirm the existing results.

(ii) Expansion of the range of applicability of the ultimate moment formula and the proposed interaction relationship between moment and axial load may be achieved by carrying out a few additional tests.

(iii) It is proposed that tests be carried out to find the ultimate circumferential moments in welded T-joints, and their interaction relationship with longitudinal moments and axial loads. This combination of load may occur in three-dimensional vierendeel structures where cross bracings may introduce torsional moments which are circumferential to the main chord members.

11.2.2. K-Joints

(i) It is proposed that tests be carried out to find the effect of moments, both primary and secondary, which may be introduced at K or N type joints.

(ii) It is proposed that an extensive study of overlapped K or N joints be carried out. This would produce a design formula and test results which might lead to less conservative joint design for this type of joint.

The present design rules for overlapped joints are generally lower bound solutions based on an estimated punching shear mechanism.

REFERENCES

1. Giddings, T.W., British Steel Corporation, Fire Resistant Construction Using H.S.S., I.S.H.S.S., May 1977.
2. Kollbrunner, C.F., Steel Buildings and Fire Protection in Europe, ASCE/IABSE Report, New York, October 1958.
3. American Society for Testing Materials, Fire Tests on Building Construction and Materials, ASTM E119-67.
4. STELCO, Implications of the Canadian Standards Association STD 640.20 on the Manufacture of Hollow Structural Sections.
5. d'Huart, J., Design of Concrete Filled H.S.S. Columns, University of Liege, I.S.H.S.S., May 1977.
6. Dundrova, V., Tubular Steel Structures, Acta Technica (Budapest) Vol. 35/36, 1961.
7. Blair Reber, J., Ultimate Strength Design of Tubular Joints, ASCE Journal of Structural Division, 1973.
8. Beale, Noel and Toprac, Stress Investigation of Welded Tubular Connections, University of Texas, 1964.
9. Toprac, A.A., Johnson and Noel, An Investigation of Stresses in T-Joints, University of Texas, 1966.
10. Toprac, A.A., Stresses at Intersections of Tubes: Cross and T-Joints, University of Texas, 1967.
11. Marshall and Toprac, Basis for Tubular Joint Design Codes, ASCE National Structural Engineering Meeting, 1973.
12. Toprac, A.A. et al., Studies on Tubular Joints in Japan - Part 1 Review of Research Reports, Report for the Welding Research Council, Tubular Structures Committee, September 1968.

13. Bouwkamp, J.C., Behaviour of Tubular Truss Joints Under Static Loads: Phase II, University of California, Berkeley, 1968.
14. Kurobane and Konomi, Fatigue Strength of Tubular K-Joints, 1974.
15. Kato, T., Design Strength of Tubular Joints, Nippon Steel Technical Report, Overseas No. 6, 1974.
16. Naka, Kato and Kanatani, Experimental Study on Welded Tubular Connections, University of Tokyo, 1966.
17. Kurobane, Y., Welded Truss Joints of Tubular Structural Members, University of Kumamoto, 1964.
18. Washio and Kurobane, Truss Joint in Tubular Steel Structures, University of Osaka, 1963, Vol. 13 No. 553.
19. Report of the Research on Node Point of Marine Steel Structures - Iran and Steel Institute of Japan. Nippon Steel Technical Report Overseas. No. 6., December 1974.
20. Washio, K., Togo, T., and Mitsui, Y., Experimental Study on Local Failure of Chords in Tubular Truss Joints, Part (I) - Technology Reports, Osaka University, Vol. 18, No. 850, (1968). Part (II) - Technology Reports, Osaka University, Vol. 19, No. 874, (1969).
21. Coutie, Davies and Dasgupta, Tubular Joints in Trusses, University of Nottingham, 1970. Private communication-Draft copy.
22. Johnson, L.P., Welded Tubular Joint Problem in Offshore Oil Structures, Journal of Petroleum Technology, May 1967, P.702.

23. Hlavacek, V., Strength of Welded Tubular Joints in Lattice Girders, Building Research Institute, University of Prague.
24. Roark, R.J., Strength and Stiffness of Cylindrical Shells Under Concentrated Loading, Journal Appl. Mech., ASME (1935), A-147.
25. Roark, R.J., Formulas for Stress and Strain, McGraw Hill.
26. Kellogg, M.W. & Co., Design of Piping Systems, Second Ed., John Wiley & Sons Inc., New York (1956) 85-86.
27. American Petroleum Industry - Recommended Practice for Planning, Designing and Constructing Fixed Offshore Platforms, Fifth Ed., 1974.
28. American Welding Society - Design of New Tubular Structures, 1974.
29. Det Norske Veritas - Rules for the Design and Construction and Inspection of Fixed Offshore Structures.
30. Visser, W., On the Structural Design of Tubular Joints, Sixth Offshore Technology Conference, Houston, Texas, 1974.
31. Harlicot, Mouty, Tournay, Joints Between Hollow Sections, CIDECT Working Group on Joints, May 1976.
32. Nedai, A., Über die Spannungsverteilung in Einer Durch Eine Einzelkraft Belasteten Rechteckigen Platte, Der Bauingenieur, January 1922, P.51.
33. Hartenberg, R.S., The Strength and Stiffness of Thin Cylindrical Shells on Saddle Supports, Doctors Dissertation, University of Wisconsin, 1941.

34. Wilson, W.M., and Olson, E.D., Tests on Cylindrical Shells, Eng. Exp. Sta. Univ. Ill. Bull. 331, 1941.
35. Dutta, Tragfähigkeit der geschweißten Verbindungen aus Hohlprofilen mit Kreisquerschnitt, Dusseldorf, 1972.
36. Lyons, L.P.R., A General Finite Element System with Special Reference to the Analysis of Cellular Structures, Ph.D., Thesis, Imperial College, London, January 1977.
37. Irons, B.M., A Frontal Solution Program for Finite Element Analysis, Int. J. Num. Meth. Eng., Vol. 2 (1970), 5-32.
38. ASKA Reference Manual, Univ. of Stuttgart, 150 - Report No. 73, 1971.
39. Zienkiewicz, O.C., The Finite Element Method in Engineering Science, London, McGraw-Hill, 1971.
40. Irons, B.M., and Kan, D.K.Y., Equation Solving Algorithms for the Finite Element Method, O.N.R. Symp. on Numerical and Computer Methods in Structural Mechanics, Univ. of Illinois, (1971).
41. Irons, B.M., The Semiloof Shell Element, Finite Elements for Thin Shells and Curved Members, Chapter 11, ed. D.G. Ashwell & R. H. Gallagher, Wiley, London, 1976.
42. Martins, R.A.F., Finite Element Eigenvalue Solution Employing the Semiloof Shell Element, M.Sc., Thesis, University of Wales, Swansea, 1974.
43. Fuchs, G., Roy, J.R., and Schrem, E., Hypermetric Solution of Large Sets of Symmetric Positive-Definite Linear Equations, Computer Methods in Applied Mechanics and Engineering 1, 1972.

44. Meyer, C., Solution of Linear Equations - State-of-the-Art, J. of Struct. Div. ASCE, July, 1973.
45. Meyer, C., Special Problems Related to Linear Equation Solvers, J. of Struct. Div. ASCE, April, 1975.
46. Wilson, E.L., Bathe, K.J., and Doherty, W.P., Direct Solution of Large Systems of Linear Equations, Computers and Structures, Vol. 4., 1974.
47. Melosh, R.J., and Bamford, R.M., Efficient Solution of Load-Deflection Equations. J. of Struct. Div. ASCE, 95, ST4, Proc. Paper 6510 (1969) 661-676.
48. Baldwin, J.T., Razzaque, A., and Irons, B., Shape Function Subroutine for an Isoparametric Thin Plate Element, Int. J. Num. Meth. in Eng., Vol. 7, 431-440, 1973.
49. Allman, D.J., Triangular Finite Elements for Plate Bending with Constant and Linearly Varying Bending Moments, IUTAM Colloquium on High-Speed Computing of Elastic Structures, Univ. of Liege, Belgium, 1970.
50. Razzaque, A., Program for Triangular Bending Elements with Derivative Smoothing, Int. J. Num. Meth. Eng., 6 (1973) 333-343.
51. Irons, B.M., and Draper, K.J., Inadequacy of Node Connections in a Stiffness Solution for Plate Bending, JAIAA, 3, 5, May 1965.
52. Bazeley, G.P. et al., Triangular Elements in Plate Bending - Conforming and Non-conforming Solutions, Proc. Conf. Matrix Methods Struct. Mech. WPAFB, Ohio, Oct. 1965.
53. Clough, R.W., and Tocher, J.L., Finite Element Stiffness Matrices for Analysis of Plates in Bending. Proc. Conf. Matrix Methods Struct. Mech. WPAFB, Ohio, Oct. 1965.

54. Clough, R.W., and Felippa, C.A., A Refined Quadrilateral Element for Analysis of Plate Bending, Proc. 2nd Conf. Matrix Methods in Struct. Mech. WPAFB 1968.
55. de Vaubeke, B.F., A Conforming Quadrilateral Element for Plate Bending, Int. J. of Solids Struct., Jan. 1968.
56. Bettess, P., The Finite Element Method for Plates in Flexure, M.Sc., Thesis, Imperial College, 1968.
57. Pian, T.H.H., Derivation of Element Stiffness Matrices by Assumed Stress Distributions, AIAA J., 2, 1333-1336, 1964.
58. Allman, D.J., A Simple Cubic Displacement Element for Plate Bending, Int. J. Numer. Meth. Eng., 1976, 10, 263-281.
59. Severn, R., and Taylor, P., The Finite Element Method for Flexure of Slabs when Stress Distributions are Assumed, Proc. Instn. Civ. Engrs. 1966, 34, pp. 153-170.
60. Wolf, J.P., Generalised Stress Models for Finite Element Analysis, Ph.D., Thesis, Institut fur Banstatik, Zurich, 1974.
61. Torbe, I., and Church, K., A General Quadrilateral Plate Element, Int. J. Num. Meth. Eng. Vol. 9, 855-868, 1975.
62. Cook, R.D., and Samaan, G.L., Observations Regarding Assumed-Stress Hybrid Plate Elements, Int. J. Num. Meth. Eng., Vol. 8, No. 3, 1974.
63. Pian, T.H.H., Hybrid Models, Conf. on Num. and Comp. Meth. In Struct. Mech. Urbana, Illinois, 1971.
64. Irons, B., and Razzaque, A., Experience with the Patch Test, from the Mathematical Foundations of the Finite Element Method with Applications to Partial Differential Equations, Academic Press, 1972.

65. Irons, B.M., The Patch Test, International Report, Univ. of Calgary, 1973.
66. Strang, G., and Fix, G.J., An Analysis of the Finite Element Method, Prentice-Hall, 1973.
67. Irons, B.M., and Razzaque, A., Shape Function Formulations for Elements Other Than Displacement Models. Conference on Variational Methods in Engineering, Southampton University, 1972.
68. Fried, I., Shear in C^0 and C^1 Bending Finite Elements, Int. J. Solids Struct., Vol. 9, 449-460, 1973.
69. Key, S.W., and Bersinger, Z.E., The Analysis of Thin Shells With Transverse Shear Strains by the Finite Element Method, Proc. Conf. Matrix. Meth. Struct. Mech., WPAFB, Ohio, 1965.
70. Melosh, R.J., A Flat Triangular Shell Element Stiffness Matrix, Proc. Conf. Matrix Meth. Struct. Tech., WPAFB, Ohio, 1965.
71. Stricklin, J.A. et al., A Rapidly Converging Triangular Plate Element, J. AIAA, Vol. 7, 1969.
72. Utku, S., Stiffness Matrix for the Triangular Elements of Non-Zero Gaussian Curvature, J. AIAA, Vol. 5, 1659-1667, 1967.
73. Irons, B.M., and Razzaque, A., A Further Modification to Ahmad's Shell Element, Int. J. Num. Meth. Eng., Vol. 5, (1973), 588-589.
74. Irons, B.M., The Semiloof Shell Element. Lecture notes, International Research Seminar on the Theory and Application of Finite Elements, July 1973, Calgary University, Canada.

75. Irons, B.M., Un Nouvel Element de Coques Generales Semiloof, Methods de Calcul Scientifique et Technique, Colloques IRIA, Rocquencourt, Paris 1973.
76. Irons, B.M., The Semiloof Shell Element, Internal Report, Univ. of Calgary, 1973.
77. Wampner, G.A., Oden, J.T., and Kross, K.K., Finite Element Analysis of Thin Shells, J. Eng. Mech. Div. ASCE 94, 1273-1294, 1968.
78. Razzaque, A., Finite Element Analysis of Plates and Shells, Ph.D., Univ. of Wales, Swansea, 1973.
79. Ahmad, S. et al., Analysis of Thick and Thin Shell Structures by Curved Finite Elements, Int. J. Numer. Meth. Eng., 1970, 2, 419-451.
80. Bates, D., Curved, Super-Parametric Finite Elements in the Analysis of Thick and Thin Plates and Slabs, M.Sc., Thesis, Imperial College, 1972.
81. Hinton, E., Razzaque, A., Zienkiewicz, O.C., and Davies, J.D., A Simple Finite Element Solution for Plates of Homogeneous, Sandwich and Cellular Construction, Proc. Instn. Civ. Engrs.
82. Pawsey, S., and Clough, R.W., Improved Numerical Integration of Thick Shell Finite Elements, Int. J. Num. Meth. Eng. Vol. 3, 1971.
83. Too, J.J.M., Two Dimensional Plate Shell and Finite Prism Isoparametric Elements and Thin Applications, Ph.D., Thesis, University of Wales, Swansea, 1971.
84. Barlow, J., Optimal Stress Locations in Finite Element Models, Int. J. Num. Meth. in Eng., Vol. 10, 243-251, 1976.

85. Javadi, F.H.S., Joints of Composite Construction in Marine Structures, Ph.D., Thesis, Imperial College, June 1979.
86. Faddeeva, V.N., Computational Methods of Linear Algebra, Dover Publications.
87. Adini, A., and Clough, R.W., Analysis of Plate Bending by the Finite Element Method and Report to Nat. Sci. Found/USA, G.7337, 1961.
88. Cowper, G.R., Gaussian Quadrature Formulas for Triangles, Int. J. for Num. Meth. Eng. 7 (1973), 405-408.
89. Cook, R.D., More on Reduced Integration and Isoparametric Elements, Int. J. Num. Meth. Eng. (8), 141-148, 1972.
90. Plantema, F.J., Sandwich Construction, Wiley, 1966.
91. Zienkiewicz, O.C., Taylor, R.L., and Too, J.M., Reduced Integration Technique in General Analysis of Plates and Shells, Int. J. Num. Meth. Eng., 1971, 3, 275-290.
92. Zienkiewicz, O.C., and Phillips, D.V., An Automatic Mesh Generation Scheme for Plane and Curved Surfaces by Isoparametric Coordinates, Int. J. Num. Meth. Eng., Vol. 3, 4, 1971, 519-528.
93. Zienkiewicz, O.C., Recent Developments, Trends and Application of Finite Element Methods, Keynote address, Int. Conf. on Finite Element Meth. in Eng., Adelaide, December 1976.
94. Danning, W.E., Statistical Adjustment of Data, John Wiley & Sons, (1946).
95. Stamenkovic, A., Sparrow, K.D., and Irving D., Review of Existing Methods for the Design of Welded Joints in Circular Hollow Sections - Part 1 - T-Joints, Internal Report to British Steel Corporation, 1979.

96. Stamenkovic, A., and Sparrow, K. D., An Experimental Investigation of the Behaviour of Welded Joints Between Circular Hollow Sections, Internal Report to the Tubes Division, British Steel Corporation, March 1975.
97. Andrian, L.E., Sewell, K.A., and Womark, W.R., Partial Investigations of Directly Loaded Pipe Joints, Unpublished Thesis, Southern Methodist University, Dallas (1958).
98. Eastwood and Wood, Recent Research on Joints in Tubular Structures, Canadian Structural Engineering Conference, 1970.
99. Private Communication of the Results of K-Joint Tests Carried out at Delft University, 1976.
100. Wardenier, J., Investigation Into the Static Strength of Welded Warren Type Joints Made of Circular Hollow Sections, Stevin Report No. 6-77-5, April 1977.
101. Pan, R.B., and Plummer, F.B., Ultimate Strength of Tubular Joints, O.T.C. 2644, Houston 1976.
102. Kurobane, Y., Makino, Y., and Mitsui, Y., Ultimate Strength Formulae for Simple Tubular Joints, Kumamoto Univ., May, 1976.
103. Irons, B.M., Numerical Integration Applied to Finite Element Methods, Conf. Use of Digital Computers in Structural Engineering, Newcastle Univ., 1966.
104. Hendry, A.W., Plastic Analysis and Design of Mild Steel Vierendeel Girders
105. B.S.449: Part II: 1969. Specification for the Use of Structural Steel in Building.

APPENDIX A

TABLE 1 INPUT DATA FOR CASE STUDIES SPECIMEN DIMENSIONS & TEST RESULTS-PAGE 1

TEST NO.	SPECIMEN NO.	EXPTAL. (PULT)		BRANCH D (IN)	T (IN)	WELD GAP (MM)		CHORD DC (IN)		JOINT ANGLE	YIELD-STRESS BASIC		PARAMETERS		
		KIPS						DC (IN)	TC (IN)		SHEAR	D/DC	DC/TC	T/TC	
1	102.00	2.88	0.200	0	12.75	0.500	90.00	33.0	19.1	0.23	25.50	0.40			
2	56.00	2.88	0.200	0	12.75	0.250	90.00	33.0	19.1	0.23	51.00	0.80			
3	54.00	3.50	0.220	0	16.00	0.250	90.00	33.0	19.1	0.22	64.00	0.88			
4	82.00	5.56	0.260	0	12.75	0.250	90.00	33.0	19.1	0.44	51.00	1.04			
5	105.00	5.56	0.190	0	8.63	0.250	90.00	33.0	19.1	0.64	34.52	0.76			
6	70.00	5.56	0.260	0	12.75	0.250	90.00	33.0	19.1	0.44	51.00	1.04			
7	82.00	5.56	0.260	0	12.75	0.250	90.00	33.0	19.1	0.44	51.00	1.04			
8	100.00	5.50	0.260	0	5.50	0.260	90.00	36.9	21.3	1.00	21.15	1.00			
9	77.30	4.50	0.180	0	5.50	0.260	90.00	36.9	21.3	0.82	21.15	0.69			
10	66.10	4.00	0.180	0	5.50	0.260	90.00	36.9	21.3	0.73	21.15	0.69			
11	47.00	3.00	0.130	0	5.50	0.260	90.00	36.9	21.3	0.55	21.15	0.50			
12	29.00	1.90	0.090	0	5.50	0.260	90.00	36.9	21.3	0.35	21.15	0.35			
13	125.40	5.50	0.260	0	5.50	0.260	90.00	36.9	21.3	1.00	21.15	1.00			
14	71.70	4.00	0.130	0	5.50	0.260	90.00	36.9	21.3	0.73	21.15	0.50			
15	62.70	3.50	0.130	0	5.50	0.260	90.00	36.9	21.3	0.64	21.15	0.50			
16	33.60	1.90	0.090	0	5.50	0.260	90.00	36.9	21.3	0.35	21.15	0.35			
17	29.12	1.63	0.090	0	5.50	0.260	90.00	36.9	21.3	0.31	21.15	0.35			
18	26.82	1.34	0.090	0	5.50	0.260	90.00	36.9	21.3	0.24	21.15	0.35			
19	82.88	5.50	0.180	0	5.50	0.180	90.00	36.9	21.3	1.00	30.56	1.00			
20	60.48	4.50	0.160	0	5.50	0.180	90.00	36.9	21.3	0.82	30.56	0.89			
21	51.52	4.00	0.160	0	5.50	0.180	90.00	36.9	21.3	0.73	30.56	0.89			
22	35.84	3.00	0.160	0	5.50	0.180	90.00	36.9	21.3	0.55	30.56	0.89			
23	23.52	1.90	0.090	0	5.50	0.180	90.00	36.9	21.3	0.35	30.56	0.50			
24	58.24	4.50	0.160	0	4.50	0.160	90.00	36.9	21.3	1.00	28.12	1.00			
25	38.10	3.50	0.130	0	4.50	0.160	90.00	36.9	21.3	0.78	28.12	0.81			
26	31.36	3.00	0.130	0	4.50	0.160	90.00	36.9	21.3	0.67	28.12	0.81			
27	24.64	2.38	0.110	0	4.50	0.160	90.00	36.9	21.3	0.53	28.12	0.69			
28	15.68	1.34	0.090	0	4.50	0.160	90.00	36.9	21.3	0.30	28.12	0.56			
29	38.80	4.50	0.190	0	8.63	0.190	90.00	36.9	21.3	0.52	45.42	1.00			
30	112.20	4.50	0.190	0	8.63	0.260	90.00	36.9	21.3	0.52	30.82	0.68			
31	192.50	4.50	0.190	0	8.63	0.410	90.00	36.9	21.3	0.52	21.05	0.46			
32	82.88	4.50	0.190	0	12.75	0.250	90.00	36.9	21.3	0.35	51.00	0.76			
33	133.90	4.50	0.190	0	12.75	0.380	90.00	36.9	21.3	0.35	33.55	0.50			
34	223.10	4.50	0.190	0	12.75	0.500	90.00	36.9	21.3	0.35	25.50	0.58			
35	31.00	4.50	0.190	0	18.00	0.300	90.00	36.9	21.3	0.25	60.00	0.63			
36	117.00	4.50	0.190	0	18.00	0.380	90.00	36.9	21.3	0.25	47.37	0.50			
37	207.00	4.50	0.190	0	18.00	0.500	90.00	36.9	21.3	0.25	36.00	0.38			
38	13.60	1.34	0.090	42	2.38	0.100	45.00	60.0	34.6	0.56	23.80	0.90			
39	14.70	1.34	0.090	42	2.38	0.100	45.00	60.0	34.6	0.56	23.80	0.90			
40	15.10	1.34	0.090	42	2.38	0.100	45.00	60.0	34.6	0.56	23.80	0.90			
41	15.40	1.34	0.090	42	2.38	0.100	45.00	60.0	34.6	0.56	23.80	0.90			
42	15.40	1.34	0.090	42	2.38	0.100	45.00	60.0	34.6	0.56	23.80	0.90			
43	14.30	1.34	0.090	47	2.38	0.100	45.00	60.0	34.6	0.56	23.80	0.90			
44	14.90	1.34	0.090	47	2.38	0.100	45.00	60.0	34.6	0.56	23.80	0.90			
45	12.50	1.34	0.090	47	2.38	0.100	45.00	60.0	34.6	0.56	23.80	0.90			
46	14.70	1.34	0.090	47	2.38	0.100	45.00	60.0	34.6	0.56	23.80	0.90			
47	14.70	1.34	0.090	47	2.38	0.100	45.00	60.0	34.6	0.56	23.80	0.90			
48	16.50	1.34	0.090	47	2.38	0.130	45.00	60.0	34.6	0.56	18.31	0.69			
49	16.50	1.34	0.090	47	2.38	0.130	45.00	60.0	34.6	0.56	18.31	0.69			
50	17.60	1.34	0.090	47	2.38	0.130	45.00	60.0	34.6	0.56	18.31	0.69			
51	16.50	1.34	0.090	47	2.38	0.130	45.00	60.0	34.6	0.56	18.31	0.69			
52	16.50	1.34	0.090	47	2.38	0.130	45.00	60.0	34.6	0.56	18.31	0.69			
53	16.50	1.34	0.090	47	2.38	0.130	45.00	60.0	34.6	0.56	18.31	0.69			
54	15.40	1.34	0.090	47	2.38	0.130	45.00	60.0	34.6	0.56	23.80	0.90			
55	16.40	1.34	0.090	47	2.38	0.100	45.00	60.0	34.6	0.56	23.80	0.90			
56	15.90	1.34	0.090	47	2.38	0.100	45.00	60.0	34.6	0.56	23.80	0.90			
57	16.50	1.34	0.090	12	2.38	0.100	45.00	60.0	34.6	0.56	23.80	0.90			
58	16.90	1.34	0.090	12	2.38	0.100	45.00	60.0	34.6	0.56	23.80	0.90			
59	16.10	1.34	0.090	12	2.38	0.100	45.00	60.0	34.6	0.56	23.80	0.90			
60	17.40	1.34	0.090	12	2.38	0.100	45.00	60.0	34.6	0.56	23.80	0.90			
61	15.40	1.34	0.090	12	2.38	0.100	45.00	60.0	34.6	0.56	23.80	0.90			
62	15.40	1.34	0.090	17	2.38	0.100	45.00	60.0	34.6	0.56	23.80	0.90			
63	16.40	1.34	0.090	17	2.38	0.100	45.00	60.0	34.6	0.56	23.80	0.90			
64	17.40	1.34	0.090	17	2.38	0.130	45.00	60.0	34.6	0.56	18.31	0.69			
65	17.60	1.34	0.090	17	2.38	0.130	45.00	60.0	34.6	0.56	18.31	0.69			
66	18.00	1.34	0.190	17	2.38	0.130	45.00	60.0	34.6	0.56	18.31	0.69			
67	17.60	1.34	0.090	17	2.38	0.130	45.00	60.0	34.6	0.56	18.31	0.69			
68	18.00	1.34	0.090	17	2.38	0.130	45.00	60.0	34.6	0.56	18.31	0.69			
69	14.40	1.34	0.090	17	2.38	0.100	45.00	60.0	34.6	0.56	23.80	0.90			
70	16.00	1.34	0.090	17	2.38	0.100	45.00	60.0	34.6	0.56	23.80	0.90			
71	15.80	1.34	0.090	17	2.38	0.100	45.00	60.0	34.6	0.56	23.80	0.90			
72	16.20	1.34	0.090	17	2.38	0.100	45.00	60.0	34.6	0.56	23.80	0.90			
73	17.30	1.34	0.090	17	2.38	0.100	45.00	60.0	34.6	0.56	23.80	0.90			
74	18.00	1.34	0.090	17	2.38	0.100	45.00	60.0	34.6	0.56	23.80	0.90			
75	18.00	1.34	0.090	17	2.38	0.130	45.00	60.0	34.6	0.56	18.31	0.69			

TABLE 1 INPUT DATA FOR CASE STUDIES SPECIMEN DIMENSIONS & TEST RESULTS-PAGE 2

SPECIMEN NO.	EXPTAL P (ULT)	BRANCH D (IN)	T (IN)	WELD GAP (MM)	CHORD		JOINT YIELD-STRESS			PARAMETERS			
	KIPS				DC (IN)	TC (IN)	ANGLE	BASIC	SHFAR	D/DC	DC/TC	T/TC	
76	17.90	1.34	0.090	17	2.38	0.130	45.00	60.0	34.6	0.56	18.31	0.69	
77	17.90	1.34	0.090	17	2.38	0.130	45.00	60.0	34.6	0.56	18.31	0.69	
78	17.60	1.34	0.090	17	2.38	0.130	45.00	60.0	34.6	0.56	18.31	0.69	
79	22.40	1.34	0.090	17	2.38	0.100	45.00	60.0	34.6	0.56	23.80	0.90	
80	20.90	1.34	0.090	17	2.38	0.100	45.00	60.0	34.6	0.56	23.80	0.90	
81	20.90	1.34	0.090	17	2.38	0.100	45.00	60.0	34.6	0.56	23.80	0.90	
82	22.00	1.34	0.090	17	2.38	0.100	45.00	60.0	34.6	0.56	23.80	0.90	
83	23.10	1.34	0.090	17	2.38	0.100	45.00	60.0	34.6	0.56	23.80	0.90	
84	19.30	1.34	0.090	17	2.38	0.100	45.00	60.0	34.6	0.56	23.80	0.90	
85	18.60	1.34	0.090	17	2.38	0.100	45.00	60.0	34.6	0.56	23.80	0.90	
86	18.00	1.34	0.090	17	2.38	0.100	45.00	60.0	34.6	0.56	23.80	0.90	
87	18.00	1.34	0.090	17	2.38	0.100	45.00	60.0	34.6	0.56	23.80	0.90	
88	18.00	1.34	0.090	17	2.38	0.100	45.00	60.0	34.6	0.56	23.80	0.90	
89	18.00	1.34	0.090	17	2.38	0.130	45.00	60.0	34.6	0.56	18.31	0.69	
90	18.70	1.34	0.090	17	2.38	0.130	45.00	60.0	34.6	0.56	18.31	0.69	
91	19.60	1.34	0.090	17	2.38	0.130	45.00	60.0	34.6	0.56	18.31	0.69	
92	19.30	1.34	0.090	17	2.38	0.130	45.00	60.0	34.6	0.56	18.31	0.69	
93	18.70	1.34	0.090	17	2.38	0.130	45.00	60.0	34.6	0.56	18.31	0.69	
94	18.70	1.34	0.090	17	2.38	0.100	45.00	60.0	34.6	0.56	23.80	0.90	
95	18.70	1.34	0.090	17	2.38	0.100	45.00	60.0	34.6	0.56	23.80	0.90	
96	18.90	1.34	0.090	-17	2.38	0.100	45.00	60.0	34.6	0.56	23.80	0.90	
97	18.80	1.34	0.090	-17	2.38	0.100	45.00	60.0	34.6	0.56	23.80	0.90	
98	19.10	1.34	0.090	-17	2.38	0.100	45.00	60.0	34.6	0.56	23.80	0.90	
99	19.40	1.34	0.090	-17	2.38	0.100	45.00	60.0	34.6	0.56	23.80	0.90	
100	19.60	1.34	0.090	-17	2.38	0.130	45.00	60.0	34.6	0.56	18.31	0.69	
101	19.30	1.34	0.090	-13	2.38	0.130	45.00	60.0	34.6	0.56	18.31	0.69	
102	20.00	1.34	0.090	-13	2.38	0.130	45.00	60.0	34.6	0.56	18.31	0.69	
103	18.70	1.34	0.090	-13	2.38	0.130	45.00	60.0	34.6	0.56	18.31	0.69	
104	15.60	1.34	0.090	-13	2.38	0.100	45.00	60.0	34.6	0.56	23.80	0.90	
105	15.60	1.34	0.090	-13	2.38	0.100	45.00	60.0	34.6	0.56	23.80	0.90	
106	16.20	1.34	0.090	-13	2.38	0.100	45.00	60.0	34.6	0.56	23.80	0.90	
107	17.10	1.34	0.090	-13	2.38	0.100	45.00	60.0	34.6	0.56	23.80	0.90	
108	17.10	1.34	0.090	-13	2.38	0.100	45.00	60.0	34.6	0.56	23.80	0.90	
109	17.60	1.34	0.090	-13	2.38	0.100	45.00	60.0	34.6	0.56	23.80	0.90	
110	17.00	1.68	0.090	-13	2.38	0.100	45.00	60.0	34.6	0.71	23.80	0.90	
111	18.70	1.68	0.090	-13	2.38	0.100	45.00	60.0	34.6	0.71	23.80	0.90	
112	17.00	1.68	0.090	-13	2.38	0.100	45.00	60.0	34.6	0.71	23.80	0.90	
113	20.40	1.68	0.090	-13	2.38	0.100	45.00	60.0	34.6	0.71	23.80	0.90	
114	20.00	1.68	0.090	-13	2.38	0.100	45.00	60.0	34.6	0.71	23.80	0.90	
115	20.30	1.68	0.090	-13	2.38	0.100	45.00	60.0	34.6	0.71	23.80	0.90	
116	22.60	1.68	0.090	-13	2.38	0.100	45.00	60.0	34.6	0.71	23.80	0.90	
117	22.90	1.68	0.090	-13	2.38	0.100	45.00	60.0	34.6	0.71	23.80	0.90	
118	23.50	1.68	0.090	-13	2.38	0.100	45.00	60.0	34.6	0.71	23.80	0.90	
119	13.70	1.07	0.100	-13	2.38	0.100	45.00	60.0	34.6	0.45	23.80	1.00	
120	13.40	1.07	0.100	-13	2.38	0.100	45.00	60.0	34.6	0.45	23.80	1.00	
121	14.60	1.07	0.100	-13	2.38	0.100	45.00	60.0	34.6	0.45	23.80	1.00	
122	13.40	1.07	0.100	-13	2.38	0.100	45.00	60.0	34.6	0.45	23.80	1.00	
123	14.10	1.07	0.100	-13	2.38	0.100	45.00	60.0	34.6	0.45	23.80	1.00	
124	13.70	1.07	0.100	-13	2.38	0.100	45.00	60.0	34.6	0.45	23.80	1.00	
125	18.40	1.07	0.100	-13	2.38	0.100	45.00	60.0	34.6	0.45	23.80	1.00	
126	18.70	1.07	0.100	-13	2.38	0.100	45.00	60.0	34.6	0.45	23.80	1.00	
127	18.70	1.07	0.100	-13	2.38	0.100	45.00	60.0	34.6	0.45	23.80	1.00	
128	13.50	1.07	0.100	-13	2.38	0.100	45.00	60.0	34.6	0.45	23.80	1.00	
129	12.30	1.07	0.100	-13	2.38	0.100	45.00	60.0	34.6	0.45	23.80	1.00	
130	13.60	1.07	0.100	-13	2.38	0.100	45.00	60.0	34.6	0.45	23.80	1.00	
131	13.70	1.07	0.100	-13	2.38	0.100	45.00	60.0	34.6	0.45	23.80	1.00	
132	14.30	1.07	0.100	17	2.38	0.100	45.00	60.0	34.6	0.45	23.80	1.00	
133	12.30	1.07	0.100	17	2.38	0.100	45.00	60.0	34.6	0.45	23.80	1.00	
134	16.90	1.07	0.100	17	2.38	0.100	45.00	60.0	34.6	0.45	23.80	1.00	
135	16.30	1.07	0.100	41	2.38	0.100	45.00	60.0	34.6	0.45	23.80	1.00	
136	15.90	1.07	0.100	41	2.38	0.100	45.00	60.0	34.6	0.45	23.80	1.00	
137	20.90	1.34	0.090	41	2.38	0.100	45.00	60.0	34.6	0.56	23.80	0.90	
138	13.60	1.34	0.090	11	2.38	0.100	45.00	60.0	34.6	0.56	23.80	0.90	
139	15.60	1.34	0.090	11	2.38	0.100	45.00	60.0	34.6	0.56	23.80	0.90	
140	22.00	1.34	0.090	11	2.38	0.100	45.00	60.0	34.6	0.56	23.80	0.90	
141	21.50	1.34	0.090	-19	2.38	0.100	45.00	60.0	34.6	0.56	23.80	0.90	
142	15.30	1.34	0.090	-19	2.38	0.100	45.00	60.0	34.6	0.56	23.80	0.90	
143	22.50	1.34	0.090	-19	2.38	0.100	45.00	60.0	34.6	0.56	23.80	0.90	
144	22.50	1.34	0.090	52	2.38	0.100	45.00	60.0	34.6	0.56	23.80	0.90	
145	33.90	1.34	0.090	52	2.38	0.100	45.00	60.0	34.6	0.56	23.80	0.90	
146	33.50	1.34	0.090	52	2.38	0.100	45.00	60.0	34.6	0.56	23.80	0.90	
147	19.10	1.34	0.090	22	2.38	0.100	45.00	60.0	34.6	0.56	23.80	0.90	
148	27.20	1.34	0.090	22	2.38	0.100	45.00	60.0	34.6	0.56	23.80	0.90	
149	17.20	1.34	0.090	22	2.38	0.100	45.00	60.0	34.6	0.56	23.80	0.90	
150	15.00	1.34	0.090	-8	2.38	0.100	45.00	60.0	34.6	0.56	23.80	0.90	

TABLE 1 INPUT DATA FOR CASE STUDIES SPECIMEN DIMENSIONS & TEST RESULTS-PAGE 3

SPECIMEN NO.	EXPTAL P (ULT)		BRANCH		WELD GAP		CHORD		JOINT YIELD-STRESS		PARAMETERS	
	KIPS	D (IN)	T (IN)	(MM)	DC (IN)	TC (IN)	ANGLE	BASIC	SHEAR	D/DC	DC/TC	T/TC
151	35.70	1.34	0.090	-8	2.38	0.100	45.00	60.0	34.6	0.56	23.80	0.90
152	16.80	1.34	0.090	-8	2.38	0.100	45.00	60.0	34.6	0.56	23.80	0.90
153	26.79	1.34	0.090	56	2.38	0.100	45.00	60.0	34.6	0.56	23.80	0.90
154	39.70	1.34	0.090	56	2.38	0.100	45.00	60.0	34.6	0.56	23.80	0.90
155	24.90	1.34	0.090	56	2.38	0.100	45.00	60.0	34.6	0.56	23.80	0.90
156	19.60	1.34	0.090	26	2.38	0.100	45.00	60.0	34.6	0.56	23.80	0.90
157	18.90	1.34	0.090	26	2.38	0.100	45.00	60.0	34.6	0.56	23.80	0.90
158	35.90	1.34	0.090	26	2.38	0.100	45.00	60.0	34.6	0.56	23.80	0.90
159	36.30	1.34	0.090	-4	2.38	0.100	45.00	60.0	34.6	0.56	23.80	0.90
160	28.30	1.34	0.090	-4	2.38	0.100	45.00	60.0	34.6	0.56	23.80	0.90
161	37.50	1.34	0.090	-4	2.38	0.100	45.00	60.0	34.6	0.56	23.80	0.90
162	16.20	1.34	0.130	12	2.38	0.100	45.00	60.0	34.6	0.56	23.80	1.30
163	18.20	1.34	0.130	12	2.38	0.100	45.00	60.0	34.6	0.56	23.80	1.30
164	17.70	1.34	0.130	12	2.38	0.100	45.00	60.0	34.6	0.56	23.80	1.30
165	16.90	1.34	0.100	36	2.38	0.100	45.00	60.0	34.6	0.56	23.80	1.00
166	16.20	1.34	0.100	36	2.38	0.100	45.00	60.0	34.6	0.56	23.80	1.00
167	14.10	1.34	0.100	36	2.38	0.100	45.00	60.0	34.6	0.56	23.80	1.00
168	20.00	1.34	0.100	6	2.38	0.100	45.00	60.0	34.6	0.56	23.80	1.00
169	19.80	1.34	0.100	6	2.38	0.100	45.00	60.0	34.6	0.56	23.80	1.00
170	19.50	1.34	0.100	6	2.38	0.100	45.00	60.0	34.6	0.56	23.80	1.00
171	21.20	1.34	0.100	-13	2.38	0.100	45.00	60.0	34.6	0.56	23.80	1.00
172	24.00	1.34	0.100	-13	2.38	0.100	45.00	60.0	34.6	0.56	23.80	1.00
173	23.60	1.34	0.100	-13	2.38	0.100	45.00	60.0	34.6	0.56	23.80	1.00
174	20.50	1.91	0.130	30	2.38	0.100	45.00	60.0	34.6	0.80	23.80	1.30
175	20.80	1.91	0.130	30	2.38	0.100	45.00	60.0	34.6	0.80	23.80	1.30
176	20.50	1.91	0.130	30	2.38	0.100	45.00	60.0	34.6	0.80	23.80	1.30
177	25.00	1.91	0.130	-8	2.38	0.100	45.00	60.0	34.6	0.80	23.80	1.30
178	24.20	1.91	0.130	-8	2.38	0.100	45.00	60.0	34.6	0.80	23.80	1.30
179	24.90	1.91	0.130	-8	2.38	0.100	45.00	60.0	34.6	0.80	23.80	1.30
180	25.70	1.91	0.130	-36	2.38	0.100	45.00	60.0	34.6	0.80	23.80	1.30
181	27.60	1.91	0.130	-38	2.38	0.100	45.00	60.0	34.6	0.80	23.80	1.30
182	27.80	1.91	0.130	-38	2.38	0.100	45.00	60.0	34.6	0.80	23.80	1.30
183	18.20	1.34	0.100	-10	2.38	0.100	90.00	60.0	34.6	0.56	23.80	1.00
184	15.70	1.34	0.100	-10	2.38	0.100	90.00	60.0	34.6	0.56	23.80	1.00
185	15.40	1.34	0.100	-10	2.38	0.100	90.00	60.0	34.6	0.56	23.80	1.00
186	17.80	1.34	0.100	4	2.38	0.100	60.00	60.0	34.6	0.56	23.80	1.00
187	17.60	1.34	0.100	4	2.38	0.100	60.00	60.0	34.6	0.56	23.80	1.00
188	17.70	1.34	0.100	4	2.38	0.100	60.00	60.0	34.6	0.56	23.80	1.00
189	22.30	1.34	0.100	24	2.38	0.100	30.00	60.0	34.6	0.56	23.80	1.00
190	22.70	1.34	0.100	24	2.38	0.100	30.00	60.0	34.6	0.56	23.80	1.00
191	21.50	1.34	0.100	24	2.38	0.100	30.00	60.0	34.6	0.56	23.80	1.00
192	100.00	2.38	0.218	53	6.62	0.432	45.00	60.0	34.6	0.36	15.34	0.50
193	103.00	2.38	0.238	11	6.62	0.432	45.00	60.0	34.6	0.36	15.34	0.55
194	99.00	2.38	0.218	-25	6.62	0.432	45.00	60.0	34.6	0.36	15.34	0.50
195	148.00	3.50	0.216	18	6.62	0.432	45.00	60.0	34.6	0.53	15.34	0.50
196	155.00	3.50	0.216	-23	6.62	0.432	45.00	60.0	34.6	0.53	15.34	0.50
197	155.00	3.50	0.216	-65	6.62	0.432	45.00	60.0	34.6	0.53	15.34	0.50
198	212.00	4.50	0.237	-11	6.62	0.432	45.00	60.0	34.6	0.68	15.34	0.55
199	212.00	4.50	0.237	-54	6.62	0.432	45.00	60.0	34.6	0.68	15.34	0.55
200	226.00	4.50	0.237	-95	6.62	0.432	45.00	60.0	34.6	0.68	15.34	0.55
201	85.00	2.38	0.218	11	6.62	0.280	45.00	60.0	34.6	0.36	23.66	0.76
202	106.00	2.38	0.218	11	6.62	0.562	45.00	60.0	34.6	0.36	11.79	0.39
203	137.00	4.50	0.237	-54	6.62	0.280	45.00	60.0	34.6	0.68	23.66	0.95
204	212.00	4.50	0.237	-54	6.62	0.562	45.00	60.0	34.6	0.68	11.79	0.42
205	105.00	2.38	0.218	11	6.62	0.344	45.00	55.0	31.8	0.36	19.26	0.63
206	275.00	4.50	0.337	-54	6.62	0.312	45.00	55.0	31.8	0.68	21.23	1.09
207	40.00	2.38	0.219	11	6.62	0.218	45.00	55.0	31.8	0.36	30.39	1.00
208	190.00	3.50	0.300	23	6.62	0.219	45.00	55.0	31.8	0.53	30.25	1.37
209	215.00	4.50	0.237	-54	6.62	0.219	45.00	55.0	31.8	0.68	30.25	1.08
210	80.00	3.50	0.300	2	6.62	0.219	45.00	55.0	31.8	0.41	39.38	1.37
211	185.00	4.50	0.337	-15	6.62	0.219	45.00	55.0	31.8	0.52	39.38	1.54
212	230.00	5.50	0.258	-61	6.62	0.220	45.00	55.0	31.8	0.64	39.20	1.17
213	45.00	3.50	0.300	29	10.75	0.188	45.00	55.0	31.8	0.33	57.18	1.60
214	70.00	4.50	0.337	-1	10.75	0.188	45.00	55.0	31.8	0.42	57.18	1.79
215	170.00	5.50	0.258	-34	10.75	0.188	45.00	55.0	31.8	0.51	57.18	1.37
216	215.00	6.62	0.219	-66	10.75	0.188	45.00	55.0	31.8	0.62	57.18	1.16
217	103.00	2.38	0.218	-28	6.62	0.219	45.00	55.0	31.8	0.36	30.25	1.00
218	175.00	3.50	0.300	-52	6.62	0.219	45.00	55.0	31.8	0.41	39.38	1.37
219	190.00	3.50	0.300	-39	10.75	0.188	45.00	55.0	31.8	0.33	57.18	1.60
220	175.00	4.50	0.250	-69	10.75	0.188	45.00	55.0	31.8	0.42	57.18	1.33
221	230.00	5.50	0.258	-102	10.75	0.188	45.00	55.0	31.8	0.51	57.18	1.37
222	48.00	1.90	0.145	-1	4.50	0.237	45.00	36.0	20.8	0.42	18.99	0.61
223	123.00	3.50	0.216	-50	4.50	0.237	45.00	36.0	20.8	0.78	18.99	0.91
224	48.00	1.90	0.145	-29	4.50	0.237	45.00	36.0	20.8	0.42	18.99	0.61
225	121.00	3.50	0.216	-78	4.50	0.237	45.00	36.0	20.8	0.78	18.99	0.91

TABLE 1 INPUT DATA FOR CASE STUDIES SPECIMEN DIMENSIONS & TEST RESULTS-PAGE 4

SPECIMEN NO.	EXPTAL P(ULT)	BRANCH		WELD GAP		CHORD		JOINT YIELD-STRESS		PARAMETERS		
	KIPS	D(IN)	T(IN)	(MM)	DC(IN)	TC(IN)	ANGLE	BASIC	SHEAR	D/DC	DC/TC	T/TC
226	71.00	4.49	0.221	22	4.49	0.221	45.00	66.1	38.2	1.00	20.37	1.00
227	55.00	2.74	0.221	22	4.49	0.221	45.00	66.1	38.2	0.61	20.37	1.00
228	45.00	1.88	0.221	22	4.49	0.221	45.00	66.1	38.2	0.42	20.37	1.00
229	69.00	4.52	0.200	22	4.52	0.200	45.00	66.6	38.4	1.00	22.60	1.00
230	54.00	2.76	0.200	22	4.52	0.200	45.00	66.6	38.4	0.61	22.60	1.00
231	39.00	1.90	0.200	22	4.52	0.200	45.00	66.6	38.4	0.42	22.60	1.00
232	52.00	4.49	0.154	22	4.49	0.154	45.00	68.0	39.3	1.00	29.17	1.00
233	33.00	2.74	0.154	22	4.49	0.154	45.00	68.0	39.3	0.61	29.17	1.00
234	27.00	1.88	0.154	22	4.49	0.154	45.00	68.0	39.3	0.42	29.16	1.00
235	71.00	4.49	0.221	17	4.49	0.221	45.00	66.1	38.2	1.00	20.37	1.00
236	55.00	2.74	0.221	12	4.49	0.221	45.00	66.1	38.2	0.61	20.37	1.00
237	45.00	1.88	0.221	7	4.49	0.221	45.00	66.1	38.2	0.42	20.37	1.00
238	69.00	4.52	0.200	7	4.52	0.200	45.00	66.6	38.4	1.00	22.60	1.00
239	54.00	2.76	0.200	7	4.52	0.200	45.00	66.6	38.4	0.61	22.60	1.00
240	39.00	1.90	0.200	7	4.52	0.200	45.00	66.6	38.4	0.42	22.60	1.00
241	52.00	4.49	0.154	2	4.49	0.154	45.00	68.0	39.3	1.00	29.17	1.00
242	33.00	2.74	0.154	3	4.49	0.154	45.00	68.0	39.3	0.61	29.17	1.00
243	27.00	1.88	0.154	0	4.49	0.154	45.00	68.0	39.3	0.42	29.17	1.00
244	49.00	1.90	0.125	0	4.50	0.212	90.00	60.0	34.6	0.42	21.23	0.89
245	80.00	3.00	0.170	0	4.50	0.212	90.00	60.0	34.6	0.67	21.23	0.80

TABLE 2 SUMMARISED RESULTS OF PARAMETRIC STUDY OF TUBE JOINT FORMULAE-PAGE 1 CALCULATED PULTRON GIVEN BY EACH METHOD IN KIPS, TEST NOS ARE THE SAME AS IN INPUT DATA TABLE

IN THIS TABLE THE FORMULAE ARE TESTED FOR APPLICABILITY
PULT=1.0 SHOWS THAT THE TEST WAS OUTSIDE THE RECOMMENDED RANGE OF THE FORMULA

FORMULAE LISTED ARE BASED ON YIELD STRESS OF CHORD

METHOD:-	REGER	ROUWKAMP	DET	NAKA,KATO,	KUROBANE	ROARK(1)	ROARK(2)	KATO	KELLOGG
			NORSKE	KANATANI					
1	1.00	33.34	1.00	69.05	1.00	1.00	1.00	1.00	23.52
2	1.00	33.34	1.00	1.00	1.00	1.00	23.02	18.55	1.00
3	1.00	44.89	1.00	1.00	1.00	1.00	21.43	18.41	1.00
4	34.75	55.72	1.00	1.00	1.00	1.00	25.89	23.65	1.00
5	45.67	43.47	40.20	52.71	1.00	1.00	1.00	1.00	1.00
6	34.75	55.72	1.00	1.00	1.00	1.00	25.89	23.65	1.00
7	34.75	55.72	1.00	1.00	1.00	1.00	25.89	23.65	1.00
8	1.00	94.76	1.00	106.88	1.00	1.00	1.00	1.00	29.04
9	1.00	54.09	48.04	66.80	1.00	1.00	1.00	1.00	23.76
10	51.88	47.83	42.48	57.33	1.00	1.00	1.00	1.00	21.12
11	37.81	25.95	31.92	41.85	1.00	1.00	1.00	1.00	15.64
12	22.87	11.33	20.13	27.19	1.00	1.00	1.00	1.00	10.03
13	1.00	94.76	1.00	106.88	1.00	1.00	1.00	1.00	29.04
14	51.88	34.99	43.04	57.36	1.00	1.00	1.00	1.00	21.12
15	44.79	30.47	37.48	49.23	1.00	1.00	1.00	1.00	16.48
16	22.87	11.33	20.13	27.18	1.00	1.00	1.00	1.00	10.03
17	19.98	9.95	17.68	24.42	1.00	1.00	1.00	1.00	8.87
18	1.00	7.82	1.00	20.21	1.00	1.00	1.00	1.00	7.68
19	1.00	66.61	1.00	61.57	1.00	1.00	1.00	1.00	16.73
20	1.00	48.30	27.60	38.48	1.00	1.00	1.00	1.00	13.69
21	28.81	42.73	24.60	33.05	1.00	1.00	1.00	1.00	12.17
22	20.99	31.61	19.19	24.11	1.00	1.00	1.00	1.00	9.17
23	12.70	11.33	11.60	15.66	1.00	1.00	1.00	1.00	5.78
24	1.00	48.30	1.00	46.67	1.00	1.00	1.00	1.00	12.68
25	1.00	30.47	20.00	27.25	1.00	1.00	1.00	1.00	9.86

METHOD:-	REGER	ROUWKAMP	DET	NAKA,KATO,	KUROBANE	ROARK(1)	ROARK(2)	KATO	KELLOGG
			NORSKE	KANATANI					
26	20.01	25.95	17.03	22.64	1.00	1.00	1.00	1.00	8.45
27	15.51	17.37	13.47	17.71	1.00	1.00	1.00	1.00	6.71
28	8.24	7.82	7.42	10.43	1.00	1.00	1.00	1.00	3.76
29	26.08	56.96	1.00	1.00	1.00	1.00	10.34	17.19	1.00
30	48.51	56.96	42.76	55.99	1.00	1.00	1.00	1.00	21.20
31	89.29	56.96	75.77	99.21	1.00	1.00	1.00	1.00	37.57
32	30.79	56.96	1.00	1.00	1.00	1.00	27.56	23.85	1.00
33	60.17	56.96	55.63	74.54	1.00	1.00	1.00	1.00	1.00
34	93.34	56.96	83.96	112.50	1.00	1.00	1.00	1.00	41.62
35	32.38	56.96	1.00	1.00	1.00	1.00	35.73	30.62	1.00
36	47.26	56.96	1.00	1.00	1.00	1.00	61.61	49.13	1.00
37	73.32	56.96	70.66	99.59	1.00	1.00	1.00	1.00	1.00
38	16.60	21.21	11.59	1.00	19.80	1.00	1.00	1.00	4.17
39	16.60	21.21	11.59	1.00	19.80	1.00	1.00	1.00	4.17
40	16.60	21.21	11.59	1.00	19.80	1.00	1.00	1.00	4.17
41	16.60	21.21	11.59	1.00	19.80	1.00	1.00	1.00	4.17
42	16.60	21.21	11.59	1.00	19.80	1.00	1.00	1.00	4.17
43	16.60	21.21	11.59	1.00	19.76	1.00	1.00	1.00	4.17
44	16.60	21.21	11.59	1.00	19.76	1.00	1.00	1.00	4.17
45	16.60	21.21	11.59	1.00	19.76	1.00	1.00	1.00	4.17
46	16.60	21.21	11.59	1.00	19.76	1.00	1.00	1.00	4.17
47	16.60	21.21	11.59	1.00	19.76	1.00	1.00	1.00	4.17
48	25.26	21.21	1.00	1.00	19.76	1.00	1.00	1.00	6.18
49	25.26	21.21	1.00	1.00	19.76	1.00	1.00	1.00	6.18
50	25.26	21.21	1.00	1.00	19.76	1.00	1.00	1.00	6.18

METHOD:-	REGER	ROUWKAMP	DET	NAKA,KATO,	KUROBANE	ROARK(1)	ROARK(2)	KATO	KELLOGG
			NORSKE	KANATANI					
51	25.26	21.21	1.00	1.00	19.76	1.00	1.00	1.00	6.18
52	25.26	21.21	1.00	1.00	19.76	1.00	1.00	1.00	6.18
53	25.26	21.21	1.00	1.00	19.76	1.00	1.00	1.00	6.18
54	16.60	12.72	11.59	1.00	19.76	1.00	1.00	1.00	4.17
55	16.60	12.72	11.59	1.00	19.76	1.00	1.00	1.00	4.17
56	16.60	12.72	11.59	1.00	19.76	1.00	1.00	1.00	4.17
57	16.60	12.72	13.37	1.00	20.04	1.00	1.00	1.00	4.17
58	16.60	12.72	13.37	1.00	20.04	1.00	1.00	1.00	4.17
59	16.60	12.72	13.37	1.00	20.04	1.00	1.00	1.00	4.17
60	16.60	12.72	13.37	1.00	20.04	1.00	1.00	1.00	4.17
61	16.60	12.72	13.37	1.00	20.04	1.00	1.00	1.00	4.17
62	16.60	12.72	12.28	1.00	20.00	1.00	1.00	1.00	4.17
63	16.60	12.72	12.28	1.00	20.00	1.00	1.00	1.00	4.17
64	25.26	21.21	1.00	1.00	20.00	1.00	1.00	1.00	6.18
65	25.26	21.21	1.00	1.00	20.00	1.00	1.00	1.00	6.18
66	25.26	21.21	1.00	1.00	20.00	1.00	1.00	1.00	6.18
67	25.26	21.21	1.00	1.00	20.00	1.00	1.00	1.00	6.18
68	25.26	21.21	1.00	1.00	20.00	1.00	1.00	1.00	6.18
69	16.60	12.72	12.28	1.00	20.00	1.00	1.00	1.00	4.17
70	16.60	12.72	12.28	1.00	20.00	1.00	1.00	1.00	4.17
71	16.60	12.72	12.28	1.00	20.00	1.00	1.00	1.00	4.17
72	16.60	12.72	12.28	1.00	20.00	1.00	1.00	1.00	4.17
73	16.60	12.72	12.28	1.00	20.00	1.00	1.00	1.00	4.17
74	16.60	12.72	12.28	1.00	20.00	1.00	1.00	1.00	4.17
75	25.26	21.21	1.00	1.00	20.00	1.00	1.00	1.00	6.18

TABLE 2 SUMMARIZED RESULTS OF PARAMETRIC STUDY OF TUBE JOINT FORMULAE-PAGE. 2 CALCULATED
 PLOT GIVEN BY EACH METHOD IN KIPS, TEST NOS ARE THE SAME AS IN INPUT DATA TABLE

IN THIS TABLE THE FORMULAE ARE TESTED FOR APPLICABILITY
 PULT=1.0 SHOWS THAT THE TEST WAS OUTSIDE THE RECOMMENDED RANGE OF THE FORMULA

FORMULAE LISTED ARE BASED ON YIELD STRESS OF CHORD

METHOD:-	REBER	ROUWKAMP	DET	NAKA,KATO,	KUROKANE	ROARK(1)	ROARK(2)	KATO	KELLOGG

			NORSKE	KANATANI					
76	25.26	21.21	1.00	1.00	20.00	1.00	1.00	1.00	6.18
77	25.26	21.21	1.00	1.00	20.00	1.00	1.00	1.00	6.18
78	25.26	21.21	1.00	1.00	20.00	1.00	1.00	1.00	6.18
79	16.60	21.21	12.28	1.00	20.00	1.00	1.00	1.00	4.17
80	16.60	21.21	12.28	1.00	20.00	1.00	1.00	1.00	4.17
81	16.60	21.21	12.28	1.00	20.00	1.00	1.00	1.00	4.17
82	16.60	21.21	12.28	1.00	20.00	1.00	1.00	1.00	4.17
83	16.60	21.21	12.28	1.00	20.00	1.00	1.00	1.00	4.17
84	16.60	21.21	12.28	1.00	20.00	1.00	1.00	1.00	4.17
85	16.60	21.21	12.28	1.00	20.00	1.00	1.00	1.00	4.17
86	16.60	21.21	12.28	1.00	20.00	1.00	1.00	1.00	4.17
87	16.60	21.21	12.28	1.00	20.00	1.00	1.00	1.00	4.17
88	16.60	21.21	12.28	1.00	20.00	1.00	1.00	1.00	4.17
89	25.26	21.21	1.00	1.00	20.00	1.00	1.00	1.00	6.18
90	25.26	21.21	1.00	1.00	20.00	1.00	1.00	1.00	6.18
91	25.26	21.21	1.00	1.00	20.00	1.00	1.00	1.00	6.18
92	25.26	21.21	1.00	1.00	20.00	1.00	1.00	1.00	6.18
93	25.26	21.21	1.00	1.00	20.00	1.00	1.00	1.00	6.18
94	16.60	21.21	12.28	1.00	20.00	1.00	1.00	1.00	4.17
95	16.60	21.21	12.28	1.00	20.00	1.00	1.00	1.00	4.17
96	16.60	21.21	11.59	1.00	20.27	1.00	1.00	1.00	4.17
97	16.60	21.21	11.59	1.00	20.27	1.00	1.00	1.00	4.17
98	16.60	21.21	11.59	1.00	20.27	1.00	1.00	1.00	4.17
99	16.60	21.21	11.59	1.00	20.27	1.00	1.00	1.00	4.17
100	25.26	21.21	1.00	1.00	20.27	1.00	1.00	1.00	6.18
METHOD:-	REBER	ROUWKAMP	DET	NAKA,KATO,	KUROKANE	ROARK(1)	ROARK(2)	KATO	KELLOGG

			NORSKE	KANATANI					
101	25.26	21.21	1.00	1.00	20.23	1.00	1.00	1.00	6.18
102	25.26	21.21	1.00	1.00	20.23	1.00	1.00	1.00	6.18
103	25.26	21.21	1.00	1.00	28.23	1.00	1.00	1.00	6.18
104	16.60	21.21	11.59	1.00	20.23	1.00	1.00	1.00	4.17
105	16.60	21.21	11.59	1.00	20.23	1.00	1.00	1.00	4.17
106	16.60	21.21	11.59	1.00	20.23	1.00	1.00	1.00	4.17
107	16.60	12.72	11.59	1.00	20.23	1.00	1.00	1.00	4.17
108	16.60	12.72	11.59	1.00	20.23	1.00	1.00	1.00	4.17
109	16.60	12.72	11.59	1.00	20.23	1.00	1.00	1.00	4.17
110	21.29	26.97	14.74	1.00	21.76	1.00	1.00	1.00	5.23
111	21.29	26.97	14.74	1.00	21.76	1.00	1.00	1.00	5.23
112	21.29	26.97	14.74	1.00	21.76	1.00	1.00	1.00	5.23
113	21.29	16.18	14.74	1.00	21.76	1.00	1.00	1.00	5.23
114	21.29	16.18	14.74	1.00	21.76	1.00	1.00	1.00	5.23
115	21.29	16.18	14.74	1.00	21.76	1.00	1.00	1.00	5.23
116	21.29	26.97	14.74	1.00	21.76	1.00	1.00	1.00	5.23
117	21.29	26.97	14.74	1.00	21.76	1.00	1.00	1.00	5.23
118	21.29	26.97	14.74	1.00	21.76	1.00	1.00	1.00	5.23
119	12.96	18.28	8.99	1.00	19.02	1.00	1.00	1.00	3.33
120	12.96	18.28	8.99	1.00	19.02	1.00	1.00	1.00	3.33
121	12.96	18.28	8.99	1.00	19.02	1.00	1.00	1.00	3.33
122	12.96	10.97	8.99	1.00	19.02	1.00	1.00	1.00	3.33
123	12.96	10.97	8.99	1.00	19.02	1.00	1.00	1.00	3.33
124	12.96	10.97	8.99	1.00	19.02	1.00	1.00	1.00	3.33
125	12.96	10.97	8.99	1.00	19.02	1.00	1.00	1.00	3.33
METHOD:-	REBER	ROUWKAMP	DET	NAKA,KATO,	KUROKANE	ROARK(1)	ROARK(2)	KATO	KELLOGG

			NORSKE	KANATANI					
126	12.96	10.97	8.99	1.00	19.02	1.00	1.00	1.00	3.33
127	12.96	10.97	8.99	1.00	19.02	1.00	1.00	1.00	3.33
128	12.96	10.97	8.99	1.00	19.02	1.00	1.00	1.00	3.33
129	12.96	10.97	8.99	1.00	19.02	1.00	1.00	1.00	3.33
130	12.96	10.97	8.99	1.00	19.02	1.00	1.00	1.00	3.33
131	12.96	10.97	8.99	1.00	19.02	1.00	1.00	1.00	3.33
132	12.96	10.97	10.07	1.00	18.80	1.00	1.00	1.00	3.33
133	12.96	10.97	10.07	1.00	18.80	1.00	1.00	1.00	3.33
134	12.96	18.28	10.07	1.00	18.80	1.00	1.00	1.00	3.33
135	12.96	18.28	8.99	1.00	18.62	1.00	1.00	1.00	3.33
136	12.96	18.28	8.99	1.00	18.62	1.00	1.00	1.00	3.33
137	16.60	12.72	11.59	1.00	19.81	1.00	1.00	1.00	4.17
138	16.60	12.72	13.75	1.00	20.05	1.00	1.00	1.00	4.17
139	16.60	12.72	13.75	1.00	20.05	1.00	1.00	1.00	4.17
140	16.60	12.72	13.75	1.00	20.05	1.00	1.00	1.00	4.17
141	16.60	12.72	11.59	1.00	20.28	1.00	1.00	1.00	4.17
142	16.60	12.72	11.59	1.00	20.28	1.00	1.00	1.00	4.17
143	16.60	12.72	11.59	1.00	20.28	1.00	1.00	1.00	4.17
144	16.60	12.72	11.59	1.00	19.72	1.00	1.00	1.00	4.17
145	16.60	12.72	11.59	1.00	19.72	1.00	1.00	1.00	4.17
146	16.60	12.72	11.59	1.00	19.72	1.00	1.00	1.00	4.17
147	16.60	21.21	11.59	1.00	19.96	1.00	1.00	1.00	4.17
148	16.60	21.21	11.59	1.00	19.96	1.00	1.00	1.00	4.17
149	16.60	21.21	11.59	1.00	19.96	1.00	1.00	1.00	4.17
150	16.60	21.21	11.59	1.00	20.29	1.00	1.00	1.00	4.17

IN THIS TABLE THE FORMULAE ARE TESTED FOR APPLICABILITY
PULT=1.0 SHOWS THAT THE TEST WAS OUTSIDE THE RECOMMENDED RANGE OF THE FORMULA

FORMULAE LISTED ARE BASED ON YIELD STRESS OF CHORD

METHOD:-	REFER	BOUWKAMP	DET	NAKA,KATO,	KUROBANE	ROARK(1)	ROARK(2)	KATO	KELLOGG
			NORSKE	KANATANI					
151	16.60	21.21	11.59	1.00	20.20	1.00	1.00	1.00	4.17
152	16.60	21.21	11.59	1.00	20.20	1.00	1.00	1.00	4.17
153	16.60	21.21	11.59	1.00	19.69	1.00	1.00	1.00	4.17
154	16.60	21.21	11.59	1.00	19.69	1.00	1.00	1.00	4.17
155	16.60	21.21	11.59	1.00	19.69	1.00	1.00	1.00	4.17
156	16.60	12.72	11.59	1.00	19.93	1.00	1.00	1.00	4.17
157	16.60	12.72	11.59	1.00	19.93	1.00	1.00	1.00	4.17
158	16.60	12.72	11.59	1.00	19.93	1.00	1.00	1.00	4.17
159	16.60	12.72	11.59	1.00	20.17	1.00	1.00	1.00	4.17
160	16.60	21.21	11.59	1.00	20.17	1.00	1.00	1.00	4.17
161	16.60	21.21	11.59	1.00	20.17	1.00	1.00	1.00	4.17
162	16.60	29.65	12.94	1.00	20.04	1.00	1.00	1.00	4.17
163	16.60	29.65	12.94	1.00	20.04	1.00	1.00	1.00	4.17
164	16.60	29.65	12.94	1.00	20.04	1.00	1.00	1.00	4.17
165	16.60	23.37	11.50	1.00	19.85	1.00	1.00	1.00	4.17
166	16.60	23.37	11.50	1.00	19.85	1.00	1.00	1.00	4.17
167	16.60	23.37	11.50	1.00	19.85	1.00	1.00	1.00	4.17
168	16.60	14.02	15.22	1.00	20.08	1.00	1.00	1.00	4.17
169	16.60	14.02	15.22	1.00	20.08	1.00	1.00	1.00	4.17
170	16.60	14.02	15.22	1.00	20.08	1.00	1.00	1.00	4.17
171	16.60	23.37	11.50	1.00	20.23	1.00	1.00	1.00	4.17
172	16.60	23.37	11.50	1.00	20.23	1.00	1.00	1.00	4.17
173	16.60	23.37	11.50	1.00	20.23	1.00	1.00	1.00	4.17
174	1.00	43.62	16.51	1.00	22.41	1.00	1.00	1.00	5.95
175	1.00	43.62	16.51	1.00	22.41	1.00	1.00	1.00	5.95

METHOD:-	REFER	BOUWKAMP	DET	NAKA,KATO,	KUROBANE	ROARK(1)	ROARK(2)	KATO	KELLOGG
			NORSKE	KANATANI					
176	1.00	43.62	16.51	1.00	22.41	1.00	1.00	1.00	5.95
177	1.00	26.17	16.51	1.00	22.75	1.00	1.00	1.00	5.95
178	1.00	26.17	16.51	1.00	22.75	1.00	1.00	1.00	5.95
179	1.00	26.17	16.51	1.00	22.75	1.00	1.00	1.00	5.95
180	1.00	43.62	16.51	1.00	23.01	1.00	1.00	1.00	5.95
181	1.00	43.62	16.51	1.00	23.01	1.00	1.00	1.00	5.95
182	1.00	43.62	16.51	1.00	23.01	1.00	1.00	1.00	5.95
183	9.87	14.02	8.13	11.03	1.00	1.00	1.00	1.00	4.17
184	9.87	14.02	8.13	11.03	1.00	1.00	1.00	1.00	4.17
185	9.87	14.02	8.13	11.03	1.00	1.00	1.00	1.00	4.17
186	12.25	14.02	14.39	1.00	16.41	1.00	1.00	1.00	4.17
187	12.25	14.02	14.39	1.00	16.41	1.00	1.00	1.00	4.17
188	12.25	14.02	14.39	1.00	16.41	1.00	1.00	1.00	4.17
189	27.92	14.02	16.26	1.00	26.20	1.00	1.00	1.00	4.17
190	27.92	14.02	16.26	1.00	26.20	1.00	1.00	1.00	4.17
191	27.92	14.02	16.26	1.00	26.20	1.00	1.00	1.00	4.17
192	158.16	38.64	1.00	1.00	136.13	1.00	1.00	1.00	39.00
193	158.16	38.64	1.00	1.00	136.94	1.00	1.00	1.00	39.00
194	158.16	38.64	1.00	1.00	139.70	1.00	1.00	1.00	39.00
195	242.30	133.71	1.00	1.00	152.74	1.00	1.00	1.00	56.05
196	242.30	133.71	1.00	1.00	153.63	1.00	1.00	1.00	56.05
197	242.30	133.71	1.00	1.00	154.49	1.00	1.00	1.00	56.05
198	319.45	190.44	1.00	1.00	165.64	1.00	1.00	1.00	75.40
199	319.45	190.44	1.00	1.00	166.78	1.00	1.00	1.00	75.40
200	319.45	190.44	1.00	1.00	167.71	1.00	1.00	1.00	75.40

METHOD:-	REFER	BOUWKAMP	DET	NAKA,KATO,	KUROBANE	ROARK(1)	ROARK(2)	KATO	KELLOGG
			NORSKE	KANATANI					
201	79.03	53.18	89.04	1.00	138.94	1.00	1.00	1.00	20.77
202	240.94	58.64	1.00	1.00	138.94	1.00	1.00	1.00	59.05
203	159.62	114.27	111.01	1.00	166.78	1.00	1.00	1.00	39.35
204	486.64	140.44	1.00	1.00	166.78	1.00	1.00	1.00	111.68
205	100.70	81.25	1.00	1.00	127.36	1.00	1.00	1.00	25.92
206	173.98	145.45	116.89	1.00	152.89	1.00	1.00	1.00	42.42
207	48.54	48.95	56.04	1.00	127.36	1.00	1.00	1.00	13.02
208	74.90	89.53	67.49	1.00	139.93	1.00	1.00	1.00	19.40
209	98.75	104.74	70.39	1.00	152.89	1.00	1.00	1.00	24.95
210	62.27	89.53	73.93	1.00	222.20	1.00	1.00	1.00	1.00
211	82.10	145.45	60.24	1.00	237.43	1.00	1.00	1.00	1.00
212	103.23	140.34	76.45	1.00	253.60	1.00	1.00	1.00	1.00
213	41.81	89.53	50.65	1.00	328.50	1.00	1.00	1.00	1.00
214	55.12	145.45	42.92	1.00	347.65	1.00	1.00	1.00	1.00
215	68.31	140.34	54.10	1.00	367.44	1.00	1.00	1.00	1.00
216	84.35	145.44	66.05	1.00	389.26	1.00	1.00	1.00	1.00
217	48.89	46.75	35.62	1.00	128.06	1.00	1.00	1.00	13.17
218	62.27	116.11	45.31	1.00	223.43	1.00	1.00	1.00	1.00
219	41.81	116.11	32.99	1.00	339.40	1.00	1.00	1.00	1.00
220	55.12	128.91	43.82	1.00	349.64	1.00	1.00	1.00	1.00
221	68.81	183.73	54.10	1.00	369.52	1.00	1.00	1.00	1.00
222	37.24	88.78	1.00	1.00	39.99	1.00	1.00	1.00	9.42
223	1.00	80.22	1.00	1.00	48.56	1.00	1.00	1.00	17.35
224	37.24	88.78	1.00	1.00	40.21	1.00	1.00	1.00	9.42
225	1.00	80.22	1.00	1.00	48.83	1.00	1.00	1.00	17.35

TABLE 2 SUMMARIZED RESULTS OF PARAMETRIC STUDY OF TUBE JOINT FORMULAE-PAGE 4 CALCULATED P(ULT) GIVEN BY EACH METHOD IN KIPS, TEST NOS ARE THE SAME AS IN INPUT DATA TABLE

IN THIS TABLE THE FORMULAE ARE TESTED FOR APPLICABILITY
PULT=1.0 SHOWS THAT THE TEST WAS OUTSIDE THE RECOMMENDED RANGE OF THE FORMULA

FORMULAE LISTED ARE BASED ON YIELD STRESS OF CHORD

METHOD:-	REHER	BOUWKAMP	DET	NAKA,KATO,	KUROBANE	ROARK(1)	ROARK(2)	KATO	KELLOGG
			NORSKE	KANATANI					
226	1.00	117.35	1.00	1.00	96.78	1.00	1.00	1.00	36.72
227	91.25	69.22	70.08	1.00	80.59	1.00	1.00	1.00	22.40
228	60.30	45.59	50.63	1.00	72.64	1.00	1.00	1.00	15.37
229	1.00	108.46	1.00	1.00	98.74	1.00	1.00	1.00	32.06
230	78.94	64.28	61.86	1.00	82.25	1.00	1.00	1.00	19.58
231	52.35	42.68	45.01	1.00	74.19	1.00	1.00	1.00	13.48
232	1.00	85.59	1.00	1.00	99.55	1.00	1.00	1.00	22.04
233	52.86	51.05	43.19	1.00	82.91	1.00	1.00	1.00	13.45
234	34.94	34.07	31.62	1.00	74.67	1.00	1.00	1.00	9.23
235	1.00	117.30	1.00	1.00	96.88	1.00	1.00	1.00	36.71
236	91.25	69.22	79.05	1.00	80.76	1.00	1.00	1.00	22.40
237	60.30	45.59	60.92	1.00	72.86	1.00	1.00	1.00	15.37
238	1.00	108.46	1.00	1.00	99.04	1.00	1.00	1.00	32.06
239	78.94	64.28	74.37	1.00	82.49	1.00	1.00	1.00	19.58
240	52.35	42.68	54.12	1.00	74.41	1.00	1.00	1.00	13.48
241	1.00	142.65	1.00	1.00	99.96	1.00	1.00	1.00	22.04
242	52.86	51.05	55.90	1.00	83.24	1.00	1.00	1.00	13.45
243	34.93	56.78	42.73	1.00	75.07	1.00	1.00	1.00	9.23
244	30.88	42.13	26.11	35.33	1.00	1.00	1.00	1.00	13.28
245	51.04	90.69	41.66	56.15	1.00	1.00	1.00	1.00	20.97

METHOD:-	VISSER	SHEAR AREA	COLUMN ANALOGY	TOPRAC	API CODE	AWS CODE	WASHIO
TEST No.1	109.15	1.00	14.30	1.00	1.00	1.00	1.00
2	273.71	1.00	3.58	1.00	1.00	1.00	1.00
3	460.33	1.00	3.50	1.00	1.00	1.00	1.00
4	812.16	1.00	6.42	12.19	16.43	30.19	1.00
5	322.90	1.00	10.65	26.66	21.99	40.72	1.00
6	812.16	1.00	6.42	12.19	16.43	30.19	1.00
7	812.16	1.00	6.42	12.19	16.43	30.19	1.00
8	390.35	1.00	25.86	1.00	1.00	1.00	1.00
9	186.60	1.00	18.74	1.00	1.00	1.00	1.00
10	170.31	1.00	15.43	37.47	26.69	48.77	1.00
11	81.48	1.00	9.87	14.80	19.16	35.48	1.00
12	28.36	1.00	6.42	14.73	12.08	22.06	1.00
13	390.35	1.00	25.86	1.00	1.00	1.00	1.00
14	94.75	1.00	15.63	37.96	27.04	48.77	1.00
15	80.09	1.00	12.60	31.69	22.57	41.94	1.00
16	28.36	1.00	6.42	14.73	12.08	22.06	1.00
17	25.57	1.00	5.74	14.64	10.62	19.46	1.00
18	20.90	1.00	4.64	1.00	1.00	1.00	1.00
19	303.74	1.00	12.58	1.00	1.00	1.00	1.00
20	236.86	1.00	9.02	1.00	1.00	1.00	1.00
21	227.74	1.00	7.43	18.05	14.36	26.10	1.00
22	193.31	1.00	4.68	7.02	10.15	18.99	1.00
23	45.35	1.00	3.07	7.06	6.47	11.81	1.00
24	214.75	1.00	9.91	1.00	1.00	1.00	1.00
25	138.31	1.00	6.56	1.00	1.00	1.00	1.00

METHOD:-	VISSER	SHEAR AREA	COLUMN ANALOGY	TOPRAC	API CODE	AWS CODE	WASHIO
26	129.81	1.00	5.10	12.60	9.78	18.22	1.00
27	81.95	1.00	3.56	5.59	7.64	14.16	1.00
28	35.43	1.00	2.10	5.46	4.21	7.82	1.00
29	464.82	1.00	4.93	7.91	12.32	22.72	1.00
30	274.33	1.00	10.71	17.18	23.81	43.92	1.00
31	168.57	1.00	22.96	36.84	45.53	83.98	1.00
32	417.30	1.00	6.07	13.70	14.94	27.15	1.00
33	233.33	1.00	14.03	31.64	30.45	55.32	1.00
34	163.43	1.00	24.29	54.78	48.55	88.21	1.00
35	399.80	1.00	6.49	19.72	16.00	28.91	1.00
36	284.16	1.00	10.41	31.64	23.92	43.21	1.00
37	194.43	1.00	18.03	54.78	38.14	68.90	1.00
38	36.55	1.00	3.78	5.40	7.48	11.06	7.44
39	36.55	1.00	3.78	5.40	7.48	11.06	7.44
40	36.55	1.00	3.78	5.40	7.48	11.06	7.44
41	36.55	1.00	3.78	5.40	7.48	11.06	7.44
42	36.55	1.00	3.78	5.40	7.48	11.06	7.44
43	36.55	1.00	3.78	5.40	7.48	11.06	7.41
44	36.55	1.00	3.78	5.40	7.48	11.06	7.41
45	36.55	1.00	3.78	5.40	7.48	11.06	7.41
46	36.55	1.00	3.78	5.40	7.48	11.06	7.41
47	36.55	1.00	3.78	5.40	7.48	11.06	7.41
48	26.41	1.00	6.39	9.12	11.68	17.27	10.91
49	26.41	1.00	6.39	9.12	11.68	17.27	10.91
50	26.41	1.00	6.39	9.12	11.68	17.27	10.91

TABLE 2 SUMMARISED RESULTS OF PARAMETRIC STUDY OF TUBE JOINT FORMULAE-PAGE 5
 (CULT) GIVEN BY EACH METHOD IN KIPS, TEST NOS ARE THE SAME AS IN INPUT DATA TABLE

IN THIS TABLE THE FORMULAE ARE TESTED FOR APPLICABILITY
 PULT=1.0 SHOWS THAT THE TEST WAS OUTSIDE THE RECOMMENDED RANGE OF THE FORMULA

FORMULAE MARKED THUS:- * ARE BASED ON SHEAR YIELD STRESS OF CHORD

METHOD:-	VISSER	SHEAR AREA	COLUMN ANALOGY	TOPRAC	API CODE	AWS CODE	WASHIO
51	26.41	1.00	6.39	9.12	11.68	17.27	10.91
52	26.41	1.00	6.39	9.12	11.68	17.27	10.91
53	26.41	1.00	6.39	9.12	11.68	17.27	10.91
54	36.55	1.00	3.78	5.40	7.48	11.06	7.41
55	36.55	1.00	3.78	5.40	7.48	11.06	7.41
56	36.55	1.00	3.78	5.40	7.48	11.06	7.41
57	36.55	1.00	3.78	5.40	7.48	11.06	8.08
58	36.55	1.00	3.78	5.40	7.48	11.06	8.08
59	36.55	1.00	3.78	5.40	7.48	11.06	8.08
60	36.55	1.00	3.78	5.40	7.48	11.06	8.08
61	36.55	1.00	3.78	5.40	7.48	11.06	7.61
62	36.55	1.00	3.78	5.40	7.48	11.06	7.61
63	36.55	1.00	3.78	5.40	7.48	11.06	7.61
64	26.41	1.00	6.39	9.12	11.68	17.27	11.21
65	26.41	1.00	6.39	9.12	11.68	17.27	11.21
66	26.41	1.00	6.39	9.12	11.68	17.27	11.21
67	26.41	1.00	6.39	9.12	11.68	17.27	11.21
68	26.41	1.00	6.39	9.12	11.68	17.27	11.21
69	36.55	1.00	3.78	5.40	7.48	11.06	7.61
70	36.55	1.00	3.78	5.40	7.48	11.06	7.61
71	36.55	1.00	3.78	5.40	7.48	11.06	7.61
72	36.55	1.00	3.78	5.40	7.48	11.06	7.61
73	36.55	1.00	3.78	5.40	7.48	11.06	7.61
74	36.55	1.00	3.78	5.40	7.48	11.06	7.61
75	26.41	1.00	6.39	9.12	11.68	17.27	11.21
76	26.41	1.00	6.39	9.12	11.68	17.27	11.21
77	26.41	1.00	6.39	9.12	11.68	17.27	11.21
78	26.41	1.00	6.39	9.12	11.68	17.27	11.21
79	36.55	1.00	3.78	5.40	7.48	11.06	7.61
80	36.55	1.00	3.78	5.40	7.48	11.06	7.61
81	36.55	1.00	3.78	5.40	7.48	11.06	7.61
82	36.55	1.00	3.78	5.40	7.48	11.06	7.61
83	36.55	1.00	3.78	5.40	7.48	11.06	7.61
84	36.55	1.00	3.78	5.40	7.48	11.06	7.61
85	36.55	1.00	3.78	5.40	7.48	11.06	7.61
86	36.55	1.00	3.78	5.40	7.48	11.06	7.61
87	36.55	1.00	3.78	5.40	7.48	11.06	7.61
88	36.55	1.00	3.78	5.40	7.48	11.06	7.61
89	26.41	1.00	6.39	9.12	11.68	17.27	11.21
90	26.41	1.00	6.39	9.12	11.68	17.27	11.21
91	26.41	1.00	6.39	9.12	11.68	17.27	11.21
92	26.41	1.00	6.39	9.12	11.68	17.27	11.21
93	26.41	1.00	6.39	9.12	11.68	17.27	11.21
94	36.55	1.00	3.78	5.40	7.48	11.06	7.61
95	36.55	1.00	3.78	5.40	7.48	11.06	7.61
96	36.55	1.00	3.78	5.40	7.48	11.06	1.00
97	36.55	1.00	3.78	5.40	7.48	11.06	1.00
98	36.55	1.00	3.78	5.40	7.48	11.06	1.00
99	36.55	1.00	3.78	5.40	7.48	11.06	1.00
100	26.41	1.00	6.39	9.12	11.68	17.27	1.00
101	26.41	1.00	6.39	9.12	11.68	17.27	1.00
102	26.41	1.00	6.39	9.12	11.68	17.27	1.00
103	26.41	1.00	6.39	9.12	11.68	17.27	1.00
104	36.55	1.00	3.78	5.40	7.48	11.06	1.00
105	36.55	1.00	3.78	5.40	7.48	11.06	1.00
106	36.55	1.00	3.78	5.40	7.48	11.06	1.00
107	36.55	1.00	3.78	5.40	7.48	11.06	1.00
108	36.55	1.00	3.78	5.40	7.48	11.06	1.00
109	36.55	1.00	3.78	5.40	7.48	11.06	1.00
110	41.39	1.00	5.46	13.29	9.81	14.10	1.00
111	41.39	1.00	5.46	13.29	9.81	14.10	1.00
112	41.39	1.00	5.46	13.29	9.81	14.10	1.00
113	41.39	1.00	5.46	13.29	9.81	14.10	1.00
114	41.39	1.00	5.46	13.29	9.81	14.10	1.00
115	41.39	1.00	5.46	13.29	9.81	14.10	1.00
116	41.39	1.00	5.46	13.29	9.81	14.10	1.00
117	41.39	1.00	5.46	13.29	9.81	14.10	1.00
118	41.39	1.00	5.46	13.29	9.81	14.10	1.00
119	39.06	1.00	2.83	5.25	5.80	8.75	1.00
120	39.06	1.00	2.83	5.25	5.80	8.75	1.00
121	39.06	1.00	2.83	5.25	5.80	8.75	1.00
122	39.06	1.00	2.83	5.25	5.80	8.75	1.00
123	39.06	1.00	2.83	5.25	5.80	8.75	1.00
124	39.06	1.00	2.83	5.25	5.80	8.75	1.00
125	39.06	1.00	2.83	5.25	5.80	8.75	1.00

TABLE 2 SUMMARISED RESULTS OF PARAMETRIC STUDY OF TUBE JOINT FORMULAE-PAGE 6
 PULTRON GIVEN BY EACH METHOD IN KIPS, TEST NOS ARE THE SAME AS IN INPUT DATA TABLE

IN THIS TABLE THE FORMULAE ARE TESTED FOR APPLICABILITY
 PULTRON=1.0 SHOWS THAT THE TEST WAS OUTSIDE THE RECOMMENDED RANGE OF THE FORMULA

FORMULAE MARKED THUS:- * ARE BASED ON SHEAR YIELD STRESS OF CHORD

METHOD:-	VISSER	SHEAR AREA	COLUMN ANALOGY	TOPRAC	API CODE	AWS CODE	WASHIO
126	39.06	1.00	2.83	5.25	5.80	8.75	1.00
127	39.06	1.00	2.83	5.25	5.80	8.75	1.00
128	39.06	1.00	2.83	5.25	5.80	8.75	1.00
129	39.06	1.00	2.83	5.25	5.80	8.75	1.00
130	39.06	1.00	2.83	5.25	5.80	8.75	1.00
131	39.06	1.00	2.83	5.25	5.80	8.75	1.00
132	38.06	1.00	2.83	5.25	5.80	8.75	6.41
133	39.06	1.00	2.83	5.25	5.80	8.75	6.41
134	38.06	1.00	2.83	5.25	5.80	8.75	6.41
135	38.06	1.00	2.83	5.25	5.80	8.75	6.27
136	38.06	1.00	2.83	5.25	5.80	8.75	6.27
137	36.55	1.00	3.78	5.40	7.48	11.06	7.45
138	36.55	1.00	3.78	5.40	7.48	11.06	8.49
139	36.55	1.00	3.78	5.40	7.48	11.06	8.49
140	36.55	1.00	3.78	5.40	7.48	11.06	8.49
141	36.55	1.00	3.78	5.40	7.48	11.06	1.00
142	36.55	1.00	3.78	5.40	7.48	11.06	1.00
143	36.55	1.00	3.78	5.40	7.48	11.06	1.00
144	36.55	1.00	3.78	5.40	7.48	11.06	7.38
145	36.55	1.00	3.78	5.40	7.48	11.06	7.38
146	36.55	1.00	3.78	5.40	7.48	11.06	7.38
147	36.55	1.00	3.78	5.40	7.48	11.06	7.58
148	36.55	1.00	3.78	5.40	7.48	11.06	7.58
149	36.55	1.00	3.78	5.40	7.48	11.06	7.58
150	36.55	1.00	3.78	5.40	7.48	11.06	1.00

METHOD:-	VISSER	SHEAR AREA	COLUMN ANALOGY	TOPRAC	API CODE	AWS CODE	WASHIO
151	36.55	1.00	3.78	5.40	7.48	11.06	1.00
152	36.55	1.00	3.78	5.40	7.48	11.06	1.00
153	36.55	1.00	3.78	5.40	7.48	11.06	7.35
154	36.55	1.00	3.78	5.40	7.48	11.06	7.35
155	36.55	1.00	3.78	5.40	7.48	11.06	7.35
156	36.55	1.00	3.78	5.40	7.48	11.06	7.55
157	36.55	1.00	3.78	5.40	7.48	11.06	7.55
158	36.55	1.00	3.78	5.40	7.48	11.06	7.55
159	36.55	1.00	3.78	5.40	7.48	11.06	1.00
160	36.55	1.00	3.78	5.40	7.48	11.06	1.00
161	36.55	1.00	3.78	5.40	7.48	11.06	1.00
162	73.81	1.00	3.66	5.23	7.24	11.06	8.08
163	73.81	1.00	3.66	5.23	7.24	11.06	8.08
164	73.81	1.00	3.66	5.23	7.24	11.06	8.08
165	44.76	1.00	3.75	5.36	7.42	11.06	7.48
166	44.76	1.00	3.75	5.36	7.42	11.06	7.48
167	44.76	1.00	3.75	5.36	7.42	11.06	7.48
168	44.76	1.00	3.75	5.36	7.42	11.06	9.90
169	44.76	1.00	3.75	5.36	7.42	11.06	9.90
170	44.76	1.00	3.75	5.36	7.42	11.06	9.90
171	44.76	1.00	3.75	5.36	7.42	11.06	1.00
172	44.76	1.00	3.75	5.36	7.42	11.06	1.00
173	44.76	1.00	3.75	5.36	7.42	11.06	1.00
174	89.63	1.00	6.60	1.00	1.00	1.00	10.04
175	89.63	1.00	6.60	1.00	1.00	1.00	10.04

METHOD:-	VISSER	SHEAR AREA	COLUMN ANALOGY	TOPRAC	API CODE	AWS CODE	WASHIO
176	89.63	1.00	6.60	1.00	1.00	1.00	10.04
177	89.63	1.00	6.60	1.00	1.00	1.00	1.00
178	89.63	1.00	6.60	1.00	1.00	1.00	1.00
179	89.63	1.00	6.60	1.00	1.00	1.00	1.00
180	89.63	1.00	6.60	1.00	1.00	1.00	1.00
181	89.63	1.00	6.60	1.00	1.00	1.00	1.00
182	89.63	1.00	6.60	1.00	1.00	1.00	1.00
183	89.51	1.00	2.41	3.44	4.77	9.15	1.00
184	89.51	1.00	2.41	3.44	4.77	9.15	1.00
185	89.51	1.00	2.41	3.44	4.77	9.15	1.00
186	67.14	1.00	2.78	3.98	5.50	9.84	9.24
187	67.14	1.00	2.78	3.98	5.50	9.84	9.24
188	67.14	1.00	2.78	3.98	5.50	9.84	9.24
189	22.38	1.00	14.46	10.33	28.60	14.00	9.90
190	22.38	1.00	14.46	10.33	28.60	14.00	9.90
191	22.38	1.00	14.46	10.33	28.60	14.00	9.90
192	59.82	1.00	44.05	98.09	75.81	113.50	80.35
193	109.13	1.00	44.05	98.09	75.81	113.50	111.57
194	99.82	1.00	44.05	98.09	75.81	113.50	1.00
195	119.13	1.00	64.41	101.34	115.41	169.15	137.48
196	119.13	1.00	64.41	101.34	115.41	169.15	1.00
197	119.13	1.00	64.41	101.34	115.41	169.15	1.00
198	165.18	1.00	95.99	235.65	152.40	221.11	1.00
199	165.18	1.00	95.99	235.65	152.40	221.11	1.00

TABLE 2 SUMMARISED RESULTS OF PARAMETRIC STUDY OF TUBE JOINT FORMULAE-PAGE 7
 PULTRUDING BY EACH METHOD IN KIPS, TEST NOS ARE THE SAME AS IN INPUT DATA TABLE

IN THIS TABLE THE FORMULAE ARE TESTED FOR APPLICABILITY
 PULT=1.0 SHOWS THAT THE TEST WAS OUTSIDE THE RECOMMENDED RANGE OF THE FORMULA

FORMULAE MARKED THUS:- * ARE BASED ON SHEAR YIELD STRESS OF CHORD

METHOD:-	VISSER	SHEAR AREA	COLUMN ANALOGY	TOPRAC	API CODE	AWS CODE	WASHIO
201	152.64	1.00	18.51	41.21	36.27	54.31	58.93
202	66.05	1.00	74.56	166.01	118.56	177.51	163.80
203	280.72	1.00	40.28	98.99	72.92	105.79	1.00
204	121.48	1.00	162.28	398.81	238.35	345.80	1.00
205	104.34	1.00	25.61	57.01	47.18	70.64	73.18
206	443.73	1.00	44.77	110.03	78.46	116.56	1.00
207	194.79	1.00	10.28	22.89	21.72	32.53	37.29
208	473.56	1.00	14.79	23.26	32.48	48.86	44.03
209	353.01	1.00	22.59	55.51	44.02	63.86	1.00
210	571.58	1.00	11.57	23.26	27.01	40.27	51.57
211	863.85	1.00	14.68	23.54	35.13	52.19	1.00
212	570.23	1.00	20.80	52.25	44.79	65.11	1.00
213	820.27	1.00	7.10	17.14	17.86	26.52	33.52
214	1265.29	1.00	8.84	17.35	23.23	34.26	1.00
215	874.36	1.00	10.84	17.87	29.28	42.19	1.00
216	710.00	1.00	14.59	37.26	35.76	51.28	1.00
217	191.95	1.00	10.38	23.11	21.90	32.78	1.00
218	571.56	1.00	11.57	23.26	27.01	40.27	1.00
219	820.27	1.00	7.10	17.14	17.86	26.52	1.00
220	710.87	1.00	9.03	17.71	23.72	34.26	1.00
221	874.36	1.00	10.84	17.87	29.28	42.19	1.00
222	35.37	1.00	9.25	18.02	17.48	25.83	1.00
223	110.72	1.00	21.28	1.00	1.00	1.00	1.00
224	35.37	1.00	9.25	18.02	17.48	25.83	1.00
225	110.72	1.00	21.28	1.00	1.00	1.00	1.00

METHOD:-	VISSER	SHEAR AREA	COLUMN ANALOGY	TOPRAC	API CODE	AWS CODE	WASHIO
226	239.55	1.00	51.73	1.00	1.00	1.00	65.15
227	204.88	1.00	22.58	57.95	40.81	61.53	43.12
228	155.51	1.00	13.94	27.36	26.88	41.55	32.31
229	227.08	1.00	43.10	1.00	1.00	1.00	57.18
230	195.02	1.00	18.91	48.51	35.24	52.67	37.88
231	149.12	1.00	11.76	22.99	23.40	35.69	28.44
232	192.47	1.00	26.34	1.00	1.00	1.00	39.41
233	166.36	1.00	11.63	29.85	23.41	34.38	26.09
234	127.92	1.00	7.28	14.28	15.63	23.23	19.55
235	239.56	1.00	51.69	1.00	1.00	1.00	72.17
236	204.88	1.00	22.58	57.95	40.81	61.53	51.54
237	155.51	1.00	13.94	27.36	26.88	41.55	41.42
238	227.08	1.00	43.10	1.00	1.00	1.00	73.17
239	195.02	1.00	18.91	48.51	35.24	52.67	48.47
240	149.12	1.00	11.76	22.99	23.40	35.69	36.40
241	192.47	1.00	26.34	1.00	1.00	1.00	54.81
242	166.36	1.00	11.63	29.85	23.41	34.38	35.73
243	127.95	1.00	7.28	14.28	15.63	23.22	27.67
244	103.24	1.00	8.01	15.61	15.66	29.35	1.00
245	248.90	1.00	14.32	35.41	25.25	47.72	1.00

METHOD:-	REER	ROUWKAMP	DET	NAKA,KATO, KANATANI	KUROBANE	ROARK(1)	ROARK(2)	KATO	KELLOGG
1	0.00	3.06	0.00	1.48	0.00	0.00	0.00	0.00	4.28
2	0.00	1.68	0.00	0.00	0.00	0.00	2.43	3.02	0.00
3	0.00	1.20	0.00	0.00	0.00	0.00	2.52	2.93	0.00
4	2.36	0.96	0.00	0.00	0.00	0.00	3.17	3.47	0.00
5	2.30	1.65	2.61	1.99	0.00	0.00	0.00	0.00	0.00
6	2.01	0.82	0.00	0.00	0.00	0.00	2.70	2.96	0.00
7	2.36	0.96	0.00	0.00	0.00	0.00	3.17	3.47	0.00
8	0.00	1.06	0.00	0.94	0.00	0.00	0.00	0.00	3.44
9	0.00	1.43	1.61	1.16	0.00	0.00	0.00	0.00	3.25
10	1.27	1.38	1.56	1.15	0.00	0.00	0.00	0.00	3.13
11	1.24	1.81	1.47	1.12	0.00	0.00	0.00	0.00	2.97
12	1.27	2.56	1.44	1.07	0.00	0.00	0.00	0.00	2.49
13	0.00	1.32	0.00	1.17	0.00	0.00	0.00	0.00	4.32
14	1.38	2.05	1.67	1.25	0.00	0.00	0.00	0.00	3.30
15	1.40	2.06	1.67	1.27	0.00	0.00	0.00	0.00	3.39
16	1.47	2.97	1.67	1.24	0.00	0.00	0.00	0.00	3.35
17	1.46	2.93	1.65	1.19	0.00	0.00	0.00	0.00	3.28
18	0.00	3.44	0.00	1.33	0.00	0.00	0.00	0.00	3.60
19	0.00	1.24	0.00	1.35	0.00	0.00	0.00	0.00	4.95
20	0.00	1.25	2.18	1.57	0.00	0.00	0.00	0.00	4.42
21	1.79	1.21	2.09	1.56	0.00	0.00	0.00	0.00	4.23
22	1.71	1.13	1.97	1.49	0.00	0.00	0.00	0.00	3.93
23	1.85	2.08	2.03	1.50	0.00	0.00	0.00	0.00	4.07
24	0.00	1.21	0.00	1.25	0.00	0.00	0.00	0.00	4.59
25	0.00	1.25	1.90	1.40	0.00	0.00	0.00	0.00	3.66

TABLE 2A SUMMARISED RESULTS OF PARAMETRIC STUDY OF THOSE JOINT FORMULAE-PAGE 1
P(CULT)EXPIL/P(CULT)THEORY RATIOS TEST NOS ARE THE SAME AS IN INPUT DATA TABLE

IN THIS TABLE THE FORMULAE ARE TESTED FOR APPLICABILITY
RATIO=0.3 SHOWS THAT THE TEST WAS OUTSIDE THE RECOMMENDED RANGE OF THE FORMULA

FORMULAE LISTED ARE BASED ON YIELD STRESS OF CHORD

METHOD:-	REGER	BOUWKAMP	DET	NAKA,KATO,	KUROBANE	ROARK(1)	ROARK(2)	KATO	KELLOGG
*****	*****	*****	NORSKE	KANATANI	*****	*****	*****	*****	*****
26	1.57	1.21	1.84	1.39	0.00	0.00	0.00	0.00	3.71
27	1.59	1.42	1.03	1.39	0.00	0.00	0.00	0.00	3.67
28	1.90	2.00	2.11	1.50	0.00	0.00	0.00	0.00	4.15
29	1.49	0.68	0.00	0.00	0.00	0.00	2.12	2.26	0.00
30	2.31	1.97	2.62	2.00	0.00	0.00	0.00	0.00	5.29
31	2.22	3.48	2.62	2.00	0.00	0.00	0.00	0.00	5.28
32	2.69	1.46	0.00	0.00	0.00	0.00	3.01	3.48	0.00
33	2.23	2.35	2.41	1.80	0.00	0.00	0.00	0.00	0.00
34	2.39	3.92	2.66	1.98	0.00	0.00	0.00	0.00	5.38
35	2.50	1.42	0.00	0.00	0.00	0.00	2.27	2.65	0.00
36	2.48	2.05	0.00	0.00	0.00	0.00	1.90	2.38	0.00
37	2.82	3.63	2.93	2.08	0.00	0.00	0.00	0.00	0.00
38	0.82	0.64	1.17	0.00	0.69	0.00	0.00	0.00	3.26
39	0.89	0.69	1.27	0.00	0.74	0.00	0.00	0.00	3.52
40	0.91	0.71	1.30	0.00	0.76	0.00	0.00	0.00	3.62
41	0.93	0.73	1.33	0.00	0.78	0.00	0.00	0.00	3.69
42	0.93	0.73	1.33	0.00	0.78	0.00	0.00	0.00	3.69
43	0.86	0.67	1.23	0.00	0.72	0.00	0.00	0.00	3.43
44	0.90	0.70	1.29	0.00	0.75	0.00	0.00	0.00	3.57
45	0.75	0.59	1.08	0.00	0.63	0.00	0.00	0.00	3.00
46	0.89	0.69	1.27	0.00	0.74	0.00	0.00	0.00	3.52
47	0.89	0.69	1.27	0.00	0.74	0.00	0.00	0.00	3.52
48	0.65	0.78	0.00	0.00	0.84	0.00	0.00	0.00	2.67
49	0.65	0.78	0.00	0.00	0.84	0.00	0.00	0.00	2.67
50	0.70	0.83	0.00	0.00	0.89	0.00	0.00	0.00	2.85

METHOD:-	PERER	BOUWKAMP	DET	NAKA,KATO,	KUROBANE	ROARK(1)	ROARK(2)	KATO	KELLOGG
*****	*****	*****	NORSKE	KANATANI	*****	*****	*****	*****	*****
51	0.65	0.78	0.00	0.00	0.84	0.00	0.00	0.00	2.67
52	0.65	0.78	0.00	0.00	0.84	0.00	0.00	0.00	2.67
53	0.65	0.78	0.00	0.00	0.84	0.00	0.00	0.00	2.67
54	0.93	1.21	1.33	0.00	0.78	0.00	0.00	0.00	3.69
55	0.99	1.29	1.41	0.00	0.83	0.00	0.00	0.00	3.93
56	0.96	1.25	1.37	0.00	0.80	0.00	0.00	0.00	3.81
57	0.99	1.30	1.23	0.00	0.82	0.00	0.00	0.00	3.95
58	1.02	1.33	1.26	0.00	0.84	0.00	0.00	0.00	4.05
59	0.97	1.27	1.20	0.00	0.80	0.00	0.00	0.00	3.86
60	1.05	1.37	1.30	0.00	0.87	0.00	0.00	0.00	4.17
61	0.93	1.21	1.15	0.00	0.77	0.00	0.00	0.00	3.69
62	0.93	1.21	1.25	0.00	0.77	0.00	0.00	0.00	3.69
63	0.99	1.29	1.34	0.00	0.82	0.00	0.00	0.00	3.93
64	0.69	0.82	0.00	0.00	0.87	0.00	0.00	0.00	2.81
65	0.70	0.83	0.00	0.00	0.88	0.00	0.00	0.00	2.85
66	0.71	0.85	0.00	0.00	0.90	0.00	0.00	0.00	2.91
67	0.70	0.83	0.00	0.00	0.88	0.00	0.00	0.00	2.85
68	0.71	0.85	0.00	0.00	0.90	0.00	0.00	0.00	2.91
69	0.87	1.13	1.17	0.00	0.72	0.00	0.00	0.00	3.45
70	0.96	1.26	1.30	0.00	0.80	0.00	0.00	0.00	3.83
71	0.95	1.24	1.29	0.00	0.79	0.00	0.00	0.00	3.79
72	0.98	1.27	1.32	0.00	0.81	0.00	0.00	0.00	3.88
73	1.04	1.36	1.41	0.00	0.87	0.00	0.00	0.00	4.15
74	1.08	1.41	1.47	0.00	0.90	0.00	0.00	0.00	4.31
75	0.71	0.85	0.00	0.00	0.90	0.00	0.00	0.00	2.91

METHOD:-	REGER	BOUWKAMP	DET	NAKA,KATO,	KUROBANE	ROARK(1)	ROARK(2)	KATO	KELLOGG
*****	*****	*****	NORSKE	KANATANI	*****	*****	*****	*****	*****
76	0.71	0.84	0.00	0.00	0.90	0.00	0.00	0.00	2.89
77	0.71	0.84	0.00	0.00	0.90	0.00	0.00	0.00	2.89
78	0.70	0.83	0.00	0.00	0.89	0.00	0.00	0.00	2.85
79	1.35	1.06	1.82	0.00	1.12	0.00	0.00	0.00	5.37
80	1.26	0.99	1.70	0.00	1.05	0.00	0.00	0.00	5.01
81	1.26	0.99	1.70	0.00	1.05	0.00	0.00	0.00	5.01
82	1.33	1.04	1.79	0.00	1.10	0.00	0.00	0.00	5.27
83	1.39	1.09	1.88	0.00	1.16	0.00	0.00	0.00	5.54
84	1.16	0.91	1.57	0.00	0.77	0.00	0.00	0.00	4.63
85	1.12	0.88	1.51	0.00	0.93	0.00	0.00	0.00	4.46
86	1.08	0.85	1.47	0.00	0.90	0.00	0.00	0.00	4.31
87	1.08	0.85	1.47	0.00	0.90	0.00	0.00	0.00	4.31
88	1.08	0.85	1.47	0.00	0.90	0.00	0.00	0.00	4.31
89	0.71	0.85	0.00	0.00	0.90	0.00	0.00	0.00	2.91
90	0.74	0.88	0.00	0.00	0.94	0.00	0.00	0.00	3.02
91	0.78	0.92	0.00	0.00	0.98	0.00	0.00	0.00	3.17
92	0.76	0.91	0.00	0.00	0.97	0.00	0.00	0.00	3.12
93	0.74	0.88	0.00	0.00	0.94	0.00	0.00	0.00	3.02
94	1.13	0.88	1.52	0.00	0.94	0.00	0.00	0.00	4.49
95	1.13	0.88	1.52	0.00	0.94	0.00	0.00	0.00	4.48
96	1.14	0.89	1.63	0.00	0.93	0.00	0.00	0.00	4.53
97	1.13	0.89	1.62	0.00	0.93	0.00	0.00	0.00	4.51
98	1.15	0.90	1.65	0.00	0.94	0.00	0.00	0.00	4.58
99	1.17	0.91	1.67	0.00	0.96	0.00	0.00	0.00	4.65
100	0.78	0.92	0.00	0.00	0.97	0.00	0.00	0.00	3.17

IN THIS TABLE THE FORMULAE ARE TESTED FOR APPLICABILITY
RATIO=0.0 SHOWS THAT THE TEST WAS OUTSIDE THE RECOMMENDED RANGE OF THE FORMULA

FORMULAE LISTED ARE BASED ON YIELD STRESS OF CHORD

METHOD:-	REBER	BOUWKAMP	DET	NAKA,KATO,	KUROBANE	ROARK(1)	ROARK(2)	KATO	KELLOGG
*****	*****	*****	NORSKE	KANATANI	*****	*****	*****	*****	*****
101	0.76	0.91	0.00	0.00	0.95	0.00	0.00	0.00	3.12
102	0.79	0.94	0.00	0.00	0.99	0.00	0.00	0.00	3.23
103	0.74	0.88	0.00	0.00	0.92	0.00	0.00	0.00	3.02
104	0.94	0.74	1.35	0.00	0.77	0.00	0.00	0.00	3.74
105	0.94	0.74	1.35	0.00	0.77	0.00	0.00	0.00	3.74
106	0.98	0.76	1.40	0.00	0.80	0.00	0.00	0.00	3.88
107	1.03	1.34	1.43	0.00	0.85	0.00	0.00	0.00	4.10
108	1.03	1.34	1.48	0.00	0.85	0.00	0.00	0.00	4.10
109	1.06	1.38	1.52	0.00	0.87	0.00	0.00	0.00	4.22
110	0.80	0.63	1.15	0.00	0.78	0.00	0.00	0.00	3.25
111	0.88	0.69	1.27	0.00	0.86	0.00	0.00	0.00	3.54
112	0.80	0.63	1.15	0.00	0.78	0.00	0.00	0.00	3.25
113	0.96	1.26	1.38	0.00	0.94	0.00	0.00	0.00	3.90
114	0.94	1.24	1.36	0.00	0.92	0.00	0.00	0.00	3.82
115	0.95	1.25	1.38	0.00	0.93	0.00	0.00	0.00	3.88
116	1.06	0.84	1.53	0.00	1.04	0.00	0.00	0.00	4.32
117	1.08	0.85	1.55	0.00	1.05	0.00	0.00	0.00	4.38
118	1.10	0.87	1.59	0.00	1.08	0.00	0.00	0.00	4.49
119	1.06	0.75	1.52	0.00	0.72	0.00	0.00	0.00	4.11
120	1.03	0.73	1.49	0.00	0.70	0.00	0.00	0.00	4.02
121	1.08	0.77	1.56	0.00	0.74	0.00	0.00	0.00	4.20
122	1.03	1.22	1.49	0.00	0.70	0.00	0.00	0.00	4.02
123	1.09	1.29	1.57	0.00	0.74	0.00	0.00	0.00	4.23
124	1.06	1.25	1.52	0.00	0.72	0.00	0.00	0.00	4.11
125	1.42	1.68	2.05	0.00	0.97	0.00	0.00	0.00	5.52
METHOD:-	REBER	BOUWKAMP	DET	NAKA,KATO,	KUROBANE	ROARK(1)	ROARK(2)	KATO	KELLOGG
*****	*****	*****	NORSKE	KANATANI	*****	*****	*****	*****	*****
126	1.44	1.70	2.08	0.00	0.98	0.00	0.00	0.00	5.61
127	1.44	1.70	2.08	0.00	0.98	0.00	0.00	0.00	5.61
128	1.04	1.23	1.50	0.00	0.71	0.00	0.00	0.00	4.05
129	0.95	1.12	1.37	0.00	0.65	0.00	0.00	0.00	3.69
130	1.05	1.24	1.51	0.00	0.72	0.00	0.00	0.00	4.08
131	1.06	1.25	1.52	0.00	0.72	0.00	0.00	0.00	4.11
132	1.10	1.30	1.42	0.00	0.76	0.00	0.00	0.00	4.29
133	0.95	1.12	1.22	0.00	0.65	0.00	0.00	0.00	3.69
134	1.30	0.92	1.68	0.00	0.90	0.00	0.00	0.00	5.07
135	1.26	0.89	1.61	0.00	0.88	0.00	0.00	0.00	4.89
136	1.23	0.87	1.77	0.00	0.85	0.00	0.00	0.00	4.77
137	1.26	1.64	1.80	0.00	1.06	0.00	0.00	0.00	5.01
138	1.12	1.46	1.35	0.00	0.93	0.00	0.00	0.00	4.46
139	0.94	1.23	1.13	0.00	0.78	0.00	0.00	0.00	3.74
140	1.33	1.73	1.60	0.00	1.10	0.00	0.00	0.00	5.27
141	1.30	1.69	1.85	0.00	1.06	0.00	0.00	0.00	5.15
142	0.92	1.20	1.32	0.00	0.75	0.00	0.00	0.00	3.67
143	1.36	1.77	1.94	0.00	1.11	0.00	0.00	0.00	5.39
144	1.36	1.77	1.94	0.00	1.14	0.00	0.00	0.00	5.39
145	2.04	2.66	2.92	0.00	1.72	0.00	0.00	0.00	8.13
146	2.02	2.63	2.89	0.00	1.70	0.00	0.00	0.00	8.03
147	1.15	0.90	1.65	0.00	0.96	0.00	0.00	0.00	4.58
148	1.64	1.28	2.35	0.00	1.36	0.00	0.00	0.00	6.52
149	1.04	0.81	1.48	0.00	0.86	0.00	0.00	0.00	4.12
150	0.90	0.71	1.29	0.00	0.74	0.00	0.00	0.00	3.60
METHOD:-	REBER	BOUWKAMP	DET	NAKA,KATO,	KUROBANE	ROARK(1)	ROARK(2)	KATO	KELLOGG
*****	*****	*****	NORSKE	KANATANI	*****	*****	*****	*****	*****
151	2.15	1.68	3.08	0.00	1.77	0.00	0.00	0.00	8.56
152	1.13	0.89	1.62	0.00	0.93	0.00	0.00	0.00	4.51
153	1.61	1.26	2.30	0.00	1.36	0.00	0.00	0.00	6.40
154	2.39	1.87	3.42	0.00	2.02	0.00	0.00	0.00	9.52
155	1.50	1.17	2.15	0.00	1.26	0.00	0.00	0.00	5.97
156	1.14	1.49	1.63	0.00	0.75	0.00	0.00	0.00	4.53
157	1.14	1.49	1.63	0.00	0.95	0.00	0.00	0.00	4.53
158	2.16	2.82	3.10	0.00	1.80	0.00	0.00	0.00	8.60
159	2.19	2.55	3.13	0.00	1.80	0.00	0.00	0.00	8.70
160	1.70	1.33	2.44	0.00	1.40	0.00	0.00	0.00	6.78
161	2.26	1.77	3.24	0.00	1.36	0.00	0.00	0.00	8.99
162	0.98	0.55	1.25	0.00	0.81	0.00	0.00	0.00	3.69
163	1.10	0.61	1.41	0.00	0.91	0.00	0.00	0.00	4.36
164	1.07	0.60	1.37	0.00	0.88	0.00	0.00	0.00	4.24
165	1.02	0.72	1.47	0.00	0.85	0.00	0.00	0.00	4.05
166	0.98	0.69	1.41	0.00	0.82	0.00	0.00	0.00	3.68
167	0.85	0.60	1.23	0.00	0.71	0.00	0.00	0.00	3.38
168	1.20	1.43	1.31	0.00	1.00	0.00	0.00	0.00	4.79
169	1.19	1.41	1.30	0.00	0.99	0.00	0.00	0.00	4.75
170	1.17	1.39	1.28	0.00	0.97	0.00	0.00	0.00	4.67
171	1.28	0.91	1.84	0.00	1.05	0.00	0.00	0.00	5.04
172	1.45	1.03	2.09	0.00	1.19	0.00	0.00	0.00	5.75
173	1.42	1.01	2.05	0.00	1.17	0.00	0.00	0.00	5.66
174	0.00	0.47	1.24	0.00	0.91	0.00	0.00	0.00	3.45
175	0.00	0.48	1.26	0.00	0.93	0.00	0.00	0.00	3.50

TABLE 2A SUMMARISED RESULTS OF PARAMETRIC STUDY OF TUBE JOINT FORMULAE-PAGE 3
 (CULT)EXPL/P(CULT)THEORY RATIOS TEST NOS ARE THE SAME AS IN INPUT DATA TABLE

IN THIS TABLE THE FORMULAE ARE TESTED FOR APPLICABILITY
 RATIO=0.0 SHOWS THAT THE TEST WAS OUTSIDE THE RECOMMENDED RANGE OF THE FORMULA

FORMULAE LISTED ARE BASED ON YIELD STRESS OF CHORD

METHOD:-	REBER	BOUWKAMP	DET	NAKA,KATO, KUROBANE	ROARK(1)	ROARK(2)	KATO	KELLOGG
			NORSKE	KANATANI				
176	0.00	0.47	1.24	0.00	0.91	0.00	0.00	3.45
177	0.00	0.96	1.51	0.00	1.10	0.00	0.00	4.20
178	0.00	0.92	1.47	0.00	1.06	0.00	0.00	4.07
179	0.00	0.95	1.51	0.00	1.09	0.00	0.00	4.10
180	0.00	0.59	1.56	0.00	1.12	0.00	0.00	4.32
181	0.00	0.63	1.67	0.00	1.20	0.00	0.00	4.64
182	0.00	0.64	1.68	0.00	1.21	0.00	0.00	4.67
183	1.84	1.30	2.24	1.65	0.00	0.00	0.00	4.36
184	1.59	1.12	1.93	1.42	0.00	0.00	0.00	3.76
185	1.56	1.10	1.89	1.40	0.00	0.00	0.00	3.69
186	1.45	1.27	1.24	0.00	1.08	0.00	0.00	4.27
187	1.44	1.25	1.22	0.00	1.07	0.00	0.00	4.22
188	1.45	1.26	1.23	0.00	1.08	0.00	0.00	4.24
189	0.80	1.59	1.37	0.00	0.79	0.00	0.00	5.35
190	0.81	1.62	1.40	0.00	0.80	0.00	0.00	5.44
191	0.77	1.53	1.32	0.00	0.76	0.00	0.00	5.15
192	0.63	1.13	0.00	0.00	0.72	0.00	0.00	2.51
193	0.65	1.07	0.00	0.00	0.74	0.00	0.00	2.59
194	0.63	1.12	0.00	0.00	0.71	0.00	0.00	2.49
195	0.61	1.11	0.00	0.00	0.97	0.00	0.00	2.52
196	0.64	1.16	0.00	0.00	1.01	0.00	0.00	2.64
197	0.64	1.16	0.00	0.00	1.00	0.00	0.00	2.64
198	0.66	1.11	0.00	0.00	1.28	0.00	0.00	2.81
199	0.66	1.11	0.00	0.00	1.27	0.00	0.00	2.81
200	0.71	1.19	0.00	0.00	1.35	0.00	0.00	3.00

METHOD:-	REBER	BOUWKAMP	DET	NAKA,KATO, KUROBANE	ROARK(1)	ROARK(2)	KATO	KELLOGG
			NORSKE	KANATANI				
201	1.08	1.60	0.95	0.00	0.61	0.00	0.00	4.09
202	0.44	1.20	0.00	0.00	0.76	0.00	0.00	1.80
203	1.17	1.64	1.68	0.00	1.12	0.00	0.00	4.75
204	0.44	1.11	0.00	0.00	1.27	0.00	0.00	1.89
205	1.04	1.29	0.00	0.00	0.82	0.00	0.00	4.05
206	1.58	1.89	2.35	0.00	1.80	0.00	0.00	6.48
207	1.65	1.63	1.43	0.00	0.63	0.00	0.00	6.12
208	2.54	1.91	2.82	0.00	1.36	0.00	0.00	9.79
209	2.18	2.05	3.05	0.00	1.41	0.00	0.00	8.62
210	1.28	0.80	1.01	0.00	0.35	0.00	0.00	0.00
211	2.25	1.27	3.07	0.00	0.78	0.00	0.00	0.00
212	2.23	1.64	3.01	0.00	0.91	0.00	0.00	0.00
213	1.08	0.45	0.89	0.00	0.14	0.00	0.00	0.00
214	1.27	0.43	1.63	0.00	0.20	0.00	0.00	0.00
215	2.47	1.21	3.14	0.00	0.46	0.00	0.00	0.00
216	2.55	1.48	3.26	0.00	0.55	0.00	0.00	0.00
217	2.11	2.11	2.89	0.00	0.80	0.00	0.00	7.62
218	2.81	1.51	3.78	0.00	0.78	0.00	0.00	0.00
219	4.31	1.55	5.46	0.00	0.54	0.00	0.00	0.00
220	3.17	1.36	3.99	0.00	0.50	0.00	0.00	0.00
221	3.34	1.40	4.25	0.00	0.62	0.00	0.00	0.00
222	1.29	1.67	0.00	0.00	1.20	0.00	0.00	5.10
223	0.00	1.53	0.00	0.00	2.53	0.00	0.00	7.09
224	1.29	1.67	0.00	0.00	1.19	0.00	0.00	5.10
225	0.00	1.51	0.00	0.00	2.48	0.00	0.00	6.97

METHOD:-	REBER	BOUWKAMP	DET	NAKA,KATO, KUROBANE	ROARK(1)	ROARK(2)	KATO	KELLOGG
			NORSKE	KANATANI				
226	0.00	0.61	0.00	0.00	0.73	0.00	0.00	1.93
227	0.60	0.79	0.78	0.00	0.69	0.00	0.00	2.46
228	0.75	0.99	0.89	0.00	0.62	0.00	0.00	2.93
229	0.00	0.64	0.00	0.00	0.70	0.00	0.00	2.15
230	0.68	0.84	0.87	0.00	0.66	0.00	0.00	2.76
231	0.74	0.91	0.87	0.00	0.53	0.00	0.00	2.69
232	0.00	0.61	0.00	0.00	0.52	0.00	0.00	2.36
233	0.62	0.65	0.76	0.00	0.40	0.00	0.00	2.45
234	0.77	0.79	0.85	0.00	0.36	0.00	0.00	2.93
235	0.00	0.61	0.00	0.00	0.73	0.00	0.00	1.93
236	0.60	0.79	0.70	0.00	0.69	0.00	0.00	2.46
237	0.75	0.99	0.74	0.00	0.62	0.00	0.00	2.93
238	0.00	0.64	0.00	0.00	0.70	0.00	0.00	2.15
239	0.68	0.84	0.73	0.00	0.65	0.00	0.00	2.76
240	0.74	0.91	0.72	0.00	0.52	0.00	0.00	2.67
241	0.00	0.36	0.00	0.00	0.52	0.00	0.00	2.36
242	0.62	0.65	0.59	0.00	0.40	0.00	0.00	2.45
243	0.77	0.48	0.63	0.00	0.36	0.00	0.00	2.93
244	0.80	0.59	0.95	0.70	0.00	0.00	0.00	1.86
245	0.78	0.44	0.96	0.71	0.00	0.00	0.00	1.91

TABLE 2A SUMMARISED RESULTS OF PARAMETRIC STUDY OF TUBE JOINT FORMULAE-PAGE 4
 P(ULT)/EXPIL/P(ULT)/THEORY RATIOS TEST NOS ARE THE SAME AS IN INPUT DATA TABLE

IN THIS TABLE THE FORMULAE ARE TESTED FOR APPLICABILITY
 RATIO=0.0 SHOWS THAT THE TEST WAS OUTSIDE THE RECOMMENDED RANGE OF THE FORMULA

FORMULAE MARKED THUS:- * ARE BASED ON SHEAR YIELD STRESS OF CHORD

METHOD:-	VISSER	SHEAR AREA	COLUMN ANALOGY	TOPRAC	API CODE	AWS CODE	WASHIO
TEST No.1	0.2345	0.0000	7.1306	0.0000	0.0000	0.0000	0.0000
2	0.2009	0.0000	15.6594	0.0000	0.0000	0.0000	0.0000
3	0.1173	0.0000	15.4345	0.0000	0.0000	0.0000	0.0000
4	0.1010	0.0000	12.7755	6.7268	4.9898	2.7159	0.0000
5	0.3252	0.0000	9.8558	3.9389	4.7746	2.5787	0.0000
6	0.0862	0.0000	10.9059	5.7424	4.2596	2.3184	0.0000
7	0.1010	0.0000	12.7755	6.7268	4.9898	2.7159	0.0000
8	0.2562	0.0000	3.8668	0.0000	0.0000	0.0000	0.0000
9	0.4143	0.0000	4.1257	0.0000	0.0000	0.0000	0.0000
10	0.3686	0.0000	4.2852	1.7641	2.4767	1.3554	0.0000
11	0.5768	0.0000	4.7609	3.1765	2.4529	1.3246	0.0000
12	1.0226	0.0000	4.5203	1.9583	2.3999	1.3144	0.0000
13	0.3213	0.0000	4.8490	0.0000	0.0000	0.0000	0.0000
14	0.7567	0.0000	4.5882	1.8888	2.6519	1.4703	0.0000
15	0.7037	0.0000	4.9762	1.9785	2.7778	1.4950	0.0000
16	1.1848	0.0000	5.2374	2.2805	2.7805	1.5229	0.0000
17	1.1390	0.0000	5.0729	1.9894	2.7432	1.4963	0.0000
18	1.2864	0.0000	5.7932	0.0000	0.0000	0.0000	0.0000
19	0.2729	0.0000	6.5861	0.0000	0.0000	0.0000	0.0000
20	0.2553	0.0000	6.7039	0.0000	0.0000	0.0000	0.0000
21	0.2262	0.0000	6.9324	2.8538	3.5882	1.9740	0.0000
22	0.1835	0.0000	7.6546	5.1073	3.5319	1.8873	0.0000
23	0.5187	0.0000	7.6491	3.3307	3.6368	1.9919	0.0000
24	0.2712	0.0000	5.8746	0.0000	0.0000	0.0000	0.0000
25	0.2755	0.0000	5.8100	0.0000	0.0000	0.0000	0.0000
METHOD:-	VISSER	SHEAR AREA	COLUMN ANALOGY	TOPRAC	API CODE	AWS CODE	WASHIO
26	0.2416	0.0000	6.1501	2.4887	3.2080	1.7214	0.0000
27	0.3007	0.0000	6.9276	4.4108	3.2250	1.7397	0.0000
28	0.4426	0.0000	7.4806	2.8699	3.7269	2.0045	0.0000
29	0.0835	0.0000	7.8706	4.9048	3.1503	1.7080	0.0000
30	0.4090	0.0000	10.4800	6.5310	4.7122	2.5549	0.0000
31	1.1776	0.0000	8.6472	5.3888	4.3594	2.3636	0.0000
32	0.1986	0.0000	13.6506	6.0516	5.5463	3.0527	0.0000
33	0.5726	0.0000	9.5454	4.2317	4.3974	2.4204	0.0000
34	1.3651	0.0000	9.1863	4.0725	4.5952	2.5292	0.0000
35	0.7026	0.0000	12.4809	4.1072	5.0613	2.8016	0.0000
36	0.4117	0.0000	11.2363	3.6976	4.8915	2.7076	0.0000
37	1.0646	0.0000	11.4825	3.7786	5.4276	3.0044	0.0000
38	0.3721	0.0000	3.5974	2.5172	1.8192	1.2301	1.8277
39	0.4022	0.0000	3.3884	2.7230	1.9663	1.3296	1.9755
40	0.4132	0.0000	3.9942	2.7971	2.0198	1.3658	2.0292
41	0.4214	0.0000	4.0736	2.8526	2.0599	1.3930	2.0696
42	0.4214	0.0000	4.0736	2.8526	2.0599	1.3930	2.0696
43	0.3913	0.0000	3.7826	2.6489	1.9128	1.2935	1.9300
44	0.4077	0.0000	3.9413	2.7600	1.9931	1.3477	2.0110
45	0.3420	0.0000	3.3065	2.3155	1.6720	1.1306	1.6871
46	0.4022	0.0000	3.8884	2.7230	1.9663	1.3296	1.9840
47	0.4022	0.0000	3.8884	2.7230	1.9663	1.3296	1.9840
48	0.6249	0.0000	2.5826	1.8085	1.4129	0.9554	1.5124
49	0.6249	0.0000	2.5826	1.8085	1.4129	0.9554	1.5124
50	0.6665	0.0000	2.7547	1.9291	1.5071	1.0191	1.6133
METHOD:-	VISSER	SHEAR AREA	COLUMN ANALOGY	TOPRAC	API CODE	AWS CODE	WASHIO
51	0.6249	0.0000	2.5826	1.8085	1.4129	0.9554	1.5124
52	0.6249	0.0000	2.5826	1.8085	1.4129	0.9554	1.5124
53	0.6249	0.0000	2.5826	1.8085	1.4129	0.9554	1.5124
54	0.4214	0.0000	4.0736	2.8526	2.0599	1.3930	2.0785
55	0.4488	0.0000	4.3381	3.0379	2.1937	1.4834	2.2135
56	0.4351	0.0000	4.2058	2.9453	2.1268	1.4382	2.1460
57	0.4515	0.0000	4.3645	3.0564	2.2071	1.4925	2.0430
58	0.4624	0.0000	4.4703	3.1305	2.2606	1.5286	2.0925
59	0.4405	0.0000	4.2547	2.9823	2.1536	1.4563	1.9935
60	0.4761	0.0000	4.6026	3.2231	2.3275	1.5739	2.1545
61	0.4214	0.0000	4.0736	2.8526	2.0599	1.3930	1.9068
62	0.4214	0.0000	4.0736	2.8526	2.0599	1.3930	2.0233
63	0.4488	0.0000	4.3381	3.0379	2.1937	1.4834	2.1547
64	0.4590	0.0000	2.7234	1.9072	1.4900	1.0075	1.5526
65	0.6665	0.0000	2.7547	1.9291	1.5071	1.0191	1.5704
66	0.6817	0.0000	2.8173	1.9729	1.5413	1.0423	1.6061
67	0.6665	0.0000	2.7547	1.9291	1.5071	1.0191	1.5704
68	0.6817	0.0000	2.8173	1.9729	1.5413	1.0423	1.6061
69	0.3940	0.0000	3.8090	2.6674	1.9262	1.3025	1.8919
70	0.4378	0.0000	4.2323	2.9638	2.1402	1.4472	2.1022
71	0.4323	0.0000	4.1794	2.9267	2.1134	1.4291	2.0750
72	0.4433	0.0000	4.2852	3.0008	2.1669	1.4653	2.1284
73	0.4734	0.0000	4.5761	3.2045	2.3141	1.5648	2.2730
74	0.4925	0.0000	4.7613	3.3343	2.4077	1.6281	2.3649
75	0.6817	0.0000	2.8173	1.9729	1.5413	1.0423	1.6061

TABLE 2A

SUMMARISED RESULTS OF PARAMETRIC STUDY OF TUBE JOINT FORMULAE-PAGE 5

P(ULT)EXPTL/P(ULT)THEORY RATIOS

TEST NOS ARE THE SAME AS IN INPUT DATA TABLE

IN THIS TABLE THE FORMULAE ARE TESTED FOR APPLICABILITY
RATIO=0.0 SHOWS THAT THE TEST WAS OUTSIDE THE RECOMMENDED RANGE OF THE FORMULA

FORMULAE MARKED THUS:- * ARE BASED ON SHEAR YIELD STRESS OF CHORD

METHOD:-	VISSER	SHEAR AREA	COLUMN ANALOGY	TOPRAC	API CODE	AWS CODE	WASHIO
76	0.6779	0.0000	2.8017	1.9620	1.5328	1.0365	1.5972
77	0.6779	0.0000	2.8017	1.9620	1.5328	1.0365	1.5972
78	0.6665	0.0000	2.7547	1.9291	1.5071	1.0191	1.5704
79	0.6129	0.0000	5.9252	4.1493	2.9963	2.0261	2.9430
80	0.5719	0.0000	5.5284	3.8714	2.7956	1.8904	2.7459
81	0.5719	0.0000	5.5284	3.8714	2.7956	1.8904	2.7459
82	0.6020	0.0000	5.8194	4.0752	2.9428	1.9899	2.8905
83	0.6321	0.0000	6.1103	4.2790	3.0899	2.0894	3.0350
84	0.5281	0.0000	5.1052	3.5751	2.5816	1.7457	2.5357
85	0.5090	0.0000	4.9200	3.4454	2.4880	1.6824	2.4438
86	0.4925	0.0000	4.7613	3.3343	2.4077	1.6281	2.3649
87	0.4925	0.0000	4.7613	3.3343	2.4077	1.6281	2.3649
88	0.4925	0.0000	4.7613	3.3343	2.4077	1.6281	2.3649
89	0.6617	0.0000	2.8173	1.9729	1.5413	1.0423	1.6061
90	0.7082	0.0000	2.9269	2.0497	1.6013	1.0828	1.6686
91	0.7423	0.0000	3.0678	2.1483	1.6784	1.1349	1.7489
92	0.7309	0.0000	3.0208	2.1154	1.6527	1.1176	1.7221
93	0.7082	0.0000	2.9269	2.0497	1.6013	1.0828	1.6686
94	0.5117	0.0000	4.9465	3.4639	2.5013	1.6914	2.4569
95	0.5117	0.0000	4.9465	3.4639	2.5013	1.6914	2.4569
96	0.5172	0.0000	4.9994	3.5010	2.5281	1.7095	0.0000
97	0.5144	0.0000	4.9729	3.4824	2.5147	1.7005	0.0000
98	0.5226	0.0000	5.0523	3.5380	2.5548	1.7276	0.0000
99	0.5308	0.0000	5.1316	3.5936	2.5950	1.7548	0.0000
100	0.7423	0.0000	3.0678	2.1483	1.6784	1.1349	0.0000
METHOD:-	VISSER	SHEAR AREA	COLUMN ANALOGY	TOPRAC	API CODE	AWS CODE	WASHIO
101	0.7309	0.0000	3.0208	2.1154	1.6527	1.1176	0.0000
102	0.7574	0.0000	3.1304	2.1921	1.7126	1.1581	0.0000
103	0.7082	0.0000	2.9269	2.0497	1.6013	1.0828	0.0000
104	0.4269	0.0000	4.1265	2.8897	2.0867	1.4110	0.0000
105	0.4269	0.0000	4.1265	2.8897	2.0867	1.4110	0.0000
106	0.4433	0.0000	4.2852	3.0008	2.1669	1.4653	0.0000
107	0.4679	0.0000	4.5232	3.1675	2.2873	1.5467	0.0000
108	0.4679	0.0000	4.5232	3.1675	2.2873	1.5467	0.0000
109	0.4816	0.0000	4.6555	3.2602	2.3542	1.5920	0.0000
110	0.4107	0.0000	3.1164	1.2788	1.7330	1.2055	0.0000
111	0.4518	0.0000	3.4230	1.4066	1.9063	1.3261	0.0000
112	0.4107	0.0000	3.1164	1.2788	1.7330	1.2055	0.0000
113	0.4928	0.0000	3.7397	1.5345	2.0796	1.4467	0.0000
114	0.4832	0.0000	3.6664	1.5044	2.0388	1.4183	0.0000
115	0.4904	0.0000	3.7213	1.5270	2.0694	1.4396	0.0000
116	0.5460	0.0000	4.1430	1.7000	2.3039	1.6027	0.0000
117	0.5532	0.0000	4.1980	1.7226	2.3345	1.6239	0.0000
118	0.5677	0.0000	4.3080	1.7677	2.3956	1.6665	0.0000
119	0.3600	0.0000	4.8422	2.6113	2.3615	1.5661	0.0000
120	0.3521	0.0000	4.7362	2.5542	2.3098	1.5318	0.0000
121	0.3679	0.0000	4.9482	2.6685	2.4132	1.6004	0.0000
122	0.3521	0.0000	4.7362	2.5542	2.3098	1.5318	0.0000
123	0.3705	0.0000	4.9836	2.6876	2.4305	1.6118	0.0000
124	0.3600	0.0000	4.8422	2.6113	2.3615	1.5661	0.0000
125	0.4835	0.0000	6.5034	3.5072	3.1717	2.1033	0.0000
126	0.4913	0.0000	6.6094	3.5644	3.2234	2.1376	0.0000
127	0.4913	0.0000	6.6094	3.5644	3.2234	2.1376	0.0000
128	0.3547	0.0000	4.7715	2.5732	2.3270	1.5432	0.0000
129	0.3232	0.0000	4.3474	2.3445	2.1202	1.4060	0.0000
130	0.3573	0.0000	4.8068	2.5923	2.3443	1.5546	0.0000
131	0.3600	0.0000	4.8422	2.6113	2.3615	1.5661	0.0000
132	0.3757	0.0000	5.0513	2.7257	2.4649	1.6347	2.2323
133	0.3232	0.0000	4.3474	2.3445	2.1202	1.4060	1.9201
134	0.4441	0.0000	5.9732	3.2213	2.9131	1.9319	2.6362
135	0.4283	0.0000	5.7611	3.1069	2.8097	1.8633	2.5994
136	0.4178	0.0000	5.6198	3.0307	2.7407	1.8176	2.5354
137	0.5719	0.0000	5.5284	3.8714	2.7956	1.8904	2.8052
138	0.5090	0.0000	4.9200	3.4454	2.4880	1.6824	2.1912
139	0.4269	0.0000	4.1265	2.8897	2.0867	1.4110	1.8378
140	0.6020	0.0000	5.8194	4.0752	2.9428	1.9899	2.5917
141	0.5883	0.0000	5.6871	3.9826	2.8759	1.9447	0.0000
142	0.4187	0.0000	4.0471	2.8341	2.0466	1.3839	0.0000
143	0.6157	0.0000	5.9516	4.1678	3.0096	2.0352	0.0000
144	0.6157	0.0000	5.9516	4.1678	3.0096	2.0352	0.0000
145	0.9276	0.0000	8.9671	6.2795	4.5345	3.0663	4.5953
146	0.9147	0.0000	8.8613	6.2054	4.4810	3.0301	4.5410
147	0.5226	0.0000	5.0523	3.5380	2.5548	1.7276	2.5200
148	0.7443	0.0000	7.1948	5.0384	3.6383	2.4603	3.5868
149	0.4706	0.0000	4.5407	3.1061	2.3007	1.5558	2.2694
150	0.4104	0.0000	3.9677	2.7785	2.0064	1.3568	0.0000

TABLE 2A SUMMARISED RESULTS OF PARAMETRIC STUDY OF TUBE JOINT FORMULAE-PAGE 6
 P(ULT)/EXPIL/P(ULT)THEORY RATIOS TEST NOS ARE THE SAME AS IN INPUT DATA TABLE

IN THIS TABLE THE FORMULAE ARE TESTED FOR APPLICABILITY
 RATIO=0.0 SHOWS THAT THE TEST WAS OUTSIDE THE RECOMMENDED RANGE OF THE FORMULA

FORMULAE MARKED THUS:- * ARE BASED ON SHEAR YIELD STRESS OF CHORD

METHOD:-	VISSER	SHEAR AREA	COLUMN ANALOGY	TOPRAC	API CODE	AWS CODE	WASHIO
151	0.0769	0.0000	9.4432	6.6129	4.7753	3.2291	0.0000
152	0.5144	0.0000	4.9729	3.4824	2.5147	1.7005	0.0000
153	0.7306	0.0000	7.0626	4.9456	3.5714	2.4151	3.6321
154	1.0863	0.0000	10.5013	7.3539	5.3103	3.5909	5.4005
155	0.6813	0.0000	6.5865	4.6124	3.3307	2.2522	3.3872
156	0.5172	0.0000	4.9994	3.5010	2.5281	1.7095	2.5024
157	0.5172	0.0000	4.9994	3.5010	2.5281	1.7095	2.5024
158	0.9823	0.0000	9.4961	6.6500	4.8020	3.2472	4.7531
159	0.9933	0.0000	9.6019	6.7241	4.8556	3.2834	0.0000
160	0.7744	0.0000	7.4856	5.2422	3.7855	2.5598	0.0000
161	1.0261	0.0000	9.9194	6.9464	5.0161	3.3919	0.0000
162	0.2195	0.0000	4.4268	3.1000	2.2386	1.4653	2.0059
163	0.2466	0.0000	4.9733	3.4829	2.5149	1.6462	2.2535
164	0.2398	0.0000	4.8367	3.3871	2.4459	1.6010	2.1916
165	0.3776	0.0000	4.5064	3.1557	2.2788	1.5286	2.2586
166	0.3620	0.0000	4.3197	3.0250	2.1844	1.4653	2.1650
167	0.3150	0.0000	3.7598	2.6329	1.9013	1.2754	1.6844
168	0.4469	0.0000	5.3330	3.7346	2.6968	1.8090	2.0197
169	0.4424	0.0000	5.2797	3.6973	2.6698	1.7909	1.9995
170	0.4357	0.0000	5.1997	3.6412	2.6294	1.7638	1.9692
171	0.4737	0.0000	5.6530	3.9587	2.8586	1.9176	0.0000
172	0.5362	0.0000	6.3996	4.4815	3.2362	2.1708	0.0000
173	0.5273	0.0000	6.2929	4.4068	3.1822	2.1347	0.0000
174	0.2313	0.0000	3.1078	0.0000	0.0000	0.0000	2.0420
175	0.2347	0.0000	3.1533	0.0000	0.0000	0.0000	2.0719
176	0.2313	0.0000	3.1078	0.0000	0.0000	0.0000	2.0420
177	0.2821	0.0000	3.7990	0.0000	0.0000	0.0000	0.0000
178	0.2730	0.0000	3.6687	0.0000	0.0000	0.0000	0.0000
179	0.2809	0.0000	3.7749	0.0000	0.0000	0.0000	0.0000
180	0.2900	0.0000	3.8961	0.0000	0.0000	0.0000	0.0000
181	0.3114	0.0000	4.1842	0.0000	0.0000	0.0000	0.0000
182	0.3137	0.0000	4.2145	0.0000	0.0000	0.0000	0.0000
183	0.2033	0.0000	7.5495	5.2868	3.8177	1.9496	0.0000
184	0.1754	0.0000	6.5125	4.5606	3.2933	1.7163	0.0000
185	0.1720	0.0000	6.3881	4.4735	3.2303	1.6835	0.0000
186	0.2651	0.0000	6.3944	4.4779	3.2335	1.8096	1.9254
187	0.2622	0.0000	6.3225	4.4276	3.1972	1.7893	1.9037
188	0.2636	0.0000	6.3585	4.4527	3.2154	1.7995	1.9146
189	0.9965	0.0000	1.5417	2.1593	0.7796	1.5928	2.2535
190	1.0144	0.0000	1.5694	2.1980	0.7936	1.6214	2.2940
191	0.9607	0.0000	1.4864	2.0818	0.7516	1.5357	2.1727
192	1.1134	0.0000	2.2699	1.0195	1.3192	0.8810	1.2446
193	0.9712	0.0000	2.3599	1.0599	1.3714	0.9075	0.9232
194	1.1023	0.0000	2.2472	1.0093	1.3060	0.8722	0.0000
195	1.2423	0.0000	2.2977	1.4605	1.2823	0.9749	1.0765
196	1.3011	0.0000	2.4063	1.5295	1.3430	0.9163	0.0000
197	1.3011	0.0000	2.4063	1.5295	1.3430	0.9163	0.0000
198	1.2835	0.0000	2.2109	0.8997	1.3911	0.9588	0.0000
199	1.2835	0.0000	2.2109	0.8997	1.3911	0.9588	0.0000
200	1.3682	0.0000	2.3569	0.9591	1.4829	1.0221	0.0000
201	0.5569	0.0000	4.5928	2.0628	2.3435	1.5652	1.4425
202	1.6048	0.0000	1.4217	0.6385	0.8941	0.5971	0.6471
203	0.6661	0.0000	4.6422	1.8890	2.5645	1.7676	0.0000
204	1.7452	0.0000	1.3063	0.5316	0.8894	0.6131	0.0000
205	0.9692	0.0000	4.1005	1.8416	2.2256	1.4864	1.4347
206	0.6198	0.0000	6.1421	2.4994	3.5051	2.3593	0.0000
207	0.4107	0.0000	7.7829	3.4955	3.6840	2.4593	2.1454
208	0.3970	0.0000	12.8499	8.1678	5.8493	3.8889	4.3151
209	0.6091	0.0000	9.5178	3.8730	4.8844	3.3666	0.0000
210	0.1400	0.0000	6.9174	3.4391	2.9624	1.9667	1.5512
211	0.2142	0.0000	12.6013	7.8598	5.2658	3.5444	0.0000
212	0.3971	0.0000	11.0562	4.4015	5.1355	3.5324	0.0000
213	0.0549	0.0000	6.3381	2.6250	2.5200	1.6969	1.3427
214	0.0953	0.0000	7.9173	4.0356	3.0133	2.0432	0.0000
215	0.1944	0.0000	15.6866	9.5126	5.8061	4.0296	0.0000
216	0.3028	0.0000	14.7329	5.7710	6.0126	4.1925	0.0000
217	0.5366	0.0000	9.9246	4.4574	4.7047	3.1419	0.0000
218	0.3062	0.0000	15.1317	7.5230	6.4902	4.3450	0.0000
219	0.2194	0.0000	25.3524	10.5001	10.0801	6.7677	0.0000
220	0.2462	0.0000	19.3851	9.8825	7.3789	5.1081	0.0000
221	0.2631	0.0000	21.2230	12.8700	7.8553	5.4519	0.0000
222	1.3570	0.0000	5.1915	2.6644	2.7455	1.8584	0.0000
223	1.1109	0.0000	5.7802	0.0000	0.0000	0.0000	0.0000
224	1.3570	0.0000	5.1915	2.6644	2.7455	1.8584	0.0000
225	1.0928	0.0000	5.6862	0.0000	0.0000	0.0000	0.0000

TABLE 2A SUMMARISED RESULTS OF PARAMETRIC STUDY OF TUBE JOINT FORMULAE-PAGE 7
 P(ULT)EXPTL/P(ULT)THEORY RATIOS TEST NOS ARE THE SAME AS IN INPUT DATA TABLE

IN THIS TABLE THE FORMULAE ARE TESTED FOR APPLICABILITY
 RATIO=0.0 SHOWS THAT THE TEST WAS OUTSIDE THE RECOMMENDED RANGE OF THE FORMULA

FORMULAE MARKED THUS:- * ARE BASED ON SHEAR YIELD STRESS OF CHORD

METHOD:-	VISSER	SHEAR AREA	COLUMN ANALOGY	TOPRAC	API CODE	AWS CODE	WASHIO
226	0.2984	0.0000	1.3724	0.0000	0.0000	0.0000	1.0897
227	0.2684	0.0000	2.4358	0.9491	1.3477	0.8939	1.2755
228	0.2894	0.0000	3.2270	1.6446	1.6739	1.0830	1.3929
229	0.3039	0.0000	1.6009	0.0000	0.0000	0.0000	1.2066
230	0.2769	0.0000	2.8554	1.1133	1.5324	1.0252	1.4256
231	0.2615	0.0000	3.3170	1.6964	1.6664	1.0927	1.3711
232	0.2702	0.0000	1.9739	0.0000	0.0000	0.0000	1.3195
233	0.1984	0.0000	2.8375	1.1057	1.4098	0.9597	1.2647
234	0.2111	0.0000	3.7098	1.8907	1.7279	1.1628	1.3813
235	0.2464	0.0000	1.3735	0.0000	0.0000	0.0000	0.9838
236	0.2684	0.0000	2.4358	0.9491	1.3477	0.8939	1.0672
237	0.2894	0.0000	3.2270	1.6446	1.6739	1.0830	1.0864
238	0.3039	0.0000	1.6009	0.0000	0.0000	0.0000	0.9430
239	0.2769	0.0000	2.8554	1.1133	1.5324	1.0252	1.1141
240	0.2615	0.0000	3.3170	1.6964	1.6664	1.0927	1.0714
241	0.2702	0.0000	1.9739	0.0000	0.0000	0.0000	0.9187
242	0.1984	0.0000	2.8375	1.1057	1.4098	0.9597	0.9237
243	0.2110	0.0000	3.7098	1.8907	1.7279	1.1628	0.9758
244	0.4746	0.0000	6.1158	3.1388	3.1280	1.6696	0.0000
245	0.3214	0.0000	5.5857	2.2594	3.1689	1.6763	0.0000

APPENDIX B

```

55      DO 66 J=1,N
56      DO 66 K=1,N

```



```

55 DO 66 J=1,N
56 DO 66 K=1,N
57 IF(J.EQ.1.OR.K.EQ.1)GOTO 66
58 SUM(J,K)=SUM(J,K)-SUM(J,1)*SUM(1,K)*T
59 66 CONTINUE
60 DO 67 K=1,N
61 SUM(1,K)=SUM(1,K)*T
62 67 SUM(K,1)=-SUM(K,1)*T
63 SUM(1,1)=T
64 GOTO 68
65 13 WRITE(4,500)
66 500 FORMAT('SINGULAR MATRIX - RUN TERMINATED')
67 68 DO 200 I=2,N
68 DO 200 J=2,I
69 200 COPY(I-1,J-1)=SUM(I,J)/(M-1)
70 WRITE(4,410)
71 410 FORMAT('TABLE OF MEANS AND STANDARD DEVIATIONS'//' VARIAD
72 1 MEAN STD.DEVIATION')
73 DO 212 I=1,N-1
74 SD=SQRT(COPY(I,I))
75 212 WRITE(4,411)NAMES(I),SUM(1,I+1),SD
76 WRITE(4,412)M
77 412 FORMAT('NUMBER OF OBSERVATIONS = ',I4/)
78 411 FORMAT(1H0,A8,3X,F9.2,9X,F9.2)
79 C MEANS AND STANDARD DEVIATIONS NOW PRINTED
80 C
81 C READ MATRIX REQUIREMENT PARAMETERS
82 WRITE(4,52)
83 52 FORMAT(' COVARIANCE MATRIX REQUIRED?')
84 WRITE(4,53)
85 53 FORMAT(' TYPE YES OR NO')
86 CALL READYESORNO(LCOV)
87 C LCOV IS FALSE IF COVARIANCE MATRIX TO BE PRINTED
88 WRITE(4,54)
89 54 FORMAT(' CORRELATION MATRIX REQUIRED?')
90 WRITE(4,53)
91 CALL READYESORNO(LCOR)
92 C LCOR IS FALSE IF CORRELATION MATRIX IS TO BE PRINTED
93 IF(LCOV)GOTO 302
94 C PRINT COVARIANCE MATRIX
95 WRITE(4,415)
96 415 FORMAT('MATRIX OF VARIANCES AND COVARIANCES'//)
97 CALL OUTPUTLTARR(COPY,NAMES,NN,20)
98 WRITE(3,55)COVN
99 55 FORMAT(A8)
100 DO 204 I=1,NN
101 204 WRITE(3,12)(COPY(I,J),J=1,I)
102 302 IF(LCOR)GOTO 310
103 C DERIVE CORRELATION MATRIX
104 DO 205 I=1,NN
105 DO 205 J=1,I
106 205 SUM(I,J)=COPY(I,J)/SQRT(COPY(I,I)*COPY(J,J))
107 C PRINT CORRELATION MATRIX
108 WRITE(4,404)
109 404 FORMAT('CORRELATION MATRIX')
110 CALL OUTPUTLTARR(SUM,NAMES,NN,21)

```



```

PROGRAM(JDCL)
INPUT1=CR0
INPUT2=TR0
INPUT3=TR1
OUTPUT4,(MONITOR)=LP0
COMPACT DATA
COMPRESS INTEGER AND LOGICAL
NOTRACE
END
MASTER REGRESSION
DIMENSION SUM(21,21),COPY(21,21),FT(30,3),GT(33,3),XM(21),COEFF(
)
INTEGER INDVARS(20),DEPVAR,TOT
REAL NAMES(20)
LOGICAL DROPOUT,LEND, LCONST,LSTEP,LFULL,LRES
COMMON/BL2/INDVARS
COMMON/BL1/NAMES
COMMON/SET/DROPOUT
COMMON/OPSET/LCONST,XM,ADJ,TOT
DATA GT/ 7.44, 7.25, 7.14, 7.06, 7.02, 6.98, 6.95, 6.91, 6.87,
        6.85, 6.84, 6.83, 6.82, 6.81, 6.8 , 6.79, 6.78, 6.77,
        6.76, 6.75, 2*6.74 , 6.73, 6.72, 6.71, 6.7 , 6.69,
        6.68, 6.67, 6.66, 6.65, 6.64, 6.63, 4.13, 4.06, 4.02,
        3.99, 3.98, 3.97, 3.95, 3.94, 3.93, 3.92, 3*3.91 ,
        3*3.9 , 3*3.89 , 3*3.88 , 3*3.87 ,
        3*3.86 , 3*3.85 , 2*3.84 , 2.86, 2.83, 2.8 ,
        2.79, 2.78, 2*2.77 , 2.76, 4*2.75 , 6*2.74 ,
        6*2.73 , 6*2.72 , 3*2.71/, FT/4052.0,
98.5 ,34.12,21.2 ,16.26,13.75,12.25,11.26,10.56,10.04,
9.65, 9.33, 9.07, 8.86, 8.68, 8.53, 8.4 , 8.29, 8.18,
8.1 , 8.02, 7.95, 7.88, 7.82, 7.77, 7.72, 7.68, 7.64,
7.6 , 7.56,161.4,18.51,10.13, 7.71, 6.61, 5.99, 5.59,
5.32, 5.12, 4.96, 4.84, 4.75, 4.67, 4.6 , 4.54, 4.49,
4.45, 4.41, 4.38, 4.35, 4.32, 4.3 , 4.28, 4.26, 4.24,
4.23, 4.21, 4.2 , 4.18, 4.16,39.86, 8.53, 5.54, 4.54,
4.06, 3.78, 3.59, 3.46, 3.36, 3.29, 3.23, 3.18, 3.14,
3.1 , 3.07, 3.05, 3.03, 3.01, 2.99, 2.97, 2.96, 2.95,
2.94, 2.93, 2.92, 2.91, 2.9 , 2.89, 2.89, 2.88/
INDEX=21
READ NN,N AND NAMES FROM FILE
LFULL,DROPOUT=.FALSE.
READ(2,50)NN,N
FORMAT(2I4)
READ(2,51)(NAMES(I),I=1,NN)
FORMAT(10A8)
N=NN+1
READ CROSS-PRODUCT MATRIX INTO SUM AND COPY
DO 209 I=1,N
READ(2,52)(SUM(I,J),J=1,I)
FORMAT(5E18.11)
DO 200 I=1,N
DO 201 J=1,N
SUM(I,J)=SUM(J,I)
DO 202 J=1,N

```

```

55 202 COPY(I,J)=SUM(I,J)
56 200 CONTINUE
57 C READ REGRESSION PARAMETERS
58 WRITE(4,70)
59 70 FORMAT(' TYPE INDEPENDENT VARIABLES')
60 CALL READINDVARS(NOINDS)
61 WRITE(4,71)
62 71 FORMAT(' TYPE DEPENDENT VARIABLE')
63 CALL READDEPVAR(NN,DEPVAR)
64 JJS=DEPVAR-1
65 C DEPVAR IS 1+(SUBSCRIPT OF D.V. IN NAMES)
66 WRITE(4,72)
67 72 FORMAT(' STEPWISE REQUIRED?')
68 WRITE(4,73)
69 73 FORMAT(' TYPE YES OR NO')
70 CALL READYESORNO(LSTEP)
71 C READ F-LEVEL IF STEPWISE TO BE PERFORMED
72 IF(LSTEP)GOTO 205
73 WRITE(4,74)
74 74 FORMAT(' F-LEVEL/' TYPE 1,5 OR 10')
75 READ(1,53)ILEVEL
76 IF(ILEVEL.EQ.1)IF2=1
77 IF(ILEVEL.EQ.5)IF2=2
78 IF(ILEVEL.EQ.10)IF2=3
79 53 FORMAT(I0)
80 205 WRITE(4,75)
81 75 FORMAT(' CONSTANT REQUIRED?')
82 WRITE(4,73)
83 CALL READYESORNO(LCONST)
84 WRITE(4,76)
85 76 FORMAT(' RESIDUALS REQUIRED?')
86 WRITE(4,73)
87 CALL READYESORNO(LRES)
88 IF(.NOT.LSTEP)LFULL=.TRUE.
89 C LCONST IS FALSE IF A CONSTANT IS TO BE INCLUDED IN THE REGR.
90 C LSTEP IS FALSE IF STEPWISE REGRESSION IS TO BE EXECUTED
91 C LFULL IS FALSE IF A FULL MULTIPLE REGRESSION IS TO BE EXECU
92 C LRES IS FALSE IF RESIDUALS ARE TO BE OUTPUT
93 ADJ=SUM(1,DEPVAR)**2/SUM(1,1)
94 TOT=M
95 XM(1)=1.0
96 DO 220 I=2,N
97 220 XM(I)=SUM(1,I)/M
98 IF(LCONST)GOTO 300
99 CALL PIVOT(COPY,INDEX,N,1)
100 IF(DROPOUT)GOTO 998
101 CALL PIVOT(SUM,INDEX,N,1)
102 IF(DROPOUT)GOTO 998
103 800 CONTINUE
104 IF(LCONST)M=M+1
105 SQY=SUM(DEPVAR,DEPVAR)
106 IF(LSTEP)GOTO 999
107 WRITE(4,60)
108 60 FORMAT('STEPWISE REGRESSION'////)
109 WRITE(4,1000)ILEVEL
110 1000 FORMAT('OLEVEL OF SIGNIFICANCE ',I2,'%')

```

```

111      WRITE(4,300)NAMES(JJS)
112      300      FORMAT('DEPENDENT VARIABLE IS ',A8/)
113      K=0
114      28      K=K+1
115      IF1=M-K-1
116      IF(IF1-30)0,0,80
117      FTEST=FT(IF1,IF2)
118      GOTO 82
119      80      IF(IF1-360)81,0,0
120      FTEST=GT(33,IF2)
121      GOTO 82
122      81      IF1=(IF1-20)/10
123      FTEST=GT(IF1,IF2)
124      82      IF(K+1-N)26,27,27
125      26      CALL HOST(SUM,INDEX,N,I,F,DEPVAR)
126      IF(DROPOUT)GOTO 998
127      F=F*(N-K-1)/(SUM(DEPVAR,DEPVAR)-F)
128      IF(F.LT.FTEST)GOTO 16
129      C      I HAS BEEN DETERMINED BY HOST
130      CALL PIVOT(SUM,INDEX,N,I)
131      IF(DROPOUT)GOTO 998
132      J=I-1
133      WRITE(4,30)NAMES(J)
134      30      FORMAT('0 ',A8,' BROUGHT INTO REGRESSION'///)
135      29      CALL OUTPUT(SUM,INDEX,N,SQY,K,FTEST,L,M,DEPVAR)
136      IF(L.EQ.0)GOTO 28
137      CALL PIVOT(SUM,INDEX,N,L)
138      IF(DROPOUT)GOTO 998
139      J=L-1
140      WRITE(4,59)NAMES(J)
141      59      FORMAT('0 ',A8,' TAKEN OUT OF REGRESSION'///)
142      K=K-1
143      GOTO 29
144      16      WRITE(4,15)
145      15      FORMAT('OREMAINING VARIABLES ARE INSIGNIFICANT')
146      GOTO 999
147      27      WRITE(4,14)
148      14      FORMAT('OALL VARIABLES NOW INCLUDED IN REGRESSION')
149      GOTO 998
150      999      IF(LFULL)GOTO 998
151      WRITE(4,61)
152      61      FORMAT('OFULL MULTIPLE REGRESSION'///)
153      WRITE(4,300)NAMES(JJS)
154      DO 42 I=2,N
155      IF(INDVARS(I-1))42,42,0
156      IF(I.EQ.DEPVAR)GOTO 42
157      CALL PIVOT(COPY,INDEX,N,I)
158      IF(DROPOUT)GOTO 998
159      42      CONTINUE
160      CALL OUTPUT(COPY,INDEX,N,SQY,NOINDS,FTEST,L,M,DEPVAR)
161      998      CALL RESIDUAL(N,DEPVAR,LRES)
162      STOP
163      END
164      SUBROUTINE HOST(A,L,N,I,BIG,DV)
165      DIMENSION A(L,L),INDVARS(20)
166      INTEGER DV

```

```

167 LOGICAL DROPOUT
168 COMMON/SET/DROPOUT/BL2/INDVARS
169 I=0
170 BIG=0.0
171 DO 61 J=2,N
172 IF(INDVARS(J-1))61,61,0
173 IF(J.EQ.DV)GOTO 61
174 IF((A(J,DV)*A(DV,J)).LE.0.0)GOTO 61
175 IF(ABS(A(J,J)).LE.1.0E-50)GOTO 62
176 PROD=A(J,DV)*A(DV,J)/A(J,J)
177 IF(PROD.LT.BIG)GOTO 61
178 I=J
179 BIG=PROD
180 61 CONTINUE
181 GOTO 63
182 62 CONTINUE
183 DROPOUT=.TRUE.
184 WRITE(4,500)
185 500 FORMAT('OSINGULAR MATRIX - RUN TERMINATED')
186 63 RETURN
187 END
188 SUBROUTINE PIVOT(A,L,N,I)
189 LOGICAL DROPOUT
190 DIMENSION A(L,L)
191 COMMON/SET/DROPOUT
192 IF(ABS(A(I,I)).LE.1.0E-50)GOTO 13
193 T=1.0/A(I,I)
194 DO 12 J=1,N
195 DO 12 K=1,N
196 IF(J.EQ.I.OR.K.EQ.I)GOTO 12
197 A(J,K)=A(J,K)-A(J,I)*A(I,K)*T
198 12 CONTINUE
199 DO 11 K=1,N
200 A(I,K)=A(I,K)*T
201 11 A(K,I)=-A(K,I)*T
202 A(I,I)=T
203 GOTO 14
204 13 DROPOUT=.TRUE.
205 WRITE(4,500)
206 500 FORMAT('OMATRIX SINGULAR - RUN TERMINATED')
207 14 RETURN
208 END
209 SUBROUTINE OUTPUT(A,L,N,SQY,K,FTEST,M2,H1,DV)
210 INTEGER DV
211 INTEGER TOT
212 REAL NAMES(20)
213 LOGICAL LCONST
214 DIMENSION A(L,L),E(2),G(2),SQ(2),IDF(2),COEFF(20),XH(21)
215 COMMON/RESSET/COEFF,CON
216 COMMON/BL1/NAMES
217 COMMON/UPSET/LCONST,XH,ADJ,TOT
218 DATA G(1)/'REGRESS RESIDUAL'/
219 RCORR=0.0
220 F1=FTEST
221 M2=0
222 WRITE(4,51)

```

```

223 51  FORMAT('0      VARIABLE      COEFFICIENT      ...')
224      1UE'///)
225      IF(LCONST)GOTO 80
226      B=A(1,DV)
227      ERROR=SQRT(A(DV,DV)*A(1,1)/(M1-K-1))
228      F=(B/ERROR)**2
229      WRITE(4,53)B,ERROR,F
230 53  FORMAT('0      CONSTANT',5X,F12.5,7X,F10.4,5X,F8.2//)
231 80  CON=B
232      IF(LCONST)CON=0.0
233      DO 510 I=1,20
234 510 COEFF(I)=0.0
235      DO 55 I=2,N
236      IF(A(I,DV)*A(DV,I).GT.0.0)GOTO 55
237      J=I-1
238      ERROR=SQRT(A(DV,DV)*A(I,I)/(M1-K-1))
239      B=A(I,DV)
240      COEFF(J)=B
241      F=(B/ERROR)**2
242      RCORR=RCORR+XII(I)*B
243      IF(F.GT.F1)GOTO 50
244      F1=F
245      M2=I
246 50  WRITE(4,48)NAMES(J),B,ERROR,F
247 48  FORMAT(1H0,4X,A8,6X,F12.5,7X,F10.4,5X,F8.2//)
248 55  CONTINUE
249      IF(LCONST)GOTO 91
250      GOTO 92
251 91  E(2)=A(DV,DV)
252      GOTO 90
253 92  RCORR=RCORR+A(1,DV)
254      E(2)=A(DV,DV)+TOT*RCORR**2-ADJ
255 90  E(1)=SQY-E(2)
256      IDF(1)=K
257      IDF(2)=M1-K-1
258      DO 56 I=1,2
259 56  SQ(I)=E(I)/IDF(I)
260      WRITE(4,57)
261 57  FORMAT('0      ANALYSIS OF VARIANCE TABLE'/'0      VARIATION
262      1UARES      D.F.      MEAN SQUARE'//)
263      WRITE(4,58)(G(I),E(I),IDF(I),SQ(I),I=1,2)
264 58  FORMAT(1H0,3X,A8,3X,F14.4,4X,I4,6X,F14.4//)
265      J=M1-1
266      R=E(1)/SQY
267      F=SQ(1)/SQ(2)
268      WRITE(4,59)SQY,J,F
269 59  FORMAT('0      TOTAL      ',F14.4,4X,I4,10X,'F = ',F8.2)
270      WRITE(4,60)R
271 60  FORMAT('0MULTIPLE CORRELATION = ',F10.7)
272      RETURN
273      END
274      SUBROUTINE RESIDUAL(N,DV,LRES)
275      DIMENSION X(20),COEFF(20)
276      INTEGER DV
277      LOGICAL LRES
278      COMMON/RESSET/COEFF,CON

```

```

279      X1,X2=0.0
280      IF(LRES)GOTO 30
281      WRITE(4,86)
282      86      FORMAT('TABLE OF RESIDUALS'//, OBSERVATION      Y(ACTUAL)
283      1ESTIMATED)      Y(ACT)-Y(EST)')
284      30      NO=1
285      26      READ(3,88,END=27)(X(J),J=1,N-1)
286      88      FORMAT(5E18.11)
287      YA=X(DV-1)
288      YH=CON
289      DO 20 I=1,N-1
290      20      YH=YH+X(I)*COEFF(I)
291      DIFF=YA*(1-COEFF(DV-1))-YH
292      X2=X2+DIFF**2
293      IF(LRES)GOTO 31
294      WRITE(4,87)NO,YA,YH,DIFF
295      31      IF(NO.EQ.1)GOTO 50
296      X1=X1+(DIFF-PDIF)**2
297      50      PDIF=DIFF
298      87      FORMAT(1H ,6X,I4,6X,F9.2,8X,F9.2,12X,F9.2)
299      NO=NO+1
300      GOTO 26
301      27      D=X1/X2
302      WRITE(4,75)D
303      75      FORMAT('DURBIN-WATSON D-STATISTIC=',F10.4)
304      RETURN
305      END
306      FINISH

```

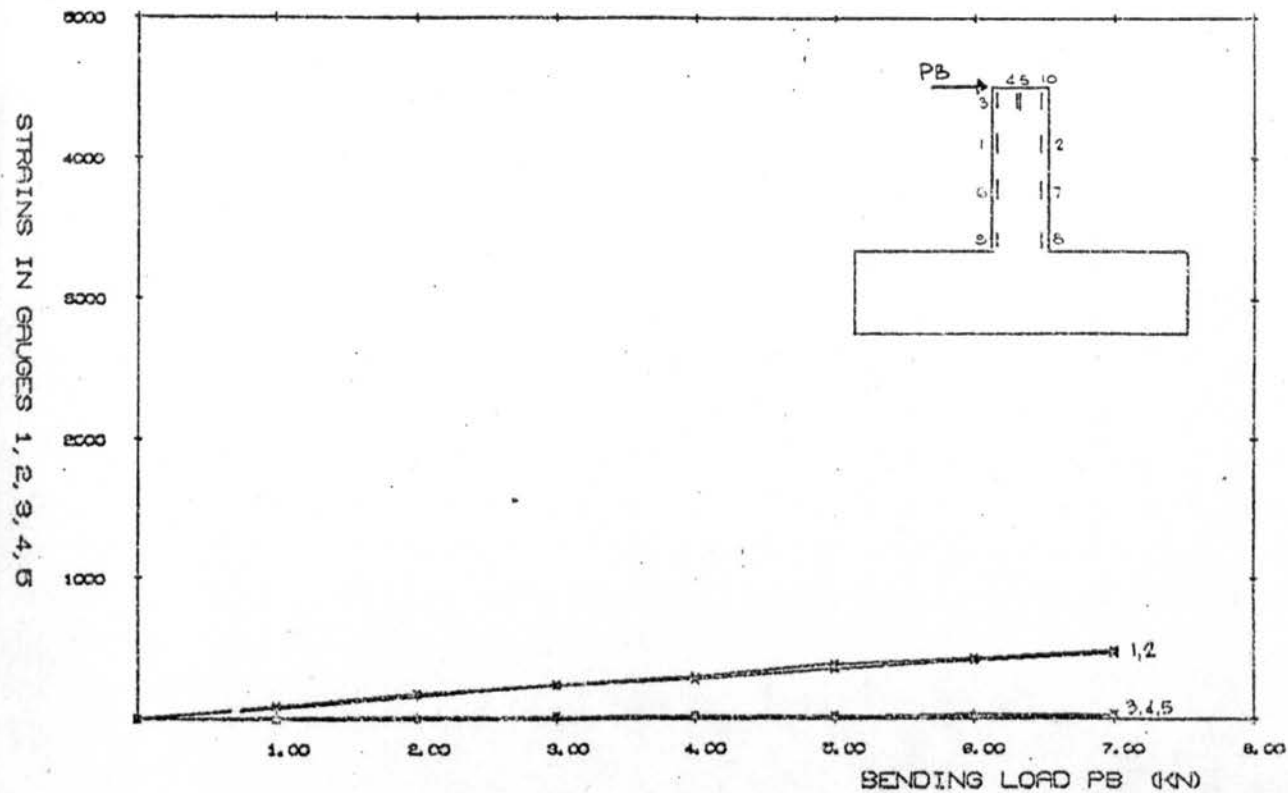
PAGE 12 21/05/79 LISTING BY EDITOR #XKYA NR 11A OU

```

SENT      @000000=00000000000000ZE)30000000000000000000000000000000
SENT      0006@000USCLF      00000000000000000000000000000000B2F400
SENT      @0000002000000000000000C72$000000000000000000000000000000
SENT      0006@000HIST      00000000000000000000000000000000B2F400
SENT      @0000007000000000000000'75200000000000000000000000000000
SENT      0006@000SCAT      00000000000000000000000000000000B2F400
SENT      @0000006000000000000000'S8!000000000000000000000000000000
SENT      0006@000ANOV      00000000000000000000000000000000B2F400
SENT      @000000?000000000000000USF=000000000000000000000000000000
SENT      0006@000TABX      00000000000000000000000000000000B2F400
SENT      @000000C000000000000000N!PZ000000000000000000000000000000
SENT      0006@000PLANSEGS      00000000000000000000000000000000
SENT      @0000001!00000000000000FV.K000000000000000000000000000000
SENT      0007000000000000000000000000000000000000000000000000000

```


BETA = 0.42 CHORD THICKNESS = 5.0



BETA = 0.53 CHORD THICKNESS = 5.0

BETA = 0.42 CHORD THICKNESS = 5.0

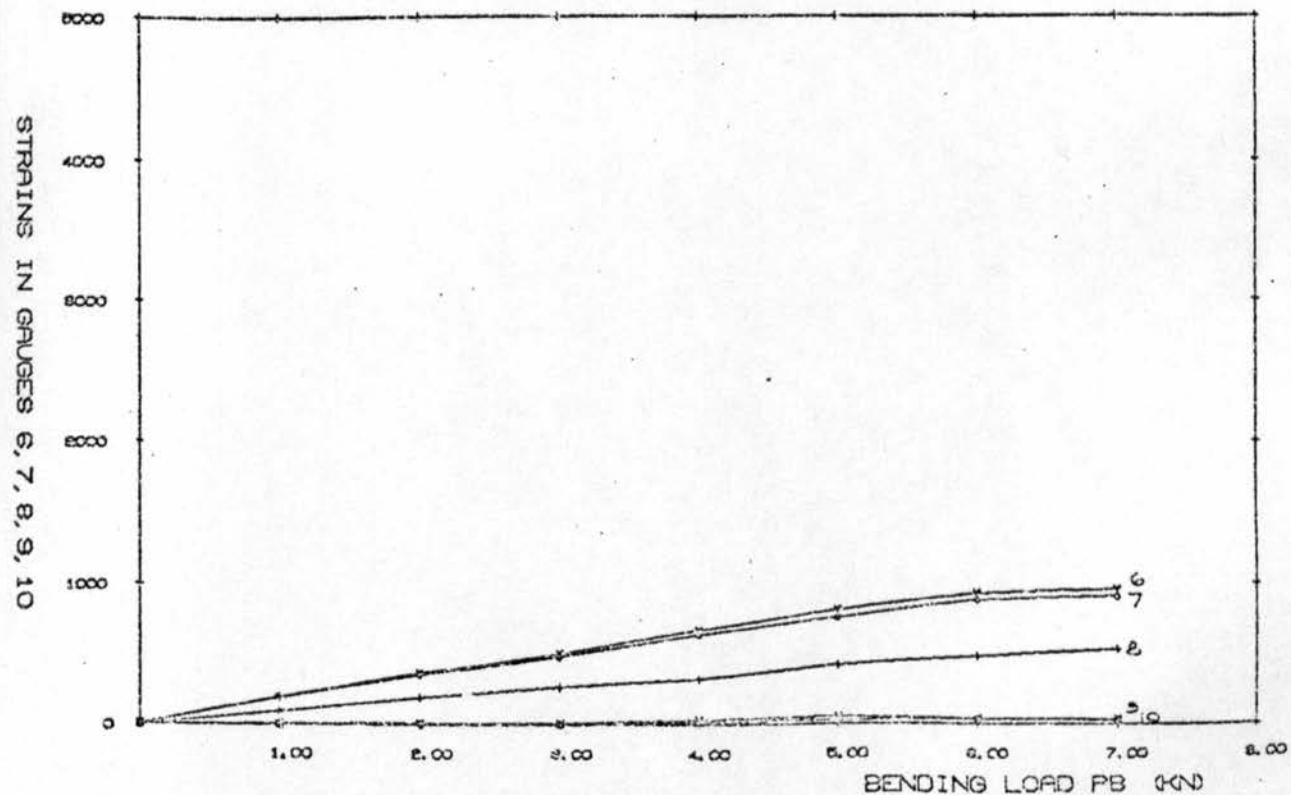
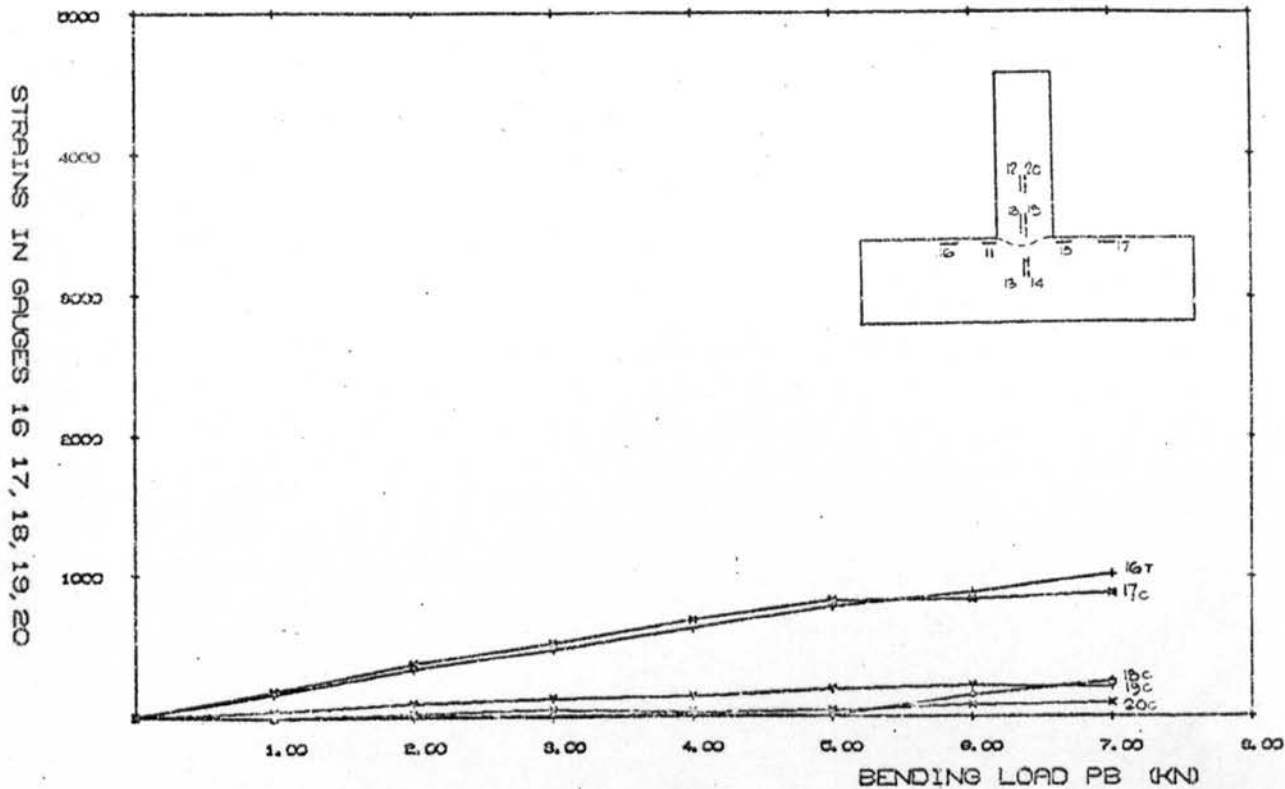


Figure 180

BETA = 0.42 CHORD THICKNESS = 5.0



BETA = 0.42 CHORD THICKNESS = 5.0

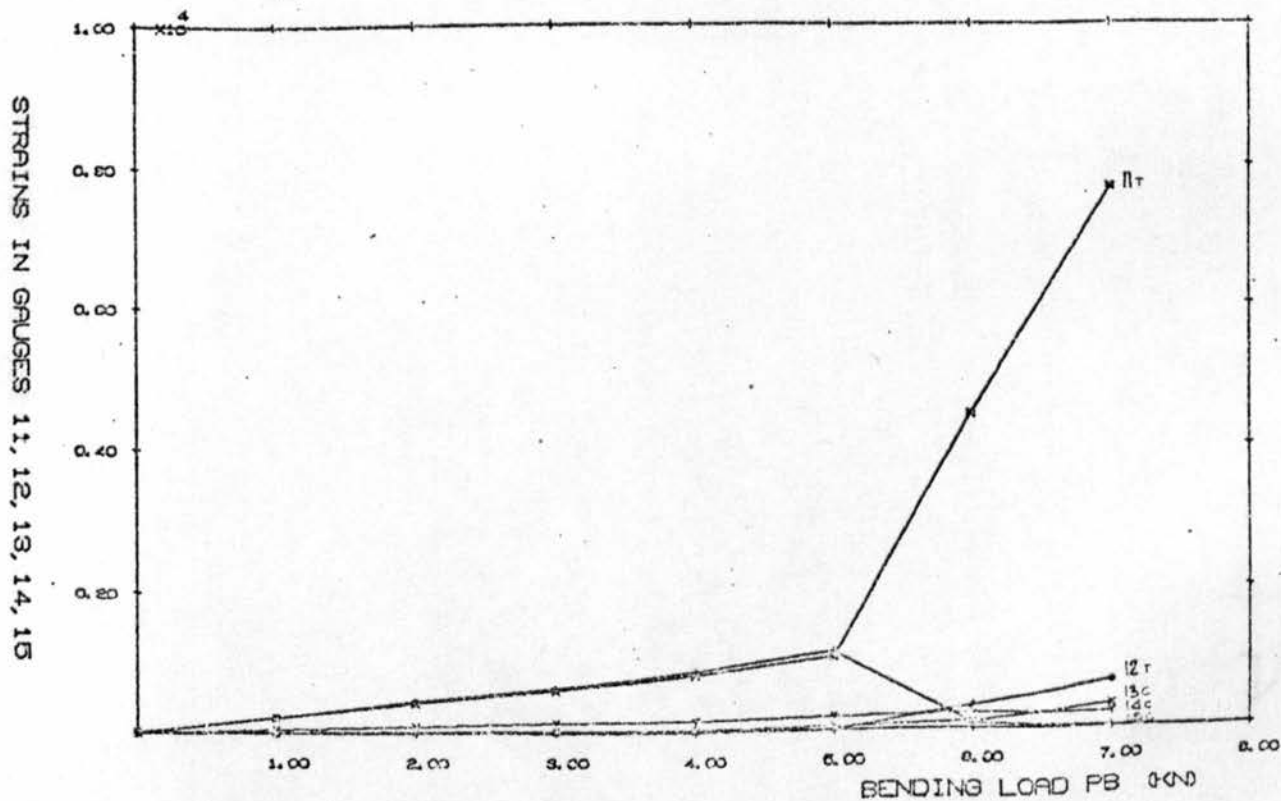
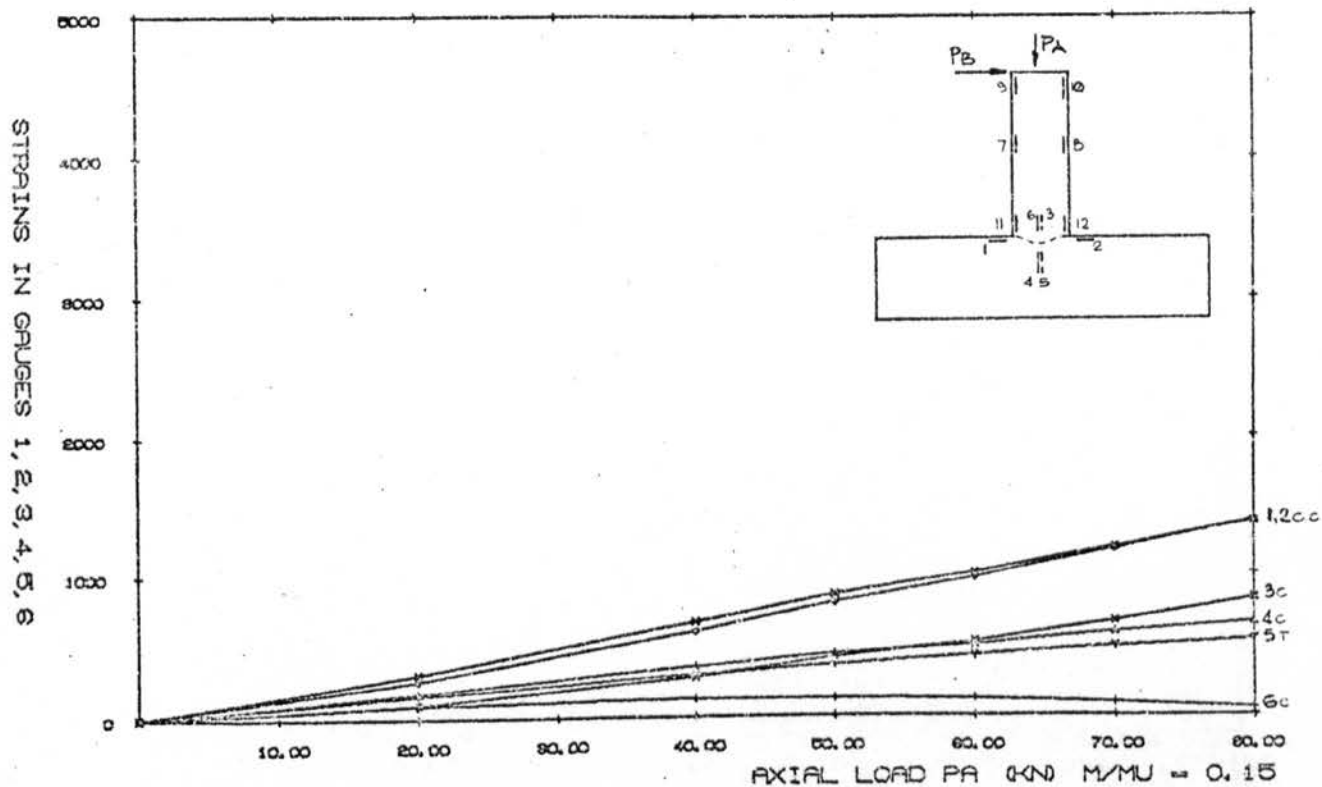


Figure 181.

BETA = 0.42 CHORD THICKNESS = 5.0



BETA = 0.42 CHORD THICKNESS = 5.0

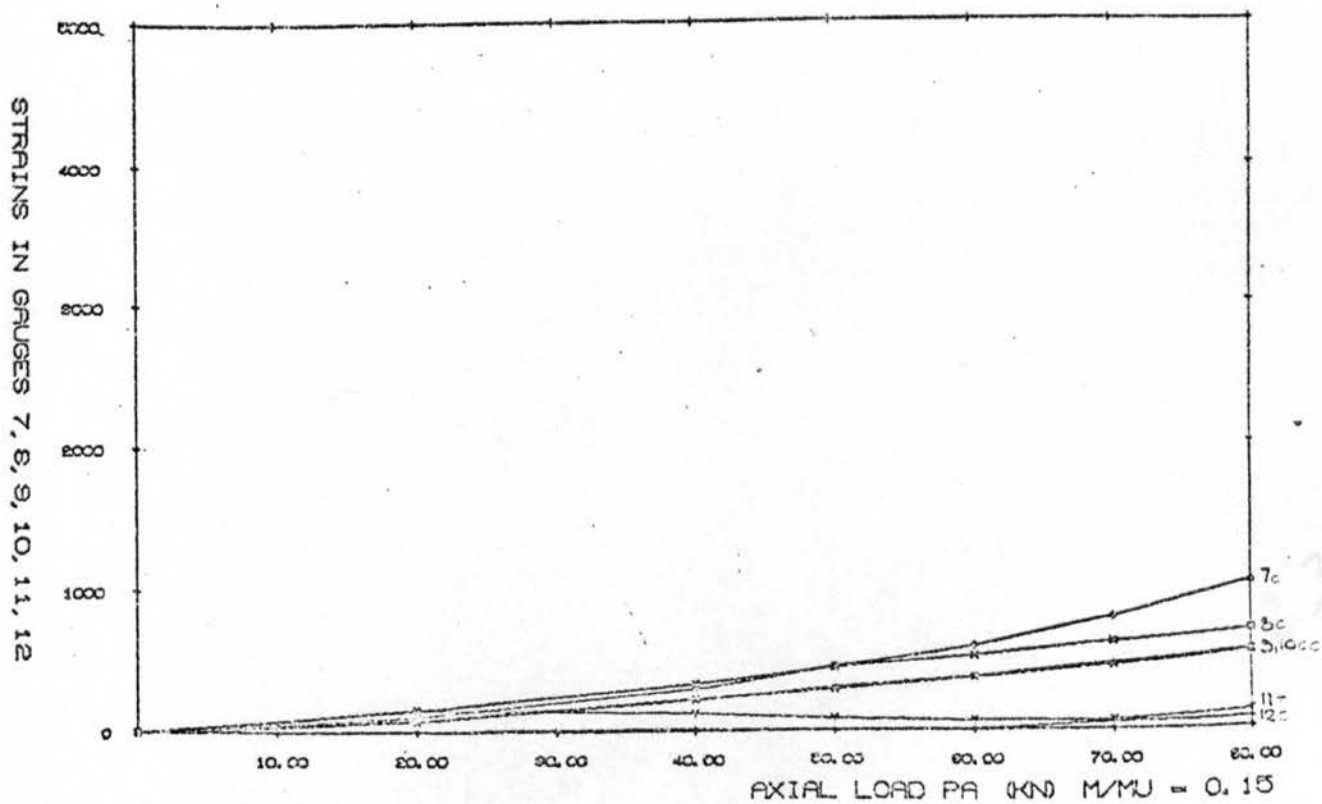
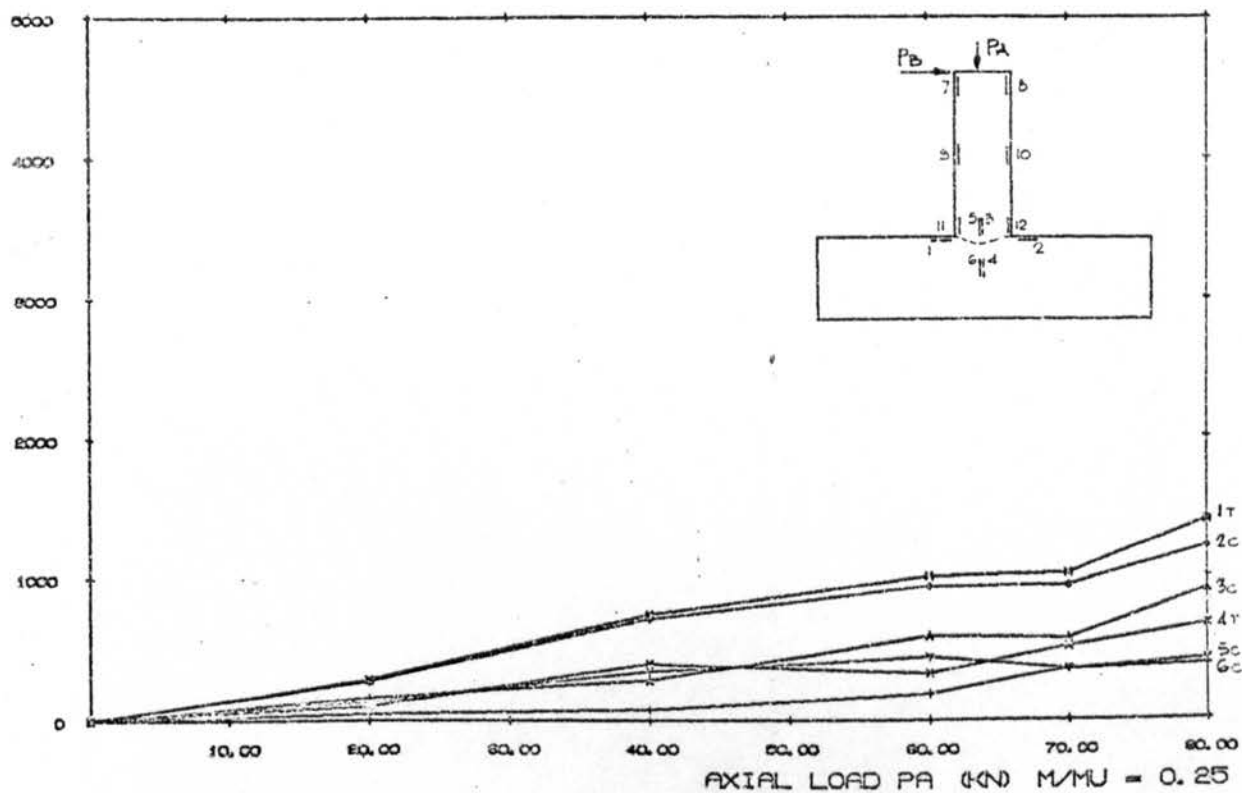


Figure 182

BETA = 0.42 CHORD THICKNESS = 5.0

STRAINS IN GAUGES 1, 2, 3, 4, 5, 6



BETA = 0.42 CHORD THICKNESS = 5.0

STRAINS IN GAUGES 7, 8, 9, 10, 11, 12

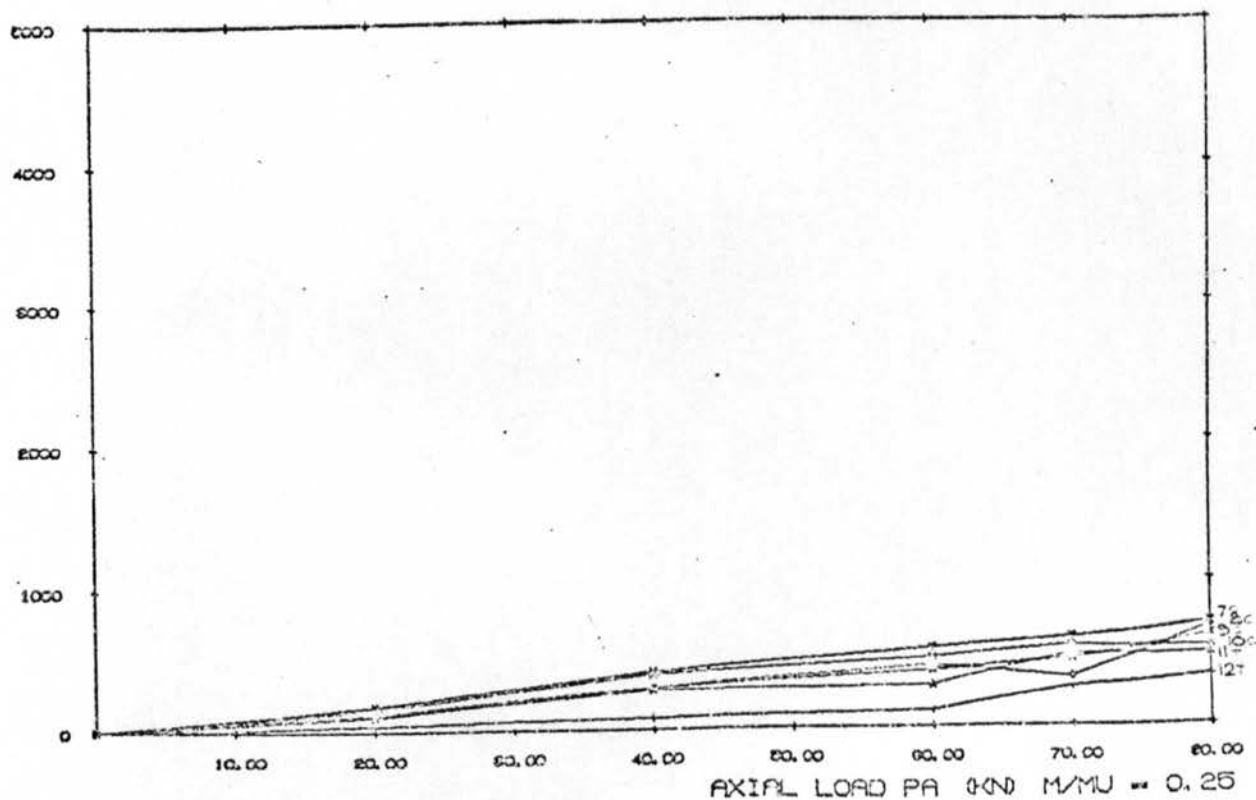
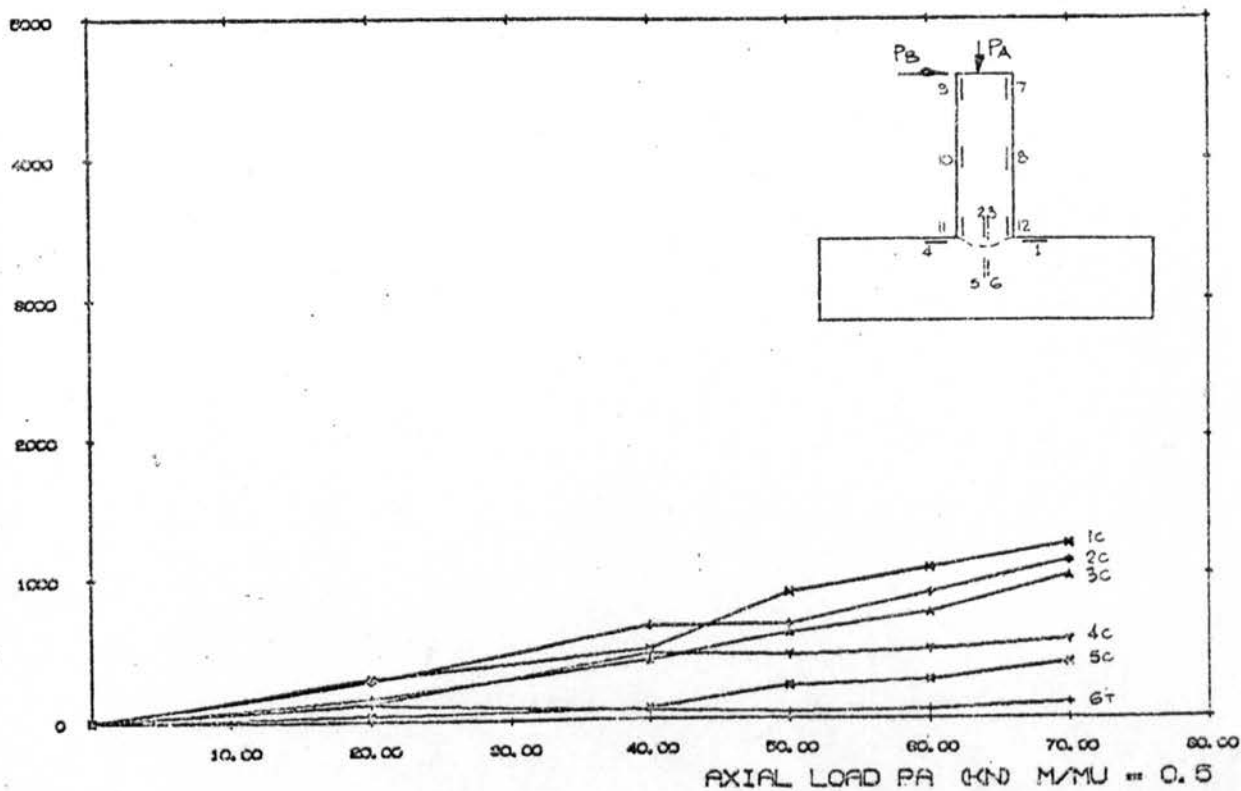


Figure 183

BETA = 0.42 CHORD THICKNESS = 5.0

STRAINS IN GAUGES 1, 2, 3, 4, 5, 6



BETA = 0.42 CHORD THICKNESS = 5.0

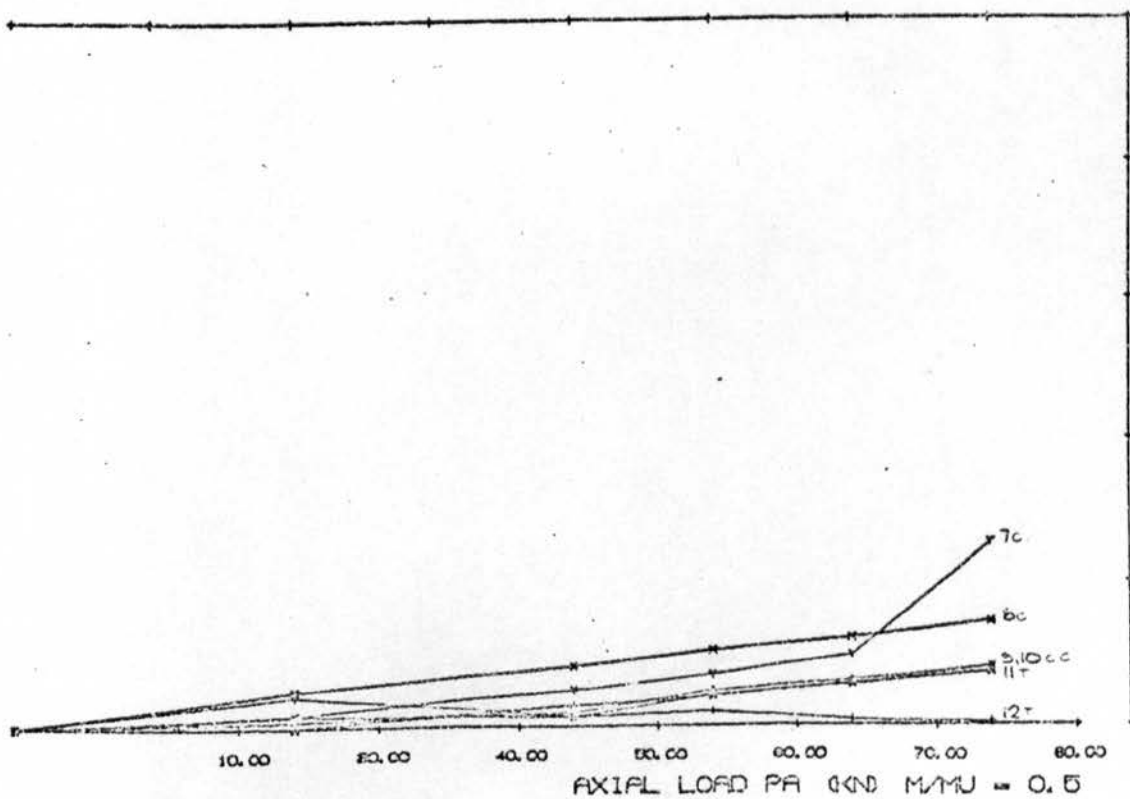
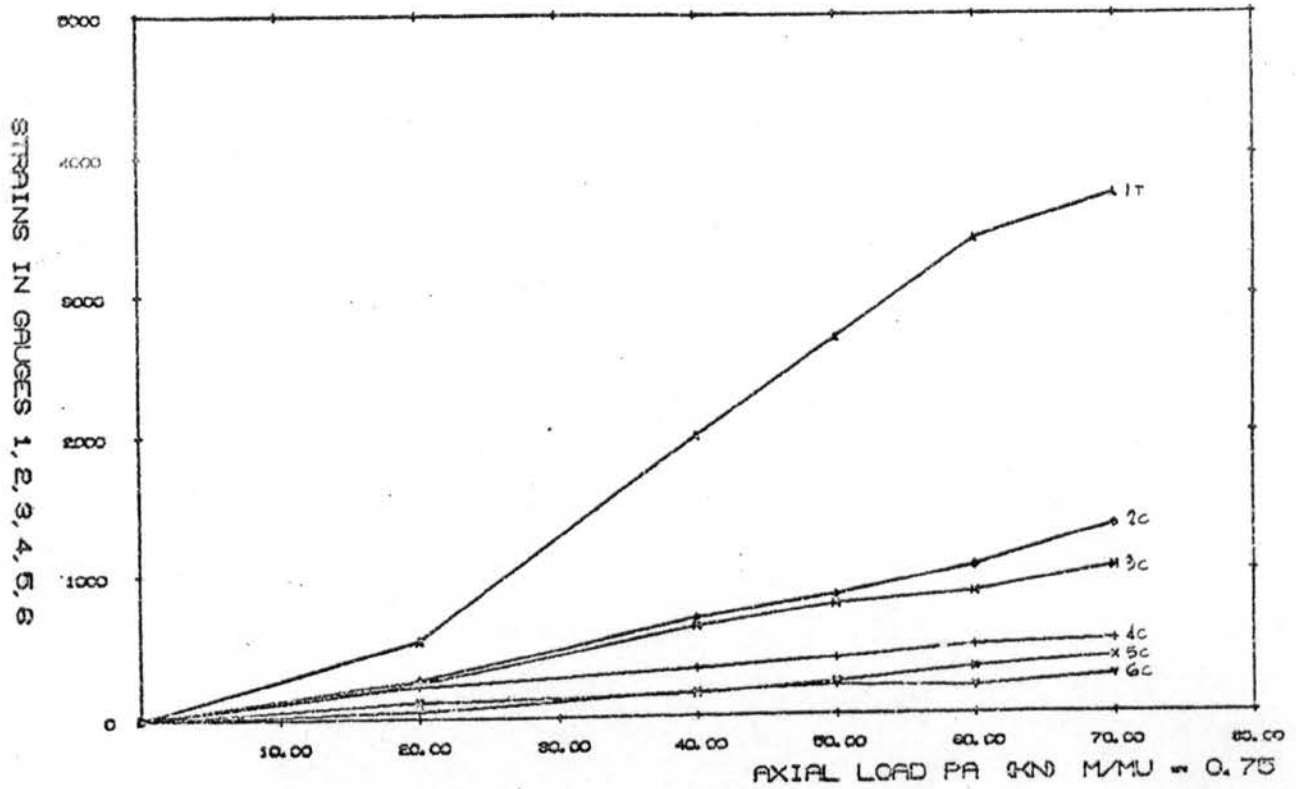


Figure 184

BETA = 0.42 CHORD THICKNESS = 5.0



BETA = 0.42 CHORD THICKNESS = 5.0

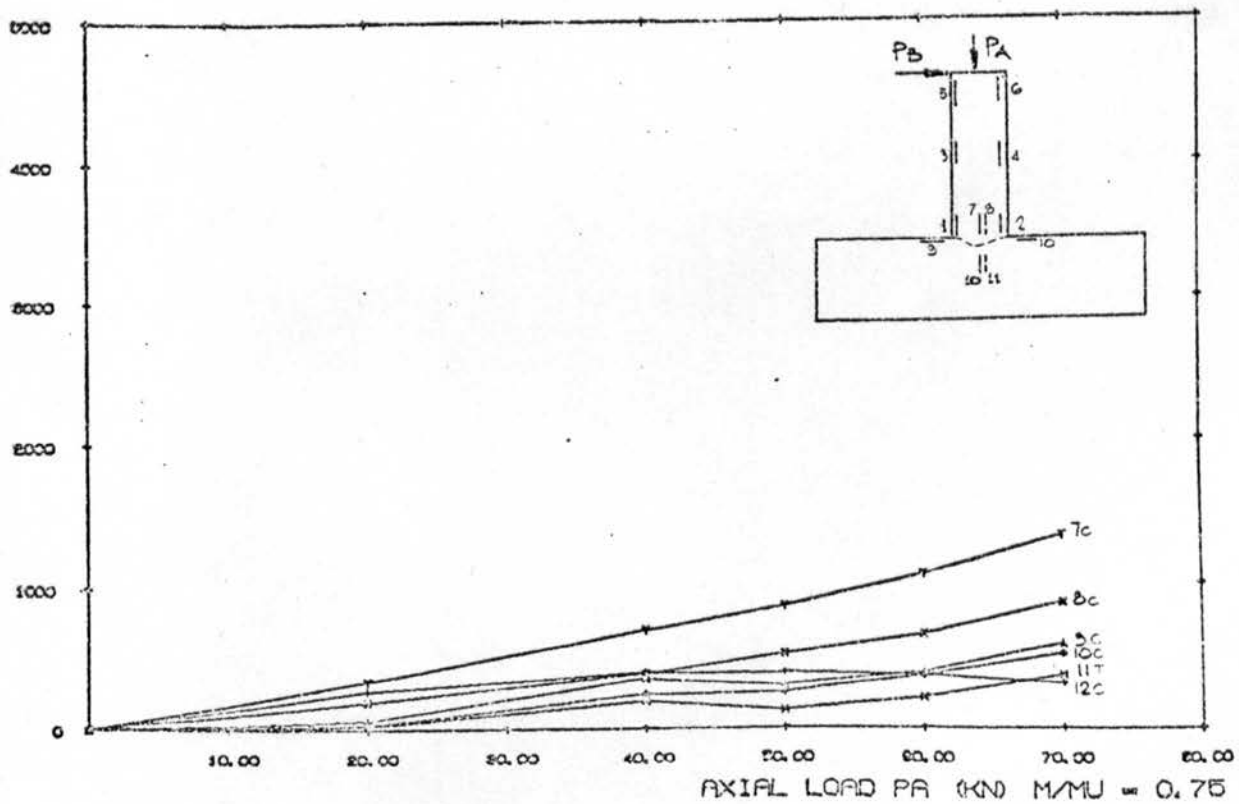
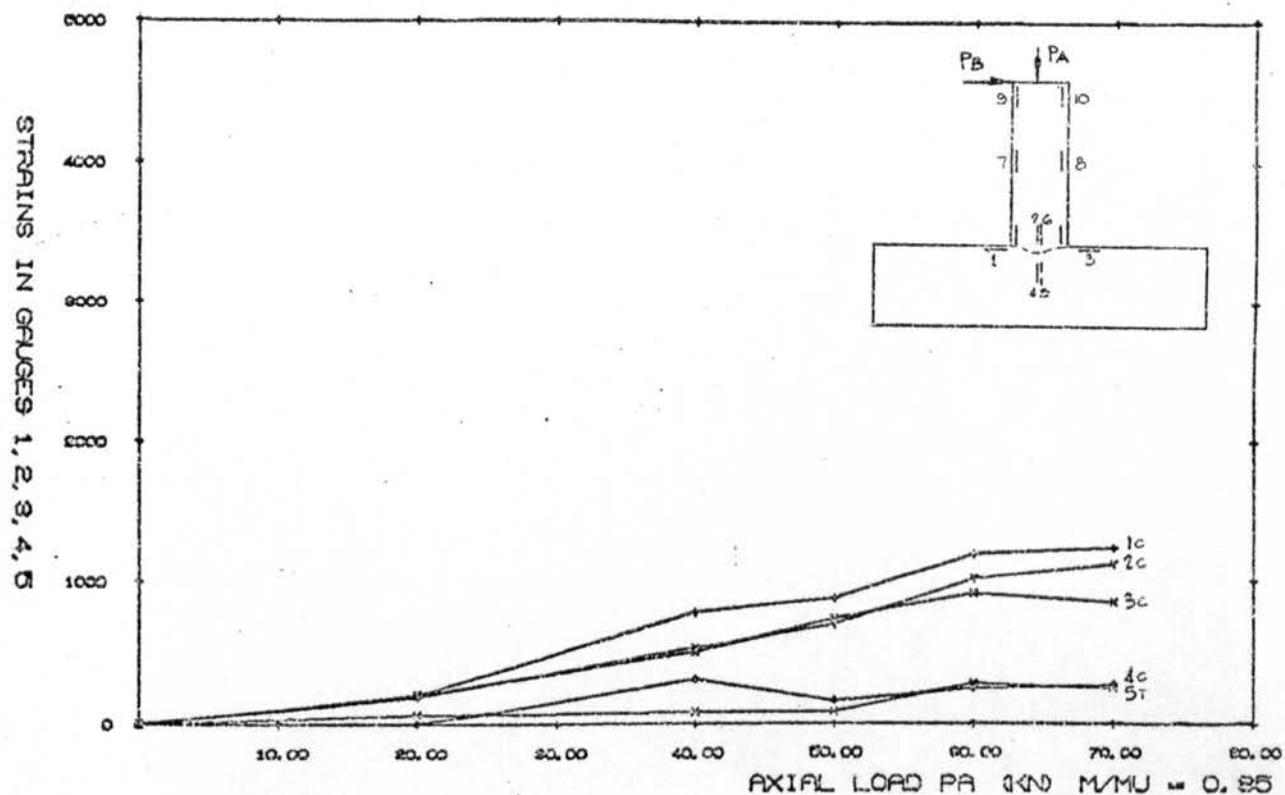


Figure 185

BETA = 0.42 CHORD THICKNESS = 5.0



BETA = 0.42 CHORD THICKNESS = 5.0

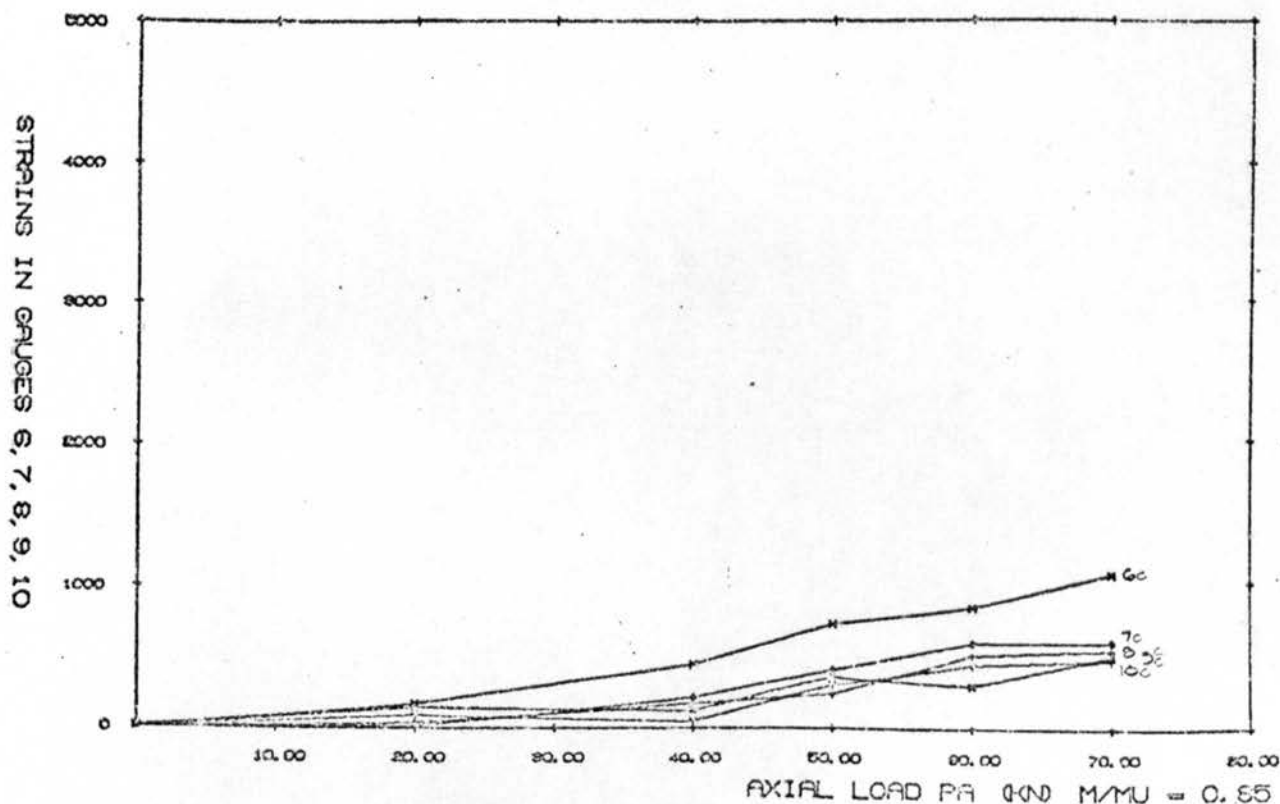
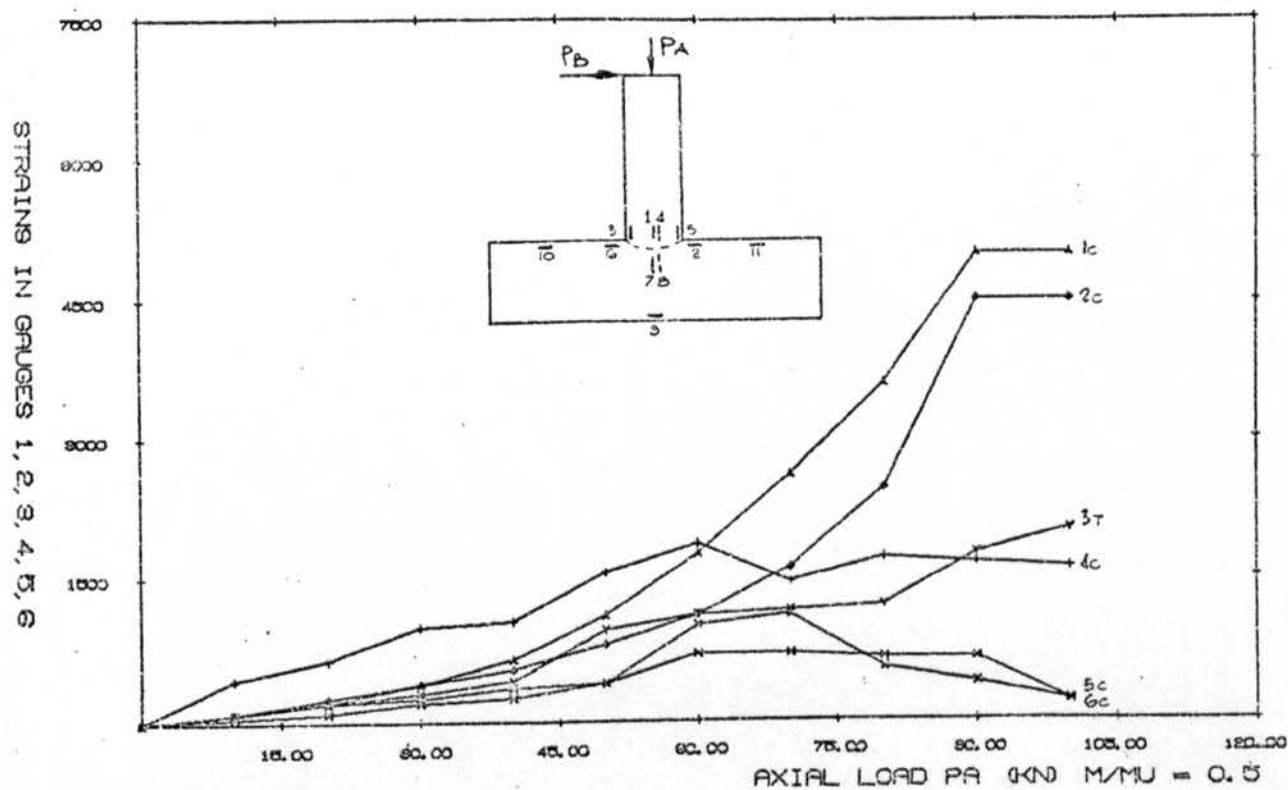


Figure 186

BETA - 0.42 CHORD THICKNESS = 5.4



BETA - 0.42 CHORD THICKNESS = 5.4

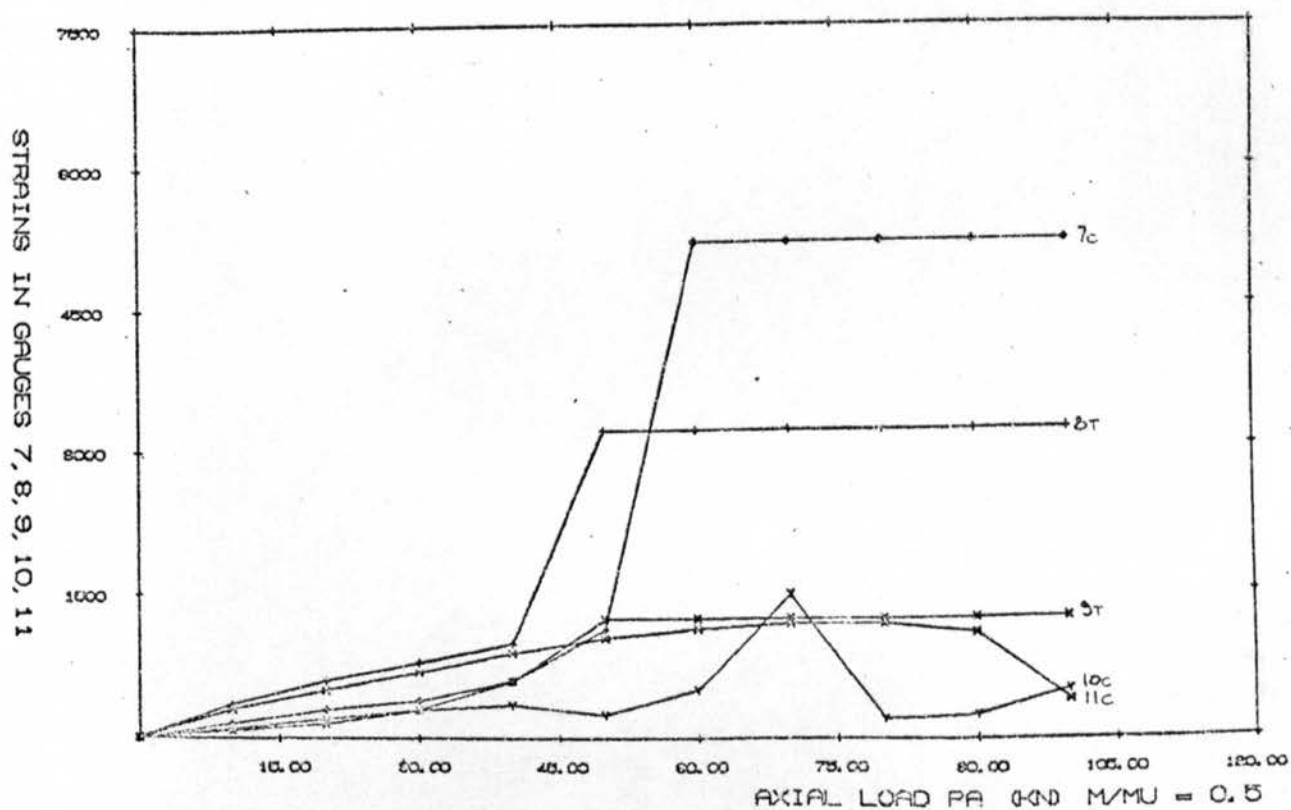
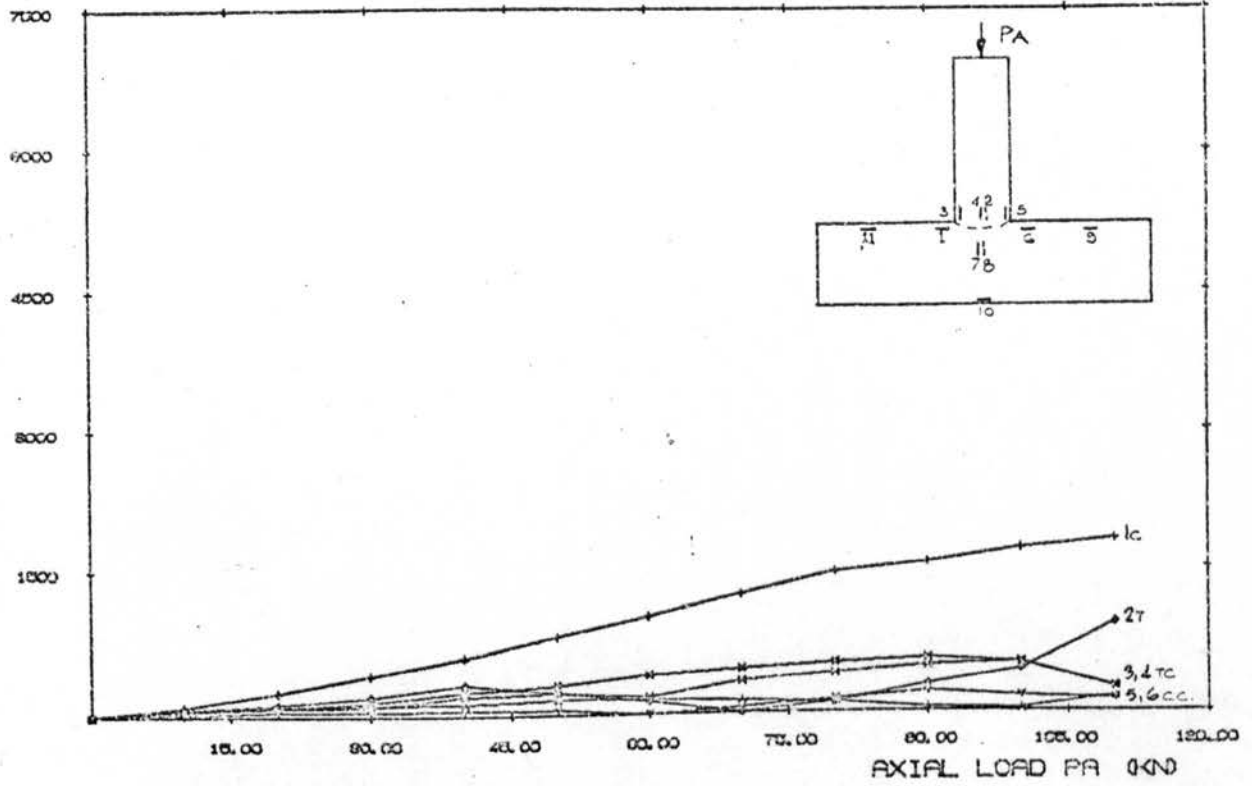


Figure 187

BETA - 0.42 CHORD THICKNESS = 5.4

STRAINS IN GAUGES 1, 2, 3, 4, 5, 6



BETA - 0.42 CHORD THICKNESS = 5.4

STRAINS IN GAUGES 7, 8, 9, 10, 11

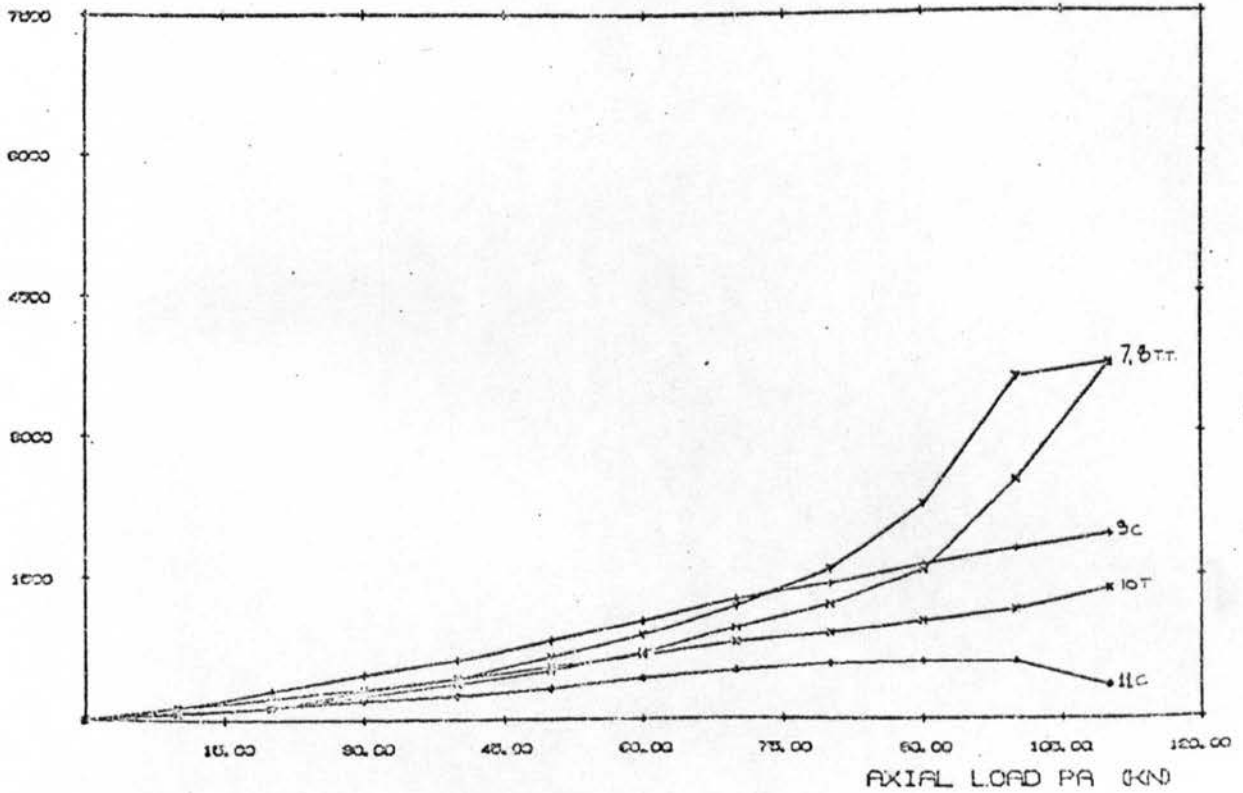


Figure 188

BETA - 0.42 CHORD THICKNESS = 5.4

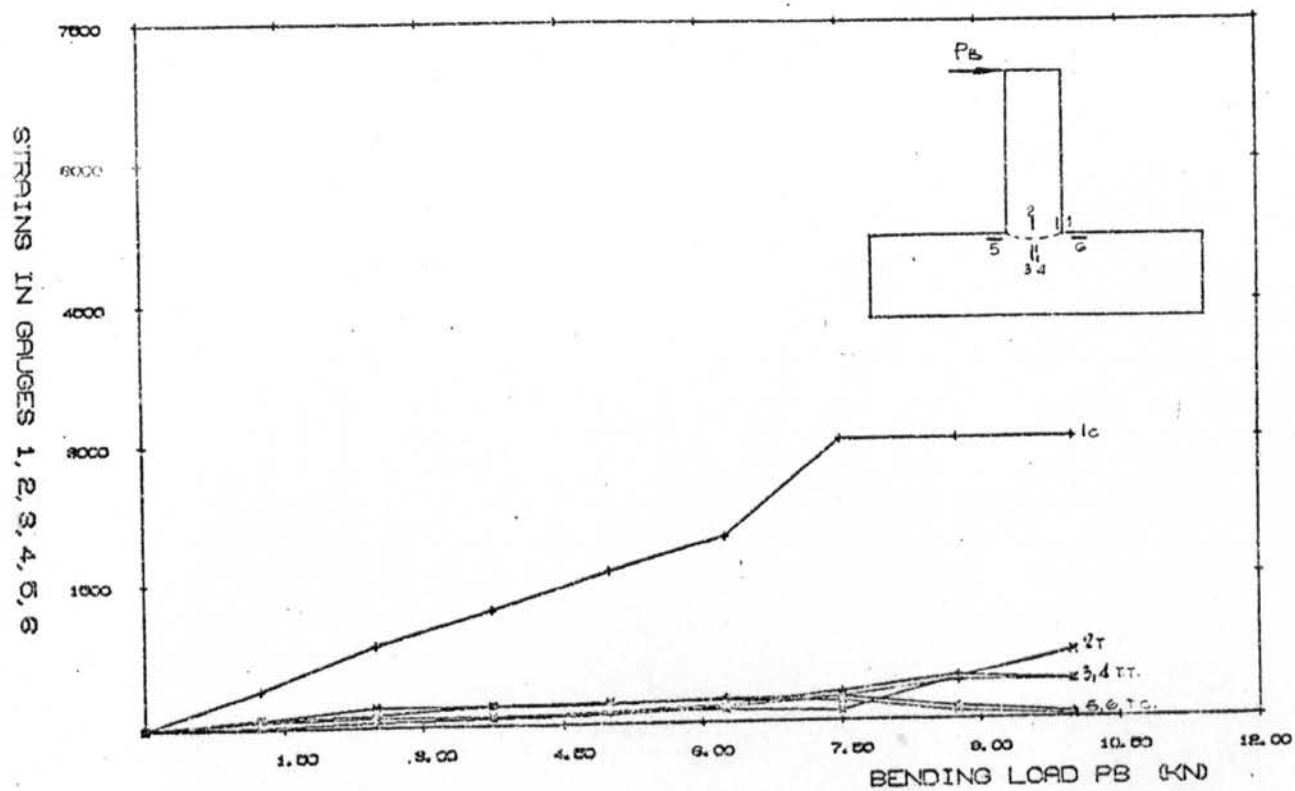
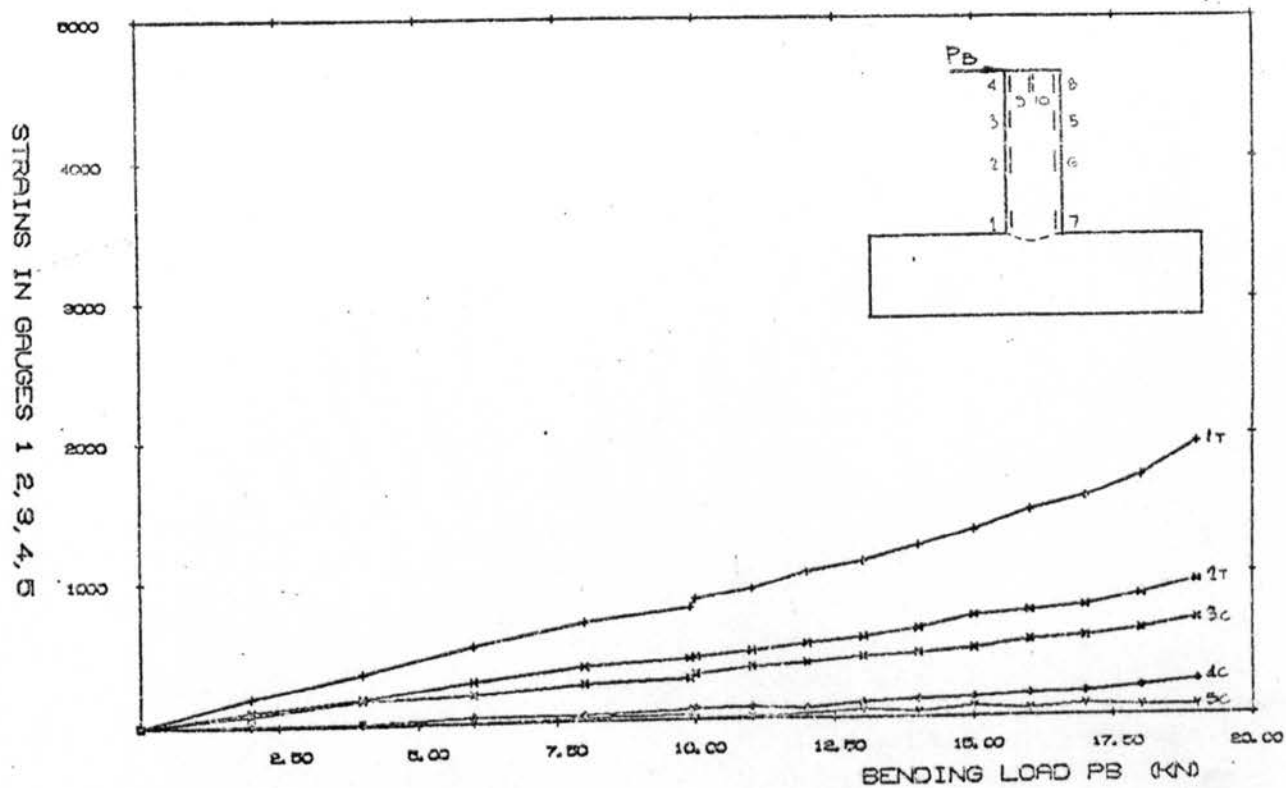


Figure 189

BETA = 0.53 CHORD THICKNESS = 5.0



BETA = 0.53 CHORD THICKNESS = 5.0

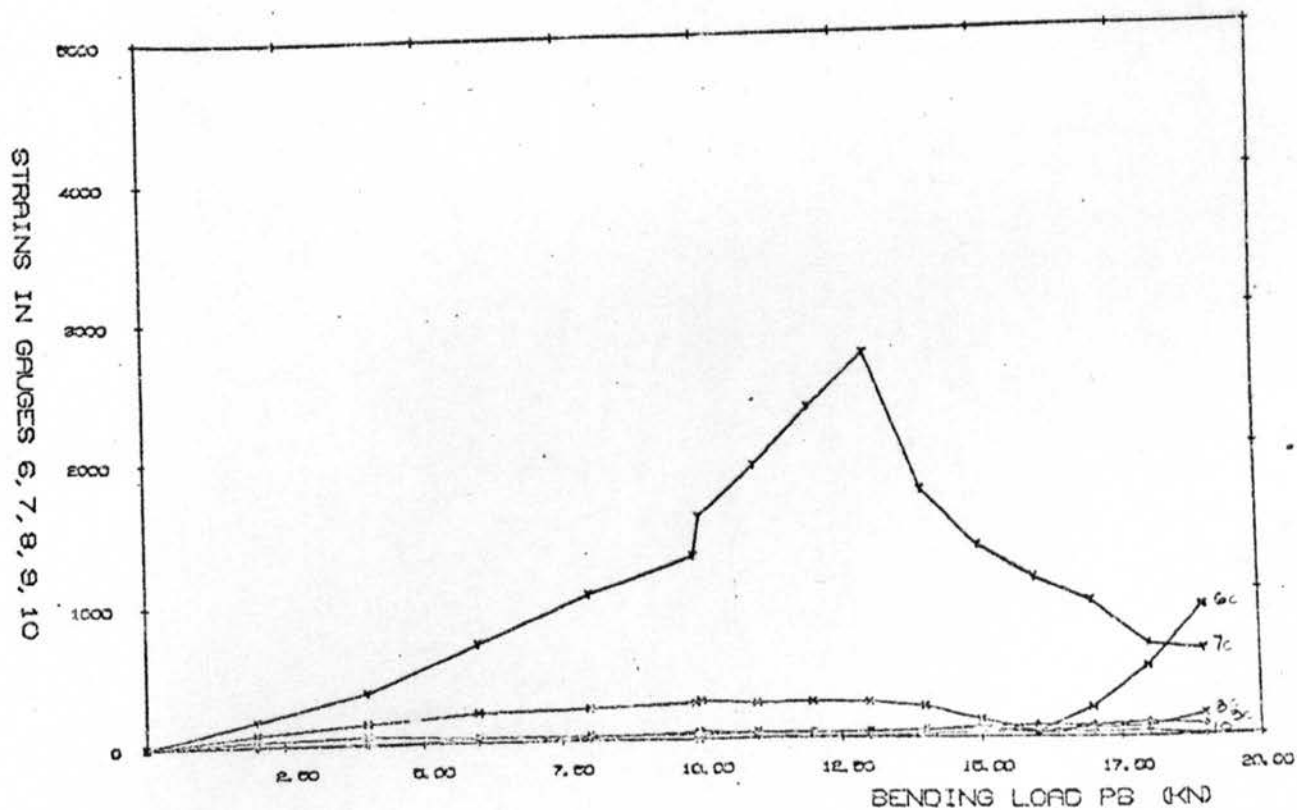
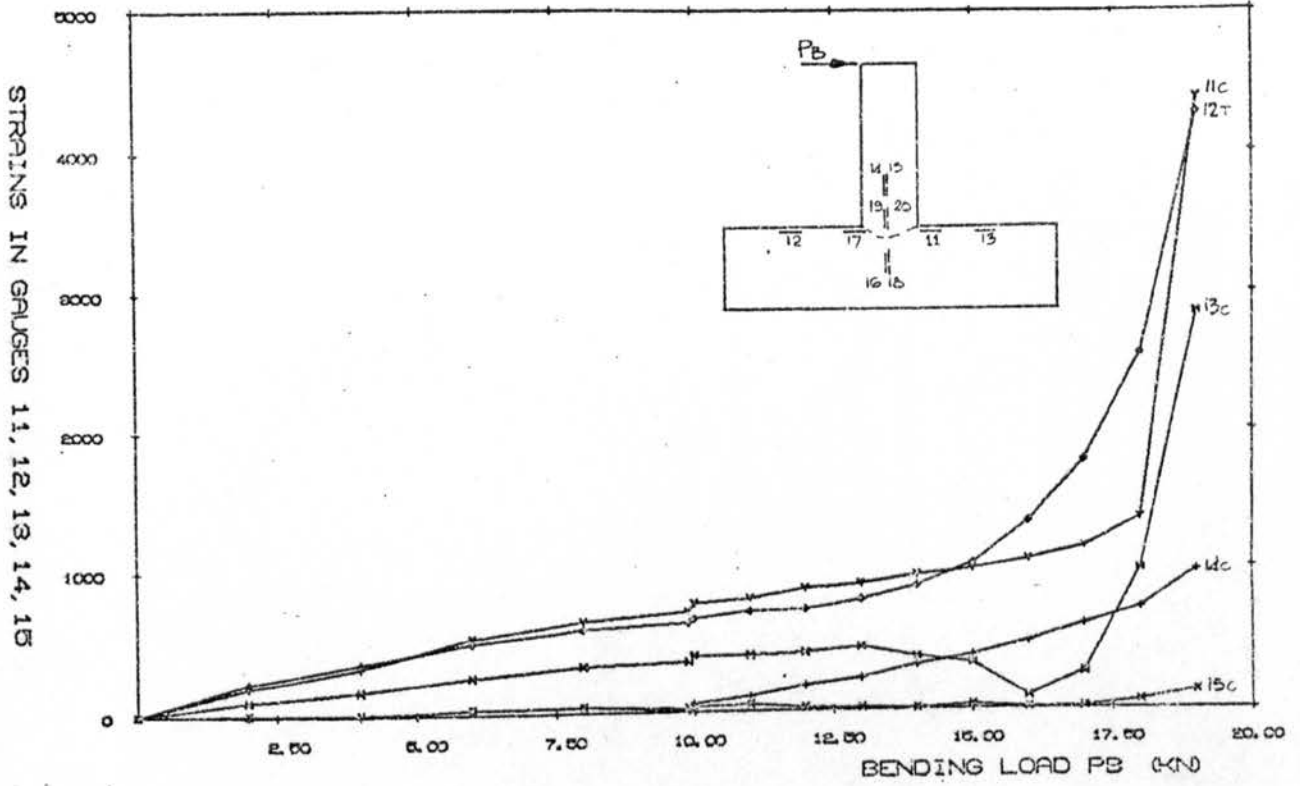


Figure 190

BETA = 0.53 CHORD THICKNESS = 5.0



BETA = 0.53 CHORD THICKNESS = 5.0

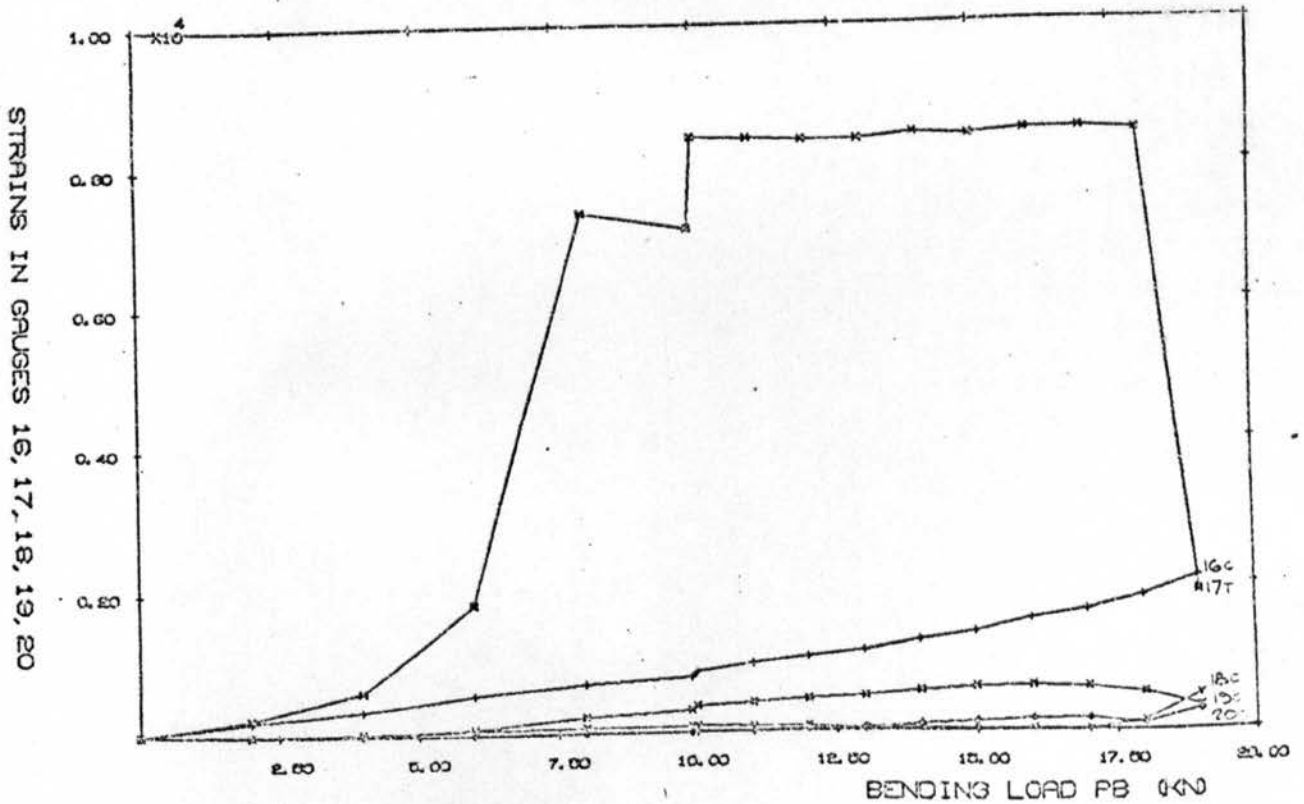


Figure 191

BETA = 0.53 CHORD THICKNESS = 5.0 mm.

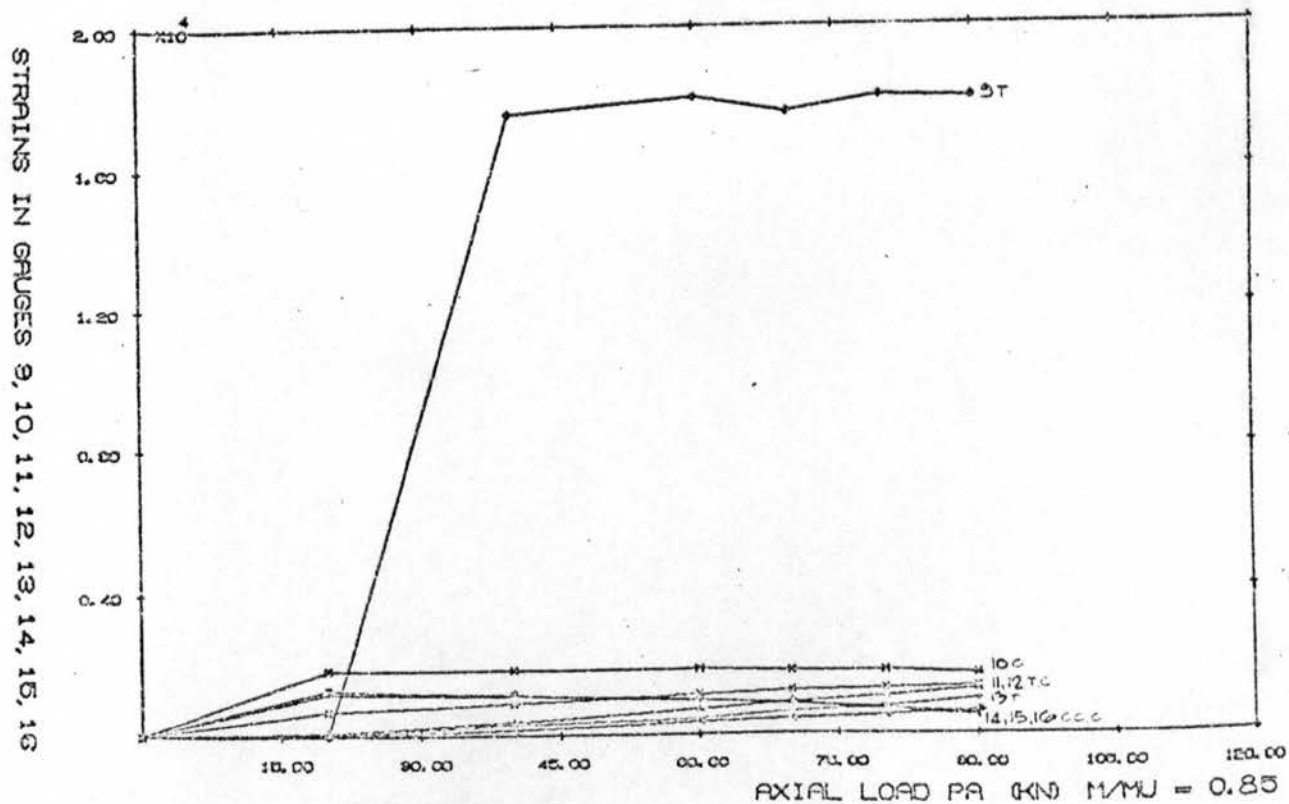
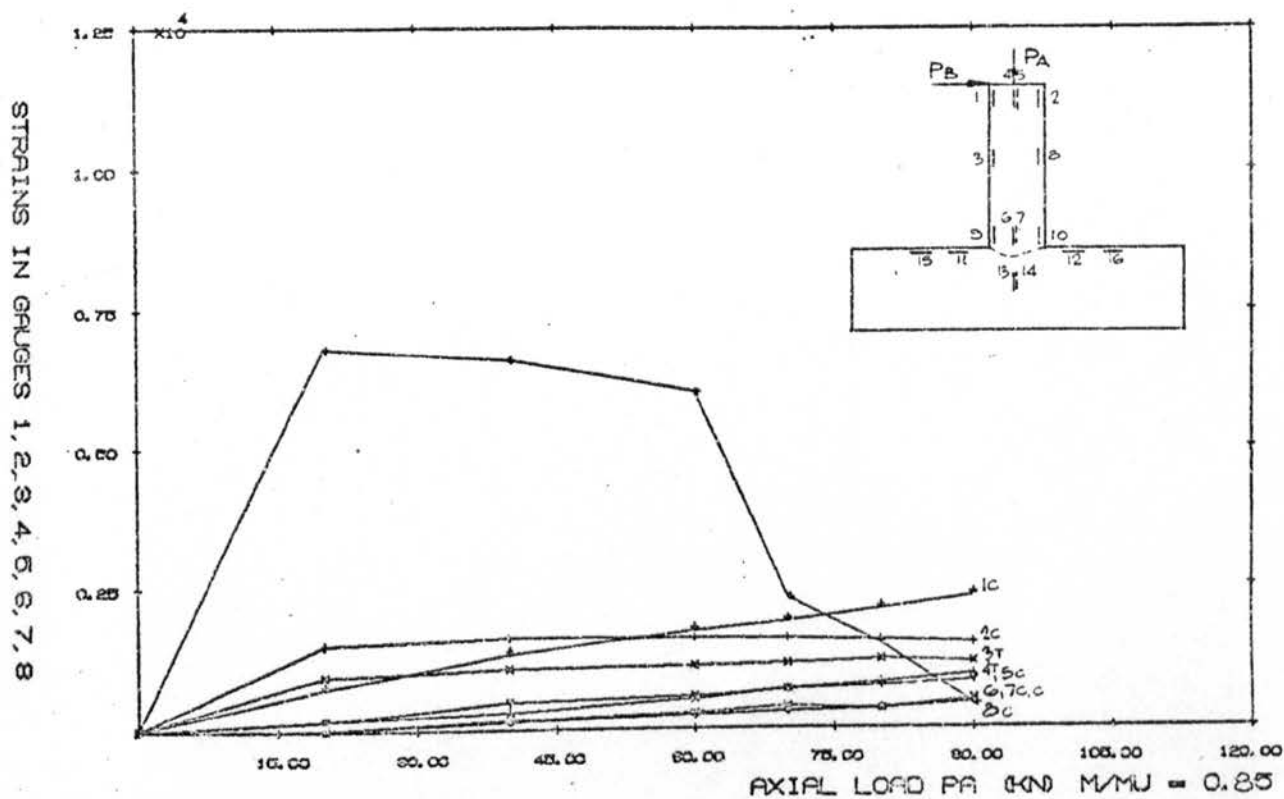


Figure 192

BETA = 0.53 CHORD THICKNESS = 5.0 MM.

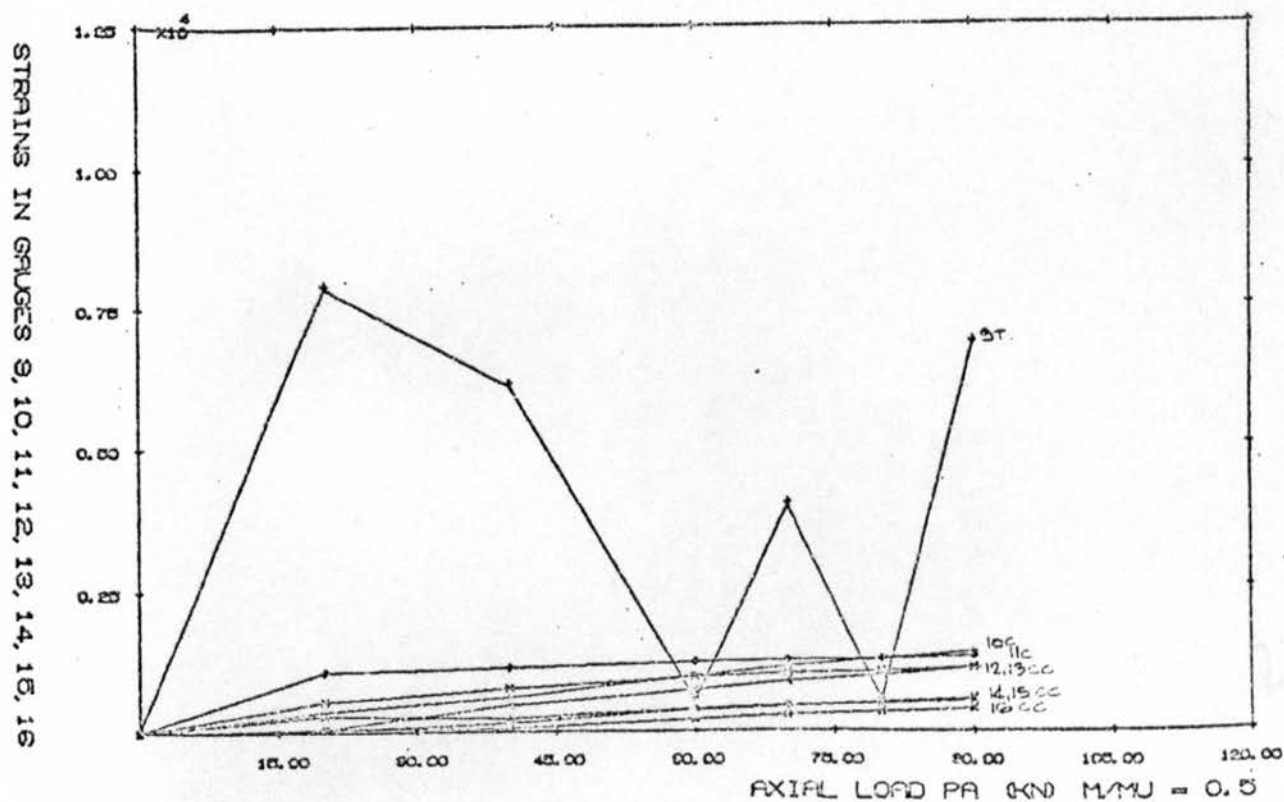
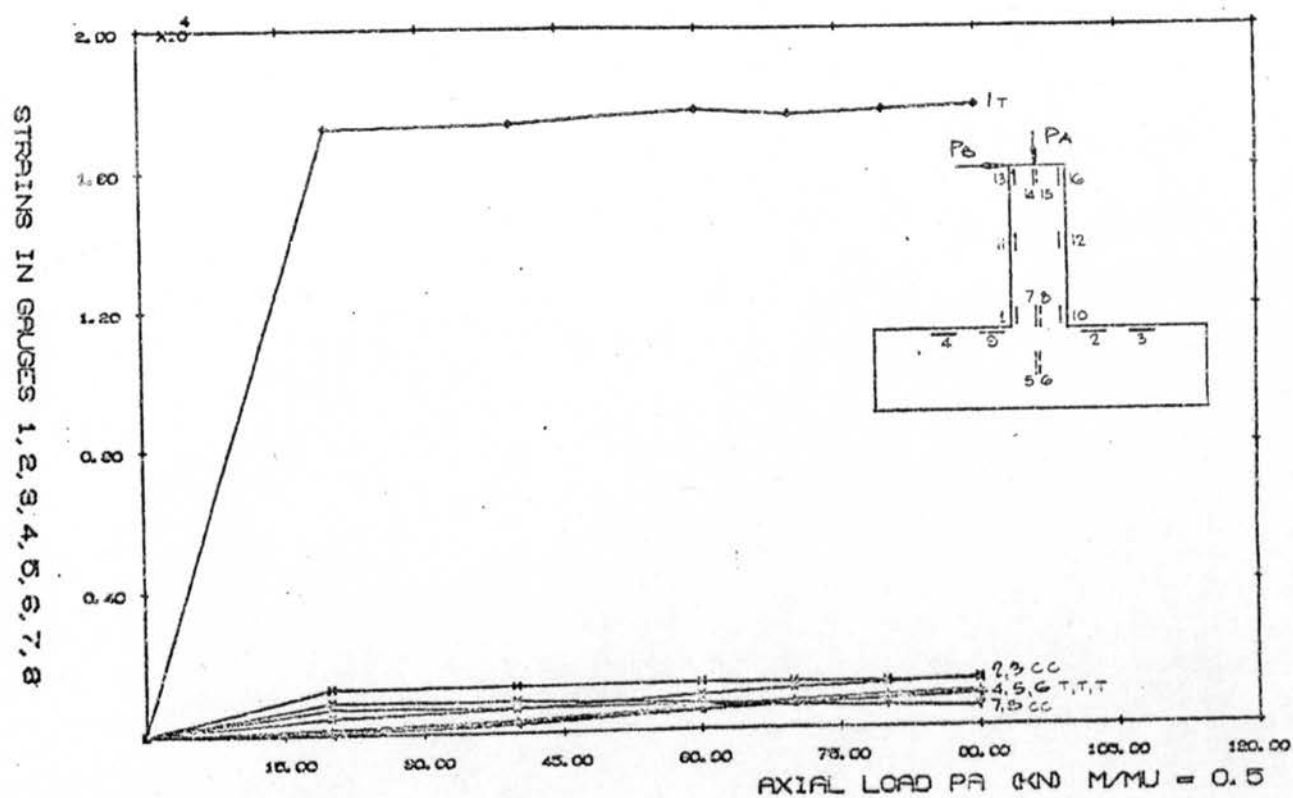


Figure 193

BETA = 0.53 CHORD THICKNESS = 5.0 mm.

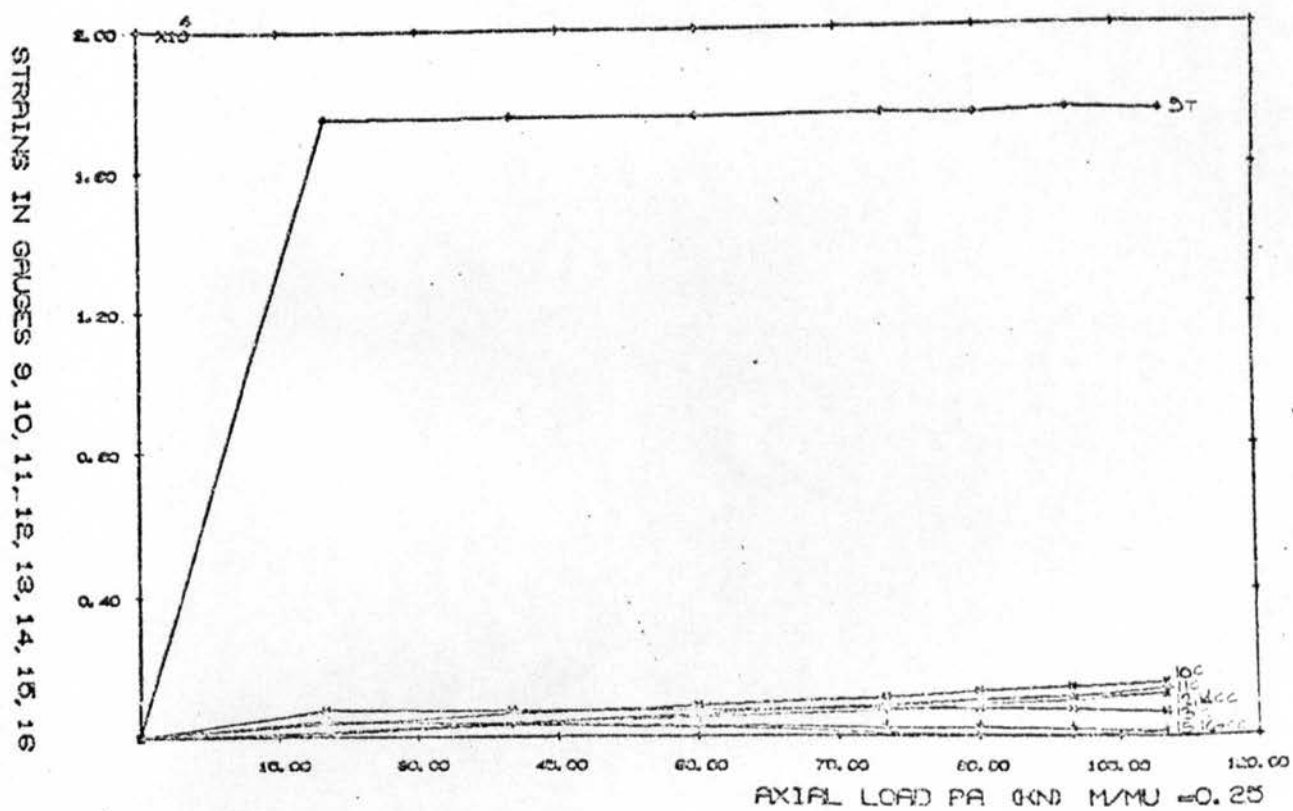
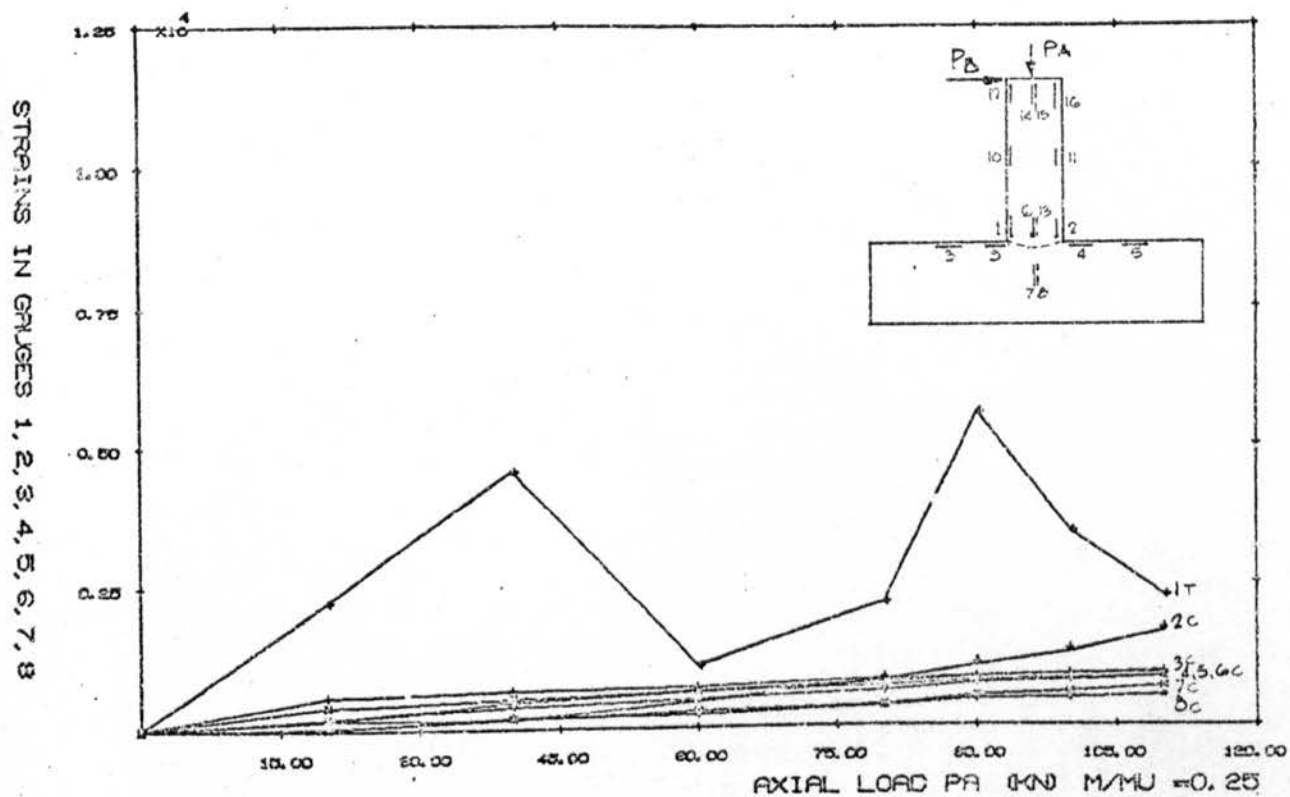


Figure 194

BETA = 0.66 CHORD THICKNESS = 5.0

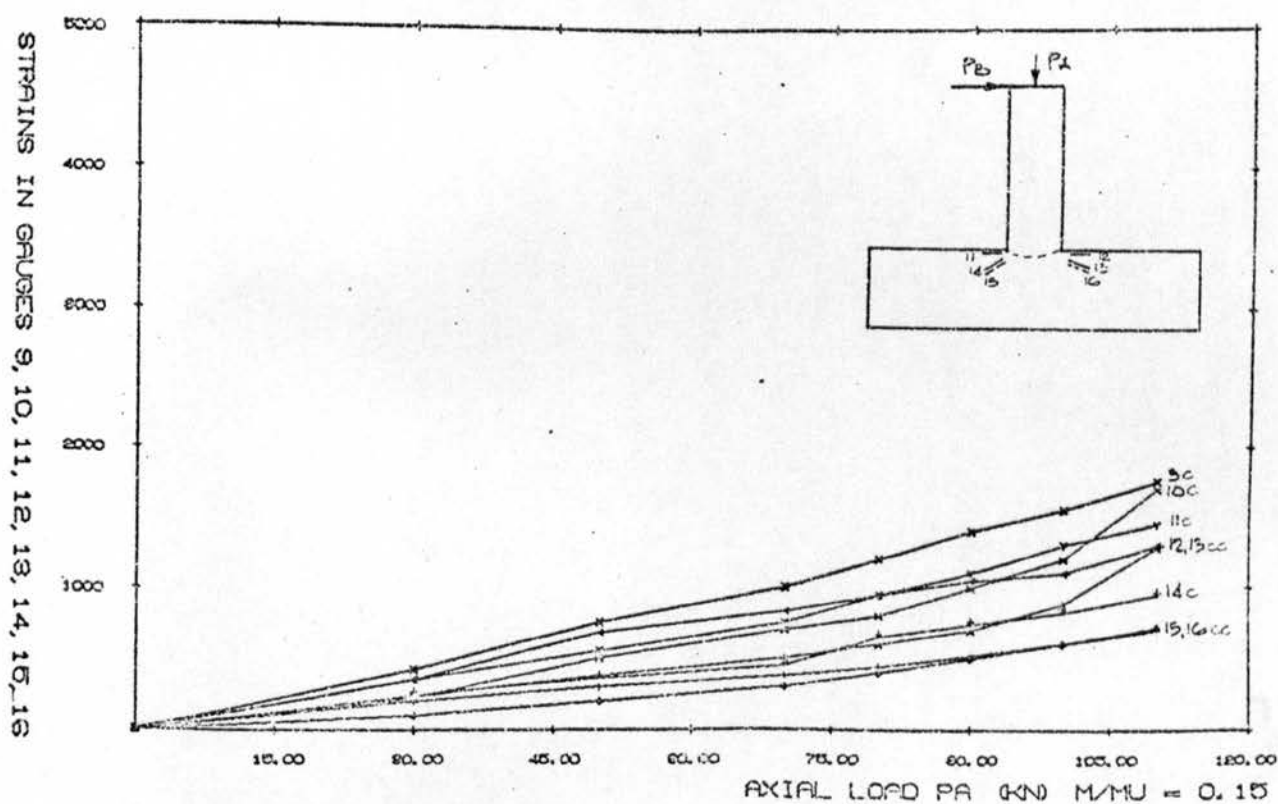
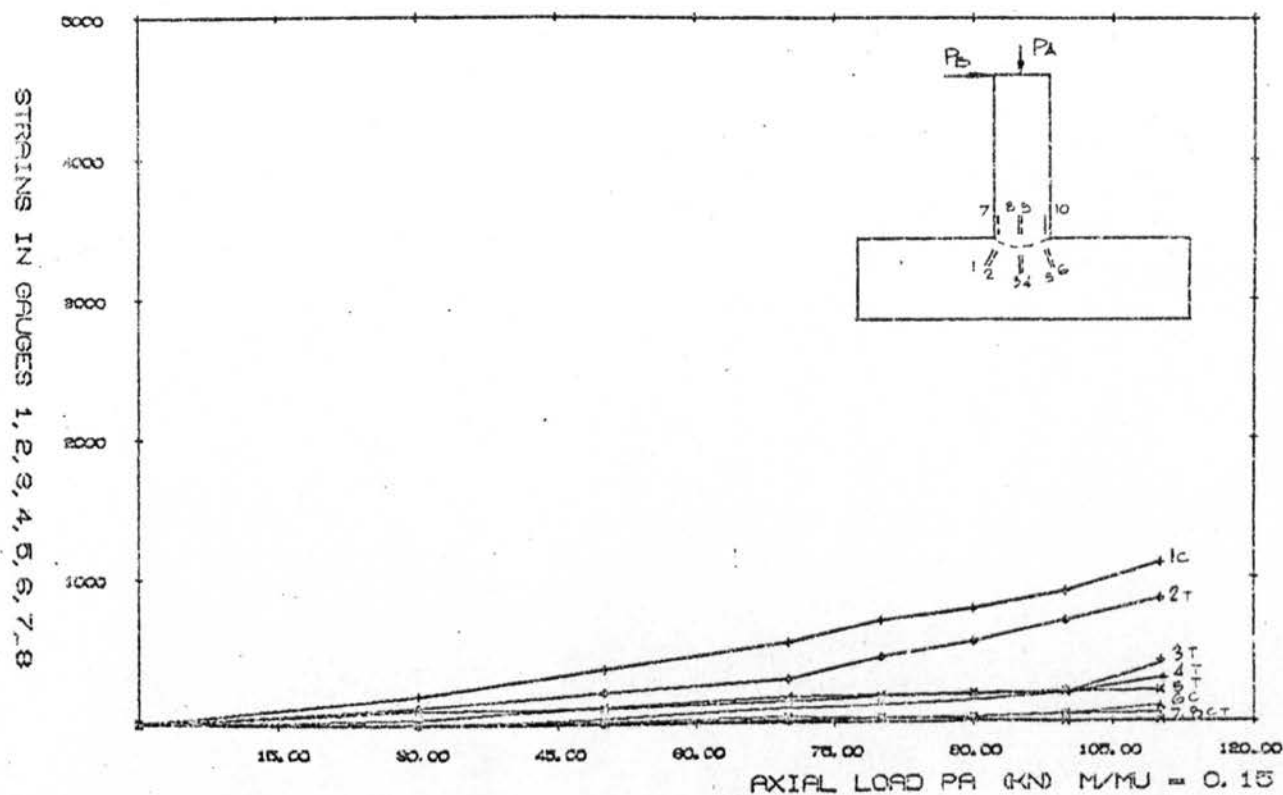
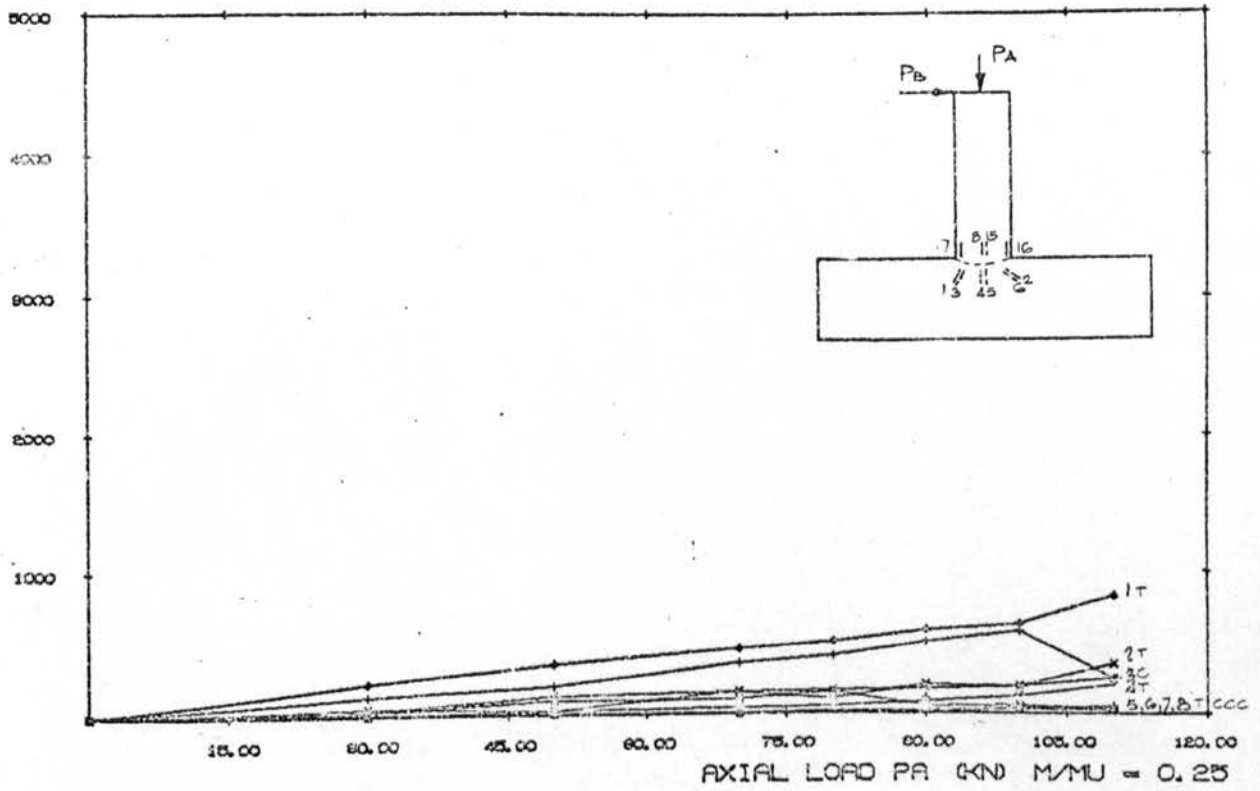
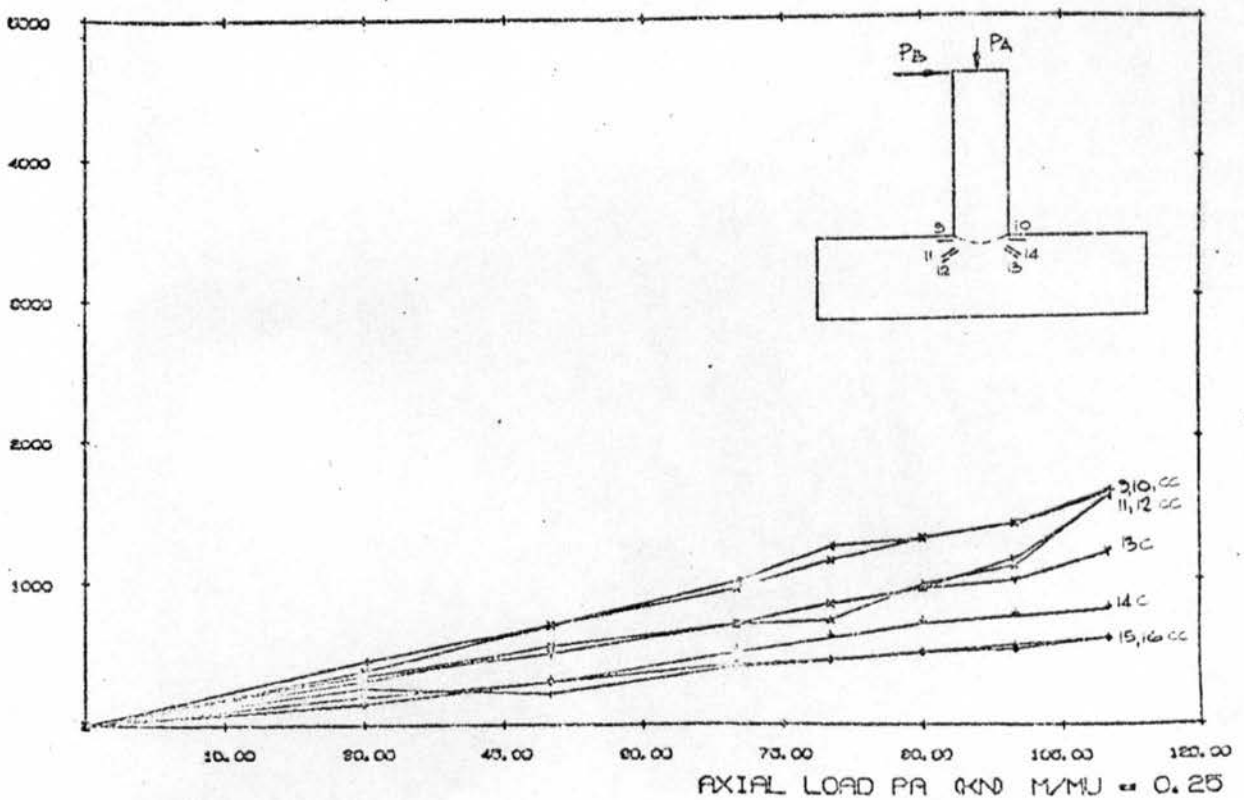


Figure 195

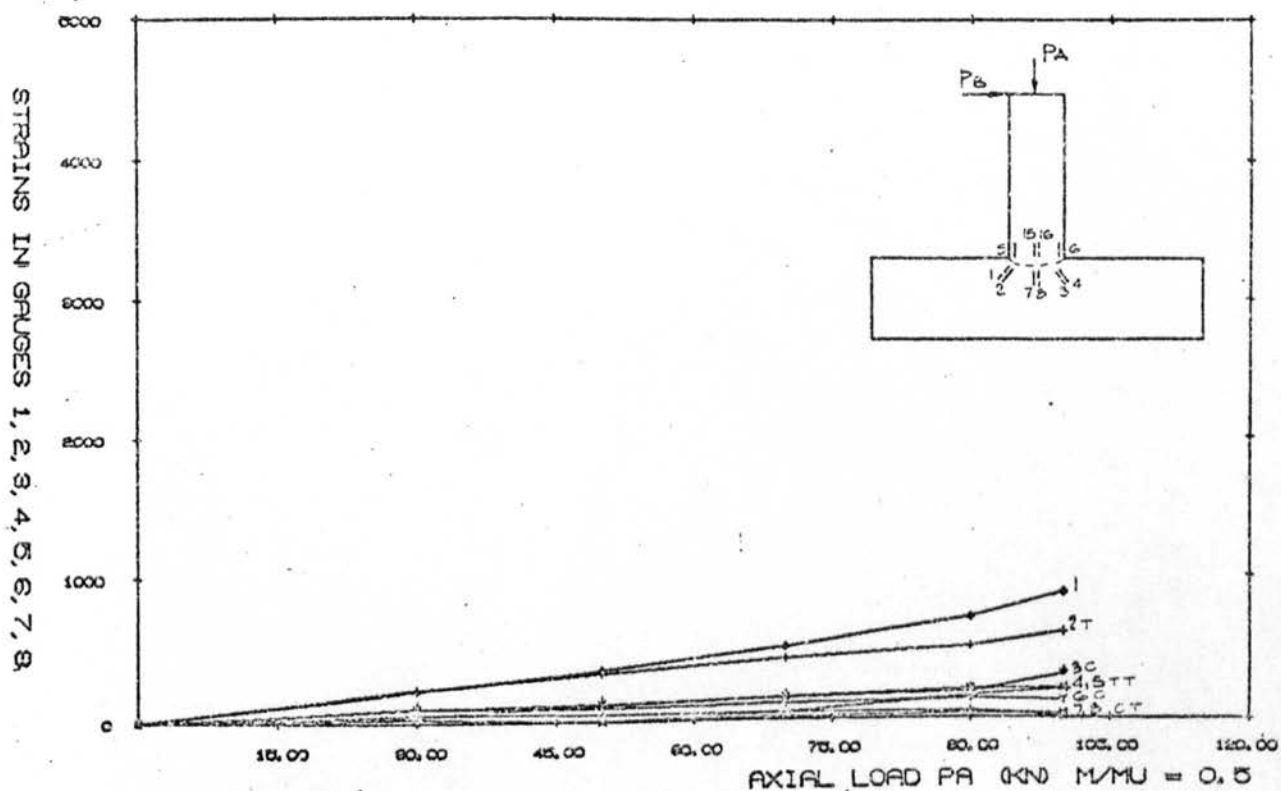
STRAINS IN GAUGES 1, 2, 3, 4, 5, 6, 7, 8



STRAINS IN GAUGES 9, 10, 11, 12, 13, 14, 15, 16



BETA = 0.66 CHORD THICKNESS = 5.0



BETA = 0.66 CHORD THICKNESS = 5.0

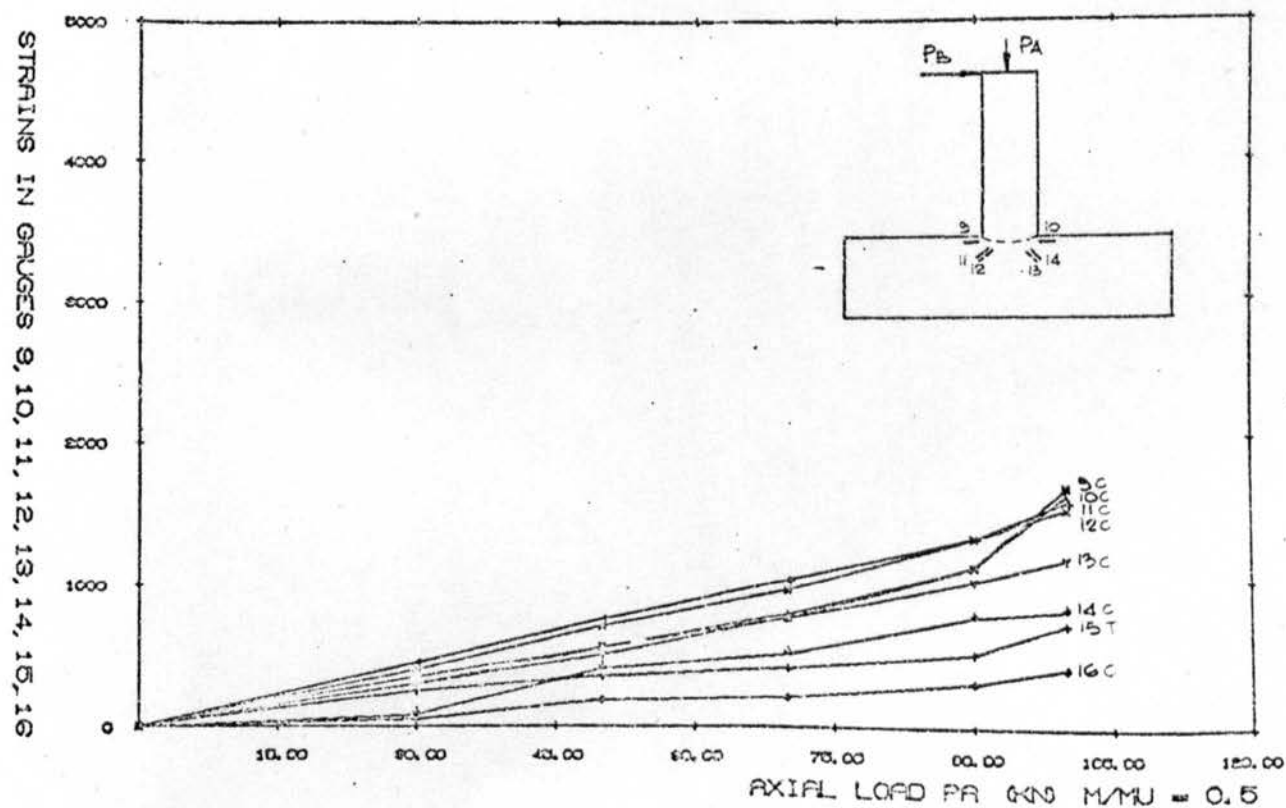
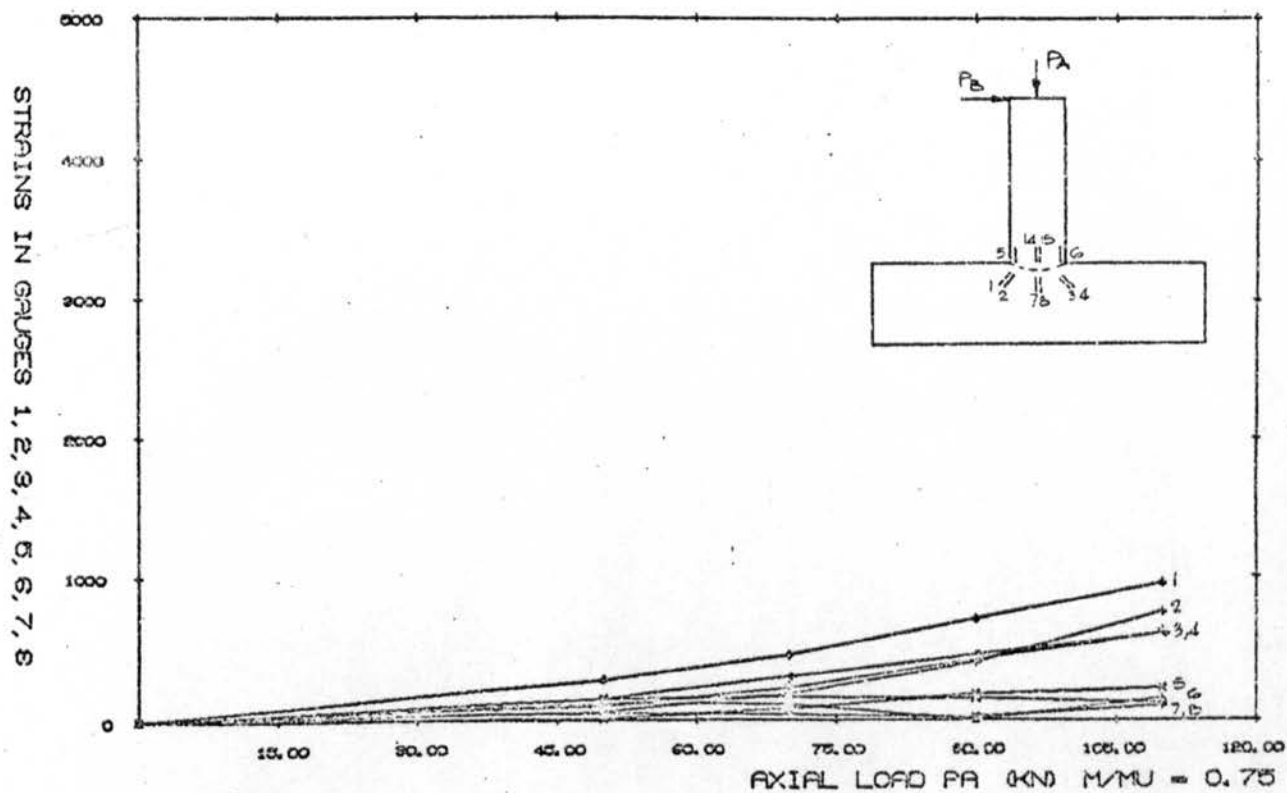


Figure 197

BETA = 0.66 CHORD THICKNESS = 5.0



BETA = 0.66 CHORD THICKNESS = 5.0

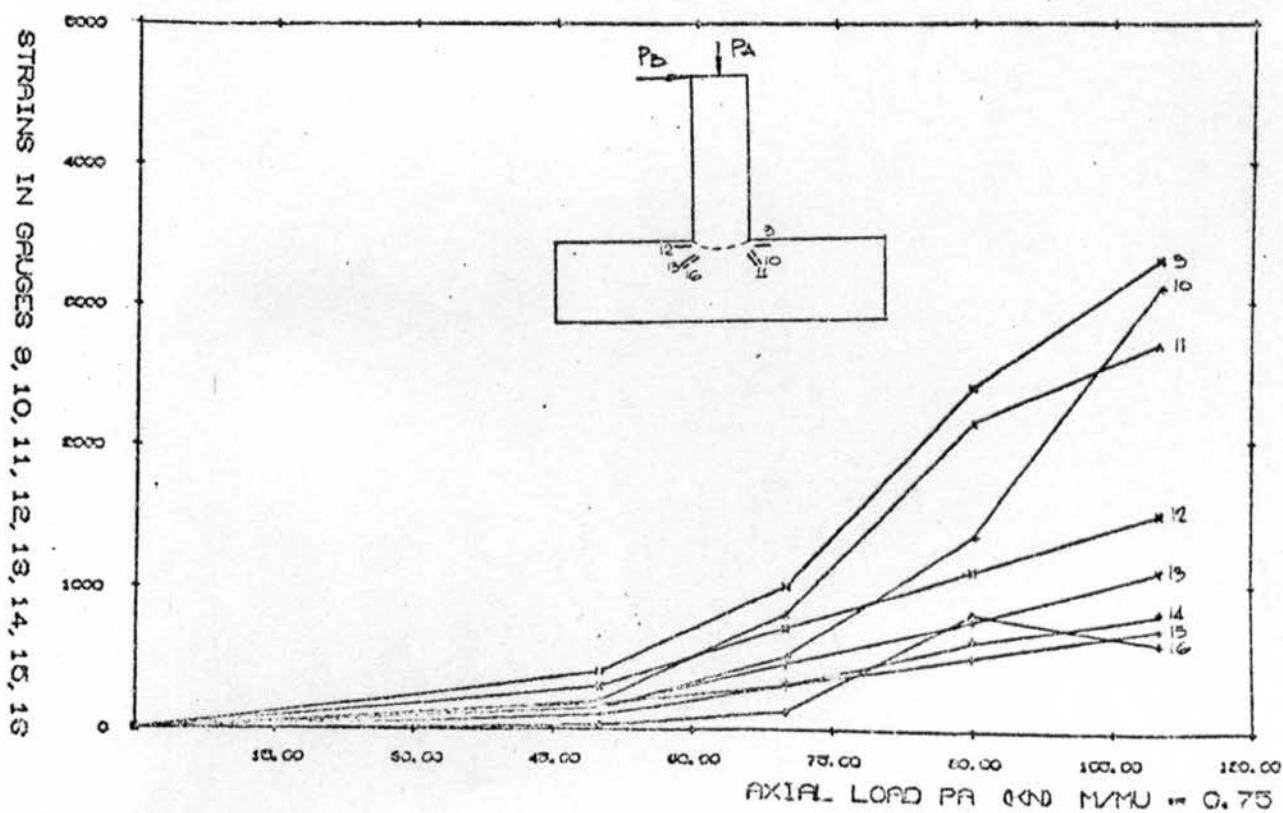
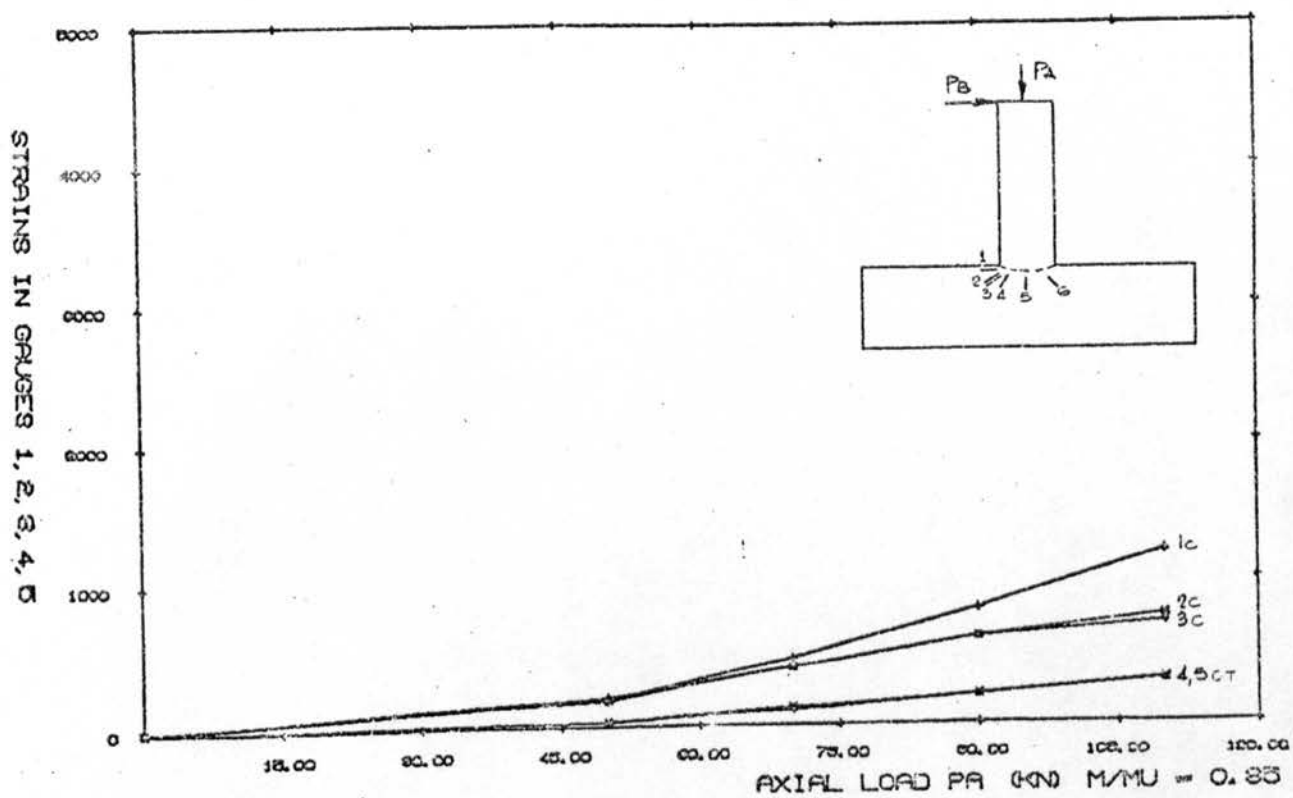


Figure 198

BETA = 0.66 CHORD THICKNESS = 5.0



BETA = 0.66 CHORD THICKNESS = 5.0

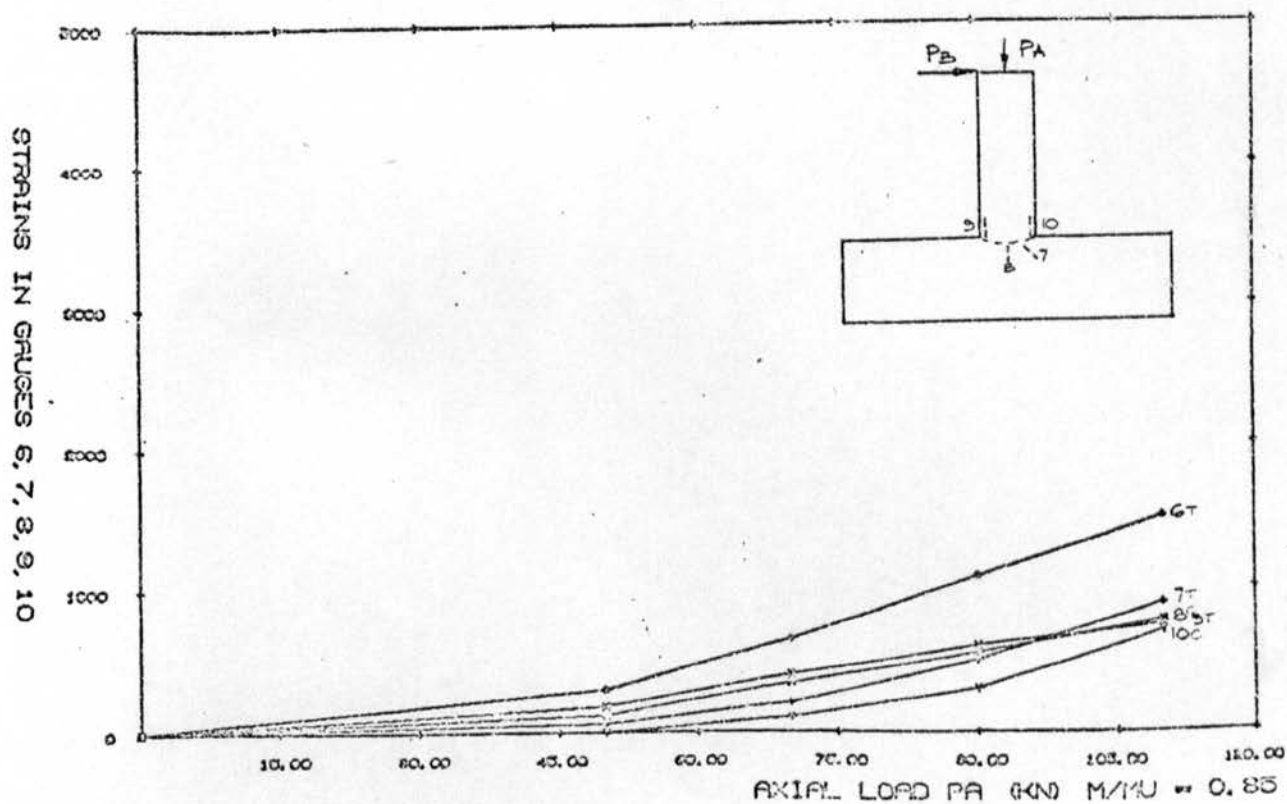
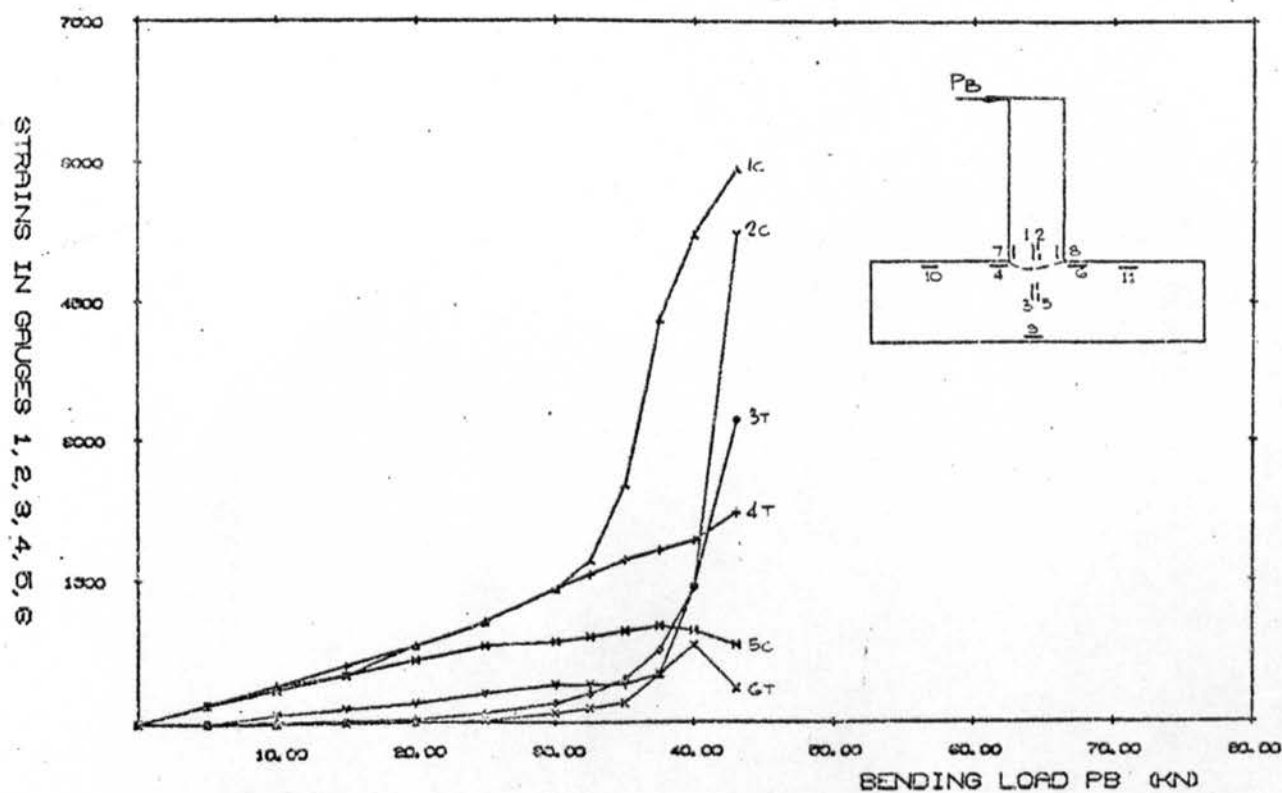


Figure 199

BETA = 0.77 CHORD THICKNESS = 5.4



BETA = 0.77 CHORD THICKNESS = 5.4

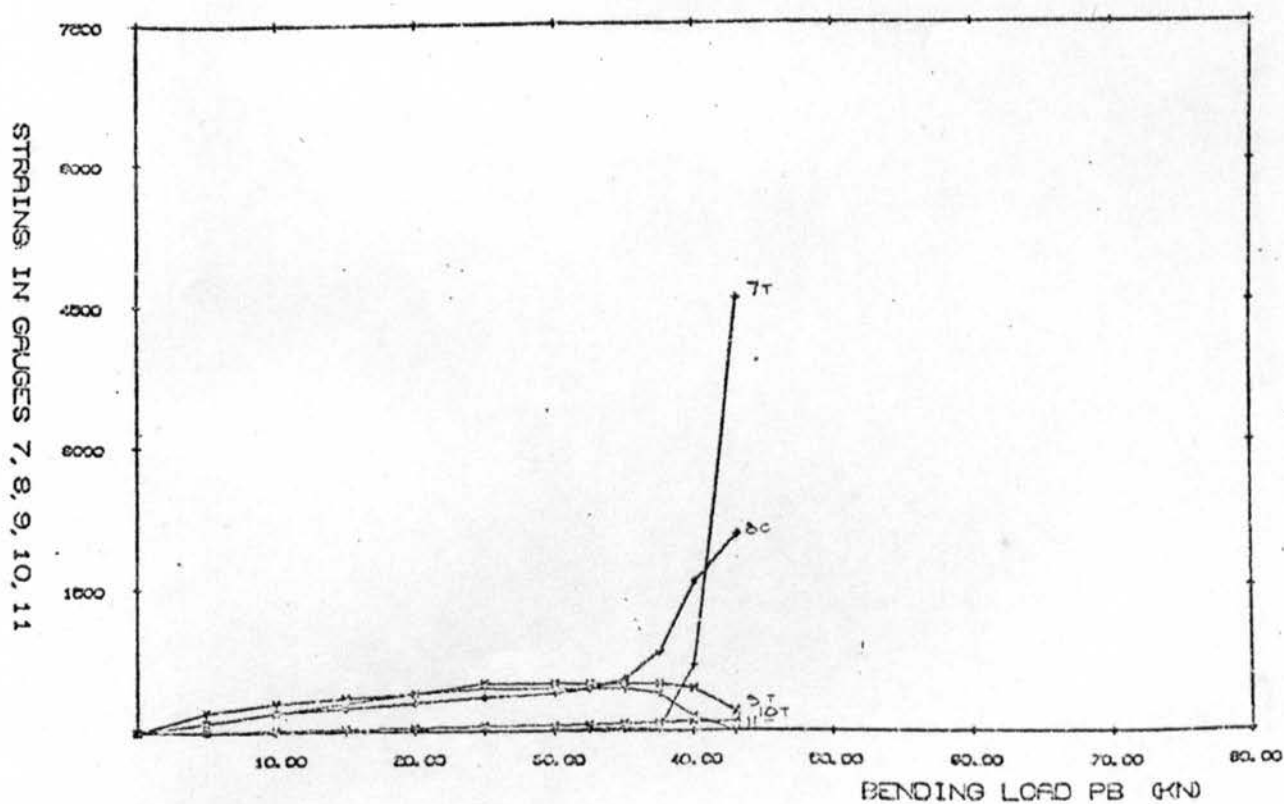
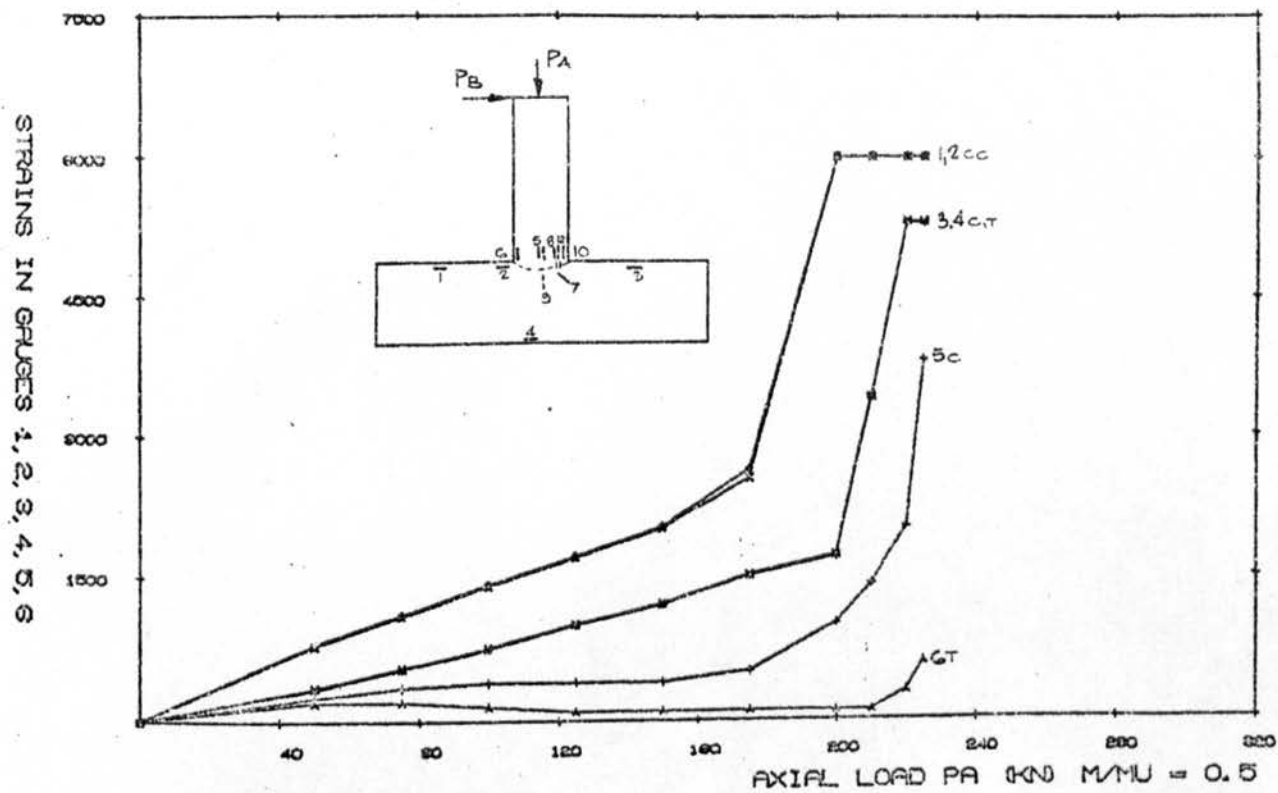


Figure 200

BETA = 0.77 CHORD THICKNESS = 5.4



BETA = 0.77 CHORD THICKNESS = 5.4

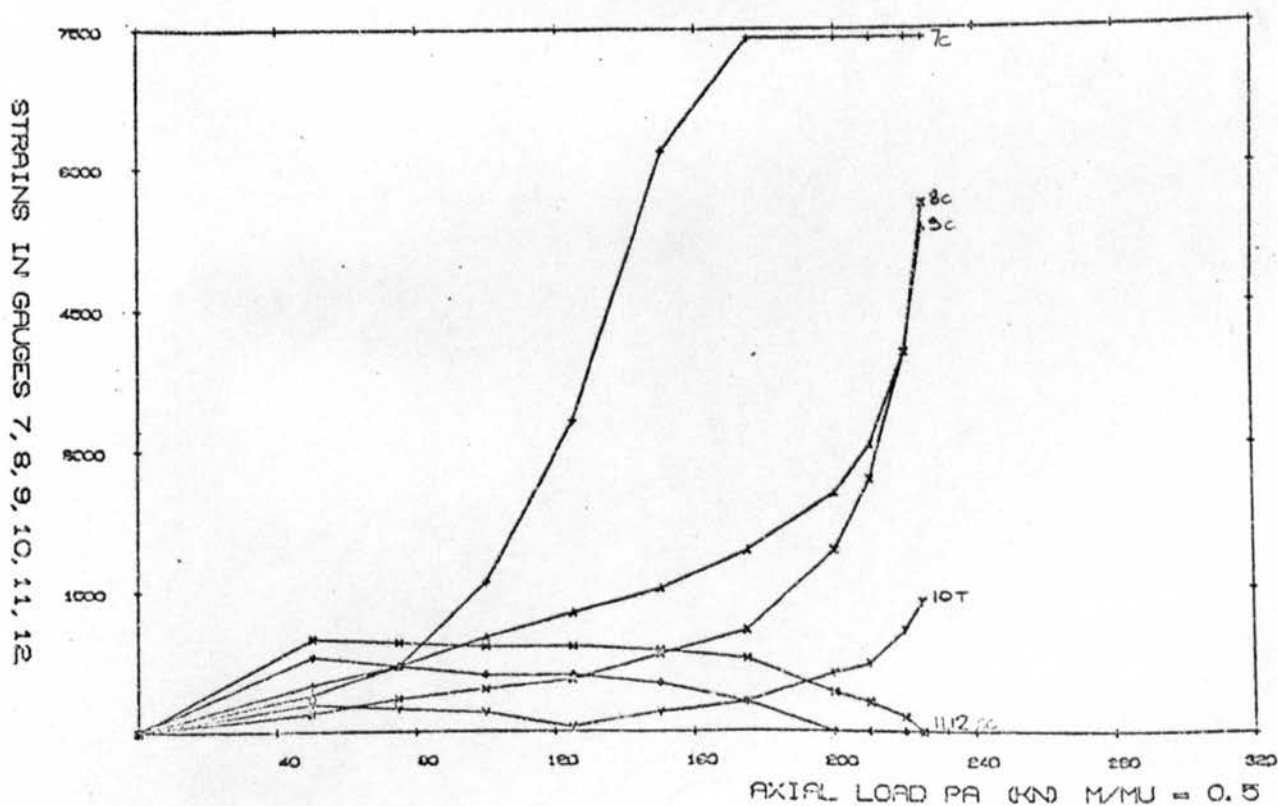


Figure 201

BETA = 0.77 CHORD THICKNESS = 5.4

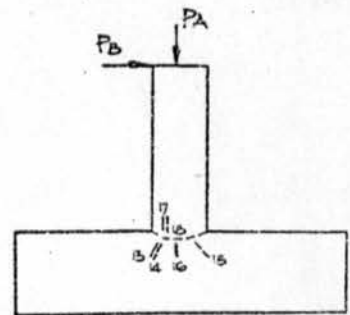
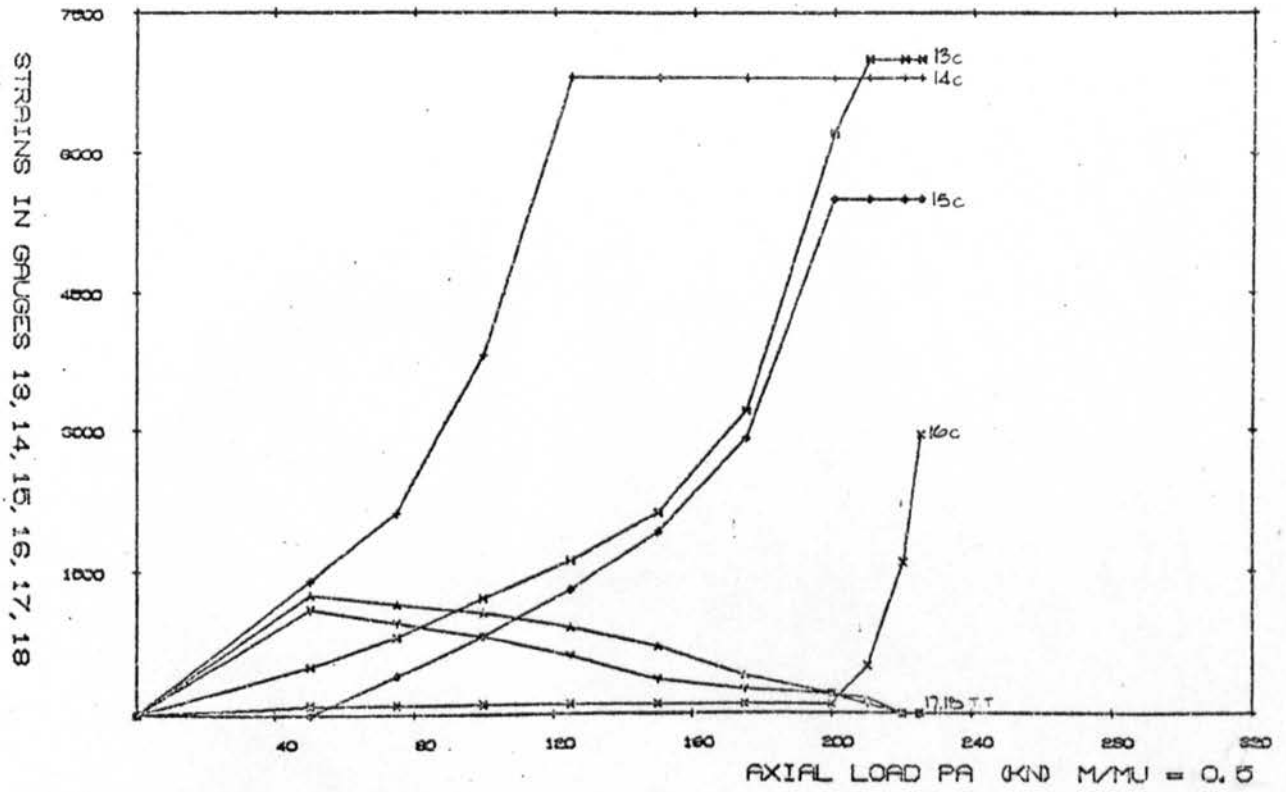
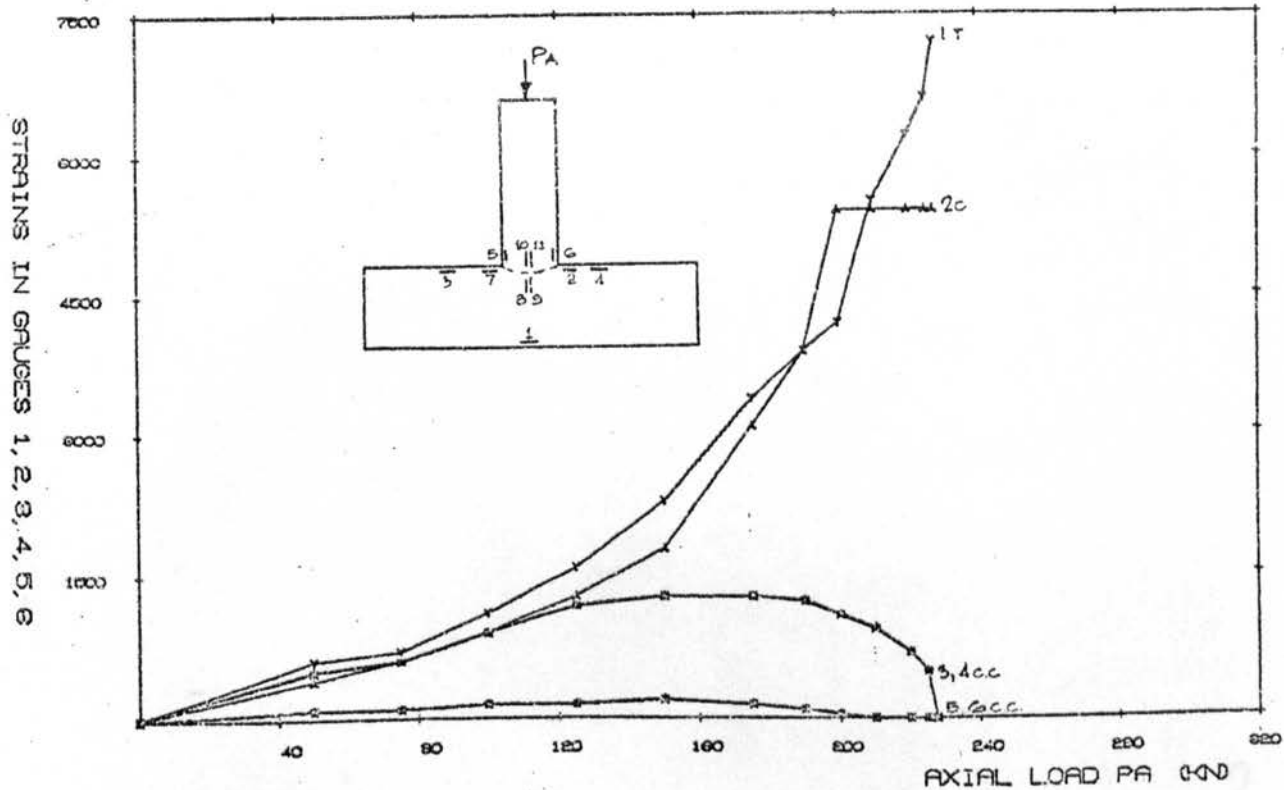


Figure 202

BETA = 0.77 CHORD THICKNESS = 5.4



BETA = 0.77 CHORD THICKNESS = 5.4

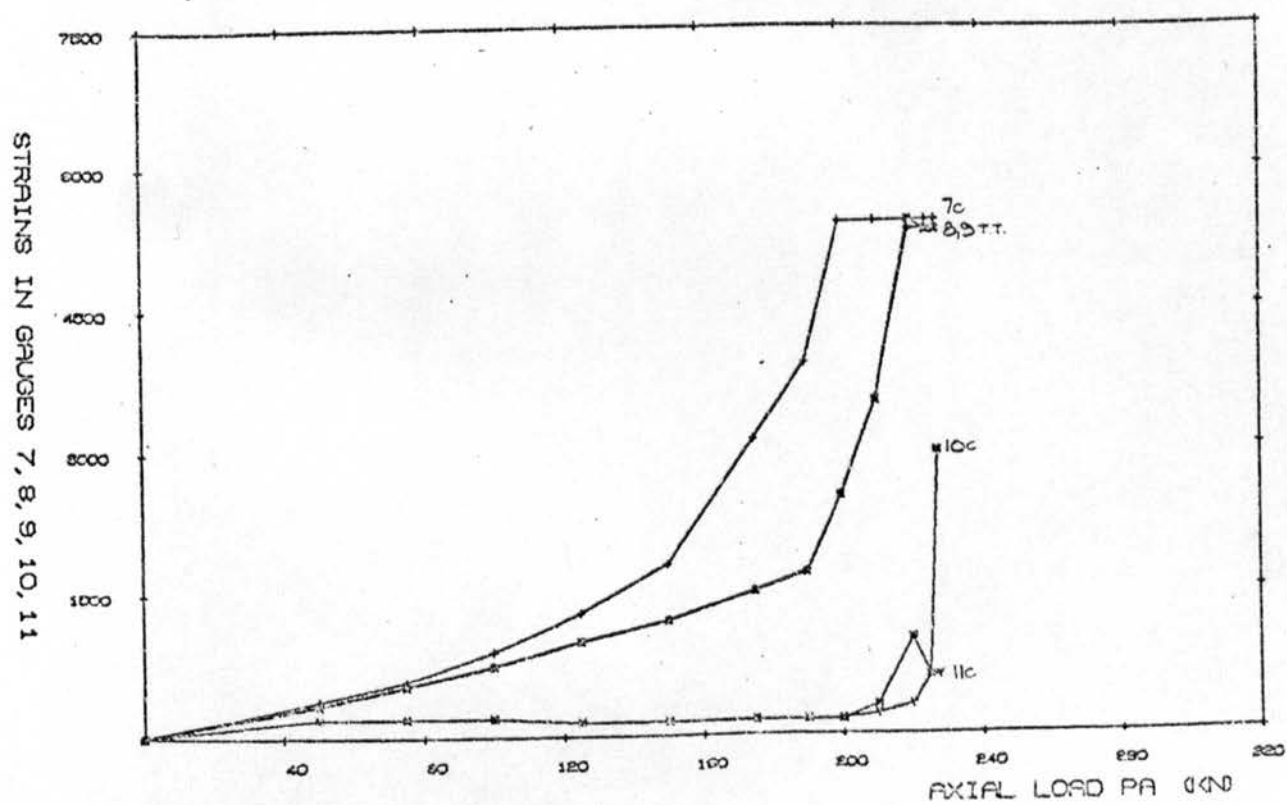
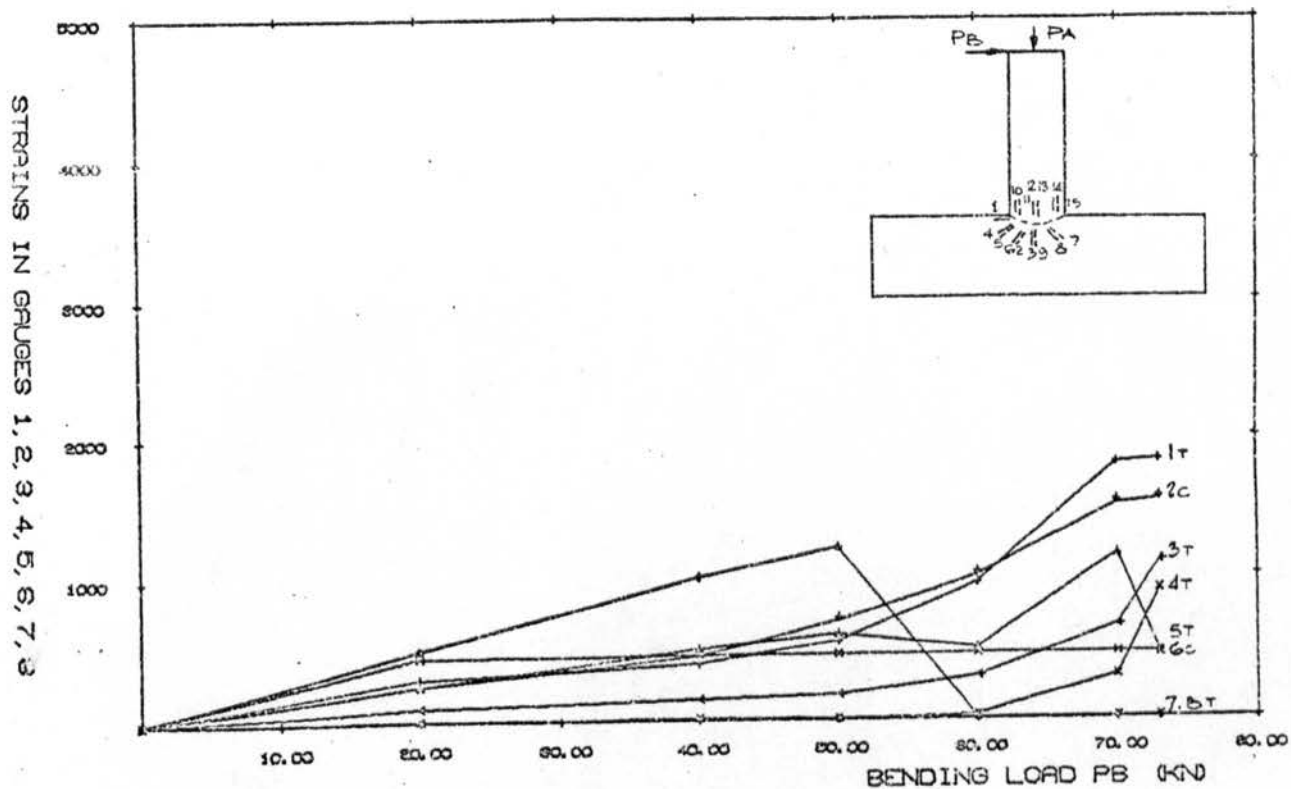


Figure 203

BETA = 1.0 CHORD THICKNESS = 5.0



BETA = 1.0 CHORD THICKNESS = 5.0

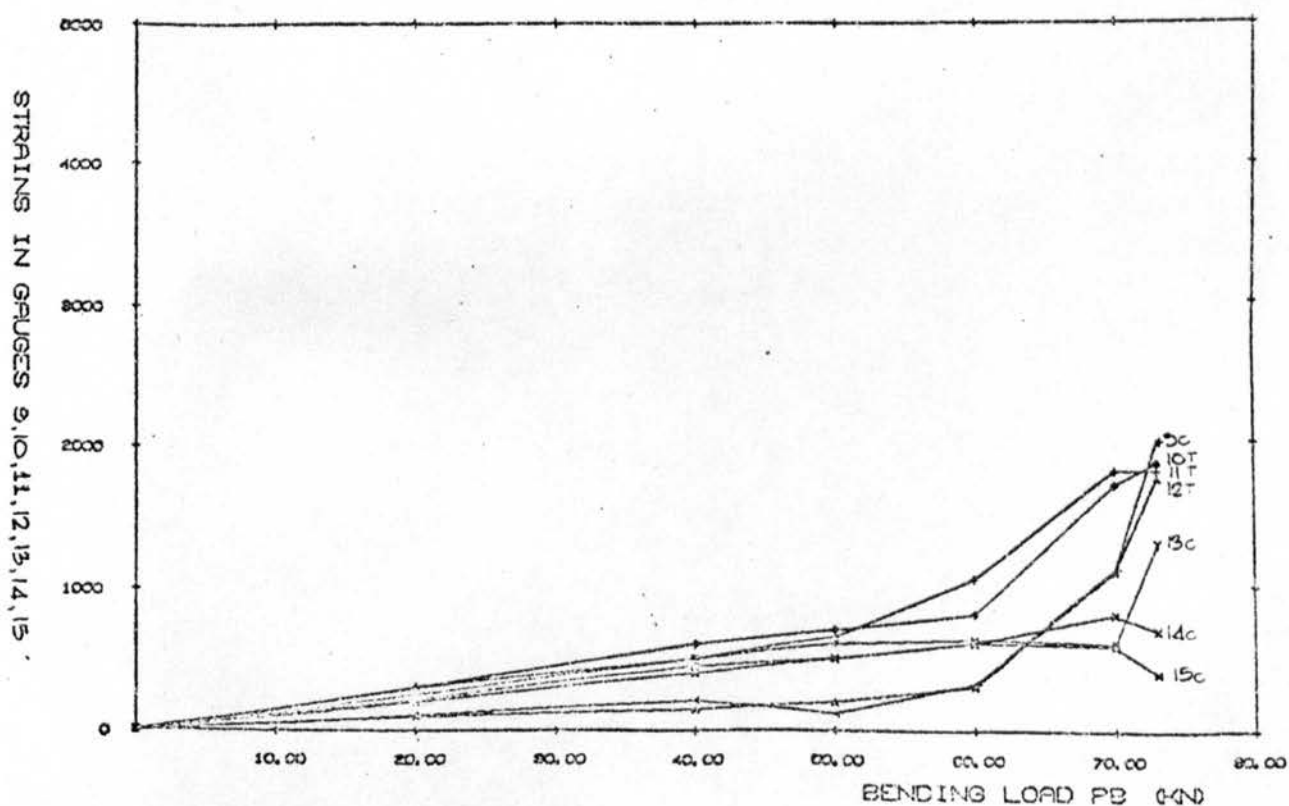
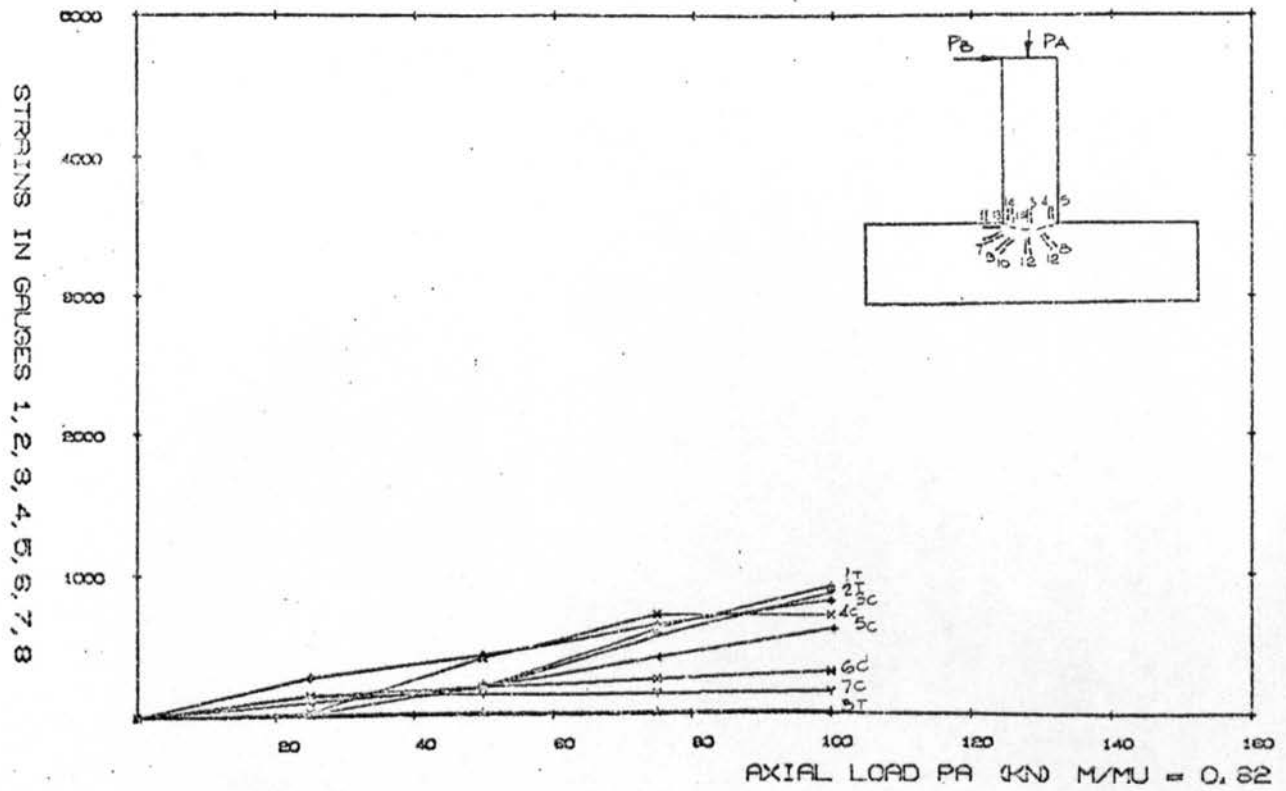


Figure 204

BETA = 1.0, CHORD THICKNESS = 5.0



BETA = 1.0, CHORD THICKNESS = 5.0

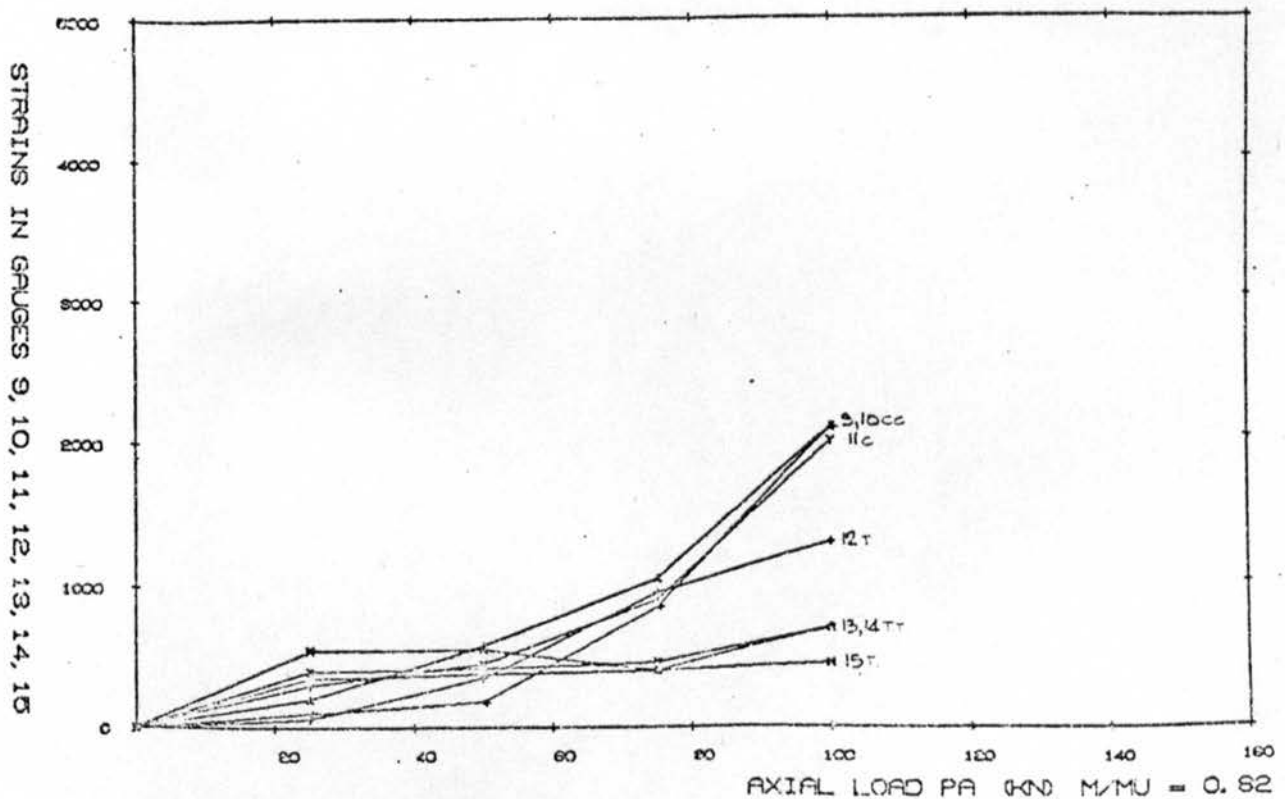
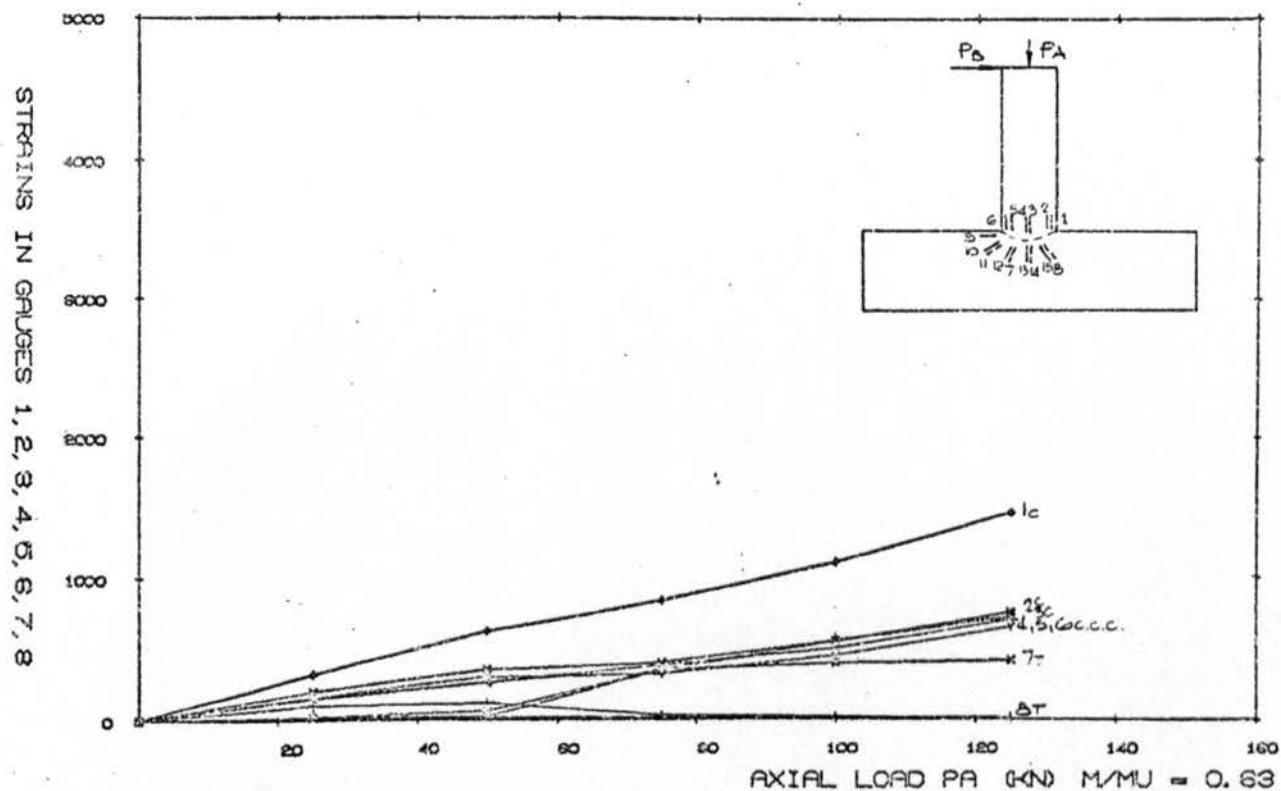


Figure 205

BETA = 1.0, CHORD THICKNESS = 5.0



BETA = 1.0, CHORD THICKNESS = 5.0

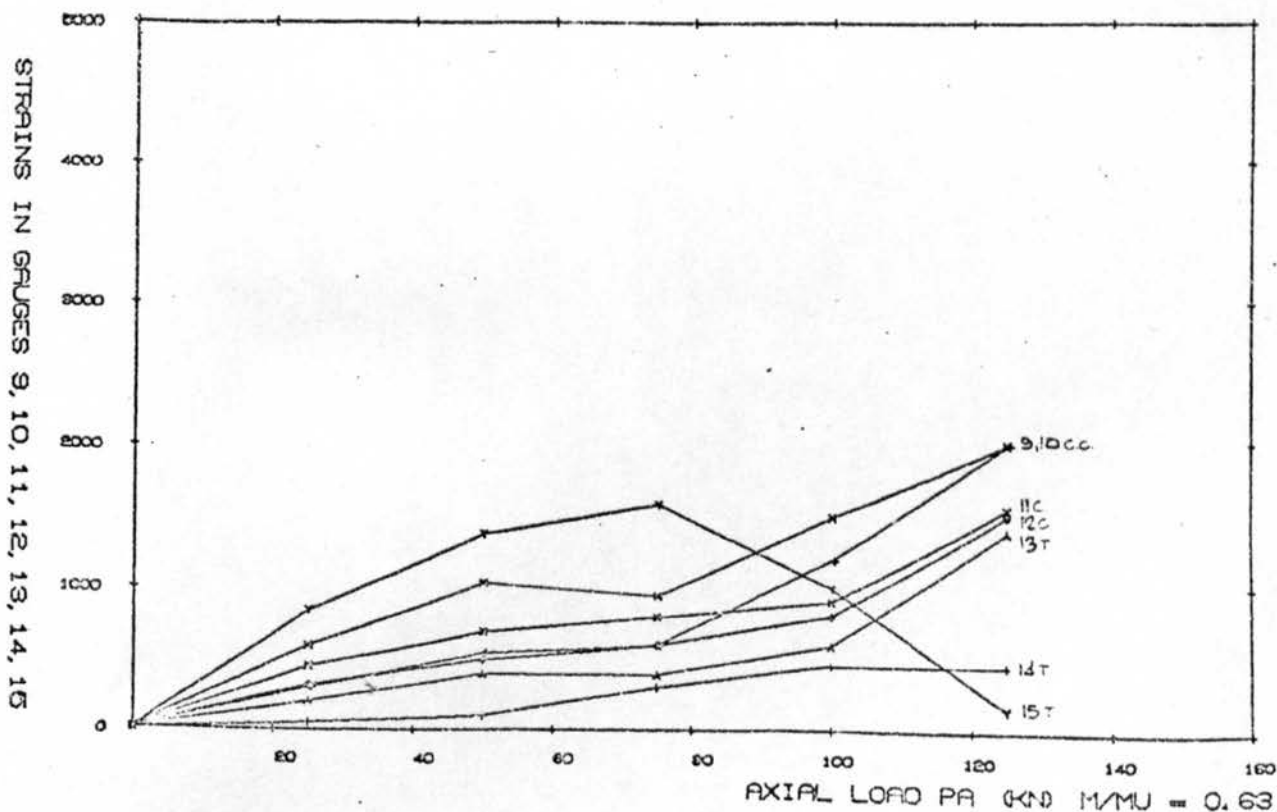
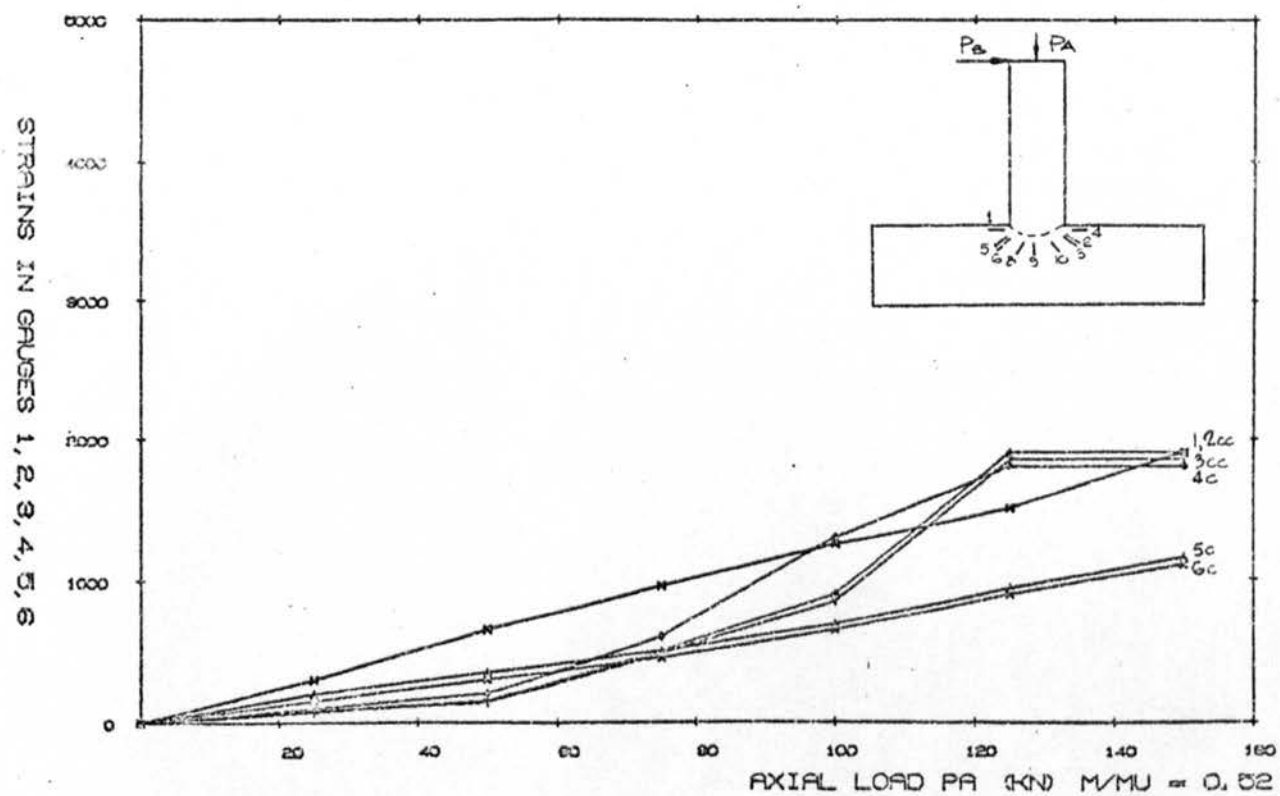


Figure 206

BETA = 1.0, CHORD THICKNESS = 5.0



BETA = 1.0, CHORD THICKNESS = 5.0

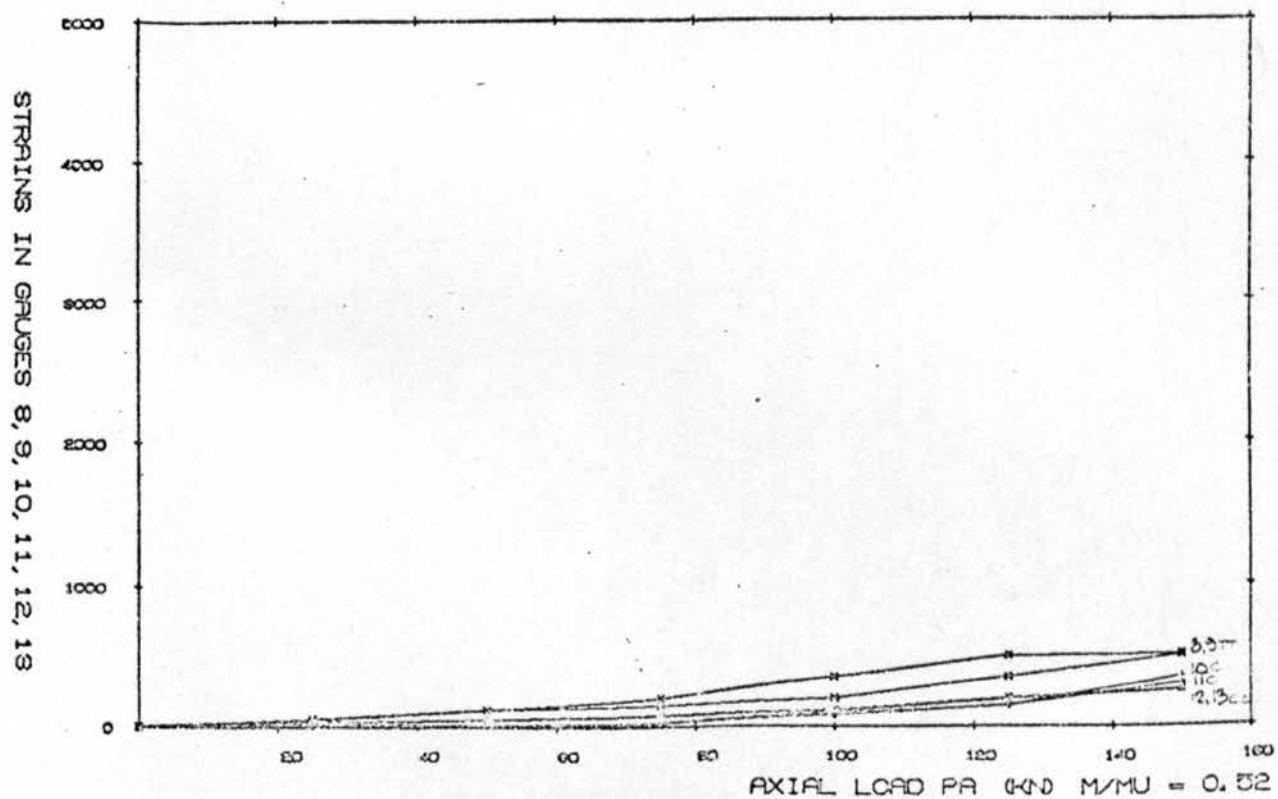


Figure 207

BETA = 1.0, CHORD THICKNESS = 5.0

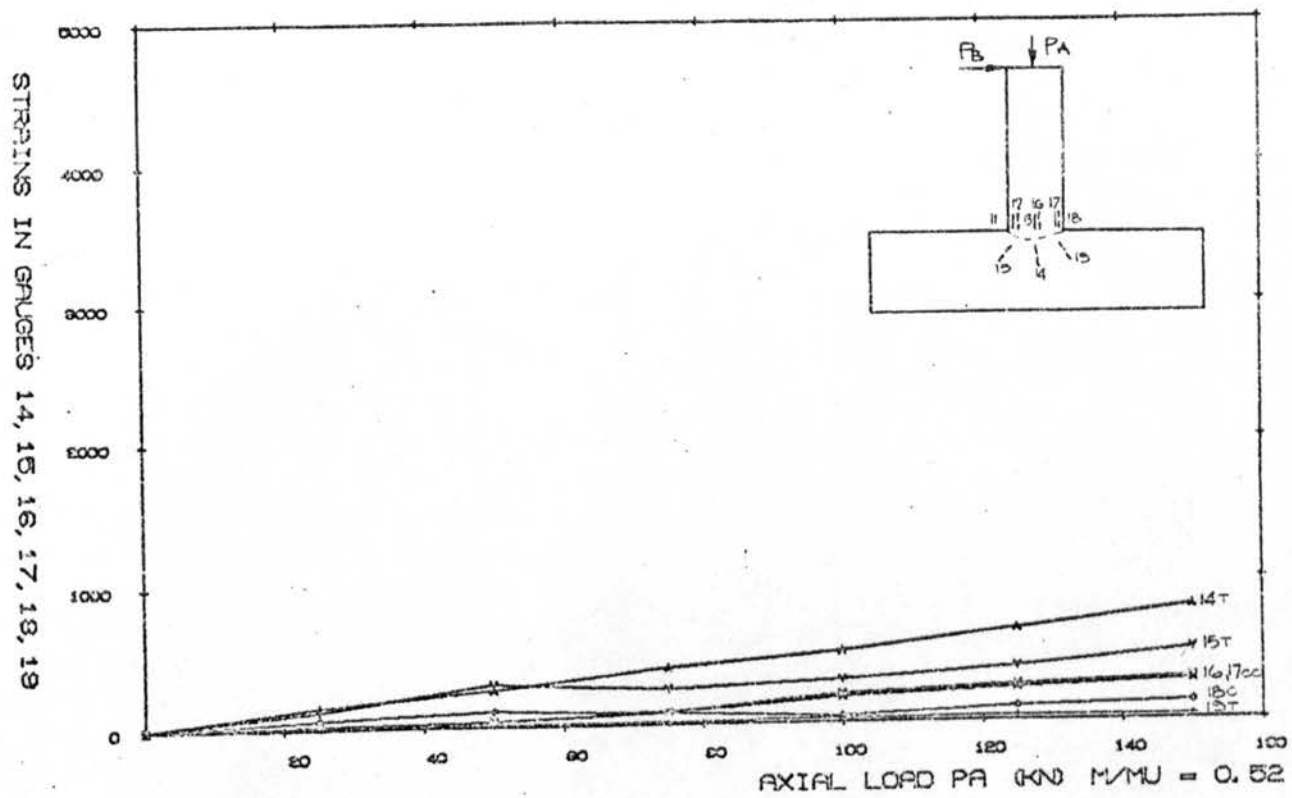
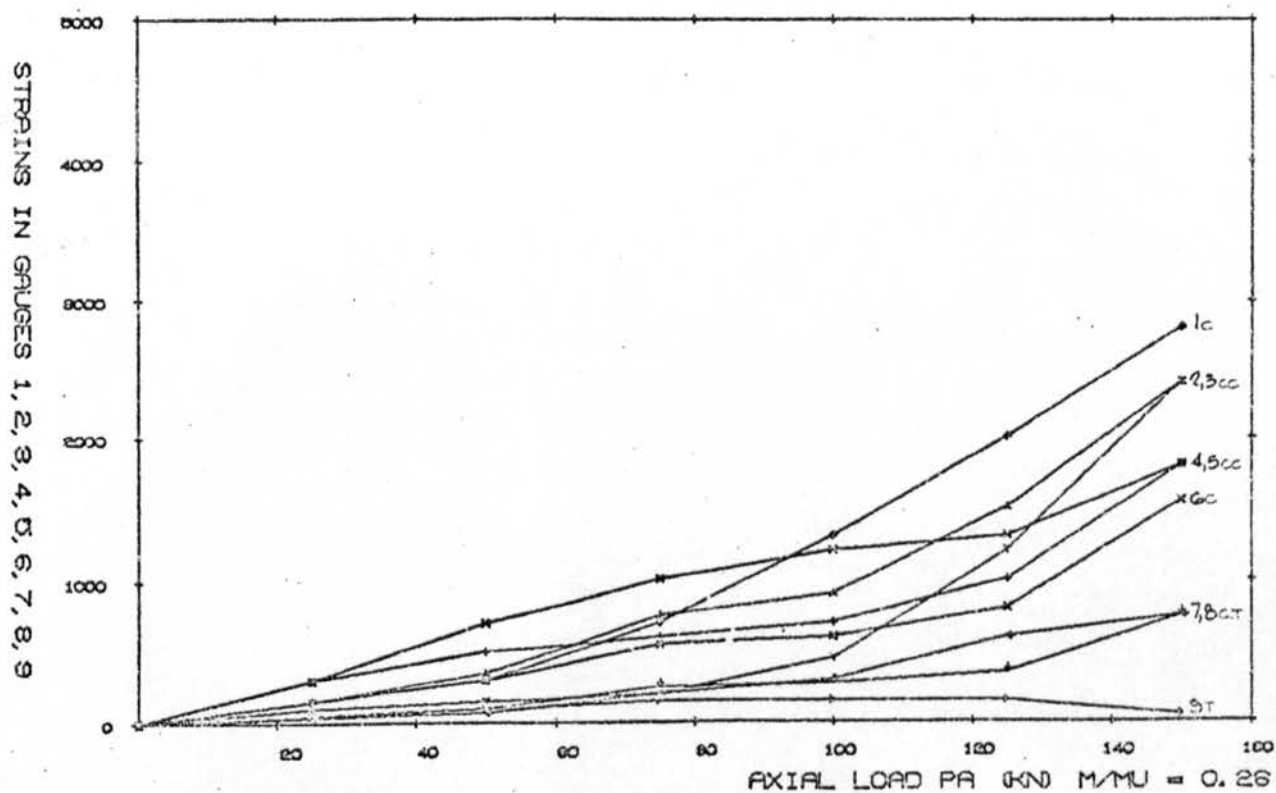


Figure 208

BETA = 1.0, CHORD THICKNESS = 5.0



BETA = 1.0, CHORD THICKNESS = 5.0

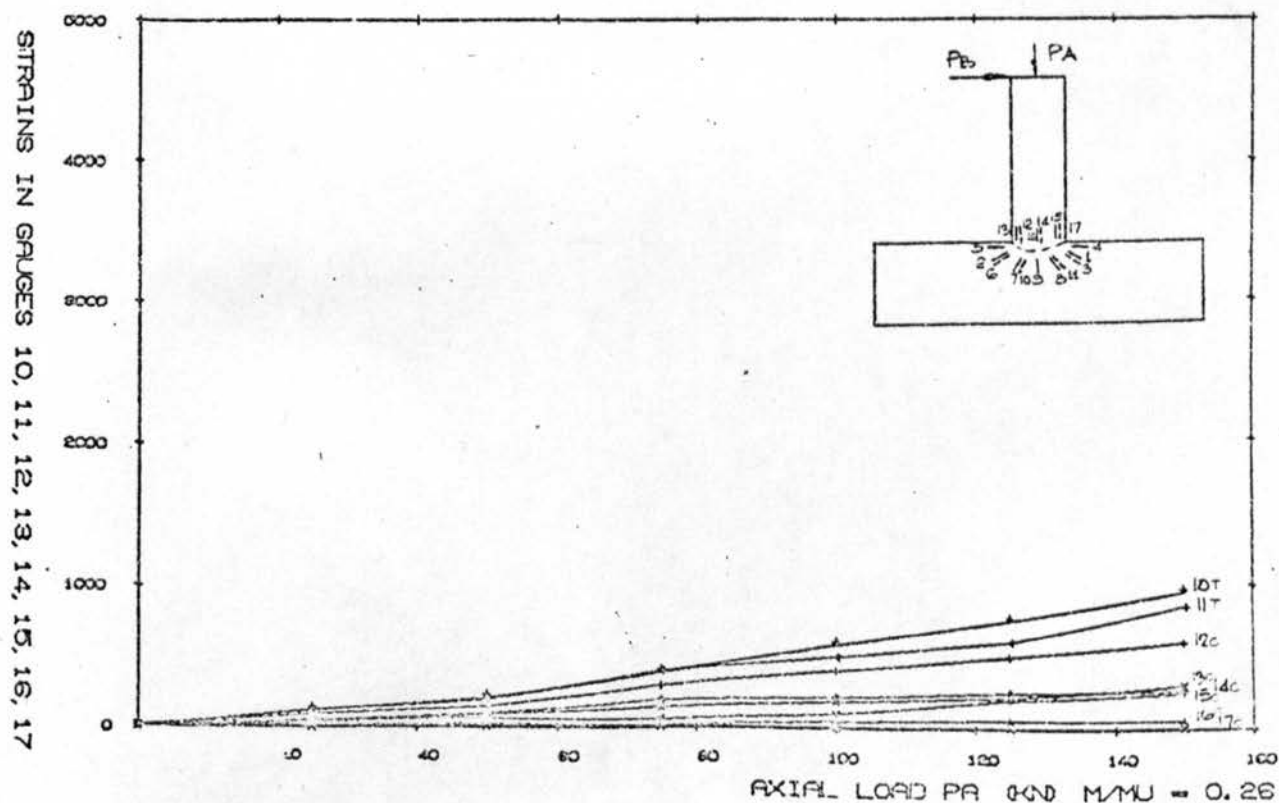


Figure 209

Intersection Lengths U_b and U_c (L_2 and L_1)

$$U_c = 3.57 Z_1 + 0.78 d_1 - 2q \left[\frac{\left(\frac{Z_2 d_2}{d_1} + 0.6 \frac{Z_2 d_2 - Z_1 d_1}{d_o} \right)}{\frac{Z_2 d_2}{d_1} + \frac{Z_2 d_1}{d_2}} \right]$$

$$Z_1 = d_1 / 2 \sin \theta_1$$

$$Z_2 = d_2 / 2 \sin \theta_2$$

$$U_b = \left(\frac{d_o}{2} + e \right) \frac{q}{y} + \frac{d \min^2}{4 d_o} \quad q \geq Z \min$$

or

$$U_b = \left(\frac{d_o}{2} + e \right) \frac{q}{y} + \frac{d \min^2 q}{4 d_o \cdot Z \min} \quad q \leq Z \min$$

$$e = \frac{2y \tan \theta_1 \tan \theta_2 - d_o (\tan \theta_1 + \tan \theta_2)}{2(\tan \theta_1 + \tan \theta_2)}$$

$$y = (Z_1 + Z_2) - q$$

when $d_1 = d_2$ and $\theta_1 = \theta_2$ the equations simplify to:-

$$U_c = 3.57 + 0.78 d_1 - q$$

$$y = 2Z - q$$

$$e = \frac{y \tan \theta - d_o}{2}$$

U_c is often called L_1 (pages 70, 77 & 88).

U_b is often called L_2 (pages 70, 77 & 88).